Momcilo Miljkovic

Electrostatic and Stereoelectronic Effects in Carbohydrate Chemistry

Springer

Electrostatic and Stereoelectronic Effects in Carbohydrate Chemistry

Momcilo Miljkovic

Electrostatic and Stereoelectronic Effects in Carbohydrate Chemistry

Springer

Momcilo Miljkovic
Pennsylvania State University
Hershey, Pennsylvania, USA

ISBN 978-1-4614-8267-3 ISBN 978-1-4614-8268-0 (eBook)
DOI 10.1007/978-1-4614-8268-0
Springer New York Heidelberg Dordrecht London

Library of Congress Control Number: 2013955044

Printed on acid-free paper

Springer is part of Springer Science+Business Media (www.springer.com)

To the memory of my parents
Prof. Dr. Adam Miljković and
Dr. Dragoslava Miljković

In Memoriam

Dr. Momcilo Miljkovic was born on December 12, 1931, in Belgrade, Serbia. He was the son of physicians Dr. Adam Miljkovic and Dr. Dragoslava Miljkovic. At the age of 14, his father bought him a chemistry kit, and soon Momcilo was passionately conducting chemistry experiments at home in the family's kitchen. He became completely fascinated with chemistry, reading college textbooks while still in high school, and developing a reputation as a young chemist, so much so that his chemistry teacher would look to him in class for his approval or disapproval regarding the correctness of her lectures.

Dr. Momcilo Miljkovic went on to pursue a B.S. in chemistry at The University of Belgrade, Serbia, and later was awarded a Ph.D. in Chemistry in 1965 at the Eidgenossische Technische Hochschule (Swiss Federal Institute of Technology) in Zurich, Switzerland. He pursued post-doctoral studies under Dr. Vladimir Prelog (Nobel Laureate) at ETH, while his informal mentor was Dr. Leopold Ruzicka (Nobel Laureate).

Another post-doctoral position brought him to the United States to the Department of Biochemistry at Duke University, and a year later he took a position as Assistant Professor in The Department of Biochemistry in the College of Medicine at The Pennsylvania State University. It is here that he spent over 40 years of his life, conducting research in carbohydrate chemistry as well as teaching graduate students and medical students.

Towards the end of his life, he preoccupied himself with writing. He published his first book *Carbohydrates: Synthesis, Mechanisms, and Stereoelectronic Effects* in 2010. He was particularly excited about writing *Electrostatic and Stereoelectronic Interactions in Carbohydrate Chemistry* due to the novelty of the material. Further, writing helped him focus away from his own terminal illness, giving him a newfound purpose in the latter stages of his life.

Acknowledgments

Several details were left unfinished, and completed after the author's death. Without the time, effort, and expertise of Dr. Stephen Benkovic, Department of Chemistry at The Pennsylvania State University, in editing portions of this book, it could not have been published.

Nor would this book have seen the light of day without the cheerful persistence of Dr. Marko Miljković, who nursed his father through his final illness, sorted through manuscripts left by his father, consulted with carbohydrate chemists when details in the manuscript were unclear, and meticulously edited portions of this book.

Contents

Chapter 1
Introduction

Stereoelectronic interactions in a molecule are important because they determine the conformation of that molecule and thus its chemical reactivity and very often the stereochemistry of its chemical transformations. These interactions involve the orbital interactions between the nonbonding orbitals.

The presence of charged or partially charged atoms (dipoles) in a molecule generates electrostatic interactions. These interactions can take place between two or more such molecules (intermolecular electrostatic interactions) or can be within a single molecule (intramolecular electrostatic interactions). The electrostatic interactions can be stabilizing or destabilizing in nature: When two opposing charges are facing each other or are next to each other, they are stabilizing, and when two identical charges are facing each other or are next to each other, they are destabilizing.

The intermolecular electrostatic interactions are found in bimolecular reactions of a charged reactant approaching a molecule with strong dipolar bonds or even charges (e.g., in enzyme-catalyzed reactions, where they are used not only to properly position a substrate in the active site of an enzyme but also to lower the activation energy barrier for the subsequent chemical transformation of a substrate).

The intramolecular electrostatic interactions play a very important role in the control of the conformation of a molecule and consequently control its chemical behavior. These interactions will be discussed first.

1.1 Intramolecular Electrostatic Interactions

In 1953, Corey [1] studied the conformational equilibrium of α-halocyclohexanones (α-bromo- and α-chlorocyclohexanones) since the C=O and the C–X (X = halogen) bonds are both strongly polarized, mutually repulsive, and next to each other. The conformer having the halogen atom equatorially oriented should be destabilized due to dipolar interactions between the C–X and the C=O dipoles which are almost coplanar and equatorially oriented, whereas the conformer having the halogen atom

M. Miljkovic, *Electrostatic and Stereoelectronic Effects in Carbohydrate Chemistry*,
DOI 10.1007/978-1-4614-8268-0_1, © Springer Science+Business Media New York 2014

Fig. 1.1

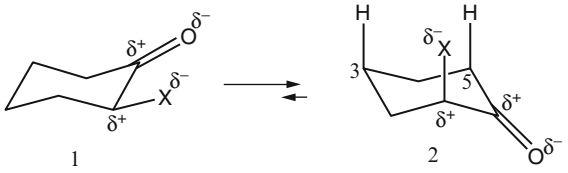

Table 1.1 The carbonyl frequency shift dependence on the conformation of the α-halo substituent

Compound	Position of carbonyl absorption, cm^{-1}	Frequencies shift due to α-halogen, cm^{-1}
Cyclohexanone	1,712	–
α-Bromocyclohexanone	1,716	4
α-Chlorocyclohexanone	1,722	10
4, 4-Dimethylcyclohexanone	1,712	–
2-Bromo-4, 4-dimethylcyclohexanone	1,728	16

in the axial orientation (*1*) (Fig. 1.1) will be subjected to nonbonding interactions with the axial C3 and C5 hydrogen atoms of a cyclohexane ring, but will not be subjected to dipolar interactions with the carbonyl group. Corey believed that the isomer with the equatorially oriented halogen will be more destabilized than the axial isomer (Fig. 1.1), because the C–X and the C=O dipoles are strong, and therefore he expected that the α-chlorocyclohexanones and α-bromocyclohexanones will, at room temperature, predominantly exist in the chair conformation in which the α-halogen atom is axially oriented (*2*) (Fig. 1.1).

In order to determine the conformational equilibrium of α-halocyclohexanones, Corey used infrared spectroscopy, since the substitution of one α-hydrogen in a cyclohexanone with a halogen produced a frequency shift in the absorption of the carbonyl group, where the frequency shift magnitudes depended upon whether or not the α-halogen atom was axial or equatorial (Table 1.1).

Calculations have shown that the equilibrium mixture of possible α-halocyclohexanone conformers, at room temperature, consists of more than 97 % of axial conformers and less than 3 % of equatorial conformers, implying that the axial conformer is more stable than the equatorial conformer by 2.3 kcal/mol.

4-Methoxycyclohexanone is another example of the intramolecular electrostatic interaction control of the conformation of a molecule. It was found that 4-methoxycyclohexanone favors, in a number of solvents, the conformation in which the strongly electronegative C4 methoxy group is axially oriented due to the presence of the strongly polarized C1 carbonyl oxygen bond [2, 3], as shown in Fig. 1.2 and Table 1.2. The axial conformer 9 is favored over the equatorial conformer 3 by 0.4 kcal/mol.

Similar conformational preferences are found in 4-halocyclohexanones, with the fluoro derivative having the highest percentage of the C4 axial conformer [4, 5].

The suggested explanation for this observation is the transannular stabilization of partial positive charge of the C1 carbonyl carbon by an axially oriented partial

Fig. 1.2

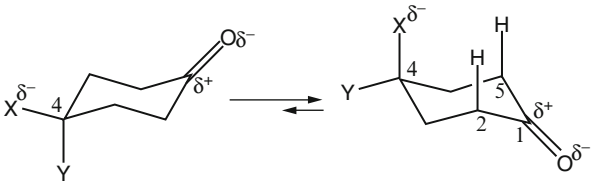

3, X = OMe; Y = D
4, X = OH; Y = D
5, X = OBz; Y = D
6, X = Cl; Y = D
7, X = Br; Y = H
8, X = I, Y = H

9, X = OMe; Y = D
10, X = OH; Y = D
11, X = OBz; Y = D
12, X = Cl; Y = D
13, X = Br; Y = H
14, X = I, Y = H

Table 1.2 Conformational equilibria of 4-substituted cyclohexanones as determined by NMR spectroscopy at 30 ± 3° [2]

X	Solvent	% axial isomer	ΔG°, kcal/mol
MeO	C_6H_6	73	−0.6
	CCl_4	70	−0.5
	CD_3COCD_3	68	−0.5
HO	C_6H_6	56	−0.15
	$CDCl_3$	54	−0.1
BzO	C_6H_6	60	−0.23
	CD_3COCD_3	59	−0.22
Cl	CCl_4	67	−0.42
	$FCCl_3$	65	−0.38
	CD_3COCD_3	57	−0.17
Br	C_6H_6	54	−0.1
I	C_6H_6	55	−0.2

negative charge of the electronegative C4 substituent. This stabilization is obviously larger than the destabilization due to the steric nonbonding 1, 3-*syn*-diaxial interaction between the axially oriented C4 substituent and the axially oriented C2 and the C6 hydrogens.

Reduction of 4-methylcyclohexanone *15* with lithium aluminum hydride gives, in 80–84 % yield, a mixture of *cis*-and *trans*-4-methylcyclohexanol *17* and *18* in which the *trans*-4-methylcyclohexanol with both the methyl and the hydroxyl group in equatorial orientation (Fig. 1.3) predominates [6–8]. Similar results were obtained when 4-methylcyclohexanone is reduced with sodium borohydride, but in this case the *cis*/*trans* ratio of obtained 4-methylcyclohexanols depended upon the solvent (see Table 1.3).

The picture dramatically changes when 4-chlorocyclohexanone is reduced with lithium aluminum hydride. Now the *cis*-4-chlorocyclohexanol is obtained as the predominant product [9] (Table 1.3).

Miljkovic et al. in their studies directed toward the stereoselective synthesis of erythronolide A, the 14-membered lactone ring of erythromycin A, from D-glucose [10], needed to introduce an axial methyl group at the C4 carbon of a methyl D-*xylo*-hexopyranosid-4-ulose derivative (this represented the synthesis of the C12

Fig. 1.3

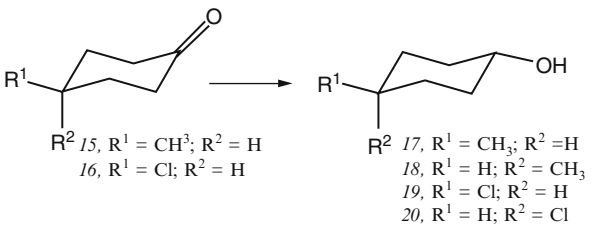

15, $R^1 = CH^3$; $R^2 = H$
16, $R^1 = Cl$; $R^2 = H$

17, $R^1 = CH_3$; $R^2 = H$
18, $R^1 = H$; $R^2 = CH_3$
19, $R^1 = Cl$; $R^2 = H$
20, $R^1 = H$; $R^2 = Cl$

Table 1.3 Ratios of *cis*/*trans*-4-substituted alcohols obtained by reduction of 4-substituted cyclohexanones

	4-methylcyclohexanol		4-chlorocyclohexanol	
	cis	*trans*	*cis*	*trans*
Sodium borohydride in				
Methanol	18	82	59	41
Tetrahydrofuran	17	83	53	47
Propan-2-ol	15	85	63	37
Acetonitrile	11	89	52	48
Diborane in				
Tetrahydrofuran	11	89	69	31
Lithium aluminum hydride in				
Tetrahydrofuran	16	84	67	33

carbon of erythronolide A) and to develop a simple and reliable method for the configurational assignment of the obtained branched carbon atom.

It was well known at that time that the addition of Grignard reagents and organolithium compounds to the carbonyl group in carbohydrates was a highly stereoselective reaction [11], but unfortunately, unpredictable. In some cases, products epimeric at the quaternary carbon were obtained [12, 13], whereas in other instances the obtained branched-chain sugars had the same configuration at the branching carbon [14].

Methyl 2, 3-di-*O*-methyl-6-*O*-triphenylmethyl-α- *21* and β-D-*xylo*-hexopyranosid-4-uloses *22* have been used as model substrates for these studies (Fig. 1.4). The reaction of glucopyranosid-4-ulose *21* with an ethereal solution of methyllithium (LiBr-free) at −80 °C afforded methyl 2, 3-di-*O*-methyl-6-*O*-triphenylmethyl-α-D-glucopyranoside *23* as the only product in which the C4 methyl group is axially oriented.

Reaction of the same oxo sugar *21* with an ethereal solution of methylmagnesium iodide at −80 °C proceeded again with high stereoselectivity, but the obtained product *24* was now the C4 epimer of the branched-chain sugar *23*, namely, methyl 2, 3-di-*O*-methyl-6-*O*-triphenylmethyl-α-D-galactopyranoside *24*.

The high stereoselectivity of the addition of methyllithium to the C4 carbonyl group was lost when an ethereal solution of methyllithium reacted with the β-anomer of *21*, at −80 °C, namely, with the methyl 2, 3-di-*O*-methyl-6-*O*-triphenylmethyl-β-D-*xylo*-hexopyranosid-4-ulose *22*, whereby a mixture of C4 epimers *25* and *26* was obtained

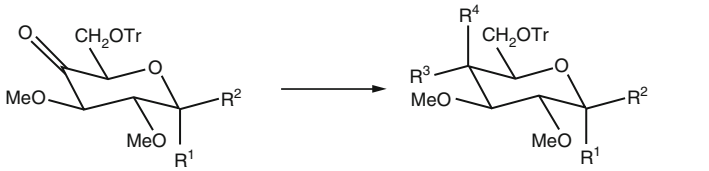

21, R^1 = OMe; R^2 = H
22, R^1 = H; R^2 = OMe

23, R^1 = OMe; R^2 = H; R^3 = OH; R^4 = Me
24, R^1 = OMe; R^2 = H; R^3 = Me; R^4 = OH
25, R^1 = H; R^2 = OMe; R^3 = Me; R^4 = OH
26, R^1 = H; R^2 = OMe; R^3 = OH; R^4 = Me

Fig. 1.4

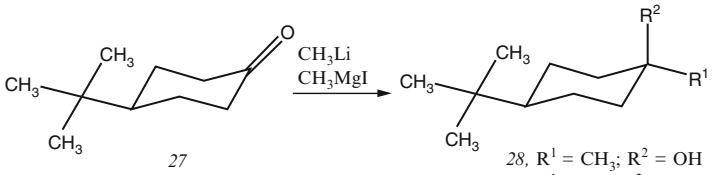

27

28, R^1 = CH_3; R^2 = OH
29, R^1 = OH; R^2 = CH_3

Fig. 1.5

in which the methyl 2, 3-di-*O*-methyl-6-*O*-triphenylmethyl-β-D-glucopyranoside *26* was again the predominant product but only in 3:1 ratio.

In contrast to the above results, the addition of methylmagnesium iodide to the C4 carbonyl group of *21* or *22* (ether and −80 °C) proceeded with high stereoselectivity, yielding in both cases methyl 2, 3-di-*O*-methyl-6-*O*-triphenylmethyl-β-D-galactopyranoside *25* as the only product, thus indicating that the stereochemistry of the addition of methylmagnesium iodide to the C4 carbonyl group did not depend upon the anomeric configuration.

Finally, both methyllithium and methylmagnesium iodide added non-stereoselectively and at a considerably slower rate to the *tert*-butyl-cyclohexanone *27* (Fig. 1.5) at −80 °C, yielded in each case a mixture of both C1 epimers: *trans*-4-*tert*-butyl-cyclohexanol *28* and *cis*-4-*tert*-butyl-cyclohexanol *29*. The isomer with the equatorial methyl group *28* (*trans*-product) was the predominant product in both reactions (*28*:*29* = 3.6:1 in the first case and 3:1 in the second case).

The above results have been rationalized in the following way. From the studies of conformational equilibria of 2-halocyclohexanones, we have seen that the conformation in which the electronegative halogen atom is axially oriented is strongly favored as compared to the conformation having the halogen atom equatorially oriented. This preference for the axial orientation was explained to be the consequence of strong dipolar interactions between the C2-Hal and the C=O dipoles when the halogen atom is equatorially oriented.

Fig. 1.6

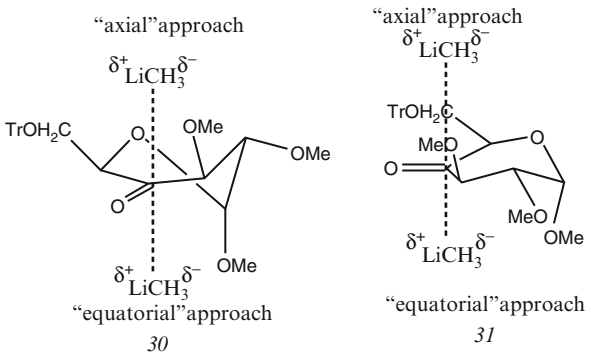

Miljkovic et al. [10] assumed that a similar situation must exist in case of oxo sugar *21* where the $^4C_1$ conformation is probably destabilized due to the strong dipolar interaction between the equatorial electronegative C3 methoxy and the polarized C4 carbonyl group dipoles which are in this conformation coplanar and equatorially oriented. Consequently, the oxo sugars *21* and *22*, at −80 °C, most likely adopt either a half-chair conformation *31* or a conformation *30* which is between the $^4C_1$ *21* and the half-chair conformation *31* as shown in Fig. 1.6.

The adoption of any conformation other than $^4C_1$ by *21* prior to the addition of methyllithium to the C4 carbonyl carbon should result in the axial addition of methyllithium, since the severe electrostatic and nonbonding steric interaction between the electronegative anomeric (C1) methoxy group and the "equatorially" approaching methyl carbanion of methyllithium will impede the equatorial addition of methyllithium. In the case of an axial attack of methyllithium to the C4 carbonyl carbon, these severe "1, 4-diaxial" electrostatic and steric interactions are avoided. This rationalization is strongly supported by the finding that methyl 2, 3-di-*O*-methyl-6-*O*-triphenylmethyl-β-D-*xylo*-hexopyranosid-4-ulose *22*, where such "1, 4-diaxial" electrostatic and nonbonded steric interactions do not exist, reacts with an ethereal solution of methyllithium at −80 °C to yield both C4 epimers (*23* and *24*, Fig. 1.4).

The reversal of stereochemistry in the addition of the Grignard reagent to the oxo sugar *21* was rationalized to be the consequence of "chelation" of the magnesium atom of the Grignard reagent with the C4 carbonyl oxygen and the C3 methoxy oxygen atom prior to the addition of methyl group to the carbonyl carbon [15, 16] (for a discussion of the relationship between chelated and non-chelated coordination transition states and the stereospecificity of the reaction between the Grignard reagent and α-alkoxy carbonyl derivatives, see Guillerm-Dron et al. [15] and Yochimura et al. [17]). Thus, the formation of the cyclic five-membered ring intermediate *32* forces the oxo sugar *21* to adopt the $^4C_1$ conformation prior to the addition of the methyl group to the C4 carbonyl carbon (Fig. 1.7). This explanation is supported by the finding that the Grignard reagent attacks also the C4 carbonyl carbon of the β-anomer of *21* (the oxo sugar *22*) exclusively equatorially. Furthermore, the addition of the Grignard reagent to the oxo sugar *22*

Fig. 1.7

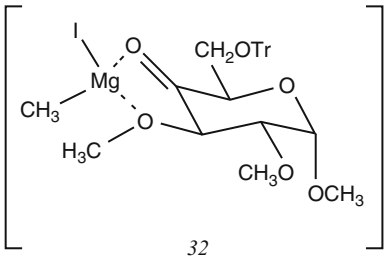

32

Table 1.4 Carbon-13 chemical shifts of the C4 methyl group in branched-chain sugars *23–26*

Branched-chain sugar	Chemical shift, ppm[a]	Methyl group at C4
23	15.4	Axial
24	21.9	Equatorial
25	15.5	Axial
26	21.8	Equatorial

[a]Downfield from TMS

is solvent dependent which also supports the idea of chelate formation prior to the addition of the methyl group to the C4 carbonyl carbon.

We would like here to briefly mention how the configurational assignment of the C4 branched-chain sugar was made. The observation made during the conformational studies of methylcyclohexanes [18–20] that the carbon-13 chemical shift of an axial methyl group is shifted 6 ppm toward a higher field than that of an equatorial methyl group prompted Miljkovic et al. [10, 21] to investigate the possibility of utilizing the carbon-13 resonance of the C4 methyl group in determining the configuration at the branching carbon atom in sugars *23–26*. Table 1.4 lists carbon-13 chemical shifts of the C4 methyl group in branched-chain sugars *23–26*.

Transition state geometry of the reactions of metal hydrides (and organometallic reagents) with a carbonyl group is thought to resemble the geometry of the starting ketone, and the nonbonded steric interactions, electrostatic interactions (dipole-dipole repulsions), and torsional strain are the controlling factors in determining the direction from which a nucleophile will approach a carbonyl group [22].

In the case of β-D-glucopyranosid-2-ulose 33 (Fig. 1.8), the axial approach of metal hydride anion to the C2 carbonyl carbon, resulting in the formation of transition state *37* (Fig. 1.9), requires that the negatively charged metal ion approaches the C2 carbonyl carbon from a direction bisecting the C_1–O_1 and C_1–O_5 torsional angle. Since the C_1–O_1 and C_1–O_5 bonds are polarized and act as two equally oriented dipoles, an approach which will appose a negatively charged ion between them should be energetically unfavorable owing to electrostatic repulsion. An "equatorial" approach of the negatively charged metal hydride ion to the C2 carbonyl carbon of *33* (Fig. 1.8) resulting in the transition state *38* (Fig. 1.9) will however not only be free from the electrostatic interactions, but the torsional strain and nonbonded steric interactions will also be at a minimum as well.

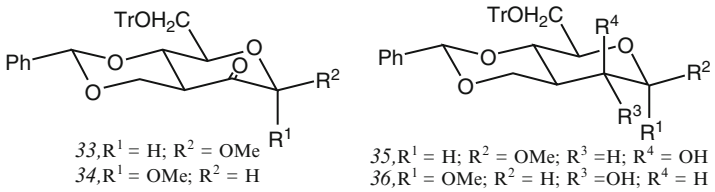

33,R^1 = H; R^2 = OMe
34,R^1 = OMe; R^2 = H

35,R^1 = H; R^2 = OMe; R^3 =H; R^4 = OH
36,R^1 = OMe; R^2 = H; R^3 =OH; R^4 = H

Fig. 1.8

Fig. 1.9

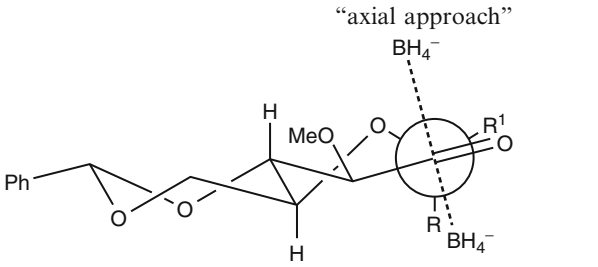

37, R =H; R^1 = OMe ("axial" approach)
38, R =H; R^1 = OMe, ("equatorial" approach)
39, R = OMe; R^1 = H, ("axial" approach)
40, R = OMe; R^1 = H; ("equatorial" approach)

In the transition state *39* (Fig. 1.9), which results from an "axial" approach of the negatively charged metal hydride ion to the C2 carbonyl carbon of the α-D-glycopyranosid-2-ulose, e.g., *34* (Fig. 1.8), the electrostatic interactions of the type described for the transition state *37* are not present. Furthermore, there will be no torsional strain. The only interaction present in *39* is one 1, 3-nonbonded steric interaction between the axially oriented C4 hydrogen atom and the incoming metal hydride anion. An "equatorial" approach of the negatively charged metal hydride ion to the C2 carbonyl carbon of *34* (Fig. 1.8) resulting in the formation of the transition state *40* (Fig. 1.9) should give rise to the generation of considerable torsional strain as well as electrostatic (dipolar) interaction between the axially oriented C1 methoxy group and the approaching metal hydride anion. Furthermore, in the transition state *40*, there will be two nonbonded steric interactions between the approaching metal hydride anion and axially oriented hydrogens at the C3 and C5 carbons.

As a consequence, the metal hydride reduction of *33* should give methyl 4, 6-*O*-benzylidene-3-*O*-methyl-α-D-glucopyranoside *36* as the preponderant, if not the only, product, whereas the metal hydride reduction of *34* should yield methyl 4, 6-*O*-benzylidene-3-*O*-methyl-β-D-mannopyranoside *35* as the preponderant product.

The experimental results were in full agreement with the above predictions. The sodium borohydride reduction in methanol of methyl 4, 6-*O*-benzylidene-3-*O*-methyl-β-D-*arabino*-hexopyranosid-2-ulose *33* gave a crude reduction product that consisted almost exclusively of methyl 4, 6-*O*-benzylidene-3-*O*-methyl-α-D-mannopyranoside *35* (Fig. 1.8) (the manno to gluco ratio was 19:1). The sodium borohydride reduction of methyl 4,6-*O*-benzylidene-3-*O*-methyl-α-D-*arabino*-hexopyranosid-2-ulose *34* in methanol afforded methyl 4, 6-*O*-benzylidene-3-*O*-methyl-β-D-glucopyranoside *36* as the only product.

References

1. Corey EJ (1953) The stereochemistry of α-haloketones. I. The molecular configurations of some monocyclic α-halocyclanones. J Am Chem Soc 75:2301–2304
2. Stolow RD, Giants TW (1971) Predominance of the axial conformation of 4-methoxycyclohexanone. J Chem Soc Chem Commun 11:528–529
3. Baldry KW, Gordon MH, Hafter R, Robinson MJT (1976) Conformational effects in compounds with six-membered rings. XI. Study of a conformational equilibrium in the gas phase and in solvents ranging from nonpolar to water:4-methoxycyclohexanone. Tetrahedron 32:2589–2594
4. Došen-Mićović LJ, Jeremić D, Allinger NL (1983) J Am Chem Soc 105:1723–1733
5. Freitas MP, Tormena CF, Oliveira PR, Rittner R (2002) Halogenated six-membered rings: a theoretical approach for substituent effects in conformational analysis. THEOCHEM 589–590:147–151
6. Noyce DC, Denney DBJ (1950) Steric effects and stereochemistry of lithium aluminum hydride reduction. Am Chem Soc 72:5743
7. Eliel EL, Ro RS (1957) Conformational analysis. III. Epimerization equilibria of alkylcyclohexanols. J Am Chem Soc 79:5992–5994
8. Dauben WG, Bozak RE (1959) Lithium aluminum hydride reduction of methylcyclohexanones. J Org Chem 24:1956–1957
9. Combe MG, Henbest HB (1961) Polar and solvent effects in the reaction of substituted cyclohexanones. Tetrahedron Lett 2:404–409
10. Miljković M, Gligorijević M, Satoh T, Miljković D (1974) Synthesis of macrolide antibiotics. I. Stereospecific addition of methyllithium and methylmagnesium iodide to methyl α-D-xylo-hexopyranosid-4-ulose derivatives. Determination of the configuration at the branching carbon atom by carbon-13 nuclear magnetic resonance spectroscopy. J Org Chem 39:1379–1384
11. Inch TD (1972) The use of carbohydrates in the synthesis and configurational assignments of optically active, non-carbohydrate compounds. Advan Carbohydr Chem Biochem 27:191–225
12. Burton JS, Overend WG, Williams NR (1965) Branched-chain sugars. III. The introduction of branching into methyl 3, 4-O-isopropylidene-β-L-arabinoside and the synthesis of L-hamamelose. J Chem Soc 3433–3445
13. Feast AAJ, Overend WG, Williams NR (1966) Branched-chain sugars. VI. The reaction of methyl 3, 4-isopropylidene-β-D-erythro-pentopyranosidulose with organolithium reagents. J Chem Soc C 303–306
14. Flaherty B, Overend WG, Williams NR (1966) Branched-chain sugars VII. Synthesis of D-mycarose and D-cladinose. J Chem Soc C 398–403
15. Guillerm-Dron D, Capmau M-L, Chodkiewicz W (1972) Assistance of methoxy group to a carbonyl in the steric course of the addition of unsaturated organometallics. Tetrahedron Lett 37–40

16. Cram DJ, Kopecky KR (1959) Studies in stereochemistry. XXX. Models for steric control of asymmetric induction. J Am Chem Soc 81:2748–2755
17. Yochimura J, Ohgo Y, Ajisaka K, Konda Y (1972) Asymmetric reactions. VI. Stereoselectivities in phenyllithium and Grignard reactions with tetrahydrofurfural derivatives. Bull Chem Soc Jap 45:916–921
18. Dalling DK, Grant DM (1967) Carbon-13 magnetic resonance. IX. Methylcyclohexanes. J Am Chem Soc 89:6612–6622
19. Anet FAL, Bradley CH, Buchanan GW (1971) Direct detection of the axial conformer of methylcyclohexane by 63.1 MHz carbon-13 nuclear magnetic resonance at low temperature. J Am Chem Soc 93:258–259
20. Stothers JB (1972) Carbon-13 NMR spectroscopy. Academic Press, New York, pp 404–426
21. Miljković M, Gligorijević M, Satoh T, Glišin D, Pitcher R (1974) Carbon-13 nuclear magnetic resonance spectra of branched-chain sugars, configurational assignment of the branching carbon atom of methyl branched-chain sugars. J Org Chem 39:3847–3850
22. House HO (1972) Modern synthetic reactions, 2nd edn. W. A. Benjamin, Menlo Park, p 56

Chapter 2
Anomeric Effect and Related Stereoelectronic Effects

There are several good books and review articles published on this subject [1–6].

In the conformational equilibria of cyclohexanols the conformer with the equatorially oriented hydroxyl group predominates. Thus, at equilibrium, the cyclohexanol conformer with an equatorially oriented hydroxyl group constitutes 89 % of the mixture and the conformer with an axially oriented hydroxyl group constitutes only 11 % of the mixture. In D-glucopyranose, the conformational composition at equilibrium is 63 % of the isomer with the equatorially oriented anomeric hydroxyl group and 36 % of the conformer with the axially oriented hydroxyl group. "...Thus, in spite of the two O_a : H_a 1,3-*syn*-axial interactions between the anomeric axial oxygen and the C3 and C5 axially oriented hydrogens present in the α-anomer, the C1 isomer in the equilibrium mixture is significantly higher than in cyclohexanol. It should be noted that the estimated destabilization energy of 0.9 kcal/mol would require that the equilibrium mixture of the two D-glucopyranose anomers does not contain more than 20 % of the α-anomer." The studies of conformational equilibria of anomers of other glycopyranoses have shown that conformers with the axial anomeric oxygen (conformationally less favored isomers) are also present in higher percentage than expected (Tables 2.1 and 2.2).

In the case of D-glucose and D-galactose, the anomer with the equatorial C1 hydroxyl group (β) is, as expected, more stable, whereas in the case of D-mannose, the anomer with the axial C1 hydroxyl group (α) is more stable. The D-mannose is a special case and it will be discussed later.

The preference for the axial orientation of the C1 substituent in D-glucopyranose was found to increase with increasing electronegativity of the C1 substituent (Table 2.3).

The first rationalization of the tendency of aglycons of alkyl glycopyranosides to assume axial orientation was proposed by Edward [12] and most probably was inspired by the Corey study on the stereochemistry of some α-halocyclohexanones [13], in which it was determined that the most stable conformation of α-chloro-and α-bromocyclohexanone is the chair form, in which the halogen substituent is axial (*2* in Fig. 2.1).

M. Miljkovic, *Electrostatic and Stereoelectronic Effects in Carbohydrate Chemistry*,
DOI 10.1007/978-1-4614-8268-0_2, © Springer Science+Business Media New York 2014

Table 2.1 Conformational equilibria of anomers of glycopyranoses [7]

	Estimated from oxidation[a] %		Calculated from optical rotation[b] %	
Sugar	α	β	α	β
D-glucose	37.4	62.6	36.2	63.8
D-mannose	68.9	31.1	68.8	31.2
D-galactose	31.4	68.6	29.6	70.4

[a]Oxidation of sugar solutions at 0 °C with bromine water in the presence of barium carbonate
[b]Calculated from optical rotation, assuming that only two sugar isomers are present in the solution

Table 2.2 Relative free energies (kcal/mol) and the percentage of α-anomer for selected D-aldohexo- and D-aldopentopyranoses in aqueous solution at equilibrium[a]

				α-anomer, %	
Pyranose	G^0_α	G^0_β	G^0_{pyranose}	Calculated	Experimental
Glucose	2.4	2.05	1.8	36	36
Galactose	2.85	2.5	2.25	36	27
Mannose	2.5	2.95	2.25	68	67
Idose	3.65	4.0	3.4	64	46
Ribose	3.1	2.3	2.15	20.5	26
Arabinose	1.95	2.2	1.65	60	63
Xylose	1.9	1.6	1.35	37	33
Lyxose	1.85	2.4	1.65	72	71

[a]Determined by ^{1}H nuclear magnetic resonance [8]

Table 2.3 Anomeric equilibria of 1-substituted D-glucopyranoses

Sugar	C1 substituent	% Axial isomer
D-Glucopyranose[a]	OH	36
Methyl D-glucopyranoside[b]	OMe	67
Penta-*O*-acetyl-D-glucopyranose[c]	OAc	86
Tetra-*O*-acetyl-D-glucopyranosyl chloride[d]	Cl	94

[a]In water at 25 °C
[b]In methanol at 25 °C
[c]In acetic acid-acetic anhydride at 25 °C using perchloric acid as catalyst [9–11]
[d]In acetonitrile at 30 °C [5]

Fig. 2.1

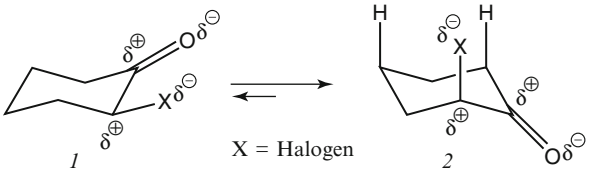

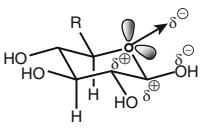

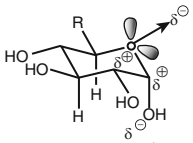

3, R = H; β-D-xylopyranose
4, R = CH_2OH, β-D-glucopyranose

5, R = H; α-D-xylopyranose
6, R = CH_2OH, α-D-glucopyranose

Fig. 2.2

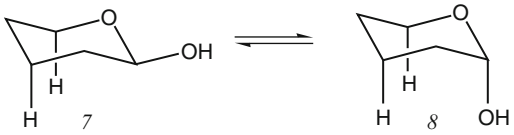

Fig. 2.3

As was shown in Chap. 1, this was explained to be the consequence of a dipole–dipole interaction between the C-halogen and the C = O group when the halogen atom is equatorially oriented, which is considered to be a more destabilizing interaction than the steric interaction between the axial halogen atom and the two axial hydrogen atoms in the conformer with the axially oriented halogen atom.

Edward explained the anomeric effect as a destabilizing effect which is the consequence of a dipolar repulsion of an equatorially oriented C1 electronegative substituent and the resultant dipole of the two unshared sp^3 electron pairs on the ring oxygen (Fig. 2.2), which is present only in the β- but not in the α-anomer. Thus the anomeric effect was originally considered to be an electrostatic effect that destabilizes the equatorially oriented C1 electronegative substituent through a dipolar interaction with the two pairs of nonbonding electrons on the ring oxygen (Fig. 2.2).

Comparison of the two anomers of D-glucopyranose (Fig. 2.2) shows that, except for the two 1,3-*syn*-axial interactions between the axial O1 and the axial C3 and C5 hydrogen atoms, which are present only in the α-anomer (*5* and *6*), both anomers have all other nonbonded interactions identical, including the gauche interaction between the C1 and the C2 hydroxyl groups. Consequently, the study of the interconversion of the two anomers of D-glycopyranose (*anomerization*, the isomerization of the anomeric carbon) can be simplified by substituting D-glucopyranose with the 2-hydroxy-tetrahydropyran as a model compound for the anomerization studies (Fig. 2.3). The free energy difference between *7* and *8* defines the conformational free energy of the hydroxyl group (the so-called *A*-value $= -\Delta G^{\circ}$) [14, 15] in 2-hydroxy-tetrahydropyran (Fig. 2.3). The *A*-value is significantly greater in protic (aqueous) solutions than in aprotic solvents, possibly because of solvation of the hydroxyl group via hydrogen bonding that increases its effective size.

The quantitative estimate of the magnitude of the anomeric effect must take into account the steric preference of an electronegative substituent larger than hydrogen for the equatorial orientation in the corresponding cyclohexane compound. In order

Fig. 2.4

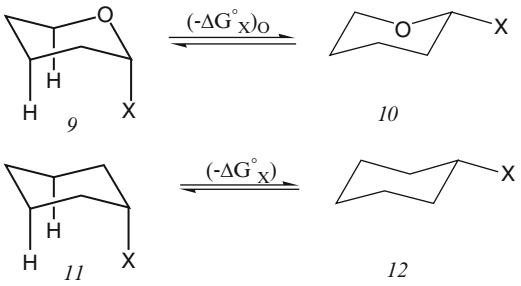

to do this it must be assumed that the conformational energy of the hydroxyl group in 2-hydroxy-tetrahydropyran and in cyclohexanol is of the same magnitude. Although this assumption ignores the difference in geometry between the cyclohexane and tetrahydropyran ring, in most cases this does not lead to a significant discrepancy.

The magnitude of the anomeric effect is thus defined as the difference between the conformational free energy $(-\Delta G^{\circ}_{X})_{O}$ of the equilibrium of 2-substituted tetrahydropyran conformers *9* and *10* (Fig. 2.4) and the conformational free energy $(-\Delta G^{\circ}_{X})$ of the equilibrium of the two analogously substituted cyclohexanes *11* and *12* (Fig. 2.4) [16].

Thus the anomeric effect, AE or O:X, where X = OH or any other electronegative substituent (such as OMe, OAc, Cl, and Br), can be expressed as,

$$(\mathrm{O{:}X}) = \left(-\Delta G^{\circ}_{X}\right) - \left(-\Delta G^{\circ}_{X}\right)_{O} \tag{2.1}$$

Rewriting the above equation gives the following expression for the magnitude of the anomeric effect:

$$(\mathrm{O{:}X}) = \left(\Delta G^{\circ}_{X}\right)_{O} - \left(\Delta G^{\circ}_{X}\right) \tag{2.2}$$

The magnitude of the anomeric effect in D-glucopyranose was determined in the following way. The internal energies of D-glucopyranosyl residues in both α- and β-anomer are identical since they have identical numbers and types of nonbonded interactions. The introduction of an electronegative anomeric substituent (hydroxyl group-, halogen, etc.) into glucopyranosyl residue introduces the difference between their respective internal energies, depending upon whether the electronegative substituent is equatorially or axially oriented. Therefore, the internal energy of an α-anomer will be the sum of the internal energy of D-glucopyranosyl residue, E^0, and the two *syn*-axial interactions between the axial anomeric hydroxyl group and the C3 and C5 axial hydrogen atoms of the pyranoside ring (2 × 0.45 kcal/mol = 0.9 kcal/mol). The internal energy of the β-anomer will be the internal energy E^0 of D-glucopyranosyl residue and the anomeric effect (AE). The number of gauche 1,2-interactions is identical in both α- and β-D-glucopyranoses. From the composition of the equilibrium mixture of α- and β-D-glucopyranose (36 % vs. 64 %, respectively) [17], one can calculate that the β-anomer has a lower free energy than the corresponding α-anomer by 0.35 kcal/mol. Therefore,

$$E_{\alpha} - E_{\beta} = 0.35 \text{ kcal/mol}$$

If now the E_{α} is substituted with (E^0 + 0.9 kcal/mol) and E_{β} with (E^0 + AE) the above equation can be rewritten to:

$$\left(E^0 + 0.9\right) - \left(E^0 + \text{AE}\right) = 0.35 \text{ kcal/mol}$$

Solving this equation for AE (O : OH) gives

$$0.9 \text{ kcal/mol} - \text{O:OH} = 0.35 \text{ kcal/mol}$$
$$(\text{O:OH}) = 0.9 \text{ kcal/mol} - 0.35 \text{ kcal/mol} = 0.55 \text{ kcal/mol}$$

Hence, the difference between the 0.9 kcal/mol and the 0.35 kcal/mol = 0.55 kcal/mol corresponds to the anomeric effect (O : OH) and represents the electronic stabilization of the axially oriented hydroxyl group in the α-anomer. Thus, in other words, this electronic interaction is thought to be responsible for the higher percentage of axial anomer in the equilibrium mixture despite the unfavorable steric 1,3-*syn*-axial interactions between the axial C1 substituent and the axial C3 and C5 hydrogens present in such anomers. This is in contrast to Edward's explanation of the anomeric effect as the electronic destabilization of the equatorially oriented anomer due to dipolar interactions between the equatorially oriented C1 electronegative substituent and the resultant dipole of the two pairs of nonbonding electrons on the ring oxygen.

Similar calculations for D-mannopyranose which at equilibrium contains 69 % of α- and 31 % of β-anomer[08] gave the value for (O : OH) of 1.0 kcal/mol, whereas calculations for 2-deoxy-D-*arabino*-hexopyranose which at equilibrium contains 47.5 % of α-anomer and 52.5 % of β-anomer[08, 18] gave the value for (O : OH) of 0.85 kcal/mol.

Thus, the magnitude of the anomeric effect determined in this way depends upon other factors such as the nature and the configuration of substituent at the C2 carbon atom. In the case of β-D-mannopyranose, the C2-oxygen bond bisects the torsional angle between the C1–O1 and the C1–O5 bonds (Fig. 2.5), and this dipolar interaction seems to introduce an additional electronic destabilization which is evident from the increased value of the anomeric effect (1.0 kcal/mol). This interaction was considered as a separate electronic interaction and was named by Reeves [19–21] Δ2 effect. It is now regarded as simpler to take as the base value for the anomeric effect the value of 0.85 kcal/mol, which is the value for the 2-deoxy-D-*arabino*-hexopyranose *14*, and then when an electronegative substituent at the C2 carbon is axial, as in *13*, to increase this value by 0.15 kcal/mol, and when the C2 substituent is equatorial to decrease it by 0.30 kcal/mol (Fig. 2.5).

In halogeno-1,4-dioxanes ($X_1 = X_4 =$ oxygen), halogeno-1,4-thioxanes ($X_1 =$ oxygen, $X_4 =$ sulfur), and halogeno-1,4-dithianes ($X_1 = X_2 =$ sulfur); (Y = Cl, Br) *16* (Fig. 2.6), halogen atoms were found to occupy preferentially the

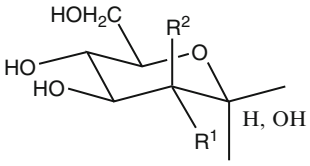

13. R^1 = H; R^2OH
14, R^1 = R^2 = H

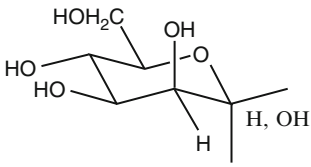

13

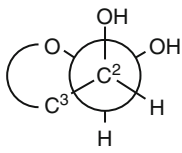

15

Fig. 2.5

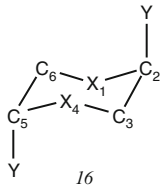

16

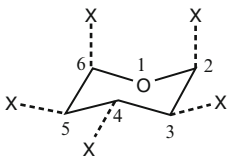

17

Fig. 2.6

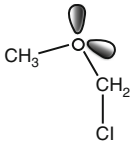

18, gauche conformation

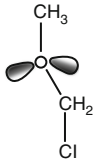

19, anti conformation

Fig. 2.7

axial orientation, which was in contradiction to the well-known situation in monohalogenocyclohexanes [22, 23]. Similarly, in 2- or 6-monochloro or monobromo tetrahydropyran (X = Cl, Br) *17* in Fig. 2.6, the halogen atom takes up the axial orientation, whereas the halogen bonded to the C3, C4, or the C5 carbon has a great preference for the equatorial orientation [24–28].

The study of a simple acyclic compound such as monochloromethoxymethane (*18, 19*) by electrondifraction [27, 28] (Fig. 2.7) has shown that the molecule does not exist in a conformationally more stable *anti* conformation *19* (Fig. 2.7) but in a *gauche* conformation *18* which is equivalent to the axial orientation of the halogen in a six-membered ring. This suggests that the anomeric effect or the preference of the C–O–C–Hal system for the gauche conformation *18* is a general phenomenon. The most intriguing finding was that the anomeric effect for Cl or Br as substituents amounts to several kcal/mol.

The anomeric effect has been defined as the sum of free-energy difference between the axial (favored) and the equatorial anomer plus the conformational preference (the "*A*-value") for the same substituent in cyclohexane [29]. Thus the

Fig. 2.8

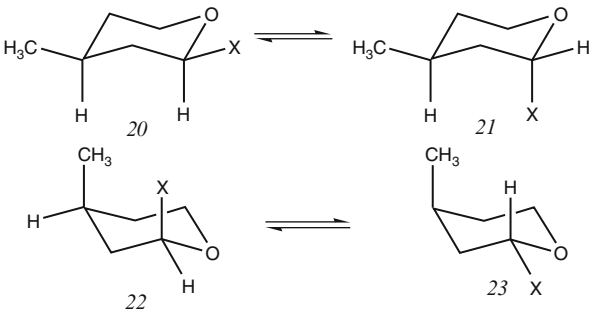

Fig. 2.9

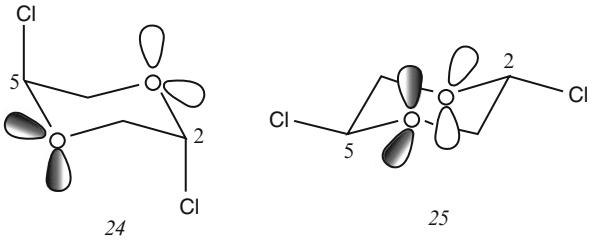

anomeric effect measures the stability of axial over an equatorial electronegative substituent in 2-substituted terahydropyran relative to the expected value in cyclohexane (where the equatorial substituent is favored). The anomeric effect for chlorine, bromine, and iodine in 2-halo-4-methyl-tetrahydropyrans (Fig. 2.8) was found by ^{1}H-NMR to be 2.65 > 3.2 and >3.1 kcal/mol, respectively26. In polar solvents, such as acetonitrile, the value for chlorine seems to be smaller (2.0 kcal/mol) than in neat liquid (2.65 kcal/mol) [26]. However, all these values are much higher than those for the anomeric effect of hydroxy, alkoxy, or acyloxy groups in the 2-substituted tetrahydropyrans (0.9–1.4 kcal/mol); the values for the anomeric effect of these substituents were also found to be significantly solvent dependent [30–34] (see also Fuchs, B. et al. [35]).

The initially proposed explanation for the anomeric effect as a simple dipole–dipole interaction [12] therefore accounts for only a part of the effect, but it does not represent the whole story. If one calculates the electrostatic interaction energy in *trans*-2,5-dichloro-1,4-dioxane (Fig. 2.9) (the molecular geometry is known from X-ray analysis) using the values of $\mu = 2.2$ and 1.4 D for the dipole moments of C–Cl and C–O bonds and $\varepsilon = 2.3$ for the dielectric constant, one arrives at the energy difference of about 1 kcal/mol in favor of the diaxial form [36]. This difference is clearly too small to account for a strong preference for the diaxial conformation [37].

Consequently it was proposed [36] that the anomeric effect consists of two contributing components. One substantial component being that in a conformer with two axially oriented chlorine atoms *24* (Fig. 2.9), there are two gauche halogen-oxygen lone pair electron interactions (Figs. 2.9 and 2.10) (one at the C2 and one at the C5 carbon) (Figs. 2.9 and 2.10).

Fig. 2.10

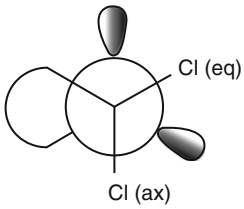

26

Fig. 2.11

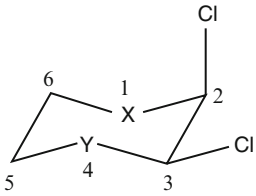

27, X = Y = O
28, X = O; Y = S
29, X = Y = S

Fig. 2.12

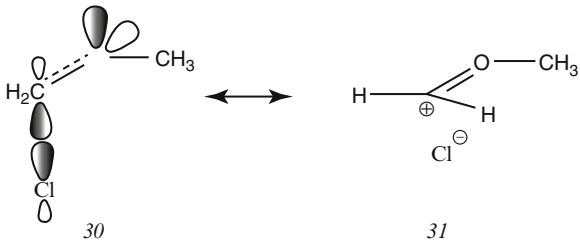

30 *31*

The other contributing component emerged from a study of the geometry of halogenodioxanes *27* (Fig. 2.11) by X-ray crystallography and chloromethoxymethane *18*, *19* (Fig. 2.7) by electron diffraction. The result of the studies of *27* and *28* was that in all cases where the accuracy of measurements was good, the C_2–O distance was significantly shorter than the C_6–O distance (*27* in Fig. 2.11). When compared to the length of C-O bonds in aliphatic ethers, the C_6–O_1 bond appears to be normal, whereas the O_1–C_2 bond appears to be shorter *27* in Fig. 2.11. A second observation was that the axial C_2–Cl bond is somewhat longer than the corresponding equatorial C_3–Cl bond (in *cis*-2,3-dichloro-1,4-dioxane *27* (Fig. 2.11)). The axial C_2–Cl bond was measured to be 1.819 Å and the equatorial C_3–Cl bond 1.781 Å; the accepted value for the aliphatic C–Cl bond is 1.79 Å. These bond length abnormalities in the C–X–C–Y system suggested [38–40] that the one nonbonding electron pair of the ring oxygen is delocalized by orbital mixing with the suitably oriented σ* anti-bonding orbital of the C–Hal bond. As a result of this delocalization (Fig. 2.12) the C–O bond between the carbon bearing the halogen and oxygen will be strengthened (shortened) and the C–Hal bond

Table 2.4 Bond distances in the group C_6–X–C_2–Y (in Angstroms) [35]

Compound	X	Y	C_6–X	C_2–X	C_2–Y
trans-2,3-Dichlorodioxane	O	Cl	1.43	1.38	1.84
cis-2,3-Dichlorodioxane	O	Cl	1.466	1.394	1.819
trans-2,5-Dichlorodioxane	O	Cl	1.428	1.388	1.845
Chloromethoxymethane	O	Cl	1.414	1.368	1.813

Fig. 2.13

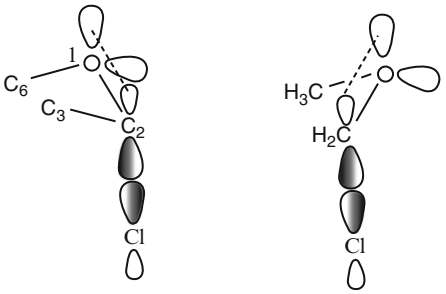

32 *33*

weakened (elongated). In Fig. 2.12 two resonance forms of this structure are shown using the concept "double bond – no bond resonance". Table 2.4 lists bond distances in the $C_6 - X - C_2 - Y$ (in Angstroms).

In Fig. 2.13 the electronic distributions in chloromethoxymethane *33* and in the partial structure of *cis*-2,3-dichloro-1,4-dioxane *32* are compared.

2.1 *Exo*-Anomeric Effect

The *exo*-anomeric effect relates to the preference of the aglycons, e.g., the methyl group of a methyl glycopyranoside, to be in near *syn*-clinal orientation to both the ring oxygen and the anomeric hydrogen, whereas the anomeric effect, which should be more correctly called *endo*-anomeric effect, relates to the preference for the axial orientation of the glycosidic oxygen of glycopyranosides. In Fig. 2.14 this is illustrated by using the C2-methoxy oxygen bond rotamers of 2-methoxy-tetrahydropyran with the methoxy group equatorially or axially oriented (*34*, *36*, *38* and *35*, *37*, *39*, respectively). The eclipsing of unshared electron pairs on glycosidic oxygen with the nonbonding electrons on the ring oxygen giving rise to destabilizing *syn*-axial lone electron pair interaction is shown with the blue double-headed arrow and denoted e://e:. The *endo*- and *exo*-anomeric effects are shown by red bonds.

Three staggered conformations are possible for the rotation about the C2–O2 bond in both equatorial and axial conformers of 2-methoxy-tetrahydropyran (Fig. 2.14). These are referred to as E1–E3 (*34, 36,* and *38*) and A1–A3 (*35*, *37*, *39*) conformers. In the E1 conformer (*34*) there are no *syn*-axial steric

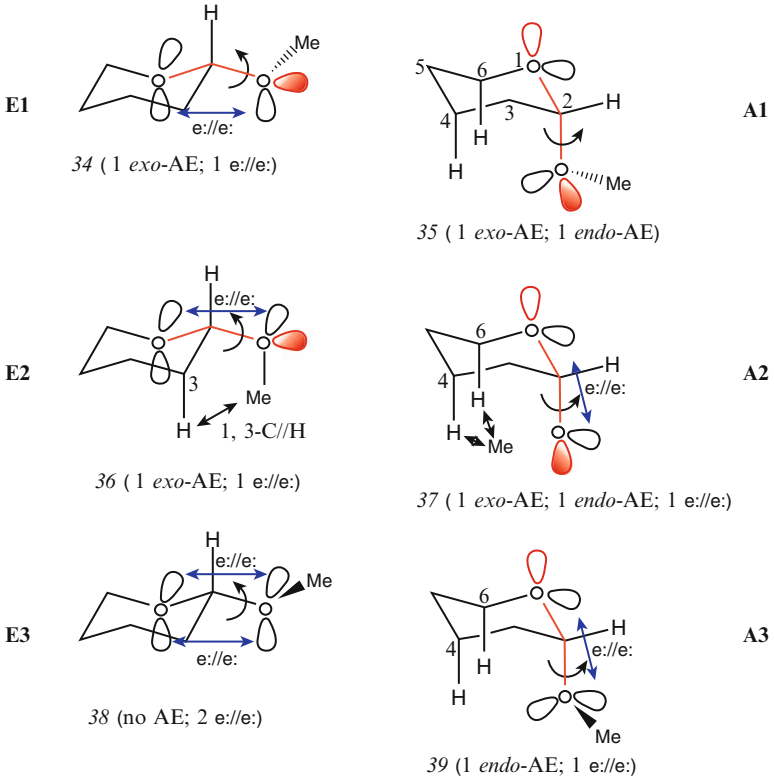

Fig. 2.14

interactions but there is one *exo*-anomeric effect (stabilizing interaction) and one destabilizing *syn*-axial lone pair (electronic) interaction. In conformer E2 *36*, there is one 1,3-*syn*-axial steric interaction between the methyl group and the axial C3 hydrogen atom, one *exo*-anomeric effect (stabilizing electronic interaction), and one destabilizing *syn*-axial interaction between two lone pair electrons (one on the methoxy oxygen and the other on the ring oxygen). In the conformer E3 *38*, there are only two destabilizing *syn*-axial interactions between four lone pair electrons (two on the methoxy oxygen and two on the ring oxygen). In the axial conformer A1 *35*, there are two stabilizing electronic interactions (one *endo*- and one *exo*-anomeric effect). In conformer A2 *37*, there is one severe steric interaction between the methyl group and the two axially oriented hydrogen atoms, one at the C4 and the other at the C6 carbon. In addition to that, there is one destabilizing electronic *syn*-axial interaction between the two lone pair electrons (one on the methoxy oxygen and the other on the ring oxygen). Finally, there is one stabilizing electronic interaction, the *endo*-anomeric effect. In conformer A3 *39*, there is one destabilizing *syn*-axial electronic interaction between two lone pair electrons (one

on the methoxy oxygen and the other on the ring oxygen) and one stabilizing *endo*-anomeric effect.

Based upon the above discussion of the three equatorial conformers, the E1 conformer should be favored, and while for three axial conformers, the A1 conformer should be favored. Thus the *exo*-anomeric effect controls the conformation of the aglycon group.

The experimental evidence for the *exo*-anomeric effect, although initially difficult to obtain, has gradually accumulated over the years, and today this phenomenon is fully accepted.

For molecules in the crystalline state, the evidence is unequivocal. It was determined that alkyl pyranoside adopts either the A1 or the E1 conformation [26] and the analysis of over 50 carbohydrate structures reveals the following regularities: For axial methyl pyranosides, the torsional angle $O_5 - C1 - O - CH_3$ (which should be 60° in A1 conformer) lies between 61° and 74° and for equatorial anomers the range is 68°–87°.

There is conflicting evidence as to whether the *exo*-anomeric effect is larger from the axially or equatorially oriented groups. Even the analysis of crystal structures quoted above does not give a clear answer for glycopyranosides in the solid state, and the results in solutions are equally ambiguous, particularly for oligosaccharides. One thing is however clear: It is a dominant short-range interaction that controls the conformation about the glycosidic bond in both α- and β-linked oligosaccharides, and therefore it is important for the conformational analysis of these molecules.

2.2 Generalized Anomeric Effect

In 1968, Hutchins et al. [41] reported that there is a widespread phenomenon in structural chemistry that the conformations are strongly disfavored if the unshared electron pairs on nonadjacent atoms are parallel or *syn*-axial, as is the case, for example, in *40* in Fig. 2.15. This effect is thought to be due to the repulsion of electric dipoles engendered by the unshared electron pairs. For obvious reasons, Eliel named this phenomenon the "rabbit-ear effect."

Although the existence of this effect has been mentioned earlier when we discussed the anomeric effect, it is the destabilizing component of the anomeric effect consisting of the electrostatic repulsion of 1,3-*syn*-axial or 1,3-parallel

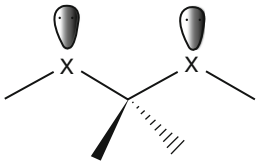

40

Fig. 2.15

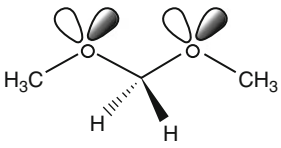

41, trans-trans

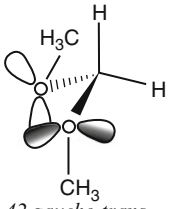

42,gauche-trans

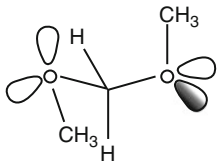

43,gauche-gauche

Fig. 2.16

Fig. 2.17

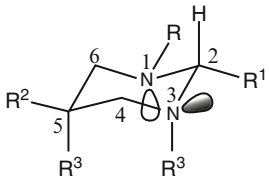

44, R = R^1= CH_3; R^2=R^3=H

45, R = R^1= R^2 = CH_3; R^3=H

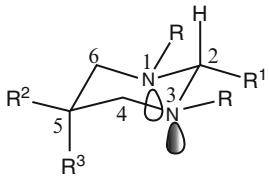

46, R = R^1= R^2 = R^3 = CH_3

unshared pairs of electrons (e://e: interaction). Support for this came from the finding that dimethoxymethane tends to exist in the *gauche–gauche* conformation *43* (Fig. 2.16) rather than in the extended *trans-trans* conformation *41* with all large groups in the *anti*-orientation or in *gauche-trans* conformation *42* (Fig. 2.16).

There are two reasons for this: First, there are two destabilizing *syn*-parallel interactions between the four pairs of unshared electrons on two oxygen atoms (rabbit-ear effect) and second, in the *gauche-gauche* conformation there are two stabilizing *endo*-anomeric effects.

Using dipole moment measurements, Kubo [42] obtained evidence that dimethoxymethane exists in the *gauche–gauche* (+sc, +sc) conformation *43* (Fig. 2.16). This conclusion was later substantiated by electron diffraction studies [43, 44].

By using NMR spectroscopy, Hutchins et al. [41] studied the conformations of variously substituted 1,3-diazanes and found striking support for the "rabbit-ear effect" (Fig. 2.17).

The introduction of one (equatorial) methyl group at the C5 carbon of *N*,*N*,2-trimethyl-1,3-diazane *44* giving the *N*,*N*,2,5-tetramethyl-1,3-diazane *45* affects very little the position of the H-2 chemical shift. However, introduction of the second (axial) methyl group at the C5 carbon (*N*,*N*,2,5,5-pentamethyl-1,3-diazane *46*) dramatically affects the position of the H-2 chemical shift. This large upfield shift of H-2 in *N*,*N*,2-trimethyldiazane upon introduction of geminal methyl groups at the C5 carbon (*N*,*N*,2,5,5-pentamethyl-1,3-diazane *46*) was explained by assuming that in *44* one methyl group is oriented axially and the other equatorially as shown in Fig. 2.17. Introduction of an equatorial C5 methyl group in *N*,*N*,2-trimethyl-1,3-diazane *44* does not significantly increase the conformational

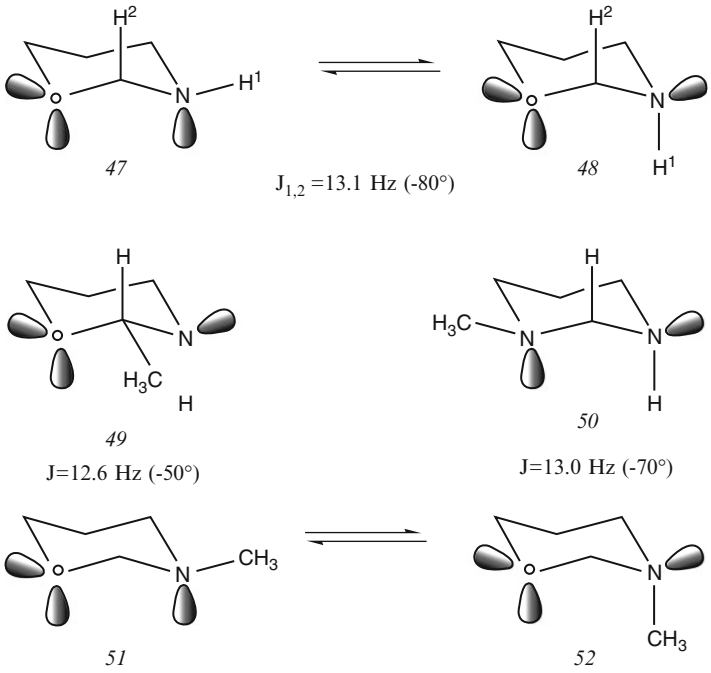

Fig. 2.18

energy, whereas the introduction of the second axial methyl group in *N*,*N*,2,5-tetramethyl-1,3-diazane must lead to it encountering a very severe nonbonding steric interaction with one of the two methyl groups on the nitrogen atom, suggesting that in *N*,*N*,2-trimethyl-1,3-diazane *44* one of the two methyl groups on the nitrogen must be oriented axially, despite the 1,3-*syn*-axial interaction of that axially oriented *N*-methyl group and the axial C5 hydrogen. This actually suggests that the *syn*-axial interaction of two unshared electron pairs on nitrogen must exist, and that it is larger than the 1,3-*syn*-axial interaction of the axially oriented *N*-methyl group and the axially oriented C5 hydrogen. It should be noted that the conformer *44* also has one *endo*-anomeric effect that additionally stabilizes the axial orientation of the C3 methyl group.

Booth and Lemieux [45] have studied the conformations of six-membered perhydro-1,3-oxazoline and 1,3-diazine compounds (Fig. 2.18) with the NMR and found that the conformer which avoids placing the unshared electron pair orbitals of both heteroatoms in axial orientation is more stable. This conclusion was based upon the magnitude of the coupling constant between the N-hydrogen and the vicinal hydrogen in the axial orientation.

For historical reasons, Lemieux proposed the term “generalized anomeric effect” for the general preference for the *gauche* conformation about the carbon-heteroatom bond in systems R–X–C–Y, which is the result of the same kind of interactions as were proposed for explaining the anomeric effect but present in noncarbohydrate structures. This proposal has now been universally adopted.

Table 2.5 Axial preference for methoxy group adjacent to sp^2 hybridized carbon atom

	% of axial isomer in CCl_4
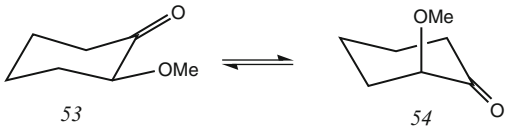 *53* *54*	63
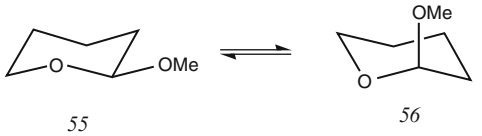 *55* *56*	69
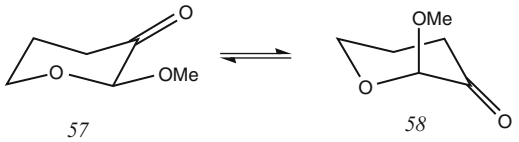 *57* *58*	100
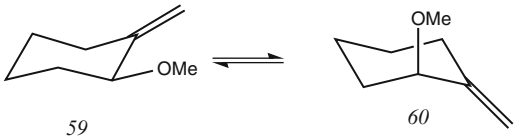 *59* *60*	78

Many cases are known where substituents on six-membered rings prefer axial orientation [46] and not all of these are the consequence of the anomeric effect. For example, the 2-halocyclohexanone system [47] where the axial preference decreases in the order Br > Cl > F and can be explained as a combination of steric effects and dipole–dipole interactions and in 2-alkoxycyclohexanones [48] which is comparable in magnitude to that caused by anomeric effect in 2-alkoxytetrahydropyrans (Table 2.5).

2.3 Reverse Anomeric Effect

In 1965, Lemieux and Morgan [49] studied the conformation of *N*-(tetra-*O*-acetyl-α-D-glucopyranosyl)-4-methyl-pyridinium bromide *61* by NMR spectroscopy and reported that the 4-methylpyridinium group is equatorially oriented and have suggested that *61* exists in the $^1C_4$ conformation *61e* (Fig. 2.19), thus forcing all other substituents to assume the axial orientation despite the presence of two large 1,3-*syn*-axial interactions (one O//O 1,3-*syn*-axial interaction between the C2 and the C4 acetyl groups and one O//C *syn*-axial interaction between the C3 acetyl and the C5 acetoxymethyl group) amounting to 1.5 + 2.5 = 4.0 kcal/mol.

Using X-ray crystallography James [50] has however found that the compound *61* in crystalline state does not exist in the $^1C_4$ conformation (*61e* in Fig. 2.19) but in the $B_{2,5}$ conformation $61B_{2,5}$, as shown in Fig. 2.20 with the methylpyridinium group oriented quasiequatorially.

Fig. 2.19

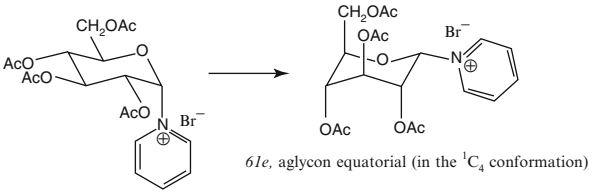

61a, aglycon axial (in the $^4C_1$ conformation)

61e, aglycon equatorial (in the $^1C_4$ conformation)

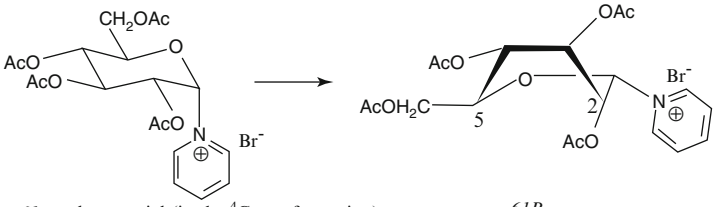

61a, aglycon axial (in the $^4C_1$ conformation)

61B$_{2,5}$

Fig. 2.20

Fig. 2.21

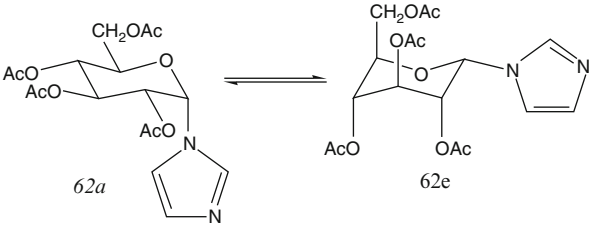

62a 62e

Since both NMR and crystallographic studies showed that the conformations of aminoglycosides with the anomeric nitrogen in axial orientation are strongly disfavored, particularly in cases where the nitrogen carries a positive charge, Lemieux concluded [51–53] that there must exist a powerful driving force for the pyridinium group to adopt the equatorial orientation.

This driving force, for the electropositive aglycon in hexopyranosides to assume the equatorial orientation, Lemieux named the reverse anomeric effect (RAE). Since the reverse anomeric effect could be either the result of steric interactions when the aglycon is axially oriented due to the bulkiness of pyridinium group, particularly if solvated, or the result of electronic interactions stemming from the presence of positively charged nitrogen, or both, Lemieux and Saluja [51, 54] suggested that the existence of the (polar) reverse anomeric effect can be established only if a clear distinction between the steric and polar effects can be made.

Soon thereafter, two groups (Lemieux et al. [51] and Paulsen et al. [55]) independently concluded that the glycosyl imidazoles (Fig. 2.21) would be more suitable substrates for these studies than pyridinium glycosides, since the protonation of an imidazole ring is not expected to significantly change its size, and

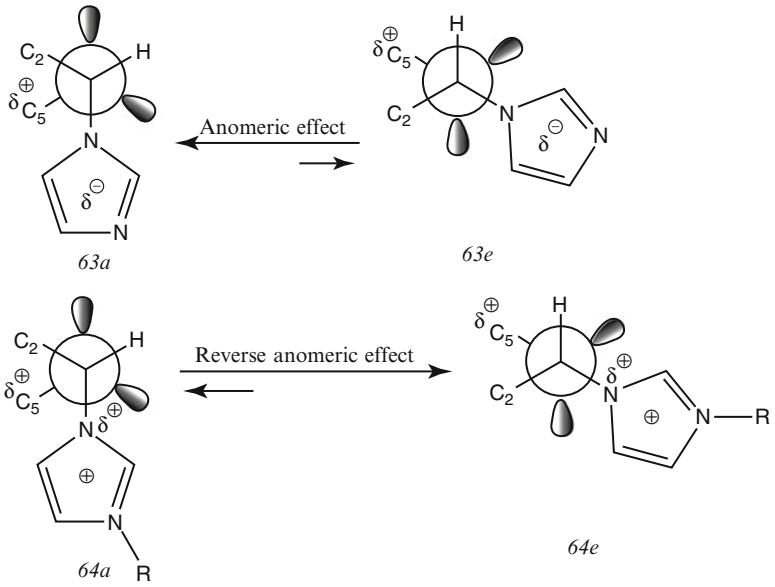

Fig. 2.22

therefore any conformational change due to protonation could be attributed to the polar effect (i.e., the reverse anomeric affect). While this argument seemed likely, it was still uncertain to what extent the association of the counterion with the positively charged imidazolium ion affects the *A*-value of the imidazolium group, as well as what effect the solvation of the imidazolium salt has on the *A*-value of the imidazolium group.

Lemieux and Saluja [54] studied the protonation of the imidazole ring of *N*-(2,3,4,6-tetra-*O*-acetyl-α-D-glycopyranosyl) imidazole *62* (Fig. 2.21) in deuterochloroform and found that the addition of equimolar amount of weak acid (acetic acid) produced a much smaller effect on the NMR spectrum than the addition of equimolar amount of a strong acid such as trifluoroacetic acid. The addition of a strong acid had an effect upon decreasing the magnitudes of $J_{2,3}$, $J_{3,4}$, and $J_{4,5}$ coupling constants that is nearly equivalent to the methylation of the imidazole group.

The distribution of electrical charge is more favorable with the imidazole group in the axial orientation when the nitrogen attached to the anomeric carbon carries a partial negative charge, and this is the anomeric effect (Fig. 2.22). However, the distribution of electrical charge is more effective in the anomer with the imidazole group in the equatorial orientation when the imidazole ring has a positive charge that was acquired either through protonation or alkylation, and this is the reverse anomeric effect.

Deslongchamps and Grein [56, 57] suggested that the equatorial orientation of aglycon is favored because of electronic stabilization via the dipolar interaction of the positively charged aglycon (N^+) with the two unshared pairs of electrons on the

Fig. 2.23

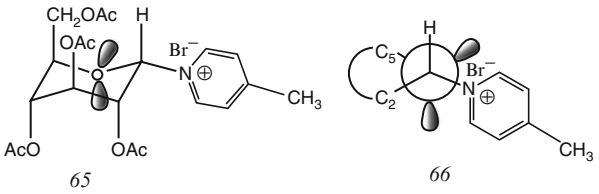

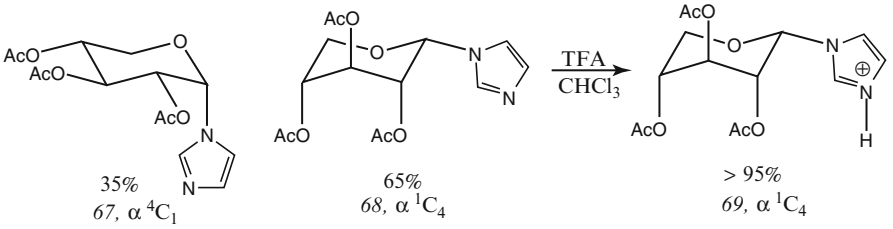

Fig. 2.24

hexopyranose ring oxygen as shown in Fig. 2.23. Apparently the lp-N^+ electrostatic attraction exceeds the desire of lp delocalization, corresponding to the *endo*-anomeric effect (Fig. 2.22).

Figure 2.23 illustrates Deslonchamps and Grein's [56, 57] explanation of the reverse anomeric effect. The imidazole ring is an electron-rich group due to the presence of two nonbonding p-electron pairs on nitrogen, and therefore tends to adopt, due to the anomeric effect, the axial orientation. However, the imidazole ring on protonation becomes positively charged and consequently adopts the equatorial orientation, because in this conformation the positively charged imidazole ring is in the *gauche* orientation relative to the two nonbonding p-electrons on the ring oxygen that stabilize the positive charge of imidazole.

The strongest support for the existence of the reverse anomeric effect (RAE) comes from the ^{1}H NMR study of conformational equilibrium of *N*-(2,3,4-tri-*O*-acetyl-α-D-xylopyranosyl) imidazole in $CDCl_3$ solution in the absence and in the presence of trifluoroacetic acid (TFA) conducted by Paulsen et al. [55]. It was found that in the absence of acid, the equilibrium mixture contained 65 % of the $^1C_4$ conformer *68* with imidazole aglycon equatorially oriented, and 35 % of the $^4C_1$ conformer *67* with the imidazole aglycon axially oriented (Fig. 2.24). In the presence of acid, the proportion of the $^1C_4$ conformer *69* with the imidazole aglycon equatorially oriented increased to more than 95 %. This difference corresponds to the free-energy change >1.4 kcal/mol. The authors attributed the shift of conformational equilibrium to the presence of the positive charge on imidazolium ring due to protonation, assuming that N-protonation did not significantly change the size of the imidazolyl group 56. Thus, they completely excluded steric effects as a possible cause for the observed conformational change.

Finch and Nagpurkar [58] studied the population of equatorial conformers in equilibrium mixtures of *N*-(α-D-glycopyranosyl) imidazole of D-glucose, D-mannose, and D-galactose in D_2O; of *N*-(α-D-glycopyranosyl) imidazole of D-glucose,

Table 2.6 The population of equatorial conformer in equilibrium mixture of *N*-(α-D-glycopyranosyl) imidazoles of D-glucose, D-galactose, and D-xylose and their tetra- and triacetyl derivatives, respectively

Glycon residue	Conformation	X	Solvent	Average % of $^1C_4$ conformer
Gluco	$^4C_1$	N	D_2O	0
Gluco	$^4C_1$	NH^+	D_2O + TFA	0
Manno	$^4C_1$ + $^1C_4$	N	D_2O	30.4
Manno	$^4C_1$ + $^1C_4$	NH^+	D_2O + TFA	31.3
Galacto	$^4C_1$	N	D_2O	0
Galacto	$^4C_1$	NH^+	D_2O + TFA	0
Ac_4 Gluco	$^4C_1$	N	$CDCl_3$	0
Ac_4 Gluco	$^4C_1$ + $^1C_4$	NH^+	$CDCl_3$ + TFA	27.4
Ac_4 Manno	$^4C_1$ + $^1C_4$	N	$CDCl_3$	Not given
Ac_4 Manno	$^4C_1$ + $^1C_4$	NH^+	$CDCl_3$ + TFA	67
Ac_4 Manno	$^4C_1$ + $^1C_4$	N	$(CD_3)_2CO$	51.1
Ac_4 Manno	$^4C_1$ + $^1C_4$	NH^+	$(CD_3)_2CO$ + TFA	71.8

D-mannose, and D-galactose tetraacetate in $CDCl_3$; and of *N*-(α-D-xylopyranosyl) imidazole triacetate in $CDCl_3$ in the absence and in the presence of acid and found that both steric factors and polar factors (reverse anomeric effect) are likely to be involved in determining the relative percentages of the two conformations at conformational equilibrium. The obtained results could in large part be accounted for by steric factors, but the operation of additional polar factors was also likely (Table 2.6).

The concept of the reverse anomeric effect (RAE) has been subject to much controversy and skepticism, because the positively charged anomeric nitrogen ought to lower the energy of the σ_{C-X^*} orbital and enhance the stabilization of axial conformer, not to destabilize it.

One of the first reports [59] that challenged the existence of RAE was the stereospecific formation of α-D-glucopyranosylacetonitrilium ion *71* when α- and β-anomers of pent-4-enyl D-glucopyranoside *70* reacted with *N*-bromosuccinimide in dry acetonitrile (68 % from β-anomer and 64 % from α-anomer). The anomeric configuration of *71* was determined by trapping the acetonitrilium ion *71*, in situ, with 2-chlorobenzoic acid and by subsequent conversion of the obtained α-imide *73* with sodium methoxide to α-2-chlorobenzamide *74* (Fig. 2.25). The exclusive formation of axially oriented α-acetonitrilium ion *71* is clearly in contrast to what would be predicted by the reverse anomeric effect.

Since both RAE and steric repulsion favor the equatorial conformer, it was essential to quantitatively assess steric factors and to determine whether the preference of pyridinium and imidazolium groups to adopt equatorial orientation is predominantly due to the steric interaction of these two groups. Since pyridinium and imidazolium groups were too bulky for this assessment to be made reliably, a protonable cyclohexyl substituent whose steric size is known in both protonated

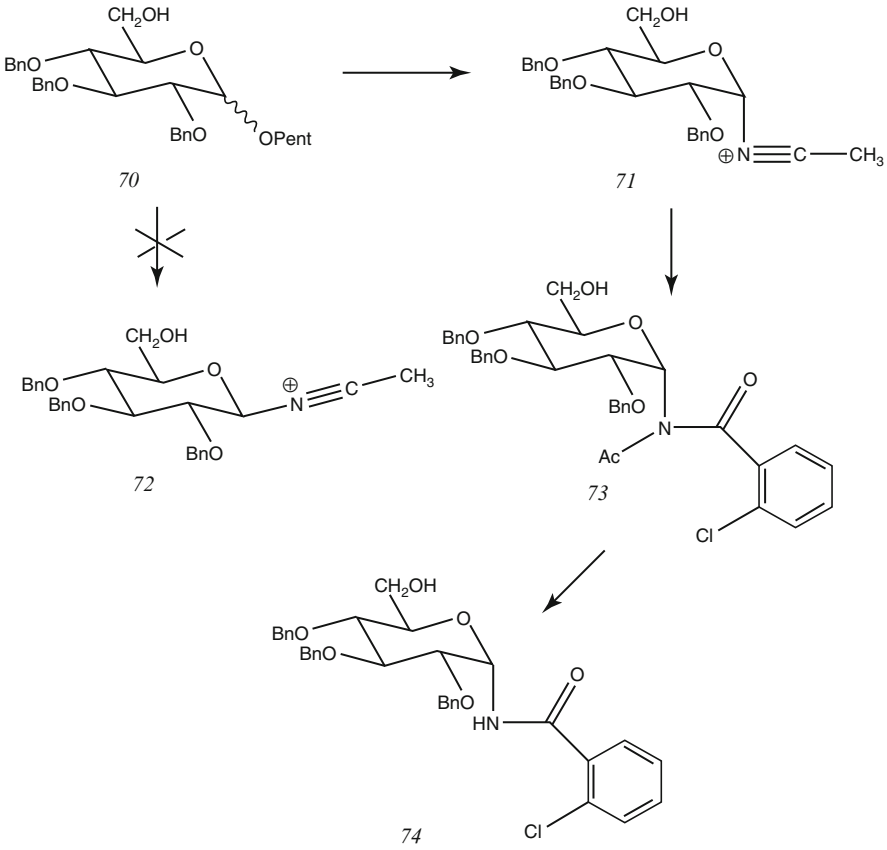

Fig. 2.25

and unprotonated forms seemed to be more suitable for probing RAE. One such substituent is NH_2 (Fig. 2.26). The conformational energy ($-\Delta G^{\circ}$ or *A*-value) [14] for NH_3^+ was found [60–62] to be larger (2.15 kcal/mol in D_2O) than the *A*-value for NH_2 (1.7 kcal/mol in D_2O and 1.65 kcal/mol in aprotic solvents, e.g., cyclohexane).

The increase of the *A*-value on protonation is the measure of the increase in size of the protonated substituent relative to the unprotonated one. This extra bulk is due to the additional proton itself and also to the additional solvent molecules attached to the positive charge needed to stabilize it. The increase in protic solvent is due to hydrogen bonding, which clusters solvent molecules around the polar group [63, 64]. Since the C–O bond is shorter than the C–C bond, steric repulsions in the tetrahydropyran system with the axially oriented 2-amino group are greater than in the cyclohexane system with the axially oriented amino group, and should be corrected to 2–2.5 kcal/mol for aprotic solvents and 2.4–2.9 kcal/mol for protic solvents.

Unlike previous experimental investigations of the reverse anomeric effect that involved the study of conformational equilibrium between the unprotonated and

Fig. 2.26

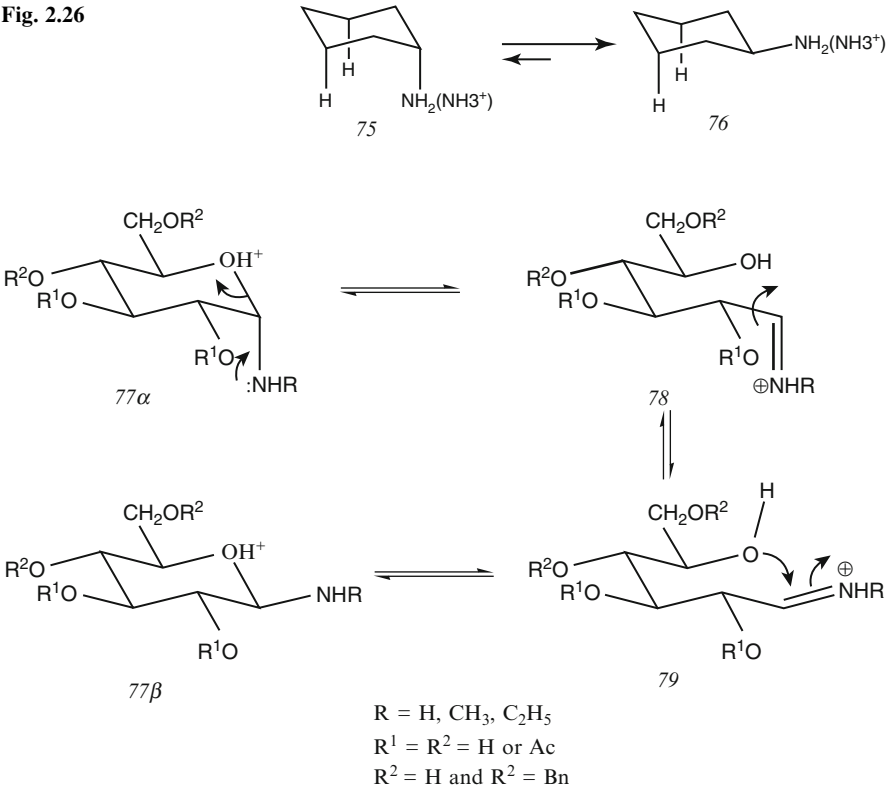

Fig. 2.27

protonated aminoglycosides, Perrin and Armstrong [65] carried out ^{1}H-NMR study of the composition of the equilibrium mixture obtained by acid-catalyzed anomerization of glycosyl amines of a wide variety of glycopyranosylamine derivatives along with their conjugate acids (Fig. 2.27).

This interconversion is known to proceed in four steps: (1) the reversible protonation of the ring oxygen *77α*, (2) the pyranoid ring opening to the imminium ion intermediate *78*, (3) the rotation about the C1–C2 bond *78* → *79*, and (4) reclosure of the pyranoid ring *79* → *77β* [66] (Fig. 2.27). The greatest experimental difficulties encountered in this work were the sensitivity of glycosylamine to hydrolysis and the problem of assignment of the ^{1}H NMR signal to the axial stereoisomer that was present only in low concentration.

The *77α*/*77β* ratio was measured by integration of the corresponding ^{1}H-NMR signals for the anomeric protons across the range of solvents, for both the unprotonated and protonated glycosylamines, and the obtained results are given in Table 2.7.

Table 2.7 Average percentage of α-anomer, free-energy change ΔG° (β → α) kcal/mol, $A(NH_2)$ or $A(NH_3^+)$ kcal/mol in glycopyranosylamine ions

Amine	α-anomer (%)	ΔG° β → α	*A* cyclohexane	*A* THP	α-Anomer (%) estimated
$-NH_2$	10	1.6 ± 0.4	1.6 or 1.3	2.5 or 2.0	–
–NHR	13	1.5 ± 0.3	1.6 or 1.3	2.5 or 2.0	–
$.H^+$, aq.	3.5	2.0 ± 0.1	1.9	2.9	0.8
$.H^+$, nonaq.	7.7	1.5 ± 0.1	ca. 1.6	ca. 2.4	1.7

The most important result of these studies is that the axial anomer *77α* is present in appreciable amounts even in acid solution: It is present in smaller percentage in aqueous solution perhaps because in water the $-NH_3^+$ or $-NH_2R^+$ is bulkier due to solvation. The fact that the ΔG° (β→α) values (the free-energy change for the conversion of equatorial *77β*-to the axial *77α*-isomer) are considerably lower than the *A*-values for $-NH_3^+$ or $-NH_2R^+$ in THP (Table 2.4) indicates that the preference of the $-NH_3^+$ for equatorial orientation can be chiefly accounted for by steric effects. These results also suggest the existence of a weak anomeric effect, but not of a reverse anomeric effect.

The reverse anomeric effect can also be determined from a difference in anomerization free-energy changes between the protonated and unprotonated glycosylamines, as shown in Eq. 2.3:

$$\Delta\Delta G^{\circ}(N \rightarrow N^+) = \Delta G^{\circ}(\beta \rightarrow \alpha)(NH^+) - \Delta G^{\circ}(\beta \rightarrow \alpha)(N) \qquad (2.3)$$

The $\Delta\Delta G^{\circ}$ is the extent to which the N-protonation increases the preference of amino substituent for the equatorial orientation. Across all glycosylamines examined, the average $\Delta\Delta G^{\circ}(N \rightarrow N^+)$ is found to be 0.1 ± 0.1 kcal/mol [65] which is not significantly different from zero. Furthermore, this value is definitely smaller than *A* (NH_3^+)-*A*(NH_2) which is what would be expected from the increase in steric bulk. Even though NH_3^+ is certainly bulkier than NH_2, the proportion of axial isomer *77α* does not decrease on protonation.

Therefore, Perrin and Armstrong [65] concluded that there is probably no reverse anomeric effect present with any cationic nitrogen substituent.

Several computational studies [4, 55, 56, 67–72] on the reverse anomeric effect have been published. Thus, conformational equilibrium of 2,3,4-tri-*O*-acetyl-D-xylopyranosylimidazole *67* ⇌ *68* (Fig. 2.28) was subjected to ab initio calculations.

In order to simplify the calculations, the axial and equatorial conformers of unprotonated and protonated 2,3,4-tri-*O*-acetyl-D-xylopyranosylimidazoles (67α, *68α*, *69α*, and *80α*, respectively) were substituted with unprotonated and protonated model substrates (*81a*, *81e*, and *82a* and *82e*) (Fig. 2.29) whose conformational energies were then calculated. Also the conformational energies of truncated acyclic models of *81a*, *81e*, *82a*, and *82e* (the structures 83″*a*″, 83″*e*″, 84″*a*″, and 84″*e*″ with X = H, F, and CH_3) were calculated [70].

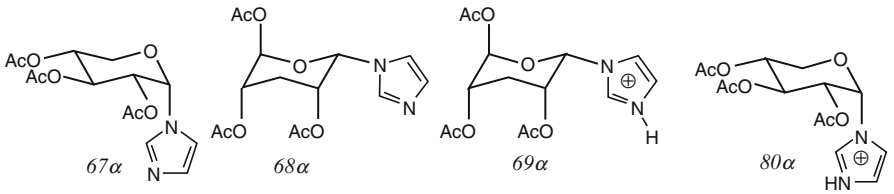

Fig. 2.28

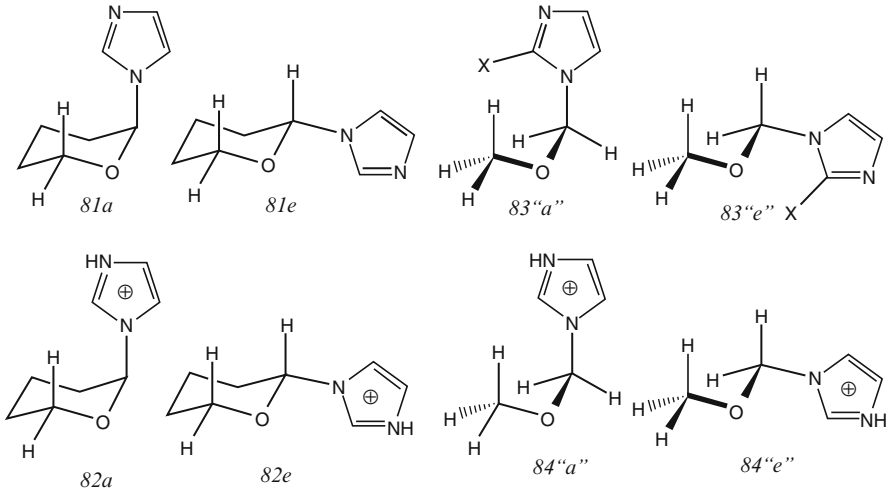

Fig. 2.29

From the calculation results it was concluded that the dominant contributions to the conformational equilibrium of *N*-pyranosylimidazoles were stabilizing anomeric hyperconjugation and destabilizing steric 1,3-interactions in the axial unprotonated conformer (*81a*). Both effects increase on N-protonation (*82a*). It was also concluded that the fine balance between these opposing contributions would allow small intramolecular electrostatic interactions to control the position of equilibrium. Stabilizing electrostatic interactions in N-protonated equatorial conformers were identified and found to be associated with ImH2-O (ring) hydrogen bonding (type 1) and dipole–dipole electrostatic stabilization between the nonbonding electrons on ring oxygen and the cationic imidazolium dipole (type 2) (see Deslonchamps and Grein proposal [56, 57]). An equatorial shift on N-protonation of 0.4–2.4 kcal/mol was predicted using models *82a and 82e*. Since Perrin [65] suggested that only 0.024–0.089 kcal/mol should result from the steric effect related to imidazole N-protonation, it was concluded that the reverse anomeric effect for the *N*-(xylopyranosyl)imidazoles is approximately 0.8–1.4 kcal/mol.

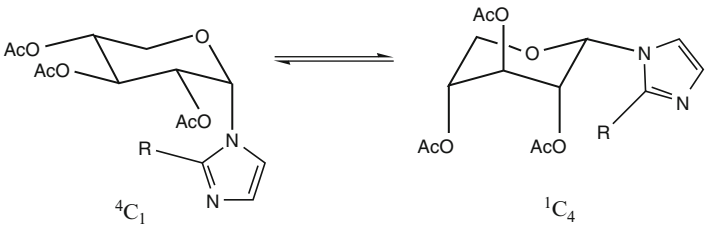

67a, R = H
85a, R = CH_3

67e, R = H
85e, R = CH_3

Fig. 2.30

Since the anomeric effect is known to be sensitive to solvent polarity, Vaino et al. [71] have reexamined the conformational equilibrium of 2,3,4-tri-*O*-acetyl-α-D-xylopyranosylimidazole 67a and 2,3,4-tri-*O*-acetyl-α-D-xylopyranosyl-2-methylimidazole *85* in the presence of trifluoroacetic acid (TFA) because protonation of imidazole by TFA increases the ionic strength of solution. The ^{1}H-NMR titration of the glycosides *67* and *85* (Fig. 2.30) with varying amounts of TFA and/or tetra-*N*-butylammonium bromide (TBAB) was undertaken in order to account for the effects of solvent ionic strength change upon equilibrium (Fig. 2.30).

From the results obtained, it was concluded that the large equatorial shifts observed for *67a* and 85*a* on N-protonation are not the results of solvent and ionic strength effects. Interestingly, the effect of increasing the solution ionic strength with TBAB produces a small axial shift for *67a*. The authors suggest that RAE does exist and that it is the result of stabilizing intramolecular electrostatic contributions to the $^1C_4$ conformer on N-protonation [56, 70]. The size of the effect in two xylopyranosyl systems studied was quantified as 0.8–1.4 kcal/mol. Since the contributions from this electrostatic RAE may be small, there may be other contributions to the conformational energy that will be diminished on transferring to solvents more polar than chloroform.

Fabian et al. [72] used an ^{1}H-NMR titration method to measure with high precision the shift of anomeric equilibrium on protonation of *N*-(D-glucopyranosyl)imidazole *86* and its tetraacetyl derivative *87* and found that $\Delta\Delta G^{\circ}_{\beta\rightarrow\alpha} = \Delta G^{\circ}_{\text{N-imidazolylH}+} - \Delta G^{\circ}_{\text{N-imidazolyl}} = -0.018$ to -0.368 kcal/mol (Fig. 2.31). This result means that the protonated imidazolyl group has a small but significantly greater preference for the axial position than does the unprotonated group. This is exactly opposite to what would be expected from the existence of RAE, leading the authors to conclude that RAE does not exist [1, 4, 73–78].

Additional experimental evidence is sparse [78, 79]. The geometric changes are consistent with an enhanced anomeric effect, not a reverse one [68, 80] Molecular orbital calculations are not conclusive because it is difficult to separate the RAE from steric effects and hydrogen bonding, which also favor the equatorial conformer [70, 81–84].

Fig. 2.31

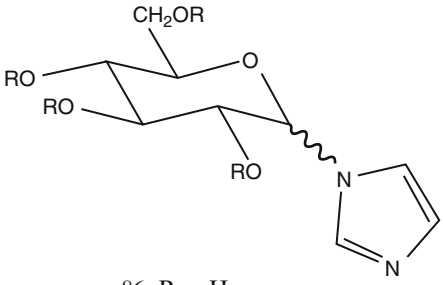

86, R = H
87, R = Ac

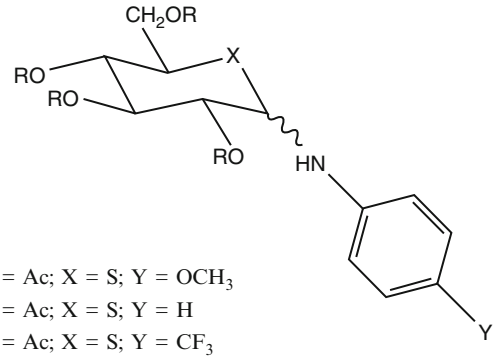

88, R = Ac; X = S; Y = OCH_3
89, R = Ac; X = S; Y = H
90, R = Ac; X = S; Y = CF_3
91, R = Ac; X = S; Y = NO_2
92, R = H; X = S; Y = OCH_3
93, R = H; X = S; Y = H
94, R = HX = S; Y = CF_3
95, R = H; X = S; Y = NO_2

96, R = Ac; X = O; Y = OCH_3
96, R = Ac; X = O; Y = H
96, R = Ac; X = O; Y = NO_2

Fig. 2.32

The question of the existence of the generalized RAE was addressed by systematic examination of substituent and solvent effects on the configurational equilibria of *N*-aryl-5-thioglucopyranosylamines *88–95* and *N*-arylglucopyranosylamines *96–98* (Fig. 2.32) and the corresponding protonated species [85].

The equilibrium population of the 5-thio compounds *88–91* and their protonated derivatives were determined by ^{1}H-NMR spectroscopy at 294° K. Equilibration of neutral species *88–91* was achieved by the $HgCl_2$ catalysis of the individual isomers only in polar solvents CD_3OD, CD_3NO_2, and $(CD_3)_2CO$, due to the limited solubility of β-anomers, in order to that the true equilibrium had been reached (Fig. 2.33).

The corresponding equilibrations of the protonated species *96–98(*96–98*)* (Fig. 2.34) were studied in the presence of 1.5 equiv. of triflic acid, in polar and nonpolar solvents. The addition of 1.5 equiv. of triflic acid would ensure the

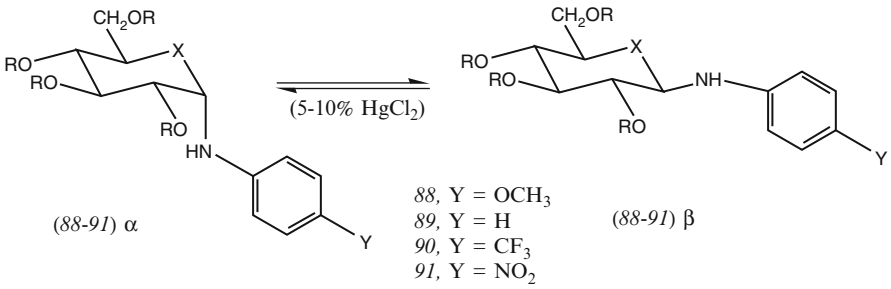

Fig. 2.33

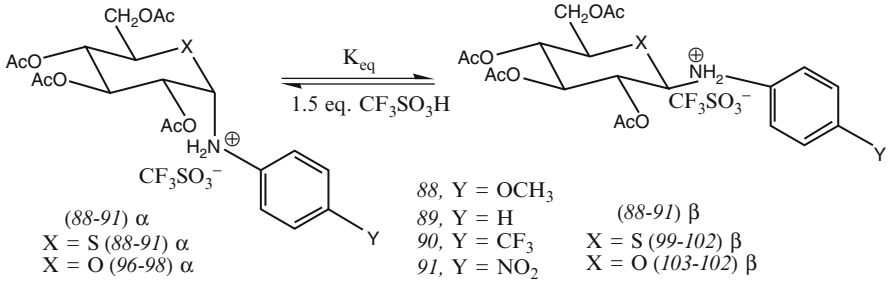

Fig. 2.34

complete protonation of amines since the pK_a of triflic acid is 5.9 [85] while the pKas of the isolated aglycons are 5.31 for p-anisidine (Y = CH_3O), 4.60 for aniline (Y = H), 2.45 for p-trifluoromethylaniline (Y = CF_3), and 1.00 for the weakest base p-nitroaniline (Y = NO_2).

The equilibration of the oxygen analogs *96–98* (Fig. 2.32) was performed at 230° K in CD_2Cl_2 and CD_3OD. In this series the choice of solvent was restricted due to the instability of compounds or line broadening effects in the spectra that did not permit unambiguous assignment of signals or their accurate integration.

The equilibration of neutral species *96–98* (Fig. 2.34) was achieved by the addition of catalytic amounts of triflic acid to the solution of individual anomers.

The conclusion based upon the obtained results is that there is no evidence to support the existence of the generalized reverse anomeric effect in neutral or protonated *N*-aryl-5-thioglucopyranosylamines and *N*-arylglucopyranosylamines.

For the neutral compounds, the anomeric effect ranges from 0.85 kcal/mol for *88* to 1.54 kcal/mol in *91*. The compounds *88–91* and *96–98* show an enhanced anomeric effect upon protonation. The anomeric effect in the protonated derivatives ranges from 1.73 kcal/mol in *90* to 2.57 in *97*. The values of K_{eq} in protonated *88–91* increase in the order OMe < H < CF_3 < NO_2, in agreement with the dominance of steric effects (due to counterion) over the *endo*-anomeric effect. The values of K_{eq} in protonated *96–98* show the trend OMe < H < NO_2 that is

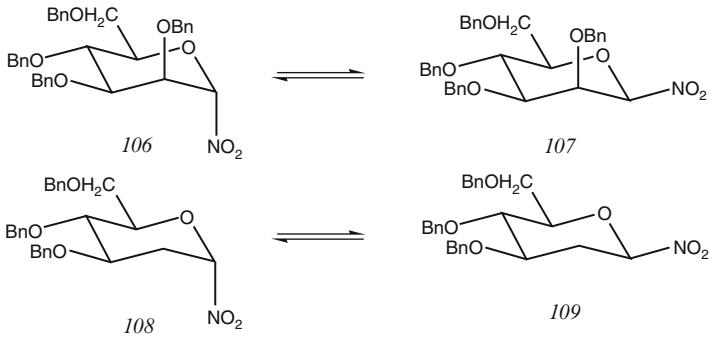

Fig. 2.35

explained by the balance of the anomeric effect and steric effects in the individual compounds.

The controversy about the existence of the reverse anomeric effect is practically impossible to resolve by using the glycosylamine type of compounds due to the solvent stabilization of the positive charge on the nitrogen. There is no way to differentiate between the relative contribution of electronic and steric effects to the magnitude of the anomeric effect. One way out of this "hopeless" situation is to use the internally stabilized positive charge on a heteroatom linked to the anomeric carbon, as is found in groups such as sulfones and nitro compounds. There are indeed studies reported with this kind of compounds, one by a Vasella group on 1-deoxy-1-nitro-glyco-pyranoses and the other by a Franck group on glycopyranosyl sulfones.

Aebischer et al. [85] reported in 1983 results of their studies on the anomeric effect of nitro group. They studied the anomeric effect of nitro group in two sugars: 1-deoxy-1-nitro-tetra-*O*-benzyl-D-mannopyranose *106* and 3,4,6-tri-*O*-benzyl-1,2-dideoxy-1-nitro-D-arabino-hexopyranose *108* (Fig. 2.35).

The compounds *106* and *108* were equilibrated in $CHCl_3$ at 37 °C with a weakly basic ion-exchange resin (Amberlite IRA 193). The progress of equilibration was periodically checked by ^{1}H-NMR spectroscopy. The relative concentrations of anomers at equilibrium (C_{eq}) were measured by integration of the H–C1 signals (200 MHz-^{1}H-NMR spectra; $\delta = 5.57$ ppm (*106a*); 5.17 ppm (*106e*); 5.58 ppm (*108a*), and 5.25 ppm (*108e*)) and the results are given in Table 2.8.

The anomeric effect of nitro group in *108* is given by the sum of "*A*-value" of the nitro group and the ΔG°-value characterizing the equilibrium between the α-D- and β-D-anomers [72, 86]. An "*A*-value" of 0.78 kcal/mol for the nitro group has been determined by Trager and Huitric [87] by equilibration of 1-(*tert*-butyl)-4-nitrocyclohexane under the same conditions as used above for the equilibration of sugars *106* and *108*. From the ΔG°-values for the equilibrium *108a* ⇌ *108e* (1.48 and 1.67 kcal/mol, respectively; see Table 2.5), one thus obtains an anomeric effect for the nitro group in *108* of 2.26 and 2.45 kcal/mol, respectively, i.e., of approximately 2.35 kcal/mol. The anomeric effect for the nitro group in *106* was

Table 2.8 Equilibration of *106a*, *e* and of *108a*, *e*

Compound	C_0 (%) α-D : β-D	C_{eq} (%) α-D : β-D	ΔG° (kcal/mol)	Conditions (mg of compound/mg resin/time)
1	11.9:88.1	93.2:6.8	1.62	31/31/159 h
	>95:5	94.0:6.0	1.70	48/48/159 h
2	48.2:51.8	91.7:8.3	1.48	65/65/370 h
	>95:5	93.7:6.3	1.67	70/70/377 h

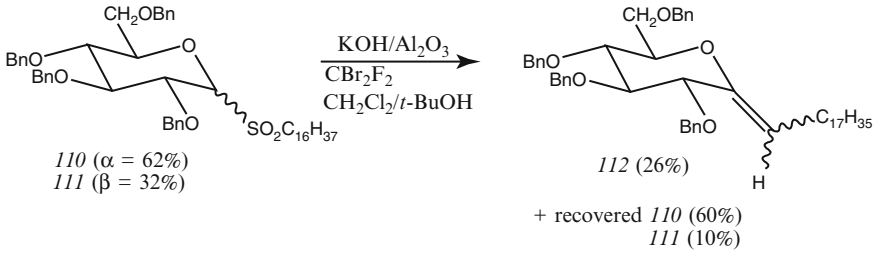

Fig. 2.36

calculated to be ca. 3.4 kcal/mol. The stronger anomeric effect of the nitro group in *106* is in keeping with the known influence on the anomeric effect of an axial 2-alkoxy group [20, 89–91].

An interesting study on the anomeric effect in glycopyranosyl sulfones was published by Chen et al. [92] in 2002. In their work on applying the Bamberg-Bäcklund reaction to carbohydrate anomeric sulfones, they observed that the α-/β-isomer ratio of unreacted sulfones *110* and *111* recovered from the basic reaction mixture was not the same as the starting ratio, since the presence of the α-anomer increased (Fig. 2.36). This observation could be explained in two ways: (i) only the β-isomer was reactive whereas the α-isomer was not and/or (ii) the β-isomer was isomerizing to the α-isomer. These two explanations could be easily verified. When pure α-isomer *110* was subjected to the Bamberg-Bäcklund conditions, no reaction was observed, which was consistent with the former explanation; however, when the pure β-isomer *111* was subjected to the same conditions, the α-isomer was recovered along with Bamberg-Bäcklund product *112* suggesting that the anomerization of β-isomer takes place together with the Bamberg-Bäcklund reaction. When pure sulfones *110* and *111* were equilibrated with *t*-BuOK-benzene, the equilibrium ratio of β-/α-isomer achieved in both directions was 57:43. This corresponds to an apparent *A*-value of 0.167 kcal/mol for the dodecyl sulfone group. Simpler tetrahydropyranyl phenyl sulfones *113–116* (Fig. 2.37) gave similar results (Table 2.9), although a different *A*-value was recorded, presumably because of the absence of the electronegative substituents found in *110* and *111*. Tetrahydropyranyl phenethyl sulfones *113* and *114* failed to equilibrate under basic conditions presumably because the proton exchange was taking place not at

Fig. 2.37

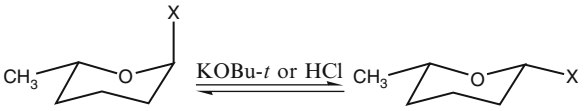

±*113*: X = $SO_2CH_2CH_2Ph$
or
±*115*: X = SO_2Ph

±*114*: X = $SO_2CH_2CH_2Ph$
or
±*115*: X = SO_2Ph

Table 2.9 Sulfone isomerizations via basic conditions

Starting material	*T* (°C)	Time	Ratio (*trans*/*cis*)	ΔG° (kcal/mol)
(±)-*115*	85	20 h	1:2.52	−0.658
		5 days	1:2.34	−0.605
(±)-*116*	85	20 h	1.5.65[a]	–
		5 days	1.252	−0.658
(±)-*114*	75	5 days	Only *cis* isomer[b]	–
(±)-*113*/(±)-*114*	75	5 days	1:1.28[b]	–

[a]No equilibrium obtained
[b]No obvious isomerization detected

Table 2.10 Sulfone isomerization via acidic conditions

Starting material	Conditions	*T* (°C)	Time	Ratio (*trans*/*cis*)	ΔG° (kcal/mol)
(±)-*113*	$CDCl_3$ (0.5 mL)	4	7 weeks	1:3.84	0.741
(±)-*113*/(±) *114*	$CDCl_3$ (1 mL), TMSCl (1.5 μL), *t*-BuOH (2 μL)	RT	2 weeks	1:3.62	0.762
(±)-*115*	$CDCl_3$ (0.5 mL)	4	3 weeks	1:1.27[a]	–
	$CDCl_3$ (1 mL), TMSCl (1.5 μL), *t*-BuOH (2 μL)	RT	2 weeks	1:3.18	0.685
(±)-*115*/(±) *116*	$CDCl_3$ (1 mL), TMSCl (12.5 μL), *t*-BuOH (10 μL)	RT	2 days	1:3.15	0.679

[a]No equilibrium obtained

the anomeric carbon but at the α′-carbon of the phenethyl group. A support for this assumption was obtained by subjecting both phenyl and phenethyl sulfones to the acid-catalyzed equilibration whereby similar *A*-values were obtained. The acid- and base-catalyzed isomerization of phenyl sulfone gave the same α-/β-isomer ratios (Table 2.10).

The evaluation of an anomeric effect for a substituent group requires a comparison of the apparent size of the group in the axial position in cyclohexane (where there can be no anomeric effect) to its apparent size in the axial position at the C1 carbon in tetrahydropyran where an effect may exist. The *A*-value for the methyl group in cyclohexane is 1.8 kcal/mol, while that for SO_2CH_3 is 2.5 kcal/mol [93]. Thus, in cyclohexane, sulfone is larger than methyl group by 0.7 kcal/mol. From the equilibration and conformational data of the simple methyl tetrahydropyranyl

sulfone, sulfone appears to be smaller than methyl group. It was estimated that the apparent *A*-value for the sulfonyl group is 0.7 kcal/mol. Assuming that the sulfone *A*-value in tetrahydropyran, in the absence of an anomeric effect, should be equal to 2.5 kcal/mol (the same as the cyclohexane value), then the anomeric effect for the sulfone is $2.5_{\text{predicted}} - 0.7_{\text{observed}} = 1.8$ kcal/mol. It is known, however, that the apparent size of axial groups in tetrahydropyran is larger than in cyclohexanes. Chen et al. [92] proposed a correction factor of 1.5 in converting a cyclohexane *A*-value to that for a tetrahydropyran. This factor has been derived by comparison of *A*-value of CH_3 group (1.8) to that of 2.7 at the C2 in tetrahydropyran [94–96]. Hence the sulfone *A*-value could be as high as $2.5 \times 1.5 = 3.75$ kcal/mol. Which leads to an anomeric effect of $3.75_{\text{predicted}} - 0.7_{\text{observed}} = 3.05$ kcal/mol. In either case, the anomeric effect is approximately 70 % of the steric effect and favors the equatorial conformer. Hence, in the parent phenylsulfonyl tetrahydropyran itself, the group will appear to be equatorial. This is a different situation from than the oxygen anomeric effect, which, although a smaller force, overrides an equivalent or somewhat smaller steric effect. It is therefore possible to detect significant amounts of axial anomeric oxygen species in the parent tetrahydropyran under equilibrium conditions.

Based upon the results of the studies of Vasella et al. [85] and Franck et al. [95], it can be concluded that the reverse anomeric effect does not exist. The electropositive substituent at the anomeric carbon produces the enhanced *endo*-anomeric effect but not a reverse anomeric effect [97]. Non-solvated electropositive axial anomeric substituents such as nitro and sulfone groups show the *endo*-anomeric effect to be much larger than the oxygen anomeric effect, namely, 2.35 kcal/mol for the nitro group and 3.05 kcal/mol for the sulfone group, as opposed to the *endo*-anomeric effect for the oxygen atom of 0.85–1.54 kcal/mol.

2.4 Anomeric Effect in Systems O–C–N

The NMR studies at low temperature of unsubstituted and the C2 substituted 1,3-oxazines such as *117* (R = H) and *119* (R = CH_3) [45] strongly suggest that the conformers *117* and *119* are the major components of the equilibrium mixture *117* ⇌ *118* and *119* ⇌ *120* (Fig. 2.38).

These results were explained in the following way. Two anomeric effects are possible for conformers *117* and *119* (one anomeric effect where the equatorial nitrogen lone pair of electrons mixes with the antibonding C–O orbital and the other where the equatorial oxygen lone pair of electrons mixes with the antibonding C–N orbital). In conformers *118* and *119*, there is only one anomeric effect possible and that is where the equatorial oxygen lone pair of electrons mixes with the C–N antibonding orbital. However, it should be noted that since the nitrogen is less electronegative than oxygen, it is a better electron donor than oxygen, and *C–N is a weaker acceptor of electrons than the *C–O bond. Consequently, the O and N anomeric effects are not of equal energy. In addition, in the conformers *118* and *120*, ring nitrogen and oxygen atoms would have their axially oriented lone pairs of

Fig. 2.38

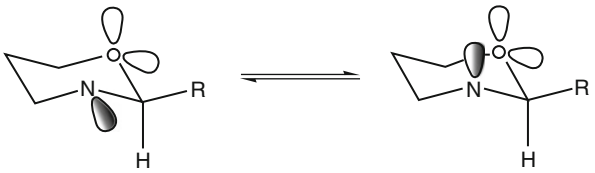

117, R = H
119, R = CH_3

118, R = H
120, R = CH_3

Fig. 2.39

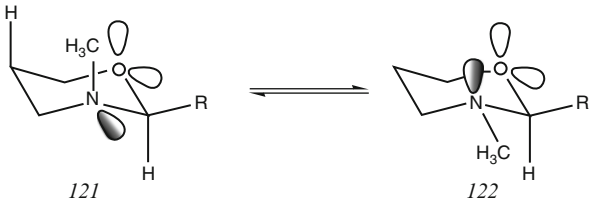

121 *122*

Fig. 2.40

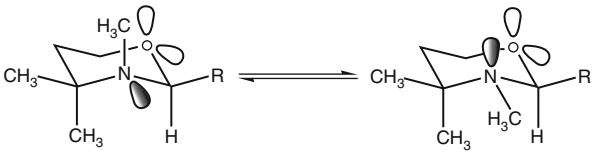

123 *124*

electrons in 1,3-*syn*-axial orientation which will further destabilize this conformation due to the generalized anomeric effect.

The NMR study of *N*-methyl tetrahydro-1, 3-oxazine such as *121* suggested that conformer *121* with the *N*-methyl group in the axial orientation is more stable than conformer *122* wherein the methyl group is equatorially oriented for the same reasons given above [98] (Fig. 2.39).

Similarly, it was found that the conformer *123* is present in appreciable concentration in the conformational equilibrium *123* ⇌ *124* (Fig. 2.40) again for the same reasons given above [98].

Kirby and Wothers [99] studied conformational equilibrium of amide acetal *125e* ⇌ *125a* to determine the magnitude of the anomeric effect of dimethylamino group by comparing the G° for ring inversion with that of its cyclohexyl analog *126e* ⇌ *126a* (Fig. 2.41).

On cooling a sample of amide acetal 125 to 140° K (in 70:30 CBr_2F_2-CD_2Cl_2), not a trace of conformer with the NMe_2 group equatorial (125e) was detected. It was concluded that the amide acetal exists as single conformer 125a and this conclusion was confirmed by NOE experiments.

If steric repulsion experienced by the methyl and dimethylamino groups increases by the same factor on going from the cyclohexane to dioxane, then the equilibrium constants for the ring inversion of the two compounds should be the same. At 185°K, cyclohexane conformation in which the NMe_2 is axially

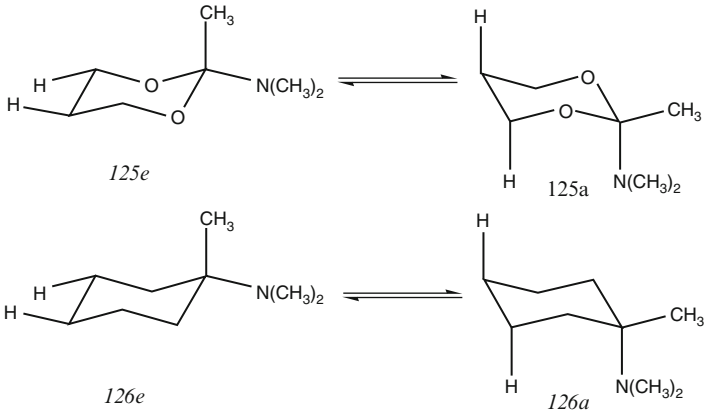

Fig. 2.41

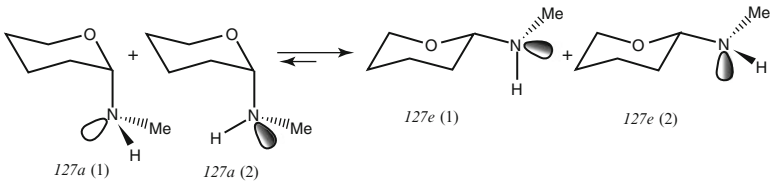

Fig. 2.42

oriented is more favored by $\Delta G^{\circ} = 1.59$ kcal.mol, whereas in a dioxane analog the axial orientation of NMe_2 group is favored by $\Delta G^{\circ} \geq 4.5$ kcal/mol. Thus, the conformation *126a* is at least 3 kJ/mol more stable at 185°K than would be expected from steric factors alone.

This result can be used to shed some light on the *exo-*/*endo*-anomeric effect in the 2-aminotetrahydropyrans studied extensively by Booth et al. [100–102]. Because nitrogen is less electronegative than oxygen, it is a better donor, and the antibonding σ*C−N orbital a weaker acceptor of electrons than the antibonding σ*C−O orbital. Consequently it could be expected that 2-methylaminotetrahydropyran exhibits a stronger *exo*-anomeric effect ($n_N - \sigma^*_{C-O}$) than *endo*-anomeric effect ($n_O - \sigma^*_{C-N}$). Thus, as shown by Booth et al. [100–102], 2-methylaminotetrahydropyran prefers the equatorial conformation (Fig. 2.42).

With the NHMe group equatorial, the rotamer *127e (1)* is stabilized by the *exo*-anomeric effect and is preferred. With NHMe axial, the preference is for rotamer *127a (2)*.

In contrast to the *N*-methyltetrahydropyrans, no *exo*-anomeric effect is expected when dimethylamino group is axial in the 2-position on dioxane ring, because in order for the nitrogen lone pair to be *anti* to the C–O bond, one methyl group will be subjected to severe steric interaction with the axially oriented C4 and C6 hydrogen atoms. This is possible for a hydrogen, but steric demands of a methyl group are prohibitive.

Fig. 2.43

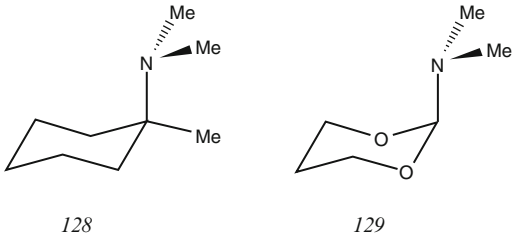

128 *129*

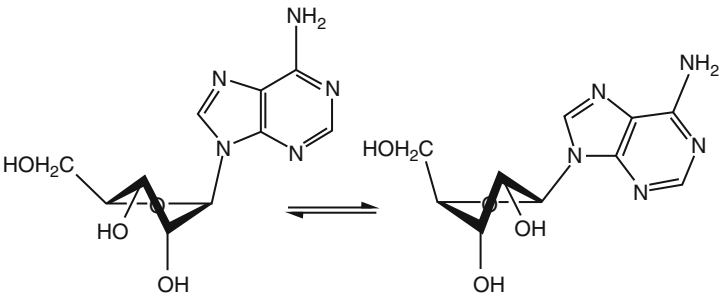

130 *131*

North (N) conformation (C_3-*endo*-C_2-*exo*)

South (S) conformation (C_2-*endo*-C_3-*exo*)

Fig. 2.44

Calculations of energies of different conformers *128* and *129* (Fig. 2.43) by using MM2 and 6-31 G * basis set have shown that the conformer with the dimethylamino group axially oriented is preferred, as shown in Fig. 2.43.

The concept of the anomeric effect in systems O–C–N is of great importance in chemical behavior of nucleosides, nucleotides, and nucleic acids since it controls the conformation of ribofuranosyl (or deoxyribofuranosyl) ring and with it the reactivity of the *N*-glycosidic bond.

The pseudorotation concept was introduced to describe the continuous interconversion of puckered forms of the cyclopentane ring [104]. The same concept is applied to the furanose geometry where the C1, O4, and C4 atoms lie in one plane and the C2 and C3 atoms lie above and below that plane. A statistical analysis of X-ray crystal structures of nucleosides and nucleotides has shown that North (N) *130* and South (S) *131* conformations are the most dominant forms, which has been the basis of the assumption of the two-state N ⇌ S pseudorotational equilibrium in solution (Fig. 2.44).

The two-state N ⇌ S pseudorotational equilibrium of the sugar moiety of β-D-ribofuranosyl-*N*-nucleoside in solution is energetically controlled by various stereoelectronic *gauche* and anomeric effects [103–110]. The *gauche* effects of O4′ − C4′ − C3′ − O3′ and O2′ − C2′ − C1′ − N fragments drive the sugar

pseudorotational equilibrium toward the S conformation [104], whereas it is driven to N conformation by the *gauche* effect of O4′ − C1′ − C2′ − O2′ (Fig. 2.44).

The X-ray crystal structures of N-nucleosides show the shortening of the O4′ − C1′ bond relative to C4′ − O4′ bond by about 0.03 Å which has been considered as a manifestation of the anomeric effect.

The preference of the 5′-CH_2OH group to occupy the pseudoequatorial orientation is manifested in the positive $\Delta H^{\neq}$ value for the pseudorotational equilibrium 111, 112 (Fig. 2.44). From the determination of the energetics of the two-state pseudorotational equilibrium in 36 nucleosides, it was found that the combined stereoelectronic and steric contributions in the anomeric effect of the nucleobases increase in the following order: adenine ≈ guanine < thymine < uracil < cytosine. One reason for the stronger anomeric effect in pyrimidine than in purine nucleosides could be that the $n_{O4'} \rightarrow \sigma^*_{C1'-N}$ delocalization is more effective in the π-deficient pyrimidine moiety compared to the relatively more electron rich purine.

The strength of the anomeric effect was enhanced upon protonation (evident by the increase in N-type sugar population) relative to the neutral state. These results are consistent with the favorable $n_{O4'} \rightarrow \sigma^*_{C1'-N}$ delocalization in the electron-deficient protonated aglycon at the acidic pH and the unfavorable $n_{O4'} \rightarrow \sigma^*_{C1'-N}$ delocalization in the electron-rich anionic aglycon at the basic pH, compared to the neutral state, as the origin of the anomeric effect.

We will discuss later in more detail the anomeric effect in nucleosides, nucleotides, and nucleic acids and its influence on the conformation of the furanose ring and the chemical consequences due to its presence.

2.5 Gauche Effect

Gauche effect can be defined as a tendency of a molecule to adopt that conformation which has the maximum number of gauche interactions between the adjacent electron pairs and/or polar bonds. The arrangement of bonding and nonbonding electron pairs about a single uncharged atom is determined mainly by the repulsive interactions, but when nonbonding electron pairs or electronegative ligands are placed on adjacent atoms, for some geometries the nuclear-electron attraction becomes sufficiently important to alter the balance between attractive and repulsive effects (Fig. 2.45).

Thus, the gauche effect will be attractive when the gauche conformation is the favored one of two equilibrium conformations, determined by the calculations of known steric and polar interactions. However, if the anti-conformation is favored more than the calculations suggest, the gauche effect is repulsive.

The attractive gauche effect has long been known in the X-C-C-Y systems, as for example when the X-Y-OCH_3 system [113], and the relationship between the gauche and anomeric effect was made some years ago [114]. However, the repulsive interactions were not initially recognized. In 1979 Zefirov et al. [114] studied

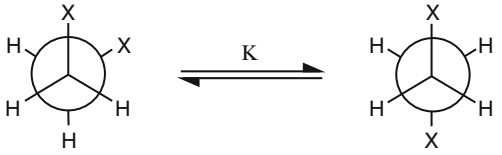

132 *133*

gauche effect is **attractive** when K is smaller than expected
gauche effect is **repulsive** when K is larger than expected
} on purely steric grounds

gauche effect is **attractive** when X = F/F, O/F, O/O
gauche effect is **repulsive** when X = S/S

Fig. 2.45

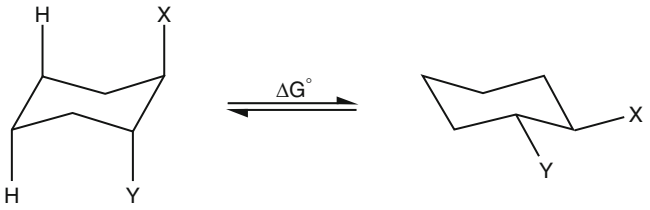

134 ($\Delta G_X + \Delta G_Y$) *135* ($E_V^{X/Y} + E_\mu^{X/Y}$)

If there is no additional effect ΔG°_{expt} = ($\Delta E_{steric} + \Delta E_{polar}$) calc' d
If ΔG°_{expt} = ($\Delta E_{steric} + \Delta E_{polar}$) calc' d, there is a ***repulsive*** *gauche* effect, and
If ΔG°_{expt} = ($\Delta E_{steric} + \Delta E_{polar}$) calc' d, there is an ***attractive*** *gauche* effect, and

Fig. 2.46

the conformational equilibrium of certain *trans*-1,2-disubstituted cyclohexanes (Fig. 2.46) by NMR spectroscopy. From the data obtained from the measurments of vicinal coupling constants, they concluded that repulsive gauche effects occur for X = Y = SR; X =SR, Y = Br; X = SCH_3, Y = Br; X = SCH_3, Y = OCH_3, X = SCH_3, Y = Cl; and X = Y = Br. They also concluded that attractive gauche effects existed when X = Y = OR or X = F, Y = I. These conclusions were arrived at by comparing the experimentally determined equilibria with those calculated on the basis of the known ΔG°-value (in cyclohexyl-X) of X and Y and calculated X/Y interaction. The steric part of the latter was estimated by the Hill equation [115] and the polar part by a charge/charge interaction [116]. For CH_3O/Cl, CH_3O/Br, CH_3O/I, and Cl/I, the calculated equilibrium agrees with the experimental findings that there is no gauche effect. An attractive gauche effect was inferred when the equilibrium was further to the right than calculated, and a repulsive effect when the equilibrium was displaced to the left. However, it should be noted that Zefirov's approach has its limitations since the calculations tend to underestimate the steric effects even in those cases where no gauche effects come into play.

Fig. 2.47

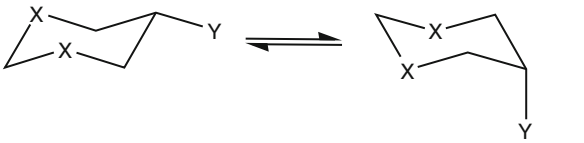

136, X = O; Y = NHMe
138, X = O; Y = OMe

137, X = O; Y = NHMe
139, X = O; Y = OMe

Table 2.11 Component analysis of ethane-type gauche effect in 5-substituted-1,3-dioxacyclohexanones

Energy difference[a]	*136, 137*	*138, 139*
e ⇌ a	X = O; Y = NHMe	X = O; Y = OMe
$\Delta G^{\circ}_{\text{steric}}$ [b]	0.74	0.26
$\Delta G^{\circ}_{\text{electrostatic}}$ [c]	−0.54	1.71
$\Delta G^{\circ}_{\text{exptl}}$ [d]	−0.36	0.19
$\Delta G^{\circ}_{\text{orbital}}$ [e]	−0.56	−1.78

[a]In kcal/mol
[b]Differences between the axial and equatorial conformers were calculated by multiplying the proportionality constants, obtained from comparing the-methyl substituted cyclohexane and 5-methyl-1,3-dioxacyclohexane, with the *A*-values of the respective substituents
[c]Differences in electrostatic energies were taken from the charge/charge interaction terms for the optimized structures, using the interactive molecular modeling program PCMODEL (PCMODEL, Serena Software, Box 3076, Bloomington, Indiana, USA). This program uses a variant of the MM2 force field
[d]Experimental ΔG°-values
[e]Differences in orbital interaction energies were calculated by substracting the $\Delta G^{\circ}_{\text{steric}}$ and $\Delta G^{\circ}_{\text{electrostatic}}$ from $\Delta G^{\circ}_{\text{exptl}}$

The interpretation of gauche interactions according to Hoffman [117] considers the effect of both through-bond and through-space orbital interactions. The interactions are illustrated for the case of 5-methylamino-1,3-dioxacyclohexane (Fig. 2.47).

In Table 2.11 the energy differences between the equatorial and axial Y substituent are given.

References

1. Kirby AJ (1983) The anomeric effect and related stereoelectronic effects on oxygen. Springer, Berlin/Heidelberg/New York
2. Szarek WA, Horton D (eds) (1979) Anomeric effect, origin and consequences, ACS symposium series 87. American Chemical Society, Washington, DC
3. Thatcher GRJ (ed) (1993) The anomeric effect and associated stereoelectronic effects, ACS symposium series 539. American Chemical Society, Washington, DC
4. Juaristi E, Cuevas G (1995) The anomeric effect. CRC Press, Boca Raton

5. Tvaroška I, Bleha T (1989) Anomeric and exo-anomeric effects in carbohydrate chemistry. Adv Carbohydr Chem Biochem 47:45–123
6. Deslongchamps P (1983) Stereoelectronic effects in organic chemistry. Pergamon Press, Oxford
7. Bates FJ and Associates (1942) Polarimetry, saccharimetry and the sugars. United States Government Printing Office, Washington, DC, p 455
8. Angyal SJ (1968) Conformational analysis in carbohydrate chemistry. I. Conformational free energies. The conformations and α: β ratios of aldopyranoses in aqueous solution. Aust J Chem 21:2737–2746
9. Bonner WA (1959) The acid-catalyzed anomerization of acetylated aldopyranoses. J Am Chem Soc 81:1448–1452
10. Lemieux RU (1963) In: de Mayo P (ed) Molecular rearrangements, vol 2. Interscience, New York, p 709
11. Lemieux RU, Hayami J-Y (1965) Mechanism of the anomerization of the tetra-*O*-acetyl-D-glucopyranosyl chloride. Can J Chem 43:2162–2173
12. Edward JT (1955) Stability of glycosides to acid hydrolysis. Chem Ind (London) 36:1102–1104
13. Corey EJ (1953) The stereochemistry of α-haloketones. The molecular configuration of some monocyclic α-haloketones. J Am Chem Soc 75:2301–2304
14. Winstein S, Holness NJ (1955) Neighboring carbon and hydrogen. XIX. t-butyl-cyclohexyl derivatives. Quantitative conformational analysis. J Am Chem Soc 77:5562–5578
15. Eliel EL (1962) Stereochemistry of carbon compounds. McGraw Hill, New York, p 236
16. Andersen CB, Sepp DT (1968) Conformation and the anomeric effect in 2-oxysubstituted tetrahydropyrans. Tetrahedron 24:1707–1716
17. Isbell HS, Pigman WW (1937) Bromine oxidation and mutarotation measurements of α- and β-aldoses. J Res Natl Bur Stand 18:141–194
18. Angyal SJ (1969) The composition and conformation of sugars in solution. Angew Chem Int Ed 8:157–166
19. Reeves RE (1949) Cupramonium-glycoside complexes. II. The angle between hydroxyl groups on adjacent carbon atoms. J Am Chem Soc 71:212–214
20. Reeves RE (1950) The shape of pyranoside rings. J Am Chem Soc 72:1499–1506
21. Reeves RE (1951) Cupramonium-glycoside complexes. Adv Carbohydr Chem 6:107–134
22. Hageman HJ (1965) Ph.D. thesis, Leiden
23. Eliel EL, Allinger NL, Angyal SJ, Morrison GA (1965) Conformational analysis. Interscience, New York, p 44
24. Planje MC (1964) Ph.D. thesis, Leiden
25. Booth GE, Oullette RJ (1966) Conformational analysis. V. 2, 2-Chloro- and 2-bromotetrahydropyran. J Org Chem 31:544–546
26. Anderson CB, Sepp DT (1967) Conformation and the anomeric effect in 2-halotetrahydropyrans. J Org Chem 32:607–611
27. Akishin PA, Vilkov LV, Sokolova NP (1960) Electronographic study of the structure of the molecules of monochloro- and monobromodimethyl ethers. Izvest Sibir Otdel Akad Nauk SSSR 5:59–60
28. Planje MC, Toneman LH, Dallinga G (1965) Electron diffraction by gases – molecular structure of monochlorodimethyl ether. Rec Trav Chim 84:232–240
29. Bishop CT, Cooper FP (1963) Glycosidation of sugars. II. Methanolysis of D-xylose, D-arabinose, D-lyxose, and D-ribose. Can J Chem 41:2743–2758
30. Anderson CB, Sepp DT (1968) Conformation and anomeric effect in 2-oxy-substituted tetrahydropyrans. Tetrahedron 24:1707–1716
31. Eliel EL, Giza CA (1968) Conformational analysis of some 2-alkoxytetrahydropyrans and 2-alkoxy-1,3-dioxanes. Anomeric effect. J Org Chem 33:3754–3758
32. Pierson GO, Runquist OA (1968) Conformational analysis of some 2-alkoxytetrahydropyrans. J Org Chem 33:2572–2574

33. Sweet F, Brown RK (1968) Cis- and trans-2,4-dimethoxy tetrahydropyran. Models for the study of the anomeric effect. Can J Chem 46:1543–1548
34. de Hoog AJ, Buys HR, Altona C, Havinga E (1969) Conformation of nonaromatic ring compounds – LII: NMR spectra and dipole moments of 2-alkoxytetrahydropyrans. Tetrahedron 25:3365–3375
35. Fuchs B, Ellencweig A, Tartakovsky E, Aped P (1986) Solvent polarity and the anomeric effect. Angew Chem Int Ed Engl 25:287–289
36. Altona C, Havinga E, cited as unpublished in Romers C, Altona C, Buys HR, Havinga E (1969) In: Eliel EL, Allinger NL (eds) Topics of stereochemistry, vol 4. Wiley-Interscience, pp 39–97
37. Altona C, Romers C, Havinga E (1959) Molecular structure and conformation of some dihalogenodioxanes. Tetrahedron Lett 1:16–20
38. Altona C (1964) Ph.D. thesis, Leiden; Altona C, Romers C (1963) The conformation of non-aromatic ring compounds. VIII. The crystal structure of cis-2,3-dichloro-1,4-dioxane at −140 °C. Acta Cryst 16:1225–1232
39. Altona C, Knobler C, Romers C (1963) The conformation of non-aromatic ring compounds. VII. Crystal structure of trans-2,5-dichloro-1,4-dioxane at 125 °C. Acta Cryst 16:1217–1225
40. de Wolf N, Romers C, Altona C (1967) The conformation of non-aromatic ring compounds. XXXIV. The crystal structure of trans-2,3-dichloro-1,4-thioxane at 185 °C. Acta Cryst 22:715–719
41. Hutchins RO, Kopp LD, Eliel EL (1968) Repulsion of syn-axial electron pairs. The "rabbit-ear effect". J Am Chem Soc 90:7174–7175
42. Kubo M (1936) Pap Inst Phys Chem Res (Tokyo) 29:179
43. Aoki K (1953) J Chem Soc (Japan), Pure Chem Sect 74:110
44. Astrup EE (1971) Molecular structure of dimethoxymethane, $MeOCH_2OME$. Acta Chem Scand 25:1494–1495
45. Booth H, Lemieux RU (1971) Anomeric effect: the conformational equilibriums of tetrahydro-1,3-oxazines and 1-methyl-1,3-diazane. Can J Chem 49:777–788
46. Zefirov NS (1977) The problem of conformational effects. Tetrahedron 33:3192
47. Eliel EL, Allinger NL, Angyal SJ, Morrison GA (1965) Conformational analysis. Wiley-Interscience, New York, p 460
48. Horton D, Turner WN (1965) Conformational and configurational studies on some acetylated aldopyranosyl halides. J Org Chem 30:3387–3394
49. Lemieux RU, Morgan AR (1965) The abnormal conformations of pyridinium α-glycopyranosides. Can J Chem 43:2205–2213
50. James MNG (1969) Proc Can Fed Biol Soc 13:71
51. Lemieux RU (1971) Effects of unshared pairs of electrons and their solvation conformational equilibria. Pure Appl Chem 27:527–548
52. Lemieux RU, Koto S (1974) The conformational properties of glycosidic linkages. Tetrahedron 30:1933–1944
53. Lemieux RU, Hendricks KB, Stick RV, James K (1975) Halide ion catalyzed glycosidation reactions. Synthesis of α-linked disaccharides. J Am Chem Soc 97:4056–4062
54. Saluja SS (1971) Ph.D. thesis, University of Alberta
55. Paulsen H, Györgdeák Z, Friedman M (1974) Konformationsanalyse, V. Einfluss des anomeren und inversen anomeren effektes auf konformationsgleichgewichte von N-substituirten N-pentopyranosiden. Chem Ber 107:1590–1613
56. Grein F, Deslonchamps P (1992) The anomeric and reverse anomeric effect. A simple energy decomposition model for acetals and protonated acetals. Can J Chem 70:1562–1572
57. Grein F (1993) Anomeric and reverse anomeric effect in acetals and related functions. In: Thatcher GRJ (ed) The anomeric effect and associated stereoelectronic effects, ACS symposium series No. 539. ACS, Washington, DC, pp 205–226
58. Finch P, Nagpurkar AG (1976) The reverse anomeric effect: further observations on N-glycosylimidazoles. Carbohydr Res 49:275–287

59. Ratcliffe AJ, Fraser-Reid B (1990) Generation of D-glucopyranosylacetonitrilium ions. Concerning the reverse anomeric effect. J Chem Soc Perkin Trans 1:747–750
60. Batchelor JG (1976) Conformational analysis of cyclic amines using carbon-13 chemical shift measurements: dependence of conformation upon ionization state and solvent. J Chem Soc Perkin Trans 2:1585–1590
61. Booth H, Jozefowicz ML (1976) The application of low temperature ^{13}C nuclear magnetic resonance spectroscopy to the determination of the a-values of amino-, methylamino-, and dimethylamino-substituents in cyclohexane. J Chem Soc Perkin Trans 2:895–901
62. Sicher J, Jonás J, Tichý M (1963) The A-values of the amino acid and dimethylamino groups. Tetrahedron Lett 4:825–830
63. Eliel EL, Della EW, Williams TH (1963) The conformational equilibrium of the amino group. Tetrahedron Lett 4:831–835
64. Ford RA, Allinger NL (1970) Conformational analysis. LXVII. Effect of solvent on the conformational energy of the carbethoxy group. J Org Chem 35:3178–3181
65. Perrin CL, Armstrong KB (1993) Conformational analysis of glycopyranosyl-ammonium ion: does the reverse anomeric effect exists? J Am Chem Soc 115:6825–6834
66. Isbel HS, Frush HL (1958) Mutarotation, hydrolysis and rearrangement reactions of glycosylamines. J Org Chem 23:1309–1319
67. Pinto BM, Leung YN (1993) In: Thatcher GRJ (ed) The anomeric effect and associated stereoelectronic effects, ACS symposium series 539. ACS, Washington, DC, pp 126–155
68. Cramer CJ (1992) Anomeric and reverse anomeric effect in the gas phase and aqueous solution. J Org Chem 57:7034–7043
69. Salzner U, Schleyer P v R (1994) Ab initio examination of anomeric effects in tetrahydropyrans, 1,3-dioxanes and glucose. J Org Chem 59:2138–2155
70. Chan SSC, Szarek WA, Thatcher GRJ (1995) The reverse anomeric effect in N-pyranosylimidazoles: a molecular orbital study. J Chem Soc Perkin Trans 2:45–60
71. Vaino AR, Chan SSC, Szarek WA, Thatcher GRJ (1996) An experimental reexamination of the reverse anomeric effect in glycosylimidazoles. J Org Chem 61:4514–4515
72. Fabian MA, Perrin CL, Sinnott ML (1994) Absence of reverse anomeric effect: conformational analysis of glycopyranosylimidazolium and glycosylimidazole. J Am Chem Soc 116:8398–8399
73. Juaristi E, Cuevas G (1992) Recent studies of anomeric effect. Tetrahedron 48:5019–5087
74. Mikolajczyk M, Graczyk P, Wieczorek MW, Bujacz G (1991) Conformational preference of 2-triphenylphosphonio-1,3-dithianes: competition between steric and anomeric effects. Angew Chem Int Ed Engl 30:578–580
75. Graczyk PP, Mikolajczyk M (1993) Anomeric effect: origin and consequences. Phosphorus Sulfur Silicon Relat Elem 78:313–316
76. Juaristi E, Cuevas G (1993) Conformational analysis of 1,3-dithiane-2-ylmethylphosphionium chloride. Origin of the S-C-P anomeric effect. J Am Chem Soc 115:1313–1316
77. Thibaudeau C, Plavec J, Watanabe KA, Chattopadhyaya J (1994) How do the aglycons drive the pseudorotational equilibrium of the pentofuranose moiety in C-nucleosides? J Chem Soc Chem Commun 537–540
78. Jones PG, Komarov IV, Wothers PD (1998) A test for the reverse anomeric effect. Chem Commun 16:1695–1696
79. Kenedy J, Wu J, Drew K, Carmichael I, Serianni AS (1997) Carbohydrate reaction intermediates: effect of ring oxygen protonation on the structure and conformation of aldofuranosyl rings. J Am Chem Soc 117:8933–8945
80. Alder RW, Carniero TMG, Mowlam RW, Orpen AG, Petillo PA, Vachon DJ, Weisman GR, White JM (1999) Evidence for hydrogen-bond enhanced structural anomeric effects from the protonation of two aminals, 5-methyl-1,5,9-triazabicyclo[7.3.1]tridecane and 1,4,8,11-tetraazatricyclo [9.3.1.1(4.8)]hexadecane. J Chem Soc Perkin Trans 2:589–599
81. Cramer CJ (1996) Hyperconjugation as it affects conformational analysis. J Mol Struct (Theochem) 370:135–146

82. Ganguly B, Fuchs B (1997) Stereoelectronic effects in negatively and positively (protonated) charged species. Ab initio studies of the anomeric effect in 1,3-dioxa-systems. J Org Chem 62:8892–8901
83. Cloran F, Zhu Y, Osborn J, Carmichael I, Serianni AS (2000) 2-Deoxy-D-ribofuranosylamine: quantum mechanical calculations of molecular structure and NMR spin-spin coupling constants in nitrogen-containing saccharides. J Am Chem Soc 122:6435–6448
84. Randell KD, Johnston BD, Green DF, Pinto BM (2000) Is there a generalized reverse anomeric effect? Substituent and solvent effects on the configurational equilibria of neutral and protonated *N*-arylglucopyranosyl amines and *N*-aryl-5-thioglucopyranosylamines. J Org Chem 65:220–226
85. Guthrie JP (1978) Hydrolysis of esters of oxy acids: pKa values for strong acids; Bronsted relationship for attack of water at methyl; free energies of hydrolysis of esters of oxyacids; and a linear relationship between free energy of hydrolysis and pKa holding over a range of 20 pK units. Can J Chem 56:2342–2354
86. Aebischer B, Hollenstein R, Vasella A (1983) 168. Deoxy-nitrosugars. The anomeric effect of the nitro group. Helv Chim Acta 66:1748–1754
87. Durette PL, Horton D (1971) Conformational analysis of sugars and their derivatives. Adv Carbohydr Chem 26:49–125
88. Trager WF, Huitric AC (1965) Conformational free-energy difference of the nitro group. J Org Chem 30:3257
89. Angyal SJ (1968) Conformational analysis in carbohydrate chemistry. I. Conformational free energies and α-β ratios of aldopyranoses in aqueous solutions. Aust J Chem 21:2737–2746
90. Reeves RE (1949) Cuprammonium-glycoside complexes. III. The conformation of the D-glucopyranoside ring in solution. J Am Chem Soc 71:215
91. Steilin H, Carmada L, Vasella A (1979) Preparation of methyl α-D-fructopyranosides and the structure of the orthoester by-products. Helv Chim Acta 62:378–390
92. Chen G, Franck RW, Yang G, Blumenstein M (2002) Anomeric affect of sulfones. Can J Chem 80:894–899
93. Hackett Bushweller C (1995) Chapter 2. In: Juaristi E (ed) Conformational analysis and stereochemistry of six-membered rings. Verlag Chemie, New York, p 25
94. Eliel EL, Hargrave KD, Pietrusiewicz KM, Manoharan M (1982) Conformational analysis. 42. Monosubstituted tetrahydropyrans. J Am Chem Soc 104:3635–3643
95. Frank RW (1983) A revision of the value for the anomeric effect. Tetrahedron 39:3251–3252
96. Frank RW (1995) In: Juaristi E (ed) Conformational analysis and stereochemistry of six-membered rings. Verlag Chemie, New York, p 157
97. Perrin CL (1995) Reverse anomeric effect: fact or fiction? Tetrahedron 51:11901–1193
98. Allingham Y, Cookson RC, Crabb TA, Vary S (1968) The NMR spectra and conformations of some tetrahydro-1,3-oxazines. Tetrahedron 24:4625–4630
99. Kirby AJ, Wothers PD (2001) Conformational equilibria involving 2-amino-1,3-dioxanes: steric control of the anomeric effect. ARKIVOC XII:58–71
100. Booth H, Khedhair KA (1985) Endo-anomeric and exo-anomeric effects in 2-substituted tetrahydropyrans. J Chem Soc Chem Commun 467–468
101. Booth H, Readshaw SA (1990) Experimental studies of the anomeric effect. Part IV. Conformational equilibria due to ring inversion in tetrahydropyrans substituted a position 2 by the groups ethoxy, 2′-fluoroethoxy, 2′, 2′-difluoroethoxy, and 2′,2′,2′-trifluoroethoxy. Tetrahedron 46:2097–2110
102. Booth H, Khedhair KA, Readshaw SA (1987) Experimental studies of the anomeric effect. I. 2-Substituted tetrahydropyrans. Tetrahedron 43:4699–4723
103. Kilpatrick JE, Pitzer KS, Spitzer R (1993) The thermodynamics and molecular structure of cyclopentane. J Am Chem Soc 115:9734–9746
104. Plavec J, Tong W, Chattopadhyaya J (1993) How do the gauche and anomeric effects drive the pseudorotational equilibrium of the pentofuranose moiety of nucleosides. J Am Chem Soc 115:9734–9746

105. Plavec J, Garg N, Chattopadhyaya J (1993) How does the steric effect drive the sugar conformation in the 3-C-branched nucleosides? J Chem Soc Chem Commun 1011–1014
106. Plavec J, Koole LH, Chattopadhyaya J (1992) Structural analysis of 2′,3′-dideoxyinosine, 2′,3′-dideoxyadsenosine, 2′,3′-dideoxyguanosine, and 2′,3′-dideoxycytidine by 500-MHz proton-NMR spectroscopy and ab initio molecular orbital calculations. J Biochem Biophys Methods 25:253–272
107. Altona C, Sundaralingam M (1972) Conformational analysis of the sugar ring in nucleosides and nucleotides. New description using the concept of pseudorotation. J Am Chem Soc 94:8205–8212
108. Altona C, Sundaralingam M (1973) Conformational analysis of the sugar ring in nucleosides and nucleotides. Improved method for the interpretation of proton magnetic resonance coupling constants. J Am Chem Soc 95:2333–2344
109. Saenger W (1988) Principles of nucleic acid structure. Springer, Berlin
110. Olson WK, Sussman JL (1982) How flexible is the furanose ring? 1. A comparison of experimental and theoretical studies. J Am Chem Soc 104:270–278
111. Plavec J, Thibaudeau C, Chattopadhyaya J (1996) How do the energetics of the stereoelectronic gauche and anomeric effects modulate the conformation of nucleo(s)tides. Pure Appl Chem 68:2137–2144
112. Eliel EL (1969) Rabbit ear effect. Polar interactions of hetero atoms. Kem Tidskr 81 (6, 7):22–27
113. Wolfe S (1972) The gauche effect. Some stereochemical consequences of adjacent electron pairs and polar bonds. Acc Chem Res 5:102–111
114. Zefirov NS, Gurvich LG, Shashkov AS, Krimer MZ, Vorob'eva EA (1976) Stereochemical studies. XX. Conformations of 1,2-trans-disubstituted cyclohexanes. Tetrahedron 32:1211
115. Eliel EL, Allinger NL, Angyal SJ, Morrison GA (1965) Conformational analysis. Interscience-Wiley, New York, p 449 ff
116. Abraham RJ, Rosetti ZL (1973) Rotational isomerism. XV. Solvent dependence of the conformational equilibriums in trans-1,2 and trans-1,4-dihalocyclohexanes. J Chem Soc Perkin II 582–587
117. Hoffman R (1971) Interaction of orbitals through space and through bonds. Acc Chem Res 4:1–9

Chapter 3
Oxocarbenium Ion

3.1 Acid-Catalyzed Hydrolysis of Glycosides

Several good reviews have been published on this subject [1–3].

Glycosides are mixed acetals wherein on one side the aldehydo C1 carbon of a sugar molecule is linked via the exocyclic oxygen atom to an alkyl, aryl, or any other group having a hydroxyl function, and on the other side is linked via the endocyclic oxygen atom to the C5 (pyranosides) or the C4 (furanosides) carbon of a sugar molecule.

The initial step of the acid-catalyzed hydrolysis of a glycoside, as well as of any acetal or ketal, is a fast and reversible protonation of one of the two acetal oxygens of a sugar glycoside (Fig. 3.1).

Depending upon the site of protonation, two reaction mechanisms could be envisioned. If the exocyclic (glycosidic) oxygen is protonated giving *2* as an intermediate (Fig. 3.1), the following step could be the unimolecular elimination of the aglycon group (in the case of alkyl glycosides the elimination of an alcohol group) with the assistance of the axially oriented nonbonding electron pair of the ring oxygen and formation of the corresponding cyclic oxocarbenium ion *6*. If water is present in the reaction mixture (which is always the case in hydrolysis reactions), then water molecules, and not alcohol molecules, will add to the positively charged carbon of the oxocarbenium ion *6* giving first the hydrolyzed monosaccharide protonated at the anomeric hydroxyl group *7* that, after deprotonation, gives the hydrolyzed sugar *8*. In the oxocarbenium ion *6*, since the C5, O5, C1, and C2 atoms lie in one plane (the sugar molecule must be in the half-chair conformation which is the consequence of the double bond character of the O5–C1 bond), the water molecules can add from either face of the oxocarbenium ion, and consequently a mixture of α- and β-glycopyranoses will be obtained (Fig. 3.2).

If the ring oxygen (the O5 in pyranosides or the O4 in furanosides) is protonated *10* (Fig. 3.3), then the C1–O5 bond can be broken in the following step with the formation of acyclic oxocarbenium ion *11* (this time by the participation of one

M. Miljkovic, *Electrostatic and Stereoelectronic Effects in Carbohydrate Chemistry*,
DOI 10.1007/978-1-4614-8268-0_3, © Springer Science+Business Media New York 2014

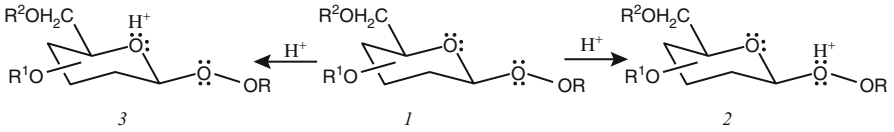

Fig. 3.1

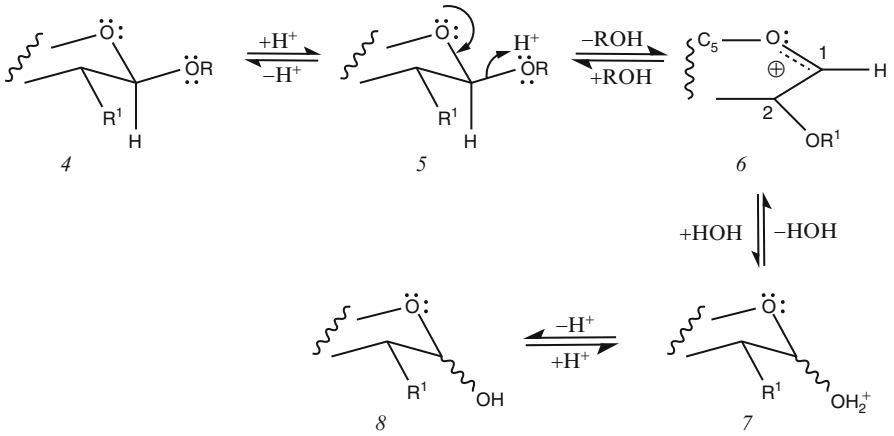

Fig. 3.2

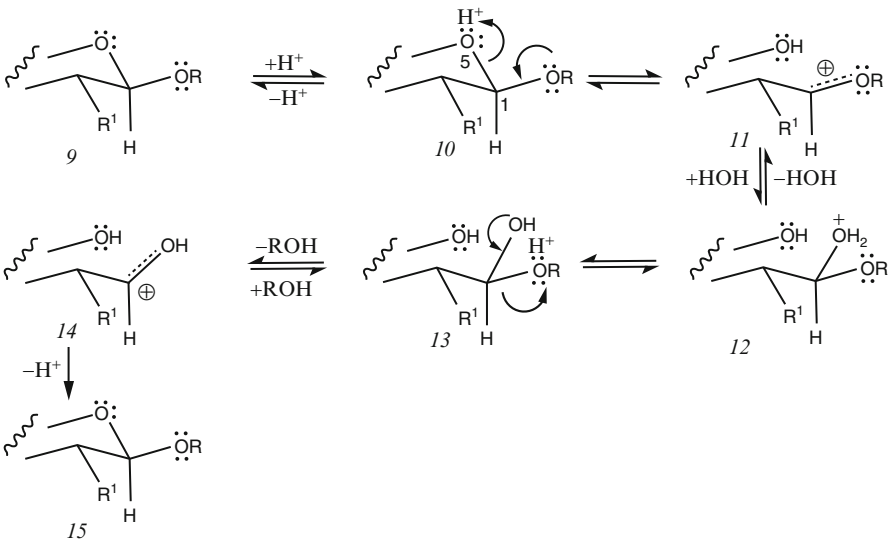

Fig. 3.3

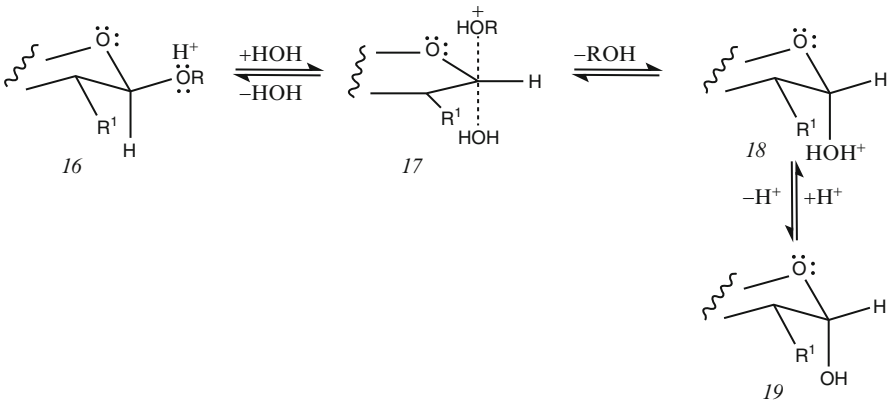

Fig. 3.4

nonbonded electron pair of the glycosidic oxygen) (Fig. 3.3). The addition of a water molecule to *11* will form the hemiacetal *12* that is protonated at the anomeric hydroxy oxygen. This intermediate will be in equilibrium with the hemiacetal protonated at the methoxy oxygen (*13*). Now, the elimination of alcohol from *13* will result in the formation of protonated aldehydo sugar *14* that by cyclization and deprotonation gives the hydrolyzed sugar *15* (Fig. 3.3).

There is, however, a third possible mechanism that can be envisioned for the hydrolysis of glycosides, and that is the nucleophilic (S_N2) displacement of the protonated methoxy group with water as the nucleophile, as is shown in Fig. 3.4.

In order to elucidate the reaction mechanism of glycoside hydrolysis, we must first fully understand the relationship between the rate of hydrolysis and steric and electronic factors present in both glycon and aglycon of a sugar glycoside. Hence, the rates of hydrolysis of many glycosides have been measured, and it has been found that they are influenced by many factors such as the type of sugar, the ring size of sugar, the anomeric configuration of glycosidic bond, the nature of substituents on the sugar ring, the conformation of sugar, and the size and the polarity of aglycon.

The observations that glycofuranosides are generally hydrolyzed much faster than glycopyranosides (ca. 50–200) [4, 5] (it should be emphasized that furanosides are also formed much faster than pyranosides) and that kinetic parameters for the acid-catalyzed hydrolysis of glycofuranosides and glycopyranosides are very different (e.g., the entropies of activations for the acid-catalyzed hydrolysis of all glycofuranosides are negative, whereas they are positive for the acid-catalyzed hydrolysis of all glycopyranosides) suggest that they are probably hydrolyzed via different mechanisms, and therefore, we will discuss these two topics separately.

3.2 The Acid-Catalyzed Hydrolysis of Glycopyranosides

The glycopyranosides with equatorially oriented aglycon are hydrolyzed roughly two times faster than glycopyranosides having the aglycon axially oriented, and this ratio seems to be dependent neither on the structure of glycon nor on the nature of aglycon. In Table 3.1 the relative rates of acid-catalyzed hydrolysis of select groups of methyl aldopyranosides are given.

The removal of the hydroxyl group from either the C2 or the C6 carbon accelerates the acid-catalyzed hydrolysis. Whereas the rate acceleration of acid-catalyzed hydrolysis is enormous for the C2 deoxy glycopyranosides (ca. 2 to 5×10^3 times), the rate acceleration for the C6 deoxy glycopyranosides is much smaller (only ca. 8 times).

The acid-catalyzed hydrolysis of pentopyranosides is generally faster than that of hexopyranosides (4.5–9.0 times) but slower than the acid-catalyzed hydrolysis of 6-deoxy-hexopyranosides.

The introduction of an electron-withdrawing group at the C6 carbon reduces the rate of acid-catalyzed hydrolysis (the acid-catalyzed hydrolysis of methyl glycoside of D-glucuronic acid is ca. 2 times slower than methyl glycoside of D-glucose).

In Table 3.2 the rate coefficients and kinetic parameters for the hydrolysis of select glycosides in 2.0N HCl extrapolated to 60 °C are given. The concentration of HCl for the hydrolysis of methyl 2-deoxy-α and β-D-glucopyranoside was 0.1N.

Table 3.1 Relative rates of acid-catalyzed hydrolysis of methyl α- and β-aldopyranosides [6] in 0.01–0.5M HCl or H_2SO_4 at 58–100°

Methyl D-glycopyranoside	Relative rates	α:β ratio	Orientation of 1-OMe group
α-D-gluco-	1.0 [7]	1:1.9	Axial
β-D-gluco	1.9 [7]		Equatorial
α-D-galacto-	2.4 [7]	1:2.4	Axial
β-D-galacto-	5.7 [7]		Equatorial
α-D-manno-	5.2 [7]	1:1.8	Axial
β-D-manno-	9.2 [7]		Equatorial
α-D-xylo-	4.5 [7]	1:2.0	Axial
β-D-xylo-	9.1 [7]		Equatorial
α-L-arabino-	13.1 [7]	1.5:1	Equatorial
β-L-arabino-	9.0 [7]		Axial
α-L-rhamno-	8.3 [7]	1:2.3	Axial
β-L-rhamno-	19.0 [7]		Equatorial
α-D-glucopyranosiduronic acid	0.47 [8]	1:1.3	Axial
β-D-glucopyranosiduronic acid	0.62 [8]		Equatorial
2-deoxy-α-D-gluco-	2,090 [9]	1:2.5	Axial
2-deoxy-β-D-gluco-	5,125 [9]		Equatorial
2,3,4,6-tetra-*O*-methyl-α-D-gluco-	0.16 [10]	1:2.5	Axial
2,3,4,6-tetra-*O*-methyl-β-D-gluco-	0.40 [10]		Equatorial

Table 3.2 Rate coefficients and kinetic parameters for the hydrolysis of select glycosides in 2.0N HCl extrapolated to 60 °C [9]

Pyranoside	$10^5 k$ s^{-1}	E (kcal/mol)	$\Delta S^{\neq}$ at 60° (cal.deg.$^{-1}$ mol^{-1})
Me α-D-gluco-	0.708	34.1 ± 1.0	+14.8
Me β-D-gluco-	1.26	34.3 ± 0.4	+16.5
Me α-D-galacto-	3.55	34.0 ± 0.3	+17.7
Me β-D-galacto-	5.13	32.3 ± 0.6	+13.3
Me α-D-manno-	2.09	31.9 ± 0.4	+10.4
Me α-D-xylo-	2.69	33.5 ± 0.9	+15.7
Me β-D-xylo-	5.89	33.6 ± 0.9	+17.5
Me 6-deoxy-α-D-galacto-	20.0	33.9 ± 0.6	+20.8

In order to elucidate the mechanism of acid-catalyzed hydrolysis of glycopyranosides, a detailed knowledge is needed of the breakdown of conjugate acid obtained after protonation of one of the two acetal oxygens, i.e., the molecularity of the rate-determining step, which is the C1–O1 or the C1–O5 bond cleavage depending upon whether the glycosidic or the ring oxygen is protonated. The experimental results suggest that the hydrolysis of glycopyranosides proceeds by an A-1 (acid-catalyzed unimolecular) mechanism (Ingold terminology [11]).

The first-order rate velocity coefficients (k_1) were found to be constant for the hydrolysis of D-glucopyranosides in perchloric acid solutions in concentrations ranging from 0.465M to 3.782M [12]. Plots of $\log k_1$ against the Hammett acidity function, H_0, and against the pH were found to be almost linear in the first instance and not linear in the second instance, suggesting that analogous to the acid-catalyzed hydrolysis of acetals [13], the hydrolysis of glycopyranosides proceeds by an A-1, and not an A-2, mechanism. However, since solvent is in large excess with respect to the reactants, both A-1 and A-2 will follow a first-order rate law, and consequently, other criteria must be used to unequivocally determine the molecularity of the reaction.

The effect of a substituent on a glycopyranoside ring upon the rate of hydrolysis of glycosidic bond is strongly dependent upon its electronegativity, its size, and its position. The nature of the substituent at the C2 and the C6 carbons of a pyranoside seems to have the most profound effect. For example, the removal of hydroxy group from the C2 carbon dramatically increases the rate of hydrolysis of the glycosidic bond. Thus, methyl 2-deoxy-β-D-*arabino*-hexopyranoside (*20* in Fig. 3.5) is hydrolyzed ca. 2,500 times faster than the parent sugar, methyl β-D-glucopyranoside *21*, whereas the replacement of the C2 hydroxyl group with a more electronegative group such as chlorine (*22* in Fig. 3.5) reduces the rate of hydrolysis by a factor of *35* [14] compared to the parent sugar (Table 3.3). The replacement of the C2 hydroxyl group with amino group, which under reaction conditions becomes positively charged, dramatically reduces the rate of hydrolysis of the glycosidic bond (see Table 3.3). From these kinetic studies, it can be concluded that the more electron-attracting group is attached to the C2 carbon, and the slower the hydrolysis of glycosidic bond, thus supporting the hypothesis that the hydrolysis

Fig. 3.5

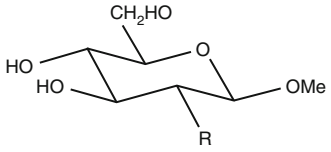

20, R=H, methyl 2-deoxy-β-D-*arabino*-hexopyranoside
21, R=OH, methyl β–D-glucopyranoside
22, R=Cl, methyl 2-chloro-2-deoxy-β-D-glucopyranoside
23, R=BH_2, methyl 2-amino-2-deoxy-β-D-glucopyranoside

Table 3.3 Rates of hydrolysis in molar acid concentration at 72.9° for the series of methyl 2-(X-substituted) glucopyranosides for various X substituents [15]

X	Anomer	Acid concentration	t °C	Rate of hydrolysis k, (s^{-1})	References
–H	α	0.10N HCl	49.7	2.4×10^{-2}	[16]
	β	0.10N HCl	49.7	3.5×10^{-2}	[16]
–OH	α	2.0N HCl	71.7	2.5×10^{-5}	[17]
	β	2.0N HCl	71.1	5.0×10^{-5}	[17]
$-NHOCCH_3$	α	pH 0.75	78.2	5.1×10^{-6}	[15]
$-NHCOCH_3$	β	1.0 N HCl	78.2	4.6×10^{3}	[15]
–Cl	β	2.0N HCl	60	3.56×10^{-7}	[14]
$-NH_3^+$	β	1.0N HCl	100	7.6×10^{-8}	[18, 19]

of glycopyranosides proceeds via oxocarbenium ion and that its formation is the rate-determining step.

The influence of the C5 substituent on the rate of glycoside hydrolysis was studied by comparing the rate of hydrolysis of methyl α-D-xylopyranoside *24* (Fig. 3.6) with that of methyl 6-deoxy-α-D-glucopyranoside *25*, methyl α-D-glucopyranoside *26* (the C5 substituent is hydroxymethyl group), methyl 6-O-methyl-α-D-glucopyranoside *27* (the C5 substituent is methoxymethyl group), methyl α-D-glucopyranosiduronic acid *28* (the C5 substituent is the carboxyl group), methyl 6-chloro-6-deoxy-α-D-glucopyranoside *29* (the C5 substituent is chloromethyl group), methyl 6-deoxy-6-iodo-α-D-glucopyranoside *30* (the C5 substituent is the iodomethyl group), and 6-amino-6-deoxy-α-D-glucopyranoside *31* (the C5 substituent is the aminomethyl group) (Fig. 3.6).

The hydrolysis of alkyl glucuronopyranosides in moderately concentrated acids has been found to proceed at a lower rate than the corresponding parent glycosides. This was attributed to the inductive effect of the electron-attracting carboxyl group (Table 3.4). Support for this explanation comes from the observation that methyl 6-amino-6-deoxy-α-D-glycopyranoside is hydrolyzed more slowly than methyl α-D-glycopyranosiduronide. As one can see, the methyl group at C5 does not introduce any significant change to rate coefficient; the C5 hydroxymethyl group, methoxymethyl group, as well as carboxyl group introduce a fivefold decrease in the rate coefficient; chloromethyl and iodomethyl introduce another sixfold decrease in reaction rate; and finally,

Fig. 3.6

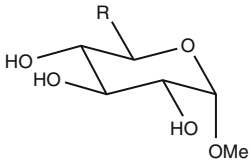

24, R=H, methyl α-D-xylopyranoside
25, R=CH_3, methyl 6-deoxy-α-D-glucopyranoside
26, R=CH_2OH, methyl α-D-glucopyranoside
27, CH_2OCH_3, methyl 6-*O*-methyl-α-D-glucopyranoside
28, R=COOH, methyl α-D-glucuronic acid
29, R=CH_2Cl, methyl 6-chloro-6-deoxy-α-D-glucopyranoside
30, CH_2I, methyl 6-deoxy-6-iodo-α-D-glucopyranoside
31, R=CH_2NH_2, methyl 6-amino-6-deoxy-α-D-glucopyranoside

Table 3.4 Rate coefficients for the hydrolysis in 0.5M sulfuric acid of methyl α-D-xylopyranosides and its homologs with different substituents at C5 [9, 20]

	$k \times 10^{-6}\ s^{-1}$		
R	60 °C	70 °C	80 °C
H	3.06	13.9	57.9
CH_3	3.22	14.4	61.8
CH_2OH	0.637	2.85	12.6
CH_2OMe	0.449	1.90	8.52
COOH	0.572	1.93	7.41
CH_2Cl	0.092	0.441	1.92
CH_2I	0.099	0.445	1.82
CH_2NH_2	0.065	0.284	1.04

6-aminomethyl introduces another twofold decrease in reaction rate. Therefore, H ≈ CH_3 > CH_2OH ≈ CH_2OMe ≈ COOH > CH_2Cl ≈ CH_2I > CH_2NH_2 [20].

There is practically no difference in rate of hydrolysis when there is no C5 substituent or if the C5 substituent is a methyl group.

The removal of a hydroxyl group from various carbon atoms of a glycopyranoside has very different effects upon the rate of glycoside hydrolysis. In general, all mono-deoxy glycopyranosides are hydrolyzed faster than parent sugars, but 2-deoxy glycopyranosides are hydrolyzed much faster than any other deoxy sugar. Thus, for example, methyl 2-deoxy-α-D-*arabino*-hexopyranoside *32* is hydrolyzed over 2,000 times faster than its parent sugar methyl α-D-glucopyranoside; methyl 3-deoxy-α-D-*ribo*-hexopyranoside *33* and methyl 3-deoxy-α-D-arabino-hexopyranoside *34* are hydrolyzed only 5 and 7 times faster, respectively, whereas methyl 4-deoxy-α-D-*xylo*-hexopyranoside *35* is hydrolyzed 40 times faster (Fig. 3.7 and Table 3.5).

Alkylation of hydroxyl group of a glycopyranoside, in general, reduces the rate of hydrolysis of the respective glycopyranoside. Although not very significant, the methylation of the C6 hydroxyl group has the largest influence on the rate of

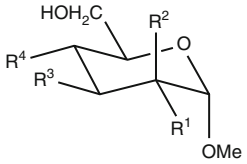

32, R^1=R^2=H; R^3=R^4=OH, methyl 2-decoxy-α-D-*arabino*-hexopyranoside
33, R^1=R^4=OH; R^2=R^3=H; methyl 3-decoxy-α-D-*ribo*-hexopyranoside
34, R^1=R^3=H; R^2=R^4=OH; methyl 3-decoxy-α-D-*arabino*-hexopyranoside
35, R^1=R^3=OH; R^2=R^4=H; methyl 4-decoxy-α-D-*xylo*-hexopyranoside

Fig. 3.7

Table 3.5 Relative rates of hydrolysis k/k_0^* of methyl deoxy-α-D-pyranosides relative to that of the parent sugar (see Fig. 3.7) (k_0 is the rate constant for the hydrolysis of parent glycoside under the same conditions)

Sugar	k/k_0	Conditions	References
2-deoxy-(*32*)	2,090	2.0 N HCl, 58°	[9]
3-deoxy-(*33*)	20	2.0N HCl, 58°	[9]
	7	1N H_2SO_4, 100°	[21]
3-deoxy-(*34*)	5	1N H_2SO_4, 100°	[21]
4-deoxy-(*35*)	40	2N H_2SO_4, 58°	[9]

hydrolysis of glycosidic bond (the 6-*O*-methyl ether is hydrolyzed at almost half the rate of the unsubstituted parent sugar ($k/k_0 = 0.6$)); monomethyl ethers at the C2, C3, and C4 carbons of methyl β-D-glucopyranoside are hydrolyzed at 0.86, 0.99, and 0.83 of the rate of the unsubstituted methyl-β-D-glucopyranoside.

Methylation of all hydroxyl groups of a hexopyranoside has a much greater effect on the rate of glycoside hydrolysis. Thus, methyl 2,3,4,6-tetra-*O*-methyl-α-D-glucopyranoside is hydrolyzed more than 6 times slower than the unsubstituted sugar, whereas the β-anomer is hydrolyzed only 3 times slower. Methyl 2,3,4,6-tetra-*O*-methyl-α-D-mannopyranoside is hydrolyzed ca. 2.5 times slower than the parent sugar, whereas the methyl 2,3,4,6-tetra-*O*-methyl-α-D-galactopyranoside is hydrolyzed almost six times slower than the parent sugar. In general, tetramethylated glycopyranosides are hydrolyzed significantly slower than monomethyl ethers (Table 3.6).

All kinetic studies have thus far strongly supported the hypothesis that the acid-catalyzed hydrolysis of glycopyranosides proceeds via formation of a positively charged oxocarbenium ion and that the cleavage of the C1–O1 bond is the rate-determining step. The initial reversible protonation of one of the two acetal oxygens and the nucleophilic attack of the water molecule to the oxocarbenium ion transition state intermediate are very fast processes.

The study of the hydrolysis rate of various glycopyranoside derivatives has clearly shown that it is most sensitive to the change of electronegativity at the C2 and the C5 carbon since the C2 carbon is vicinal to the C1 carbon and the C5 carbon

Table 3.6 Rates of hydrolysis in 0.5M sulfuric acid, at 70° of monomethyl ethers of methyl-β-D-glucopyranoside [22]

	$k \times 10^{-6}$, s^{-1}				
Sugar	60°	70°	80°	E(kcal/mol)	$\Delta S^{\neq}$ at 60° (cal deg^{-1} mol^{-1})
2-*O*-methyl	1.19	5.22	20.8	33.4	+12.9
3-*O*-methyl	1.27	5.66	23.8	34.0	+41.9
4-*O*-methyl	1.15	4.97	21.2	33.8	+41.1
6-*O*-methyl	0.84	3.88	16.1	34.9	+16.8
Unsubstituted	1.38	–	–		

is vicinal to the O5 ring oxygen atom, the chief players in the formation of the oxocarbenium ion. Thus, the C2 electron-attracting substituent directly inhibits the formation of a positive charge on the C1 carbon, via the inductive effect (positively charged C2 carbon will prevent the formation of a positively charged C1 carbon). The C5 electron-attracting substituent reduces the rate of hydrolysis, again via the inductive effect. If the hydrolysis proceeds via a cyclic oxocarbenium ion transition state, the C5 electron-attracting substituent will reduce the ability of the ring (O5) oxygen to donate its nonbonding electron pair needed to stabilize the carbonium ion intermediate formed after the cleavage of the C1–O1 bond. If the acid-catalyzed hydrolysis of a glycopyranoside proceeds via the C1–O5 bond cleavage, the C5 electron-attracting substituent will lower the basicity of the ring oxygen and thus its ability to be protonated, which will reduce the concentration of the reactive conjugate acid that is transformed to the acyclic oxocarbenium ion transition state.

Feather and Harris published in 1965 a paper [6] suggesting that the conversion of a $^4C_1$ or $^1C_4$ glycopyranoside conformation into the ^4H (half-chair) conformation with the C5–O5–C1–C2 atoms lying in one plane (this is presumably the conformation of the oxocarbenium ion in the transition state) requires rotation about the C2–C3 and the C5–C4 bonds. Thus, they proposed that there is a correlation between the ease of rotation about these bonds and the rate of hydrolysis of glycosidic bonds. The conversion of a chair conformation ($^4C_1$ or $^1C_4$) of a glycopyranoside into a half-chair (^4H or ^1H) conformation requires the counterclockwise rotation about the C1–O5 bond (if looked along the C1–O5 bond from the direction of the C1 carbon). This rotation is accompanied by a counterclockwise rotation about the C2–C3 bond if looked along the C2–C3 bond and from the direction of the C2 carbon in which case the substituents at the C2 and the C3 carbon assume a new conformation increasing or decreasing the distance between them. The rates of hydrolysis are therefore expected to be influenced by the configurations of the C2 and C3 carbon on a pyranoside ring (Fig. 2.52). Thus, counterclockwise rotation about C2–C3 bond (if looked along the C2–C3 bond and from the direction of the C2 carbon) predicts that the acid-catalyzed hydrolysis of methyl α-D-mannopyranoside should be slower than the hydrolysis of methyl α-D-glucopyranoside, since the conversion of their $^4C_1$ conformations to the respective half-chair conformation shall bring the R^2 and R^3 substituents into closer proximity, thus increasing the Pitzer strain. However, the

Fig. 3.8

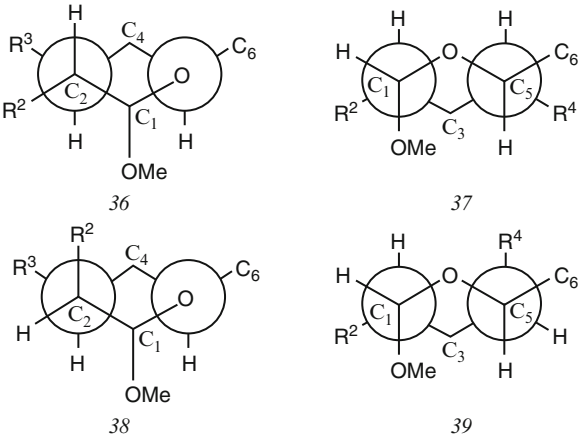

rate coefficients of acid-catalyzed hydrolysis of methyl α-D-manno- and methyl α-D-glucopyranoside (2.0N HCl, 60°; Table 2.7) are 2.09×10^{-5} and 0.78×10^{-5}, respectively, i.e., methyl α-D-mannopyranoside is hydrolyzed ca. 2.7 times more rapidly than methyl α-D-glucopyranoside [9], indicating that the stereoelectronic effects are more important than the Pitzer strain in the acid-catalyzed hydrolysis of methyl α-D-mannopyranoside (e.g., the participation of the axial C2 oxygen in the stabilization of the oxocarbenium ion).

The counterclockwise rotation about the C5–C4 bond (if looked along the C5–C4 bond from the direction of the C5 carbon) predicts that the acid-catalyzed hydrolysis of methyl α-D-galactopyranoside should be slower than that of methyl α-D-glucopyranoside. This is however again contrary to experimental findings. The acid-catalyzed hydrolysis (2.0N HCl, 60°, Table 3.2) of methyl α-D-galactopyranoside is found to be ca. 5.0 times faster than that of methyl α-D-glucopyranoside (5.13×10^5 and 0.708×10^5, Table 3.2) [23]. Furthermore, there is no correlation between the size of the C5 substituent and the rate of acid-catalyzed hydrolysis of a glycopyranoside. Thus, for example, there is a very little difference in the rate of acid-catalyzed hydrolysis of methyl α-D-xylopyranoside and methyl 6-deoxy-α-D-glucopyranoside (3.06×10^{-6} and 3.22×10^{-6}, respectively) (Table 3.4) although the difference in the size of C5 substituents is very large (hydrogen vs. methyl group). Also the rates of acid-catalyzed hydrolyses of methyl 6-chloro-6-deoxy- and 6-deoxy-6-iodo-α-D-glucopyranoside are very similar (0.092×10^{-6} and 0.099×10^{-6} respectively, Table 3.4) despite the very large difference in size of the C5 substituent ($-CH_2Cl$ vs. $-CH_2I$) (Fig. 3.8).

The above experimental results are in full agreement with the conclusions that can be drawn from studying molecular models. Namely, the conversion of a chair conformation of a hexopyranoside to the corresponding half-chair conformation requires counterclockwise rotation about the C1–O5 bond and the counterclockwise rotation about the C2–C3 bond, but not about the C5–C4 bond. The slight increase in the Pitzer strain that results from these rotations in the course of conversion of a chair to a half-chair conformation of oxocarbenium ion transition state is not

Table 3.7 Rates of hydrolysis in 0.01N HCl at 95–100° of tetra-*O*-methyl ethers of α- and β-D-hexopyranosides [10], $k \times 10^5$ min^{-1}

Sugar	$k \times 10^5$ min^{-1} ($k \times 10^5$ s^{-1})	
Methyl α-D-glucopyranoside	25	(0.42)
Methyl 2,3,4,6-tetra-*O*-methyl-α-D-glucopyranoside	4	(0.067)
Methyl β-D-glucopyranoside	30	(0.5)
Methyl 2,3,4,6-tetra-*O*-methyl-β-D-glucopyranoside	10	(0.17)
Methyl α-D-mannopyranoside	10	(0.17)
Methyl 2,3,4,6-tetra-*O*-methyl-α-D-mannopyranoside	4	(0.067)
Methyl α-D-galactopyranoside	23	(0.38)
Methyl 2,3,4,6-tetra-*O*-methyl-α-D-galactopyranoside	4	(0.067)

sufficient to significantly influence the rate of acid-catalyzed hydrolysis of a glycopyranoside.

On the other side, the electronegativity of the C2 or the C5 substituent has a profound influence on the rate of acid-catalyzed hydrolysis of glycopyranosides, as is shown in Tables 3.5, 3.6, and 3.7.

3.3 Acid-Catalyzed Hydrolysis of Glycofuranosides

Unlike numerous kinetic and mechanistic studies of acid-catalyzed hydrolysis of glycopyranosides [5, 7, 9, 12, 16, 24–30] that led to the conclusion that glycopyranosides are hydrolyzed via an A-1 mechanism (the molecularity of the reaction and the entropy of activation (positive $\Delta S^{\neq}$), dissociation of methanol, and the formation of oxocarbenium ion transition state intermediate) (*42* in Fig. 3.9), the acid-catalyzed hydrolysis of glycofuranosides has been studied much less [4, 9, 31–34].

Although there were a number of kinetic studies of the acid-catalyzed hydrolysis of sucrose (containing a ketofuranoside) [35–38] and of methyl and benzyl fructofuranoside [39], the first systematic kinetic and mechanistic study of acid-catalyzed hydrolysis of glycofuranosides was reported by Capon and Thacker [40] (see Table 3.8).

The first thing that can be seen from Table 3.8 is that the entropies of activation for the hydrolysis of all glycofuranosides studied are negative. This is in strong contrast to the positive values obtained with pyranosides [9, 12, 16, 29, 30], suggesting that glycofuranosides and glycopyranosides must react via different mechanisms.

The solvent deuterium isotope effect for the hydrolysis of methyl α-D-xylofuranoside in 1M hydrochloric acid at 25° is $k_{D_2O}/k_{H_2O} = 2.5$ is consistent with the initial rapid and reversible proton transfer to form a conjugate acid of the furanoside which could be theoretically either *43* or *44* (Fig. 3.10).

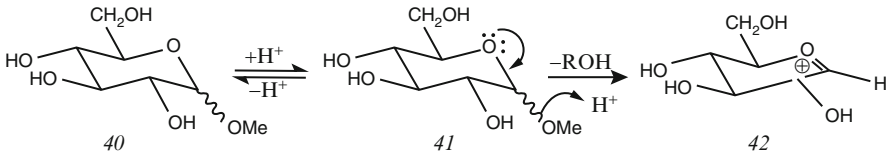

Fig. 3.9

Table 3.8 The rate coefficients and kinetic parameters for the hydrolysis of select methyl furanosides in 1M perchloric acid [40]

Methyl furanoside	t °C	$10^5 k(s^{-1})$	E_a (kcal $mol^{-1} \pm 1$)	$\Delta S^{\neq}$ (e.u. ± 2)
α-D-xylo-	25.03	39.5	20.2	−8.3
	35.04	120		
β-D-xylo-	25.01	26.3	20.3	−8.9
	35.04	79.4		
β-L-arabino-	24.92	4.46	23.1	−2.8
	35.12	16.2		
α-D-galacto-	25.03	3.35	21	−9.4
	34.91	10.8		
β-D-galacto-	25.02	0.405	22.8	−8.7
	35.12	1.43		
α-D-gluco-	24.92	59.7	19.2	−11.0
	35.12	175		
β-D-gluco-	25.00	21.0	20.5	−9.0
	34.00	64.3		

Fig. 3.10

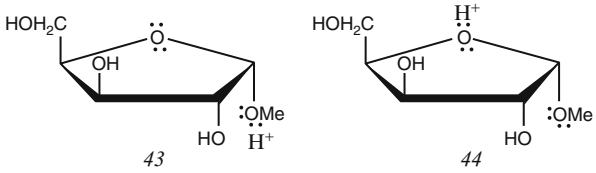

There are two possible mechanisms for the hydrolysis of glycofuranosides that are compatible with the negative entropy of activation: one that proceeds via a cyclic transition state intermediate (protonation of the glycosidic oxygen) and the other that proceeds via an acyclic transition state intermediate (protonation of the ring oxygen) (Fig. 3.10).

In the first case, the large difference in entropy of activation between the acid-catalyzed hydrolysis of glycopyranosides and glycofuranosides, as well as its negative sign, is explained by postulating that glycofuranosides are hydrolyzed via an A-2 mechanism [9] (Fig. 3.11). It is namely envisioned that the hydrolysis takes place via the protonation of the glycosidic oxygen but without the formation of a cyclic oxocarbenium ion transition state intermediate in the next step, as shown

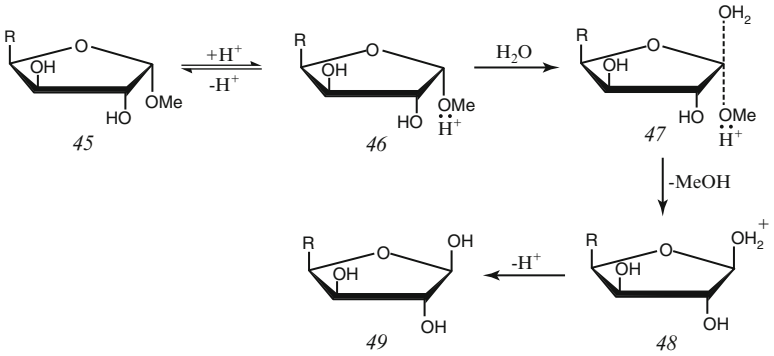

Fig. 3.11

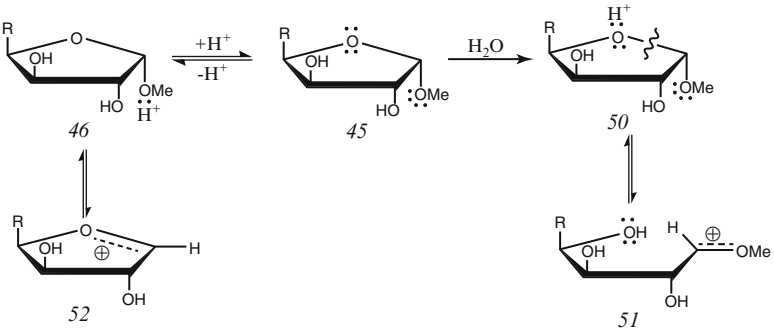

Fig. 3.12

in Fig. 3.11. Instead, the protonated methoxy group undergoes nucleophilic displacement with a water molecule, i.e., the transition state of hydrolysis resembles the transition state of an S_N2 displacement. The A-2 mechanism is supported by the Bunnett *w* values (+1.0 to +2.4) falling in the range considered to indicate a mechanism in which water acts as a nucleophile.

However, there has been proposed an alternative explanation for the observed negative entropies of activation in the acid-catalyzed hydrolysis of glycofuranosides [40]. According to this explanation, after protonation of the ring oxygen of a furanoside *45*, the C1–O4 bond ruptures and an acyclic oxocarbenium ion *51* is formed in the transition state, indicating that the conjugate acid obtained by protonation of a glycofuranoside that leads to the hydrolysis of glycosidic bond is *51* and not *52* (Fig. 3.12).

The formation of the acyclic oxocarbenium ion *51* is supported by the results obtained from the study of acid-catalyzed hydrolysis of a number of 1, 3-dioxolanes where it has been shown that the entropies of activation are also negative [41–44], although it is obvious that the hydrolysis must proceed with the ring opening.

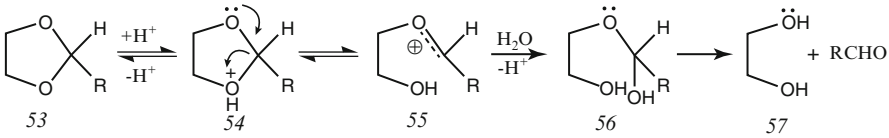

Fig. 3.13

Fig. 3.14

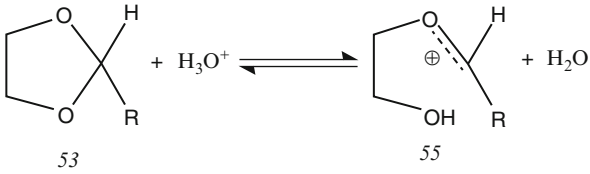

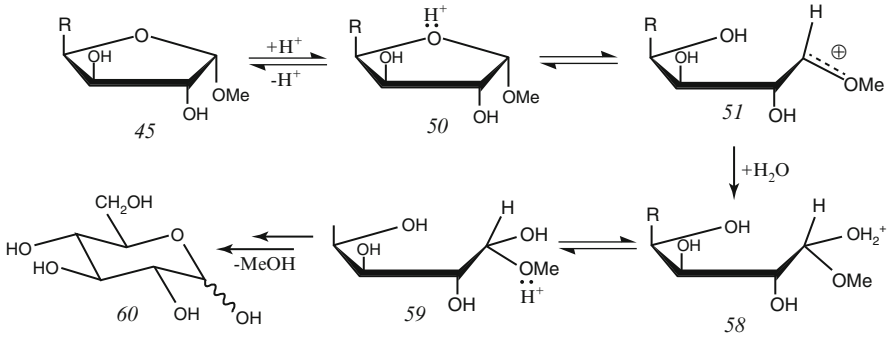

Fig. 3.15

An explanation suggested by Capon and Thacker [40] is that the initial rupture of the C–O bond of the conjugate acid *50* is reversible, since the resulting hydroxyl group in *51* is part of the same molecule as the oxocarbenium ion. Hence, the reaction could be written as described in Fig. 3.13.

The observed rate constant for the above reaction then would be given by $k_{obs} = k_2 K$, where K is the equilibrium constant for the equilibrium (Fig. 3.14).

The observed entropy of activation then would be $\Delta S^{\pm} = \Delta S^{\circ} + \Delta S_2^{\neq}$, where ΔS° is the standard entropy change for the above equilibrium. This would presumably have a positive value. The value of $\Delta S_2^{\neq}$ would be, however, strongly negative since it is the entropy of activation for a bimolecular reaction between the oxocarbenium ion *51* and the water molecule to give an oxonium ion *58* (Fig. 3.15). The overall value for $\Delta S^{\pm}$ could therefore be negative.

3.4 Some Recent Developments Regarding the Mechanism of Glycoside Hydrolysis

In 1980, van Eikeren [45] undertook a study of acid-catalyzed hydrolysis of conformationally rigid methyl acetals *61* and *62* (Fig. 3.16), arguing that the rates of anomer hydrolysis may be affected by the conformation of a glycoside.

From the composition of the equilibrium mixture obtained after the acid-catalyzed equilibration of *61* and *62* (68 ± 1 % of axial *61* and 32 ± 1 % of equatorial *62* anomer), it was calculated that the axial *α*-anomer *61α* is more stable than β-anomer *62β* by 0.45 kcal/mol which was in full agreement with the concept of the anomeric effect. On the other hand, in contrast to the results for alkyl glycosides, a comparison of the second-order rate constants showed that the axial anomer hydrolyzes 1.51 ± 0.22 times faster than the equatorial anomer, indicating that the TS energy of the transition state in the hydrolysis of *61* is lower by 0.25 kcal/mol than the TS energy of the transition state in the hydrolysis of *62*. Thus, the difference in energy between the TS of *61α* and *62β* is 0.7 kcal/mol (Fig. 3.17).

The acid-catalyzed hydrolyses of the axial and equatorial anomers *61* and *62* were studied in aqueous HCl/acetone solvent mixtures maintained at constant temperature in a water bath. The dependence of k_{obs} on acid concentration and temperature was measured because the conclusions are justified only if the anomers show similar variations in rate with changes in the catalyzing acid and temperature.

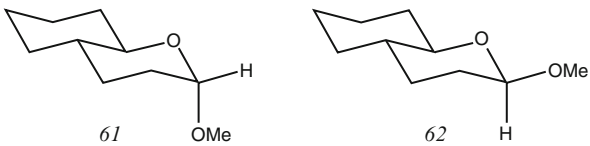

Fig. 3.16

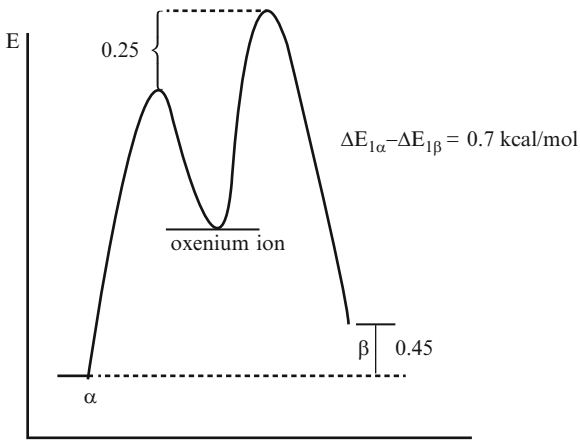

Fig. 3.17

Table 3.9 Activation parameters[a] for the hydrolysis of *61* and *62*

$[H^+]$[b], M	$\Delta H^{\neq^\circ}_{Ax}$ kcal/mol	$\Delta H^{\neq^\circ}_{Eq}$ kcal/mol	$\Delta S^{\neq^\circ}_{Ax}$ cal/mol K	$\Delta S^{\neq^\circ}_{Eq}$ cal/mol K
7.5×10^{-3}	+25.7	+24.6	+17	+13
2.5×10^{-2}	+26.1	+24.6	+21	+16

Ax axial, *Eq* equatorial

[a]Calculated from the slope and intercept of ln k_2 versus $(\text{temperature})^{-1}$; temperature range 20–55 °C

[b]Aqueous HCl/acetone mixtures (1/1 v/v)

The examination of activation parameters for the hydrolysis of *61* and *62* (Table 3.9) shows that both anomers exhibit positive enthalpies and entropies of activation as what would be expected for a dissociative mechanism. The observation that the axial anomer exhibits both a larger positive enthalpy and entropy of activation than the equatorial anomer suggests that the rate-determining transition state of the axial anomer involves more extensive C–O bond cleavage.

Thus, van Eikeren [45] concludes that the axial and equatorial anomers *61* and *62* (Fig. 3.16) must hydrolyze via different transition states and that the difference in their hydrolysis rates may be explained by postulating an early transition state for the equatorial anomer with little C–O bond breakage and a late transition state for the axial anomer with more extensive C–O bond breakage.

In order to shed some more light on the mechanism of acid-catalyzed hydrolysis of α- and β-D-glucopyranosides, Deslongchamps and Dory [46] carried out the molecular modeling study of various endocyclic and exocyclic cleavage pathways of tetrahydropyranyl acetals *59α* and *59β* (R = H in Fig. 3.18) during acid-catalyzed hydrolysis, and then they compared the reached theoretical conclusions with the experimental results obtained by using the conformationally rigid bicyclic tetrahydropyranyl acetals (R = $(CH_2)_4$ in Fig. 3.18). The reason for selecting the bicyclic conformationally rigid tetrahydropyranyl acetals for their experimental study was again to limit the effect of conformational change of a tetrahydropyranyl acetal upon the rate of its acid-catalyzed hydrolysis (see Eikeren [45]).

Deslongchamps et al. [46] have calculated the energies of the four possible transition structures *64α, 64β, 67α,* and *67β* and two intermediates *65* and *68* in the hydrolysis of the glycoside models *63α* and *63β* (Fig. 3.18).

For the hydrolysis of acetal *63α* → *66*, both the exocyclic (via *64α*) and the endocyclic (via *67α*) C–O bond cleavages take place via a chair-like transition state structure conformation with stereoelectronic assistance (Fig. 3.19) where one electron lone pair is antiperiplanar to the leaving group. Molecular modeling indicates that the free energy of transition structure *64α* for the exocyclic mechanism is 1.72 kcal/mol lower than that of the endocyclic mechanism (*67α*). In addition, an entropy effect also favors the exocyclic mechanism (formation of two molecules: the oxocarbenium ion *65* and methanol). Therefore, it can be expected that the transition structure for the exocyclic cleavage process for α-D-glycopyranosides will be highly favored, which is in agreement with published results [47–51].

For the hydrolysis of *63β* → *66*, calculation indicates that the transition structure *64β* for the exocyclic C–O bond cleavage takes place via a sofa conformation

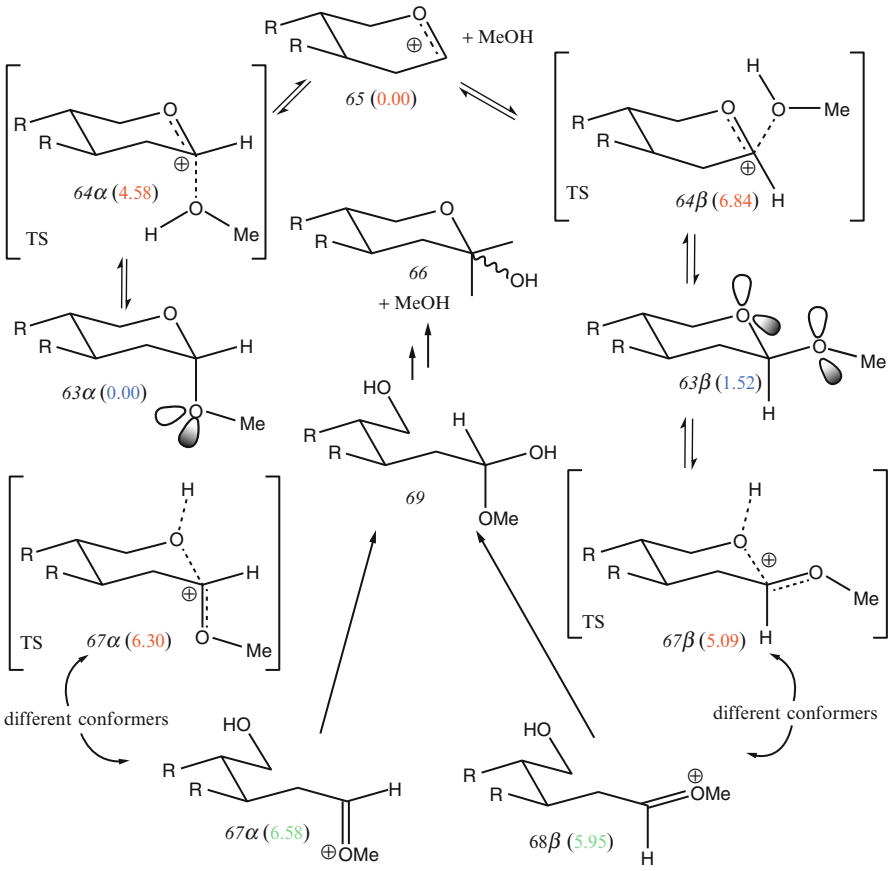

[a]Numbers in *red* are relative energies (kcal/mol) of charged species *64*, *65*, *67α* and *67β*; the numbers in *blue* are relative energies of acetals *59α* and *59β*, R=H (calculations), R=$(CH_2)_4$ (experimental). Numbers in *green* are for cations *64α* and *64β* in extended conformations (no interaction between cation and alcohol).

Fig. 3.18

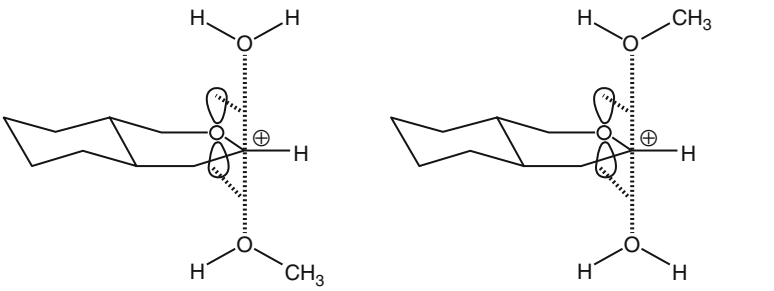

69,α-D-glucopyranoside TS (S_N2)

69, β-D-glycopyranoside TS (S_N2)

Fig. 3.19

with an endocyclic oxygen lone pair periplanar to the C–O bond (*syn* or *anti*) to be cleaved [52, 53].

For the endocyclic C–O bond cleavage, calculation shows that the transition structure geometry *67β* remains close to the chair ground-state conformation. This is the result of the participation of the exocyclic oxygen lone pair antiperiplanar to the leaving group. The enthalpy difference between the two transition state structures *64β* and *63β* is 1.75 kcal/mol, now favoring the endocyclic C–O bond cleavage. On the other hand, entropy disfavors the opening of a ring over the exocyclic C–O bond cleavage, which leads to the formation of two molecules. Since the enthalpy favors *63β* → *67β* process and the entropy favors the *63β* → *64β*, both processes are likely to take place concurrently, which is in accord with published experimental observations [54].

The results of calculations are in full agreement with the fact that the relative rate of hydrolysis of the α-anomer in a conformationally rigid model is faster than that of the β-anomer (rate ratio 3/2) [46, 55]. The transition structure *64α* for the exocyclic C–O bond cleavage has a lower energy (4.58 kcal/mol) than the β-anomer, *64β* (6.84 kcal/mol); it has also slightly lower energy than the other competing endocyclic C–O bond cleavage of the β-isomer (*67β*, 5.09 kcal/mol). The calculations also show that there is a small energy difference (0.63 kcal/mol) between the conformers *68β* and *68α* of the corresponding oxocarbenium ion *68*. The relative energy difference of these ions is increased in the corresponding transition structures *67β* and *67α*, respectively (1.21 kcal/mol favoring *67β*). During the endocyclic hydrolysis of *63β*, the hydroxy-oxocarbenium ion *68β* could undergo a rotation and recyclize via conformer *68α* to give the more stable anomer *63α*. However, experimental results show that the isomerization of the β-anomer into the α-anomer does not take place concurrently with hydrolysis [56]. This suggests that either the exocyclic cleavage via *64β* is much more favored entropically than the endocyclic cleavage via *63β* or the recyclization barrier is too high.

The experimental and theoretical studies of acid-catalyzed hydrolysis of various conformationally rigid acetal models [44–46] such as *61* and *62* (Fig. 3.16) have shown that it takes place via a late transition state.

From this study, Deslongchamps et al. [46] concluded that the α-glycosides undergo hydrolysis in their ground-state chair-like conformation via an exocyclic C–O bond cleavage while following the principle of kinetic stereoelectronic control (proper orbital alignment). β-Glycosides can be however hydrolyzed either by an exocyclic C–O bond cleavage via distorted twist-boat or sofa conformation or by an endocyclic C–O bond cleavage in the ground-state chair-like conformation. While van Eikeren [45] suggested an early transition state for the cleavage of equatorial anomer with little C–O bond breakage and a late transition state for the cleavage of axial anomer with more extensive C–O bond breakage, Deslongchamps et al. [46] suggested that both cleavages take place via late transition states and with stereoelectronic control whereby the cleavage of equatorial anomer takes place somewhat earlier. The exocyclic cleavage is favored by entropy, and the endocyclic cleavage might be disfavored because the resulting hydroxy-oxocarbenium ion (like *68β*) might undergo a fast cyclization to give back the β-glycoside rather than undergoing a reaction with water to produce the hydrolysis product. On that basis,

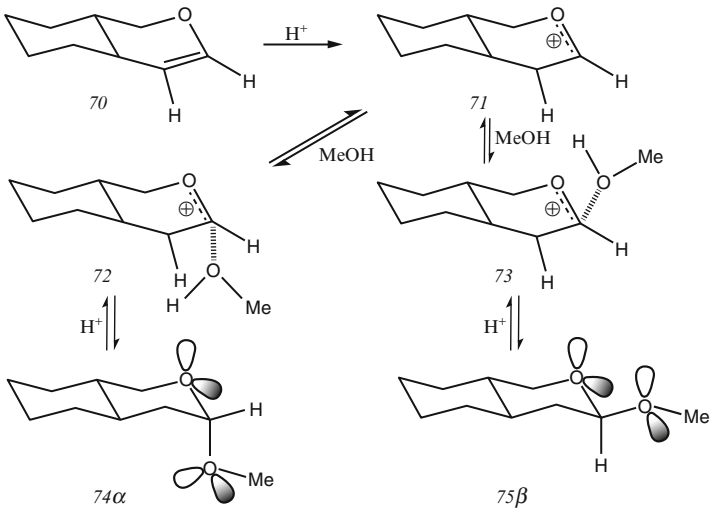

Fig. 3.20

the hydrolysis of β-glycosides can take place via both the exocyclic and endocyclic pathways [57], the choice depending upon the specific structure of the substrate and upon the reaction conditions (acid catalyzed or enzymatic [58]).

In hydrolyses that are carried out in water or in solvents containing water, it is now generally accepted [59] that an oxocarbenium ion is too reactive to have a real lifetime in the presence of a nucleophile such as water [60, 61].

Consequently, a glycopyranosidic bond cleavage very likely proceeds via a transient [62] *oxocarbenium-like transition state*, with an sp^2-hybridized geometry at both the C1 and the O5 atoms, allowing thus a considerable double bond character between the O5 and the C1 atoms and forcing the C5, O5, C1, and C2 atoms to assume a coplanar conformation. Hence, this process does not involve a discrete carbocation in a first-order reaction but is borderline S_N1–S_N2 reaction. In other words, the C1–OMe bond breaking is taking place simultaneously with the C1–OH_2 bond making (S_N2-like) (Fig. 3.19).

In the late transition state, both α- and β-D-glycopyranosides have essentially the same oxocarbenium ion with a CH_3OH group at a long distance ($\geq$1.80 Å). In this way, the CH_3OH in α- or β-transition state will have small steric interactions with the oxocarbenium ion. As a result, it is not surprising that ΔE between TSα and TSβ is only about 0.7 kcal/mol (see Fig. 3.19).

The above rationalization is confirmed experimentally by the addition of methanol in mild acid to enol ether *71* (Fig. 3.20). Under these kinetically controlled conditions, a mixture of *74α* and *75β* was obtained in 76:24. This ratio corresponds to the energy difference of 0.70 kcal/mol for the transition state favoring the formation of *72α* which is in complete agreement with the AM1 [46] and 6.31G [47] calculation. This value is in agreement with that found by van Eikeren [45]. In addition, these calculations also show that the transition states are definitely late transition states and resemble the geometry of the oxocarbenium ion.

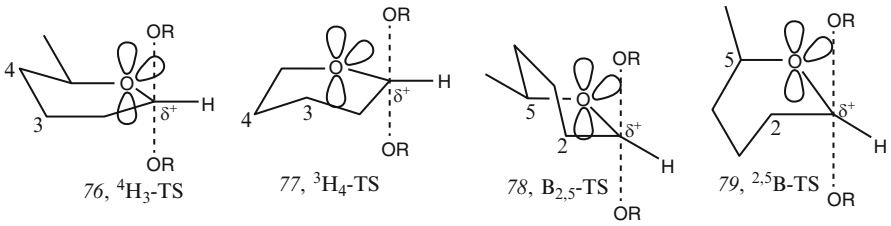

Fig. 3.21

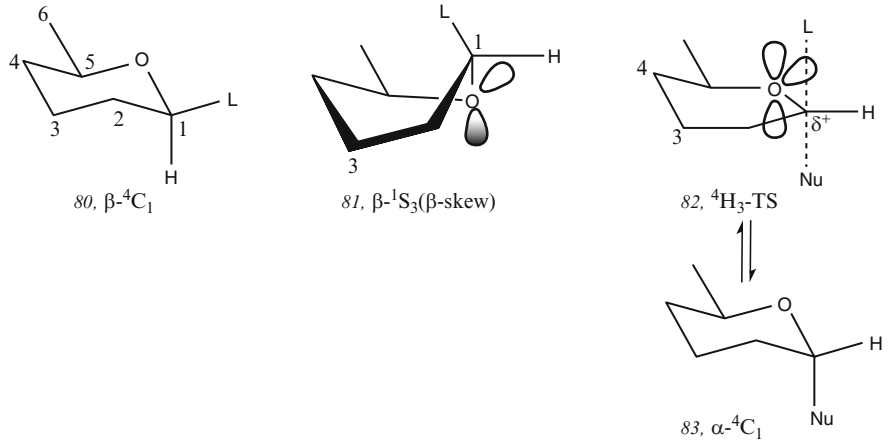

Fig. 3.22

The primary ^{13}C [63, 64], as well as secondary α-deuterium [65] isotope effects, were consistent with this S_N2-type itinerary. The conformation of oxocarbenium ion requires the coplanarity of the C5, O5, C1, and C2 atoms of pyranoside ring, and there are four possible conformations of transition state structure in which the C5, O5, C1, and C2 will be coplanar (Fig. 3.21): the $^4H_3$ (*76*), the $^3H_4$ (*77*), the $B_{2,5}$ (*78*), and the ^{2,5}B (*79*) conformer. The route from reactant to the product via transition state TS is called the substitution pathway.

By examining these TS geometries, Nerinckx et al. [59] have recently suggested an explanation as to why there is such a small difference in energy between these transition states and also as to why the rates of acid-catalyzed hydrolysis of α- and β-D-glycopyranosides are so close.

According to antiperiplanar lone pair hypothesis (ALPH) pathway, the substitution of β-equatorial glycopyranosides is preceded by a conformational change from ground-state chair to a skew conformation in which the leaving group is in the axial orientation and in antiperiplanar orientation with regard to the *trans*-lone electron pair of the ring oxygen. This sp^3 lone electron pair will hybridize at the TS into 2pz orbital and thus allow the formation of the partial double bond toward the anomeric carbon [47, 49, 66]. The reaction then proceeds through an ALPH-compliant β-skew → $^4H_3$−TS → α−$^4C_1$ pathway (Fig. 3.22).

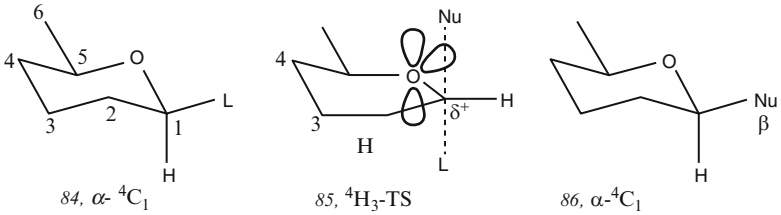

84, α- $^4C_1$ *85*, $^4H_3$-TS *86*, α-$^4C_1$

Fig. 3.23

Fig. 3.24

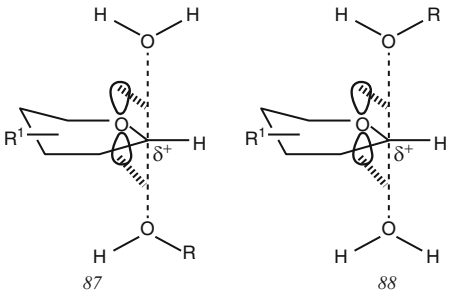

87 *88*

In the case of α-axial D-glycopyranosidic bond substitutions, the leaving group already has an ALPH-compliant orientation when the carbohydrate ring is in the ground-state chair conformation. Thus, the α-glycosides must hydrolyze via their ground-state conformation, as explicitly stated by Deslongchamps [47] (Fig. 3.23).

Thus, the energies of transition state intermediates for the hydrolysis of α- and β-D-glycopyranosides *80* and *81* must be very close, as shown in Fig. 3.24.

It was established that both transition states are late and have essentially the same oxocarbenium ion in which the MeOH is at the long distance from the C1 carbon (≥1.80 Å). What happens is while the MeOH is leaving, the H_2O is entering (S_N2-like reaction). But one should realize that TS energy is lowered by the fact that at TS, there is a p-orbital on O5 that assists this S_N2 reaction. Thus, the anomeric effect still plays the same key role. In that case, the competing TS resemble *87* and *88* (Fig. 3.24) which again have to have very close energy.

3.5 Acetolysis of Glycosides

The cleavage of a glycosidic bond by acetolysis is an alternative method to hydrolysis. Although both methods are acid-catalyzed, and presumably in the case of glycopyranosides involve the formation of a cyclic oxocarbenium transition state, they also have their differences. Thus, for example, the most important difference is that the hydrolysis is always performed either in aqueous solutions or in a solvent containing water, whereas the acetolysis is performed in nonaqueous

solvents, typically acetic anhydride. In the case of acid-catalyzed hydrolysis, the activation of glycosidic bond is effected by protonation of one of the two acetal oxygens (glycosidic or the ring oxygen), whereas in acetolysis, the attacking species is not (H^+) but most likely the acetylium ion (Ac^+) [67–70]. Acetolysis can also be catalyzed by Lewis acids, such as ferric chloride ($FeCl_3$) [71, 72].

A review on acetolysis has been published by Guthrie and McCarthy [73].

The study of the mechanism of acid-catalyzed hydrolysis of glycosidic bonds failed to answer two very important questions: first, why are the β-anomers of D-glycopyranosides (having the glycosidic oxygen equatorially oriented) hydrolyzed ca. 2–3 times more rapidly than α-anomers (having the glycosidic oxygen oriented axially) irrespective of the glycopyranoside structure, and second, why do the configurations of hydroxyl groups of the pyranoid ring (e.g., D-gluco-, D-galacto-) have very little or no influence upon the rates of hydrolysis of their glycosidic bonds. The postulated mechanism also contradicts the importance of relative basicities of ring and glycosidic oxygen in a glycopyranoside upon the rate of hydrolysis of the corresponding glycoside and thus challenges the well-documented concept of the anomeric effect. The one explanation for this "anomaly" could be that perhaps the electronic effects that do exist in all glycopyranoside structures are significantly "neutralized" in aqueous solution, or in solvents containing water, due to hydrogen bonding between the sugar polar groups (hydroxyl groups and ring oxygen) and water molecules. This assumption is supported by the fact that the magnitude of the anomeric effect is solvent dependent [74–78]. Another possible explanation could be that the energies of transition states for the hydrolysis of both anomers are close but the ground-state energies are different due to the anomeric effect whereby the α-anomer is more stable than the β-anomer. Since both transition states are late, the β-anomer should reach the transition state easier and thus sooner than α-anomer, because its ground-state energy is higher than ground-state energy of the α-anomer (the α-anomer being more stable will reach the transition state slightly later than β-anomer).

The observed behavior of glycosidic bonds toward acid-catalyzed hydrolysis is contrary to what one would expect from the existence of the anomeric effect and ALPH. Namely, it is known that due to the anomeric effect, the axially oriented oxygen should have a higher basicity than the equatorial one, due to the mixing of the axially oriented nonbonding electron pair of the ring oxygen with the antibonding orbital of the C1–O1 bond. Consequently, the concentration of conjugate acid resulting from protonation of the glycosidic oxygen should be higher in solutions of glycopyranosides having the glycosidic oxygen axially oriented (α-D-anomers) than in solutions of glycopyranosides having the glycosidic oxygen equatorially oriented (β-D-anomers). As a result, α-D-glycopyranosides should be hydrolyzed more rapidly than β-D-glycopyranosides, which is opposite to what is observed.

The mechanism of acid-catalyzed cleavage of glycosidic bonds could be perhaps better understood by studying the mechanism of acetolysis, since the acetolysis is performed in the absence of water (most often in acetic anhydride), and thus, the electronic effects that exist in each glycopyranoside structure will not be

Fig. 3.25

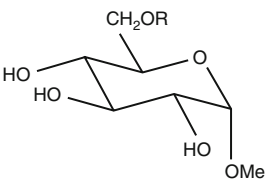

89, R=H
90, R=Ts

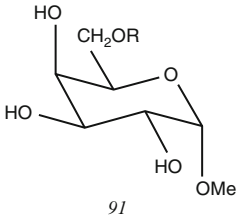

91

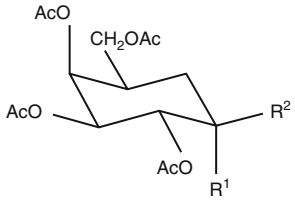

92, R^1=OAc; R^2=H
93, R^1=H; R^2=OAc

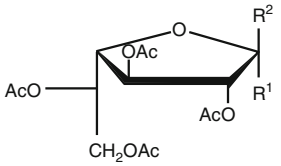

94, R^1=OAc; R^2=H
95, R^1=H; R^2=OAc

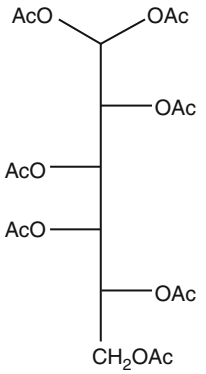

96

Fig. 3.26

"neutralized" by the solvent, and their influence upon the reactivity of glycosidic bond could be hopefully evaluated.

Dasgupta et al. [72] have studied the acetolysis of methyl α-D-glucopyranoside *89*, methyl 6-*O*-p-toluenesulfonyl-α-D-glucopyranoside *90*, and methyl α-D-galactopyranoside *91* in acetic anhydride at 60 °C using ferric chloride as a catalyst (Fig. 3.25). Methyl α-D-glucopyranoside *89* gave only two products, α- and β-penta-*O*-acetyl-D-glycopyranoses, whereas the acetolysis of methyl α-D-galactopyranoside *91* gave, under the same reaction conditons, gave five products, of which the two major products were α- and β-penta-*O*-acetyl-D-galactopyranoses (*92* and *93*), the next two products were α- and β-D-galactofuranose pentaacetates (*94* and *95*), and the last product was the acyclic hepta-*O*-acetyl-aldehydo-D-galactose (*96*) (Fig. 3.26). Furthermore, they observed that the acetolysis of methyl 6-*O*-p-toluenesulfonyl-α-D-glucopyranoside *90* was, under the same reaction conditions, ca. 4 times slower than the acetolysis of *89*. The authors suggested two reaction mechanisms: one proceeding via the formation of a cyclic oxocarbenium ion (the initial attack of the acetylium ion taking place at the glycosidic oxygen) and the other via the formation of an acyclic oxocarbenium ion (the initial attack of the acetylium ion taking place at the ring oxygen). Both of these pathways are actually unsubstantiated.

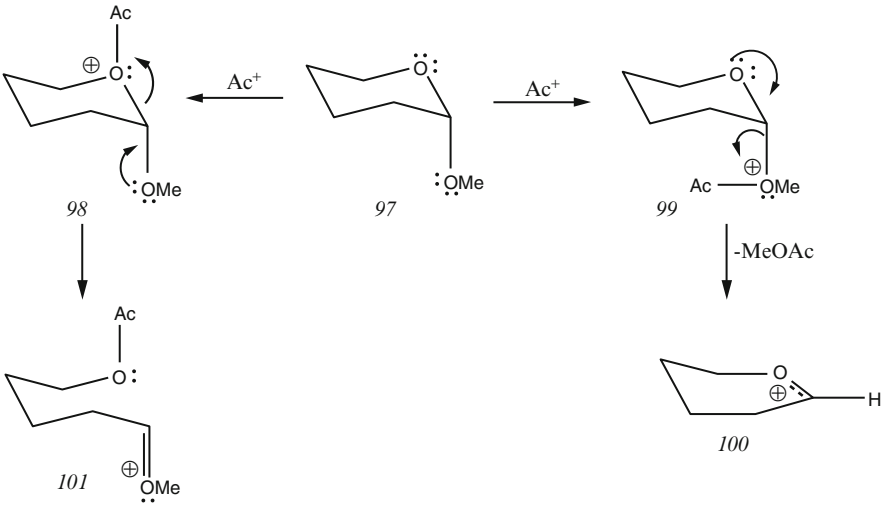

Fig. 3.27

With a slightly modified experimental procedure, McPhail et al. [79] repeated the study of Dasgupta et al. [72] on the acetolysis of methyl α- and β-D-glucopyranosides. The discussion of reaction mechanism of acetolysis based on their experiments is described in Fig. 3.27.

The site of anomeric activation in glycoside cleavage has been a subject of a long-standing controversy [80–85]. Early experiments were supporting the view that the activation occurs at the glycosidic oxygen (*99*), leading to the formation of cyclic oxocarbenium ion *100* rather than at the ring oxygen (*98*) giving the acyclic counterpart *101* (Fig. 3.27).

The question of activation site is directly related to the question of relative basicities of glycosidic and the ring oxygen, which is, in turn, related to the anomeric effect [49, 86]. MO rationalization of the anomeric effect invokes the donation of axially oriented nonbonding pair of ring oxygen to the antibonding orbital of the C1–O1 bond (n→σ* donation) (antiperiplanar orientation of these two entities), thus making the glycosidic oxygen more basic than the ring oxygen and hence the preferred site for the attack of an electrophile (Ac^+) [87]. An *ab initio* study of dimethoxymethane has provided support for this postulate by determining the proton affinities for oxygens in a *gauche* and in an *anti*-orientation of methyl group and one oxygen, as shown in Fig. 3.28. As indicated by broken lines, these rotamers correspond to axial and equatorial glycosides, respectively, and as observed by Lemieux [88], the nσ* donations in *102* are in competition. Accordingly, Praly and Lemieux [89] found that for β-D-glycosides (*103*) the exo-anomeric effect was stronger than in α-D-glycosides. In view of these differences in oxygen basicities, a β-D-glycoside might be expected to be activated on the ring oxygen and react via the formation of an acyclic oxocarbenium ion *105*, whereas an α-D-glycoside would be expected to be activated at both oxygens (glycosidic and the

Fig. 3.28

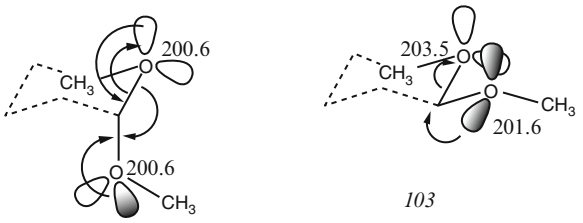

102 *103*

arrows indicate $n\sigma^8$ interstions

numbers represent calculated proton affinities (in kcal/mol)

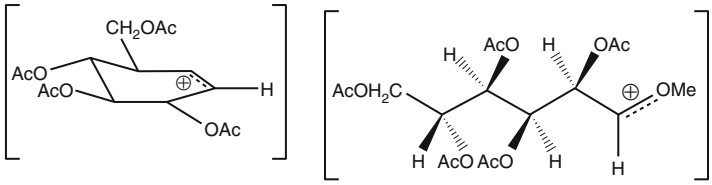

104 *105*

Fig. 3.29

ring oxygen) and consequently react by formation of either a cyclic *104* or an acyclic oxocarbenium ion *105* (Fig. 3.29).

Their conclusion is that α- and β-D-glucopyranosides react through different mechanisms. From the fact that the ratio of the α- and β-D-glucopyranosyl acetates is 4:1 in both cases, they concluded that the cyclic oxocarbenium ion is produced from both anomers that is trapped by acetate anion. The acyclic oxocarbenium ion is responsible for the formation of both acyclic heptaacetate and the penta-*O*-acetyl furanose derivatives.

In their study of acetolysis of methyl α-D-glucopyranoside using modified acetolysis medium (acetic anhydride, ferric chloride, and a small amount of concentrated sulfuric acid), McPhail et al. [79] found (by using gas chromatography and ^{1}NMR spectroscopy) that peracetylated α- and β-D-glucopyranoses were obtained in 73 % and 18 % yield, the mixture of α- and β-D-glucofuranose pentaacetates was obtained in 8 % yield, and the acyclic D-glucose heptaacetate was obtained only in traces. For the β-D-glucopyranoside, the same four products were obtained but in different amounts: peracetylated α- and β-D-glucopyranoses were obtained in 19 % and 5 % yield, the mixture of α- and β-D-glucofuranose pentaacetates was obtained in 48 % yield, and the acyclic D-glucose heptaacetate was obtained in 23 % yield.

From this, they concluded that contrary to what might be expected on the sole consideration of oxygen basicities, it is the β-anomer, and not the α-anomer, that gives rise to both cyclic and acyclic oxocarbenium ions and therefore, there are

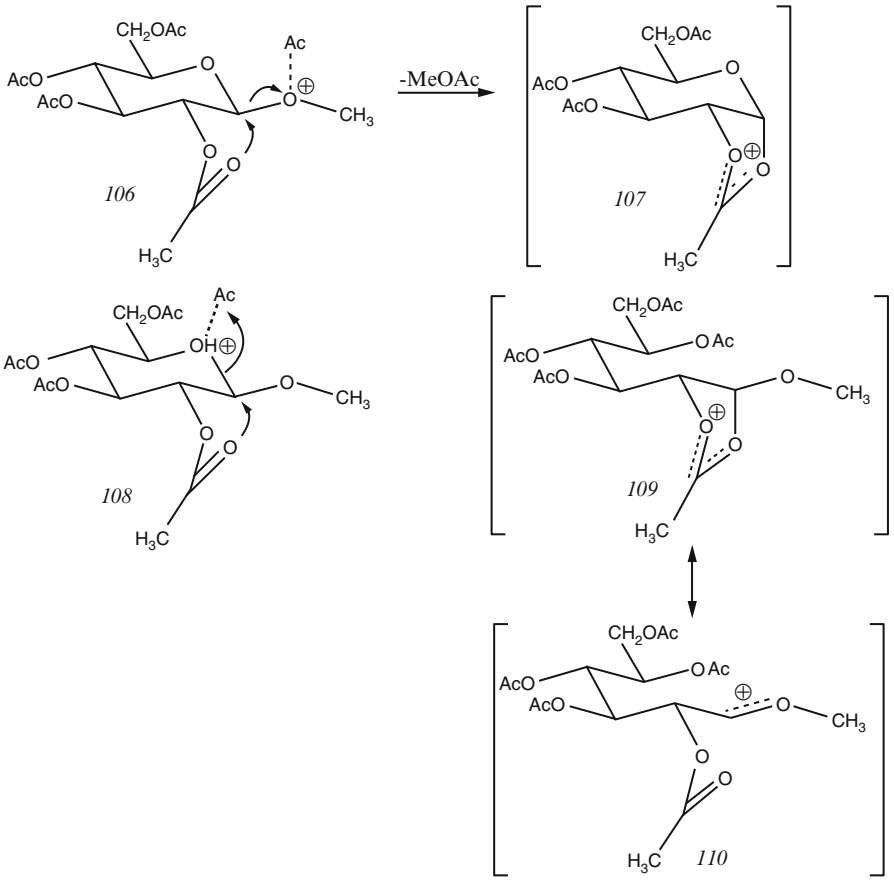

Fig. 3.30

factors other than basicities of two acetal oxygens in glycosides that determine the course of glycosidic bond cleavage.

The major objection to these studies is the choice of methyl α- and β-D-glucopyranosides as substrates because the acetylation of free hydroxyl groups is faster than acetolysis, and hence, their model compounds were actually the peracetylated or partially acetylated methyl α- and β-D-glucopyranosides. The presence of acetate at the C2 carbon will enormously complicate the acetolysis reaction pathway since the acetate is known to be an excellent participating group capable of altering the reaction pathway of activated glycosides as shown in Fig. 3.30. Thus, the formation of both cyclic and acyclic oxocarbenium ion by the activation of β-glycoside via the attack of acetylium ion either to the ring or to the glycosidic oxygen will most likely be assisted by the C2 equatorial acetate via neighboring group participation. Trans-diaxial orientation of acetylium-activated

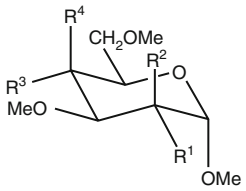

111, $R^1=R^3=OMe$; $R^2=R^4=H$
113, $R^1=R^4=OMe$; $R^2=R^3=H$
115, $R^1=R^4=H$; $R^2=R^3=OMe$

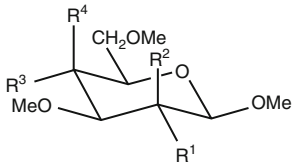

112, $R^1=R^3=OMe$; $R^2=R^4=H$
114, $R^1=R^4=OMe$; $R^2=R^3=H$
116, $R^1=R^4=H$; $R^2=R^3=OMe$

Fig. 3.31

ring oxygen and the carbonyl oxygen of C2 acetate would favor the opening of the pyranoside ring with the formation of *109* over the displacement of acetylium-activated equatorially oriented glycosidic oxygen by the C2 acetate (*106* → *107*). Therefore, it can be expected that the β-glucopyranoside would prefer a pathway that would involve the formation of acyclic oxocarbenium ion transition state.

In the case of α-D-glucopyranoside, the displacement of acetylium-activated ring oxygen or the acetylium-activated glycosidic oxygen by C2 acetate via neighboring group participation is not possible due to stereochemical reasons. So the only role of the C2 acetate in the acetolysis of α-D-glucopyranosides would be to stabilize the cyclic oxocarbenium ion.

The results reported in this study are consistent with this interpretation: the predominant products of acetolysis of methyl α-D-glucopyranoside is a 4:1 mixture of penta-*O*-acetyl-α- and β-D-glucopyranoses (91 %) with only 8 % of penta-*O*-acetyl-D-glucofuranose and traces of acyclic heptaacetate. The acetolysis of methyl β-D-glucopyranoside gave a 4:1 mixture of penta-*O*-acetyl-α- and β-D-glucopyranoses in only 24 %, whereas the penta-*O*-acetyl-D-glucofuranose and the acyclic heptaacetate were obtained in 48 % and 23 %, respectively. The 4:1 ratio of penta-*O*-acetyl-α- and β-D-glucopyranose obtained by acetolysis of both methyl α- and β-D-glycopyranoside is due to the anomerization of the reaction mixture after the acetolysis since, the authors modified the $FeCl_3$–Ac_2O original reagent of Dasgupta [72] by adding a small amount of sulfuric acid to speed up the reaction.

In 1983, Miljkovic et al. [90, 91] studied the acetolysis of permethylated methyl α- and β-D-gluco-(*111* and *112*), methyl α- and β-D-galacto-(*113* and *114*), and methyl α- and β-D-mannopyranosides (*115* and *116*) (Fig. 3.31) in acetic anhydride solution at 75 °C containing 3.33 % of methanesulfonic acid. Since the C2 substituent in these glycopyranosides was a nonparticipating methoxy group, the acetolyses of permethylated methyl glycopyranosides of glucose, galactose, and mannose were very clean reactions, giving, in addition to the starting material, a mixture of α- and β-1-acetates as the only products. In all kinetic measurements, the progress of acetolysis was monitored by a change of relative concentration of

Table 3.10 Kinetic data for acetolysis of permethylated methyl glycopyranosides of D-glucose, D-galactose, and D-mannose (*111–116*) with acetic anhydride-methanesulfonic acid (30:1 v/v) at 75 °C

Sugar	$10^3 k_1$, s^{-1}	$10^3 \times$ standard deviation	α/β ratio of 1-acetates
α-D-gluco	1.87	0.0734	3.17
β-D-gluco	0.12	0.00462	3.36
α-D-galacto	37.10	1.43	2.97
β-D-galacto	0.84	0.0709	3.22
α-D-manno	1.08	0.0456	Only α-acetate
β-D-manno	3.06	0.0631	Only α-acetate

starting material, using HPLC and C18 column. The kinetic data are presented in Table 3.10.

From Table 3.10, it can be seen that the α-anomers of permethylated methyl D-gluco- and D-galactopyranosides are acetolyzed considerably faster than the corresponding β-anomers (15.58 and 44.17 times, respectively) which is in contradiction with the results obtained for the acid-catalyzed hydrolysis of these two compounds where β-anomers are hydrolyzed ca. 1.9 times more rapidly than the α-anomer. The second observation is that permethylated methyl α- and β-D-galactopyranosides *113* and *114* are acetolyzed much faster than permethylated methyl α- and β-D-glucopyranosides *111* and *112* ($\alpha - \text{gal}/\alpha - \text{glc} \approx 20$ and $\beta - \text{gal}/\beta - \text{glc} \approx 7$). The permethylated methyl β-D-mannopyranoside *116* is, however, acetolyzed 2.83 times faster than the α-anomer *115* (Fig. 3.31). It is reasonable to assume that stereoelectronic interactions that are characteristic for a given alkyl- or aryl glycopyranoside structure must play an important role in determining the overall chemical behavior of its glycosidic bond. In protic and polar solvents (e.g., in water), these electronic interactions must be "neutralized" by intermolecular interactions with solvent dipoles (solvation), whereas in aprotic solvents, particularly those having a relatively low dielectric constant (e.g., acetic anhydride $\varepsilon = 20.7$, as opposed to water $\varepsilon = 84.2$), the intramolecular electronic interactions must be fully operative and could be expected to influence the chemical behavior of the anomeric carbon of a glycopyranoside. The basicity of the glycosidic oxygen, which is directly related to the anomeric effect, in nonpolar solvents with low dielectric constant can be expected to be higher than in polar protic solvents [91–93], and consequently, the difference in relative basicities between the ring and glycosidic oxygen could be expected to be considerably larger. Thus, the attack of acetylium cation could be expected to occur at the glycosidic rather than at the ring oxygen of a glycopyranoside. This activation will be then followed by formation of the oxocarbenium ion that will, in the presence of acetate anion, give a mixture of α- and β-1-acetates. Due to the presence of methanesulfonic acid in acetolyzing solution, the anomerization of 1-acetates will take place until the equilibrium is reached (α : β ratio ≈ 3 : 1, except for the mannose). This rationale is supported by findings that an acetic anhydride solution of D-glucose pentaacetate contains, after equilibration with sulfuric acid, approximately 87 % of the α-anomer

Fig. 3.32

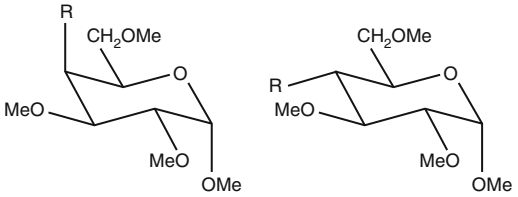

106, R=OMe
110, R=AcO
111, R=NHAc

105, R=OMe
112, R=AcO
113, R=NHAc

Table 3.11 Kinetic data for the acetolysis of methyl 4-*O*-methyl, 4-*O*-acetyl-, and 4-acetamido-4-deoxy derivatives of methyl 2,3,6-tri-*O*-methyl-α-D-galacto- (*106*, *110*, and *111*, respectively) and α-D-glucopyranosides (*105*, *112*, *113*, respectively)

Sugar	10^3k (s^{-1})
Methyl 2,3,4,6-tetra-*O*-methyl-α-D-galactopyranoside (*106*)	22.18
	25.79
Methyl 4-*O*-acetyl-2,3,6-tri-*O*-methyl-α-D-galactopyranoside (*110*)	2.44
	2.39
Methyl 4-acetamido-4-deoxy-2,3,6-tri-*O*-methyl-α-D-galactopyranoside (*111*)	0.44
	0.50
Methyl 2,3,4,6-tetra-*O*-methyl-α-D-glucopyranoside (*105*)	1.67
	1.63
Methyl 4-*O*-acetyl-2,3,6-tri-*O*-methyl-α-D-glucopyranoside (*112*)	0.63
	0.61
Methyl 4-acetamido-4-deoxy-2,3,6-tri-*O*-methyl-α-D-glucopyranoside (*113*)	0.56
	0.47

and 13 % of the β-anomer (α : β ratio ≈ 6.7), whereas in aqueous solution of D-glucose, there is 36 % of α-anomer and 64 % of β-anomer (β : α ratio ≈ 1.78). It is clear that the magnitude of anomeric effect that favors the α-anomer in the anomeric mixture is decreased in water.

The observed higher acetolysis rate of permethylated methyl β-D-mannopyranoside as compared to the α-anomer (β:α ratio 2.83) may seem to contradict the above explanation. However, there may be other reasons for such a behavior. First, it could be the much higher ground-state energy of the β-anomer as compared to α-anomer due to unfavorable electrostatic interactions of the axially orientated C2 methoxy group with the C1–OMe and C1–O5 dipoles (Δ2 effect) and due to unfavorable torsional strain between the ring, glycosidic, and C2 oxygens. Second, the nσ* orbital mixing in permethylated methyl-α-D-mannopyranoside could be expected to be less favored because this orbital mixing forces the flattening of the pyranoside ring and that will, in the case of mannopyranoside, result in increased torsional strain between the C2 and the C3 methoxy groups.

In order to understand why permethylated methyl α- and β-D-galactopyranosides acetolyzed 20 and 7 times more rapidly than the corresponding D-gluco derivatives, the rates of acetolysis of methyl 4-*O*-methyl- (*106*), 4-*O*-acetyl- (*110*), and 4-deoxy-4-acetamido-2,3,6-tri-*O*-methyl-α-D-galacto- (*111*) and the corresponding

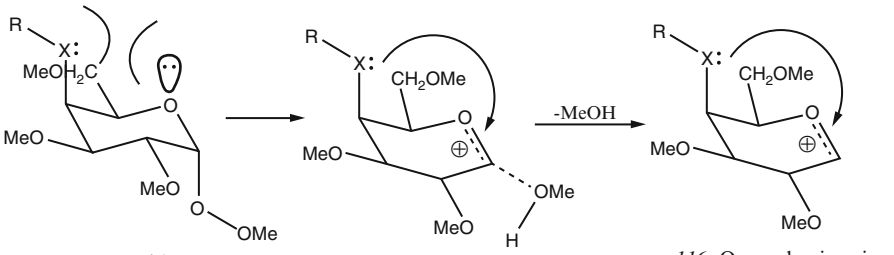

114, Pyranoside GS *115,* TS *116,* Oxocarbenium ion

Fig. 3.33

α-D-glucopyranosides (*105*, *112*, *113*) were compared (Fig. 3.32), and the results are given in Table 3.11 [91].

The data in Table 3.11 suggest that for 4-X-derivatives of methyl 4-*X*-2,3,6-tri-*O*-methyl-α-D-galactopyranoside the increase in electronegativity of the C4 substituent results in the increase of the rate of acetolysis. Thus, the 4-*O*-methyl derivative acetolyzes ca. 10 times faster than the 4-*O*-acetyl derivative, and the 4-*O*-acetyl derivative acetolyzes ca. 5 times faster than the 4-acetamido derivative. When the C4 substituent is equatorial, as is the case in the D-glucopyranoside series, the influence of change in electronegativity of the C4 substituent on acetolysis rates is much smaller. Thus, the 4-*O*-methyl derivative acetolyzes only 2.9 and 3.3 times faster than 4-*O*-acetyl- and 4-*O*-acetamido-derivatives, respectively. In the D-gluco series, the dependence of acetolysis rates upon the electronegativity of the C4 substituent can only be explained as a "through-bond" electronic interaction (inductive effect) with the ring oxygen, which is apparently rather small. However, in the D-galacto series, the very large influence of electronegativity of the axially oriented C4 substituent on the acetolysis rate cannot be ascribed to this small through-bond interaction. The only possible explanation for the unusually large kinetic effect observed in the D-galacto series is a strong through-space electron donation of the axially oriented electronegative substituent at the C4 carbon to the oxocarbenium ion under formation. This effect, which is destabilizing in the neutral galactopyranoside due to electrostatic repulsion (*114*), becomes stabilizing as the oxocarbenium ion appears (*115*, *116*) (Fig. 3.33).

The *ab initio* calculations at the 6-31G* level of theory fully supported the above conclusions [91].

Calculations were conducted on model oxocarbenium ions corresponding to D-gluco- and D-galacto series (*117–122*) (Fig. 3.34) and olefin analogs (*123–128*) stereochemically identical to oxocarbenium models of these two series. Finally, the 4-substituted 2-alkoxytetrahydropyrans (*129–134*) were used to calculate the difference in ground-state energy of 4-axially substituted and 4-equatorially substituted tetrahydropyrans. When considering only the low-energy conformers of acetals *129–134*, it was found that the compound in which the C4 methoxy group is equatorially oriented (*130*) is 0.88 kcal/mol more stable than the compound *129*

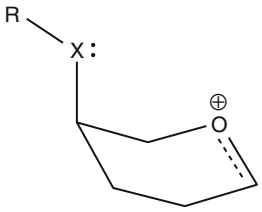

117, X=O; R=Me
119, X=O; R=Ac
121, X=NH; R=Ac

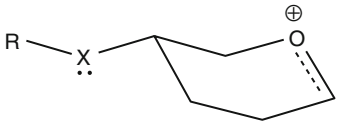

118, X=O; R=Me
120, X=O; R=Ac
122, X=NH; R=Ac

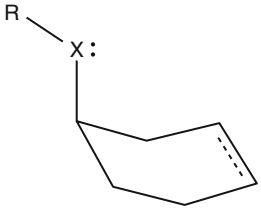

123, X=O; R=Me
125, X=O; R=Ac
127, X=NH; R=Ac

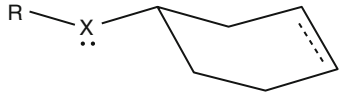

124, X=O; R=Me
126, X=O; R=Ac
128, X=NH; R=Ac

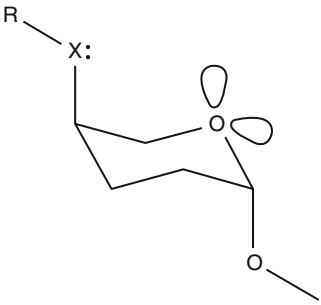

129, X=O; R=Me
131, X=O; R=Ac
133, X=NH; R=Ac

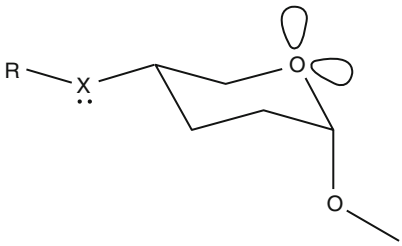

130, X=O; R=Me
132, X=O; R=Ac
134, X=NH; R=Ac

Fig. 3.34

having the C4 methoxy group axial. This trend is reversed for the C4 acetamido derivatives: axial isomer *133* is now more stable, by 0.55 kcal/mol, than the equatorial isomer *130*. The C4 acetates fall between these two extremes since the axial and equatorial acetates (*131* and *132,* respectively) are almost equally stable. These observations are in complete agreement with the idea of repulsion between an electron-rich C4 axial substituent and the axially oriented sp^3-hybridized lone pair of electrons on the ring oxygen. In the case of acetamido acetal, there exists an electronic attraction between the axially oriented sp^3-hybridized lone pair of

electrons on the ring oxygen and the axially oriented C4 acetamido nitrogen since the axial isomer is preferred. The most likely reason for this is that the nitrogen atom has a partial positive charge due to donation of its nonbonding pair of electrons to the carbonyl oxygen of the acetamido group through delocalization involving carbonyl carbon and carbonyl oxygen. While the electronic interactions are rather small in neutral acetals, they are much more significant in corresponding oxocarbenium ions which are both geometrically and energetically very similar to the acetolysis transition structures. Thus, the oxocarbenium ion having the C4 methoxy group axially oriented (*117*) was found to be 4.06 kcal/mol more stable than the oxocarbenium ion with the C4 methoxy group equatorially oriented (*118*). The same electronic interaction can be seen in the oxocarbenium ion having the C4 acetoxy group axially oriented (*119*); however, it is somewhat smaller: the axial isomer is now favored by 2.89 kcal/mol over the equatorial isomer (*120*). In the case of acetamido derivatives, this interaction seems to no longer exist. Thus, the oxocarbenium ions having the C4 acetamido group axially or equatorially oriented (*121* and *122*, respectively) have very similar energies: the axial isomer, however, is again favored but only by 0.20 kcal/mol. It is interesting that while the nitrogen atom is sp^2 hybridized in all acetamido compounds (*121*, *122*, *127*, *128*, *133*, *134*) as expected, in two rotamers around the C4–X bond of oxocarbenium ions *121* in which the C4 acetamido group is axially oriented, the nitrogen atom exhibits a high degree of sp^3 hybridization and the nitrogen lone pair of electrons points toward the oxocarbenium ion.

References

1. Shafizadeh F (1958) Formation and cleavage of the oxygen ring in sugars. Adv Carbohydr Chem 13:9–61
2. Capon B, Overend WG (1960) Constitution and physicochemical properties of carbohydrates. Adv Carbohydr Chem 15:11–51
3. BeMiller JN (1967) Acid-catalyzed hydrolysis of glycosides. Adv Carbohydr Chem 22:25–108
4. Haworth WN (1932) The constitution of some carbohydrates. Chem Ber 65A:43–65
5. Heidt LJ, Purves CB (1944) Thermal rates and activation energies for the aqueous acid hydrolysis of α- and β-methyl, phenyl and benzyl-D-glucopyranosides, α- and β-methyl and β-benzyl-D-fructopyranosides, and α-methyl-D-fructofuranoside. J Am Chem Soc 66:1385–1389
6. Feather MS, Harris JF (1965) The acid-catalyzed hydrolysis of glycopyranosides. J Org Chem 30:153–157
7. Isbell HS, Frush HL (1940) α- and β-methyl lyxosides, mannosides, gulosides and heptosides of like configuration. J Res Natl Bur Stand 24:125–151
8. Nakano J, Rånby BG (1962) Acid hydrolysis of methyl glucosides and methyl glucuronosides. Svensk Papperstid 65:29–33
9. Overend WG, Rees CW, Seqeuira JS (1962) Reactions at position 1 of carbohydrates. Part III. The acid-catalysed hydrolysis of glycosides. J Chem Soc 3429–3440
10. Haworth WN, Hirst EL (1930) The structure of carbohydrates and their optical rotatory power. Part I. General introduction. J Chem Soc 2615–2635

11. Day JNE, Ingold CK (1941) Mechanism and kinetics of carboxylic ester hydrolysis and carboxyl esterification. Trans Faraday Soc 37:686–705
12. Bunton CA, Lewis TA, Llewellyn DR, Vernon CA (1955) Mechanisms of reactions in the sugar series. Part I. The acid-catalysed hydrolysis of α- and β-methyl and α- and β-phenyl D-glucopyranosides. J Chem Soc 4419–4423
13. McIntyre D, Long FA (1954) Acid-catalyzed hydrolysis of methylal. I. Influence of strong acids and correlation with Hammett acidity function. J Am Chem Soc 76:3240–3242
14. Buncell E, Bradley PR (1967) The acid-catalyzed hydrolysis of methyl 2-chloro-2-deoxy-β-D-glucopyranoside. Can J Chem 45:515–519
15. Marshall RD (1963) Rates of acid hydrolysis of 2-substituted methyl glucopyranosides. Nature 199:998–999
16. Armour C, Bunton CA, Patai S, Selman LH, Vernon CA (1961) Mechanisms of reactions in the sugar series. Part III. The acid-catalysed hydrolysis of t-butyl β-D- glucopyranoside and other glycosides. J Chem Soc 412–416
17. Moelwyn-Hughes EA (1929) The kinetics of the hydrolysis of certain glucosides, part III.; β-methylglucoside, cellobiose, melibiose, and turanose. Trans Faraday Soc 25:503–520
18. Moggridge RCG, Neuberger A (1938) Methylglucosaminide: its structure, and the kinetics of its hydrolysis by acids. J Chem Soc 745–750
19. Foster AB, Horton D, Stacey M (1957) Amino-sugars and related compounds. Part II. Observations on the acidic hydrolysis of derivatives of 2-amino-2-deoxy-D-glucose (D-glucosamine). J Chem Soc 81–85
20. Timell TE, Enterman W, Spencer F, Soltes EJ (1965) The acid hydrolysis of glycosides. II. Effect of substituents at C-5. Can J Chem 43:2296–2305
21. Richards GN (1955) Hydrolysis of glycosides and cyclic acetal. Chem Ind (Lond) 228
22. Dee KK, Timell TE (1967) The acid hydrolysis of glycosides: III. Hydrolysis of O- methylated glucosides and disaccharides. Carbohydr Res 4:72–77
23. Kahne D, Walker S, Cheng Y, Van Engen DJ (1989) Glycosylation of unreactive substrates. J Am Chem Soc 111:6881–6882
24. Riiber CN, Sørensen NA (1938) Anomeric sugars. Kgl. Norske Videnskab. Selskabs, Skrifter 1:38pp
25. Moelwyn-Hughes EA (1928) The kinetics of the hydrolysis of certain glucosides (Salicin, arbutin and phloridzin). Trans Faraday Soc 24:309–321
26. Moelwyn-Hughes EA (1929) The kinetics of the hydrolysis of certain glucosides, part II.- Trehalose, a- methylglucoside and tetramethyl-a-methylglucoside. Trans Faraday Soc 25:81–92
27. Nath RL, Rydon HN (1954) The influence of structure on the hydrolysis of substituted phenyl β-d-glucosides by emulsin. Biochem J 57:1–10
28. Hall AN, Hollingshead S, Rydon HN (1961) The acid and alkaline hydrolysis of some substituted phenyl α-D-glucosides. J Chem Soc 4290–4295
29. Banks BEC, Meinwald Y, Rhind-Tutt AJ, Sheft I, Vernon CA (1961) Mechanism of reactions in the sugar series. Part IV. The structure of the carbonium ions formed in the acid-catalysed solvolysis of glucopyranosides. J Chem Soc 3240–3246
30. Timell TE (1964) The acid hydrolysis of glycosides: I. General conditions and the effect of the nature of the aglycone. Can J Chem 42:1456–1472
31. Augestad I, Berner E, Weigner E (1953) Chromatographic separations of anomeric glycosides. Chem Ind (Lond) 376–377
32. Augestad I, Berner E (1954) Chromatographic separation of anomeric glycosides. II. New crystalline methylfuranosides of galactose, arabinose, and xylose. Acta Chem Scand 8:251–256
33. Augestad I, Berner E (1956) Chromatographic separation of anomeric glycosides. III. Crystalline methylfuranosides of L-fucose, D-ribose, and L-rhamnose. Acta Chem Scand 10:911–916

34. Blom J (1961) Ein Beitrag zur Kenntnis der Konfiguration und der Konformation anomerer Aldosen und deren Glykoside. Acta Chem Scand 15:1667–1675
35. Krieble VK (1935) Activities and the hydrolysis of sucrose with concentrated acids. J Am Chem Soc 57:15–19
36. Krieble VK, Holst KA (1938) Amide hydrolysis with high concentrations of mineral acids. J Am Chem Soc 60:2976–2980
37. Leiniger PM, Kilpatrick M (1938) The inversion of sucrose. J Am Chem Soc 60:2891–2899
38. Moelwyn-Hughes EA (1934) The temperature coefficient of the inversion of cane sugar. Z Phys Chem B26:281–287
39. Heidt LJ, Purves CB (1938) The unimolecular rates of hydrolysis of 0.01 molar methyl- and benzylfructofuranosides and -pyranosides and of sucrose in 0.00965 molar hydrochloric acid at 20 to 60°. J Am Chem Soc 60:1206–1210
40. Capon B, Thacker D (1967) The mechanism of the hydrolysis of glycofuranosides. J Chem Soc B Phys Org 185–189
41. Ceder O (1954) A kinetic study of the acid hydrolysis of cyclic acetals. Arkiv Kemi 6:523–535
42. Salomaa P, Kankaanperä A (1961) Hydrolysis of 1,3-dioxolane and its alkyl-substituted derivatives. I. Structural factors influencing the rates of hydrolysis of a series of methyl-substituted dioxolanes. Acta Chem Scand 15:871–878
43. Fife TH, Jao LK (1965) Substituent effects in acetal hydrolysis. J Org Chem 30:1492–1495
44. Fife TH, Hagopian L (1966) Steric effects in ketal hydrolysis. J Org Chem 31:1772–1775
45. van Eikeren P (1980) Models for glycoside hydrolysis. Synthesis and hydrolytic studies of the anomers of a conformationally rigid acetal. J Org Chem 45:4641–4645
46. Deslongchamps P, Li S, Dory YL (2004) Hydrolysis of α- and β-glycosides. New experimental data and modeling of reaction pathways. Org Lett 6:505–508
47. Deslongchamps P (1983) Stereoelectronic effects in organic chemistry. Pergamon Press, Oxford
48. Kirby AJ (1985) Stereoelectronic effects on acetal hydrolysis. Acc Chem Res 17:305
49. Kirby AJ (1983) The anomeric effect and related stereoelectronic effects at oxygen. Springer, New York
50. Cordes EH, Bull HG (1978) In: Gandour DR, Showen RL (eds) Transition state in biochemical processes. Plenum Press, New York
51. BeMiller JN, Doyle ER (1971) Acid-catalyzed hydrolysis of alkyl α-D- glucopyranosides. Carbohydr Res 20:23–30
52. Li S, Kirby AJ, Deslongchamps P (1993) First experimental evidence for a synperiplanar stereoelectronic effect in the acid hydrolysis of acetal. Tetrahedron Lett 34:7757–7758
53. Ratcliffe AJ, Mootoo DR, Webster C, Fraser-Reid B (1989) Concerning the anti-periplanar lone pair hypothesis: oxidative hydrolysis of conformationally restrained 4-pentenyl glycosides. J Am Chem Soc 111:7661–7662
54. Gupta RB, Franck RW (1987) Direct experimental evidence for cleavage of both exo-and endo-cyclic carbon-oxygen bonds in the acid-catalyzed reaction of alkyl β- tetrahydropyranyl acetals. J Am Chem Soc 109:6554–6556
55. Deslongchamps P, Dory YL, Li S (1994) 1994 R.U. Lemieux Award Lecture Hydrolysis of acetals and ketals. Position of transition states along the reaction coordinates, and stereoelectronic effects. Can J Chem 72:2021–2027
56. Ishij T, Ishizu A, Nakano J (1976) Acid hydrolysis of methyl chlorodeoxyglycosides. Carbohydr Res 48:33–40
57. Liras JL, Anslyn EV (1994) Exocyclic and endocyclic cleavage of pyranosides in both methanol and water detected by a novel probe. J Am Chem Soc 116:2645–2646
58. Frank RW (1992) The mechanism of β-glycosidases: a reassessment of some seminal papers. Bioorg Chem 20:77–88
59. Nerinckx W, Desmet T, Claessens M (2006) Itineraries of enzymatically and non- enzymatically catalyzed substitutions at O-glycopyranosidic bonds. Arkivoc 13:90–116
60. Sinnot ML, Jencks WP (1980) Solvolysis of D-glucopyranosyl derivatives in mixtures of ethanol and 2, 2, 2-trifluoroethanol. J Am Chem Soc 102:2026–2032

61. Amyes TL, Jenks WP (1989) Concerted bimolecular substitution reactions of acetal derivatives of propionaldehyde and benzaldehyde. J Am Chem Soc 111:7900–7909
62. Kurzynski M (1993) Enzymic catalysis as a process controlled by protein conformational relaxation. FEBS Lett 328:221–224
63. Huang X, Tanaka KSE, Bennet AJ (1997) Glucosidase-catalyzed hydrolysis of α-D-glucopyranosyl pyridinium salts: kinetic evidence for nucleophilic involvement at the glucosidation transition state. J Am Chem Soc 119:11147–11154
64. Berti PJ, Tanaka KSE (2002) Transition state analysis using multiple kinetic isotope effects: mechanisms of enzymatic and non- enzymatic glycoside hydrolysis and transfer. Adv Phys Org Chem 37:239–314
65. Vocadlo DJ, Wicki J, Rupitz K, Withers SG (2002) Mechanism of Thermoanaerobacterium saccharolyticum -Xylosidase: kinetic studies. Biochemistry 41:9727–9735
66. Lorthiois E, Meyyappan M, Vasela A (2000) β -Glycosidase inhibitors mimicking the pyranoside boat conformation. Chem Commun 1829–1830
67. Murray TF, Kenyon WO (1940) The rates of formation of sulfoaliphatic acids. J Am Chem Soc 62:1230–1233
68. Jeffery EA, Satchell DPN (1962) The mechanism of sulphoacetic acid formation in the system H_2SO_4–Ac_2O–AcOH. J Chem Soc 1913–1917
69. Germain A, Commeyras A (1973) Mechanism of the C-acylation of aromatic and ethylenic compounds. XV. Kinetic study of the formation of acetylium ion in acetic anhydride solutions in the presence of trifluoromethanesulfonic and fluorosulfonic acids. Bull Soc Chim (France) 2532–2537
70. Germain A, Commeyras A, Casadevall A (1973) Mechanism of the C-acylation of aromatic and ethylenic compounds. XVI. Kinetic study of the acetylation of aromatic compounds by acetic anhydride in the presence of strongly protonating acids. Bull Soc Chim (France) 2537–2543
71. Dasgupta F, Singh PP, Srivastava HC (1980) Acetylation of carbohydrates using ferric chloride in acetic anhydride. Carbohydr Res 80(1980):346–349
72. Dasgupta F, Singh P, Srivastava HC (1988) Use of ferric chloride in carbohydrate reactions. Part V. Acetolysis of methyl hexopyranosides using ferric chloride in acetic anhydride. Indian J Chem 27B:527–529
73. Guthrie RD, McCarthy JF (1967) Acetolysis. Adv Carbohydr Chem 22:11–23
74. Zaccari DG, Snyder JP, Peralta JE, Taurian OE, Coutreras RH, Barone V (2002) Natural J Coupling (NJC) analysis of the electron lone pair effect on NMR couplings. Part 2. The anomeric effects on 1J (C, H) couplings and its dependence on solvent. Mol Phys 100:705–715
75. Pinto BM, Johnston BD, Nagelkerke R (1988) Solvent and temperature dependence of the anomeric effect in 2[(4-methoxyphenyl)seleno]-1, 3-dithianes. Dominance of the orbital interaction component. J Org Chem 53:5668–5672
76. Franks F, Lillford PJ, Robinson G (1989) Isomeric equilibration of monosaccharides in solution: influence of solvent and temperature. J Chem Soc Faraday Trans 1 85:2417–2426
77. Paulsen H, Friedmann M (1972) Conformational analysis. I. Dependence of the syn-1,3-diaxial interaction on the substituents and solvents. Conformational equilibria of D-idopyranose derivatives. Chem Ber 105:705–717
78. Bailey WF, Eliel EL (1974) Conformational analysis. XXIX. 2-substituted and 2,3-disubstituted 1,3-dioxanes. Generalized and reverse anomeric effects. J Am Chem Soc 96:1798–1806
79. McPhail DR, Lee JR, Fraser-Reid B (1992) Exo and endo activation in glycoside cleavage: acetolysis of methyl α- and β-glucopyranosides. J Am Chem Soc 114:1905–1906
80. Lemieux RU (1954) Some implications in carbohydrate chemistry of theories relating to the mechanisms of replacement reactions. Adv Carbohydr Chem 9:1–57
81. Capon B (1969) Mechanism in carbohydrate chemistry. Chem Rev 69:407–498

82. Lindberg B (1949) Action of strong acids on acetylated glucosides. III. Strong acids and aliphatic glucoside tetraacetates in acetic anhydride-acetic acid solutions. Acta Chem Scand 3:1153–1169
83. Asp L, Lindberg B (1950) Action of strong acids on acetylated glycosides. VII. Trans-glycosidation of xylosides. Acta Chem Scand 4:1446–1449
84. Lonnberg H, Kankaanperä A, Haapakka K (1977) The acid-catalyzed hydrolysis of β-D-xylofuranosides. Carbohydr Res 56:277–287
85. Lonnberg H, Kulonpaa A (1977) Mechanisms for the acid-catalyzed hydrolysis of some alkyl aldofuranosides with the trans-1,2-configuration. Acta Chem Scand A31:306–312
86. Lemieux RU (1964) Rearrangements and isomerizations in carbohydrate chemistry. In: de Mayo P (ed) Molecular rearrangements, Part two. Interscience, New York, pp 709–769
87. Altona C (1964) Ph.D. thesis, University of London, London
88. Lemieux RU (1985) personal communication to H. Booth in 1983, as quoted by Booth, H.; Khedhair, K. A. in Endo-Anomeric and exo-anomeric effects in 2-substituted tetrahydropyrans. J Chem Soc Chem Commun 467–468, reference 13
89. Praly J-P, Lemieux RU (1987) Influence of solvent on the magnitude of the anomeric effect. Can J Chem 65:213–223
90. Miljkovic M, Habash-Marino M (1983) Acetolysis of permethylated O-alkyl glycopyranosides: kinetics and mechanism. J Org Chem 48:855–860
91. Miljkovic M, Yeagley D, Deslongchamps P, Dory YL (1997) Experimental and theoretical evidence of through-space electrostatic stabilization of the incipient oxocarbenium ion by an axially oriented electronegative substituent during glycopyranoside acetolysis. J Org Chem 62:7597–7604
92. Tvaroška I, Bleha T (1989) Anomeric and exo-anomeric effects in carbohydrate chemistry. Adv Carbohydr Chem Biochem 47:45–123
93. Fuchs B, Ellencweig A, Tartakovsky E, Aped P (1986) Solvent polarity and the anomeric effect. Angew Chem Int Engl 25:287–289

Chapter 4
Conformations and Chemistry of Oxocarbenium Ion

While the conformational analysis of stable compounds has been studied in detail, determining the conformational preferences of reactive intermediates is much more difficult. For example, knowledge of the three-dimensional structures of cyclic oxocarbenium ions is very important for understanding both uncatalyzed and enzymatic reactions of carbohydrates involving the anomeric carbon, since these reactions often involve oxocarbenium ion intermediates [1–5]. Since the charged intermediates are generally much too reactive, it is impossible to directly observe oxocarbenium ions, particularly in aqueous environments [6, 7].

Theoretical studies of oxocarbenium ions suggested that electrostatic effects control the conformational preferences of these reactive intermediates [8–11]. Computational studies of carbohydrate-derived oxocarbenium ions revealed that methyl substituents favor equatorial positions in oxocarbenium ions, while hydroxyl groups prefer axial orientation particularly at certain positions (Fig. 4.1) [8]. These conclusions were reinforced by *ab initio* calculations (RHF/6-31G**) on C4 alkoxy-substituted oxocarbenium ions [11]. The authors conclude that the through-space electrostatic effect [12, 13], not anchimeric assistance, stabilizes the axial conformation *1* (X = OMe) by about 4 kcal/mol relative to the equatorial conformer *2* (Fig. 4.1) [11]. It is important to note that although oxocarbenium ions are typically drawn with a formal positive charge on the oxygen atom (as shown in Fig. 4.1), it is the anomeric carbon atom that bears positive charge and not the ring oxygen atom [12, 13].

Consideration of the preference for alkoxy groups to adopt axial conformers at certain positions, as shown in Fig. 4.1, explains the relative rates of monosaccharide hydrolysis [8, 11]. For example, the reactivity pattern exhibited by methyl pyranosides *3*–*5* (Fig. 4.2) showed a trend that the more axial hydroxyl groups are present in the acetal, the faster the rate of hydrolysis (Fig. 4.2) [14, 15].

Since the transition state structures of exocyclic C–O bond cleavage resemble the oxocarbenium ion intermediates, favorable interactions that stabilize the charged intermediates would facilitate hydrolysis [16]. The pyranoside *5* bearing axial substituents at the C3 and C4 carbons reacted at the highest rate via an

M. Miljkovic, *Electrostatic and Stereoelectronic Effects in Carbohydrate Chemistry*,
DOI 10.1007/978-1-4614-8268-0_4,

Fig. 4.1

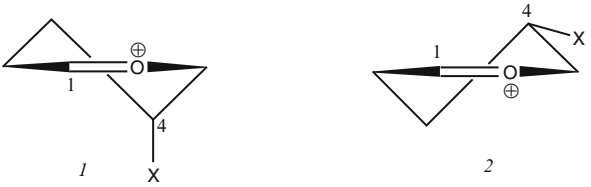

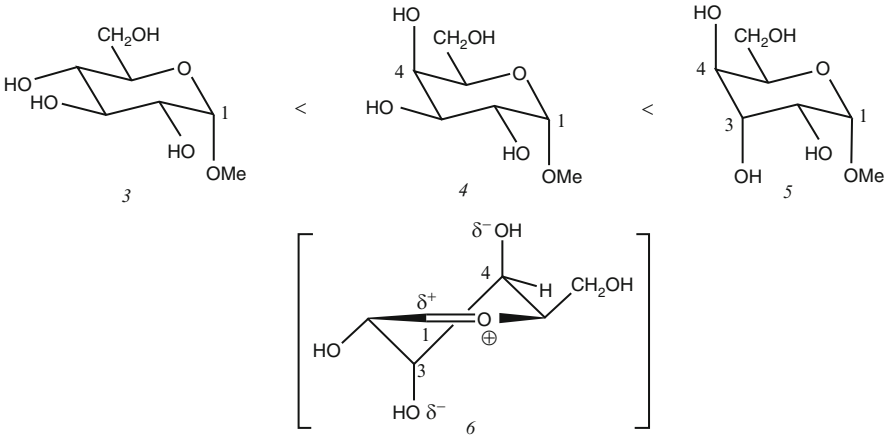

Fig. 4.2

oxocarbenium ion *6* stabilized by two partially negatively charged oxygen atoms positioned near the positively charged carbon atom of oxocarbenium ion [12, 13].

Chamberland et al. [17] provided unambiguous evidence for the preferred axial orientation of a partially negatively charged substituent in an oxygen-substituted carbocation. The isolable but unstable benzyloxy-substituted cation *8* was prepared by ethylation of the corresponding lactone *7* (Fig. 4.3) [18]. ^{1}H-NMR spectrum of dioxocarbenium ion *8* revealed that H_b exhibited a splitting pattern characteristic of an equatorial proton, suggesting that the C4 alkoxy substituent preferred the axial orientation in solution (Fig. 4.3). An X-ray crystal structure of cation *8* confirmed that the low-energy ground-state conformer orients the alkoxy substituent proximal to the electron-deficient carbon. The distance between the C4 oxygen and the cationic carbon (3.301 Å) is consistent with a through-space Coulombic interaction, excluding stabilization from covalent bond formation between the two charged atoms [19].

When the corresponding alkyl-substituted cation was prepared, the alkyl group was equatorially orientated both in solution and in the solid state.

The strong preference for an alkoxy substituent to reside in the axial position (Figs. 4.1 and 4.3) can be utilized to control the conformation of oxocarbenium

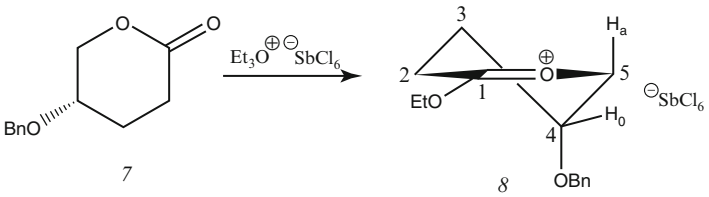

Fig. 4.3

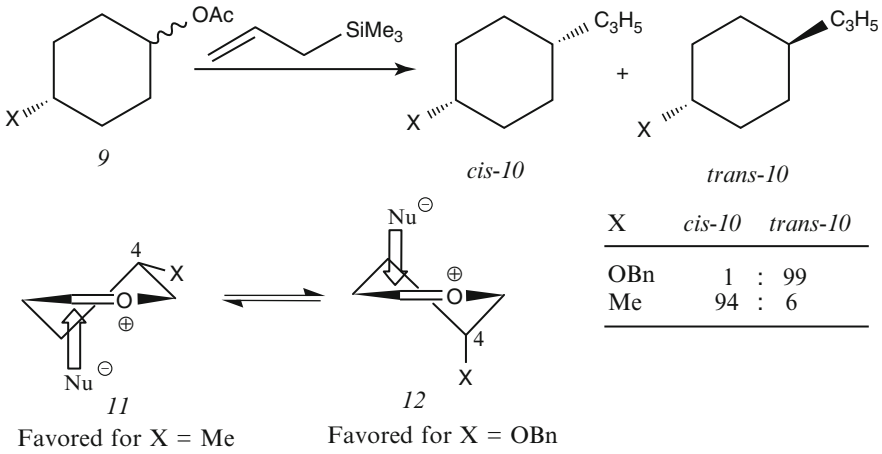

Fig. 4.4

ions, so that carbon-carbon bonds can be formed in a contrasteric manner. Nucleophilic substitution of acetate *9* (X = OBn) in the presence of a Lewis acid afforded the 1,4-*trans* product *10* with high diastereoselectivity (Fig. 4.4) [19, 20]. Similar selectivities have been observed with vinyl oxocarbenium ion [21, 22].

"Control experiments indicate that these reactions proceed via free oxocarbenium ions and not contact ion pairs [23]. This *trans*-selective outcome can be understood by considering that the alkoxy-substituted oxocarbenium ion favors the axial conformer *12*, in accord with the structure *17* of the dioxocarbenium ion *8* (Fig. 4.3). The product selectivity is in accord with computational predictions (Fig. 4.1) [8, 11]." Nucleophilic addition to the lower energy conformer *12* (Fig. 4.4) through the stereoelectronically preferred chair-like transition structure leads to the observed *trans* product [24–26]. The reaction of the corresponding alkyl-substituted acetate *11* (X = Me) in the presence of a Lewis acid afforded 1,4-*cis* product *10*, consistent with an equatorial preference for the substituent at C4 (viz. *11*) followed by the stereoelectronically controlled nucleophilic addition [23, 24, 26].

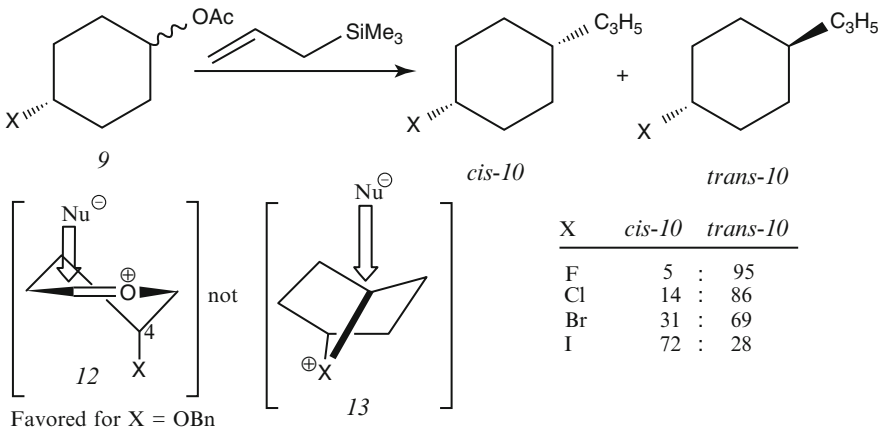

X	*cis-10*		*trans-10*
F	5	:	95
Cl	14	:	86
Br	31	:	69
I	72	:	28

Fig. 4.5

The examination of halogen-substituted C4 analogs confirmed that stabilization of the C1 center does not occur through anchimeric assistance but rather is more consistent with a through-space electrostatic stabilization (Fig. 4.5). The *trans*-selectivity of substitution decreased as the halogen atom became less electronegative (F > Cl > Br > I, Fig. 4.5). If the high *trans*-selectivities were attributable to anchimeric assistance through formation of a bond as shown in *13* (Fig. 4.5), the iodine substituent should lead to the highest *trans*-selectivity. Instead, the iodinated acetate *9* (X = I) provided mostly the *cis* product *cis-10*, similar to the outcome for the alkyl-substituted substrate *9* (X = Me, Fig. 4.4). This outcome requires the iodine to favor an equatorial position in the oxocarbenium ion. The highly selective reaction of the fluorinated substrate *9* (X = F) suggests that the conformational preference for the halogen atom is caused by electrostatic effects holding the electronegative atom closer to the oxocarbenium ion (as in *12*). The more negatively charged the halogen atom, the greater the preference for the axial orientation.

Conformational control through electrostatic stabilization is also observed with an alkoxy substituent at the C3 carbon of a six-membered ring oxocarbenium ion intermediate. In contrast to the *trans* product obtained with an alkyl substituent, nucleophilic addition to *14* (X = OBn, Fig. 4.6) in the presence of a Lewis acid afforded the contrasteric 1,3-*cis* product: *cis-15* (Fig. 4.6). The *cis* product arises from addition of the nucleophile to the pseudoaxial conformer *16*, which would be favored for X = OBn [8]. The high selectivity for the contrasteric *cis* product indicates that the electrostatic stabilization compensates for the development of steric interactions between C3 alkoxy substituents and the approaching nucleophile in the chair-like transition structure [27]. Without the electrostatic stabilization, substituents at the C3 carbon reside in pseudoequatorial orientation of the oxocarbenium ion *17* to give the sterically preferred 1,4-*trans* product *trans-15*.

The conformational preferences exerted by a single alkoxy substituent are found also in systems with several alkoxy groups [28]. In their studies of carbohydrate

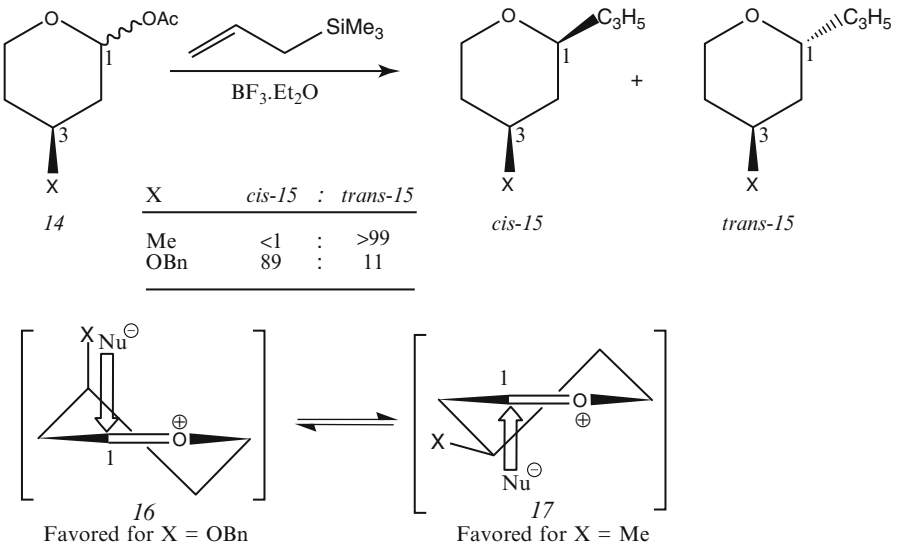

Fig. 4.6

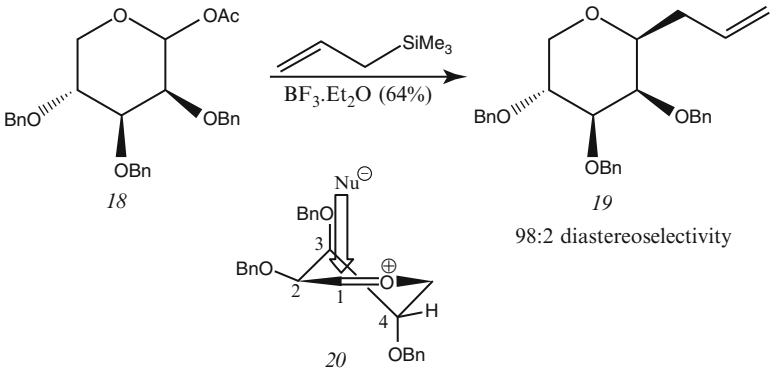

Fig. 4.7

oxocarbenium ions that served as models for enzyme inhibitors [29], Lucero and Woerpel [28] treated the pentose acetal *18* with allyltrimethylsilane in the presence of a Lewis acid to provide the product *19* with high diastereoselectivity (Fig. 4.7) [28]. This stereochemical outcome can be analyzed by considering that the oxocarbenium cation prefers the conformation *20*, where the alkoxy groups at C2, C3, and C4 are all in their favored orientations [8, 19, 20].

Analyzing the reactions involving highly oxygenated five-membered ring oxocarbenium ions added another level of complexity. For example, analyzing the C-glycosylation reactions of ribose derivatives (Fig. 4.7) [30] required not

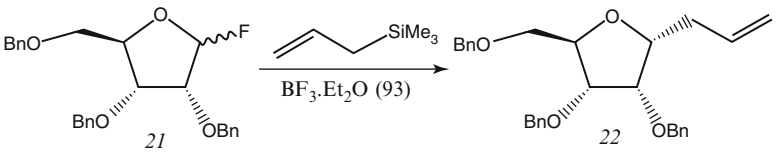

Fig. 4.8

only understanding of the conformational preferences of the intermediate carbocations, but also the preferred direction of nucleophilic attack. The reason for this is that in the half-chair conformation shown in Fig. 4.7, both H3 and the H4 benzyloxy groups are oriented axially, thus maximally stabilizing the oxocarbenium ion while impeding the approach of the negatively charged nucleophile which is to react with the carbocation C1, since it is subjected to electrostatic and steric interaction with the electronegative benzyloxy groups. A reliable, predictive stereochemical model would be necessary to analyze which face of the cation would be attacked. Unfortunately, a few systematic studies of stereoselective reactions of five-membered ring oxocarbenium ions were available [31–33] and it was not clear how to adapt the available models to analyze the selectivity shown in Fig. 4.8. This topic will be addressed at the end of this chapter.

Knowledge of the three-dimensional structures, relative energies, and reactivities of oxocarbenium ions would make it much easier to design selective glycosylation reactions [34–39].

In addition, the understanding of conformational preferences of oxocarbenium ions would have an impact on glycobiology and medicinal chemistry. Enzymes that catalyze glycosyl transfer, which can operate by stabilizing transition states with substantial oxocarbenium ion character [1, 40–46], have emerged as potential targets for the treatment of influenza [47, 48], diabetes [49, 50], and cancer [51]. Although transition state analogs of glycosyl transfer have been identified [52–54] and many inhibitors of glycosidases have been developed [55–60], the three-dimensional structures of carbohydrate-derived oxocarbenium ions are not very well understood, and only recently have computational studies of these structures emerged [10, 45, 46, 61, 62]. A better understanding of the three-dimensional structures of these cations would clarify the roles of these intermediates and transition states and facilitate the design of therapeutic glycosidase inhibitors [10, 46, 63, 64].

Studies of Woerpel et al. of conformational preferences of oxocarbenium ions revealed that electronic effects exert strong influences on the conformational preferences of these cations. For reactions involving C3 and C4 alkoxy-substituted tetrahydropyran cations, the pseudoaxial conformations of the oxocarbenium ion intermediates *23* and *24* (Fig. 4.9) were consistent with the formation of the 1,4-*trans*- and the 1,3-*cis* products, respectively (Fig. 4.9) [19, 20]. The pseudoaxial conformations of the oxocarbenium ions are favored because they are stabilized by electrostatic interactions between the positively charged atoms of the cations and the partially negatively charged substituents [8, 11, 19, 20, 65]. The results with

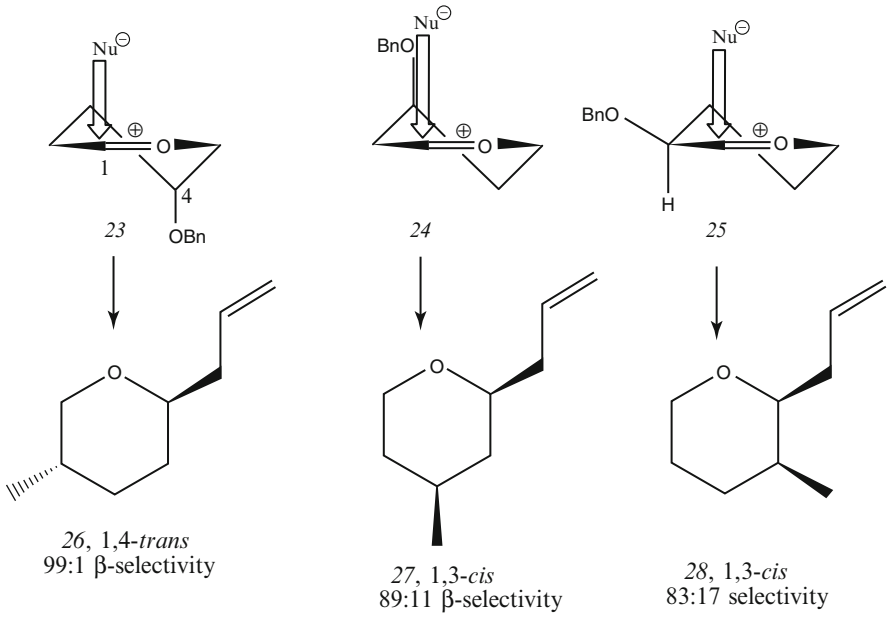

Fig. 4.9 Preferred conformations of the oxocarbenium ioon intermediates in nucleophilic substitution reaction of monosubstituted tetrahydrophyran oxocarbenium ions

substrates bearing an alkoxy group at C2 revealed that although electrostatic effects are similar between the pseudoaxial and pseudoequatorial conformers [In the pseudoaxial and pseudoequatorial conformers, the position of the C2 substituent changes through a C2–C1 bond rotation. Consequently, the distance between the C2 oxygen atom and the cationic C1 carbon atom should remain essentially the same.] Previous calculation showed that the distance between the C2 oxygen atom and the C1 carbon atom is 2.30 Å when the substituent is axial and 2.33 Å when the substituent is equatorial [8]; the pseudoequatorial conformation *25* is stabilized by hyperconjugation from the C2 carbon-hydrogen bond [66].

Knowledge of the contributions of individual substituents to the conformational preferences of oxocarbenium ions, however, is not sufficient to predict the reactivities of highly substituted systems such as those formed from carbohydrates. [Other intermediates, aside from discrete oxocarbenium ions, could also lead to the nucleophilic substitution products. For an example involving ion-pair intermediate, see Crich et al. [15].] For the type of substrates presented in this work, neither the Lewis acid nor the solvent has significant influence upon product distribution as described in Ref. [19]. For instance, although the influences of the C2, C3, and C4 substituents on the mannopyranosyl cation should reinforce each other to favor β-product, α-selectivity was observed upon allylation of the mannosyl phosphate *29* (Fig. 4.10) [Allylation of mannosyl phosphate *29* has been shown to be highly α-selective with Me_3SiOTf [67]. C-Mannosylation reactions are generally α-selective [68–76]. α-Selectivity was also observed with acetate-protected

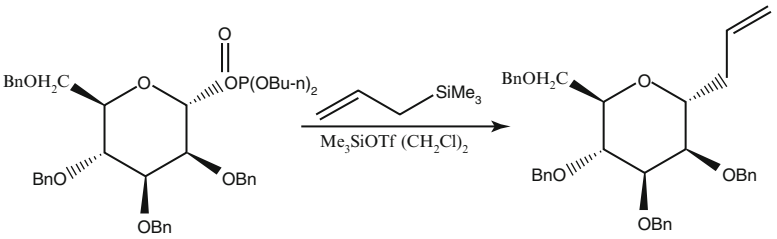

29 *30*

Fig. 4.10

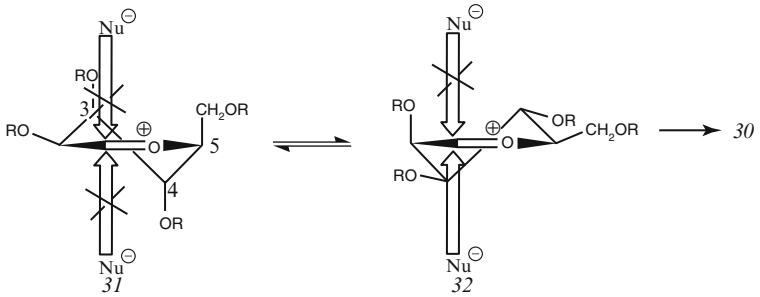

Fig. 4.11

mannose derivatives in which the protecting group could be involved in selectivity [77–80]. Allylation of mannosyl phosphate with no selectivity has also been reported [81].]

This observation could be the result of a change in the conformational equilibria of the oxocarbenium ion such that the cationic intermediate now prefers the conformation *30* with the C3, C4, and C5 substituents in the equatorial orientation (Fig. 4.11) to avoid 1, 3-diaxial interaction between the C3 and C5 substituents. Alternatively, the reversal in facial selectivity could be the result of Curtin-Hammett scenario [82, 83] where the product distribution was dictated by the relative reactivities of the low-energy conformers. In this case, nucleophilic addition would occur via the higher energy conformer *32*, given that the kinetic barriers to the stereoelectronically disfavored twist transition states were too high in energy and that the lower energy conformer *31* was too sterically congested to react. Although the selectivities exhibited by multiply substituted cations suggested that the observation shown in Fig. 4.11 was the result of reaction through intermediate *32* [84], the additional evidence to confirm this hypothesis was required.

Although oxocarbenium ions are too reactive [6] to be observed in many cases (alkyl oxocarbenium ions have previously been characterized by various means as superacidic solutions [85–87], electrochemical oxidation [88–90]), the related

Fig. 4.12

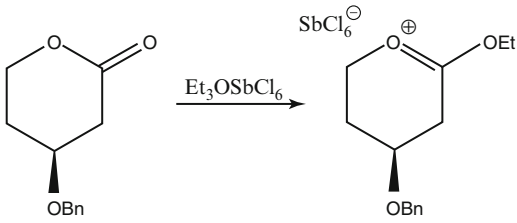

dioxocarbenium ions [91, 92] serve as isolable structural homologs, with conformational preferences that are also sensitive to electronic effects [17]. From the comparison of the ^{1}H-NMR coupling constants of dioxocarbenium ions with those predicted by computational methods, there were established conformational preferences of both monosubstituted and multiply substituted dioxocarbenium ions with structures related to glycosyl cations [93]. In the absence of severe steric interactions, electrostatic forces dictate the conformational preferences of dioxocarbenium ions. This conclusion underscores the importance of considering electrostatic influence as well as steric effects when predicting conformational preferences in structurally flexible molecules.

To study the conformational equilibria of the mannosyl oxocarbenium ion in solution, Yang and Woerpel [93] prepared a series of monosubstituted and multiply substituted tetrahydropyran dioxocarbenium ions and analyzed their conformational preferences. This approach was employed successfully for determining that the C4 alkoxy-substituted dioxocarbenium ion preferred the pseudoaxial conformation [17].

Yang and Woerpel [93] prepared a series of lactones which were then converted into dioxocarbenium ions by alkylation with Meerwein salts [91, 92].

Studies of the simplified dioxocarbenium ions such as monosubstituted systems indicated that correlation of spectroscopic data with theoretical calculations could identify low-energy conformers. Spectroscopic studies of the C3 alkoxy-substituted dioxocarbenium ion *34* (Fig. 4.12) confirmed the earlier proposal [19] that the 3-alkoxy group in 3-alkoxy oxocarbenium ion adopts a pseudoaxial orientation. The dioxocarbenium ion *34* (Fig. 4.12) was synthesized by alkylation of lactone *33*. It was found that it is not very stable at room temperature (it decomposes over 5 h) but it could be spectroscopically analyzed at 0° C. The small magnitude of the vicinal (^{3}J) coupling constants of the hydrogen at C3 suggested that the alkoxy group was oriented pseudoaxially. This observation is consistent with the computational studies (B3LYP/6-31G*) of the corresponding methyl derivative, which showed that the pseudoaxial conformer *35-ax* is favored by 1.4 kcal/mol over the equatorial conformer *35-eq* (Fig. 4.13).

The coupling constants for the computationally preferred conformer *35-ax* are in agreement with experimental J-values (Fig. 4.14) and with the observed stereoselectivities of additions to the corresponding oxocarbenium ion [19]. The preference for the pseudoaxial conformer *35-ax* was again attributed to electrostatic attraction

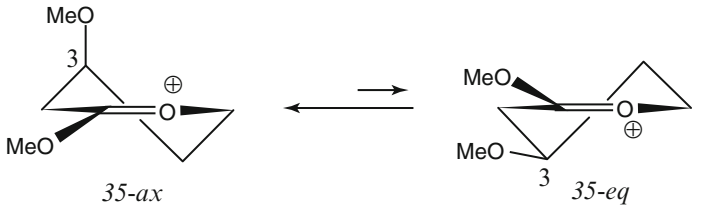

35-ax *35-eq*

E_{rel} = 0 kcal/mol E_{rel} = + 1.4 kcal/mol

Fig. 4.13

Fig. 4.14 Theoretical and experimental J-values for C3 alkoxy dioxocarbenium ion (B3LYP/6-31G*)

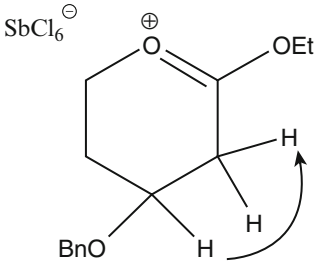

36

4.3, 2.7 Hz (Experimental J values)
3.9, 1.8 Hz (Theoretical J values)
8.7, 5.5 Hz (Theoretical J values for *35-ax*)

between the positively charged oxygen atom of the dioxocarbenium ion and the partially negatively charged oxygen atom of the alkoxy group, in agreement with the earlier studies on the C4 benzyloxy-substituted dioxocarbenium ions [17, 19, 20].

The influence of an alkoxymethyl group at C5 of a carbohydrate-derived oxocarbenium ion is more complicated than the influence of an alkoxy group at either C3 or C4. In addition to the ability to adopt either a pseudoaxial or a pseudoequatorial orientation, the substituent has additional conformational flexibility about the exocyclic C5–C6 bond, as illustrated in cation *37* (Fig. 4.15). This exocyclic dihedral angle can significantly influence the reactivity of carbohydrates [94].

Computational studies on monosubstituted dioxocarbenium ion *37* (X = OEt) indicated that the conformational distribution could not be simply explained by invoking steric effects. Although the pseudoequatorial half-chair conformer *38* (which is in the $^4H_3$ conformation) would minimize steric interactions, it was not the lowest energy structure (Fig. 4.16). Despite incurring two gauche interactions, conformers *36* and *37* remained approximately isoenergetic with conformer *38* [conformers *36–38* are considered to be isoenergetic because errors associated with

Fig. 4.15

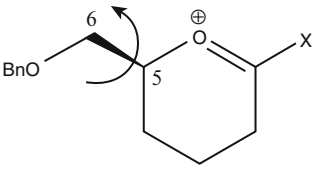

37

X = H, OEt

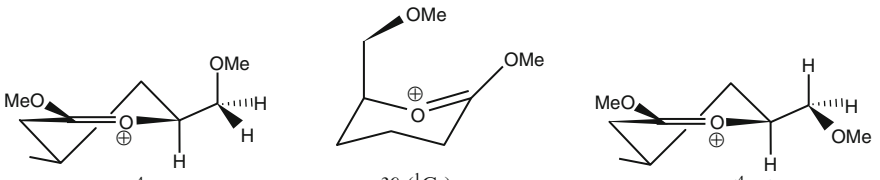

	38 ($^4H_3$)	*39* ($^1C_4$)	*40* ($^4H_3$)
E_{rel}	0 kcal/mol	+ 0.3 kcal/mol	+ 0.4 kcal/mol
Distance ()6-Cl)	3.7 A	3.0 A	4.1 A

Fig. 4.16 Relative low-energy confomrers od C-5 alkoxymethyl dioxocarbenium ion (B3LYP/6-31G*)

the B3LYP method can approach 1 kcal/mol [95, 96]]. The relative energies of the low-energy structures *36* and *37* are consistent with the proposal that electrostatic effects stabilize these cations in spite of the presence of some steric interactions [8, 11, 19, 65]. The decrease in distance between the electronegative oxygen substituent at C5 and the carbocationic carbon C1 compensated for the steric penalties associated with additional gauche interactions.

The computational predictions illustrated in Fig. 4.16 are consistent with the NMR coupling constant data obtained for dioxocarbenium ion *37* (X = OEt). The comparison of experimentally determined and calculated coupling constants for conformers *38–40* showed good correlation between the theoretical and experimental values. The experimental J-values for conformer *38*, where the dioxocarbenium ion adopted a half-chair conformation ($^4H_3$) with the electronegative 5-alkoxymethyl group oriented toward the positive charge, agreed most closely with the predicted coupling constants. The substantial deviation between the experimentally determined $J_{H5,H6'}$ value and that calculated for cation *40* indicates that the alkoxymethyl substituent does not adopt this orientation. This discrepancy can be rationalized by considering the expected magnitude of $^3J_{H5,H6}$ and $^3J_{H5,H6'}$ based on Karplus equation (Fig. 4.17). Both *gt* and *tg* rotamers would have one large and one small J-value, while two small coupling constants would be expected for the *gg* rotamer. The experimental vicinal coupling constants of 4.1 and 2.8 Hz are consistent with a *gg* conformation as found in both *38* ($^4H_3$) and *39* ($^1C_4$) (Fig. 4.16). The small energy differences between conformers *38* and *39* suggest the

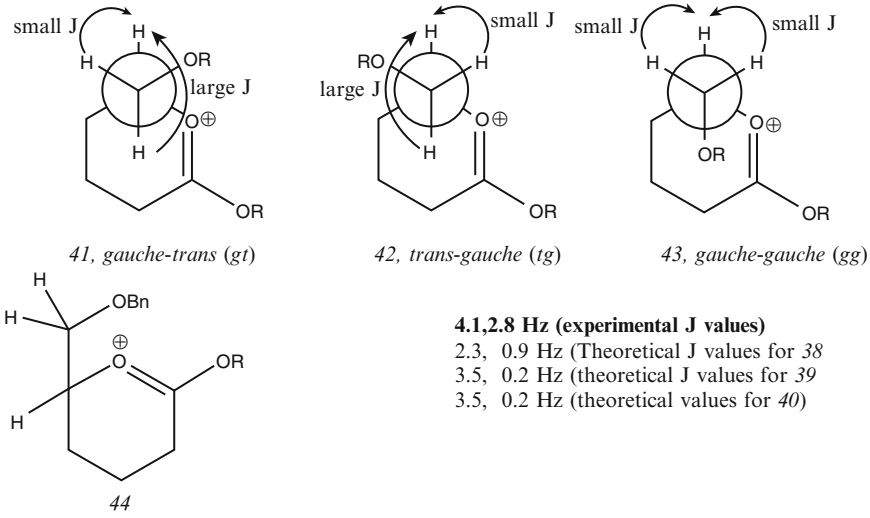

Fig. 4.17

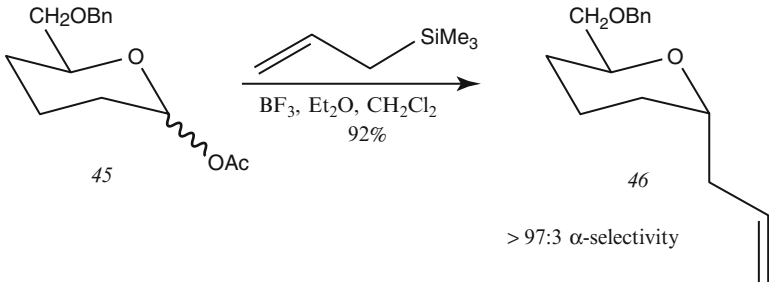

Fig. 4.18

presence of all three conformers in solution. Statistically relevant averaged coupling constants were determined from a weighted average of their populations (based upon their calculated relative energies).

The conclusion from spectroscopic evidence that dioxocarbenium ion with an alkoxymethyl group at C5 adopts a pseudoequatorial conformation is consistent with reactivity of the related oxocarbenium ion. Lewis acid-catalyzed nucleophilic substitution of acetate *45* afforded the 1,5-*trans* product *46* with high diastereoselectivity (Fig. 4.18). This result is inconsistent with the product ratio (70:30) previously reported for this reaction [84] (Fig. 4.18). In that paper, a minor product observed in the unpurified reaction mixture was assumed to be a diastereomer of *46*. It was later found that the minor product formed in the reaction mixture is not the *cis* isomer. This result can be explained by stereoelectronically controlled addition to the half-chair conformer analogous to *38* (or even *40*) in which the alkoxymethyl

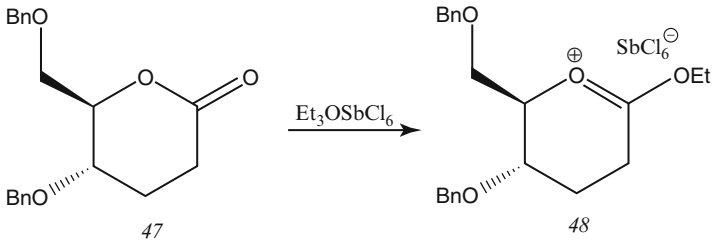

Fig. 4.19

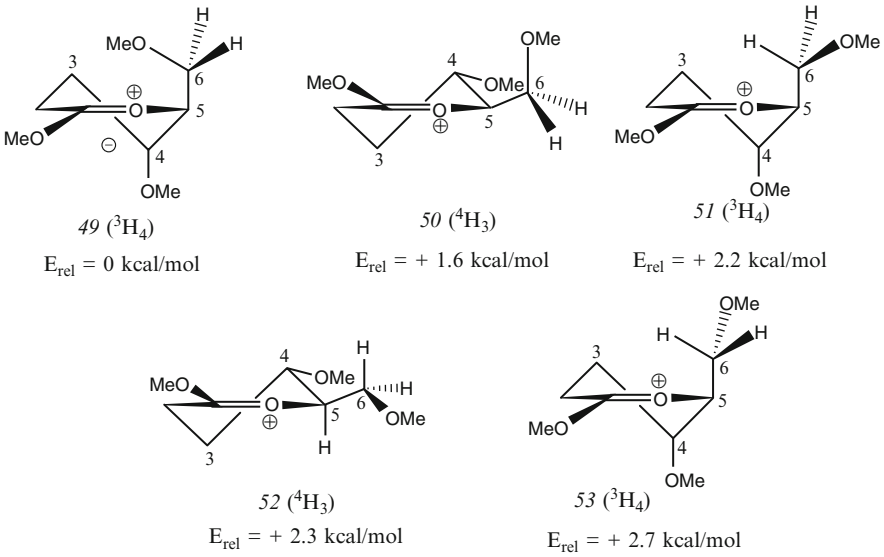

Fig. 4.20 Relative low-energy conformers of hte 4, 5-disubstituted dioxocarbenium ion (B3LYP/6-31G*)

substituent adopts a pseudoequatorial orientation. Nucleophilic addition to the oxocarbenium ion analogous to *39* might give similar selectivity because the alkoxymethyl substituent would hinder approach of the nucleophile to the top face.

The importance of the exocyclic electrostatic effect of the C5 alkoxymethyl-substituted dioxocarbenium ion *37* (Fig. 4.15) was demonstrated by results for the *trans*-4, 5-disubstituted dioxocarbenium ion *48* (Fig. 4.19). Computational studies suggested that the dioxocarbenium ion strongly favored the diaxial half-chair conformer *54* (a $^3H_4$ conformer) over other possible conformers (Fig. 4.20). The preference for this diaxial conformation demonstrates that the powerful electrostatic effect of the C4 alkoxy group can overwhelm the steric preference of the C5 substituent to reside pseudoequatorially (vide supra). As with the C5 alkoxymethyl-substituted dioxocarbenium ion *42*, the exocyclic alkoxymethyl group of *46* (Fig. 4.18) assumes a gauche orientation to maximize electrostatic interactions

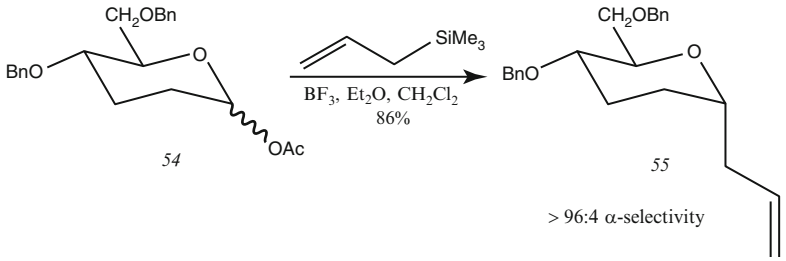

Fig. 4.21

between the C6 alkoxy group and the cationic carbon atom (as depicted by conformer *46*, Fig. 4.18). Consistent with this argument, conformers *48*, *49*, and *51*, which are stabilized by only one electrostatic interaction, are considerably higher in energy. Although both conformers *47* and *51* have the proper alignment for a σ C6-H to σ* $C5^+$ donation, a 2.7 kcal/mol difference in their energy suggests that the stabilization is electrostatic rather than hyperconjugative in nature. Without electrostatic benefits, the diequatorial conformer *50* ($^4H_3$) is predicted to be higher in energy than the diaxial conformer *47* ($^3H_4$).

In accordance with the calculated energy differences of the low-energy conformers, experimental coupling constants confirmed that the diaxial conformation *49* is the predominant species in solution. The fact that all $^3J_{H,H}$ coupling constants could be obtained for this molecule permitted a thorough analysis of its conformational preferences. The experimental coupling constants are in good agreement for most of the values expected for a $^3H_4$ half-chair conformation (*49*, *51*, and *53*), but they corresponded poorly with the $^4H_3$ half-chair conformers (*50* and *52*). The diaxial orientation of the 4, 5-disubstituted dioxocarbenium ion was further substantiated by the observed 1.5 Hz W-coupling between the hydrogen atom at C5 and the equatorial hydrogen atom at C3. This coupling is only possible when the C5 substituent is pseudoaxial. The two half-chair conformers *49* and *51* can be distinguished by examination of the $J_{H5,H6'}$ region. The preference for conformer *49*, with gauche orientations of the hydrogen at C5 to both hydrogens at C6, indicates that the alkoxy group at C6 must be positioned over the ring of the cation, presumably to maximize electrostatic stabilization.

The discrepancy between the conformational preference of the dioxocarbenium ion *48* (Fig. 4.19) and the selectivity of the reaction of the analogous oxocarbenium ion derived from *52* could be explained with the Curtin-Hammett principle [82, 83]. Although it might be expected that nucleophilic substitution of acetate *52* via its oxocarbenium ion would occur with β-selectivity through a conformer resembling *49*, α-selectivity was observed in this reaction (Fig. 4.21). Because interconversion among the different conformers is fast relative to the rate of nucleophilic addition [8], the major product would rise from the conformer with the lowest transition state [82, 83]. Reaction through the diaxial half-chair conformers analogous to *49, 51,* and *53* would involve higher energy transition states due to

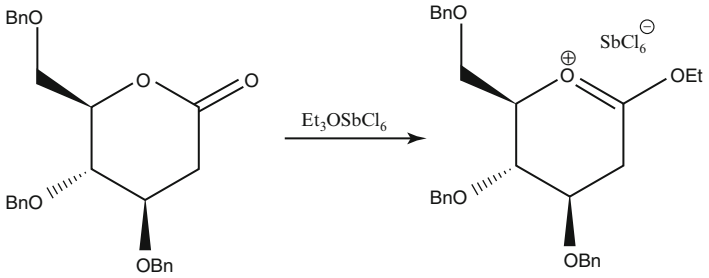

Fig. 4.22

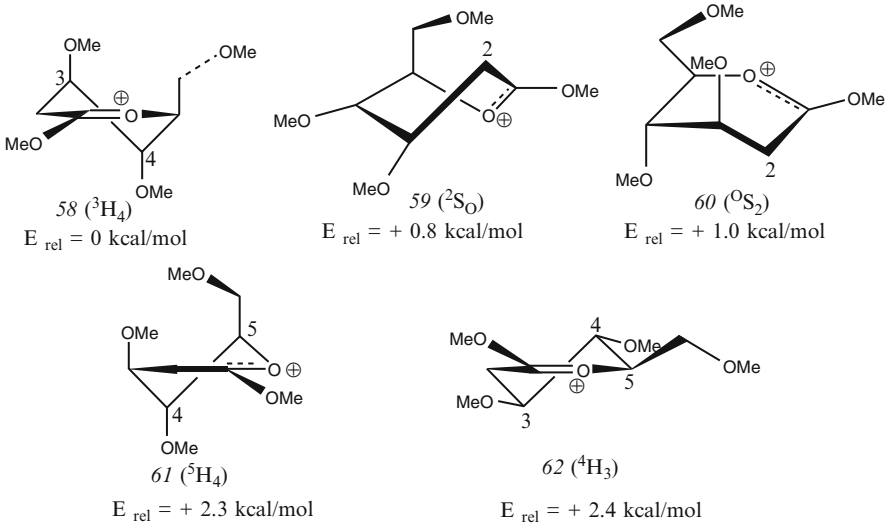

Fig. 4.23

developing 1, 3-diaxial interactions. Therefore, the product likely resulted from α-attack of the $^{4}H_{3}$ diequatorial conformers (*50* or *52*).

Examination of the conformational bias of the dioxocarbenium ion *57* derived from 2-deoxy-D-mannolactone *56* (Fig. 4.22) [this lactone may be considered to be 2-deoxy-D-gluconolactone also, because mannose and glucose differ only in the configuration at C2] revealed the limits of the electronic stabilization by an exocyclic alkoxy group. The lowest energy conformer identified by density functional methods (B3LYP/6-31G*) was the $^{3}H_{4}$ conformer *58* (Fig. 4.23). The $^{3}H_{4}$ conformation is similar in structure to ^{3}E conformation, a calculated minimum for the mannosyl oxocarbenium ion [10]. Conformer *58* is electrostatically stabilized by both C3 and C4 alkoxy groups. It does not, however, bring the alkoxy group at C6 close to the cationic center, presumably to avoid interactions with the pseudoaxial

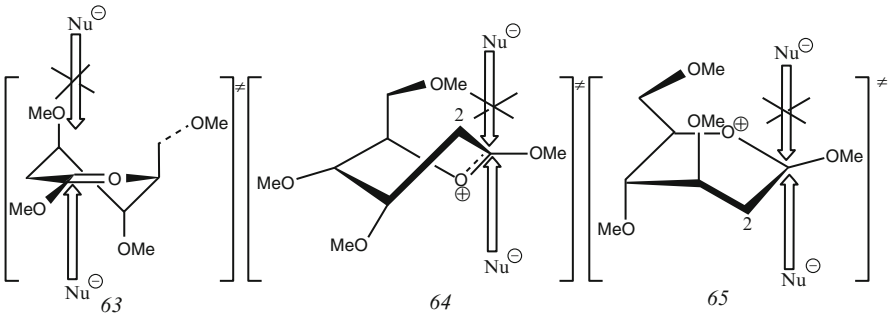

Fig. 4.24 Nucleophilic addition to oxocarbenium ions derived from 2-deoxymannoloctone

C3 substituent. This conformer would be destabilized not only by *syn*-butanol interactions [27] but also by bringing two oxygen atoms into proximity [97]. In contrast, although both *60* (the $^{O}S_2$ conformer) and *61* ($^{5}H_4$) place all three substituents in positions to maximize their electrostatic influences, they remain higher in energy than the half-chair conformer *58*. The conformation predicted based solely on steric grounds, *62* (the half-chair conformer $^{4}H_3$), was considerably less stable.

Experimental coupling constants for the 2-deoxymannosyl dioxocarbenium ion *57* are more consistent with a weighted average of the low-energy conformers than they are with any particular conformer. On the basis of the energy differences between low-energy conformers, *58* ($^{3}H_4$) should dominate the solution-phase equilibrium with some contributions from the twist conformers *59* and *60* (conformers *61* and *62* would, combined, represent less than 3 % of the mixture at 298° K). The experimental coupling constants, however, do not match well with any individual conformer. A weighted average of their populations was again employed to determine statistically relevant averaged coupling constants.

If conformations resembling the half-chair conformer *58* ($^{3}H_4$) and the twist conformers *59* and *60* were also responsible for the reactivity of the related oxocarbenium ion, nucleophilic addition to the oxocarbenium ion should be α-selective. Nucleophilic attacks from the β-face to conformers analogous to *56–58* should be disfavored over the corresponding attacks from the α-faces, because they would lead to transition states with 1, 3-diaxial interactions (Fig. 4.24). Alternatively, if any of these modes of nucleophilic attack were slow relative to stereoelectronically controlled addition to the higher energy half-chair conformer *60*, α-selectivity would still be predicted based upon the Curtin-Hammett principle [82, 83]. This interpretation was supported by the nucleophilic substitution reaction of acetate *66*, which yielded the α-product *67* (Figs. 4.25 and 4.26).

The strategy employed to discern the conformational preference of the less substituted oxocarbenium ions described above was not suitable for studying oxocarbenium ions with alkoxy groups at C2. When the lactone precursors *70* and *71* (Fig. 4.25) were subjected to alkylation conditions, the dioxocarbenium ion products *74* and *75* were not observed (Fig. 4.27). Instead, the reaction yielded a

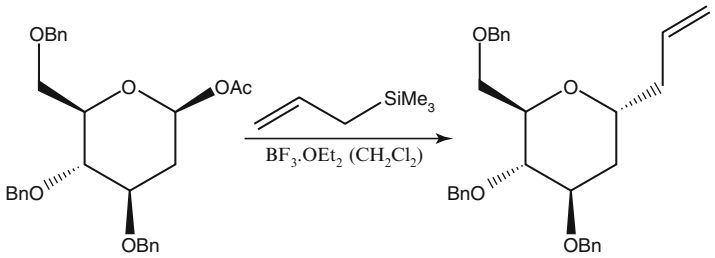

66 *67*

Fig. 4.25

Fig. 4.26

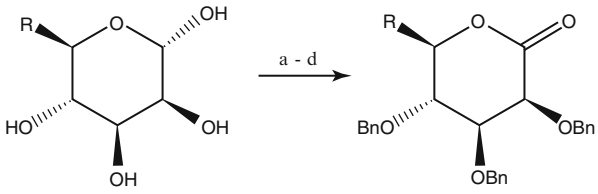

68, R = H
69, R = CJH_2OH

70, R = H
71 , R = CH_2OBn

Reagents: a) Dowex-50 resin, MeOH; b) NaH, BnBr;
c) cat. H_2SO_4 in 3:1 AcOH-H_2O; d) TPAP, NMO

Fig. 4.27

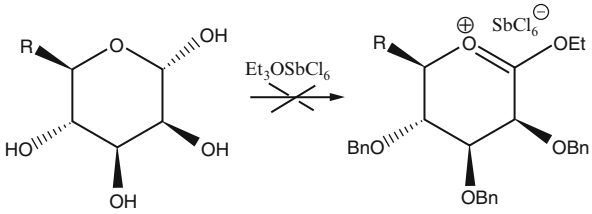

72, R = H
73, R = CJH_2OH

74, R = H
75, R = CH_2OBn

complex mixture of byproducts. It is possible that dioxocarbenium ions were formed, but the neighboring electronegative C2 substituent [98] made these intermediates much more reactive than their deoxy analogs (such as *48* and *57*, vide supra).

As we already mentioned, a few systematic studies of stereoselective reactions of the five-membered ring oxocarbenium ions are available [31–33], and it was not clear how to rationalize the selectivity shown in Fig. 4.28.

Woerpel et al. [65, 99–101] conducted studies of the reactions of the five-membered ring oxocarbenium ions and postulated a stereoelectronic model to

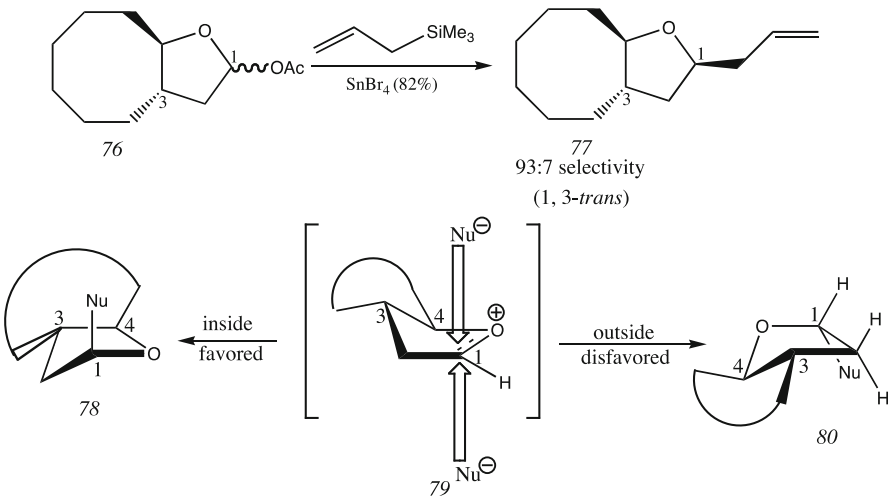

Fig. 4.28

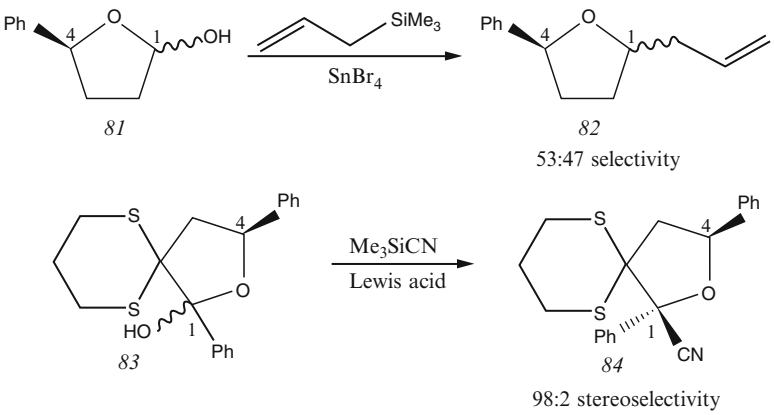

Fig. 4.29

explain these processes. This model is illustrated by analyzing the stereoselective reaction of the bicyclic lactol acetate *76* (Fig. 4.29) [100]. The intermediate oxocarbenium ion was constrained to one possible envelope conformation (as shown in *79* (Fig. 4.29)). Although this system provides no impediment to approach from either inside or outside the envelope, the reaction was highly selective (Fig. 4.29). Formation of the 1,3-*trans* diastereomer demonstrated that an inherent stereoelectronic preference directs nucleophilic addition from the inside face of the five-membered ring oxocarbenium ion envelope structure. This preference arises from the development of destabilizing eclipsing interactions upon nucleophilic attack from outside the envelope conformation (as shown in *79*, Fig. 4.29).

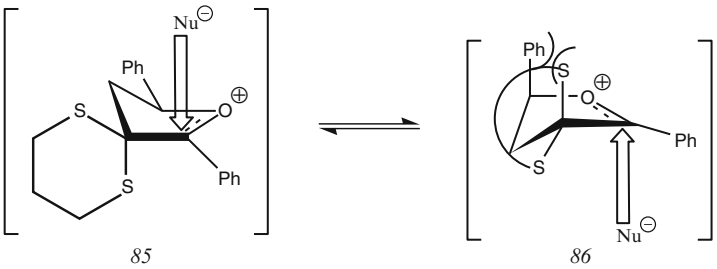

85 *86*

Fig. 4.30

Fig. 4.31

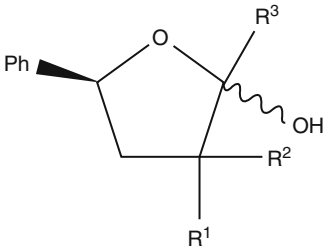

87

Inside attack instead provides a staggered product *78*, so transition states leading to this favored product should be lower in energy.

Reissig and Schmitt [102] and others [99, 103] demonstrated that the presence of a substituent at the C4 position of an oxocarbenium ion is not sufficient to control the selectivity in nucleophilic substitution reactions (e.g., *81* → *82*, Fig. 4.30 proceeded with 53:47 selectivity). Nishiyama et al. [104] have, however, reported that the addition of Me_3SiCN to acetal *81*, in the presence of a Lewis acid, proceeds with high selectivity (98:2) to give the 1,4-cis product [104]. Because acetal *83* has a single stereocenter at C4, the selective formation of *84* contradicted the results observed for the nucleophilic substitution of acetal *81*. The stereochemical outcome for acetal *83* was attributed to the steric bias imparted by Lewis acid coordination for the oxonium oxygen and the C2 heteroatom [105]. An oxocarbenium ion intermediate with Lewis acid blocking one face has been invoked to account for the facial selectivity of a nucleophile [106].

Woerpel and Smith [101] assumed that the sulfur substituents might not participate in the chelated transition structure but would instead influence the conformational preference of the oxocarbenium ion intermediate. According to that hypothesis and the stereoelectronic model [101, 102], contrasteric 1,4-*cis* product *84* would arise from inside attack of the nucleophile to the lower energy diequatorial oxocarbenium ion *85* (Fig. 4.30). This reaction pathway would provide a lower energy transition structure relative to inside attack of the nucleophile on the diaxial conformer *86* (*vide infra*) [84, 107] (Figs. 4.30 and 4.31).

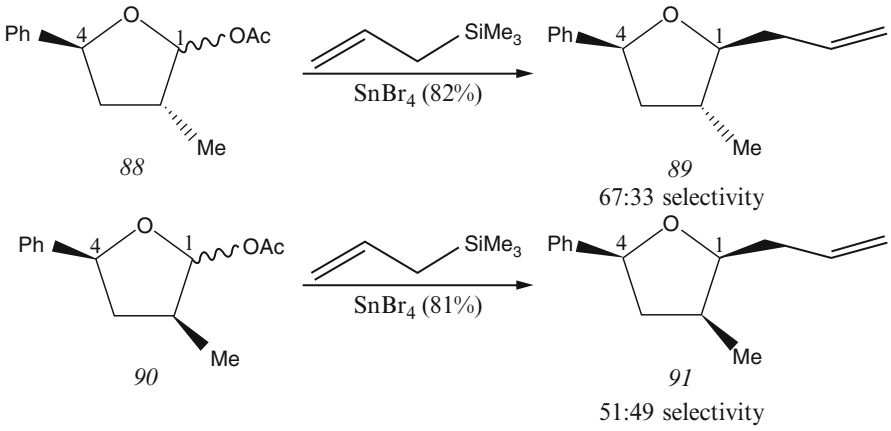

Fig. 4.32

To prove this hypothesis of inside attack and to elucidate the factors that contribute to the selective reaction of acetal *83*, alkyl analogs *85* (R^1, R^2 = Me, Fig. 4.30) with various substitution pattern at C1 and C2 were investigated. Experiments with alkyl substituents at C2, in place of the sulfur heteroatoms, eliminate the viability of a chelation-controlled selectivity and reveal the significance of geminal substitution [geminal substitution influenced the selectivity in other oxocarbenium ion systems [108]]. Perturbation of the C1 substituent of the oxocarbenium ion intermediate has little effect on reaction stereoselectivity, and analysis of this observation lends additional support for stereoelectronically preferred inside attack of the nucleophile. The results demonstrate that selective formation of the 1,4-*cis* product *84* does not require a chelated transition structure, reinforcing the utility of the inside attack model to analyze the reactivity of complex five-membered ring oxocarbenium ion intermediates.

Nucleophilic substitution reactions of acetates *88* and *90* (Fig. 4.32) indicate that a single substituent at C2 is not the origin of stereoselectivity for acetal *83* (Fig. 4.32). Treatment of the *trans* acetate *88* with allyltrimethylsilane in the presence of $SnBr_4$ provided the 1,4-*cis* product *89* with 67:33 stereoselectivity (Fig. 4.32). Use of BF_3OEt_2 and Me_3SiOTf as the Lewis acid provided similar selectivities. The reaction of the related *cis* acetate *90* also afforded a mixture of diastereoisomers. Low selectivity with C2 and C4-*cis*-substituted five-membered ring oxocarbenium ions has been observed [108].

Both the conformational preference of the oxocarbenium ion intermediate and steric interactions that arise in the transition structure for nucleophilic attack influence the stereochemical outcomes observed with acetates *88* and *90*. While the two ground-state conformers of the cation derived from *trans* acetate *88*, namely, *92* and *93*, are comparable in energy, developing steric interactions between the approaching nucleophile and the pseudoequatorial methyl of intermediate *93* slightly disfavor the formation of 1,4-*trans* product (Fig. 4.33). The selectivity obtained from the reaction

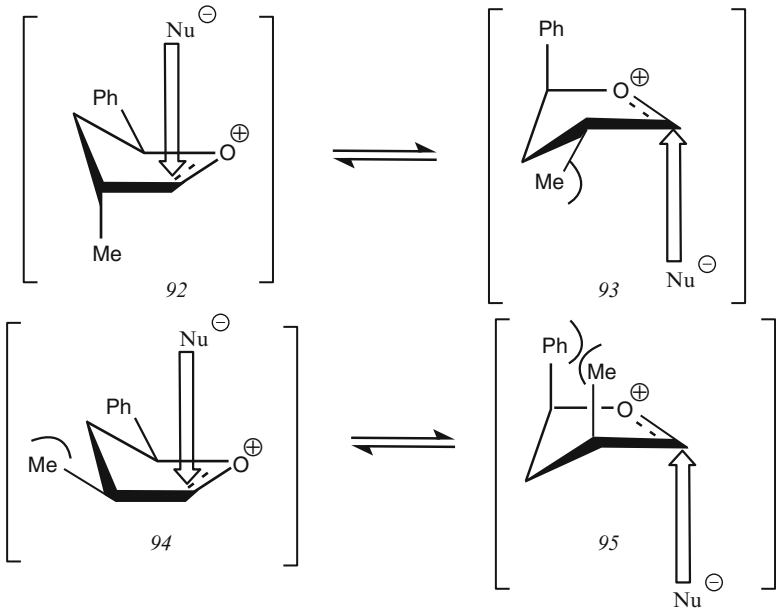

Fig. 4.33

of *cis* acetate *88* indicates that the difference in transition state energies ($\Delta\Delta G^{\neq}$) is negligible. Inside attack of the nucleophile to each of the two ground-state conformers *94* and *95* involves destabilized transition structures. The transition structure for inside attack on the lower energy conformer *94* develops a destabilizing gauche-butane interaction between the nucleophile and the pseudoequatorial C2 methyl substituent. [Low selectivity with C2 and C4-*cis*-substituted five-membered ring oxocarbenium ions has been observed [108]. For a study on the developing steric interactions between C2 substituents and the incoming nucleophile in six-membered ring oxocarbenium ion intermediates, see Ref. [19]. While the inside attack on conformer *95* circumvents an unfavorable interaction [19], with the steric interactions between the methyl and phenyl, the groups destabilize the transition structure leading to the product [80]. [In accordance with the Curtin-Hammett principle, the relative energies of the transition state structures dictate the stereochemical outcome, not the relative energies of the ground-state structures.]

The origin of the contrasting selectivities exhibited by acetal *81* [33] and acetal *83* [105] is not attributable to the presence of an alkyl substituent at the acetal carbon (C1). Treatment of acetal *96* with allyltrimethylsilane in the presence of $SnBr_4$ afforded tetrahydrofuran *97* with 65:35 selectivity (Fig. 4.34). Although the two anomers of acetal *96* were isolated in various ratios, the control experiments have shown that the starting anomer ratio does not affect the stereochemical outcome of the product, which is consistent with the intermediacy of oxocarbenium ions.

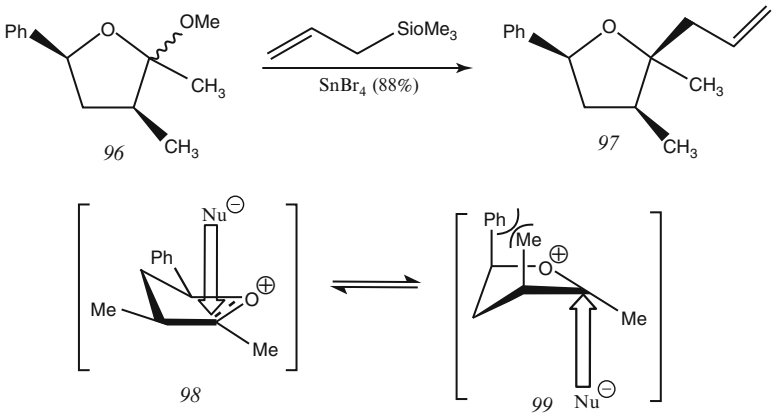

Fig. 4.34

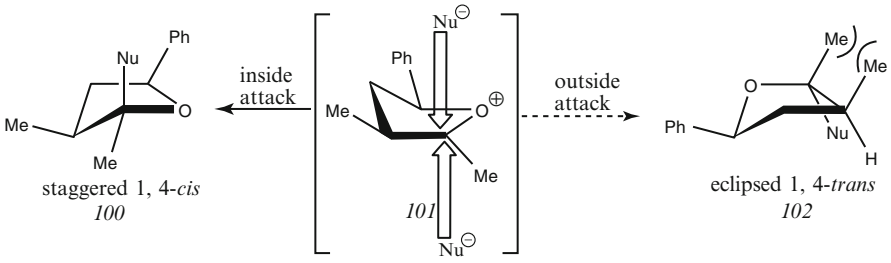

Fig. 4.35

The use of $BF_3.OEt_2$ as the Lewis acid afforded a 54:46 ratio of *cis*/*trans* isomers for the allylation of *94*. The C1 substituent exerts minimal influence on the equilibrium of the conformers *96* and *97* and the respective transition state structures for inside attack, resulting in a similar reactivity for the reaction of the C1-unsubstituted substrate *90* (Fig. 4.32).

The selectivities for reactions of acetate *90* and acetal *96* provide experimental support for stereoelectronically preferred inside attack on five-membered ring oxocarbenium ions, confirming the importance of torsional angle effects in addition reactions [101, 109, 110]. A potential reaction pathway leading to the minor 1,4-*trans* product obtained with acetal *90* could involve outside attack of the nucleophile to the lower energy conformer *94*. The reaction of acetate *96* resolves this ambiguity because formation of the 1,4-*trans* product *100* via outside attack on conformer *98* would be disfavored due to a more severe eclipsing interaction (Me ↔ Me and a M ↔ H) that develops in the transition structure (Fig. 4.35) [The energy difference between a Me ↔ Me and Me ↔ H eclipsing interaction is estimated to be 2 kcal/mol. This approximation was extrapolated from the rotational barriers of n-butane and n-propane. For n-butane, see Allinger et al. [110]. For n-propane, see Bürgi et al. [111].] If outside attack occurred, acetal *96* should have

Fig. 4.36

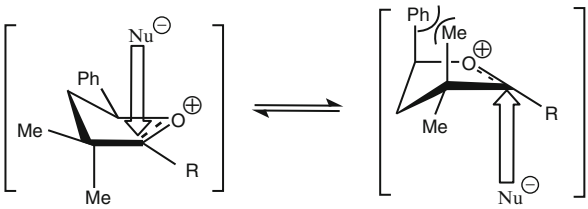

103 *104*

shown considerably higher selectivity for the staggered 1,4-*cis* product *99*. The selectivity for the nucleophilic substitution reaction of methyl-substituted acetal *96* confirms that the minor product obtained with acetate *90* is the result of inside attack on the higher energy conformer of the cation and not outside attack on the lower energy conformer (for an investigation of torsional angle effects (eclipsing strain energy on the reaction selectivity of hydromercuration of substituted cyclohexenes), see Pasto et al. [112].).

Because the C4-substituted acetals in this study exhibit low selectivity as was observed for acetal *81* [33] (Fig. 4.28), the unique feature of acetal *83* [104] that contributes to high selectivity may be geminal substitution at C2. With a pseudoequatorial methyl groups in both ground-state conformers *103* and *104* (Fig. 4.36), steric interactions with the approaching nucleophile would be comparable in both transition structures. Therefore, the energy difference between the transition structures of inside attack would reflect the relative energy difference between the ground-state oxocarbenium ion conformers *103* and *104*. Inside attack on the favored diequatorial conformer *103* should afford the 1,4-*cis* product with high selectivity, consistent with acetal *83*.

The above experiments confirm that geminal substitution at the C2 position, regardless of the substitution pattern at C1, is required to obtain high stereoselectivity for this series of substrates. Allylation of geminal dimethyl acetate *103* (Fig. 4.36) in the presence of $SnBr_4$ afforded the 1,4-*cis* product *104* with high selectivity (Fig. 4.36). [(a) Use of BF_3OEt_2 and Me_3SiOTf as the Lewis acid provided similar selectivities; (b) the solvent employed for these nucleophilic substitution reactions was CH_2Cl_2. With toluene as the solvent, selectivities were optimized to a 96:4 ratio of *cis*/*trans* isomers for the reaction of acetate *103* (Fig. 4.36).] To mimic the experiments reported for the nucleophilic substitution reaction of dithianes-substituted acetal *81* (Fig. 4.30), the reaction of C1 phenyl acetal *105* with Me_3SiCN was studied. In accord with experiments described previously, the substituent at C1 exerted little influence on the selectivity. The kinetically controlled addition of Me_3SiCN to *105* in the presence of $SnBr_4$ afforded the 1,4-*cis* product *106* with high selectivity.

In conclusion, the dissimilar selectivities exhibited by the two related tetrahydrofuran acetals shown in Fig. 4.30 are not the result of chelation of the Lewis acid. Instead, the substituent at C4 biases the conformation of the oxocarbenium ion, and inside attack provides the product with high *cis*-selectivity.

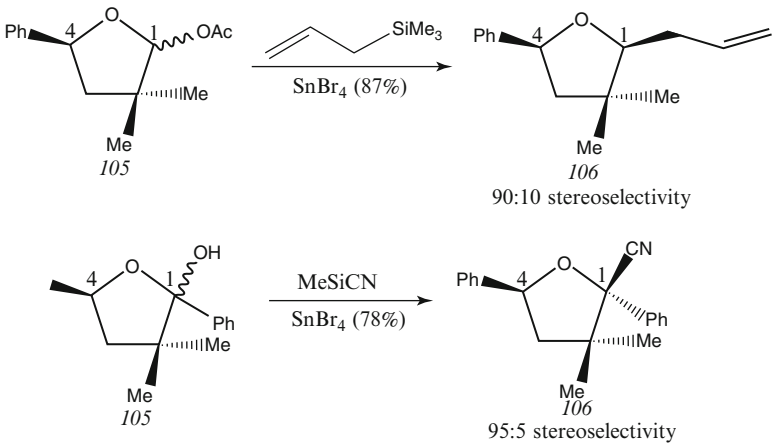

Fig. 4.37

References

1. Zechel DL, Withers SG (2000) Glycosidase mechanisms: anatomy of a finely tuned catalysts. Acc Chem Res 33:11–18
2. Allart B, Gatel M, Guillerm D, Guillerm G (1998) The catalytic mechanism of adenosylhomocysteine/methylthioadenosine nucleosidase from Escherichia coli. Chemical evidence for a transition state with substantial oxocarbenium character. Eur J Biochem 256:155–162
3. Banait NS, Jencks WP (1991) Reactions of anionic nucleophiles with α-D-glucopyranosyl fluoride in aqueous solution through a concerted, ANDN (SN2) mechanism. J Am Chem Soc 113:7951–7958
4. Zhu J, Bennet AJ (1998) Hydrolysis of (2-Deoxy-α-D-Glucopyranosyl) pyridinium salts: the 2-Deoxyglycosyl oxocarbenium is not solvent-equilibrated in water. J Am Chem Soc 120:3887–3893
5. Vasella A, Davies GJ, Böhm M (2002) Glycosidase mechanism. Curr Opin Chem Biol 6:619–629
6. Amyes TL, Jencks WP (1989) Lifetime of oxocarbenium ions in aqueous solution from common ion inhibition of the solvolysis of α-azido ethers by added azide ion. J Am Chem Soc 111:7888–7900
7. Richard JP, Williams KB, Amyes TL (1999) Intrinsic barriers for the reactions of oxocarbenium ion in water. J Am Chem Soc 121:8403–8404
8. Woods RJ, Andrews CW, Bowen JP (1992) Molecular mechanical investigations of the properties of oxocarbenium ions. 2. Application to glycoside hydrolysis. J Am Chem Soc 114:859–864
9. Nukada T, Bérces A, Whitfield DM (2002) Can the stereochemical outcome of glycosylation reactions be controlled by the conformational preferences of the glycosyl donor? Carbohydr Res 337:765–774
10. Nukada T, Bérces A, Wang L, Zgierski MZ, Whitfield DM (2005) The two-conformer hypothesis: 2, 3, 4, 6-tetra-O-methyl-mannopyranosyl-and glucopyranosyl oxocarbenium ions. Carbohydr Res 340:841–852
11. Miljković M, Yeagley D, Deslongchamps P, Dory Y (1997) Experimental and theoretical evidence of through-space electrostatic stabilization of the incipient oxocarbenium ion by an

axially oriented electronegative substituent during glycopyranoside acetolysis. J Org Chem 62:7597–7604
12. Woods RJ, Andrews CW, Bowen JP (1992) Molecular mechanical investigations of the properties of oxocarbenium ions. 1. Parameter development. J Am Chem Soc 114:850–858
13. Dudley TJ, Smoliakova IP, Hoffmann MR (1999) Theoretical study of 1-methoxy-2-sulfanylethan-1-yl cation: insight into intermediates in glycosidation reactions. J Org Chem 64:1247–1253
14. McDonnell C, Lopez O, Murphy P, Bolaños JGF, Hazell R, Bols M (2004) Conformational effects on glycoside reactivity: study of the high reactive conformer of glucose. J Am Chem Soc 126:12374–12385
15. Crich D, Chandrasekera NS (2004) Mechanism of 4, 6-O-benzylidene beta- mannosylation as determined by alpha-deuterium kinetic isotope effects. Angew Chem Int Ed Engl 43:5386–5389
16. Jensen HH, Bols M (2003) Steric effects are not the cause of the rate difference in hydrolysis of stereoisomeric glycosides. Org Lett 5:3419–3421
17. Chamberland S, Ziller JW, Woerpel KA (2005) Structural evidence that alkoxy substituents adopt electronically preferred pseudoaxial orientations in six-membered ring dioxocarbenium ions. J Am Chem Soc 127:5322–5323
18. Wiberg KB, Waldron RF (1991) Lactones. 3. A comparison of the basicities of lactones and esters. J Am Chem Soc 113:7705–7709
19. Ayala L, Lucero CG, Romero JAC, Tabacco SA, Woerpel KA (2003) Stereochemistry of nucleophilic substitution reactions depending upon substituent: evidence for electrostatic stabilization of pseudoaxial conformers of oxocarbenium ions by heteroatom substituents. J Am Chem Soc 125:15521–15528
20. Romero JAC, Tabacco SA, Woerpel KA (2000) Stereochemical reversal of nucleophilic substitution reactions depending upon substituent: reactions of heteroatom-substituted six-membered-ring oxocarbenium ions through pseudoaxial conformers. J Am Chem Soc 122:168–169
21. Hosokawa S, Kirschbaum B, Isobe M (1998) 1, 4-anti induction in C-glycosylation of pentose glycals. Tetrahedron Lett 39:1917–1920
22. Isobe M, Saeeng R, Nishizawa R, Konobe M, Nishikawa T (1999) Electronic factors in the C-glycosidation with silylacetylene. Chem Lett 6:467–468
23. Shenoy SR, Woerpel KA (2005) Investigation into the role of ion pairing in reactions of heteroatom-substituted cyclic oxocarbenium ions. Org Lett 7:1157–1160
24. Stevens RV, Lee AWM (1979) Stereochemistry of the Robinson-Schoepf reaction. A stereospecific total synthesis of the ladybug defense alkaloids precoccinelline and coccinelline. J Am Chem Soc 101:7032–7035
25. Stevens RV (1984) Nucleophilic additions to tetrahydropyridinium salts. Applications to alkaloid syntheses. Acc Chem Res 17:289–296
26. Deslongchamps P (1983) Stereoelectronic effects in organic chemistry. Pergamon Press, New York, pp 209–221
27. Ohno K, Yoshida H, Watanabe H, Fujita T, Matsuura H (1994) Conformational study of 1-butanol by the combined use of vibrational spectroscopy and ab initio molecular orbital calculation. J Phys Chem 98:6924–6930
28. Lucero CG, Woerpel KA unpublished
29. Asano N (2003) Glycosidase inhibitors: update and perspectives on practical use. Glycobiology 13:93R–104R
30. Araki Y, Kobayashi N, Ishido Y, Nagasawa J (1987) Synthetic studies with fluorinated intermediates. 3. Highly stereoselective C-α-D-ribofuranosylation. Reactions of ribofuranosyl fluoride derivatives with enol trimethylsilyl ethers and with allyl trimethylsilane. Carbohydr Res 171:125–139
31. Schmitt A, Reissig H-U (1990) Highly diastereoselective route to disubstituted tetrahydrofuran derivatives by substitution of γ-lactols with silylated nucleophiles. Synlett 40–42

32. Schmitt A, Reissig H-U (1995) Stereoselective substitution at phenyl-substituted γ-lactols with organometallic reagents. Chem Ber 128:871–876
33. Schmitt A, Reissig H-U (2000) On the stereoselectivity of γ − lactol substitutions with allyl and propargylsilanes-synthesis of disubstituted tetrahydrofuran derivatives. J Org Chem 23:3893–3901
34. Jensen HH, Pedersen CM, Bols M (2007) Going to extremes: "super"armed donors in glycosylation chemistry. Chem Eur J 13:7576–7582
35. Jensen HH, Bols M (2006) Stereoelectronic substituent effects. Acc Chem Res 39:259–265
36. Roush WR, Sebesta DP, Bennett CE (1997) Stereoselective preparation of 2-deoxy-β-glycosides from glycal precursors. 1. Stereochemistry of the reactions of D-glycal derivatives with phenylsulfenyl chloride and phenylselenyl chloride. Tetrahedron 53:8825–8836
37. Durham TB, Roush WR (2003) Stereoselective synthesis of 2-deoxy-beta-galactosides via 2-deoxy-2-bromo- and 2-deoxy-2-iodogalapyranosyl donors. Org Lett 5:1871–1874
38. Arnés X, Diaz Y, Castillón S (2003) Phenyl-2-deoxy-2-iodo-1-thio-glycosides: new glycosyl donors for the stereoselective synthesis of 2-deoxy-oligosaccharides. Synlett 14:2143–2146
39. Morales Serna JA, Boutureira O, Díaz Y, Matheu MI, Castillón S (2007) Recent advances in the glycosylation of sphingosines and ceramides. Carbohydr Res 342:1595–1612
40. Ünligil UM, Rini JM (2000) Glycosyltransferase structure and mechanism. Curr Opin Struct Biol 10:510–517
41. Rye CS, Withers SG (2000) Glycosidase mechanism. Curr Opin Chem Biol 4:573–580
42. Sinott ML (1990) Catalytic mechanism of enzymic glycosyl transfer. Chem Rev 90:1171–1202
43. Kempton JB, Withers SG (1992) Mechanism of Agrobacterium beta-glucosidase: Kinetic studies. Biochemistry 31:9961–9969
44. Tull D, Withers SG (1994) Mechanisms of cellulases and xylanases: a detailed kinetic study of the exo-beta-1, 4-glucanase from Cellulomonas fimi. Biochemistry 33:6363–6370
45. Ionescu AR, Whitfield DM, Zgierski MZ, Nukada T (2006) Investigation into the role of oxacarbenium ions in glycosylation reactions by ab initio molecular dynamics. Carbohydr Res 341:2912–2920
46. Ionescu AR, Whitfield DM, Zgierski MZ (2007) O-2 Substituted pyrano oxacarbenium ions are C-2-O-2–2-fold rotors with a strong syn preference. Carbohydr Res 342:2793–2800
47. Moscona A (2005) Neuraminidase inhibitors for influenza. New Engl J Med 353:1363–1373
48. von Itzstein M, Wu WY, Kok GB, Pegg MS, Dyason JC, Jin B, Phan TV, Smythe ML, Hume F et al (1993) Rational design of potent sialidase-based inhibitors of influenza virus replication. Nature 363:418–423
49. Breuer H-WM (2003) Review of acarbose therapeutic strategies in the long-term treatment and in the prevention of type 2 diabetes. Int J Clin Pharm Th 41:421–440
50. Scott LJ, Spencer CM (2000) Miglitol: a review of its therapeutic potential in type 2 diabetes mellitus. Drugs 59:521–549
51. Goss PE, Baker MA, Carver JP, Dennis JW (1995) Inhibitors of carbohydrate processing: a new class of anticancer agents. Clin Cancer Res 1:935–944
52. Lillelund VH, Jensen HH, Liang X, Bols M (2002) Recent developments of transition-state analogue glycosidase inhibitors of non-natural product origin. Chem Rev 102:515–554
53. Gloster TM, Meloncelli P, Stick RV, Vasella A, Davies GJ (2007) Glycosidase inhibition: an assessment of the binding of 18 putative transition-state mimics. J Am Chem Soc 129:2345–2354
54. Wicki J, Williams SJ, Withers SG (2007) Transition-state mimicry by glycosidase inhibitors: a critical kinetic analysis. J Am Chem Soc 129:4530–4531
55. Svansson L, Johnston BD, Gu J-H, Patrick B, Pinto BM (2000) Synthesis and conformational analysis of a sulfonium-ion analogue and the glycosidase inhibitor castanospermin. J Am Chem Soc 122:10769–10775

56. Heck M-P, Vincent SP, Murray BW, Bellamy F, Wong C-H, Moskowski CJ (2004) Cyclic amidine sugars as transition-state analogue inhibitors of glycosidases: potent competitive inhibitors of mannosidases. J Am Chem Soc 126:1971–1979
57. Davis BG, Hull A, Smith C, Nash RJ, Watson AA, Winkler DA, Griffiths RC, Fleet GWJ (1998) 5-epi-deoxyrhamnojirimycon is a potent inhibitor of an α-L-rhamnosidase: 5-epi-deoxymannojirimycin is not potent inhibitor of an α-D-mannosidase. Tetrahedron Asymmetr 9:2947–2960
58. Tong MK, Papandreou G, Ganem B (1990) Potent, broad-spectrum inhibition of glycosidases by an amidine derivative of D-glucose. J Am Chem Soc 112:6137–6139
59. Ganem B, Papandreou G (1991) Mimicking the glucosidase transition state: shape/charge consideration. J Am Chem Soc 113:8984–8985
60. Williams SJ, Notenboom V, Wickl J, Rose DR, Withers SG (2000) A new, simple, high-affinity glycosidase inhibitor: analysis of binding through x-ray crystallography, mutagenesis, and kinetic analysis. J Am Chem Soc 122:4229–4230
61. Amat L, Carbó-Dorca RJ (2000) Molecular electronic density fitting using elementary Jacobi rotations under atomic shell approximation. Chem Inf Comput Sci 40:1188–1198
62. Winkler DA (1996) Molecular modeling studies of "flap up" mannosyl cation mimics. J Med Chem 39:4332–4334
63. Jung KH, Schmidt PR (2003) In: Wong C-H (ed) Carbohydrate based drug discovery, vol 2. Wiley VCH, Weinheim, pp 609–660
64. Davies GJ, Ducros VM-A, Varrot A, Zechel DL (2003) Mapping the conformational itinerary of β-glycosidases by X-ray crystallography. Biochem Soc Trans 31:523–527
65. Larsen CH, Ridgway BH, Shaw JT, Smith DM, Woerpel KA (2005) Stereoselective C-glycosylation reactions of ribose derivatives: electronic effects of five-membered ring oxocarbenium ions. J Am Chem Soc 127:10879–10884
66. Alabugin IV (2000) Stereoelectronic interactions in cyclohexane, 1, 3-dioxane, 1.3-oxathiane, and 1, 3-dithian: W-effect, σC-X↔σ*-H interactions, anomeric effect-what is really important? J Org Chem 65:3910–3919
67. Plante OJ, Palmacci ER, Andrade RB, Seeberger PH (2001) Oligosaccharide synthesis with glycosyl phosphate and dithiophosphate triesters as glycosylating agents. J Am Chem Soc 123:9545–9554
68. Lee YJ, Baek JY, Lee B-Y, Kang SS, Paek H-S, Jeon HB, Kim KS (2006) 2′-Carboxybenzyl glycosides: glycosyl donors for C-glycosylation and conversion into other glycosyl donors. Carbohydr Res 341:1708–1716
69. Beignet J, Tierman J, Woo CH, Kariuki BM, Cox LR (2004) Stereoselective synthesis of allyl-C-mannosyl compounds: use of a temporary silicon connection in intramolecular allylations strategies with allyl silanes. J Org Chem 69:6341–6356
70. Brunel FM, Taylor KG, Spatola AF (2003) Synthesis of permethylated α-D- mannosyl-acetic acid, a new type of bio-conjugate. Tetrahedron Lett 44:1287–1289
71. Nishikawa T, Ishikawa M, Isobe M (1999) Synthesis of a α-C-mannosyltryptophan derivative, naturally occurring C-glycosyl amino acid found in human ribonuclease. Synlett 123–125
72. Roche D, Bänteli R, Winkler T, Casset F, Ernst B (1998) Synthesis of benzylated (R)-and (S)-aminoethyl-C-α-D-mannosides as conformationally restricted building blocks for the preparation of E- and P-selectin antagonists. Tetrahedron Lett 39:2545–2548
73. Bertozzi C, Bednarski M (1992) C-Glycosyl compounds bind to receptors on the surface of Escherichia coli and can target proteins to the organism. Carbohydr Res 223:243–253
74. Panek JS, Sparks MA (1989) Oxygenated allylic silanes: useful homoenolate equivalents for the stereoselective C-glycosidation of pyranoside derivatives. J Org Chem 54:2034–2038
75. Hosomi A, Sakata Y, Sakurai H (1987) Stereoselective synthesis of 3-(D- glycopyranosyl) propenes by use of allylsilanes. Carbohydr Res 171:223–232

76. Akira H, Yasuyuki S, Hideki S (1984) Highly stereoselective C-allylation of glycopyranosides with allylsilanes catalyzed by silyl triflate or iodosilane. Tetrahedron Lett 25:2383–2386
77. McDevitt JP, Lansbury PT (1996) Glycosamino acids: new building blocks for combinatorial synthesis. J Am Chem Soc 118:3818–3828
78. Marron TG, Woltering TJ, Weitz-Schmidt G, Wong C-H (1996) C-mannose derivatives as potent mimics of sialyl Lewis X. Tetrahedron Lett 37:9037–9040
79. Nicolaou KC, Hwang C-K, Duggan ME (1985). J Am Chem Soc 111:6682–6690
80. Giannis A, Sandhoff K (1985) Stereoselective synthesis of α-C-allylglycopyranosides. Tetrahedron Lett 26:1479–1482
81. Singh G, Vankayalapati H (2001) Efficient stereocontrolled synthesis of C-glycoside using glycosyl donors substituted by propane 1,3-diyl phosphate as the leaving group. Tetrahedron Asymmetr 12:1727–1735
82. Seeman JI (1983) Effect of conformational change on reactivity in organic chemistry. Evaluations, applications, and extensions of Curtin-Hammett Winstein-Holness kinetics. Chem Rev 83:83–134
83. Seeman JI (1986) The Curtin-Hammett principle and the Winstein-Holness equation. New definition and recent extensions to classical concepts. J Chem Educ 63:42–48
84. Lucero CG, Woerpel KA (2006) Stereoselective C-glycosylation reactions of pyranoses: the conformational preference and reactions of the mannosyl cation. J Org Chem 71:2641–2647
85. Olah GA, Dunne K, Mo YK, Szilagyi PJ (1972) Stable carbocations. CXXVIII protonated acyclic carboxylic acid anhydrides and their cleavage to oxocarbenium ions. Question of the formyl cation in superacid media. J Am Chem Soc 94:4200–4205
86. Olah GA, Berrier AL, Prakash GKS (1982) Onium ions. 24. Oxygen-17 NMR spectroscopic study of oxonium and carboxonium ions. J Am Chem Soc 104:2373–2376
87. Prakash GKS, Rasul G, Liang G, Olah GA (1996) 13C NMR spectroscopic and Density Functional Theory (DFT), ab initio, and IGLO theoretical study of protonated cycloalkylcarboxylic acids (carboxonium ions) and their acyl cations (oxocarbenium ions). J Phys Chem 100:15805–15809
88. Suga S, Suzuki S, Yamamoto A, Yoshida J (2000) Electrooxidative generation and accumulation of alkoxycarbenium ions and their reactions with carbon nucleophiles. J Am Chem Soc 122:10244–10245
89. Suzuki S, Matsumoto K, Kawamura K, Suga S, Yoshida J (2004) Generation of alkoxycarbenium ion pools from thioacetals and applications to glycosylation chemistry. Org Lett 6:3755–3758
90. Yoshida J, Suga S (2002) Basic concepts of “cation pool” and “cation flow” methods and their applications in conventional and combinatorial organic synthesis. Chem Eur J 8:2650–2658
91. Deslongchamps P, Chêvert R, Taillefer RJ, Moreau C, Saunders JK (1975) Hydrolysis of cyclic orthoesters. Stereoelectronic control in the cleavage of hemiorthoester tetrahedral intermediates. Can J Chem 53:1601–1615
92. Childs RF, Kostyk MD, Lock CJ, Mahedran M (1991) Structural studies on 6-ethoxytetrahydropyrylium cations; stereoelectronic control in the reactions of lactonium salts. Can J Chem 69:2024–2032
93. Yang MT, Woerpel KA (2009) The effect of electrostatic interactions on conformational equilibria of multiply substituted tetrahydropyran oxocarbenium ions. J Org Chem 74:545–553
94. Jensen HH, Nordstrøm LU, Bols M (2004) The disarming effect of the 4,6-acetal group on glycoside reactivity: torsional or electronic? J Am Chem Soc 126:9205–9213
95. Weldon AJ, Vickrey TL, Tschumper GS (2005) Intrinsic conformational preferences of substituted cyclohexanes and tetrahydropyrans evaluated at the CCSD(T) complete basis set limit: implications for the anomeric effect. J Phys Chem 109:11073–11079

96. Woodcock HL, Moran D, Pastor RW, McKerell AD Jr, Brooks BR (2007) Ab initio modeling of glycosyl torsions and anomeric effects in a model carbohydrate: 2-ethoxy tetrahydropyran. Biophys J 93:1–10
97. Law RW, Sasanuma Y (1996) Nature of the non-bonded (C-H):. . .O interaction of ethers CH3O-(CH2)n-OCH3 (n = 4–8). J Chem Soc Faraday Trans 92:4885–4888
98. Namchuk MN, McCarter JD, Becalski A, Andrews T, Withers SG (2000) The role of sugar substituents in glycoside hydrolysis. J Am Chem Soc 122:1270–1277
99. Larsen CH, Ridgway BH, Shaw JT, Woerpel KA (1999) A stereoelectronic model to explain the highly stereoselective reactions of nucleophiles with five-membered-ring oxocarbenium ions. J Am Chem Soc 121:12208–12209
100. Smith DM, Tran MB, Woerpel KA (2003) Nucleophilic additions to fused, bicyclic five-membered ring oxocarbenium ions: evidence for preferential attack on the inside face. J Am Chem Soc 125:14149–14152
101. Smith DM, Woerpel KA (2004) Using stereoelectronic effects to explain selective reactions of 4-substituted five-membered ring oxocarbenium ions. Org Lett 6:2063–2066
102. Schmitt A, Reissig H-U (2000) On the stereoselectivity of γ-lactol substitutions with allyl- and propargylsilanes – synthesis of disubstituted tetrahydrofuran derivatives. Eur J Org Chem 3893–3901
103. Frank X, Hocquemiller R, Figadére B (2002) Access to 2,5-disubstituted tetrahydrofurans from Grignard reagents and hemiacetal derivatives. Chem Commun 160–161
104. Nishiyama Y, Katoh T, Deguchi K, Morimoto Y, Itoh KJ (1997) Stereoselective synthesis of 2,2,5-trisubstituted tetrahydrofurans via the Lewis acid assisted reaction of cyclic hemiketals with nucleophiles. J Org Chem 62:9339–9341
105. Mukaiyama T, Shimpuku T, Takashima T, Kobayashi S (1989) Stereoselective 1,2-cis glycosylation reaction of 1-O-acetylribose with silylated nucleophiles promoted by a new catalyst system. Chem Lett 145–148
106. Curtin DY (1954) Stereochemical control of organic reactions. Differences in behavior of diastereoisomers. I. Ethane derivatives. The cis effect. Rec Chem Prog 15:111–128
107. Shaw JT, Woerpel KA (1999) Divergent diastereoselectivity in the addition of nucleophiles to tetrahydrofuran-derived oxonium ions. Tetrahedron 55:8747–8756
108. Smith DM, Woerpel KA (2003) Nucleophilic additions to fused bicyclic five-membered ring oxocarbenium ions: evidence for preferential attack on the inside face. J Am Chem Soc 125:14149–14152
109. Houk KN, Paddon-Row MN, Rondan NG, Wu Y-D, Brown FK, Spellmeyer DC, Metz JT, Li Y, Loncharich RJ (1986) Theory and modeling of stereoselective organic reactions. Science 231:1108–1117
110. Allinger NL, Fermann JT, Allen WD, Shaefer III HF (1997) The torsional conformations of butane: definitive energetics from ab initio methods. J Chem Phys 106:5143–5250
111. Bürgi H-B, Houshell WD, Nachbar RB Jr, Mislow K (1983) Conformational dynamics of propane, di-tert-butylmethane, and bis(9-triptycyl)methane. An analysis of the symmetry of two threefold rotors on a rigid frame in terms of nonrigid molecular structure and energy hypersurfaces. J Am Chem Soc 105:1427–1438
112. Pasto DJ, Gontarz JA (1971) Characterization of torsional angle effects as the dominant steric effect in the hydroxymercuration of substituted cyclohexenes. J Am Chem Soc 93:6909–6913

Chapter 5
Armed-Disarmed Concept in the Synthesis of Glycosidic Bond

Fraser-Reid et al. reported [1] that n-pentenyl glycosides undergo chemospecific cleavage *1* → *2* → 3, with *N*-bromosuccinimide under conditions that leave a wide variety of other protecting groups unaffected (Fig. 5.1).

According to the proposed mechanism (Fig. 5.1), the addition of water to the reaction mixture will lead to hydrolysis but the addition of alcohol or another sugar having a free hydroxyl group will lead to the formation of glycoside or a disaccharide. In the course of these studies, Fraser-Reid et al. [1] observed that sugar molecules having an acyloxy group at the C2 carbon (*6* in Fig. 5.2) hydrolyzed much more slowly than if they had an alkoxy group (*7* in Fig. 5.2). This observation suggested that the n-pentenyl glycoside could be made more or less reactive (it could be *armed or disarmed*) by the type of protecting group placed on the C2 oxygen.

The ability of the C2 acyloxy group to disarm the n-pentenyl glycoside was rationalized as shown in Fig. 5.3. Thus, it can be assumed that the cyclic halonium ions *8* and *9* are formed reversibly [2] and that the electron density on the glycosidic oxygen is depleted in 2-*O*-acyl derivatives so that nucleophilic attack of this oxygen on the halonium ion is less favored than in the 2-*O*-alkyl counterpart *9*. The reason for this is that the electron-withdrawing group at the C2 carbon makes the C2 carbon slightly positively charged so that the formation of another positive charge at the C1 carbon is not a favorable process [there cannot exist two positive charges on two neighboring carbons (C1 and C2) (Fig. 5.3).].

Consequently, the armed glycosyl donors react with electrophiles faster than the disarmed ones, and therefore in a solution containing both an armed and disarmed glycosyl donor molecules, whereby disarmed glycosyl donor molecules have one free hydroxyl group, the reaction with an electrophile will result in cross-coupling and not self-coupling, i.e., an armed glycosyl donor will react with the disarmed one, whereas a disarmed donor will not react with itself [3] as illustrated in Fig. 5.5. The promoters for the activation of n-pentenyl group [4, 5] are iodonium dicollidine perchlorate (IDCP) and *N*-iodosuccinimide/triethylsilyl triflate (NIS/Et_3SiOTf).

M. Miljkovic, *Electrostatic and Stereoelectronic Effects in Carbohydrate Chemistry*,
DOI 10.1007/978-1-4614-8268-0_5, © Springer Science+Business Media New York 2014

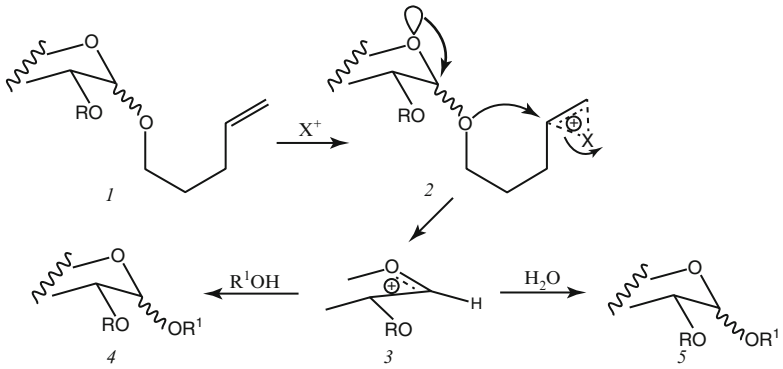

Fig. 5.1

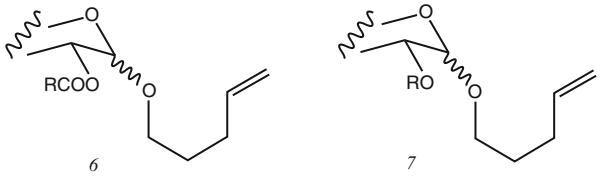

Fig. 5.2

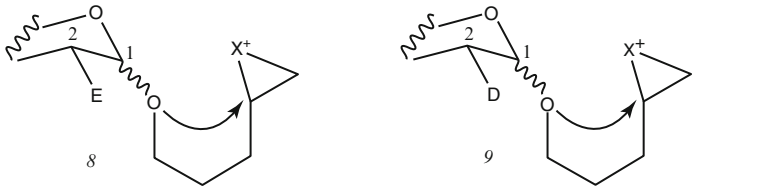

a) E = OAc
b) E = Br (electron withdrawing group)

a) D = OBn
b) D = H (electron donating group)

Fig. 5.3

An example for the synthesis of a trisaccharide using armed-disarmed concept is given in Fig. 5.6. Pent-4-enyl-2,3,4,6-tetra-*O*-benzyl-α,β-D-glucopyranoside *20* is coupled to pent-4-enyl-2,3,4-tri-*O*-acetyl-α,β-D-glucopyranoside *21* in the presence of IDCP giving the disaccharide *22* as a mixture of anomers. Disarmed disaccharide could be further glycosylated without prior modification with another acceptor, which will terminate the oligosaccharide chain because the acceptor is not pent-4-enyl glycoside (Fig. 5.6).

Veeneman and van Boom [6] have attempted to synthesize L-rhamnose-containing fragments from *Streptococcus pneumoniae* type-specific capsular

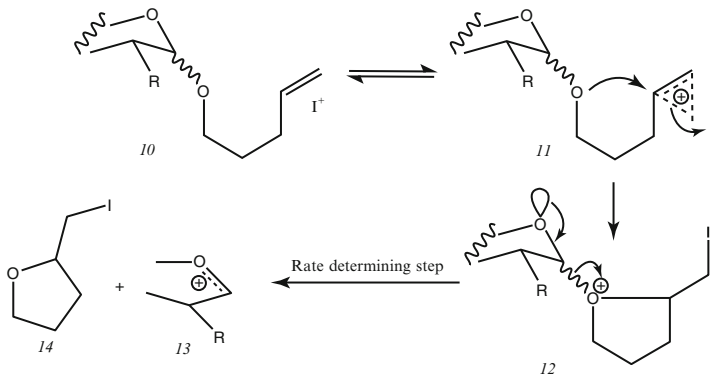

Fig. 5.4

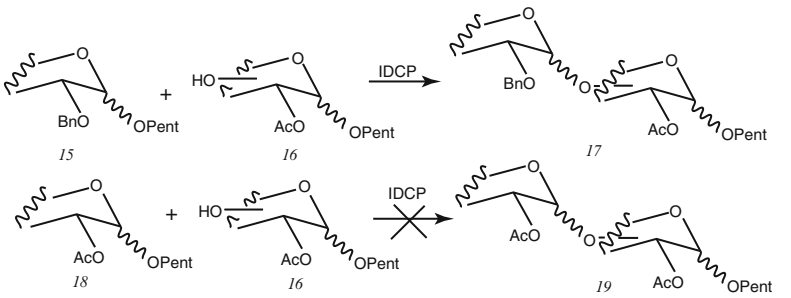

IDCP = Iodonium dicolidine perchlorate

Fig. 5.5

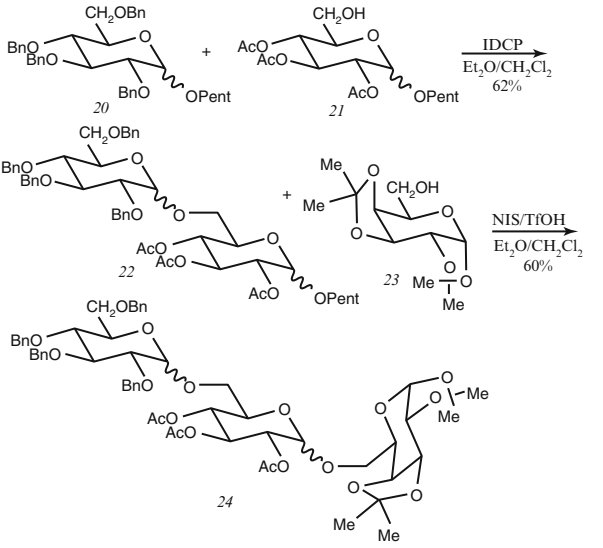

Fig. 5.6

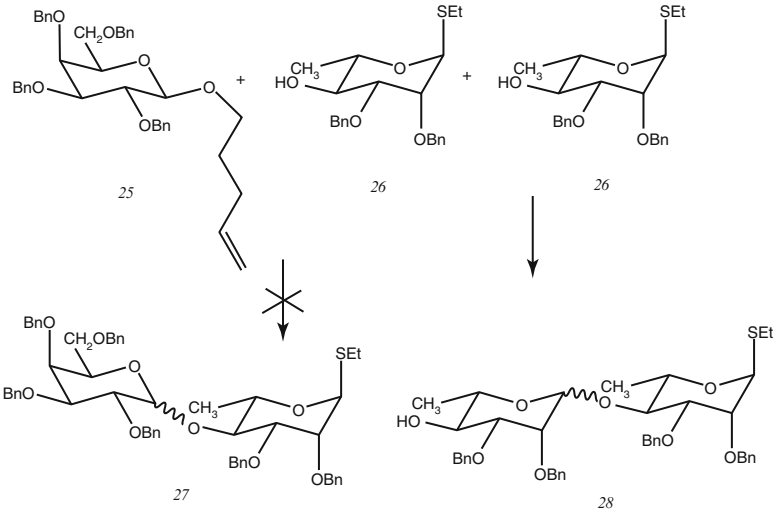

Fig. 5.7

Fig. 5.8

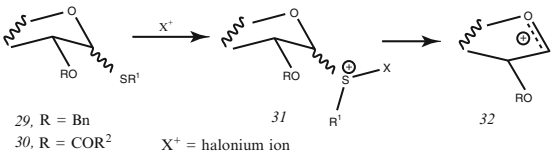

polysaccharide using the Fraser-Reid et al. approach [7]. They attempted to condense the n-pentenyl galactosyl donor *25* (Fig. 5.7) with ethyl 1-thio-L-rhamnopyranoside acceptor *26* in the presence of activator iodonium dicollidine perchlorate (IDCP). However, analysis of the glycosidation reaction revealed no formation of the expected disaccharide *27*, but merely products arising from self-condensation of *26*, the disaccharide *28* (Fig. 5.7). In the same year (1990), Konradsson et al. [5]. published their studies on armed-disarmed thioglycoside donors for synthesis of oligosaccharides.

In the view of the well-known reaction of thioglycosides with NBS (*N*-bromosuccinimide), which generates the unstable cationic species *31* in the course of formation of oxocarbenium ion *32* (Fig. 5.8), Konradsson et al. [5]. reported that *N*-iodosuccinimide/trifluoromethanesulfonic acid induces the same reactivity with disarmed thioglycosides as substrates. (NIS/AgOTf or NIS/Et_3SiOTf also proves to be an excellent source of iodonium ion.)

Thus, by treating an armed thioglycosyl donor with a disarmed thioglycosyl donor that has one hydroxyl group free in the presence of NIS/TfOH, NIS/AgOTf, or NIS/Et_3SiOTf, they synthesized disaccharides in good yields (Fig. 5.9).

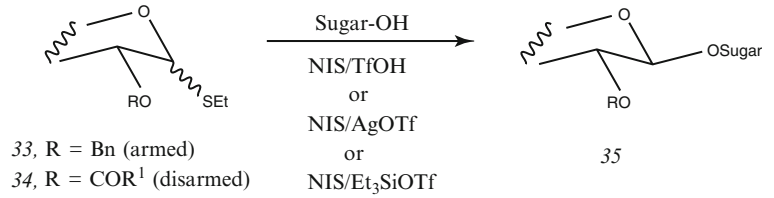

Fig. 5.9

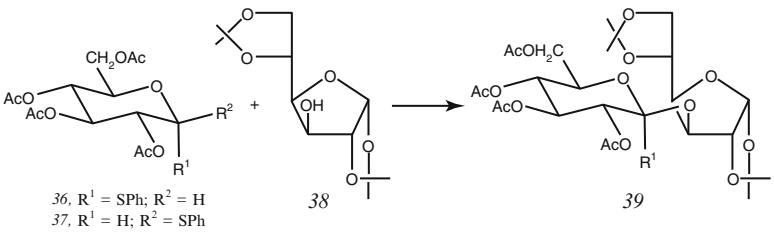

Fig. 5.10

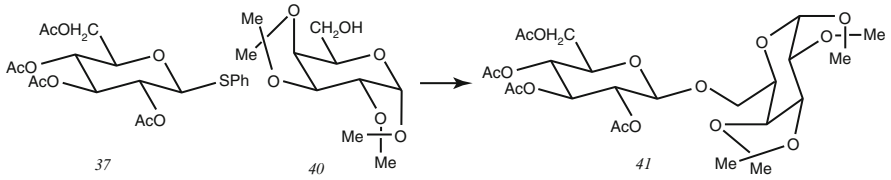

Fig. 5.11

The reaction of phenyl 2,3,4,6-tetra-*O*-acetyl-α-D-thioglucopyranoside *36* with 1,2:5,6-di-*O*-isopropylidene-α-D-glucofuranose *38* in the presence of NIS/TfOH as promoter gave the corresponding disaccharide *39* in 86 % yield (Fig. 5.10).

The same disaccharide *39* was obtained in 83 % yield by reaction of phenyl 2,3,4,6-tetra-*O*-acetyl-β-D-thioglucopyranoside *37* with 1,2:5,6-di-*O*-isopropylidene-α-D-glucofuranose *38* in the presence of NIS/TfOH. Reaction of phenyl 2,3,4,6-tetra-*O*-acetyl-β-D-thioglucopyranoside *37* with 1,2:3,4-di-*O*-isopropylidene-α-D-galactopyranose *40* gave in the presence of NIS/TfOH as promoter disaccharide *41* in 90 % yield (Fig. 5.11).

The discovery of thioglycoside-mediated formation of α-glycosidic linkages promoted by IDCP led to the development of a new chemoselective glycosylation strategy, the so-called one-pot sequential glycosylation [8–17]. This approach is based on the observation that a large disparity between the reactivities of different glycosyl donors can be achieved by varying the protecting groups and the electron-donating or electron-withdrawing character of the leaving group within a given class of glycosyl donors (e.g., thioglycosides). As a result, at each glycosidic

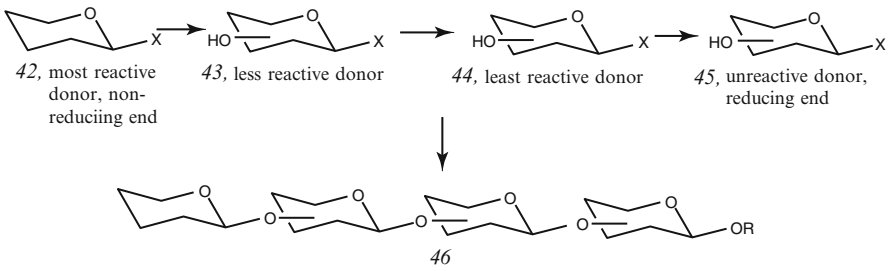

Fig. 5.12

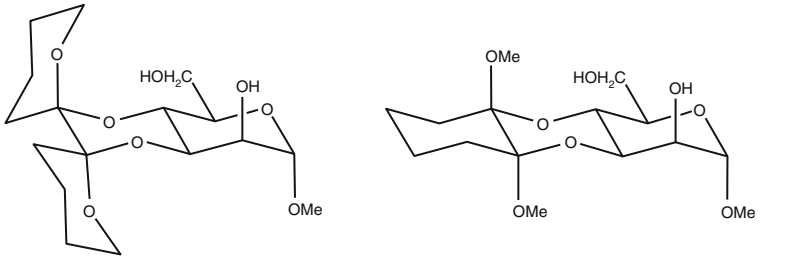

Fig. 5.13

coupling step, a high degree of sequence selectivity can be achieved between competing donors, even though identical chemistry is performed, thus eliminating thus the need for protecting group manipulation between coupling steps. A synthetic approach is designed such that the choice of protecting groups on monosaccharide components [8–10] or the combination of protecting groups and the anomeric substituent [11, 12] leads to a decrease in donor reactivity over the course of a synthetic sequence. The most reactive donor is used for the nonreducing end, and the most unreactive donor is used for the reducing end of the given target oligosaccharide (Fig. 5.12).

Wilson and Fraser-Reid [18] studied the rates of hydrolysis of variously substituted n-pentenyl glucopyranosides and found that cyclic acetals and acetyl groups exert profound effect upon the relative and absolute rates of anomeric activation.

Douglas et al. [19] and Zhang et al. [17]. published studies on the dependence of the activation of glycosyl donor on the nature of protecting groups in donor molecule making thus a major contribution toward the development of the so-called "one-pot synthesis of oligosaccharides".

Douglas et al. [19]. discovered that the cyclohexane-1,2-diacetal (CDA) protection group (e.g., *48*) (Fig. 5.13) as well as the octahydro-2,2′-bi-2H-pyran-2,2′-diyl (dispoke) group (e.g., *47*) had a reactivity tuning effect between that of the fully

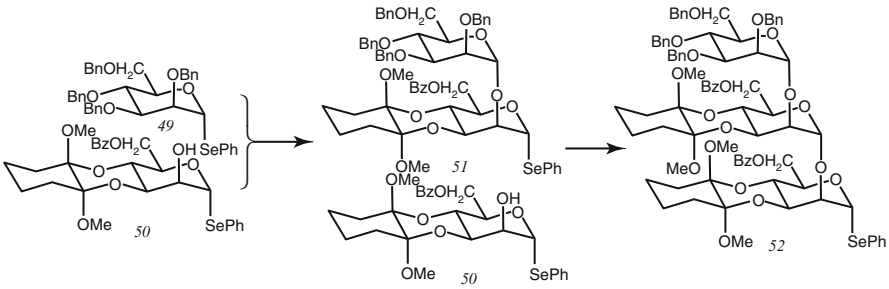

Fig. 5.14

benzylated and fully benzoylated system. This discovery immediately led to the development of preparing tri-and tetrasaccharides without the need for protective group manipulations [16, 20]. The general strategy is illustrated [16] in Fig. 5.14 by the preparation of a trisaccharide *52*.

Friesen and Danishefsky [21] reported an interesting application of armed-disarmed concept in their methodology for the synthesis of oligosaccharides via controlled oxidative coupling of glycals. Thus, a glycal which serves as glycosyl acceptor (*54*) shall have one free hydroxyl group that will be glycosidically linked to a glycosyl donor *53* and all the other hydroxyl groups acylated. For example, *53* (3,4,6-tri-*O*-benzyl-D-*arabino*-glycal) which serves as glycosyl donor has all of its hydroxyl groups benzylated, since the electron-donating C3 alkoxy group enhances the nucleophilicity of the C1–C2 double bond toward the iodonium cation, whereas in the 3,6-di-*O*-benzoyl-D-*arabino*-glycal *54* that serves as a glycosyl acceptor, the electron-withdrawing C3 acyl group deactivates (disarms) the nucleophilicity of the C1–C2 double bond toward electrophiles such as the iodonium cation. So in an equimolar mixture of glycosyl donor and glycosyl acceptor with the equimolar amount of iodonium cation, the electrophile will attack much faster the C1–C2 double bond of glycosyl donor *53* than the C1–C2 double bond of glycosyl acceptor *54* (Fig. 5.15). The result is the formation of the glycosidic bond between *53* and *54*. To reiterate the scheme with another glycal, the two acyl groups of *55* are cleaved and the hydroxyl groups are alkylated (*55* → *56*). The AC glycal *56* became now glycosyl donor, and diacylmonohydroxyglycal *54* is the glycosyl acceptor. In this way a trisaccharide ACD *57* is readily produced. The coupling reactions, presumably involving a 1,2-iodonium ion intermediate, proceed in a stereoselective 1,2-diaxial fashion yielding only the α-glycosides. This process can be reiterated.

The glycosyl donor 53 and glycosyl acceptor *54* gave on iodoglycosylation the 3,4,6-tri-*O*-benzyl-2-deoxy-2-iodo-α-D-mannopyranosyl-D-*arabino*-glycal *55* as the exclusive product. No other glycals or stereoisomers of *55* were detected. As we have seen this disaccharide chain can be further extended by hydrolyzing the two benzoyl groups in ring B and protecting the two obtained hydroxyl groups as TBS ethers (*55* → *56*). In this way the glycal *56* will be armed again. The coupling of *56* with *54* produces the trisaccharide *57* (Figs. 5.15 and 5.16). By repeating the same steps again, tetrasaccharide, pentasaccharide, etc. can be synthesized.

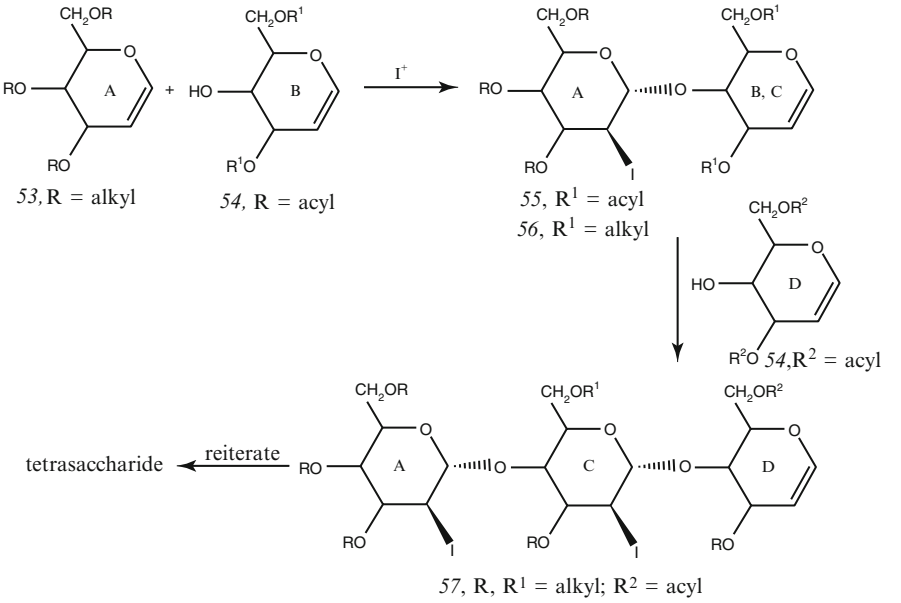

Fig. 5.15

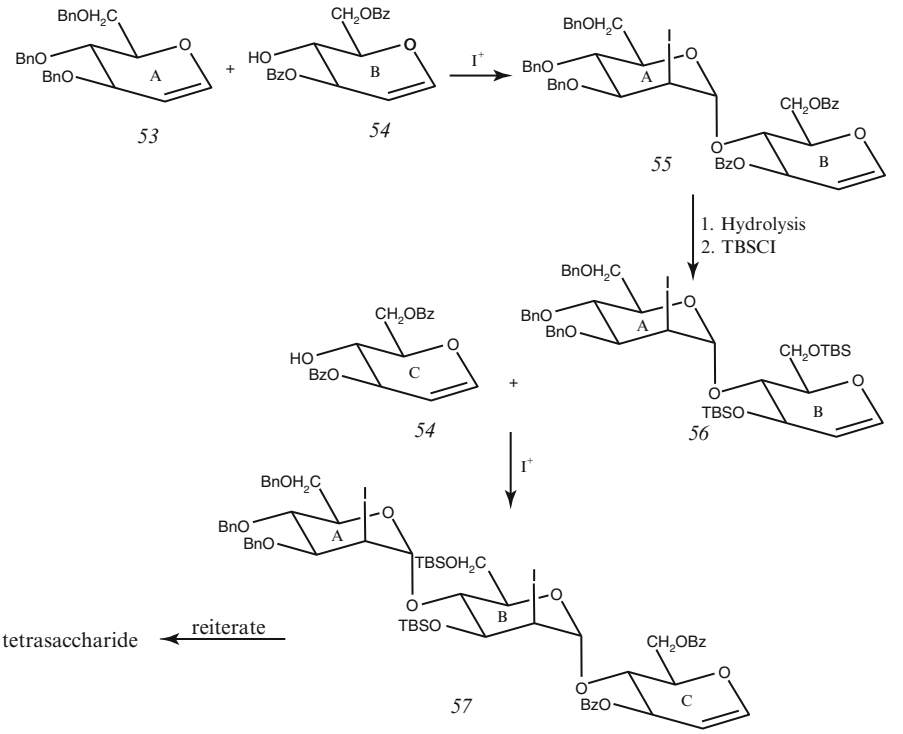

Fig. 5.16

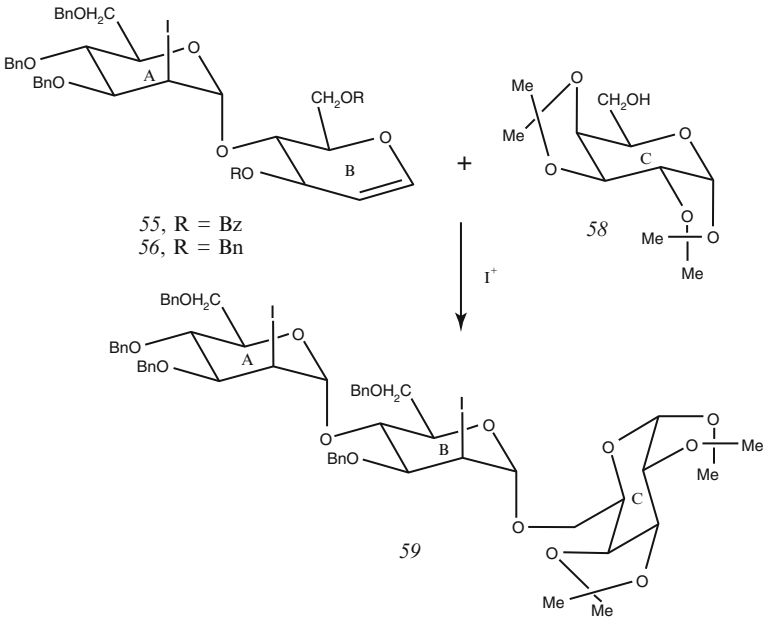

Fig. 5.17

On the other hand, glycal *55* can be coupled to a non-glycal acceptor, such as 1,2:3,4-di-*O*-isopropylidene-α-D-galactopyranose *58,* in the presence of I^+ terminating thus the chain elongation (Fig. 5.17).

5.1 Stereoelectronic Effects of Substituents: Polyhydroxylated Piperidines and Sugars

A very interesting article on the stereoelectronic substituent effect appeared recently [22] in which Jensen and Bols examined the influence of the orientation of a substituent on a pyranose, piperidine, isofagomine, etc., ring upon the chemical properties and the reactivity of this six-membered ring molecule. Thus, they compared the pK_a values of isofagomine *60* and its three stereoisomers *61*, *62*, and *63* (Fig. 5.18) [23, 24].

As can be seen from Fig. 5.18, the pK_a in the series of conjugate acids of isofagomine *60* and its stereoisomers *61–63* increased with the increasing number of axial hydroxyl groups [23, 25] and their proximity to the positively charged nitrogen. An axial OH-3 group appeared to increase the base strength [it should be noted that this increase (0.8 pH units) in base strength is taking place only when the axial OH is compared to the equatorial OH group at the same location].

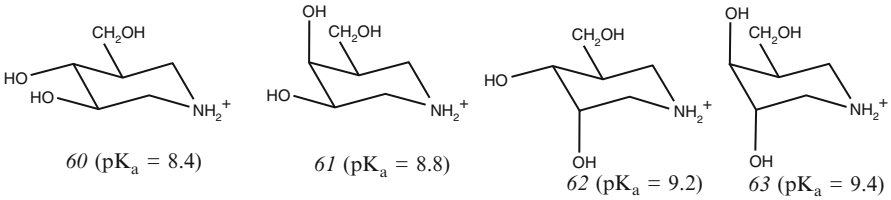

60 (pK_a = 8.4) *61* (pK_a = 8.8) *62* (pK_a = 9.2) *63* (pK_a = 9.4)

Fig. 5.18

Table 5.1 Axial and equatorial substituent effect on piperidine base strength in water at 25 °C[a]

R group	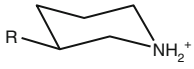	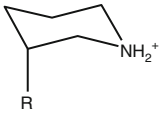	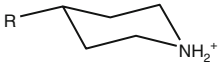	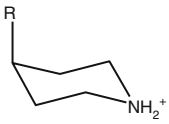
H	0	0	0	0
OH (eq)	1.3	–	0.6	–
OH(ax)	–	0.5	–	0.2
F(eq)	2.3	–	1.7	–
COO^- (eq)	0.5	–	0.2	–
COOMe (eq)	1.2	–	–	–
COOMe (ax)	0.2	–	–	–
CN	2.8	3.0	–	–
CH_2OH	0.4	0.5	–	–

[a]The numbers are σ_s values and are in pH units. The pK_a of the piperidine conjugate acid is decreased by the indicated substituent. Thus, base strength can be calculated as pK_a (substituted amine) = pK_a (unsubstituted amine) $-\sum\sigma_s$

Overall, the axial OH groups decrease the base strength when compared to the corresponding deoxy derivative. A 4-OH increases basicity by 0.4 pH units when placed axially rather than equatorially.

Jensen et al. [23]. studied more than 60 different hydroxylated piperidine and hexahydropyridazines, and the measured stereoelectronic effects are summarized in Table 5.1. The σ_s value of each substituent is the basicity decreasing effect in pK units. As can be seen, the axial OH decreases the base strength of the amine by 0.5 and 0.2 units when it is in the β- and γ-position, respectively, relative to the amine, while the equatorial OH decreases the pK_a by 1.3 and 0.6 in those instances. Thus, the equatorial OH is significantly more electron-withdrawing than the axial OH.

Other substituents, such as F, ester, and carboxylate functions were also found to result in considerable variation of pK_a depending on whether they were axial or equatorial, while epimerization of CH_2OH, $CONH_2$, and CN did not cause a great deal of change to base strength.

The observed differences are possibly caused by several effects, but can be, nevertheless, largely and satisfactorily explained by differences in charge-dipole

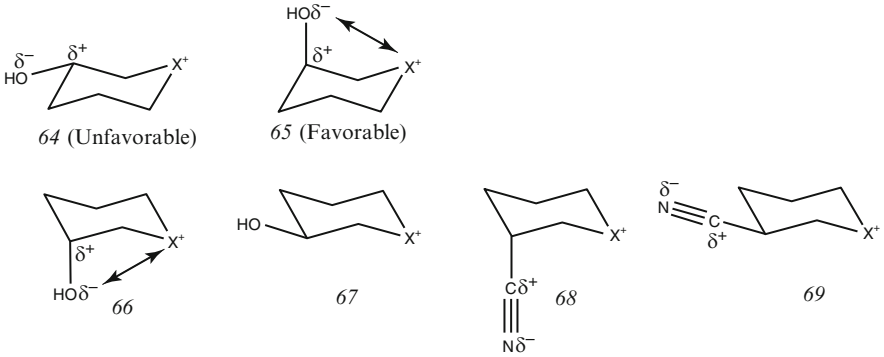

64 (Unfavorable) *65* (Favorable) *66* *67* *68* *69*

Fig. 5.19

interactions. This is particularly evident by analyzing the effect of the 3-cyano substituent compared to the 3-hydroxyl group. As can be seen from Table 5.1, the electron-withdrawing power of the 3-OH increases almost threefold when it is placed equatorially. However, this is not true for the cyano group, which actually has an essentially unchanged substituent effect. The reason for this is probably that despite having a large dipole moment, which does result in a large substituent effect, no stereoelectronic effect is displayed by the cyano group, because the dipole is more distant than the C–O dipole (Fig. 5.19).

We have already seen that the hydrolysis of glycopyranosides are known to involve the oxocarbenium ion intermediates and oxocarbenium ion-like transition states, having a high degree of positive charge in the pyranoside ring. The transition state of the C–O bond cleavage reaction is late, thus resembling the oxocarbenium ion (vide supra) with most of the charge located on the anomeric carbon and ring oxygen. The difference in electron-withdrawing effect from axial and equatorial hydroxyl groups should be reflected in different reactivity of monosaccharide derivatives with axial and equatorial OH groups in these reactions. Indeed, the variation in rate of various hydrolytic reactions of glycosides was found to closely parallel the variations in base strength of isofagomines. Thus, the acidic hydrolysis of methyl α-D-galactopyranoside is five times faster than the hydrolysis of methyl α-D-glucopyranoside [26] indicating that the formation of positive charge at the anomeric center is easier in the *galacto*pyranose, which indeed coincides with *61* ($pK_a = 8.8$) being more basic than *60* ($pK_a = 8.4$) (Fig. 5.19). Likewise, the methyl α-D-idopyranoside undergoes acidic hydrolysis more readily than the corresponding altroside, which is again in agreement with the higher base strength of *63* ($pK_a = 9.4$) than *60* ($pK_a = 8.4$) (the difference is 1 pK unit).

From this it was concluded that electronic effects are the major reason that the stereoisomeric glycosides hydrolyze with different rates. This is also in agreement with the work of Namchuk et al. [27] who found that the rate of hydrolysis of dinitrophenyl glycosides depends mainly on electronic effects. In his work it was also shown that the variations in rate differences observed by different

stereoisomers could be satisfactorily explained using the Kirkwood-Westheimer analysis, that is, the rate differences that are the result of stereoisomerism could be explained by charge-dipole interactions. Also in agreement with this is the work of Woods et al. [28] who, by using a molecular mechanics approach, showed that a saccharide containing an axial OH group is more reactive than one with an equatorial group for electronic reasons.

Thus, the increased reactivity of galactosides over glucosides is caused by the axial C4 hydroxyl group being less electron-withdrawing than the equatorial one.

These findings are in agreement with the findings of Miljkovic et al. [29, 30] who studied the acetolysis of methyl 2,3,4,6-tetra-*O*-methyl-α- and β-D-gluco- and galactopyranosides and found that α-D-galactopyranoside acetolyzed ca. 20 times faster than α-D-glucopyranoside. The influence of the electronegativity of the C4 substituent upon the rate of acetolysis was examined [30] by comparing the C4–OCH_3 with the C4–OAc and C4–NHAc substituent (see also Chap. 3). In the D-gluco series the dependence of acetolysis rates upon the electronegativity of the C4 substituent can be explained as a "through-bond" electronic interaction (inductive effect) with the ring oxygen, which is rather small. However, in the D-galacto series, the very large influence of electronegativity of the axially oriented C4 substituent on the acetolysis rate cannot be ascribed to this rather small through-bond interaction. The only possible explanation for the unusually large kinetic effect observed in D-galacto series is a strong through-space electron donation of the axially oriented electronegative substituent at the C4 carbon to the oxocarbenium ion under formation. This effect, which is destabilizing in the neutral galactopyranoside due to the electrostatic repulsion of axially oriented C4 oxygen and the axially oriented p-electron pair of the ring oxygen, as well as steric interactions, becomes stabilizing as the oxocarbenium ion is being formed (see Fig. 3.33 in Chap. 3).

If the axial and equatorial OH groups have different electron-withdrawing power, then different glycoside conformers must have different hydrolytic lability. Therefore, a glycoside may become more (or less) reactive by simply changing its conformation from one chair conformation to the other. From σ_s values it is estimated that a glycoside containing equatorial groups at C2, C3, and C4 carbons of a pyranoside ring will become 100 times more reactive when it is flipped into the conformation where these OH groups become axial. To verify this theoretical finding, the 3,6-anhydroglycoside derivatives were investigated, because the 3,6-anhydro bridge can force glucose that exists in stable $^4C_1$ conformation into $^1C_4$ chair conformation. The hydrolysis of methyl 3,6-anhydroglucopyranoside *70* in 2 M HCl was found to be 446 times faster than the hydrolysis of methyl α-D-glucopyranoside confirming that changing the conformation has a remarkable effect (Fig. 5.20) [31]. In contrast, 3,6-anhydrogalactose derivative *72*, which is in a boat conformation and therefore does not have more hydroxyl groups axially oriented than the methyl β-D-galactoside, does not hydrolyze faster than methyl β-D-galactoside; in fact, it hydrolyzes slightly slower (for a possible explanation, see the discussion above of the acetolysis of permethylated methyl α-D-galactopyranoside).

The high reactivity toward hydrolysis of sugar residues with axial groups can be illustrated by the observation that oligosaccharides containing a

Fig. 5.20

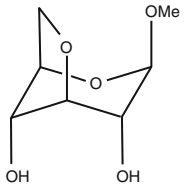

70
rel. Rate: 446

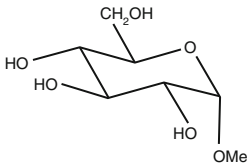

71
rel. Rate: 1

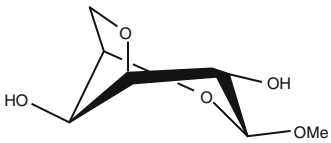

72
rel. Rate: 3.8

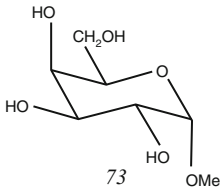

73
rel. Rate: 7.8

Fig. 5.21

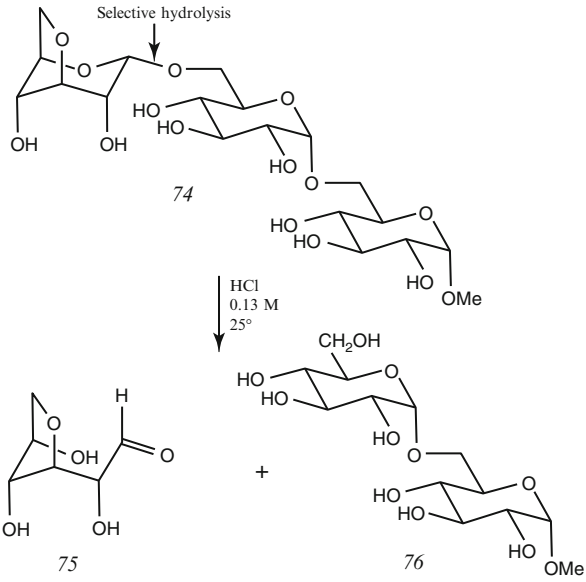

3,6-anhydrosaccharide, such as *74*, are selectively hydrolyzed at the anhydro sugar residue under mild conditions [31] (Fig. 5.21).

It is known that 4,6-*O*-benzylidene protection group in a saccharide reduces its reactivity (i.e., it "disarms" it) in glycosylation reactions. Thus, a thiosaccharide glycosyl donor with 4,6-*O*-benzylidene group *77* is less reactive toward reaction with methanol than its fully benzylated analog *78* (Fig. 5.22) [17]. This phenomenon, which has been attributed to torsional effects or more specifically to the

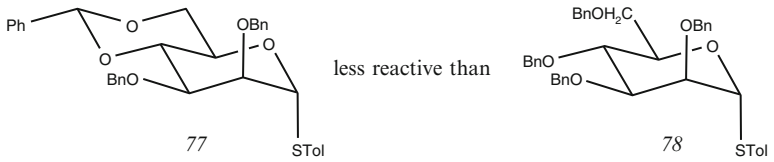

Fig. 5.22

Fig. 5.23

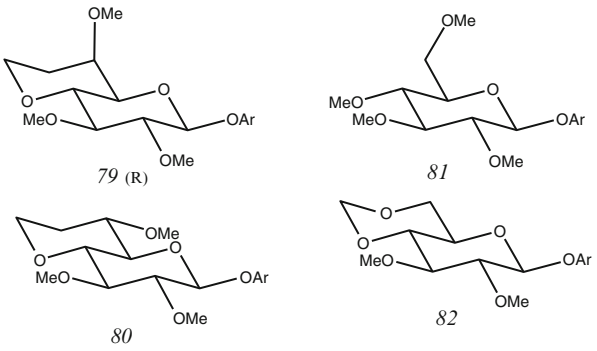

locking together of the C6 hydroxymethyl and the C4 hydroxyl group, is believed to make the molecule's transition to a half chair transition state conformation more difficult [32, 33]. However, on the basis of directional electronic effects observed from the ring hydroxyl groups, it was suggested that the conformation of the exocyclic C6 hydroxymethyl group of hexopyranosides may be important for their reactivity. Looking at the possible conformers of the exocyclic hydroxymethyl group, it is clear that in the *tg* conformer, the C6–OH C–O bond is dipole directed away from the ring oxygen and anomeric carbon, while in the *gg* and *gt* conformers, this dipole is much closer to being perpendicular. Therefore, it was expected that a glycoside with its C6 OH in *tg* conformation to be less reactive, and the low reactivity of the 4,6-*O*-benzylidene protected saccharides could be the result of this electronic deactivation rather than torsional effect. To determine which of these effects were responsible for the low reactivity of the 4,6-*O*-benzylidene protected saccharides, the two probe molecules were prepared, *79* and *80* (Fig. 5.23) [34].

These two molecules contain a ring fused to the pyranoside similar to a benzylidene and should be just as torsionally disarmed, but they do not have the methoxymethyl group in the potentially deactivating *tg* conformation. The rates of uncatalyzed hydrolysis of *79*(*R*) and *80*(S) were compared with those of *81* and *82*, the unrestrained and the 4,6-acetal-protected analogs, respectively (Fig. 5.23). The relative hydrolysis order was found to be *81* > *79* (R) > *80* (S) > *82* with the relative hydrolysis rates being 1:0.24:0.16:0.07, respectively. The same order and relative rates were found for acid-catalyzed hydrolysis of the corresponding methyl α-D-glycosides [34]. In other words, the most reactive glycoside is the unrestrained glucoside *81*,

the 4,6-*O*-protected saccharide is the least reactive, and the probe molecules *79*(R) and *80*(S) are in between. This means that there exist both a "torsional disarming" effect, which causes *79*(R) and *80*(S) to be less reactive than *81*, and "electronic disarming" effect, which causes *82* to be less reactive than *79*(R) and *80*(S) [34].

5.2 Glycosylation Reactions with Conformationally Armed Glycosyl Donors

Although glycosyl coupling reactions are performed in organic solvents and under very different conditions than those of the hydrolytic reactions, it is nevertheless found that the reactivity of glycosyl donors containing axial O-substituents are more reactive than their equatorial epimers. This is clearly seen from the large collection of relative rate data for reaction of thioglycosides with methanol upon activation with NIS (*N*-iodosuccinimide), which has been reported by Zhang et al. [17]. For example, a benzylated tolyl thiogalactoside has been found to react 6.4 times faster than the corresponding thioglucoside, which is a surprisingly similar value to the ratio of relative hydrolysis rates between dinitrophenyl galactosides and glucosides (4.7 times) [27] and methyl galactosides and glucoside toward acidic hydrolysis (5.0 times) [26]. Bulow et al. [35] looked at the difference in reactivity between other galactosyl and glucosyl donors and found a Gal/Glu ratio of 5 times for benzyl-protected trichloroacetimidates and 4.1 times for the benzylated glycosyl chlorides. Notably, this ratio is only 1.3 times between the benzyl-protected galacto and glucosyl 4-pentenylglucosides toward NIS activation. It is suggested that the reason for this could be that in this case, the rate-determining step is not C1–O1 bond cleavage but a step involved in the pentenyl activation.

The higher reactivity observed in glycosylations with donors having axial OR groups should make it possible to conformationally "arm" glycosyl donors by forcing their oxygen substituents into axial orientation. This was achieved by using bulky silyl protection groups such as TBDMS or TBDPS in glycosyl donor, which cannot be accommodated in $^4C_1$ conformation and thus force the molecule into a $^1C_4$ conformation. The idea for this conformational change came from the work of Eliel and Satici [36] who observed in their studies of conformational equilibria of silyloxycyclohexanes *86* that the greater the bulk of the substituents on silicon, the greater the population of the chair conformation with the silyloxy substituent *axial* (Fig. 5.25). The donor *83* is an example of such a "conformationally armed" glycosyl donor (Fig. 5.24). The armament in this case exceeds the armament of having equatorially placed benzyl ethers, which makes it possible to selectively couple it with an armed glycosyl donor *84* to give adduct *85* without any self-coupling of *84* taking place (Fig. 5.24) [37]. This example very clearly shows the very considerable difference in electronic effect of the axial and equatorial OR groups.

Fig. 5.24

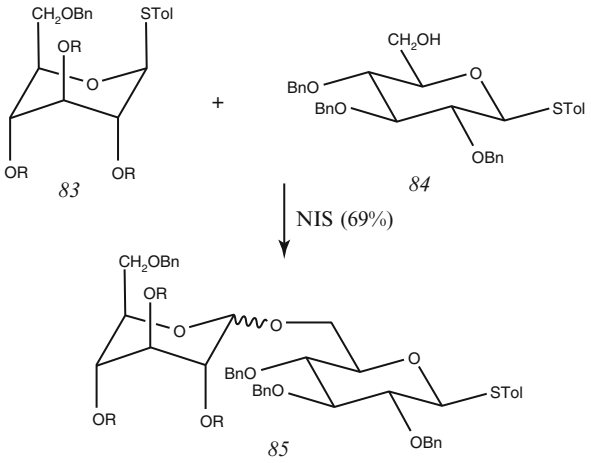

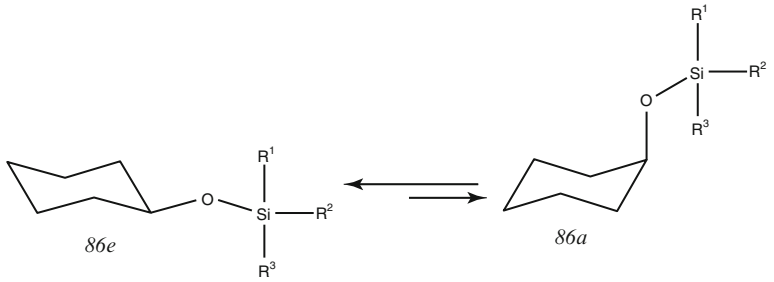

Compounds	R^1	R^2	R^3	Percentage axial conformation
86a	Me	Me	Me	3.6
86b	Et	Et	Et	4.0
86c	Me	Me	*t*-Bu	6.5
86d	*i*-Pr	*i*-Pr	*i*-Pr	8.6
86e	Ph	Ph	Ph	14.3
86f	Ph	Ph	*t*-Bu	19.6

Fig. 5.25

The main findings can be summed up as follows: first, in a six-membered ring in chair conformation, the axial OH group is less electron-withdrawing than the equatorial OH group in relation to another ring atom 2–3 positions away. This is also true for other electronegative substituents. Second, the two chair forms of a six-membered ring with electronegative substituents will have different properties such as different acidity or different reactivity.

The implications of these findings are quite far-reaching. The large boost in reactivity found caused by ring inversion of some saccharides suggests that

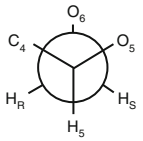

87, *gg* C5-C6 rotamer

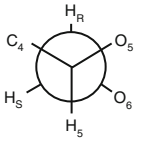

88, *gt* C5-C6 rotamer

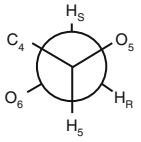

89, *tg* C5-C6 rotamer

Fig. 5.26 The Newmans projections outlining the nomenclature for C5–C6 rotamers

glycosides may spontaneously undergo conformational change during hydrolysis or glycosylation reactions, which of course may affect the stereochemical outcome of the latter reactions.

These findings, furthermore, offer a new explanation that does not rely on the questioned stereoelectronic effect as to why enzymes may change the conformation of a monosaccharide's unit or possibly preferentially stabilize the 6-OH in the *gg* orientation *87* (O6–C6–C5–O5) to make the substrate more reactive (Fig. 5.26).

5.3 Superarmed Glycosyl Donors in Glycosylation Reactions

Mydock and Demchenko [38] have developed a concept of superarmed glycosyl donors by strategic placement of common protecting groups on the sugar pyranoside ring. This is illustrated in Fig. 5.27. It was determined that *S*-benzoxazyl glycosyl donors having both a participating moiety at C2 and an electronically armed lone pair at O5, such as the superarmed glycosyl donor shown above, were exceptionally reactive.

The armed-disarmed concept, although discovered with *O*-pentenyl glycosides, has been found to be applicable to many other classes of glycosides such as thioglycosides [6], selenoglycosides [39], fluorides [40], phosphoroamidates [41], substituted thioformimidates [42], glycals [21], *S*-benzoxazolyl (SBox), and *S*-thiazolinyl (STaz) [43, 44].

When a glycosyl donor with the mixed protecting group patterns such as 2-*O*-benzyl-3,4,6-tri-*O*-acyl derivative *95* was compared in reactivity with 2,3,4,6-*O*-tetra-*O*-acyl-derivative *94* and 2,3,4,6-tetra-*O*-benzyl derivative *93*, it was found that it is less reactive than either one [43] (Fig. 5.28). This was the first indication that the reactivity of the glycosyl donor was not dependent only upon the electron-withdrawing/donating properties of its protecting groups. This finding ultimately resulted in postulating the "O2/O5 cooperative effect" [43] wherein it is stated that glycosyl donor reactivity is also dependent upon the stability of the glycosyl cation that is formed upon the leaving group departure. In the case of the armed, benzylated glycosyl donor *93*, stabilization can be efficiently achieved through resonance with the electronically "armed" lone pair of electrons of ring oxygen (O5) via the oxocarbenium intermediate (Fig. 5.29).

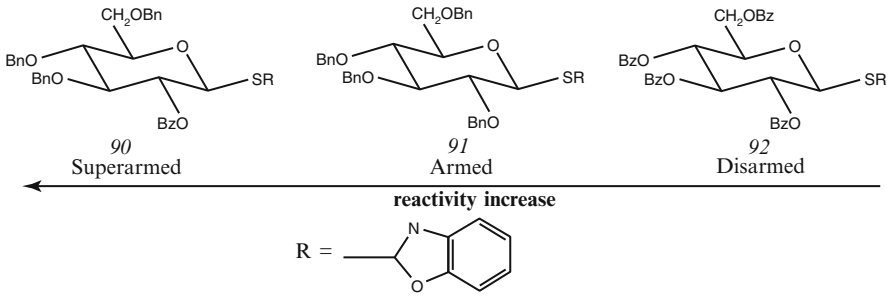

Fig. 5.27

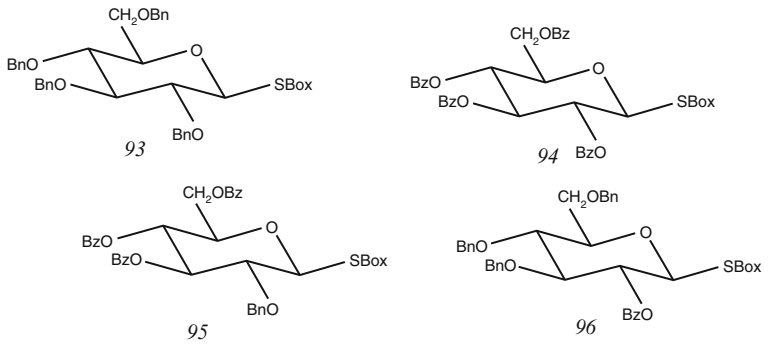

Fig. 5.28

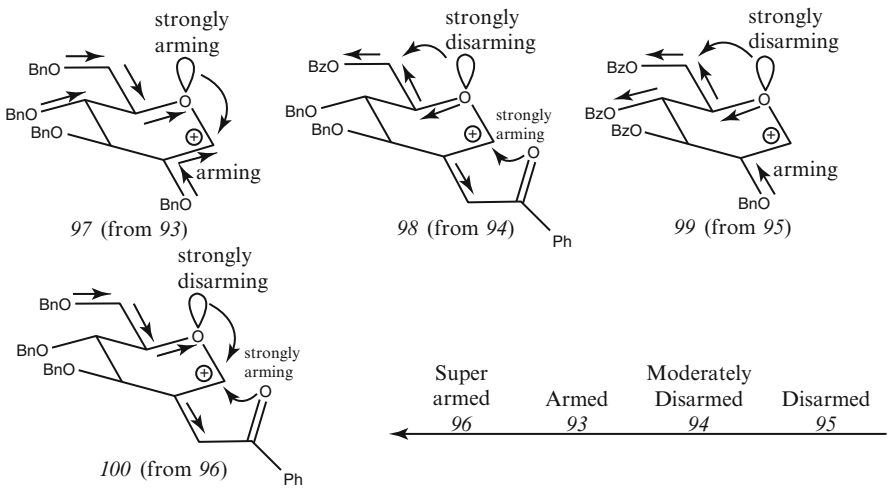

Fig. 5.29

However, in the case of perbenzoylated derivative *94*, this type of stabilization is less likely due to the electron-withdrawing substituents at C4 and C6. Instead, the acyl substituent at C2 allows for stabilization via acyloxonium ion intermediate. In combination, these two competing effects result in an overall moderate disarming of glycosyl donor *94*. Additionally, Crich and Li [45] recently suggested the importance of the 1,2-*trans* anomeric configuration for the SBox glycosyl donors of the D-gluco series, in order for this stabilizing participation to occur. In the case of glycosyl donor *95*, the O5 disarming effect is only slightly compensated by electron-donating 2-*O*-benzyl group, whose arming effect is mild. The anticipated "lack of cooperation" is in agreement with experimental results, which indicate a strong disarming effect for compound *95* [43]. In comparison to the application of traditional perbenzylated armed glycosyl donor *93*, the "superarmed" (the term "superarmed" was originally coined by Bols et al. in their recent publications dedicated to conformationally modified glycosyl donors [46, 47]) glycosyl donor *96* would offer advantages that could significantly enhance the way we currently obtain oligosaccharide sequences.

Glycosidation of the perbenzylated donor *93* with glycosyl acceptor *101* in the presence of dimethyl(methylthio)sulfonium triflate (DMTST) as promoter proceeded smoothly and was completed in 2 h affording the corresponding disaccharide *102* in 91 % yield (Table 5.2). In reaction of moderately armed and disarmed glycosyl donors *95* and *94*, respectively, with glycosyl acceptor *101* under the same experimental conditions, no formation of the corresponding coupling products was observed (Table 5.2). However, the superarmed glycosyl donor *96* reacted, under the same reaction conditions, almost instantaneously to give disaccharide *103* in 90 % yield (Table 5.2). The reaction of the superarmed glycosyl donor *96* with less reactive secondary glycosyl acceptors *104–108* were also efficient resulting in the formation of the respected disaccharides *105*, *107*, and *109* in high yield (88–97 %) (Table 5.2).

As expected the superarmed galacto derivative *110* was found to be significantly more reactive than the armed galacto derivative *112*. Thus, disaccharides *111* and *113* were formed in 5 min (92 %) and 40 min (85 %), respectively. As in the case of D-glucose, no reaction took place with the perbenzoylated galactoside *114*. Similar observations were made with mannosides *115–119*: disaccharides *116* and *118* were formed in 50 min (79 %) and 90 min (79 %), respectively, whereas no glycosidation with the disarmed donor *119* took place. To this end, it was determined that not only did the 2-*O*-benzoyl-3,4,6-tri-*O*-benzyl donors *96*, *110*, and *115* readily react, while disarmed glycosyl donors *94*, *114,* and *119* did not, but also, as postulated, they proved to be more reactive than their armed counterparts *93*, *112*, and *117*.

Mydock and Demchenko [48] studied whether the enhanced reactivity of superarmed donors *96*, *110*, and *115* was sufficient to allow for direct chemoselective couplings. As acceptors were chosen armed benzylated glycosides *123, 124, and 125*, all bearing the same leaving group (SBox) (Fig. 5.30).

The superarmed concept was validated by direct coupling of the superarmed glycosyl donor *96* and benzylated ("armed") acceptor *101* whereby the corresponding disaccharide *103* was obtained in 70 % yield (Fig. 5.31). No self-condensation products were detected.

Table 5.2 Comparitive glycosydation of glycosyl donors *101–106* and *113–122* in presence of DMTST

Donor	Acceptor	Temperature (°C)	Time	Product and yield
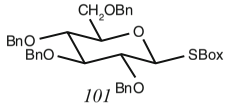 *101*	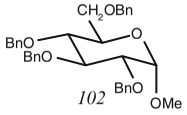 *102*	0 → 25	2 h	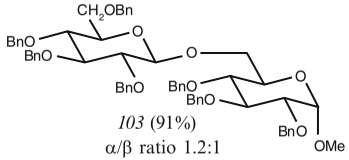 *103* (91%) α/β ratio 1.2:1
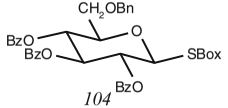 *104*	*102*	0 → 25	16 h	No reaction
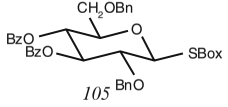 *105*	*102*	0 → 25	16 h	No reaction
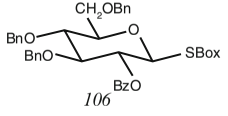 *106*	*102*	0	>5 min	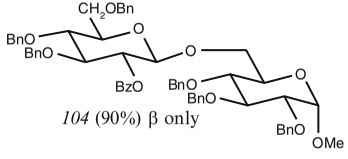 *104* (90%) β only
106	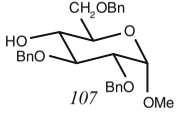 *107*	0	>5 min	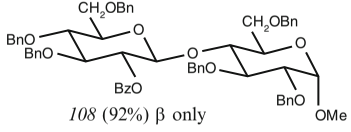 *108* (92%) β only
106	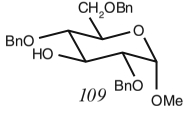 *109*	0	>5 min	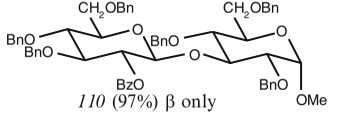 *110* (97%) β only

106	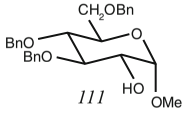 *111*	0	>5 min	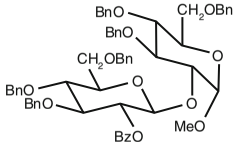 *112* (88%) β only
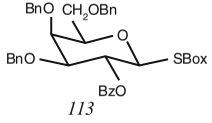 *113*	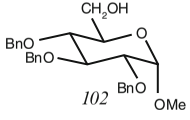 *102*	0	<5 min	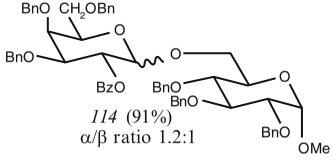 *114* (91%) α/β ratio 1.2:1
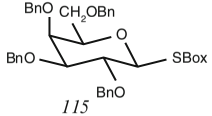 *115*	*102*	0 → 13	40 min	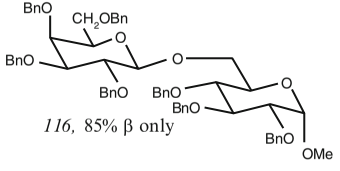 *116*, 85% β only
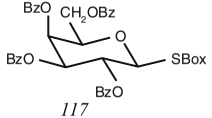 *117*	*102*	0 → 25	16 h	No reaction
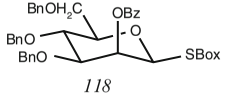 *118*	*102*	0 → 18	50 min	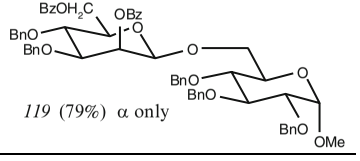 *119* (79%) α only

(continued)

Table 5.2 (continued)

Donor	Acceptor	Temperature (°C)	Time	Product and yield
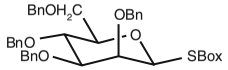 *120*	*102*	0 → 22	1.5 h	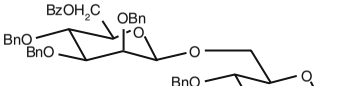 *121* (79%) α/β ratio 1.1:1
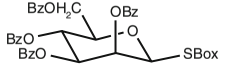 *122*	*102*	0 → 25	16 h	No reaction

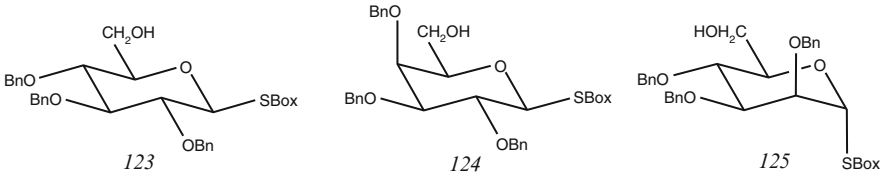

Fig. 5.30

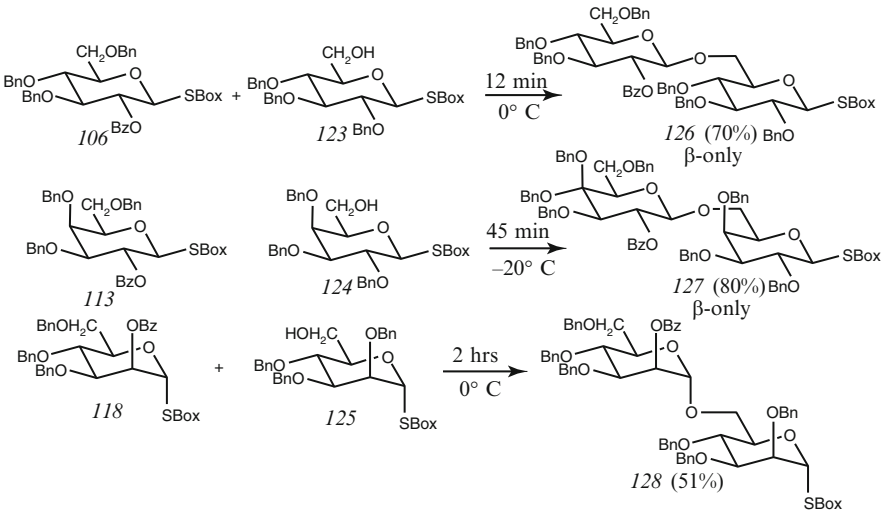

Fig. 5.31

The superarmed galactosyl donor *113* reacted with benzylated galactosyl acceptor *124* giving the corresponding disaccharide *127* in 80 % yield (Fig. 5.31). The reaction was conducted at −20 °C in order to minimize the competing side reaction of the isomerization of galactosyl donor *113* into its corresponding unreactive *N*-linked (NBox) counterpart. Coupling between the superarmed mannosyl donor *118* and benzylated mannosyl acceptor *125* was somewhat less efficient. Although the self-condensation products were not observed, the disaccharide *128* was isolated in only 51 % yield (Fig. 5.31).

Competitive glycosylation of glycosyl acceptor *102* with glycosyl donors *106* (superarmed) and *101* (armed) demonstrated that the superarmed glycosyl donor reacted much faster than the armed glycosyl donor giving the corresponding disaccharide *104* in 95 % yield. Armed glycosyl donor gave the corresponding disaccharide *103* only in traces (Fig. 5.32).

Sequential trisaccharide syntheses were carried out [48] with the use of the superarmed glycosyl donor *106*, thus allowing to introduce a 1,2-*trans* linkage prior to other linkages. This is not possible in classic armed-disarmed approach. In the first sequence, a stepwise coupling of building blocks *106* and *129* and the

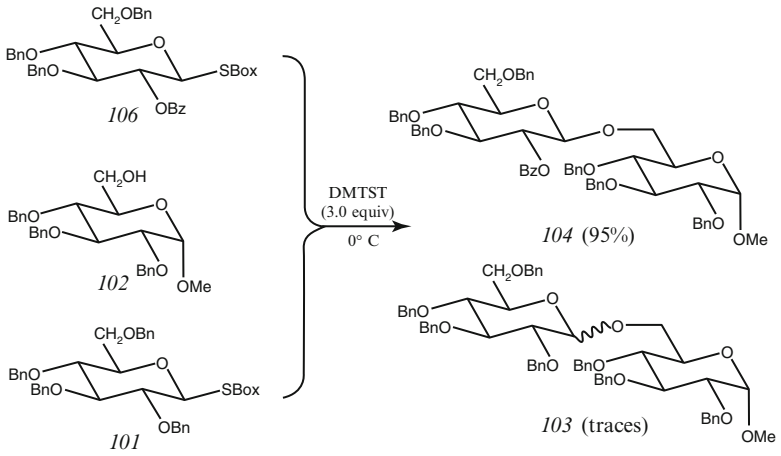

Fig. 5.32

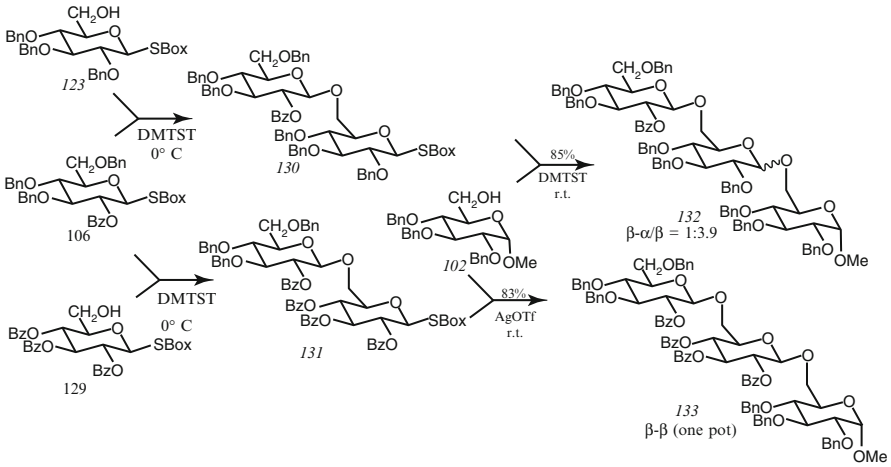

Fig. 5.33

isolated disaccharide *131* was reacted with glycosyl acceptor *102*, at room temperature, to afford trisaccharide *133* in 60 % overall yield (Fig. 5.33). The same sequencing could also be performed in a one-pot fashion without isolating the intermediate. In this case, trisaccharide *133* was isolated in a 74 % yield. Similarly, a one-pot synthesis of the *trans-trans*-linked trisaccharide *132*, from building blocks *106*, *130*, and *102*, was accomplished in 83 % overall yield.

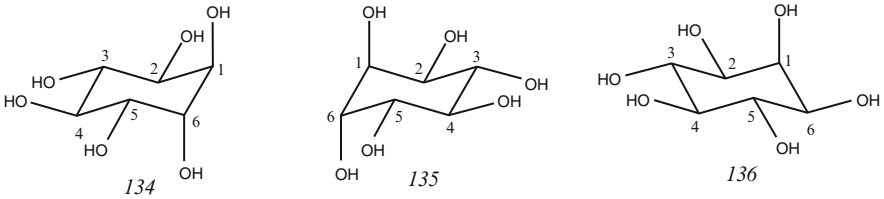

Fig. 5.34

5.3.1 Regio- and Stereoselectivity in Glycosylation

Cid et al. [49] have studied the glycosylation of 1,2-*trans*-diequatorial diols derived from tetrabenzoylated and tetrabenzylated D- and L-*chiro*-inositol with several glycosyl donors. They found that the regioselectivity depended on the absolute configuration of the acceptor. However, this trend has been modulated by the nature of the protecting groups on both the donor and acceptor, with benzoylated acceptor affording higher levels of regioselectivity.

Although the outcome of glycosylations depends on both the donor and acceptor [50], most glycosylation studies have focused on the role of glycosyl donors in controlling the stereoselectivity of the process. A remarkable exception is the glycosylation with glycosylidene diazirines where the key factor is the kinetic acidity of the acceptor OH group. In this case, the emphasis is shifted to the role of polyol glycosyl acceptors in controlling the regioselectivity of glycosylation [51].

In the course of their work on the synthesis of inositolphosphoglycans (IPGs) as potential mediators in the insulin signaling process, Martin-Lomas et al. [52–58] have extensively studied the glycosylation reactions of *myo*-inositol and D- and L-*chiro*-inositol derivatives (Fig. 5.34) with different glycosyl donors, in particular 2-azido-2-deoxy-glycopyranosyl trichloroacetimidates. In an attempt to extend the applicability of the double stereodifferentiation principle [59] to glycosylation reactions [60], Martin-Lomas et al. studied the stereoselectivity of the glycosylation of D- and L-*chiro*-inositol derivatives with several glycosyl donors [61]. The authors observed that when differently protected 1,2-diols, derived from both *chiro*-inositol enantiomers, are used as acceptors, both the absolute configuration of the acceptor as well as the nature of the donor's and acceptor's protecting groups plays a key role in the regiochemistry of the coupling. A few examples of regioselective glycosylation of 1,2-*cis*-axial/equatorial [51, 62, 63] and 1,2-*trans*-diequatorial diols [51, 53, 64] have been described, and the influence of the donor's protecting groups on the regiochemistry of polyol glycosylation has been investigated [65, 66]. A notable example of regioselective glycosylation of 1,2-*trans*-diequatorial diol is the virtually complete regioselective galactosylation of the OH-4 group of p-methoxyphenyl 6-*O*-benzyl-2-deoxy-2-tetrachlorophthalimido-β-D-glucopyranoside *137* (Fig. 5.35) using a thiophenyl 2,3,4-tri-*O*-acetyl-6-*O*-benzyl-galactopyranoside *138* as glycosyl

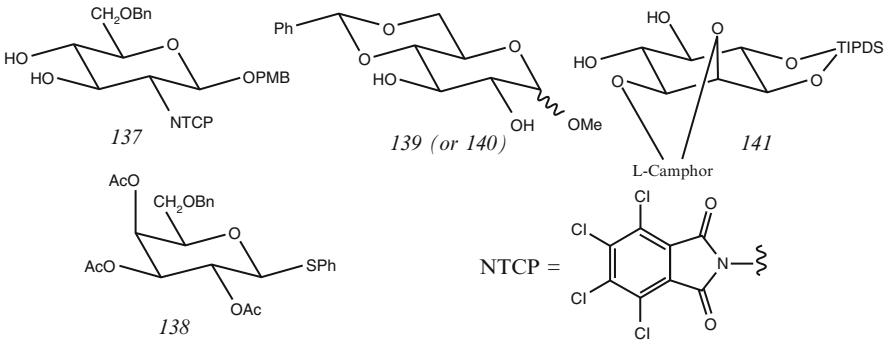

Fig. 5.35

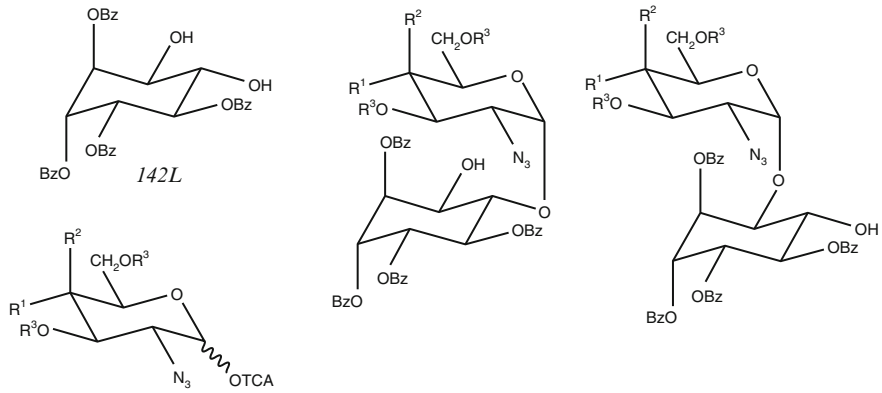

143, R^1 =OBn; R^2= H; R^3 = Bn
146, R^1 =H; R^2= OBn; R^3 =Bn
149, R^1 =OAc; R^2 = H; R^3 = Ac

144 (58%)
147 (42%)
150 (52%)

145 (9%)
148 (6%)
151 (26%)

Fig. 5.36

donor [64]. In this case it was also reported that OH–3 and OH–4 in *137* (Fig. 5.35) show different preferences for fucosylation reactions depending upon the nature of the protecting groups in the fucosyl donor. This was later observed in the mannosylation of the diequatorial diols of methyl 4,6-*O*-benzylidene-α- and β-D-glucopyranosides (*139* and *140*) in the course of RDAS studies [65].

The glycosylation of the OH–6 group of the *myo*-inositol derivative *141* with 2-azido-2-deoxy-D-glucopyranosyl trichloroacetimidates is another case of regioselective glycosylation of a 1,2-*trans*-*O*-diequatorial diol system *141* which is frequently performed for the preparation of building blocks for IPG synthesis [53].

Martin-Lomas et al. have already shown that the coupling of L-*chiro*-inositol tetrabenzoate *142L* with 2-azido-2-deoxy-3,4,6-tri-*O*-benzyl-D-glucopyranosyl trichloroacetimidate *143* gave a 6.4:1 mixture of the α(1 → 3) *144* and α(1 → 2) *145* pseudodisaccharides in 67 % combined yield (Fig. 5.36). Similarly,

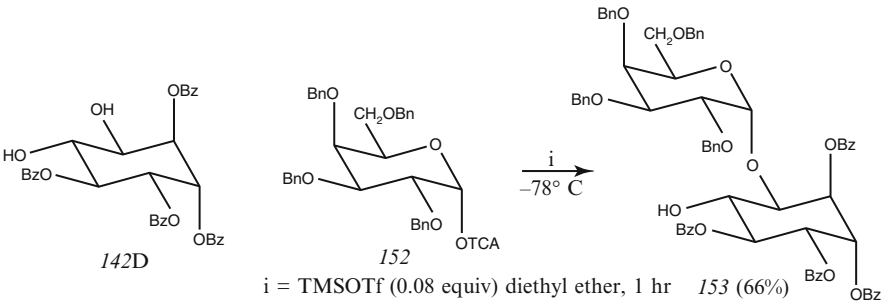

Fig. 5.37

the glycosylation of *140L* with 2-azido-2-deoxy-3,4,6-tri-*O*-benzyl-D-galactopyranoside *146* gave a 7:1 mixture of the α(→3) *147* and the α(1 → 2) *148* compounds in 48 % overall yield [54]. The regioselectivity was poorer but followed the same trend in the glycosylation with the less reactive 3,4,6-tri-*O*-acetyl-2-azido-2-deoxy-D-glycopyranosyl trichloroacetimidate *149* which afforded a 2:1 mixture of the α(1 → 3) *150* and the α(1 → 2) *151* pseudodisaccharides in 78 % overall yield. Interestingly, the glycosylation of the corresponding D-*chiro*-inositol diol *142D* with trichloroacetimidate *152* under the same conditions gave α/β mixture. Here, the 2-*O*-glycosylated products predominated and afforded the α(1 → 2) pseudodisaccharide *153* (Fig. 5.37) as the only product in 65 % yield when the reaction temperature was decreased from −40 °C to −78 °C [67]. In neither case were transbenzoylation processes detected.

In order to confirm the influence of the absolute configuration of the acceptor on the regioselectivity of these glycosylations, we may observe the results of the reactions of *142D* with *152* (see Fig. 5.37), *142D* with *154* (see Table 5.3) (for structures see Fig. 5.38), and *140L* with *155* (not shown).

In the glycosylations of *142D*, the α(1 → 2) compounds (*165* and *167*) (Fig. 5.38) slightly predominated over the α(1 → 3) pseudodisaccharides (*164* and *166*) (Fig. 5.38), thus confirming that the absolute configurations of the acceptor play a role in the regioselectivity process. Although, in these cases the regioselectivity was poorer than for *140L*. In the glycosylation of *140L* with *155,* a mixture of the α(1 → 2) (*161*), β(1 → 2), and α(1 → 3)(*164*) pseudodisaccharides was observed even when the reaction was performed at −78 °C. Thus, the tendency for the D-enantiomer (*140D*) to form α(1 → 2) pseudodisaccharide, as observed in the glycosylation with *155*, was also observed in the glycosylation with *155* and *156*.

However, the tendency for the L-enantiomers (*140L*) to form the α(1 → 3) glycosidic linkage, as observed in the glycosylation with *154* and *155*, was not observed in the glycosylation with *157*. The reason for this could possibly be that other factors like the nature of the protecting group at C2 in the glycosyl donor play a role in the regiochemistry of the process (Table 5.3).

At this point, the glycosylation of *142D* and *142L* with trichloroacetimidate *157*, bearing a trifluoroacetamide participating group at C2, was investigated.

Table 5.3 Glycosylation reactions of acceptors *142L* and *142D* with donors *154*, *155*, *156*, and *157*. Reaction conditions: TMSOTf (0.08 equiv.), −14 °C, diethyl ether, 1 h, −40 °C; *TCA* trichloracetimidate

	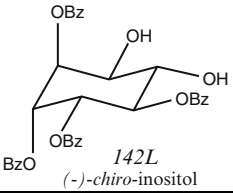 *142L* *(-)-chiro*-inositol	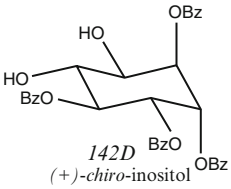 *142D* *(+)-chiro*-inositol
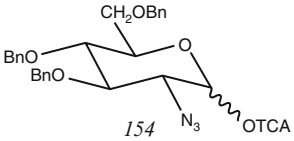 *154*	α(1 → 3) *158* (*58* %) α(1→2) *159* (9 %) 67 % (overall yield) C2/C3 = 6:4:1	α(1 → 3) *164* (*27* %) α(1→2) *165* (40 %) 67 % (overall yield) C3/C2 = 1:1.5
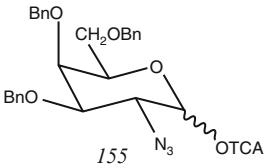 *155*	α(1 → 3) *160* (*42* %) α(1→2) *161* (6 %) 48 % (overall yield) C3/C2 = 7:1	α(1 → 3) *166* (*28* %) α(1→2) *167* (35 %) 63 % (over yield) C3/C2 = 1:1.25
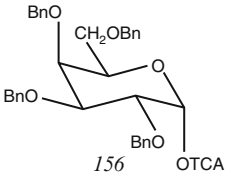 *156*	α(1→2) *162* (24 %) α(1 →3) *163* (6 %) α(1 → 3) *169* (21 %) 51 %(overall yield) C3/C2=1:1.4	α(1 → 3) *168* (66 %) 63 %[a] (overall yield) C3/C2 = 0:1
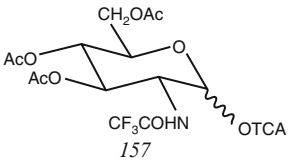 *157*	α(1 → 3) *172* (30 %) 30 %[b] (overall yield) C3/C2 = 100.0	*170* β(1 → 2) *171* β(1 → 3) 95 %[c] (overall yield) C3/C2 = 1:5[d]

[a]T = −78 °C
[b]Reaction timie 3 h at −40 °C, 1 h at −10 °C
[c]Reaction time 3 h at −40 C
[d]Determined b y ^{1}H NMR spectroscopy

The results are also shown in Table 5.3 and Fig. 5.38. In this case, the regiochemistry of the glycosylation followed the same trend as already observed for donors *154* and *155*; the reaction with *142D* afforded a 5:1 mixture of the β(1 → 2) (*168*) and β(1 → 3) (*169*) compounds with excellent yield, while the reaction with *142L* yielded the β(1 → 3) derivative *170* as the only product, albeit in lower yield (Fig. 5.39).

Therefore, with the only exception of the reaction of *140L* with *156* (with a benzyloxy group in position 2), in all the cases studied with tetrabenzoylated acceptors, the regiochemistry of the glycosylation seems to be dictated by the absolute configuration of the glycosyl acceptor. These results constitute the first

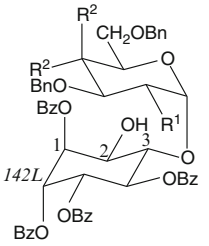

158, α (1→3), $R^1 = N_3$; R^2 = OBn; R^3 = H (58%)
67% overall yield; C2/C3 = 6.4:1

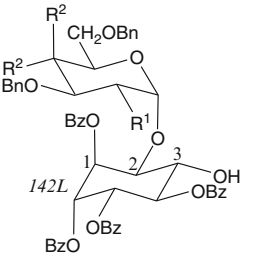

159, α (1→2)$R^1 = N_3$; R^2 = OBn; R^3 = H (9%)
67% overall yield; C3/C2 = 1:1.5

160, α (1→3), $R^1 = N_3$; R^2 = H; R^3 = OBn (42%)
48% overall yield; 3/C2 = 7:1

161, α (1→2), $R^1 = N_3$; R^2 = H; R^3 = OBn (6%)
48% overall yield; C/C2 = 1:1.25

162, α (1→3), $R^1 = R^3$ = OBn; R^2 = H; (30%)
51% overall yield; C3/C2 = 1.14

163, α (1→2), $R^1 = R^3$ = OBn; R^2 = H (21%)

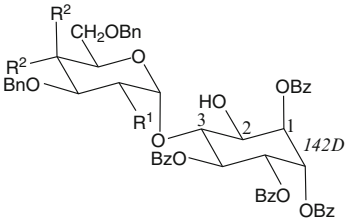

164, α (1→3), $R^1 = N_3$; R^2 = H; R^3 = OBn (28%)
63% overall yield; C3/C2 = 1:1.25

166, α (1→3), R^1 = OBn: R^2 = H; R^3 = OBn (6%)
66% overall yield; C3/C2 = 0:1

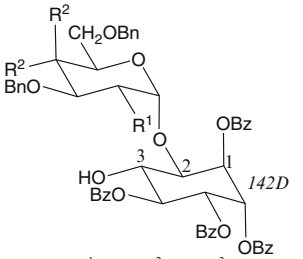

165, α (1→2), $R^1 = N_3$: R^2 = H; R^3 = OBn (35%)
63% overall yield; C3/C2 = 1:1.25

167, α (1→2), R^1 = OBn: R^2 = H; R^3 = OBn
51% overall yield; C3/C2 = 1:1.14

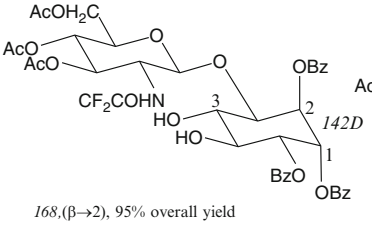

168,(β→2), 95% overall yield

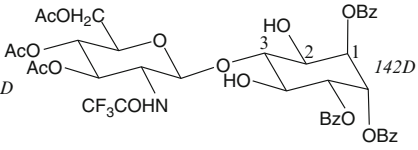

169, β(1→3), 30% overall yield; C3/C2 = 100%
C3/C2 = 1:5

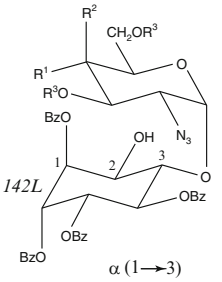

α (1→3)

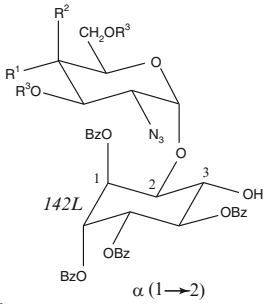

α (1→2)

170 R^1 = OBn; R^2 = H; R^3 = Bn *172*
171 R^1 = H; R^2 = OBn; R^3 = Bn *173*

Fig. 5.38

Fig. 5.39

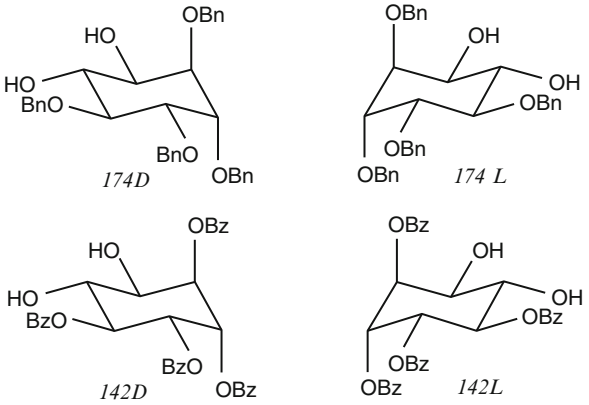

Table 5.4 Glycosylation reactions of acceptors *174L* and *174D* with donors 154 and 155. Reaction conditions: TMSOTY (0.08 equiv.). −40 °C, diethyl ether. 1 h, −40 °C; *TCA* trichloracetimidate

	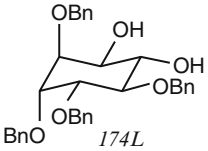	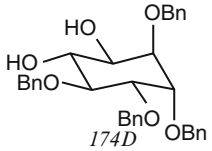
	174L	174D
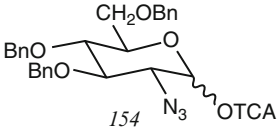 154	α (1–2) *181* 21 % β (1–2) *182* 13 % α (1–3) *183* 8 % β (1–3) *184* 2 % αβ-Trisaccharide 4 % 48 % C3/C2 = 1:3.4	α (1.2) *173* 23 % β (1–2) *174* 16 % α (1–3) *175* 13 % β (1–3) *176* 13 % . . . . . . *65 %* *C3/C2 = 1:1.5*
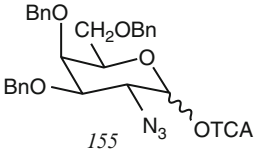 155	α (1–2) *185* 5 % β (1–2) *186* 20 % β (1–3) *187* 10 % . . . . . . αβ-Trisaccharide 4 % 39 % C3/C2 = 1: 2.5	α (1–2) *177* 12 % β (1–2) *178* 14 % α (1–3) *179* 6 % β (1–3) *180* 22 % αβ-Trisaccharide 17 % 71 % C3/C2 = 1.1:1

experimental evidence of simultaneous regio- and enantiodifferentiation in carbohydrate coupling.

The clear influence of the absolute configuration of the acceptor could not be observed when a similar study was carried out with the tetrabenzylated glycosyl acceptors *172D* and *172L*. The results of the glycosylation reactions with acceptors *172D* and *172L* are presented in Table 5.4 and Fig. 5.40.

Substituting benzoyl for benzyl groups resulted in an increase of the proportions of the β-anomers and small amounts of uncharacterized pseudotrisaccharides,

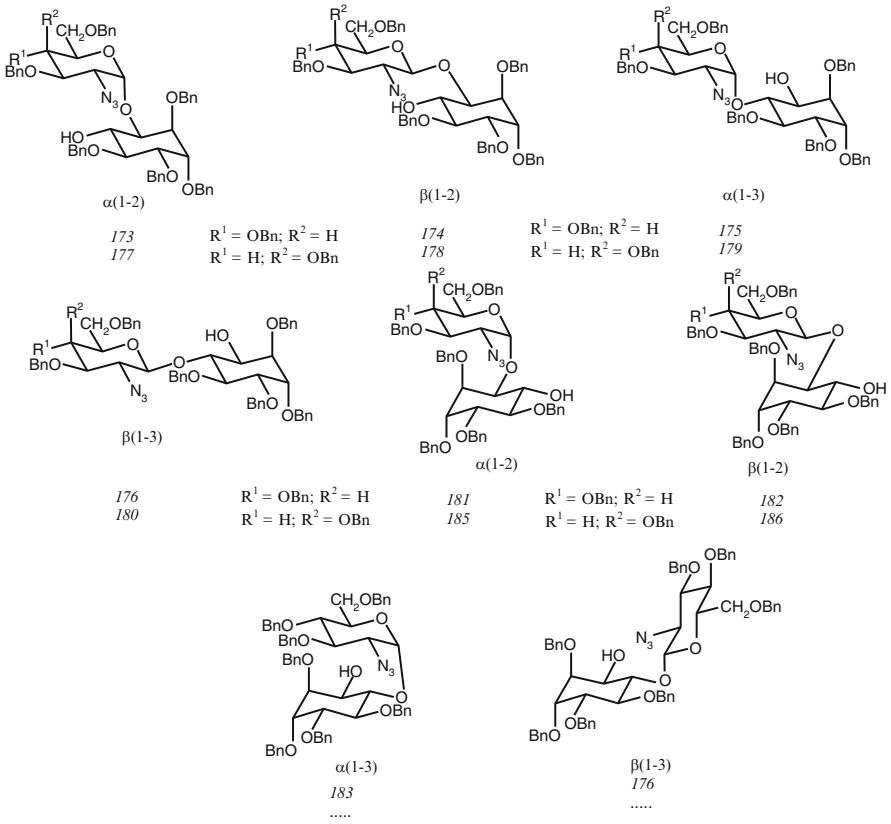

Fig. 5.40 Structures of Table 5.5

probably due to the higher reactivity of the benzylated acceptors [56]. Compared to the results described above for *142D*, the yield and the regioselectivity for the glycosylation of *172D* were similar when using donor *153* affording the α(1 → 2) *173* and β(1 → 2) *174* pseudodisaccharides in a slightly higher proportion than the α(1 → 3) *175* and β(1 → 3) *176* compounds (C3/C3 = 1:1.5). No selectivity at all was observed with donor *154* where the 1 → 2 (*177* and *178*) and the 1 → 3 (*179* and *180*) compounds were formed in similar proportions (C3/C2 = 1.1:1). For *172L*, the regioselectivity observed in the reactions with both *153* and *154* was reversed compared to *140L*. The mixture of 1 → 2 pseudodisaccharides (α*181* and β*182* in the glycosylation with *142* and α*179* and β*180* in the glycosylation with *153*) predominated (C3/C2 = 1:2.5) over the 1 → 3 compounds (*α177* and *β178* in the glycosylation with *153* and α185 and β*186* in the glycosylation with *154*), and the yields were considerably decreased (Table 5.4 and Fig. 5.40).

Therefore, the nature of the protecting group in the glycosyl acceptor also seems to exert an important influence on the regiochemical outcome of these

glycosylations. While a comparison of the results obtained for *142L* and *142D* under identical experimental conditions evidences the importance of stereoelectronic factors on the regiochemistry of the process, a comparison of the behavior of *142L* and *172L* also provides experimental evidence for the importance of the protecting groups on the donor-acceptor match [50] affecting the yield and the stereoselectivity, and also the regioselectivity of the coupling.

In an attempt to rationalize the above experimental results, the interactions taking place in the process of glycosidic bond formation were analyzed by means of DFT calculations [Conformational analyses of donor and acceptor models were performed using semiempirical PM3 ™ procedure as implemented in HyperChem 6.02; see [68–70]; the low-energy structures found were reoptimized by using hybrid density functional theory (B3LYP); see [71, 72]; all of the atoms were described by means of the 6-31G(d) basis set as implemented in Gaussian 03; see [73–76]. The same method was used for the optimization of all model complexes. Frequencies were also computed at the same level of theory/basis to characterize stationary points (all of the models presented here were characterized as minima) and to determine the zero-point energy (ZPE).] Glycosyl oxocarbenium ions with 2-azide and 2-methoxy groups without substituents at positions 3 and 4 (far from the reaction center) and methyl instead of benzyl ether at position 6 were used as glycosyl donor models. The benzoylated glycosyl acceptors were modeled by removing the substituents at positions 5 and 6 of the cyclitol ring and changing the benzoyl to acetyl groups. Methoxylated glycosyl acceptors were used as models for benzylated derivatives. Several nucleophile-carbonium ion complexes differing in the nucleophile orientation, acceptor configuration (D or L), and attacking OH group (OH–2 or OH–3 of the *chiro*-inositol ring) were optimized. Most of the complexes showed a C1′–O2(O3) bond length around 2 Å. However, some slightly more stable complexes with shorter distances for the incipient glycosidic bond were found. Complexes obtained with 2-azide (denoted as **A**) and 2-methoxy (denoted as **M**) substituted donors and L and D acetylated acceptors are named **AL** and **ML** and **AD** and **MD** and are shown in Figs. 5.42 and 5.43, respectively. In each case the approximation through position 2 or 3 is indicated by the corresponding number. Complexes obtained from L methoxylated acceptor (denoted as L′) with 2-azide donor are also shown in Fig. 5.41. The equivalence between models and real systems is also indicated.

Two main interactions seem to control all these approximations. First is a very strong hydrogen bond, according to the usual criteria [77] which is present in all the complexes with acetylated acceptors between the O–H group to be glycosylated and the adjacent acyl group. In complexes **AL′3 and AL′2,** an equivalent but weaker interaction is also present with the adjacent methoxy group. Second is an important hydrogen bond between C1′ and the closest O2 (O3)–H group, the directionality of which determines the conformation (especially Φ angle) of the pseudodisaccharide being formed. This interaction is present in all the complexes except **AD2** and **MD2** where there is an equivalent interaction between C5′–H and O3.

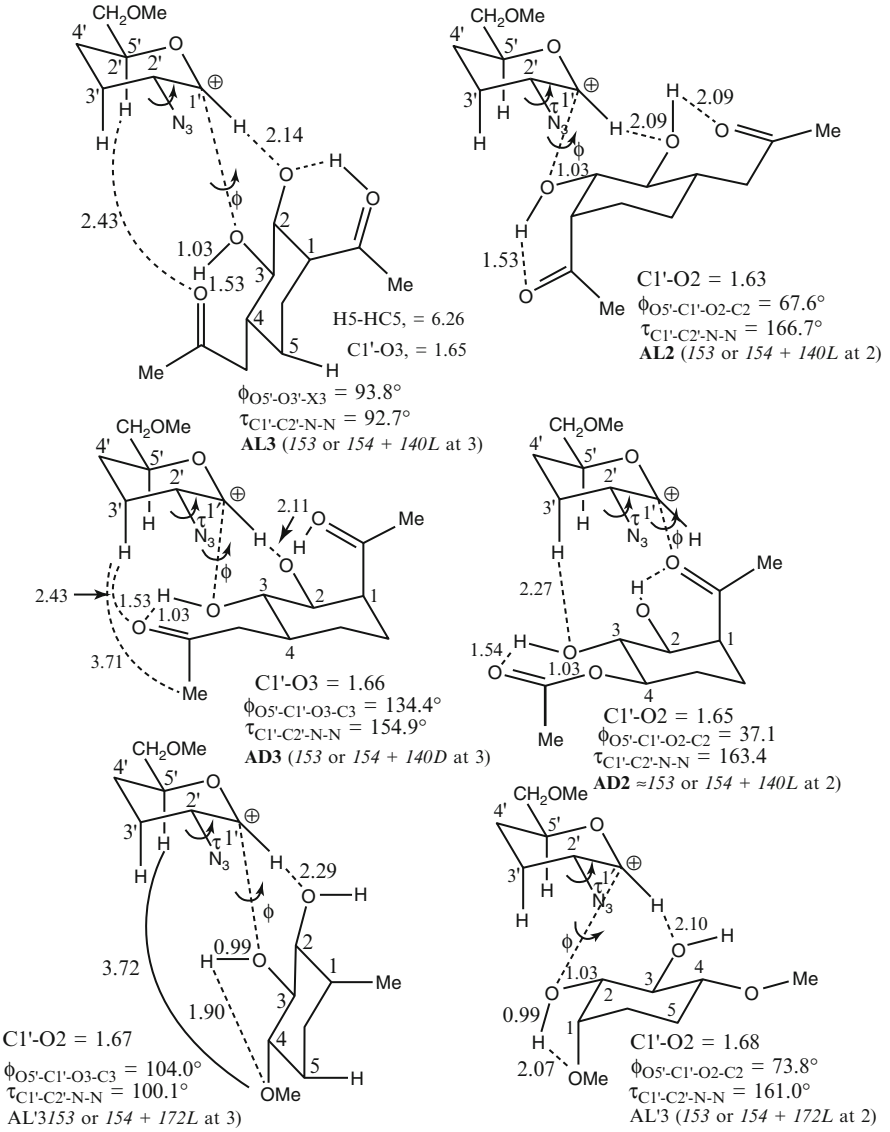

Fig. 5.41 Significant interactions between groupsat short and long distances (in Angstroems) deermined on model complexes AL3AL2, AD3, AD2, AL'3, and AL'2

Comparing the hydrogen bond between the O3(O2)–H bond and the adjacent acyl group in complexes with acetylated acceptors, with respect to the situation in the acceptor model, the hydrogen atom seems to be partially transferred to the carbonyl group [distances and angles in the acceptor model: d(C = O. . .H) = 2.11, 2.14 Å, Θ(O. . .H−O) = 132.1, 133.8°, φ(X = . . .O−H) = 98.2, 99.2°.] NBO

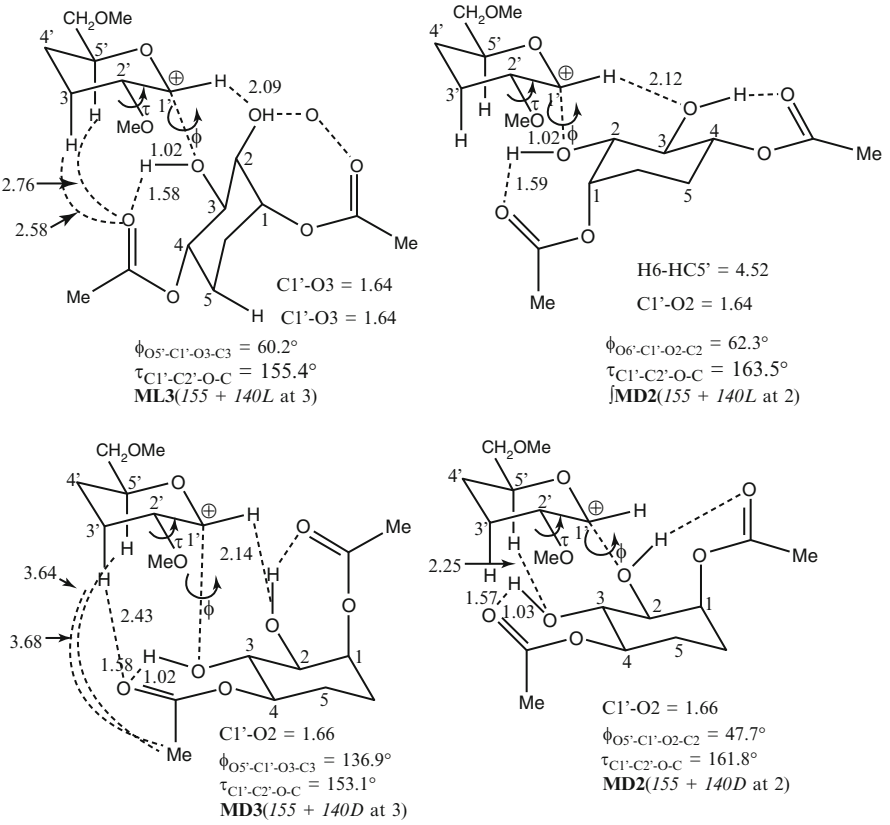

Fig. 5.42

analysis [78, 79] shows an important charge donation from a lone pair of the carboxylic oxygen to the O–H antibonding orbital that weakens this bond (Wiberg bond indexes of O–H bonds involved in glycosidic bond formation are in the range 0.50 − 0.52 Å, whereas the values for the other O–H group are in the range 0.65 − 0.66 Å) [Wiberg bond indexes of O–H bonds in the acceptor model are 0.72 and 0.73 Å]. The second-order perturbation energy associated with these stabilizing donations are in the range 43–46 kcal/mol, a big value compared with the interactions found for other O–H groups (7–12 kcal/mol) that participate in a normal hydrogen bond. This suggests that glycosylation may be assisted by the basic character of the adjacent acyl group. In agreement with this, when the acyl groups in complexes **AL3** and **AL2** were substituted by methyl groups (see complexes **AL′3** and **AL′2** in Fig. 5.51), the complexation process was less favorable, and a slight elongation of the distances C′–O3(O2) (1.67 and 1.68 Å)

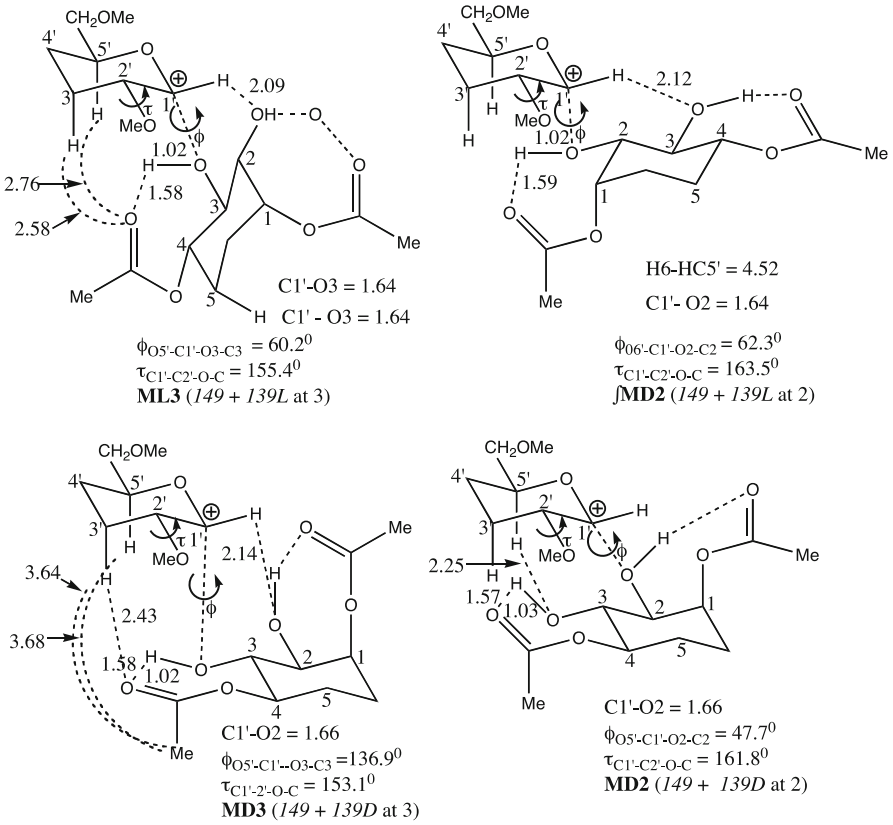

Fig. 5.43

and C′–H–O2(O3) (2.29 and 2.10 Å) was observed. Although there also exists an interaction between the O–H group to be glycosylated and the adjacent methoxy group, this must be weaker according to the values of distances and angles [77]. For complexes shown in Fig. 5.51 CO. . .H distance is 1.53–1.54 Å, O. . .H–O angle (Θ) 155 − 166°, X = O. . .H angle (φ) 111 − 116°. For complexes **AL′3** and **AL′2** shown in Fig. 5.52, CO. . .H distance 1.90 and 2.07 Å, O. . .H–O angle (θ) 120.9 and 119.5°, C–O. . .H angle (θ) 130.3 and 129.5°, respectively [80] (van der Waals radii values: H = 1.20 Å, O = 1.52 Å, N = 1.55 Å).

Complexes shown in each figure are quite similar in energy and do not seem to have important differences in electronic interactions. However, a careful analysis of these structures may help to understand most of the experimental results presented in Table 5.4. First, the high regioselectivity to position 3 shown by acceptor *142L* in reaction with 2-azide substituted donors *153* and *154*, which is inverted to position 2 with benzylated acceptor *172L* and the same donors. Second, the low regioselectivity observed for acceptor *142D* with 2-azide substituted donors *153*

and *154*. Third, the role of the group at C2 of the glycosyl donor azide group induces high 3-regioselectivity with acceptor L, whereas the benzyloxy group induces high 2-regioselectivity with acceptor D.

The interactions that takes place during the approach of the acceptor to the lower face of the donor can be related to the value of the dihedral angle Φ as well as to the distances between certain groups indicated in Figs. 5.41 and 5.42.

In order to analyze the results from the **AL3** and **AL2** approximations (see Fig. 5.42), it must be mentioned that in complex **AL2,** the axial substituent at C6 of the acceptor (that has been eliminated in the model) should be closer to the lower face of the donor (distance H6–NC5′ 4.70 Å) than in complex **AL3** where the closest substituent, at C5 in this case, shows a longer distance (H5–HC5′ 6.26 Å). Additionally, complex **AL3** shows a stabilizing interaction between the 4-acyl group and C5′-H (distance C = O–HC5′ 2.43 Å). These factors would afford a high C3/C2 ratio which is in agreement with the experimental results (see highly regioselective reaction of *142L* with *153* and *154*, Table 5.3).

When methoxylated glycosyl acceptors were used, an increase in the dihedral angle Φ was observed. Thus, the dihedral angle $\phi_{O5'\text{-}C1'\text{-}O3\text{-}C3}$ increased from 93.8 (in **AL3**) to 104.0° (in **AL′3**) (see Fig. 5.42). In the case of approximation through position 2, the dihedral angle $\phi_{O5'\text{-}C1'\text{-}O2\text{-}C2}$ varied from 67.6 (in **AL2**) to 73.8° (in **AL′2**). These variations provide fewer interactions between groups on the acceptor and the lower face of the donor in both **AL′** complexes. The absence of the carbonyl group in **AL′3** produces the loss of the stabilizing interaction that was present in **AL3** (the equivalent distance O–HC5′ with the OMe group in **AL′3** is 3.72 Å). The possible steric hindrance in **AL′2** would decrease (distance between axial H6 and C5′ = 5.54 Å) with respect to the situation in **AL2** (4.70 Å). These facts agree with the reverse stereoselectivity experimentally observed for benzylated acceptors (see the results of the reaction of *172L* with *153* and *154* in Table 5.3).

On the other hand, in the case of the acceptor with D-configuration, complex **AD3** also shows a stabilizing interaction (analogous to the one found in **AL3**) between the 4-acyl group and in this case C3′–H (distance C =)–HC3′ 2.43 Å. However, due to the orientation of this acyl group, steric effects should become important when the size of the acyl group increases (distance COCH3–HC3′ 3.71 Å). The approximation shown for complex **AD2** is almost totally free of steric interactions but does not present any additional favorable electronic interaction. The experimental result in this case is poor regioselectivity (see reaction of *142D* with *153* and *154* in Table 5.3).

In order to study the role of the group at C2 of the glycosyl donor, complexes shown in Figs. 5.42 and 5.43 must be compared. Both types of complexes are quite similar. However, there exists a remarkable difference between complex **AL3** and **ML3** regarding the orientation of the C2 substituent (torsional angles: C1′–C2–N–N = 92.7°; C1′–C2′–O–CH_3 = 155.4°) [this torsion angle is in the range 153–167° for the rest of the structures shown in Figs. 5.42 and 5.46

(**AL2**, **AD3**, **AD2**, and **ML2**, **MD3**, **MD2**)]. Probably with this orientation, the nitrogen atom on the azide group can avoid electronic repulsion with O2, whereas the methoxy group cannot reach this conformation due to steric reasons. The different conformation of the C2 substituent causes a dramatic decrease in the value of $\Phi_{O5'-C1'-O3-C3}$ from 93.8° in complex **AL3** to 60.2° [Φ changes only in the range 2–10° for the rest of the complexes (**AL2**, **AD3, AD2** and **ML2**, **MD3**, **MD2**) in complex **ML3**]. Thus, complex **ML3** shows an orientation similar to **ML2** (and also to **AL2**, compare Φ angle values in Figs. 5.42 and 5.43), and therefore they present similar interactions between the axial substituent at C5 in **ML3** and C6 in **ML2** and **AL2** of the acceptor and the lower face of donor. Additionally, **ML3** shows the 4-acyl group inside the lower face of the donor (distances C=O–HC5′ 2.76 Å and C=O–HC3′ 2.58 Å) and thus the stabilizing interaction should be smaller than in complex **AL3**. Therefore, with these 2-methoxy **ML** complexes, no regioselectivity should be expected as can be experimentally observed in the reaction of *142L* with *155* (Table 5.3). For the D-enantiomer, the approximation through OH–2 seems to be slightly favored according to the distance of the incipient bond (1.66 Å in complex **MD2** vs. 1.68 Å in complex **MD3**). The relatively unfavorable situation in **MD3** may also be ascribed to steric factors. The distance between methyl groups of the C2′-methoxy substituent and 4-acetyl is only 3.68 Å. In comparison with **AD3**, the COCH3–HC3′ distance in **MD3** is 3.64 Å. Most likely the influence of these effects on the regioselectivity of the glycosylation will increase as the size of the substituent at the 2-position of the glycosyl donor increases.

These calculations have highlighted the importance of hydrogen bonds on the acceptor residue in the regiochemical outcome of the glycosylation of diol acceptors. Particularly interesting is the assistance of an acyl group close to the hydroxyl group to be glycosylated. This effect can help to explain the results presented herein, as well as some others already described in the literature. For example, a methoxycarbonyl group at the 6-position facilitates regioselective glycosylation at the 3-position of a 3,4 diol of a glucuronic derivative in a $^1C_4$ conformation [80]. The higher ratio of glycosylation at C2 of the 2,4-mannosyl diol acceptors, when a benzoyl group is at C3 compared with a benzyl group, is also in agreement with these observations [81].

As can be seen in complexes **AL′3** and **AL′2**, the hydrogen bond assistance can also be found, although to a lesser extent, with alkoxy substituents. This effect could explain the lower degree of glycosylation of hydroxyl groups with either no possible or favorable hydrogen bond assistance described in the literature. That could be the case of the higher ratio of glycosylation of hydroxyl groups at C3 position even being the most hindered one, compared to OH–2 in α-altrose diol acceptor derivatives described by Fraser-Reid et al. [66]. This fact could also explain the glycosylation tendency of the axial hydroxyl group at C1 versus C2 in D-*chiro*-inositol 1,2-*syn* diol acceptors [54].

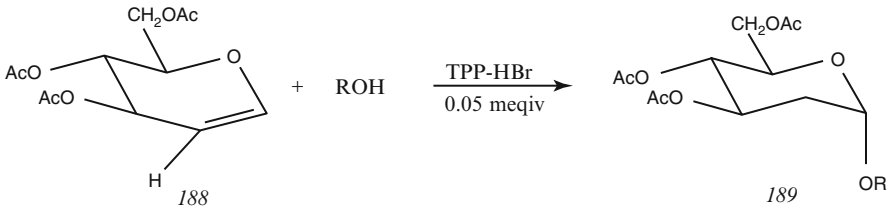

Fig. 5.44

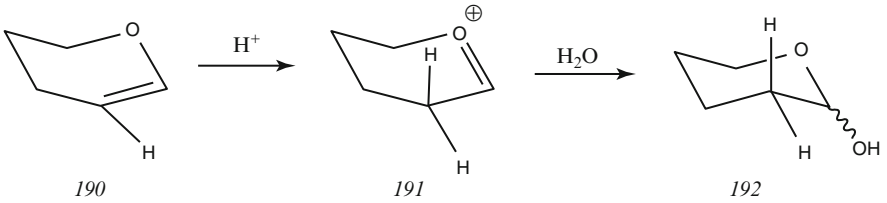

Fig. 5.45

5.3.2 Proton-Catalyzed Addition of Alcohols to Glycals: Glycals as Glycosyl Donors

The proton-catalyzed addition of alcohols to glycals is shown not to be *trans* diaxial addition. Bollitt et al. [83] reported that triphenylphosphine hydrobromide (TPP-HBr) was the catalyst of choice for mild and high-yield protonation and subsequent glycosidation of glycals (Fig. 5.44).

They observed mainly α-glycoside products in their examples using glycals with all equatorial substituents. Danishefsky [84] has obtained, in allal series, a β-glycoside with the BMLF protocol. Earlier physical organical studies had shown that the hydration of enol ethers occurs via an Ad_E2 (addition-electrophilic-bimolecular) mechanism, i.e., a first step of protonation to form an oxocarbenium ion followed by a second step of nucleophilic addition [85, 86] (Fig. 5.45).

In the protonation step in a polar medium, no strong bridging of the proton can occur. Thus, there was no good reason to expect direct *trans* addition in cases where stereochemistry was observable. In order to completely determine the stereochemistry of nonenzymatic protonation of glycals, the BLMF procedure in deuterated media was used [87]. Thus, the glycals listed in Table 5.5 were treated with catalytic amount of TPP-HBr in the presence of nucleophiles having O–D functions. The stereochemistry and yield of the products were determined by NMR spectroscopy (both ^1H and ^2H) (Lemieux has reported the synthesis of 2-deuterioglycosides by Pd-catalyzed deuterogenolysis of 2-iodosaccharides and has reported their 60-MHz proton spectra which are in good agreement with the obtained data [88]).

Table 5.5 Sugar stereochemistry at C1 and C2 resulting from protonation of glycals

Entry	Glycal	R (equiv)	Anomer ratio α/β	Equatorial D/axial D
1	*193*		70/30	87/13[a, b]
2	*193*		90/10	92/8[a, b]
3	*194*		75/25	67/33[a–c]
4	*195*		77/23	33/67[a, d]
5	*196*		88/12	87/13[a, d]
6	*196*		98/2	85/15[a, d]
7	*190*		21/79	<5/0.95[e]

[a]Since the NMR peaks for axial and equatorial D did not give baseline resolution, the peak areas were determined by a visual curve-fitting program; hence, the disparities in the e/a ratios in entries 1–2 and 5–6 indicate the imprecision of the curve-fitting
[b]The ratios were identical in both α- and β-anomers; hence the ^{2}H spectra are of α/β mixtures
[c]The ratio was determined after deacetylation and rebenzylation
[d]The ratio was determined for α-anomer only
[e]The ratio was determined for the β-anomer only

From the obtained results it is clear that, except for the case of 3-deoxyglycal *194* and allal *198,* deuteron delivery is largely from below the plane to afford what becomes the equatorial ligand at C2 (Fig. 5.46). Hence, the stereochemistry at the anomeric center of the product glycoside is not due to *trans* addition. The predominant axial stereochemistry at C1 probably arises from the kinetic anomeric effect (KAE) expected for trapping the intermediate oxocarbenium ions *198* and *201* (Fig. 5.46) [89, 90]. Hence, the differing ratios are due to differing magnitudes of the KAE inherent in the developing C1-nucleophile bonding. One can interpret the observation of a β-glycoside in the allal series simply as a result of the steric repulsion of the 3-axial substituent overriding the KAE. These results are consistent with the Ad_E2 mechanism with a kinetically (sterically?) controlled protonation followed by glycosyl transfer directed by KAE. They are only surprising to the extent that the intuition of many practicing organic chemists assumes that *trans* diaxial addition of electrophilic reagents to alkenes is the common behavior. The presented results confirm a related experiment with similar mild conditions where Borowiecka et al. [91] added deuterated thiophosphoric acid to glycal to afford cleanly a 2-deoxypyranose thiophosphate product resulting from *cis* addition from the α-face. Treatment of the triacetate of galactal-2-d *204* (Fig. 5.47) with a melt of phenol and p-TosH at 60 °C afforded largely an α-glycoside with no stereoselectivity in the proton delivery [92, 93].

It is interesting to compare the acid-catalyzed results with those of enzyme-catalyzed additions. Lehmann [92, 93] (β-galactosidase, *trans*-"diequatorial") and Hehre [94] (α-glucosidase, *trans* "diaxial" and β-glucosidase, *trans*-"diequatorial") in a pioneering series of experiments that anticipated recent work applying enzymology to preparative glycoside chemistry (the Lehmann-Hehre discoveries have been applied to the synthesis of disaccharides in the β-2-deoxy series [95–98]) demonstrated that glycals could be stereospecifically converted to 2-deoxyglycosides using glycosidase enzymes. For example, the galactal-2-d (*204* in Fig. 5.47) was cleanly transferred to glycerol using a β-galactosidase,

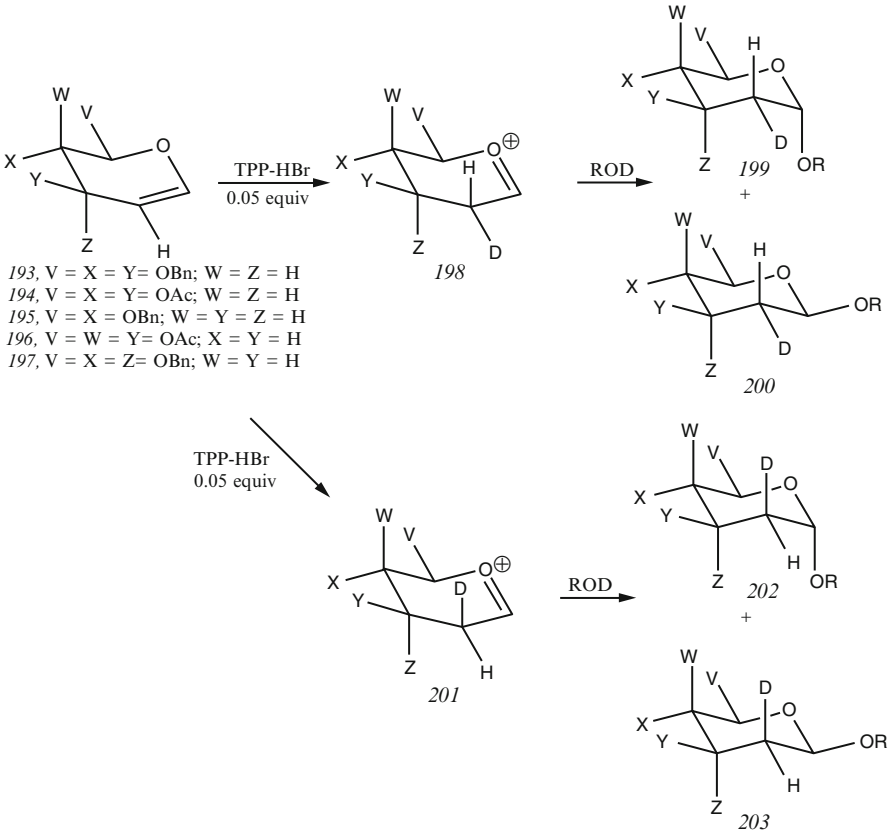

Fig. 5.46

affording glyceryl 2-deoxy-β-galactoside *205* (Fig. 5.47). Delivery of the proton to C2 of the galactal took place specifically from the bottom face to afford apparent *trans* addition. Although it would be simple to explain the observation as a direct *trans* addition, the accepted interpretation is more complex. Thus, it has been shown that the enzyme delivers the glycerol to the β-face of the galactosyl anomeric carbon in a step subsequent to the initial bonding of an enzymic nucleophile on the α-face [99, 100], ostensibly the microscopic reversal of the enzyme's natural and stereospecific cleavage mechanism [101, 102]. The attachment of a proton at C2 and the presumed enzymic nucleophile at the intermediate stage must have been via *cis* addition. It is now possible to speculate that the β-galactosidase-promoted addition with an overall *trans* outcome was really a more stereoselective version of a simple acid-catalyzed *cis* addition, subject to stereoelectronic control, with the β-enzyme affording below-plane protonation corresponding to the previous observation. In contrast, the above-plane protonation with the α-glucosidase enzyme is not consistent with the simple acid-catalyzed chemistry of glycals followed by

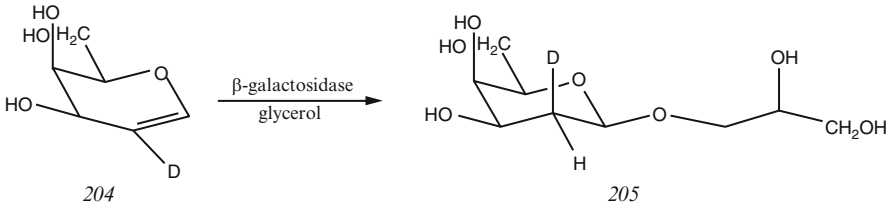

Fig. 5.47

glycosyl transfer. The unanswered question concerning the described chemical results and also the larger field of electrophilic addition to glycals is what is the basis for "below plane" of "equatorial-developing" attack at C2. One popular explanation, namely, pyramidalization of the alkene carbon [103], is belied by the reported crystal structures for glycals [104, 105]. A rationalization, commonly known as Cieplak effect [106], where the more electron-rich bond vicinal and anti-parallel to the forming bond, directs the attack, can explain the outcome only in the 3-deoxyglycal case. Some as yet undefined steric effect of the 3-equatorial substituent and the 4-axial proton may be a part of the explanation in the glycal series, while in the galactal and allal cases, a steric repulsion of 4-axial and 3-axial groups, respectively, is probably determinant. More work remains to be done to discover the balance of forces that controls the face-selectivity of electrophilic attack in glycals.

The use of neighboring group participation to control the stereoselectivity of a glycosylation reaction is a powerful method for the stereoselective synthesis of glycosides [107, 108]. This method provides an efficient synthesis of 2-deoxysugar glycosides, because after a substituent at the C2 has directed the stereochemistry at the anomeric carbon (C1), the substituent can be removed [107, 108]. Figure 5.48 summarizes the selective conversion of thioglycoside *206* into both glycosyl acceptor *210* and glycosyl donor *212*; the 1,2-migration developed by Nicolaou et al. [109, 110] was employed. Thioglycosides *207* and *211* underwent smooth 1,2-migration on exposure to DAST to furnish glycosyl fluorides *208* (mixture of α- and β-anomers, ca. 1:17) and *212* (mixture of α- and β-anomers, ca. 1:14), respectively, in quantitative yields. As expected, glycosylation of *208* with MeOH and $SnCl_2$ in ether was directed by the PhS group at C2 to give predominantly the β-anomer *209* (91 %, ca. 10:1). Desilylation of *209* gave compound *210*.

The assembly of the A_1BC ring of everninomycin *213* (Fig. 5.49) from building blocks *203*, *207* (Fig. 5.50) was effected as described in Fig. 5.50. Thus, carbohydrates *203* and *207* undergo highly stereoselective glycosidation giving the corresponding β-glycoside due to the presence of the PhS groups at the C2 carbon which directs the stereochemistry. The 2-phenylthio group is removed in the next step by reaction with Raney nickel providing the pure β-linked 2-deoxy disaccharide *209* which otherwise would be impossible to obtain.

Other substituents, such as PhSe groups [111, 112] and halogens (particularly I [113–116]), have also been employed. The stereochemical outcomes of these

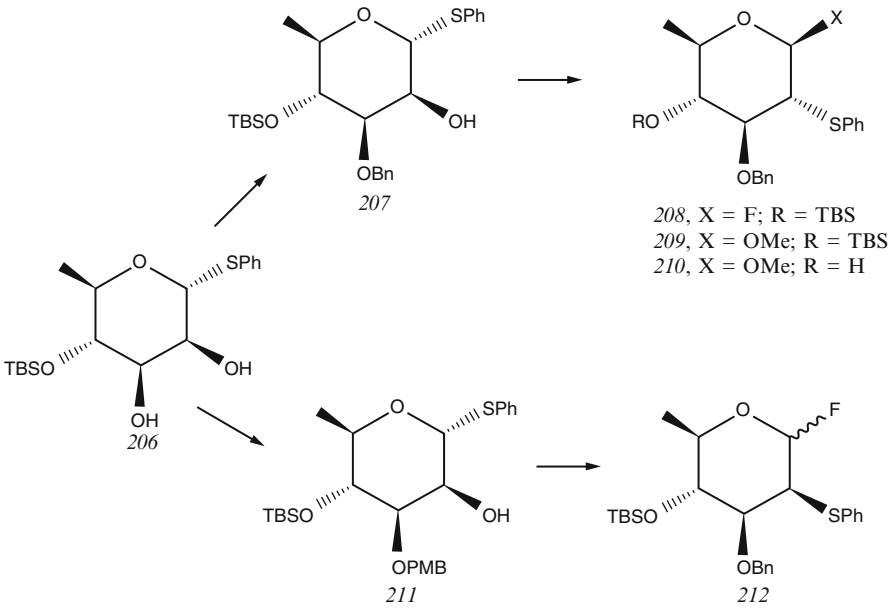

Fig. 5.48

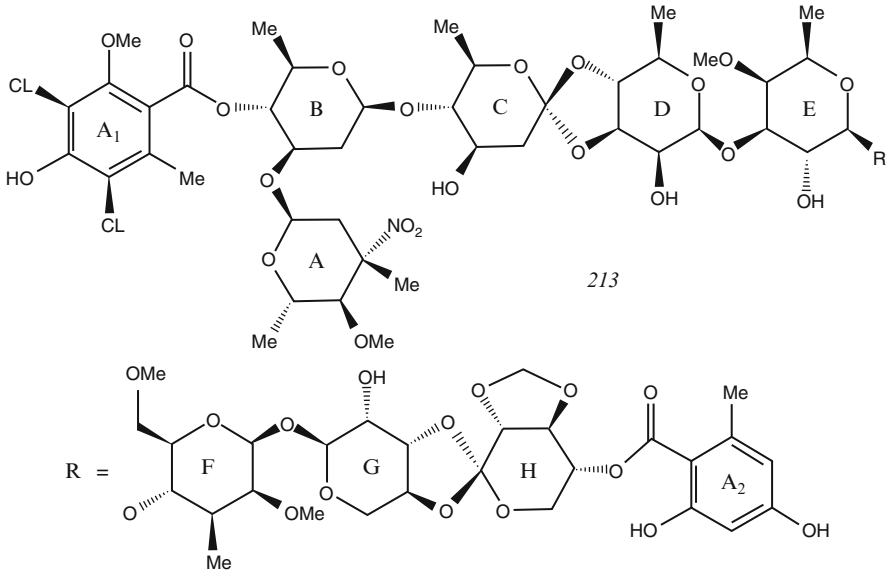

Fig. 5.49

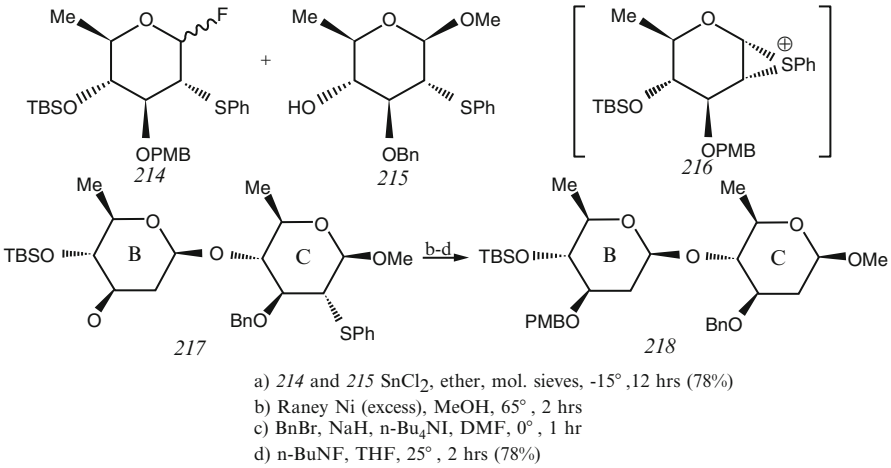

Fig. 5.50

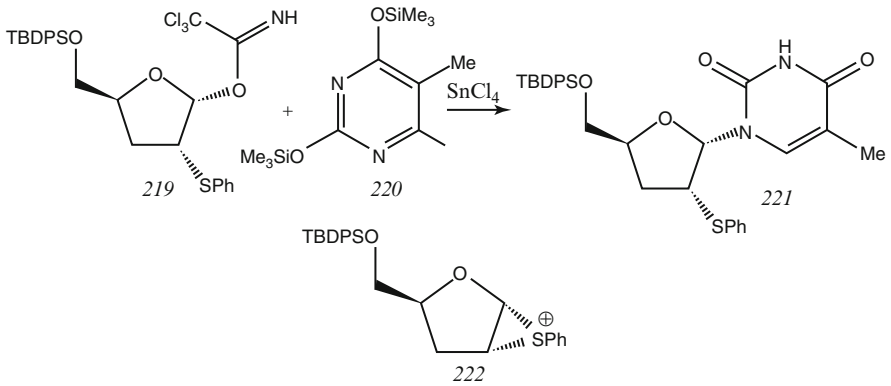

Fig. 5.51

reactions are typically considered to result from stereospecific ring opening of bridged intermediates [108] such as *216* and *222* (Figs. 5.50 and 5.51) with inversion of configuration.

The high selectivities exhibited by many of these processes make this explanation strongly compelling [117].

Although mechanisms involving bridged intermediates such as the episulfonium ions *216* (Fig. 5.50) and *222* (Fig. 5.51) provide satisfying explanations for observations such as those shown in Figs. 5.50 and 5.51, accumulating evidence suggests that such intermediates may not be involved in stereoselective substitution processes. The fact that the reactions that would be expected to proceed through episulfonium [111, 112, 118–120], episelenonium [118, 121], or iodonium ions

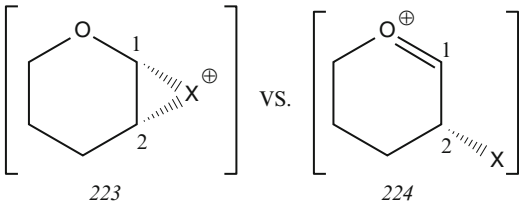

Fig. 5.52

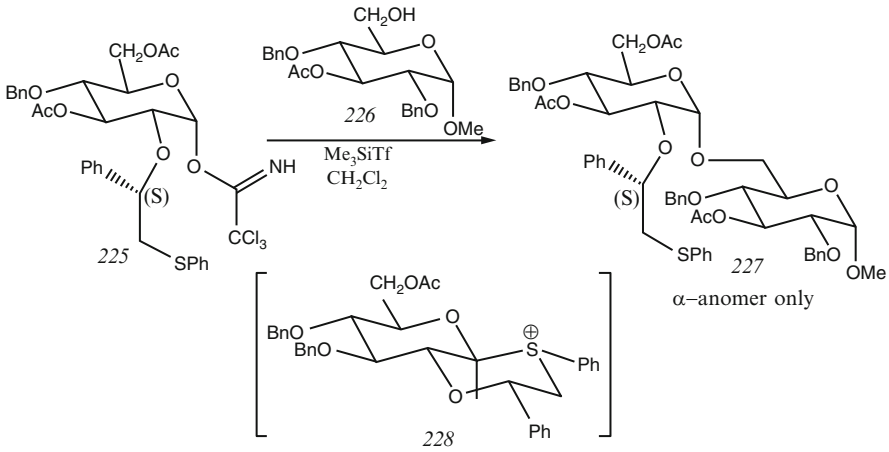

Fig. 5.53 1, 2-*cis*-Glycosylation using a tethered sulfide

[114, 115] are not completely selective [122] indicates that these reactions may occur by a different pathway or through multiple pathways (Fig. 5.52).

Carbohydrate-derived episulfonium ions have been observed spectroscopically. Boons et al. [123–125] have developed methods for 1,2-*cis* *O*-glycosylation, a challenging problem in carbohydrate chemistry [126]. The glycosyl donor *225*, which bears a pendant sulfide group at C2, exhibited high α-selectivity in glycosylation reactions [124] (Fig. 5.53).

The intermediate sulfonium ion *228* was observed by low-temperature NMR spectroscopy in the absence of a nucleophile. The stereochemical outcome of the glycosylation reaction implies a mechanism involving ring opening of sulfonium ion *228* with inversion at the anomeric carbon. The Boons laboratory, however, noted that the precise structure of the sulfur-bearing directing group is critical. When the directing group possessed the (R)-configuration at the benzylic stereocenter, the disaccharide product was obtained with no selectivity. Consequently, the formation, stability, and reactivity of sulfonium ions resembling *228* are sensitive to the exact nature of the cation.

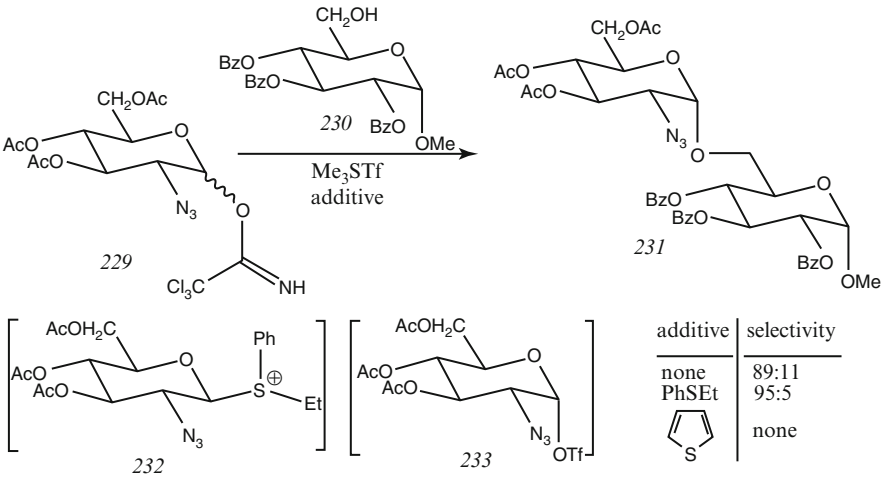

Fig. 5.54 1, 2-*cis*-Glycosylation of 2-azidosugars using exogenous sulfides

The addition of exogenous sulfides can increase the selectivity of some glycosylation reactions [124] and sulfonium ion intermediates may be involved in these reactions [125] and related processes [127]. For example, the selectivities of reactions of the 2-azido sugar *229* can be enhanced with the appropriate choice of a sulfide additive [125] (Fig. 5.54). As with the glycosyl donor bearing a tethered sulfide *225* (Fig. 5.53), a sulfonium ion *232* was observed by low-temperature NMR spectroscopy, along with the glycosyl triflate *225* [125]. The stereochemical course of this glycosylation reaction is also consistent with direct displacement of the anomeric sulfonium ion. The observation of inversion at the anomeric carbon, however, can also be the result of a transition state with considerable oxocarbenium character, as demonstrated for mannosyl triflates [128] and iodides [129].

Nicolaou et al. [109] reported a new synthetic technology for the following: (a) introduction of fluorine at C1 [for some previous syntheses and/or utilizations of glycosyl fluorides, see [130–139]]; (b) introduction of *O*-, *S*-, and *N*-containing substituents at C2; (c) inversion of configuration at C2; (d) deoxygenation at C2; and (e) stereocontrolled synthesis of α- and β-glycoside bonds including the hitherto difficult to construct 2-deoxy-β-glycosides (for some previous efforts for synthesis of 2-deoxy-β-D-glycosides, see [140]).

Figure 5.55 outlines the mechanistic considerations that led to the design of these stereospecific migrations. Thus, it was anticipated that a migratory group at C1 might be induced to shift to the neighboring position (C2) by (a) a "pull" from the "host" carbon initiated by the departure of a leaving group and (b) a "push" from the ring oxygen lone pairs of electrons, provided the groups involved were stereoelectronically oriented in the proper fashion. In consideration of practical means to realize this scenario from simple and readily available starting materials, and in order to maximize the synthetic potential of the resulting products, (diethylamino)

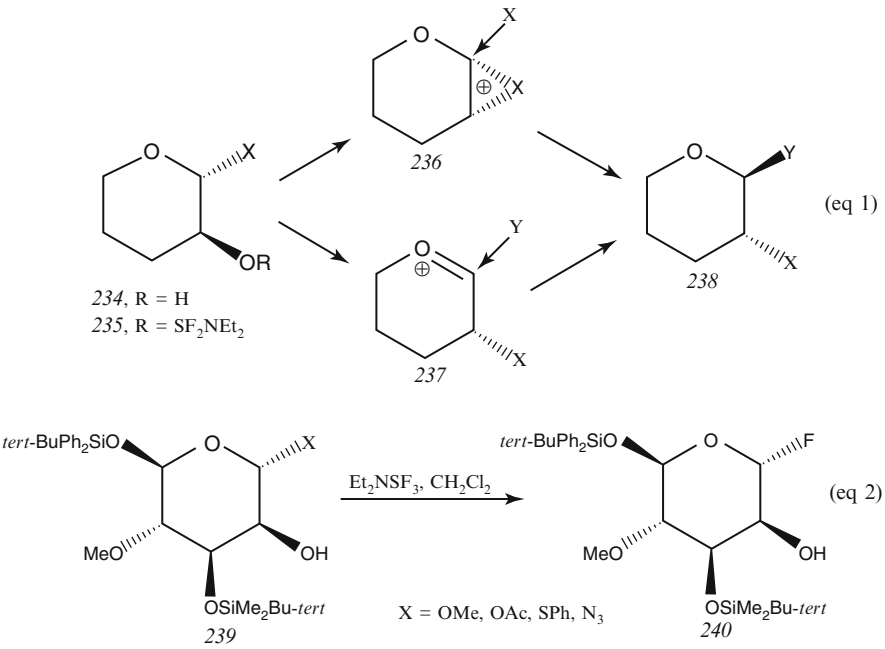

Fig. 5.55

sulfur trifluoride (Et_2NSF_3, DAST) was chosen to operate on the hydroxy substrates *234* (Fig. 5.55) (for use of DAST to prepare α-fluoro-β-amino acids from β-hydroxy-α-amino acids via nitrogen 1,2-shift, see [141]). Indeed, when compounds *239* (X = OMe, OAc, SPh, N_3; Fig. 5.55, Eq. 2) were treated with excess DAST in CH_2Cl_2 at 0–45 °C, the glycosyl fluorides *240* were obtained in high yields (see Table 5.7) (for a previous report of C1 to C2 shift involving a thiophenyl and mesylated group under basic conditions, see [142]). Furthermore, a number of other substrates and substituents (e.g., OCH_2Ph, OCOPh, O-sugar) were found to undergo the C1 to C2 shift, as Table 5.6 demonstrates. Thus, in one step, this operation introduces a variety of useful functional groups at C2 and simultaneously a fluorine substituent at C1 with inversion of stereochemistry at both centers.

These facile migrations have a number of obvious and useful applications. Thus, the glycosyl fluorides obtained can be used in coupling reactions (vide supra) to afford various types of *O*-, *S*-, *N*-, and *C*-glycosides. This powerful reaction also offers the possibility of transplanting a group in a predictable stereochemical fashion at C2 after introduction at C1, the most activated position of the carbohydrate framework. Easy deprotection of some of these groups (e.g., OAc, OCH_2Ph) results in a new and practical method for inversion of stereochemistry at C2, whereas the successful introduction of the azido group has important implications in the synthesis of amino sugars. The PhS group with its rich and synthetically

Table 5.6 1,2-Migration in carbohydrates

Substrate	Product	Yield
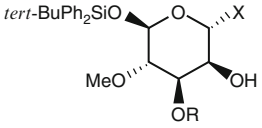	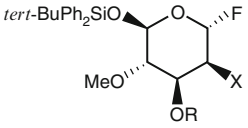	
241a, X = OMe; R = $SiMe_2Bu$-*tert*	*242a*, X = OMe; R = $SiMe_2Bu$-*tert*	77 % (at 45°)
241b, X = OMe; R = CH_2Ph	*242b*, X = OMe; R = CH_2Ph	81 % (at 45°)
241c, X = OAc; R = $SiMe_2Bu$-*tert*	*242c*, X = OAc; R = $SiMe_2Bu$-*tert*	91 % (at 0°)
241d, X = SPh; R = $SiMe_2Bu$-*tert*	*242d*, X = SPh; R = $SiMe_2Bu$-*tert*	88 % (at 0°)
241e, X = N_3; R = $SiMe_2Bu$-*tert*	*242e*, X = N_3; R = $SiMe_2Bu$-*tert*	78 % (at 45°)
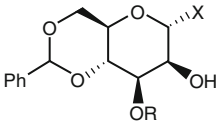	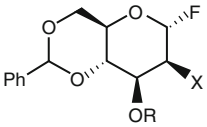	
243a, X = OMe; R = $SiMe_2Bu$-*tert*	*244a*, X = OMe; R = $SiMe_2Bu$-*tert*	70 % (at 45°)
243b, X = SPh; R = $SiMe_2Bu$-*tert*	*244b*, X = SPh; R = $SiMe_2Bu$-*tert*	93 % (at 0°)
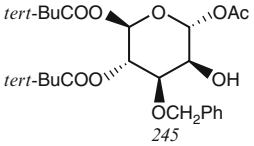 *245*	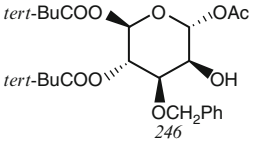 *246*	88 % (at 0°)
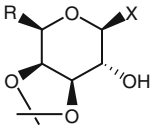	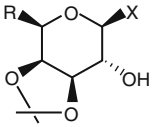	
247a, X = SPh; R = Me	*248a*, X = SPh; R = Me	86 % (at 0°)
247b, X = N_3; R = Me	*248b*, X = N_3; R = Me	75 % (at 45°)
247c, X = OCH_2Ph; R = H	*248c*, X = OCH_2Ph; R = H	65 % (at 25°)
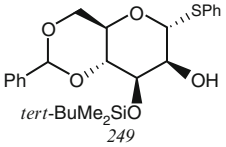 *249*	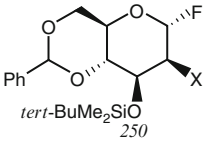 *250*	88 % (at 0°)
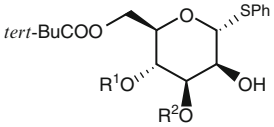	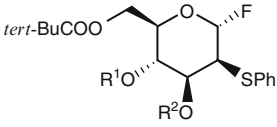	
251, R^1 = CH_2Ph; R^2 = $SiMe_2Bu$-*tert*	*252*, R^1 = CH_2Ph; R^2 = $SiMe_2Bu$-*tert*	85 % (at 0°)
251, R^1 = $SiMe_2Bu$-*text*; R^2 = Me	*252*, R^1 = $SiMe_2Bu$-*tert*; R^2 = $SiMe_2Bu$-*tert*	86 % (at 0°)

In entries *233c* and *233d*, *245*, *247a* and *249* the indicated anomer was exclusively formed, whereas in the remaining entries the indicated anomer predominated in an anomeric mixture Z (α/β ratio): *241a*(40:60), *241b*(40:60), *241e*(50:50), *242a*(25:75), *247b*(50:50), *247c* (60:40), *250*(62:38)

Table 5.7 Stereocontrolled synthesis of α- and β-glycosides

Entry	Reactants	Solvent/reagents[a]	Yield, %	α:β ratio[b]
1	*246*, *247*	Et_2O	92	1:16
2		CH_2Cl_2	90	10:1
3		CH_2Cl_2/20 equiv Me_2S	90	1:13
4		THF (1.2 equiv of $AgClO_4$)[c]	(50)	(1:3)
5	*254*, *247*	Et_2O	93	1:0
6		CH_2Cl_2	91	1:0

[a]Reaction conditions: 1.8 equivalent of $SnCl_2$, 4 Å MS, −15° C
[b]Determined by ^1H NMR spectroscopy
[c]In the absence of $AgClO_4$, the reaction did not proceed

fertile chemistry promises new ventures in carbohydrate chemistry including deoxygenation at C2 and control of glycosidation stereochemistry.

The application of this technology to the stereocontrolled construction of α- and β-glycosides was then demonstrated by the efficient syntheses of two isomeric disaccharides. This objective was achieved by (a) introduction of a PhS group at C2, (b) α- or β-directed glycosidation by neighboring group and/or solvent participation, and (c) desulfurization to afford the 2-deoxy-α-glycoside or its β-isomer. Figure 8.84 illustrates this three-step sequence which is of particular importance for 2-deoxy-β-glycosides, compounds normally not directly accessible from 2-deoxy-sugars (for some previous entries into 2-deoxy-β-glycosides, see [140]), leading to the α-linked disaccharides *249* and *252* [in both entries *234* and *235*, Fig. 5.55, the α-anomer is expected as observed, since sulfur participation and the anomeric effect direct the stereochemistry to the α-configuration] and the β-linked isomer *236* with high stereocontrol. Of special interest was the solvent effect on the stereochemical outcome of these glycosidation reactions in the presence of $SnCl_2$ as Table 5.7 shows. It appears that in the presence of a tin-complexing solvent or reagent (e.g., entries 1, 3, and 5, Table 5.7), the SPh group remains free to direct the glycosidation via a transient intermediate such as *255* (Fig. 5.56), whereas in the absence of a complexing medium (e.g., entries 2 and 6, Table 5.7), the catalyst may be engaging the sulfur, thus preventing it from participating in the coupling reaction [in both entries 5 and 6, Table 5.7, the α-anomer is expected as observed, since sulfur participation and the anomeric effect direct the stereochemistry to the α-configuration].

The described chemical transformations are expected to (a) increase the usefulness of carbohydrates in organic synthesis, (b) enhance our ability to synthesize various useful and/or rare sugars from other readily available carbohydrates, and (c) facilitate the construction of oligosaccharide chain with stereocontrol at the glycoside bond.

Numerous approaches to the synthesis of *C*-glycosides have been proposed [143–164] and reviewed [143–152]. A majority of these methods have led to mixture of α- and β-isomers. One viable approach to improve the stereoselectivity in organic synthesis has been the use of epoxides [165, 166] or three-membered cyclic cations (e.g., episulfoniium [167–171] and episelenonium [172, 173]). Reactions of nucleophiles with these species are expected to proceed with high stereoselectivity as a

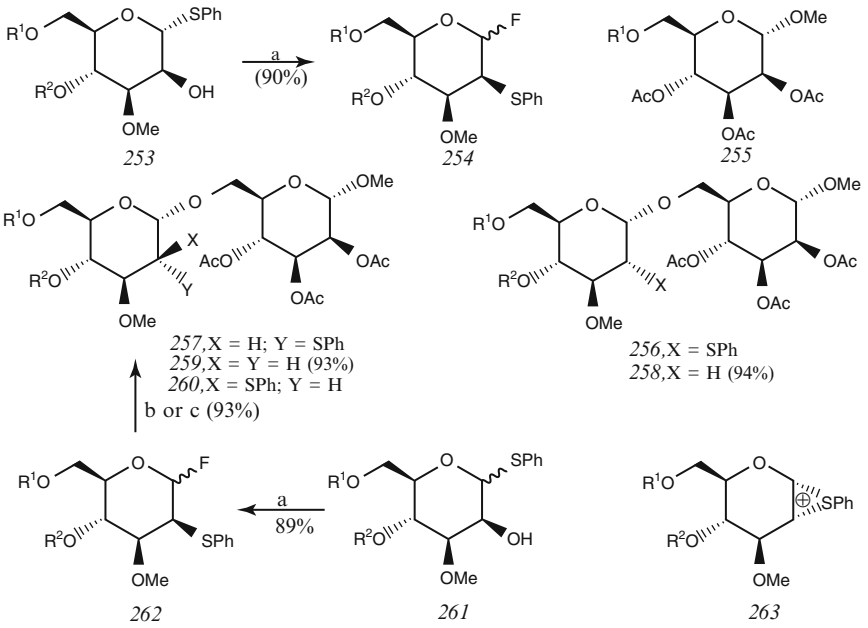

(a) 3 equiv DAST, CH_2Cl_2, 0°C; (b) 0.9 equiv of *253*, 1.8 equiv of $SnCl_4$, 4A MS, Et_2O, - 15°C; (c) 0.9 equiv. of *253*, 1.8 equiv of $SnCl_4$, 4A MS, CH_2Cl_2, - 15°C; (d) Raney Ni, EtOH, Δ; (e) yield based on *253*

Fig. 5.56

result of *trans*-opening of the rings [165, 166] or three-membered cyclic cations (e.g., episulfonium [167–171] and episelenonium [172, 173]). Epoxides and three-membered cyclic ions have been the precursors for the preparation of *O*-glycosides [174–177]. For the use of 1,2-episulfonium intermediates for the synthesis of *O*-glycosides, see [109, 110, 112, 178–188]. For the nucleoside preparation via episulfonium ions, see [189, 190]. For the use of 1,2-episelenonium ions for the synthesis of *O*-glycosides, see [191–193]. For 1,2-iodonium ions in *O*-glycoside synthesis, see [21, 194–197]. For cyclization via halonium ions providing *O*-glycosides, see [198]. For mercury-assisted cyclizations forming *O*-glycosides, see [199, 200] and for other carbohydrate derivatives, see [201–203]. In the *C*-glycoside synthesis, the use of these cyclic species has been based on three major approaches. The first is the formation of a cyclic intermediate from a 1,2-unsaturated sugar derivative, glycal, with subsequent attack of a carbon nucleophile (C–Nu, Fig. 5.57). In the second, rather limited method, epoxides or three-membered cyclic ions obtained from *exo*-glycals react with C–Nu (Fig. 5.58). The third approach includes electrophile-mediated cyclization reactions of alkenols (Fig. 5.59).

For cyclizations via epoxide opening leading to *C*-glycosides and related compounds, see [2, 204–206]. For the synthesis of *C*-glycosides and related compounds by episelenonium-mediated cyclizations, see [2, 207]. For episulfonium ion promoted cyclizations of hydroxy alkenes, see [2]. For the preparation of *C*-glycosides

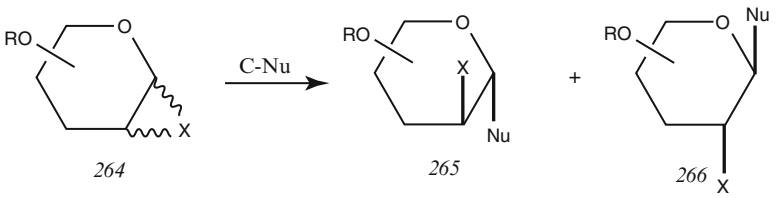

Fig. 5.57

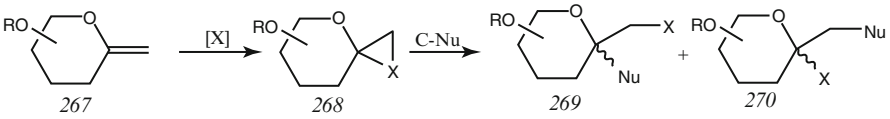

Fig. 5.58

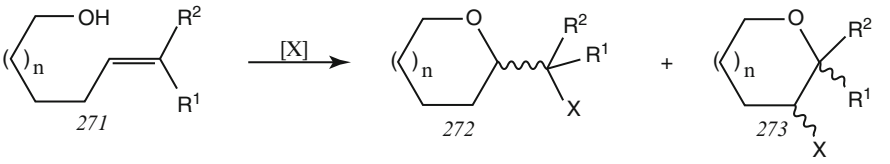

Fig. 5.59

and related compounds using cyclization reactions via halonium ions, see [198, 207–211]. For mercury-assisted cyclizations forming *C*-glycosides and related compounds, see [2, 200, 213].

Among a variety of possible glycal-based three-membered cyclic intermediates, only glycal epoxides and 1,2-episulfonium ions have been employed in the synthesis of *C*-glycosides and related compounds.

Carbohydrate-derived epoxides have found a great use in the synthesis of *O*-glycosides [174–177].

Glycal epoxides have also served as *C*-glycosides precursors as well. Bellosta and Czernecki [214, 215] have studied the reaction of 3,4,6-tri-*O*-acetyl-1,2-anhydro-α-D-glucopyranose *260,* 1,2-anhydro-3,4,6-tri-*O*-benzyl-α-D-glucopyranose *261*, and 1,2-anhydro-3,4,6-tri-*O*-benzyl-β-D-mannopyranose *265* with four organocuprate reagents, R_2CuLi and $R_2CuCNLi_2$ (R = Me, Ph, Fig. 5.60). For all the reactions studied, Me_2CuLi gave higher yields than the other three reagents. This was explained by higher reactivity of this reagent compared to the phenyl analog [215, 216]. The most significant result of this study is that for both epoxides D-gluco (*260* and *261*) and D-manno (*265*), the isolated products were 1,2-*trans* isomers *262*, *263*, *266*, and *267*. It is important that the reaction did not require the use of a Lewis acid.

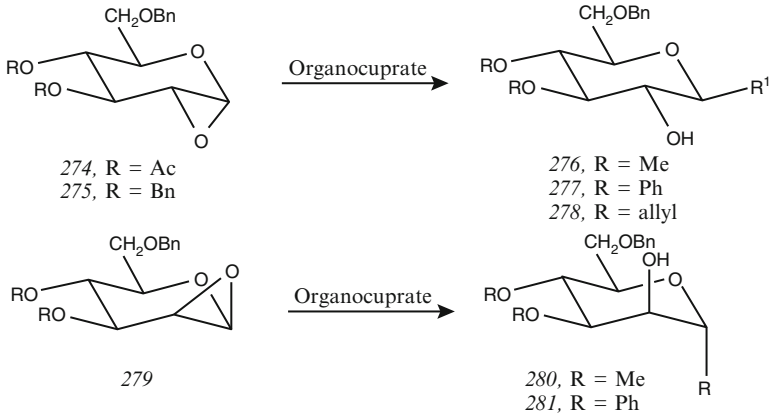

Entry	Epoxide	Organocuprate	Yield % and Reference
1	*274*	$Me_2CuCNLi_2$	26 [29a, b]
2	*274*	$Me_2CuCNLi_2.BF_3.Et_2O$	23 [29b]
3	*274*	Me_2CuLi	65.5 [29a, b]
4	*274*	$Ph_2CuCNLi$	27 [29b]
5	*274*	Ph_2CuLi	23 [29b]
6	*279*	Me_2CuLi	90 [29a, b]
7	*279*	Ph_2CuLi	70 [29a, b]
8	*275*	$(allyl)_2CuCNLi$	43 [31], 0 [32]

Fig. 5.60

There are limited data on 1,2-epoxy of glycal epoxide ring opening reaction with C-nucleophiles other than organocuprate, e.g., Grignard reagents [217, 218], organolithium compounds [217–219], allylstannane [217], and sodio di-*tert*-butyl malonate [219, 220].

Thus, the reaction of allylmagnesium bromide with epoxide *275* in FHF gave β-*C*-D-glucopyranoside *278* in a 75 % yield [217]. It has been also found that the addition of $ZnCl_2$, Li_2CuCl_4, and $Yt(OTf)_3$ increased the yield of the reaction by 9–15 % [218]. However, the use of other Lewis acids, such as CuI, $CuBrSMe_2$, and $BF_3.Et_2O$, caused the opposite effect [218]. The influence of the Lewis acid on stereoselectivity of these reactions has not been studied.

In contrast to the known data for the reactions of glycal epoxides with other C–Nu, the ring opening using lithium alkynyl derivatives gave α-*C*-D-glucopyranosides. The formation of 1, 2-*cis* products was explained by suggesting that (1) the actual nucleophiles in this fraction are organozinc derivatives and (2) the ring opening takes place before the C–C bond formation (Fig. 5.61).

A number of different nucleophiles have been used for opening of glycal epoxide and introducing an allylic residue [217, 218]. Evans et al. proposed a highly stereoselective method for ring opening of glycal epoxides using allylstannanes [217]. This reaction was promoted by a number of Lewis acids.

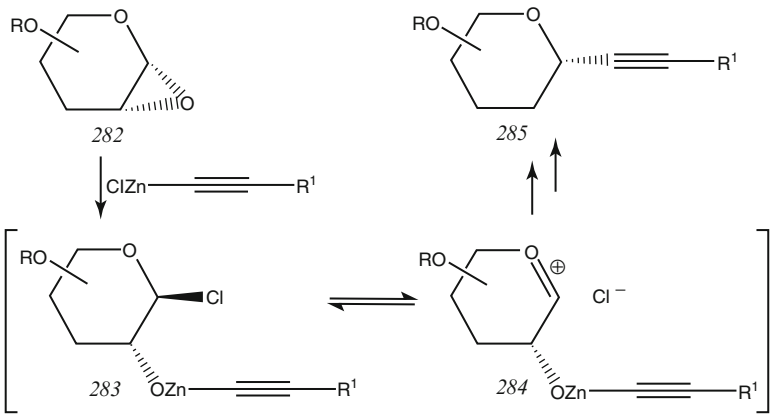

Fig. 5.61

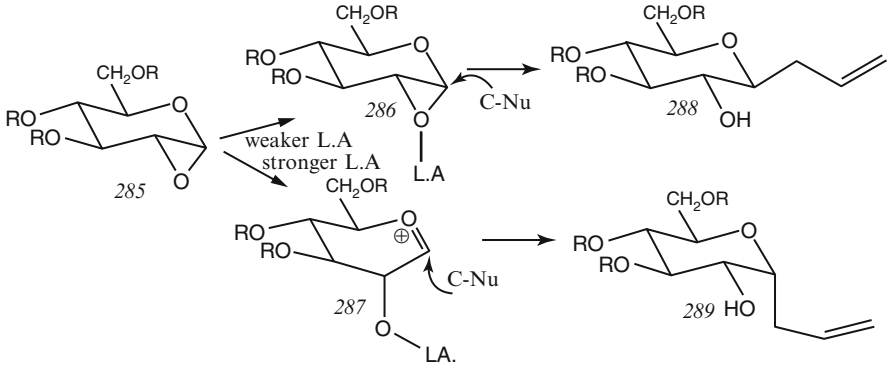

Fig. 5.62

It was found that the stronger acid, $SnCl_4$, provided a trace amount (3 %) of two isomeric *C*-allyl glycosides in the ratio of 1.4:1 (β:α). Tributylstannyl triflate, the weakest among the Lewis acids studied, afforded 57 % of the product as a mixture of β- and α-isomers in a ratio 95:5. The author's explanation [217] of the Lewis acid effect on stereoselectivity is illustrated in Fig. 5.62.

It has been also reported that the reaction of sodio di-*tert*-butyl malonate with epoxide *290* in the presence of a rather weak Lewis acid $ZnCl_2$ stereoselectively afforded β-*C*-D-glycoside *291* (Fig. 5.63).

Thus, the reaction of glycal epoxides with strong nucleophiles, such organocuprates, allylmagnesium bromide, and allyllithium, did not require the use of Lewis acid and proceeded with the formation of 1,2-*trans*-*C*-glycosides.

Episulfonium ions have been known to react with a variety of nucleophiles of different natures and strengths [2, 167, 169–171].

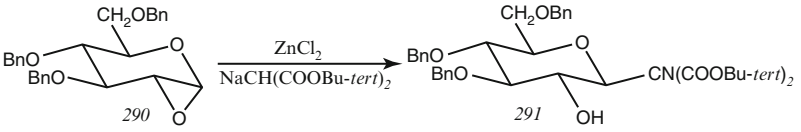

Fig. 5.63

References

1. Mootoo DR, Date V, Fraser-Reid BJ (1988) n-Pentenyl glycosides permit the chemospecific liberation of the anomeric center. J Am Chem Soc 110:2662–2663
2. Reitz AB, Nortey SO, Maryanoff BE, Liotta D, Monahan R III (1987) Stereoselectivity of electrophile-promoted cyclizations of γ-hydroxyalkenes. An investigation of carbohydrate-derived and model substrates. J Org Chem 52:4197–4202
3. Fraser-Reid B, Wu Z, Udodong UE, Ottosson H (1990) Armed/disarmed effects in glycosyl donors; rationalization and sidetracking. J Org Chem 55:6068–6070
4. Konradsson P, Mootoo DR, McDevitt RE, Fraser-Reid B (1990) Iodonium ion generated in situ from N-iodosuccinimide and trifluoromethanesulfonic acid promotes direct linkage of disarmed pent-4-enyl glycosides. J Chem Soc Chem Commun 1990:270–272
5. Konradsson P, Udodong UE, Fraser-Reid B (1990) Iodonium promoted reactions of disarmed thioglycosides. Tetrahedron Lett 30:4313–4316
6. Veeneman GH, van Boom JH (1990) An efficient thioglycoside-mediated formation of α-glycosidic linkages promoted by iodonium dicollidine perchlorate. Tetrahedron Lett 31:275–278
7. Mootoo DR, Fraser-Reid B (1989) Pentenyl 2-amino-2-deoxy glycosides undergo stereoselective coupling under mild, chemospecific conditions. Tetrahedron Lett 30:2363–2366
8. Fraser-Reid B, Udodong UE, Wu Z, Ottosson H, Merritt JR, Rao CS, Roberts C, Madsen R (1992) n-Pentenyl glycosides in organic chemistry: a contemporary example of serendipity. Synlett 1992:927–942
9. Raghavan S, Kahne D (1993) A one step synthesis of the cyclamycin trisaccharide. J Am Chem Soc 115:1580–1581
10. Yamada H, Harada T, Miyazaki H, Takahashi T (1994) One-pot sequential glycosylation: a new method for the synthesis of oligosaccharides. Tetrahedron Lett 35:3979–3982
11. Yamada H, Harada T, Takahashi T (1994) Synthesis of an elicitor-active hexaglycoside analog by one-pot, two-step glycosidation procedure. J Am Chem Soc 116:7919–7920
12. Chenault HK, Castro A (1994) Glycosyl transfer by isopropenyl glycosides: trisaccharide synthesis in one pot by selective coupling of isopropenyl and n-pentenyl glycopyranosides. Tetrahedron Lett 35:9145–9148
13. Ley SV, Priepke HWM (1994) Cyclohexane 1,2-diacetals in synthesis. 2. One-pot synthesis of a trisaccharide unit of the common polysaccharide antigen of group-B streptococci using cyclohexane 1,2-diacetal (CDA)-protected rhamnosides. Angew Chem Int Ed Engl 33:2292–2294
14. Grice P, Ley SV, Pietruszka J, Priepke HWM, Walther EPE (1995) Cyclohexane-1, 2-diacetals in synthesis. 3. Tuning the reactivity of glycosides: efficient one-pot oligosaccharide synthesis. Synlett 1995:781–784
15. Geurtsen R, Holmes DS, Boons G-J (1997) Chemoselective glycosylations. 2. Differences in size of anomeric leaving groups can be exploited in chemoselective glycosylations. J Org Chem 62:8145–8154

16. Grice P, Ley SV, Pietruszka J, Osborn MI, Henning WM, Priepke HWM, Warriner SL (1997) A new strategy for oligosaccharide assembly exploiting cyclohexane-1, 2-diacetal methodology: an efficient synthesis of a high mannose type nonasaccharide. Chem Eur J 3:431–440
17. Zhang Z, Ottmann IR, Ye X-S, Wischnat R, Baasov T, Wong CH (1999) Programmable one-pot oligosaccharide synthesis. J Am Chem Soc 121:734–753
18. Wilson BG, Fraser-Reid B (1995) n-Pentenyl glycoside based methodology for determining the relative reactivities of variously protected pairs of glycosides. J Org Chem 60:317–320
19. Douglas NL, Ley SV, Lücking U, Warriner SL (1998) Tuning glycoside reactivity: new tool for efficient oligosaccharide synthesis. J Chem Soc Perkin Trans 1998(1):51–65
20. Cheung MK, Douglas NL, Hinzen B, Ley SV, Pannecoucke X (1997) One-pot synthesis of tetra- and pentasaccharides from monomeric building blocks using the principles of orthogonality and reactivity tuning. Synlett 1997:257–260
21. Friesen RW, Danishefsky SJ (1989) On the controlled oxidative coupling of glycals: a new strategy for the rapid assembly of oligosaccharides. J Am Chem Soc 111:6656–6660
22. Jensen HH, Bols M (2006) Stereoelectronic substituent effects. Acc Chem Res 39:259–265
23. Jensen HH, Lyngbye L, Jensen A, Bols M (2002) Stereoelectronic substituent effects in polyhydroxylated piperidines and hexahydropyridazines. Chem Eur J 8:1218–1226
24. Pedersen CM, Bols M (2005) Stereochemical substituent effects: investigation of the cyano, amide and carboxylate group. Tetrahedron 61:115–122
25. Jensen HH, Lyngbye L, Bols M (2001) A free energy relationship between the rate of acidic hydrolysis of glycosides and the pK_a of isofagomines. Angew Chem Int Ed 40:3447–3449
26. Overend WG, Rees CW, Sequeira JS (1962) Reactions at position 1 of carbohy drates. III. The acid catalyzed hydrolysis of glycosides. J Chem Soc 1962:3429–3440
27. Namchuk MN, McCarter JD, Bacalski A, Andrews T, Withers SG (2000) The role of sugar substituents in glycoside hydrolysis. J Am Chem Soc 122:1270–1277
28. Woods RJ, Andrews CW, Bowen JP (1992) Molecular mechanical investigations of the properties of oxocarbenium ions. 2. Application to glycoside hydrolysis. J Am Chem Soc 114:859–864
29. Miljkovic M, Habash-Marino M (1983) Acetolysis of permethylated *O*-alkyl- glycopyranosides: kinetics and mechanism. J Org Chem 48:855–860
30. Miljkovic M, Yeagley D, Deslongchamps P, Dory Y (1997) Experimental and theoretical evidence of through-space electrostatic stabilization of the incipient oxocarbenium ion by an axially oriented electronegative substituent during glycopyranoside acetolysis. J Org Chem 62:7597–7604
31. McDonnell C, Lopez OL, Murphy P, Bolanos JF, Hazell R, Bols M (2004) Conformational effects on glycoside reactivity: study of the high reactive conformer of glucose. J Am Chem Soc 126:12374–12385
32. Fraser-Reid B, Wu Z, Andrews CW, Skowronski E, Bowen JP (1991) Torsional effects in glycoside reactivity: saccharide couplings mediated by acetal protecting groups. J Am Chem Soc 113:1434–1435
33. Ley SV, Baeschlin DK, Dixon DJ (2001) 1,2-diacetals: a new opportunity for organic synthesis. Chem Rev 101:53–80
34. Jensen HH, Nordstrøm LU, Bols M (2004) The disarming effect of the 4, 6-acetal group on glycoside reactivity. Torsional or electronic? J Am Chem Soc 126:9205–9213
35. Bulow A, Meyer T, Olszewski TK, Bols M (2004) The C-4 configuration as a probe to study glycosylation reactions. Eur J Org Chem 2:323–329
36. Eliel EL, Satici H (1994) Conformational analysis of cyclohexylsilyl ethers. J Org Chem 59:688–689
37. Nordstrøm LU, Bols M Unpublished work cited in Ref. [23]
38. Mydock LK, Demchenko AV (2008) Superarming the *S*-benzoxazolyl glycosyl donors by simple 2-*O*-Benzoyl-3, 4, 6-tri-*O*-benzyl protection. Org Lett 10:2103–2106

39. Baeschlin DK, Chaperon AR, Charbonneau V, Green LG, Ley SV, Lucking U, Walther E (1998) Rapid assembly of oligosaccharides: 1,2-diacetal- mediated reactivity tuning in the coupling of glycosyl fluorides. Angew Chem Int Ed 37:3423–3428
40. Barrena MI, Echarri R, Castillon S (1996) Synthesis of disaccharides by selective metallocene promoted activation of glycosyl fluorides. Synlett 1996:675–676
41. Hashimoto SI, Sakamoto H, Abe H, Nakamura SI, Ikegami S (1997) "Armed- Disarmed" glycosidation strategy based on glycosyl donors and acceptors carrying phosphoramidate as a leaving group: a convergent synthesis of globotriaosylcera mide. Tetrahedron Lett 38:8969–8972
42. Chiba H, Funasaka S, Kiyota K, Mukaiyama T (2002) Catalytic and chemoselective glycosylation between "armed" and "disarmed" glycosyl p-trifluoromethylben zylthio-p-trifluoromethylphenyl formimidates. Chem Lett 2002:746–747
43. Kamat MN, Demchenko AV (2005) Revisiting the armed-disarmed concept rationale: *S*-benzoxazolyl glycosides in chemoselective oligosaccharide synthesis. Org Lett 7:3215–3218
44. Smoot JT, Pornsuriyasak P, Demchenko AV (2005) Development of an arming participating group for stereoselective glycosylation and chemoselective oligosaccharide synthesis. Angew Chem Int Ed 44:7123–7126
45. Crich D, Li M (2007) Revisiting the armed-disarmed concept: the importance of anomeric configuration in the activation of *S*-benzoxazolyl glycosides. Org Lett 9:4115–4118
46. Pedersen CM, Nordstrom LU, Bols M (2007) "Super armed"glycosyl donors; conformational arming of thioglycosides by silylation. J Am Chem Soc 129:9222–9235
47. Jensen HH, Pedersen CM, Bols M (2007) Going to extremes: "super" armed glycosyl donors in glycosylation chemistry. Chem Eur J 13:7576–7582
48. Mydock LK, Demchenko AV (2008) Application of superarmed glycosyl donor to chemoselective oligosaccharide synthesis. Org Lett 11:2107–2110
49. Cid MB, Alonso I, Alfonso F, Bonilla JB, Lopes-Prados J, Martin-Lomas M (2006) Simultaneous regio- and enantio-differentiation in carbohydrate coupling. Eur J Org Chem 2006:3947–3959
50. Paulsen H (1984) In: Bartmann W, Trost BM (eds) Selectivity a goal for synthetic efficiency. Verlag Chemie, Basel
51. Vasella A, Bernet B, Weber M, Wenger W (2000) In: Ernst B, Hart GW, Sinaÿ P (eds) Carbohydrates in chemistry and biology, vol 1. Wiley-VCH, Weinheim, pp 154–175
52. Khiar N, Martin-Lomas M (1998) In: Chapleur Y (ed) Carbohydrate mimics, concepts and methods. Wiley-VCH, Weinheim, pp 433–462, and references cited therein
53. Dietrich H, Espinosa JF, Chiara JL, Jimenéz-Barbero J, León Y, Varela- Nieto I, Mato H-M, Cano FH, Foces-Foces C, Martin-Lomas M (1999) Glycosyl inositol derivatives related to inositolphosphoglycans mediators: synthesis, structure, and biological activity. Chem Eur J 5:320–336
54. Cid MB, Bonilla JB, Alfonso F, Martin-Lomas M (2003) Synthesis of new hexosaminyl D- and L-chiro-inositols related to putative insulin mediators. Eur J Org Chem 2003:3505–3514
55. Reichard NC, Martin-Lomas M (2003) A practical solid-phase synthesis of glycosyl phosphatidylinositol precursors Angew Chem Int Ed 42:4674–4677, Angew Chem 115:4822–4825
56. Cid MB, Alfonso F, Martin-Lomas M (2005) A comparative sturdy of the influence of protecting groups on the reactivity of chiro-inositol glycosyl acceptors. Synlett 2005:2052–2056
57. Cid MB, Bonilla JB, Dumarcay S, Alonso F, Martin-Lomas M (2002) New synthesis of 1-D-O-(2-amino-2-deoxy-D-gluco- and –galactopyranosyl)-chiro- inositols. Eur J Org Chem 2002:881–888
58. Bonilla JB, Muñoz-Ponce JL, Nieto PM, Cid MB, Martin-Lomas M (2002) Synthesis and structure of 1-D-6-*O*-(2-amino-2-deoxy-α- and β-D-gluco- and – galactopyranosyl)-3-*O*-methyl-D-chiro-inositol. Eur J Org Chem 2002:889–898

59. Masamune S, Choy W, Petersen JC, Sita LR (1985) Double stereodifferentiation and a new strategy for stereocontrol in organic syntheses. Angew Chem 97:1–31
60. Spijker NM, Van Boeckel CAA (1991) Double stereodifferentiation in sugar reactions. Mismatched reactions of donors and acceptors. As yet unconsidered factors of the influence of α/β-ratios on glycoside synthesis. Angew Chem 103:179–182
61. Cid MB, Alfonso F, Martin-Lomas M (2005) A study on the influence of the structure of the glycosyl acceptors on the stereochemistry of the glycosylation reactions with 2- azido-2-deoxy-hexopyranosyl trichloroacetimidates. Chem Eur J 11:928–938
62. Haines AH (1976) Relative reactivities of hydroxyl groups in carbohydrates. Adv Carbohydr Chem Biochem 33:11–109
63. Collins P, Ferrier R (1955) Monosaccharides. Wiley, New York
64. Ellervirk U, Magnusson G (1998) A high yielding chemical synthesis of silyl Lewis x Tetrasaccharide; examples of regio- and stereodifferentiated glycosylations. J Org Chem 63:9314–9322
65. Fraser-Reid B, López JC, Radhakrishnan KV, Mach M, Schlueter U, Gómez A, Uriel C (2002) Reciprocal donor acceptor selectivity (RDAS): a new concept for "matching" donors with acceptors. Can J Chem 80:1075–1087
66. Fraser-Reid B, López JC, Gómez AM, Uriel C (2004) Reciprocal donor acceptor selectivity (RDAS) and Paulsen's concept of "match" in saccharide coupling. Eur J Org Chem 2004:1387–1395 and references cited therein
67. Cid MB, Alfonso F, Martin-Lomas M (2004) Synthesis of fagopyritols A1 and B1 from D-chiroinositol. Carbohydr Res 339:2303–2307
68. Stewart JJP (1989) Optimization of parameters for semiempirical methods. I. Methods. J Comput Chem 10:209–220
69. Stewart JJP (1989) Optimization of parameters for semiempirical methods. II. Applications. J Comput Chem 10:221–264
70. (1999) HyperChem 6.02; Hypercube, Inc., Gainesville
71. Becke AD (1993) A new mixing of Hartree-Fock and local-density functional theories. J Chem Phys 98:1372–1377
72. Lee C, Yang W, Parr RG (1988) Development of the Colle-Salvetti correlation-energy formula into a functional of the electron density. Phys Rev B 37:785–789
73. Ditchfield R, Hehre WJ, Pople JA (1971) Self-consistent molecular orbital methods. IX. Extended Gaussian-type basis for molecular –orbital studies of organic molecules. J Chem Phys 54:724–728
74. Hehre WJ, Ditchfield R, Pople JA (1972) Self-consistent molecular orbital methods. XII. Further extensions of the Gaussian-type basis sets for use in molecular orbital studies of organic molecules. J Chem Phys 56:2257–2261
75. Hariharan PC, Pople JA (1973) Influence of polarization functions on MO hydrogenation energies. Theor Chim Acta 28:213–222
76. Frisch MJ, Trucks GW, Schlegel HB, Seuseria GE, Robb MA, Cheeseman JR, Montgomery Jr. JA, Vreven T, Kudin KN, Burant JC, Millam JM, Iyengar SS, Tomasi J, Barone V, Mennucci B, Cossi M, Scalmani G, Rega N, Petersson GA, Nakatsuji H, Hada M, Ehara M, Toyota K, Fukuda R, Hasegawa J, Ishida M, Nakajima T, Honda Y, Kitao O, Nakai H, Klene M, Li X, Knox JE, Hratchian HP, Cross JB, Adamo C, Jaramillo J, Gomperts R, Stratmann RE., Yazyev O, Austin AJ., Cammi R, Pomelli C, Ochterski JW, Ayala PY, Morokuma K, Voth GA, Salvador P, Dannenberg JJ, Zakrzewski VG, Dapprich S, Daniels AD., Strain MC, Farkas O, Malick DK, Rabuck AD, Raghavachari K, Foresman JB, Ortiz JV, Cui Q, Baboul AG, Clifford S, Cioslowski J, Stefanov BB, Liu G, Liashenko A, Piskorz P, Komaromi I, Martin RL, Fox DJ., Keith T, Al-Laham MA, Peng CY, Nanayakkara A, Challacombe M, Gill PMW, Johnson B, Chen W, Wong MW, Gonzalez C, Pople JA (2003) Gaussian 03, revision B.03. Gaussian, Inc., Pittsburgh
77. Cosp A, Larrosa I, Anglada JM, Bofill JM, Romea P, Urpi F (2003) Studies on the intramolecular C-H...X (X = O, S) interactions in (S)-N-acyl-4-isopropyl-1, 3- thiazolidine-

2-thiones and related 1, 3-oxazolidin-2-ones. Org Lett 5:2809–2812 and references cited therein
78. Reed AE, Curtiss LA, Weinhold F (1988) Intermolecular interactions from a natural bond orbital, donor-acceptor viewpoint. Chem Rev 88:899–926
79. Reed AE, Weinstock RB, Weinhold F (1985) Natural population analysis. J Chem Phys 83:735–746
80. Bondi A (1964) van der Waals volumes and radii. J Phys Chem 68:441–451
81. Yu HN, Furukawa J, Ikeda T, Wong CH (2004) Novel efficient routes to heparin monosaccharides and disaccharides achieved via regio- and stereoselective glycosidation. Org Lett 6:723–726
82. Cid MB, Valverde S, López C, Gómez AM, Garcia M (2005) Study of the regioselectivity of intra- and intermolecular glycosylations of mannoside diol acceptors. Synlett 2005:1095–1100
83. Bollitt V, Mioskowski C, Lee S-G, Falck JR (1990) Direct preparation of 2-deoxy- D-glucopyranosides from glucals without Ferrier rearrangement. J Org Chem 55:5812–5813
84. Danishefsky SJ, Halcomb RL (1991) The synthesis of the core trisaccharide of esperamicin: corroboration of the proposed structure for its rearrangement product and stabilization of the core trisaccharide domain. J Am Chem Soc 113:5080–5802
85. Salomaa P, Kankaanpena A, Lajunen M (1966) Protolytic cleavage of vinyl ethers. General acid catalysis, structural effects, and deuterium solvent isotope effects. Acta Chem Scand 20:1790–1801
86. Kresge AJ, Chiang Y (1967) Hydrolysis of ethyl vinyl ether. I. Reaction mechanism. J Chem Soc B 1967:53–57 and 58–61
87. Kaila N, Blumenstein M, Bielawska H, Franck RW (1992) Face selectivity of the protonation of glycals. J Org Chem 57:4576–4578
88. Lemieux RU, Levin S (1964) Synthesis of alkyl 2-deoxy-α-D-deoxy-glycopyranosides and their 2-deuterio derivatives. Can J Chem 42:1473–1480
89. Kirby AJ (1983) Anomeric effect and related stereoelectronic effects at oxygen. Springer Verlag, New York
90. Deslongchamps P (1983) Stereoelectronic effects in organic chemistry. Pergamon Press, Oxford
91. Borowiecka J, Lipka P, Michalska M (1988) Stereoselective synthesis of S-(2-deoxy-α-D-glycosyl) phosphorodithioates and of their (2R)-2-deoxy-2-deuterio analogs. Novel route to C-2 deuterium labeled 2-deoxymonosaccharides. Tetrahedron 44:2067–2076
92. Lehmann J, Schroter E (1972) Reactions of enolic sugar derivatives. VIII. Action of β-D-galactosidase an D-glucal and D-galactal. Carbohydr Res 23:359–368
93. Lehmann J, Zieger B (1977) Uncommon results of glycosidase action. Part IV. The stereochemistry of the addition of glycerol to D-galactal, catalyzed by β-D-galactosidase. Carbohydr Res 58:73–78
94. Hehre EJ, Ganghof DS, Sternlicht H, Brewer CF (1977) Scope and mechanism of carbohydrase action: stereospecific hydration of D-glucal catalyzed by α- and β-glucosidase. Biochemistry 16:1780–1787
95. Petit J-M, Paquet F, Beau J-M (1991) Syntheses of 2-deoxy-D-glycosides assisted by glycosidases. Tetrahedron Lett 32:6125–6128
96. Berkowitz DB, Danishefsky SJ (1991) Enzymic resolution of racemic glycals: an application of the Wong acylation method. Tetrahedron Lett 32:5497–5500
97. Thiem J, Wiemann T (1991) Galactosyl transferase-catalyzed synthesis of 2′-deoxy-*N*-acetyllactosamine. Angew Chem 103:1184–1186
98. Ichikawa Y, Look GC, Wong C-H (1992) Enzyme catalyzed oligosaccharide synthesis. Anal Biochem 202:215–238
99. Viratelle OM, Yon J (1980) Comparison of the β-galactosidase conformations induced by D-galactal and by magnesium ions. Biochemistry 19:4143–4149

100. Sinnott ML (1987) In: Page MI, Williams MA (eds) Enzyme mechanisms. Royal Society of Chemistry, London, p 259
101. Sinnott MJ (1990) Catalytic mechanism of enzymic glycosyl transfer. Chem Rev 90:1171–1202
102. Frank RW (1992) The mechanism of β-glycosidases: a reassessment of some seminal papers. Bioorg Chem 20:77–88
103. Seebach D, Zimmerman J, Gysel U, Ziegler R, Ha T-K (1988) Totally stereoselective additions to 2,6-disubstituted 1,3-dioxin-4-ones (chiral acetoacetic acid derivatives). Synthetic and mechanistic aspects of remote stereoselectivity. J Am Chem Soc 110:4763–4772
104. Voelter W, Fuchs W, Stezowski JJ, Schott-Kollat P (1981) Molecular structures of tri-*O*-acetyl-D-glucal and ethyl 4, 6-di-*O*-acetyl-2, 3—dideoxy-α-D-erythro-2-hexenopyranoside. Angew Chem 93:1070–1071
105. Krajewski JW, Urbanczuk-Lipkowska Z, Gluzinski P (1979) The structure of 3,4-dideoxy-α-DL-threo-hex-3-enopyranoside. Acta Crystalogr B 35:519–522
106. Cieplak AS, Tait BD, Johnson CR (1989) Reversal of n-facial diastereoselection upon electronegative substitution of the substrate and the reagent. J Am Chem Soc 111:8447–8462
107. Marzabadi CH, Franck RW (2000) The synthesis of 2-deoxyglycosides:1988–1999. Tetrahedron 56:8385–8417
108. Smoliakova IP (2000) Synthesis of *C*-glycosylic compounds using three-membered cyclic intermediates. Curr Org Chem 4:589–608
109. Nicolaou KC, Ladduwahetty T, Randall JL, Chucholowski A (1986) Stereospecific 1,2-migration in carbohydrates. Stereocontrolled synthesis of α- and β-2-deoxyglycosides. J Am Chem Soc 108:2466–2467
110. Nicolaou KC, Hummel CW, Bockovich NJ, Wong C-H (1991) Stereocontrolled synthesis of sialyl lex, the oligosaccharide binding ligand to ELAM-1 (Sialyl = *N*-acetylneuramin). J Chem Soc Chem Commun 1991:870–872
111. Roush WR, Sebesta DP, Bennett CE (1997) Stereoselective preparation of 2-deoxy–βglycosides from glycal precursors. 1. Stereochemistry of the reactions of D-glucal derivatives with phenylsulfenyl chloride and phenylselenyl chloride. Tetrahedron 53:8825–8836
112. Roush WR, Sebesta DP, James RA (1997) Stereoselective preparation of 2-deoxy-β-glycosides from glycal precursors. 2. Stereochemistry of glycosidation reactions of 2-thiophenyl- and 2-selenophenyl-α-D-glucopyranosyl donors. Tetrahedron 53:8837–8852
113. Roush WR, Bennett CE (1999) A highly stereoselective synthesis of 2-deoxy-β-glycosides using 2-deoxy-2-iodo-glucopyranosyl acetate donors. J Am Chem Soc 121:3541–3542
114. Chong PY, Roush WR (2002) Concerning the origin of the high β-selectivity of glycosidation reaction reactions of 2-deoxy-2-iodo-glucopyranosyl trichloroacetim idates. Org Lett 4:4523–4526
115. Durham TB, Roush WR (2003) Stereoselective synthesis of 2-deoxy-β-galactosides via 2-deoxy-2-bromo- and 2-deoxy-2-iodo-galactopyranosyl donors. Org Lett 5:1871–1874
116. Durham TB, Blanchard N, Savall BM, Powel NA, Roush WR (2004) Total synthesis of formamicin. J Am Chem Soc 126:9307–9317
117. Smoliakova IP, Caple R, Gregory D, Smit WA, Shashkov AS (1995) Highly selective formation of a β-*C*-glycosidic bond in the reactions of ArSCl-glucal adducts with silicon-containing nucleophiles. J Org Chem 60:1221–1227
118. Viso A, Poopeiko N, Castillón S (2000) Stereoselective synthesis of nucleosides from 1-thio and 1-seleno glycosides through consecutive 1,2-migration and glycosylation under Mitsunobu conditions. Tetrahedron Lett 41:407–411
119. Johnston BD, Pinto BM (2000) Synthesis of thio-linked disaccharides by 1 → 2 intramolecular thioglycosyl migration: oxocarbenium versus episulfonium ion intermediates. J Org Chem 65:4607–4617
120. Sajtos F, Lázár L, Borbás A, Bajza I, Lipták A (2005) Glycosyl azides of sugar 2-sulfonic acids. Tetrahedron Lett 46:5191–5194

121. Poopeiko N, Fernández R, Barrena MI, Castillón S, Forniés-Cámer J, Cardin J (1999) Stereoselective synthesis of 2′,3′-dideoxy-3′-fluoro-2′- phenylselenenyl-β – nucleosides from phenyl 1-seleno-α-arabino-furanosides through consecutive 1,2-migration and glycosylation under Mitsunobu conditions. A new entry to 2′,3′-dideoxy-3′-fluoro-nucleosides. J Org Chem 64:1375–1379
122. Toshimitsu A, Hirosawa C, Tamao K (1994) Retention of configuration in the Ritter-type substitution reaction of chiral β-arylthio alcohols through the anchimeric assistance of the arylthio group. Tetrahedron 50:8997–9008
123. Kim J-H, Yang H, Boons G-J (2005) Stereoselective glycosylation reactions with chiral auxiliaries. Angew Chem Int Ed Engl 44:947–949
124. Kim J-H, Yang H, Park J, Goons G-J (2005) A general strategy for stereoselective glycosylations. J Am Chem Soc 127:12090–12097
125. Park J, Kawatkar S, Kim J-H, Boons G-J (2007) Stereoselective glycosylations of 2-azido-2-deoxy-glucosidses using intermediate sulfonium ions. Org Lett 9:1959–1962
126. Demchenko AV (2003) 1, 2-cis *O*-glycosylation: methods, strategies, principles. Curr Org Chem 7:35–79
127. Krüger A, Pyplo-Schneiders J, Redlich H, Winkelmann P (2004) 2-haloethylglycosides as new tools in glycoside syntheses. Part 1. Preparation, characteristics, general reactions. Coll Czech Chem Commun 69:1843–1876
128. Crich D, Chandrasekera DS (2004) Mechanism of 4,6-*O*-benzylidene-directed beta-mannosylation as determined by alpha-deuterium kinetic isotope effects. Angew Chem Int Ed Engl 43:5386–5389
129. El Badri MH, Willenbring D, Tantillo DJ, Garvay-Hague J (2007) Mechanistic studies on the stereoselective formation of β-mannosides from mannosyl iodides using α-deuterium kinetic isotope effects. J Org Chem 72:4663–4672
130. Nicolaou KC, Dolle RE, Papahatjis DP, Randall JL (1984) Practical synthesis of oligosaccharides. Partial synthesis of avermectin B1a. J Am Chem Soc 106:4189–4192 and references cited therein
131. Nicolaou KC, Dolle RE, Chucholowski A, Randall JL (1984) Reactions of glycosyl fluorides. Synthesis of *C*-glycosides. J Chem Soc Chem Commun 1984:1153–1154
132. Nicolaou KC, Chucholowski A, Dolle RE, Randall JL (1984) Reactions of glycosyl fluorides. Synthesis of *O*-, *S*-, and *N*-glycosides. J Chem Soc Chem Commun 1984:1155–1156
133. Hashimoto S, Hayashi M, Noyori R (1984) Glycosylation using glucopyranosyl fluorides and silicon-based catalysts. Solvent dependency of the stereoselection. Tetrtahedron Lett 25:1379
134. Rosenbrook W, Riley DA, Lartey PA (1985) A new method for the synthesis of glycosyl fluorides. Tetrahedron Lett 26:3–4
135. Posner GH, Haines SA (1985) A convenient, one-step, high-yield replacement on an anomeric hydroxyl group by a fluorine atom using DAST. Preparation of glycosyl fluorides. Tetrahedron Lett 26:5–8
136. Mukayama T, Murai Y, Shoda S (1981) An efficient method for glycosylation of hydroxy compounds using glucopyranosyl fluorides. Chem Lett 1981:431
137. Mukayama T, Hashimoto Y, Shoda S (1983) Stereoselective synthesis of 1,2-cis- glycofuranosides using glycofuranosyl fluorides. Chem Lett 1983:935–938
138. Kunz H, Sager W (1985) Stereoselective glycosylation of alcohols and silyl ethers using glycosyl fluorides and boron trifluoride etherate. Helv Chim Acta 68:283–287
139. Araki Y, Watanabe K, Kuan F-H, Itoh K, Kobayashi N, Ishido Y (1984) Synthetic studies by the use of fluorinated intermediates, Part 1. A novel procedure for *C*-glycosylation involving Lewis acid-catalyzed coupling-reactions of glycosyl fluorides with enol trimethylsilyl ethers. Carbohydr Res 127:C5–C9
140. Bock K, Lundt I, Pedersen C (1984) 2-Bromo-2-deoxy sugars as starting materials for the synthesis of α- and β-glycosides of 2-deoxy sugars. Carbohydr Res 130:125–134 and references cited therein

141. Somekh L, Shanzer A (1982) A facile stereospecific synthesis of α-fluoro β-amino acids. Am Chem Soc 104:5836–5837
142. Ryan KJ, Acton EM, Goodman L (1971) Synthesis of 2-thiio-D-ribose and 2′-thioadenosine derivatives. J Org Chem 36:2646–2657
143. Levy DE, Tang C (1995) The chemistry of *C*-glycosides, vol 13, Tetrahedron organic chemistry series. Elsevier, Tarrytown
144. Postema MHD (1995) C-glycoside synthesis. CRC Press, Boca Raton
145. Bertozzi C, Bednarski M (1996) In: Kahn SH, O'Neill RA (eds) Modern methods in carbohydrate synthesis. Hardwood Academic, Amsterdam, pp 316–351
146. Nicotra F (1997) Synthesis of *C*-glycosides of biological interest. Top Curr Chem 187:55–83
147. Du Y, Linhardt RJ, Vlahov IR (1998) Recent advances in stereoselective *C*-glycoside synthesis. Tetrahedron 54:9913–9959
148. Beau J-M, Gallagher T (1998) Nucleophilic *C*-glycosyl donors for *C*-glycoside synthesis. Top Curr Chem 187:1–54
149. Togo H, He W, Waki Y, Yokoyama M (1998) *C*-glycosidation technology with free radical reactions. Synlett 1998:700–717
150. Jaramillo C, Knapp S (1994) Synthesis of *C*-aryl glycosides. Synthesis 1994:1–20
151. Suzuki K (1994) Pure Appl Chem 66:2135
152. Parker KA (1994) Novel methods for the synthesis of *C*-aryl glycoside natural products. Pure Appl Chem 66:2135–2138
153. Gaertzen O, Misske AM, Wolbers P, Hoffmann HMR (1999) Synthesis of enantiopure *C*-glycosides and pseudo *C*-glycosides: Lewis acid mediated heterolysis of methyl acetals. Tetrahedron Lett 40:6359–6363
154. Yamago S, Miyazoe H, Yoshida J (1999) Synthesis of vinylic *C*-glycosides from telluroglycosides. Addition of photochemically and thermally generated glycosyl radicals to alkynes. Tetrahedron Lett 40:2343–2346
155. Wolbers P, Hoffmann HMR (1999) *Trans-C*-glycosides from 8-oxabicyclo [3.2.1] oct-6-en-3-one – synthesis of the C3–C13 segment of the phorboxazoles A and B. Tetrahedron 55:1905–1914
156. Kuribayashi T, Ohkawa N, Satoh S (1998) AgOTfa/$SnCl_4$: a powerful new promoter combination in the aryl *C*-glycosidation of a diverse range of sugar acetates and aromatic substrates. Tetrahedron Lett 39:4537–4540
157. Kuribayashi T, Ohkawa N, Satoh S (1998) The sequential double aryl *C*-glycosidation: introduction of a second sugar unit onto mono aryl *C*-glycosides using $SnCl_4$/AgOTfa. Tetrahedron Lett 39:4541–4542
158. Khan N, Cheng X, Mootoo DR (1999) 1-Thio-1,2-*O*-isopropylidene acetals: novel precursors for the synthesis of complex *C*-glycosides. J Am Chem Soc 121:4918–4919
159. Kuribayashi T, Ohkawa N, Satoh S (1998) Aryl *C*-glycosides: physiologically stable glycomimetics of sialyl Lewis X. Bioorg Med Chem Lett 8:3307–3310
160. Gross P (1998) New synthetic pathways to *C*-glycosides. Carbohydr Polymer 37:215–217
161. Urban D, Skrydstrup T, Beau J-M (1998) First synthesis of a *C*-glycoside analog of a tumor-associated carbohydrate antigen employing samarium diiodide promoted *C*-glycosylation. Chem Commun 1998:955–956
162. Dios A, Geer A, Marzabadi CH, Franck RW (1998) Novel heterocycloaddition reaction of glycals. J Org Chem 63:6673–6679
163. López-Herrera FJ, Sarabia-Garcia F, Heras-López A, Pino-Gonzáles MS (1997) Stereoselective synthesis of *C*-amino-substituted D-mannopyranosides. Easy preparation of novel inhibitors for mannosidases. J Org Chem 62:6056–6059
164. Holzapfel CW, Portwig M (1997) Heterocycles 45:1433
165. Behrens CH, Sharpless KB (1983) New transformations of 2,3-epoxy alcohols and related derivatives. Easy route to homochiral substances. Aldrichimica Acta 16:67–80
166. Bartok M, Lang KL, in Supplemental E (1980) In: Patai S (ed) The chemistry of ethers, crown ethers, hydroxyl groups, and their sulfur analogs. Part 2, Wiley, Chichester, p 609

167. Smit WA, Caple R, Smoliakova IP (1994) Stepwise electrophilic addition. Some novel synthetic ramifications of an old concept. Chem Rev 94:2359–2382
168. Smit VA, Zefirov NS, Bodrikov IV, Krimer MZ (1979) Episulfonium ions: myth and reality. Acc Chem Res 12:282–288
169. Lucchini V, Modena G, Pasquato L (1997) Thiiranium and thirenium ions. From reaction intermediates to building blocks in organic synthesis. Gazz Chim Ital 127:177–188
170. Harring SR, Edstrom ED, Livinghouse T (1992) Episulfonium ions and episelenonium ions. Versatile heterocyclic cations for the synthesis of natural products. Adv Heterocycl Nat Prod Synth 2:299–376
171. Rayner CM (1995) In: Page P (ed) Organosulfur chemistry. Synthetic aspects, Academic, San Diego, vol 1. p 89
172. Sonoda N, Ogawa A (1987) In: Patai S (ed) The chemistry of organic selenium and tellurium compounds, vol 1. Wiley, Chichester, pp 619–665
173. Liotta D (1984) New organoselenium methodology. Acc Chem Res 17:28–34
174. Danishefsky SJ, Bilodeau MT (1996) Glycals in organic synthesis: the evolution of comprehensive strategies for the assembly of oligosaccharides and glycoconjugates of biological consequence. Angew Chem Int Ed Engl 35:1380–1419
175. Timmers CM, Verheijen JC, van der Marel GA, van Boom JH (1997) Use of furanoid glycals in oligosaccharide synthesis. Synlett 1997:851–853
176. Horton D, Priebe W, Sznaidman M (1990) Iodoalkoxylation of 1,5-anhydro-2-deoxy-1-hexenitols (glycals). Carbohydr Res 205:71–86
177. Timmers CM, Wigchert SCM, Leewenburgh MA, van der Marel GA, Boom JH (1998) Synthesis of tetrameric arabinogalactans based on 1,2-anhydro sugars. Eur J Org Chem 1998:91–97
178. Roush WR, Briner K, Kesler BS, Murphy M, Gustin DJ (1996) Studies on the synthesis of aureolic acid antibiotics: acyloin glycosidation studies. J Org Chem 61:6098–6099
179. Ito Y, Ogawa T (1990) Highly stereoselective glycosylation of sialic acid aided by stereocontrolling auxiliaries. Tetrahedron 46:89–102
180. Grewal G, Kaila N, Franck RW (1992) Arylbis(arylthio)sulfonium salts as reagents for the synthesis of 2-deoxy-β-glycosides. J Org Chem 57:2084–2092
181. Ramesh S, Kaila N, Grewal G, Franck RW (1990) Aureolic acid antibiotics: a simple method for 2-deoxy-β-glycosidation. J Org Chem 55:5–7
182. Kondo T, Abe H, Goto T (1988) Synthetic studies on gangliosides. 9. Efficient synthesis of 2α-glycoside of *N*-acetylneuraminic acid via phenylsulfonyl chloride adduct of 2-deoxy-2,3-dehydro-*N*-acetylneuraminic acid methyl ester tetra-*O*-acetate. Chem Lett 1988:1657–1660
183. Sebesta DP, Roush WR (1992) Synthesis of C-D-E-trisaccharide precursors of olivomycin A. J Org Chem 57:4799–4802
184. Ito Y, Ogawa T (1987) Tetrahedron Lett 28:4799
185. Ito Y, Ogawa T (1987) Novel approaches to glycoside synthesis. Sulfenate esters as glycosyl acceptors: a novel approach to the synthesis of 2-deoxyglycosides. Tetrahedron Lett 28:2723–2726
186. Preuss R, Schmidt RR (1988) Glycosylimidates. Part 38. A convenient synthesis of 2-deoxy-β-D-glucopyranosides. Synthesis 1988:694–697
187. Ramesh S, Franck RW (1989) Aureolic acid antibiotics: synthesis of model 2-deoxy-β-glycosides of α-hydroxytetralone. J Chem Soc Chem Commun 1989:960–962
188. Franck RW, Kaila N (1993) Synthesis of C′D′ disaccharide of aureolic acid. Carbohydr Res 239:71–83
189. Wilson LJ, Liotta D (1990) A general method for controlling glycosylation stereochemistry in the synthesis of 2′-deoxtribose nucleosides. Tetrahedron Lett 31:1815–1818
190. Kawakami H, Ebata T, Koseki K, Okano K, Matsushita H, Ebata T, Koseki K, Okano K, Matsumoto K, Matsushita H (1993) Nucleoside synthesis from furanoid glycals. Heterocycles 36:665–669

191. Jaurand G, Beau J-M, Sinaÿ P (1981) Glycosyloxyselenation-deselenation of glycals: a new approach to 2′-deoxy-disaccharides. J Chem Soc Chem Commun 1981:572–573
192. Kaye A, Neidle S, Reese CB (1988) Oxidative ring contraction of benzeneselenenate adducts of glycal ethers. Synthesis of showdomycin analogs. Tetrahedron Lett 29:2711–2714
193. Perez M, Beau J-M (1989) Selenium-mediated glycosidations. A selective synthesis of β-2-deoxyglycosides. Tetrahedron Lett 30:75–78
194. Thiem J, Karl H, Schwentner J (1978) Synthesis of α-linked 2′-deoxy-2′-iododisaccharide. Synthesis 1978:696–698
195. Thiem J, Klaffke W (1990) Synthesis of deoxyoligosaccharides. Top Curr Chem 154:285–332
196. Ogawa Y, Hinou H, Matsuoka K, Terenuma D, Kuzuhara H (1998) Synthetic conversion of cellobiose into the glycal-type monomers and their polymerization. Tetrahedron Lett 39:5789–5792
197. Izumi M, Ichikawa Y (1998) Combinatorial synthesis of oligosaccharide library of 2,6-dideoxysugars. Tetrahedron Lett 39:2079–2082
198. Freeman F, Rabarge KD (1985) Electrophile-mediated cyclizations in carbohydrate chemistry: synthesis of highly functionalized ribofuranose and ribopyranose compounds. Tetrahedron Lett 26:1943–1946
199. Suzuki K, Mukaiyama T (1982) A novel method for the synthesis of 2-deoxydisaccharide by stereoselective cyclization of acyclic precursor. Chem Lett 1982:683–686
200. Lay L, Nicotra F, Panza L, Verani A (1992) Synthetic studies on α-*C*-glycosides of D-glucosamine. Gazz Chim Ital 122:345–348
201. Witczak ZJ (1987) In: Patai S (ed) The chemistry of organic selenium and tellurium compounds, vol 2. Wiley, Chichester, pp 765–793
202. Link JT, Raghavan S, Gallant M, Danishefsky SJ, Chou TC, Ballas LM (1996) Staurosporine and ent-staurosporine: the first total syntheses, prospects for a regioselective approach, and activity profiles. J Am Chem Soc 118:2825–2842
203. Zagelaar-Jaarsveld K, Smits SAW, van Straten NCR, van der Marel GA, van Boom JH (1996) Iodonium ion-assisted synthesis of tetrameric fragment corresponding to the cell wall phenolic glycolipids of Mycobacterium kansasii Serovar I. Tetrahedron 52:3593–3608
204. Frèchou C, Dheilly L, Beaupère D, Uzan R, Demailly G (1992) Reaction of sulfur ylides on reducing sugars: application to the synthesis of hydroxymethyl *C*-glycosides. Tetrahedron Lett 33:5067–5070
205. Nicolaou KC, Prasad CVC, Somers PK, Hwang C-K (1989) Activation of 6-endo over 5-exo hydroxy epoxide openings. Stereoselective and ring selective synthesis of tetrahydrofuran and tetrahydropyran systems. J Am Chem Soc 111:5330–5334
206. Boschetti A, Panza L, Ronchetti F, Russo G (1988) Synthesis of ketofuranosides by epoxidation-ring closure of enol ethers. J Chem Soc Perkin Trans 1:3353–3357
207. Hart DJ, Leroy V, Merriman GH, Young DGJ (1992) *C*-aryl glycosides: electrophile-initiated cyclizations of 6-aryl-5-hexen-2-ols. J Org Chem 57:5670–5680
208. Khan AT, Ahmed W, Schmidt RR (1996) A method for the synthesis of C-(2-deoxy-β-glycosyl) arenes. Carbohydr Res 280:277–286
209. Armstrong RW, Teegarden BR (1992) Synthesis of α-methyl 1′,2′-dideoxycellobioside: a novel *C*-disaccharide. J Org Chem 57:915–922
210. Nicotra F, Panza L, Ronchetti F, Russo G, Toma L (1987) Synthesis of *C*-glycosyl compounds by the Wittig iodocyclization procedure. Differences from mercuriocyclization. Carbohydr Res 171:49–57
211. Tamaru Y, Hojo M, Kawamura S, Sawada S, Yoshida Z (1987) Stereoselective intramolecular iodoetherification of 4-pentene-1,3-diols: synthesis of *cis*-2-(iodomethnyl)-3-hydroxytetrahydrofurans. J Org Chem 52:4062–4072π
212. Ting PC, Bartlett PA (1984) Stereocontrolled synthesis of trans-2,5-disubstituted tetrahydrofurans. J Am Chem Soc 106:2668–2671

213. Pougny JR, Nassr MAM, Sinaÿ PJ (1981) Mercuricyclization in carbohydrate chemistry. A highly stereoselective route to α-D-*C*-glucopyranosyl derivatives. J Chem Soc Chem Commun 1981:375–376
214. Bellosta V, Czernecki S (1989) Stereocontrolled synthesis of *C*-glycosides by reaction of organocuprates with protected 1,2-anhydrosugars, and their transformation into 2-deoxy-*C*-glycosides. J Chem Soc Chem Commun 1989:199–200
215. Bellosta V, Czernecki S (1993) *C*-glycosyl compounds. Part X. Reaction of organocuprate reagents with protected 1,2-anhydro sugars. Stereocontrolled synthesis of 2-deoxy-*C*-glycopsyl compounds. Carbohydr Res 244:275–284
216. Lipschutz BH, Wilhellm RS, Kozlovski JA, Parker D (1984) Substitution reaction of secondary halides and epoxides with higher order, mixed organocuprates, R2Cu(CN)Li2: synthetic, stereochemical, and mechanistical studies. J Org Chem 49:3928–3938
217. Evans DA, Trotter BW, Côte B (1998) Addition of allylstannanes to glycal epoxides. A diastereoselective approach to β-*C*-glycosidation. Tetrahedron Lett 39:1709–1712
218. Best WM, Ferro V, Harle J, Stick RV, Tilbrook MG (1997) The synthesis of some epoxyalkyl β-*C*-glycosides as potential inhibitors of β-glucan hydrolases. Aust J Chem 50:463–472
219. Leeuwenburgh MA, Timmers CM, van der Marel GA, van Boom JH, Mallet J-M, Sinaÿ PG (1997) Stereoselective preparation of α-*C*-(alkynyl)-glycosides via ring-opening of α-1,2-anhydro sugars. Tetrahedron Lett 38:6251–6254
220. Timmers CM, Dekker M, Buijsman RC, van der Marel GA, Ethell B, Anderson G, Burchell B, Mulder GJ, van Boom JH (1997) Synthesis and inhibitory effect of a trisubstrate transition state analog for the UDP glucosyltransferases. Bioorg Med Chem Lett 7:1501–1506

Chapter 6
Stereoelectronic Effects in Nucleosides and Nucleotides

An excellent review of this subject was published in 2005 by Chattopadhyaya et al. [1].

It has been shown that stereoelectronic effects play an important role in many enzyme-catalyzed biochemical reactions, as, for example, in ribozymes [2–4], serine proteases [5], lysozymes [6], and ribonucleases [3, 7]. While most of the studies on stereoelectronic effects were conducted on pyranoid forms of sugars, the relationship between stereoelectronic effects and furanoid ring conformations, to the best of our knowledge, is almost totally neglected. This is a big void since the conformations of furanoid forms of sugars are of great importance for overall conformations of ribo- and deoxyribonucleic acids (RNA and DNA).

The reason for this is most likely due to the fact that the saturated five-membered rings are very flexible due to pseudorotation and are involved in complex conformational equilibria in which the individual conformations were very difficult if not impossible to identify, whereas the pyranoid rings are rather stiff and consequently have much simpler conformational equilibria.

Early experimental studies have shown qualitatively how the anomeric and gauche effect control the conformational equilibria of pentofuranoses in nucleo(s)tides. Chattopadhyaya et al. [8–40] made accurate estimates of the magnitude of stereoelectronic effects driving the two-state North $\rightleftharpoons$ South pseudorotational equilibrium in nucleos(t)ides (Fig. 6.1).

Recent studies on modified oligonucleotides have shown that a modification of one of the three components of the constituent nucleotides, i.e., the nucleobase, the sugar moiety, and the phosphate backbone, alters both their stability and overall structure. The actual involvement of stereoelectronic effects in the observed structural changes has been initially addressed only qualitatively [41–45].

The ultimate goal of modifying oligonucleotides is to develop antisense compounds with increased nuclease resistance compared to the parent DNA and RNA and with improved hybridization with the target RNA. Thus, design of new oligonucleotides that would have the desired therapeutic properties requires a study of magnitude and origin of stereoelectronic effects in the pentofuranose

M. Miljkovic, *Electrostatic and Stereoelectronic Effects in Carbohydrate Chemistry*,
DOI 10.1007/978-1-4614-8268-0_6, © Springer Science+Business Media New York 2014

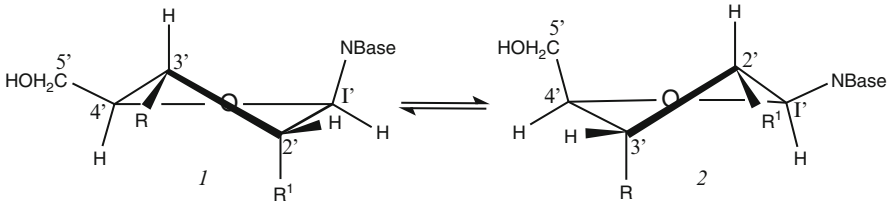

Fig. 6.1

ring in nucleosides and nucleotides in order to understand their role in the self-organization of DNA, RNA, and their analogs.

Three-dimensional structure and biological function of oligonucleotides is controlled by several factors. First, it is controlled by the conformation of the constituent pentofuranoses, which in turn is controlled by stereoelectronic factors, such as the anomeric and gauche effects that determine the position of pseudorotational equilibria in nucleos(t)ides. Second, it is controlled by the nature or by the configuration of one of their constituents, i.e., a heterocyclic nucleobase, a pentofuranose moiety, or C2′ and C3′ substituents, and finally it is controlled by the pH of the medium.

Saturated heterocyclic six-membered rings are much less flexible than their five-membered counterparts [46]. The activation energy barrier for the conversion of one chair form of cyclohexane into the alternate form is ca. 42 kJ/mol [47, 48]. The activation energy for the interconversion barrier between the two puckered conformations, i.e., N- and S-type pseudorotamers, of the pentofuranose moiety in purine nucleosides is much smaller in comparison, i.e., below 20–25 kJ/mol.

The pseudorotation concept has been introduced by K. S. Pitzer [49] to describe the continuous interconversions between an infinite number of indefinite puckered conformations of the cyclopentane ring. Pseudorotation [50] allows cyclopentane to relieve the ring strain, which would be induced by a 120° bond angle and the torsional strain by an eclipsed methylene group, if it were to adopt a planar conformation. A barrier to the planarity of cyclopentane of 22 kJ/mol has been reported [51]. The concept of pseudorotation has been applied for the first time to sugar furanoses by Hall et al. [52] studying the conformational analysis of pentofuranosyl fluorides.

In Fig. 6.2, four distinct puckered conformations of pentofuranosyl D-nucleosides are shown. Interconversions between N- and S-type puckered furanose conformers most likely occur along the pseudorotational cycle (i.e., via puckered geometries) rather than through a planar intermediate, which is disfavored as a result of high strain energies [53–55]. The fact that only a few E-type puckered conformations and no W-type pseudorotamer were identified among the 178 crystal structures of β-D-nucleos(t)ides suggests that N- to S-interconversion proceeds via an E-type puckered geometry intermediate, and not through the W conformation.

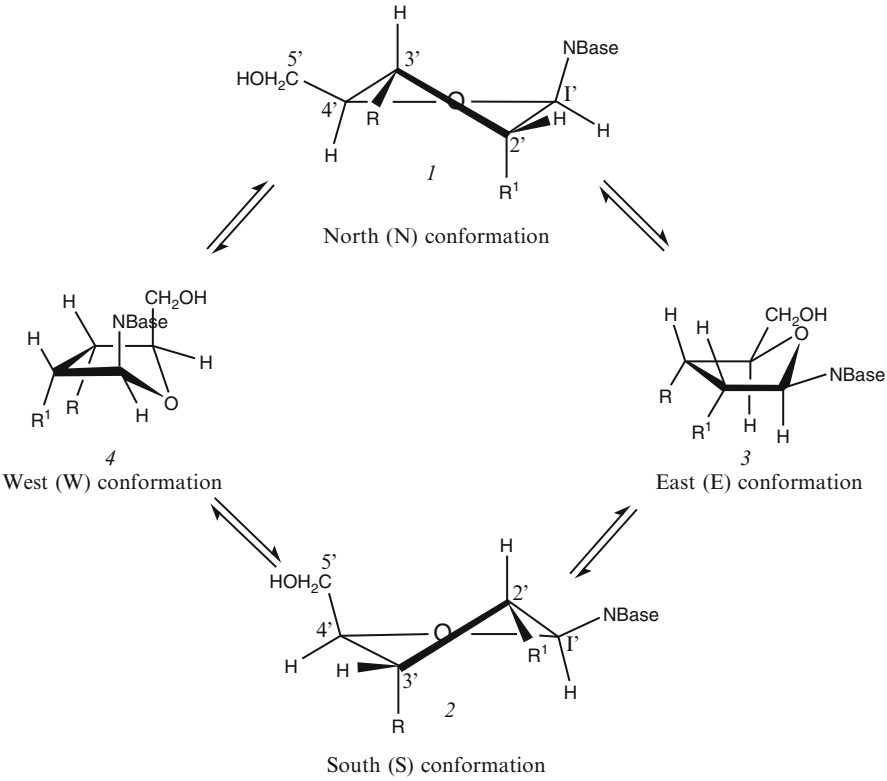

Fig. 6.2

The effect of packing forces and hydrogen bonds upon the observed puckered conformations of nucleosides in the solid state is well-known [56, 57]. [the anomeric effect across the 3′O-P-O-ester fragment in the sugar-phosphate backbone see references cited therein]. Solution and solid-state conformations of pentofuranose differ dramatically for some nucleosides: adenosine [58] crystallizes as the N-type conformer, whereas its hydrochloride salt crystallizes as the S-type conformer [59].

The inspection of the three molecular fragments in nucleotides (i.e., the aglycon, the sugar, and the phosphate) permits the bias of the two-state N ⇌ S pseudorotational equilibrium of the constituent pentofuranose moiety to be estimated on the basis of various steric and stereoelectronic effects.

The N-nucleobase influences the conformation of a pentofuranose through its inherent steric effect and counteracting stereoelectronic interactions within O4′–C1′–N1/9 fragment. In β-D-nucleosides, among all pseudorotamers, steric repulsions penalize O4′-*exo* (W-type) conformation [60–63] mostly owing to the 1, 3-diaxial orientation of the nucleobases and the 5′CH_2OH group and to the eclipsed arrangement of the C2′ and C3′ substituents (Fig. 6.2). In O4′-*endo*

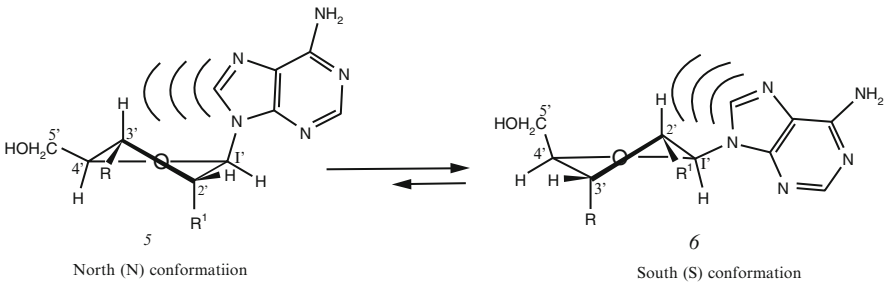

Fig. 6.3 The drive of the two-state N ⇌ S equilibrium toward S-over N-type pseudorotamer by steric effect of the nucleobase

(E-type) pseudorotamers, the steric repulsions between the nucleobase and 5′CH_2OH group are minimized; however, the substituents at C2′ and C3′, just as in the case of W-type conformers, are in the unfavorable eclipsed orientation (Fig. 6.2). Conformational analyses of nucleos(t)ides in aqueous solution assuming a two-state N ⇌ S equilibrium model suggest for β-D-nucleosides, in terms of steric effects alone, S-type pseudorotamers to be energetically favored in comparison with N-type counterparts, since the pseudoequatorially oriented nucleobases in the former exert less steric repulsions with the other substituents on the pentofuranose ring than when it is pseudoaxial (Figs. 6.2 and 6.3).

In α-D-nucleosides, the nucleobases and 5′CH_2OH group are on the opposite sides of the pentofuranose ring; therefore, their steric interactions will be minimal in comparison with the β-D-nucleosides. In N-type conformers, the nucleobases and the 3′-OH are pseudoequatorial while the 2′-OH is pseudoaxial, whereas the opposite is true for S-type pseudorotamers. Both in W- and E-type conformers, the 2′-OH and 3′-OH are pseudoaxial, whereas the nucleobase is pseudoequatorial in the W-type geometry and pseudoaxial in the E-type counterpart. In α-D-2′-deoxynucleosides, the nucleobases exert a stronger steric repulsion with 3′-OH and H4′ in the N-type than in the S-type pseudorotamers. Therefore, in solution, taking into consideration the two-state N ⇌ S equilibrium model, S-type pseudorotamers would be energetically favored over the N-type counterparts if the steric effects alone were considered.

The O4′–C1′–N1/9 anomeric effects in nucleosides and nucleotides may be explained either (1) by stabilizing $n_{O4'} \rightarrow \sigma^*_{C1'-N1/9}$ orbital interactions between the orbital of one of the endocyclic O4′ electron lone pairs ($n_{O4'}$) and the antibonding orbital of the C1′–N1/9 glycosyl bond ($\sigma^*_{C1'-N1/9}$) (Fig. 6.5) or (2) by the destabilizing electrostatic repulsion between two dipoles (i.e., the dipole of the furanose ring, which is the result of C4′–O4′, O4′–C1′ individual dipole moments and the dipoles induced by O4′ lone pairs) on the one hand, and the dipole oriented from C1′– to N1/9 on the other hand (Fig. 6.4)).

In β-D-nucleosides, O4′–C1′–N1/9 stereoelectronic interactions are most efficient in the W-type pentofuranose conformations, where one of the O4′ lone pairs is in an optimal antiperiplanar orientation with respect to the C1′–N1/9 bond, and the

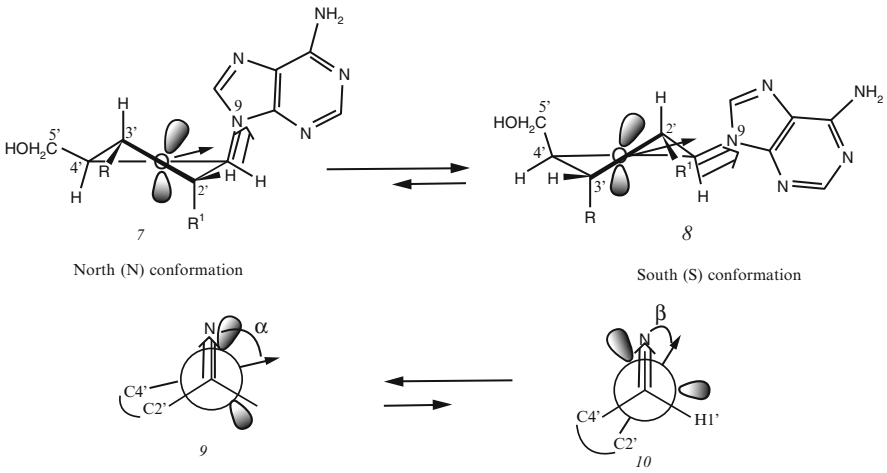

Fig. 6.4 Stronger electrostatic repulsions between the pentofuranose ring oxygen dipole (*black arrow*) C1′-N9 dipole (*white arrow*) in S-than in N-type conformation. Both dipoles are nearly parallel in the S-type pseudorotamers whereas they are nearly perpendicular in N-type pseudorotamers ($\beta \ll \alpha$)

same dipole-dipole repulsions are minimal since the angle between both dipoles is nearly 90°. However, for the steric reasons stated above, the West-type conformers have neither been found in crystal structures of β-D-nucleos(t)ides nor in the conformational equilibria in solution. Conversely, in E-type pseudorotamers, both O4′ lone pairs are gauche with respect to the C1′–N1/9 bond, which makes hyperconjugation (or molecular orbital overlap) least efficient. Simultaneously, dipole-dipole repulsions are maximal, owing to the fact that both dipoles are nearly parallel.

The anomeric effect is therefore often invoked as one of the factors responsible for the activation energy barrier encountered in the East region of the pseudorotational cycle for β-D-nucleosides, which, besides the stronger barrier in the West region, also hampers free pseudorotation of the constituent pentofuranose.

The comparison of the geometries of N- and S-type pseudorotamers of β-D-nucleosides shows that dipole-dipole repulsion (Fig. 2.4) and O4′–C1′–N1/9 hyperconjugative interaction (Fig. 6.5) are reduced and enhanced respectively, in the former compared to the latter. Therefore, O4′–C1′–N1/9 stereoelectronic interactions drive the two-state N ⇌ S pseudorotational equilibrium in the β-D-nucleosides, in aqueous solution, toward N-type conformations.

In Fig. 6.5 the O4′–C1′–N1/9 anomeric effect in nucleos(t)ides is rationalized in terms of molecular orbital overlap and hyperconjugation, as shown for β-D-dA. The O4′ lone-pair orbitals are represented using either the sp^2 (i.e., higher energy $^1n_{sp}2_{(s\text{-}type)}$ lone pair with predominant p-type character and lower energy $^2n_{sp}2_{(p\text{-}type)}$ lone pair with predominant s-type character) or sp^3 (i.e., $^1n_{sp}3$ and $^2n_{sp}3$ lone pairs with the same energy hybridization models) [64–69]. Molecular overlap model (*11* ⇌ *12)* [70] envisions the overlap (i.e., $n_{O4'} \rightarrow \sigma^*_{C1'-N9}$) of a lone-pair orbital of O4′ [$^1n_{sp}2_{(p\text{-}type)}$] with the

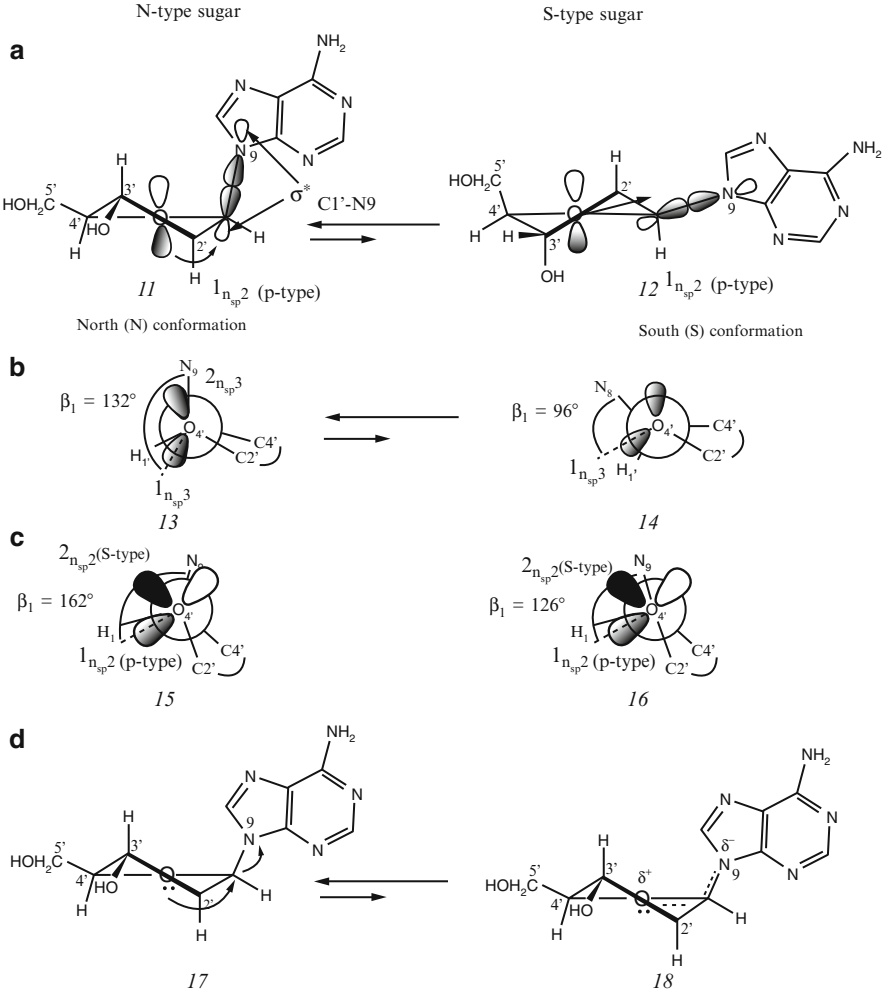

Fig. 6.5

$\sigma^*_{C1'–N9}$ antibonding orbital of the glycosyl bond resulting in the stabilization of N- over S-type pseudorotamers and shifts the pseudorotational equilibrium toward N (panel **A**). Further shown is the influence of the sp^3 (i.e., $^1n_{sp}3$ and $^2n_{sp}3$ (panel **B**) *versus* sp^2 ($^1n_{sp}2_{(p\text{-type})}$ and $^2n_{sp}2_{(s\text{-type})}$ (panel **C**) hybridization of the O4′ lone pair orbitals on N- and S-type pseudorotamer conformations with respect to the glycosidic bond and on the efficiency of the O4′-C1′-N9 stereoelectronic interactions. For a typical N-type pseudorotamer, the O4′→$\sigma^*_{C1'–N9}$ interaction is possible due to the near antiperiplanar orientation of either $^1n_{sp}3$ ($\beta \approx 132°$) or $^1n_{sp}2_{(p\text{-type})}$ ($\beta \approx 162°$) with respect to $\sigma^*_{C1'\text{-}N9}$ orbital, whereas in the S-type sugar counterpart, the efficiency of the interaction is much reduced as the result of the more acute β_1 and β_2 angles compared to those in the N-type

sugar. The double-bond ⇌ no-bond resonance results from the hyperconjugation of one of the lone pairs to the glycosyl C1′–N9 bond [70]. This model is consistent with the shortening of O4′–C1′ bond observed in crystal structures [71–73] of β-nucleos(t)ides. This overlap, which results in the formation of stabilizing (occupied) and destabilizing (unoccupied) orbitals, becomes more efficient as the square of the overlap (S) between both orbitals increases and as the difference (ΔE) between their respective energies decreases [74, 75]; maximal interaction requires an antiperiplanar orientation of $n_{O4'}$ relative to the C1′–N9 bond (panel **E**).

The crystal structures of β-D-*N*-nucleosides show that C1′–O4′ bond is 0.03–0.04 Å shorter than the C4′–O4′ bond, which goes hand in hand with the possible hyperconjugative origin for the anomeric effect in nucleosides (Fig. 6.5, panel **D**).

The effect of the aglycon on the conformation of nucleos(t)ides was observed in several ways. It was observed that the UV spectrum of 1-methylcytosine and cytosine nucleosides varies with the nature of carbohydrate component, thus establishing the crosstalk between the aglycon and the constituent sugar [76]. Guschlbauer et al. [77] showed that the conformation of the ribose moiety changes with the protonation of the guanin-9-yl base at N7 in 2′-GMP. Sarma et al. [78] have shown that the sugar conformation is different in the oxidized and reduced β-nicotinamide mononucleotides. Remin and Shugar showed [79] that the protonation of cytidine or arabinocytidine changes the $^3J_{1'2'}$ value by about 0.2 Hz. Altona and Sundaralingam did an important qualitative correlation on the nature of sugar pucker depending upon the nature of the aglycon based upon their X-ray crystal structure data [53]. Altona and Sundaralingam [80] extended their X-ray correlation data to the coupling constant correlation, showing again the qualitative dependence of $^3J_{1'2'}$ with the nature of the aglycon. The preference of S versus N conformers is pH dependent, as demonstrated for the first time by Guschlbauer et al. [81] on guanosine phosphate. A similar observation was also made by Hruska et al. [82] on 2′-*O*-methyladenosine.

Chattopadhyaya et al. [8] have shown based upon thermodynamic estimates on a set of four isomeric 2′/3′-deoxynucleosides that the net result of the gauche effect and the anomeric effect is of major importance in determining the overall furanose conformation. Many qualitative studies have been conducted [83–88] to understand how the electronic nature, protonation state [89], bulkiness or substitution pattern [90–95], and configuration of the nucleobases [96–115] or C1 substituent [116] modulate the sugar conformation in nucleosides and nucleotides, as well as furanosides [117–121]. The conformational analysis [122] in solution of a dimer containing a 4′-oxofuran derivative [123], based upon the analysis of vicinal $^3J_{HH}$, has shown that the modified nucleoside adopts exclusively (89 %) the S-type puckered geometries, as a result of the cooperative drive by the O5′–C4′–O4′ anomeric effect and the [O3′–C3′–C4′–O4′] gauche effect.

The NMR spectroscopic studies, based upon the interpretation of $^3J_{HH}$, $^3J_{CH}$, and $^3J_{CC}$ coupling constants [117, 119, 124], have shown that the α- and β-anomers of D-ribofuranose (and of their methyl glycosides) adopt preferentially the S- and N-type puckered conformations, respectively, due to the O4–C1–O1 anomeric

effect, which places the anomeric group in a pseudoaxial or nearly pseudoaxial orientation. The contribution of the exo-anomeric effect to the relative stabilities and preferred conformations of α- and β-D-erythro- and threofuranose, as obtained from *ab initio* calculation, has also been studied [118].

It has already been shown with various glycopyranosyl derivatives that the magnitude of the anomeric effect increases as the anomeric group becomes more electronegative. In nucleosides and nucleotides, it has been found that this similar trend exists.

Thus, Egert et al. [86] have shown by using analysis of crystallographic data, NMR spectroscopy, and quantum-chemical calculations on 5-substituted uridines that the electron-withdrawing substituent at the C5 induces the lengthening and shortening of N1–C1′ and O4′–C1′ bonds, respectively, in comparison with the reference compound, uridine. For electron-donating substituents, the opposite situation was observed. This was in agreement with the previously observed dependence of the magnitude of the anomeric effect upon the electronegativity of aglycon.

Uhl et al. [87] have shown by studying 5-substituted uridine derivatives in aqueous solution by ^{1}H-NMR spectroscopy that the population of N-type pseudorotamers (% N) increases from 44 % to ≈90 % going from the NH_2 to NO_2 substituent at C5. This is consistent with the proposal that electron-withdrawing (electron-donating) groups at C5 are expected to strengthen $n_{O4'} \rightarrow \sigma^*_{C1'-N9}$ interactions, i.e. the anomeric effect, and therefore stabilize the N- over S-type pseudorotamers. This is also supported by the observation that the protonation of the nucleobases in adenosine, guanosine, and cytidine nucleosides and their deoxy derivatives, strengthens the anomeric effect, i.e. increases the N-type conformation, whereas deprotonation, i.e. decreases the N-type conformation, weakens it when compared to the neutral state.

The sugar conformation can be controlled not only by altering the electronic character of nucleobases but also by changing the electronegativity of the sugar substituents.

The protonation of a nucleobase in a nucleotide controls its hydrogen-bonding abilities, and thus the three-dimensional structure of oligonucleotides is controlled by the pH of the medium.

The acid–base character of nucleobases in nucleosides and nucleotides varies widely [125–138]. Thus, adenosine ($pK_a \approx 3.5$) [125] and cytidine [125] ($pK_a \approx 4.2$) can be easily protonated in an acidic solution at N1 and N3, respectively; uridine [125] ($pK_a \approx 9.4$) and thymidine [125] ($pK_a \approx 9.9$) are deprotonated at N3 in an alkaline solution. Guanosine is either protonated at N7 [136] ($pK_a \approx 1.9$) in an acidic medium or deprotonated at N1 [125] in an alkaline solution ($pK_a \approx 9.4$).

As a consequence of protonation, the local DNA triple helix formed [139, 140] by the binding of natural homopyrimidine oligonucleotides to a target DNA duplex is much more stable to the acidic solution than at neutral pH, owing to the fact that Hoogsteen base pairing with the third pyrimidine strand requires that the cytosin-1-yl nucleobase be protonated. However, substitution of cytidine in the Hoogsteen strand for 5-methylcytosine allows it to increase its affinity for the DNA duplex under physiological pH [141, 142]. The pH-dependent conformational transitions and stabilities of C.A and G.A mismatches in DNA [143–147] have been extensively studied.

It has been also suggested [148, 149] that although the secondary structure of the oligo-DNA d$(A^+\text{-}G)_{10}$ is presumably helical, it is stabilized not by stacking bases or hydrogen-bonding base pairs , but instead by ionic bonds between positively charged 2′-deoxyadenosine residues and distal negatively charged phosphates.

References

1. Thibaudeau C, Acharya P, Chattopadhyaya J (2005) Stereoelectronic effects in nucleosides and nucleotides and their structural implications, 2nd edn. Department of Bioorganic Chemistry, Biomedical Center, Upsala University Press, Upsala
2. Taira K, Uebayasi M, Maeda H, Furukawa K (1990) Energetics of RNA cleavage: implications for the mechanism of action of ribozymes. Protein Eng 3:691–701
3. Storer JW, Uchimaru T, Tanabe K, Uebayasi M, Nishikawa S, Taira K (1991) Existence of a marginally stable intermediate during the base-catalyzed methanolysis of methylene phosphate and ab initio studies of the monohydration of the pentacoordinated oxyphosphorane intermediate. J Am Chem Soc 113:5216–5219
4. Zhou D-M, Taira K (1998) The hydrolysis of RNA: from theoretical calculations to the hammerhead ribozyme-mediated cleavage of RNA. Chem Rev 98:991–1026
5. Bizzozero SA, Dutler H (1981) Stereochemical aspects of peptide hydrolysis catalyzed by serine proteases of the chymotrypsin type. Bioorgan Chem 10:46–62
6. Post CB, Karplus M (1986) Does lysozyme follow the lysozyme pathway? An alternative based on dynamic, structural, and stereoelectronic considerations. J Am Chem Soc 108:1317
7. Taira K (1987) Stereoelectronic control in the hydrolysis of RNA by imidazole. Bull Chem Soc Japan 60:1903
8. Koole LH, Buck HM, Nyilas A, Chattopadhyaya J (1987) Structural properties of modified deoxyadenosine structures in solution. Impact of the gauche and anomeric effects on the furanose conformation. Can J Chem 65:2089–2094
9. Koole LH, Buck HM, Bazin H, Chattopadhyaya J (1987) Conformational studies of 3′-*C*-methyl and 2′-*C*-methyl analogs of cordycepin. Tetrahedron 43:2989–2997
10. Koole LH, Moody HM, Buck HM, Groullier A, Essadiq H, Vial J-M, Chattopadhyaya J (1988) Synthesis and conformation of 1-(3′-*C*-methyl-2′-deoxy-β-D-xylofuranosyl)uracil and 9-(3′-*C*-methyl-2′-deoxy-β-D-xylofuranosyl) adenine; two novel sugar-methylated nucleoside analogs. Recl Trav Chim Pays-Bas 107:343–346
11. Plavec J, Koole LH, Sandström A, Chattopadhyaya J (1991) A mild and general method for the synthesis of 2-substituted-5-hydroxypyrimidines. Tetrahedron 47:7363–7365
12. Plavec J, Buet V, Groullier A, Koole L, Chattopadhyaya J (1991) Structural studies on 1-(1-deoxy-β-D-psicofuranosyl)thymine. Tetrahedron 47:5847–5856
13. Plavec J, Koole LH, Chattopadhyaya J (1992) Structural analysis of 2′,3′-dideoxyinosine, 2′,3′-dideoxyadenosine, 2′,3′-dideoxyguanosine, and 2′,3′-dideoxycytidine by 500-MHz proton NMR spectroscopy and ab initio molecular orbital calculations. J Biochem Biophys Methods 25:253–272
14. Plavec J, Tong W, Chattopadhyaya J (1993) How do the gauche and anomeric effects drive the pseudorotational equilibrium of the pentofuranose moiety of nucleosides? J Am Chem Soc 115:9734–9746
15. Plavec J, Garg N, Chattopadhyaya J (1993) How does the steric effect drive the sugar conformation in 3′-*C*-branched nucleosides. J Chem Soc Chem Commun (1993) :1011–1014
16. Plavec J, Fabre-Buet V, Uteza V, Grouiller A, Chattopadhyaya J (1993) Conformational studies on some C1′-branched β-D-nucleosides by proton-NMR spectroscopy and molecular mechanics calculations. J Biochem Biophys Methods 26:317

17. Plavec J, Thibaudeau C, Viswanadham G, Sund C, Chattopadhyaya J (1994) How does the 3′-phosphate drive the sugar conformation in DNA? J Chem Soc Chem Commun (1994):781–783
18. Thibaudeau C, Plavec J, Watanabe KA, Chattopadhyaya J (1994) How do the aglycons drive the pseudorotational equilibrium of the pentofuranose moiety in C-nucleosides? J Chem Soc Chem Commun (1994):537–540
19. Thibaudeau C, Plavec J, Chattopadhyaya J (1994) Quantitation of the anomeric effect in adenosine and guanosine by comparison of the thermodynamics of the pseudorotational equilibrium of the pentofuranose moiety in N- and C-nucleosides. J Am Chem Soc 116:8033–8037
20. Thibaudeau C, Plavec J, Garg N, Papchikhin A, Chattopadhyaya J (1994) How does the electronegativity of the substituent indicate the strength of the gauche effect? J Am Chem Soc 116:4038–4043
21. Plavec J, Thibaudeau C, Chattopadhyaya J (1994) How does the 2′-hydroxy group drive the pseudorotational equilibrium in nucleoside and nucleotide by the tuning of the 3′-gauche effect? J Am Chem Soc 116:6558–6560
22. Plavec J, Thibaudeau C, Viswanadham G, Sund C, Sandström A, Chattopadhyaya J (1995) The interaction of the 2′-OH group with the vicinal phosphate in ribonucleoside 3′-(ethylphosphate) drives the sugar phosphate backbone into unique (S, ε) conformational state. Tetrahedron 51:11775–11792
23. Plavec J, Thibaudeau C, Chattopadhyaya J (1996) How do the energetics of the stereoelectronic gauche and anomeric effects modulate the conformation of nucleosides and nucleotides? Pure Appl Chem 68:2137–2144
24. Thibaudeau C, Plavec J, Chattopadhyaya J (1996) Quantitation of the pD dependent thermodynamics of N.dblarw. S pseudorotational equilibrium of the pentofuranose moiety in nucleosides gives a direct measurement of the strength of the tunable an omeric effect and the pKa of the nucleobase. J Org Chem 61:266–286
25. Chattopadyaya J (1996) The nature of intramolecular stereoelectronic forces in nucleosides and nucleotides. Nucleic Acids Res Symp Ser 35:111–112
26. Luyten I, Thibaudeau C, Sandström A, Chattopadhyaya J (1997) The tunable transmission of the aromatic character of the aglycon through the anomeric effect in *C*-nucleosides drives-its own sugar conformation: a thermodynamic study. Tetrahedron 53:6433–6464
27. Luyten I, Thibaudeau C, Chattopadhyaya J (1997) The strength of the anomeric effect in adenosine, guanosine and their 2′-deoxy counterparts is medium-dependent. J Org Chem 62:8800–8808
28. Luyten I, Thibaudeau C, Chattopadhyaya J (1997) The determination of the ionization constants of *C*-nucleosides. Tetrahedron 53:6903
29. Thibaudeau C, Chattopadhyaya J (1997) Nucleosides Nucleotides 16:523
30. Thibaudeau C, Földesi A, Chattopadhyaya J (1997) The first experimental evidence for a larger medium-dependent flexibility of natural β-D-nucleosides compared to the α-D-nucleosides. Tetrahedron 53:14043–14072
31. Thibaudeau C, Földesi A, Chattopadhyaya J (1998) The quantitation of the competing energetics of the stereoelectronic and steric effects of the 3′-OH and the aglycon in the α- versus β-D- and L-2′-deoxyribonucleosides by 1H NMR. Tetrahedron 54:1867–1900
32. Thibaudeau C, Chattopadhyaya J (1998) The information transmission from the nucleobase drives the sugar-phosphate backbone conformation in the nucleotide wire. Nucleosides Nucleotides 17:1589–1603
33. Thibaudeau C, Plavec J, Chattopadhyaya J (1998) A new generalized Karplus-type equation relating vicinal proton-fluorine coupling constants to H-C-C-F torsion angles. J Org Chem 63:4967–4984
34. Luyten I, Matulic-Adamic J, Biegelman L, Chattopadhyaya J (1998) The electronic nature of the aglycon dictates the drive of pseudorotational equilibrium of the pentofuranose moiety in *C*-nucleosides. Nucleosides Nucleotides 17:1605–1611

35. Thibaudeau C, Kumar A, Bekiroglu S, Matsuda A, Marquez VE, Chattopadhyaya J (1998) NMR conformation of (-)-β-D-aristeromycin and its 2′-deoxy and 3′-deoxy counterparts in aqueous solution. J Org Chem 63:5447–5462
36. Thibaudeau C, Nishizono N, Sumita Y, Matsuda A, Chattopadhyaya J (1999) Determination of the group electronegativity of CF3 group in 3′-*O*-CF3-thymidine by 1H-NMR. Nucleosides Nucleotides 18:1035–1053
37. Acharya P, Nawrot B, Thibaudeau C, Chattopadhyaya J (1999) The strength of the 3′-gauche effect dictates the structure 3′-*O*-anthraniloyladenosine and its 5′-phosphate, two analogs of the 3′-end of aminoacyl-tRNA. J Chem Soc Perkin Trans II (1999) :1531–1536
38. Acharya P, Trifonova A, Thibaudeau C, Földesi A, Chattopadhyaya J (1999) The transmission of the electronic character of guanine-9-yl the sugar-phosphate backbone torsions in guanosine 3′,5′-biphosphate. Angew Chem Int Ed 38:3645–3650
39. Velikian I, Acharya P, Trifonova A, Földesi A, Chattopadhyaya J (2000) The RNA molecular wire: the pH-dependent change of the electronic character of adenin-9-yl is transmitted to drive the sugar and phosphate torsions in adenosine 3′,5′-biphosphate. J Phys Org Chem 13:300–305
40. Polak M, Plavec J, Trifonova A, Földesi A, Chattopadhyaya J (1999) The change in the electronic character upon cisplatin binding to guanine nucleotide is transmitted to drive the conformation of the local sugar-phosphate backbone – a quantitative study. J Chem Soc Perkin I (1999) :2835–2843
41. Griffey RH, Lesnik E, Freier S, Sanghvi YS, Teng K, Kawasaki A, Guinosso C, Wheeler P, Mohan V, Cook PD (1994) In: Sanghvi YS, Cook PD (eds) Carbohydrate modifications in antisense research, new twists on nucleic acids; structural properties of modified nucleosides incorporated into oligonucleotides, vol 580. American Chemical Society, Washington, DC, p 212
42. Freier SM, Altmann K-H (1997) The ups and downs of nucleic acid duplex stability: structure-stability studies on chemically-modified DNA:RNA duplexes. Nucleic Acids Res 25:4429–4443
43. Tereshko V, Gryaznov S, Egli M (1998) Consequences of replacing the DNA 3′-oxygen by an amino group: high-resolution crystal structure of a fully modified N3 → P5′ phosphoramidate DNA dodecamer duplex. J Am Chem Soc 120:269–283
44. Berger I, Tereshko V, Ikeda H, Marquez VE, Egli M (1998) Crystal structures of B-DNA with incorporated 2′-deoxy-2′fluoro-arabino-furanosyl thymines: implications of conformational preorganization for duplex stability. Nucleic Acids Res 26:2473–2480
45. Ikeda H, Fernandez R, Wilk A, Barchi JJ Jr, Huang X, Marquez VE (1998) The effect of two antipodal fluorine-induced sugar puckers on the conformation and stability of the Dickerson-Drew dodecamer duplex[d(CGCGAATTCGCG)]2. Nucleic Acids Res 26:2237–2244
46. Angyal SJ (1984) The composition of reducing sugars in solution. Adv Carbohydr Chem Biochem (Tipson RS, Horton D (ed) Academic Press, London) 42:15–68
47. Squillacote M, Sheridan OL, Chapman OL, Anet FAL (1975) Spectroscopic detection of the twist-boat conformation of cyclohexane. Direct measurement of the free energy difference between the chair and the twist-boat. J Am Chem Soc 97:3244–3246
48. Anderson JE (1974) Top Curr Chem 45:139
49. Kilpatrick JE, Pitzer KS, Spitzer R (1947) The thermodynamics and molecular structure of cyclopentane. J Am Chem Soc 69:2483
50. Strauss HL (1983) Pseudorotation: a large amplitude molecular motion. Ann Rev Phys Chem 34:301–328
51. Carreira LA, Jiang GJ, Person WB, Willis JN (1972) Spectroscopic determination of the barrier to planarity in cyclopentane. J Chem Phys 56:1440–1443
52. Hall LD, Steiner PR, Pedersen C (1970) Specifically fluorinated carbohydrates. VI. Pentofuranosyl fluorides. Can J Chem 48:1155–1165

53. Altona C, Sundaralingam M (1972) Conformational analysis of the sugar ring in nucleosides and nucleotides. New description using the concept of pseudorotation. J Am Chem Soc 94:8205–8212
54. Westhof E, Sundaralingam M (1980) Interrelationship between the pseudorotation parameters P and Tm and the geometry of the furanose ring. J Am Chem Soc 102:1493
55. Sasisekharan V (1973) Jerus Symp Quant Chem Biochem 5:247
56. Saenger W (1988) Principles of nucleic acid structure. Springer, Berlin
57. Saenger W (1988) Principles of nucleic acid structure. Springer, Berlin, pp. 9396
58. Lai TF, Marsh RE (1972) Crystal structure of adenosine. Acta Cryst B28:1982–1989
59. Shikata K, Ueki T, Mitsui T (1973) Crystal and molecular structure of adenosine hydrochloride. Acta Cryst 29:31–38
60. Olson WK, Sussman JL (1982) How flexible is the furanose ring? 1. A comparison of experimental and theoretical studies. J Am Chem Soc 104:270–278
61. Olson WK (1982) How flexible is furanose ring? An updated potential energy estimate. J Am Chem Soc 104:278–286
62. Pearlman DA, Kim S-H (1985) Conformational studies of nucleic acids. II. The conformational energetics of commonly occurring nucleosides. J Biomol Struct Dyn 3:99
63. Jalluri RK, Yuh H, Taylor EW (1993) O-C-N anomeric effect in nucleosides. A major factor underlying the experimentally observed eastern barrier to pseudorotation. In: Thatcher GRJ (ed) The anomeric effects and associated stereoelectronic effects, vol 539. American Chemical Society, Washington, DC, pp 277–293
64. Sweigart DA (1973) Lone pair orbital in group VI and VII hydrides. J Chem Educ 50:322
65. David S, Eisenstein O, Hehre WJ, Salem L, Hoffman R (1973) Superjacent orbital control. Interpretation of the anomeric effect. J Am Chem Soc 95:3806–3807
66. Laing M (1987) No rabbit ears on water. The structure of the water molecule: what should we tell the students? J Chem Educ 64:124–128
67. Brundle CR, Turner DW (1968) High resolution molecular photoelectron spectroscopy. II. Water and deuterium oxide. Proc R Soc Lond A A307:27–36
68. Cossé-Barbi A, Dubois JE (1987) Anomeric orbital and steric control in static conformations and systems dynamics: rotations of methoxy groups in 2,2-dimethoxypropane and similar crystallographic COCOC fragments. J Am Chem Soc 109:1503–1511
69. Cossé-Barbi A, Watson DG, Dubois JE (1989) Anomeric effect in carbohydrates: non-equivalence of endocyclic oxygen lone pairs. Tetrahedron Lett 30:163–166
70. Romers C, Altona C, Buys HR, Havinga E (1969) In: Eliel EL, Allinger NL (eds) Topics in stereochemistry, vol 4. Willey Science, New York, p 39
71. de Leeuw HPM, Haasnoot CAG, Altona C (1980) Empirical correlations between conformational parameters in β-D-furanoside fragments derived from a statistical survey of crystal structures of nucleic acid constituents. Full description of nucleoside molecular geometries in terms of four parameters. Isr J Chem 20:108–126
72. Allen FH, Davies JE, Galloy JJ, Johnson O, Kennard O, MacRae CF, Mitchell EM, Mitchell GF, Watson DG (1991) The development of versions 3 and 4 of the Cambridge Structural Database System. J Chem Inf Comput Sci 31:187–204
73. Lo A, Shefter E, Cochran TG (1975) Analysis of *N*-glycosyl bond length in crystal structures of nucleosides and nucleotides. J Pharm Sci 64:1707–1710
74. Juaristi E, Cuevas G (1992) Recent studies on the anomeric effect. Tetrahedron 48:5019–5087
75. Thatcher GRJ (1993) In: Thatcher GRJ (ed) Anomeric effect and associated stereoelectronic effects. Scope and controversy, vol 539. American Chemical Society, Washington, DC, pp 6–25
76. Fox JJ, Sugar D (1952) Spectrometric studies of nucleic acid derivatives and related compounds as a function of pH. II. Natural and synthetic pyrimidine nucleosides. Biochim Biophys Acta 9:369–384

77. Tran-Dinh S, Thiéry J, Guschlbauer J-J (1972) Nucleoside conformations. VIII. Conformation of guanosine 2′-phosphate in aqueous solution by proton magnetic resonance spectroscopy. Biochim Biophys Acta 281:289–298
78. Sarma RH, Mynott RJ (1973) Conformation of pyridine nucleotides studied by phosphorus-31 and hydrogen-1 Fourier transform nuclear magnetic resonance spectroscopy. I. Oxidized and reduced mononucleotides. J Am Chem Soc 95:1641–1649
79. Remin M, Shugar D (1973) Conformational analysis of cytidine 1-β-D-(arabinofuranosyl) cytosine and their O′-methyl derivatives by proton magnetic resonance spectroscopy. J Am Chem Soc 95:8146–8156
80. Altona C, Sundaralingam S (1973) Conformational analysis of the sugar ring in nucleosides and nucleotides. Improved method for the interpretation of proton magnetic resonance coupling constants. J Am Chem Soc 95:2333–2344
81. Tran-Dinh S, Guschlbauer W (1975) Nucleoside conformations. 19. Temperature and pH effects on the conformation of guanosine phosphates. Nucleic Acids Res 3:873–886
82. Hruska FE, Wood DJ, Singh H (1977) Effect of temperature and protonation upon the conformation of 2′-*O*-methyladenosine. Correlation of conformational parameters in purine nucleosides. Biochim Biophys Acta 474:129–140
83. Jalluri RK, Yuh YH, Taylor EW (1993) O-C-N anomeric effect in nucleosides. A major factor underlying the experimentally observed eastern barrier to pseudorotation. In: Thatcher GRJ (ed) The anomeric effect and associated stereoelectronic effects, vol 539. American Chemical Society, Washington, DC, pp 277–293
84. Seela F, Becher G, Rosemeyer H, Reuter H, Kastner G, Mikhailopulo I (1999) The high-anti conformation of 7-halogenated 8-aza-7-deaza-2′-deoxyguanosines. A study of the influence of modified bases on the sugar structure of nucleosides. Helv Chim Acta 82:105–124
85. Hillen W, Gassen HG (1978) 5-substituents in the uridine moiety and their effect on the conformation of ApU-type dinucleoside phosphates. Biochim Biophys Acta 518:7–16
86. Egert E, Lindner HJ, Hillen W, Böhm MC (1980) Influence of substituents at the 5 position on the structure of uridine. J Am Chem Soc 102:3707–3713
87. Uhl W, Reiner J, Gassen HG (1983) On the conformation of 5-substituted uridines as studied by proton magnetic resonance. Nucleic Acids Res 11:1167–1180
88. O'Leary DJ, Kishi Y (1994) Preferred conformation of *C*-glycosides. 13. A comparison of the conformational behavior of several *C*-, *N*-, and *O*-furanosides. J Org Chem 59:6629–6636
89. Ekiel I, Remin M, Darzynkiewicz E, Shugar D (1979) Correlations of conformational parameters and equilibrium conformational states in a variety of β-D-arabinonucleosides and their analogs. Biochim Biophys Acta 562:177–191
90. Yamamoto Y, Yokoyama S, Miyazawa T, Watanabe K, Higuchi S (1983) FEBS Lett 157:95
91. Allore BD, Queen A, Blonski WJ, Hruska FE (1983) A kinetic and nuclear magnetic resonance study of methylated pyrimidine nucleosides. Can J Chem 61:2397–2402
92. Birnbaum GI, Blonski WJP, Heuska FE (1983) Structure and conformation of anticodon nucleoside 5-methoxyuridine in the solid state and in solution. Can J Chem 61:2299–2304
93. Cadet J, Ducolomb R, Taieb C (1975) NMR at 250 MHz of 6-methyl-2′-deoxyuridine. Preferential syn-configuration in aqueous solution. Tetrahedron Lett 40:3455–3458
94. Birnbaum GI, Hruska FE, Niemczura WP (1980) A pyrimidine nucleoside constrained in the syn form. Structure and conformation of 6-methyl-2′-deoxyuridine. J Am Chem Soc 102:5586–5590
95. Bergström DF, Zhang P, Toma PH, Andrews PC, Nichols R (1995) Synthesis, structure, and deoxyribonucleic acid sequencing with a universal nucleoside: 1-(2′-deoxy-β-D-ribofuranosyl)-3-nitropyrrole. J Am Chem Soc 117:1201–1209
96. Swarna Latha Y, Yathindra N (1992) Stereochemical studies on nucleic acid analogs. I. Conformations of α-nucleosides and α-nucleotides: interconversion of sugar puckers via O4′-exo. Biopolymers 32:249–269
97. Post ML, Birnbaum GI, Huber CP, Shugar D (1977) α-Nucleosides in biological systems. Crystal structure and conformation of α-cytidine. Biochim Biophys Acta 479:133–142

98. Sundaralingam M (1971) Stereochemistry of nucleic acids and their constituents. XVIII. Conformational analysis of α nucleosides by X-ray crystallography. J Am Chem Soc 93:6644–6647
99. Rohrer DC, Sundaralingam M (1970) Stereochemistry of nucleic acids and their constituents. XII. Crystal and molecular structure of α-D-amino-2′-deoxyadenosine monohydrate. J Am Chem Soc 92:4956–4962
100. Remin M, Ekiel I, Shugar D (1975) Proton-magnetic-resonance study of the solution conformation of the α and β anomers of 5-ethyl-2′-deoxyuridine. Eur J Biochem 53:197–206
101. Seto H, Otake N, Yonehara H (1972) Tetrahedron Lett 38:3991
102. Ruzic-Toros Z (1979) [Crystal structure of]5,6-dimethyl-1-(α-D-ribofuranosyl)benzimidazole. Acta Cryst B35:1277–1280
103. Crowfoot Hodgkin D, Lindsey J, Sparks RA, Trueblood KN, White JG (1962) Structure of vitamin B12. V. Structure of the air-dried crystals of vitamin B12. Proc R Soc A266:494
104. Brink-Shoemaker C, Cruickshank DWJ, Crowfoot Hodgkin D, Kamper MJ, Pilling D (1964) Structure of vitamin B12. VI. Structure of crystals of vitamin B12 grown from and immersed in water. Proc R Soc Lond A A278:1–26
105. Hawkinson SW, Coulter CL, Greaves ML (1979) Structure of vitamin B12. VIII. Crystal structure of vitamin B12-5′ phosphate. Proc Roy Soc A318:143
106. Savage HFJ, Lindley PF, Finney JL, Timmins PA (1987) High-resolution neutron and X-ray refinement of vitamin B12 coenzyme, C72H100CoN18O17P.17H2O. Acta Cryst B43:280–295
107. Lenhert PG (1968) Structure of vitamin B12. VII. X-ray analysis of the vitamin B12 coenzyme. Proc R Soc Lond A A303:45–84
108. Hamor TA, O'Leary MK, Walker RT (1977) The crystal and molecular structure of α-5-acetyl-2′-deoxyuridine. Acta Cryst B33:1218–1223
109. Shefter E, Kotick MP, Bardos J (1967) Crystal and molecular structure of 5-[1(2-deoxy-α-D-erythro-pentofuranosyl)acyl]disulfide. J Pharm Sci 56:1293–1299
110. Ide H, Shimzu H, Kimura Y, Sakamoto S, Makino K, Glackin M, Wallace SS, Nakamuta H, Sasaki M, Sugimoto N (1995) Influence of α-deoxyadenosine on the stability and structure of DNA. Thermodynamic and molecular mechanics studies. Biochemistry 34:6947–6955
111. Gutowski GE, Chaney MO, Jones ND, Hamill RL, Davis FA, Miller RD (1973) Pyrazomycin B: isolation and characterization of an *–C*-nucleoside antibiotic related to pyrazomycin. Biochim Biophys Res Commun 51:312–317
112. Armstrong VW, Dattagupta JK, Eckstein F, Saenger W (1976) The base catalyzed anomerization of β-5-formyluridine; crystal and molecular structure of α-5-formyluridine. Nucleic Acids Res 3:1791–1810
113. Cline SJ, Hodgson DJ (1979) The crystal and molecular structure of 9-α-D-arabinofuranosyladenine. Biochim Biophys Acta 563:540–544
114. Post ML, Huber CP, Birnbaum GI, Shugar D (1981) Crystal structures and conformations of 1-α-D-xylofuranosylcytosine and its protonated form (hydrogen chloride salt). Can J Chem 59:238–245
115. Piper IM, MacLean DB, Faggiani R, Lock CJL, Szarek WA (1985) Configurational and conformational studies on condensation products of biogenic amines with 2,5-anhydro-D-mannose. Can J Chem 63:2915–2921
116. Hoffman RA, van Wijk J, Leeflang BR, Kamerling JP, Altona C, Vliegenthart JFG (1992) Conformational analysis of the α-L-arabinofuranosides present in wheat arabinoxylans from proton-proton coupling constants. J Am Chem Soc 114:3710–3714
117. Serianni A, Barker R (1984) [13C]-Enriched tetroses and tetrofuranosides: an evaluation of the relationship between NMR parameters and furanosyl ring conformation. J Org Chem 49:3292–3300
118. Serianni AS, Chipman DM (1987) Furanose ring conformation: the application of ab initio molecular orbital calculations to the structure and dynamics of erythrofuranose and threofuranose rings. J Am Chem Soc 109:5297–5303

119. Kline PC, Serianni AS (1990) 13C-enriched ribonucleosides: synthesis and application of 13C-1H and 13C-13C spin-coupling constants to asses furanose and *N*-glycoside bond conformations. J Am Chem Soc 112:7373, 7381
120. Raap J, van Boom JH, van Lieshoiut HC, Haasnoot CAG (1988) J Am Chem Soc 110:2736–7381
121. Ellervik U, Magnussonm G (1994) Anomeric effect in furanosides. Experimental evidence from conformationally restricted compounds. J Am Chem Soc 116:2340–2347
122. Griffey RH, Lesnik E, Freier S, Sanghvi YS, Teng K, Kawasaki A, Guinoso C, Wheeler P, Mohan V, Cook PD (1994) In: Sanghvi VS, Cook PD (eds) Carbohydrate modifications in antisense research, new twist on nucleic acids; structural properties of modified nucleosides incorporated into oligonucleotides, vol 580. American Chemical Society, Washington, DC, p 212
123. Teng K, Cool PD (1994) Nucleic acid mimics. Synthesis of ethylene glycol- and propoxy-linked thymidyl-tetrahydrofuranylthymine dimers via a Vorbruggen-type glycosylation reaction. J Org Chem 59:278–280
124. Cyr N, Perlin AS (1979) The conformations of furanosides. A carbon-13 nuclear magnetic resonance study. Can J Chem 57:2504–2511
125. Saenger W (1988) Principles of nucleic acids structure. Springer, Berlin
126. Izatt RM, Christensen JJ, Ryttiing JH (1971) Sites and thermodynamic quantities associated with proton and metal ion interaction with ribonucleic acid, deoxyribonucleic acid, and their constituent bases, nucleosides, and nucleotides. Chem Rev 71:439–482
127. Garcia B, Palacios JC (1988) Protonation study of biological bases of DNA. Ber Bunsenges Phys Chem 92:696–700
128. Taylor R, Kennard O (1982) The molecular structures of nucleosides and nucleotides. Part 1. The influence of protonation on the geometries of nucleic acid constituents. J Mol Struct 78:1–28
129. Jardetzky CD, Jardetzky O (1960) Investigation of the structure of purines, pyrimidines, ribose nucleosides and nucleotides by proton magnetic resonance.II. J Am Chem Soc 82:222–229
130. Angell CL (1961) An infrared spectroscopic investigation of nucleic acid constituents. J Chem Soc (1961) :504–515
131. Tsuboi M, Kyogoku Y, Shimanouchi T (1962) Infrared absorption spectra of protonated and deprotonated nucleosides. Biochim Biophys Acta 55:1–12
132. Kartritzky AR, Wariing AJ (1962) Tautomeric azines. Tautomerism of 1-methyluracil and 5-bromo-1-methyluracil. J Chem Soc (1962) :1540–1544
133. Lord RC, Thomas GJJ (1967) Raman studies of nucleic acids. II. Aqueous purine and pyrimidine mixtures. Biochim Biophys Acta 142:1–11
134. Clauwaert J, Stockx J (1968) Interactions of polynucleotides and their components. I. Dissociation constants of the bases and their derivatives. Z Naturforsch 23B:25–30
135. Wagner R, von Philipsborn W (1970) Protonation of amino and hydroxypyrimidines. NMR-spectra and structures of mono and dications. Helv Chim Acta 53:299–320
136. Christensen JJ, Rytting H, Izatt RM (1970) Thermodynamic pK, ΔH.deg, ΔS.deg, and ΔCp. deg values for proton dissociation from several purines and their nucleosides in aqueous solution. Biochemistry 9:4907–4913
137. Poulter CD, Anderson RB (1972) Direct observation of uracil dication and related derivatives. Tetrahedron Lett 36:3823–3826
138. Dunn DB, Hall RH (1975) In: Fassman GD (ed) Handbook of biochemistry and molecular biology, vol 1. CRC Press, Cleveland, p 65
139. Le Doan T, Perrouault L, Praseuth D, Habhoub N, Decout J-L, Thouong NT, Lhomme J, Hélène C (1987) Sequence-specific recognition, photocrosslinking and cleavage of the DNA double helix by an oligo-[α]-thymidylate covalently linked to an azidoproflavine derivative. Nucleic Acids Res 15:7749–7760
140. Moser HE, Dervan PB (1987) Sequence-specific cleavage of double helical DNA by triple helix formation. Science 238:645

141. Povsic TJ, Dervan PB (1989) Triple helix formation by oligonucleotides on DNA extended to the physiological pH range. J Am Chem Soc 111:3059–3061
142. Xodo LE, Manzini G, Quadrifoglio F, van der Marel GA, van Boom JH (1991) Effect of 5-methylcytosine on the stability of triple-stranded DNA – a thermodynamic study. Nucleic Acids Res 19:5625–5631
143. Brown T, Leonard GA, Booth ED, Kneale G (1990) Influence of pH on the conformation and stability of mismatch base-pairs in DNA. J Mol Biol 212:437
144. Boulard Y, Cognet JAH, Gabarro-Arpa J, LeBret M, Sowers LC, Fazakerley GV (1992) The pH dependent configurations of the C′A mispair in DNA. Nucleic Acid Res 20:1933–1941
145. Wang C, Gao H, Gaffney BL, Jones RA (1991) Nitrogen-15 labeled oligodeoxynucleotides. 3. Protonation of the adenine N1 in the A′C and A′G mispairs of the duplexes {d[CG(15N1)AGAATTCCCG]}2 and {d[CGGGAATTC(15N1)ACG]}2. J Am Chem Soc 113:5486–5488
146. Macaya RF, Gilbert DE, Malek S, Sinsheimer JS, Feigon J (1991) Structure and stability of X′G′C mismatches in the third strand of intramolecular triplexes. Science 254:270–273
147. Gao X, Patel DJ (1988) G(syn)′A(anti) mismatch formation in DNA dodecamers at acidic pH: pH-dependent conformational transition of G′A mispairs detected by proton NMR. J Am Chem Soc 110:5178–5182
148. Dolinnaya NG, Fresco JR (1992) Single stranded nucleic acid helical secondary structure stabilized by ionic bonds: d(A^+-G)10. Proc Natl Acad Sci U S A 89:9242–9246
149. Dolinnaya NG, Braswell EH, Fosella JA, Klump H, Fresco JR (1993) Molecular and thermodynamic properties of d(A^+-G)10, a single-stranded nucleic acid helix without paired or stacked bases. Biochemistry 32:10263–10270

Chapter 7
Free Radical Cyclizations

The free radical cyclizations of hex-5-enes (*1* in Fig. 7.1) were accomplished some time ago, and although the origin of selectivity was not initially understood, the stereochemistry at the newly created centers was predictable in some of the cases.

In the 1980s, Beckwith had published the first pioneering studies on this subject [1, 2] in which he postulated two transition states for this cyclization, as shown in Fig. 7.2.

RajanBabu and coworkers have undertaken a systematic study of these control elements in highly functionalized and synthetically useful systems. On the basis of their work, models for transition states that can be utilized to rationalize the stereochemistry of hex-5-enyl radical cyclizations have been proposed, including a number of seemingly anomalous reported results.

In his papers, Beckwith proposed general guidelines to predict the stereochemical outcome of the reactions of simple substituted hex-5-enyl radicals [1, 2]. The cyclization of 1- and 3-substituted hex-5-enyl radicals leads mostly to *cis*-disubstituted cyclopentyl products, whereas 2- and 4-substituted radicals give predominantly *trans* products. The observed stereochemical results were rationalized by invoking theoretically derived transition states *4* and *5* (Fig. 7.2), which have a long incipient bond (ca. 2.3 Å), in accordance with an early transition state predicted for these reactions. This distance is not much different from that between C1 and C5 in cyclohexane (ca. 2.5 Å). Beckwith argued that this and other geometric parameters are comparable in the two cases, and therefore conformational features that are well-known in substituted cyclohexanes can be used to rationalize stereochemical results in the hex-5-enyl radical cyclizations. Thus, the major products arise via a conformation where the substituents occupy quasiequatorial positions. Also, in the absence of any special effects, a "chair-like" transition state will be preferred. (It should be noted here that a similar and perhaps more realistic transition state model can be constructed based upon the folded envelope-like conformations of methylene-cyclopentane. However, the cyclohexane model seems to be more useful, albeit less precise, simply because the conformational preferences are better understood in the cyclohexane system than in methylenecyclopentanes.)

M. Miljkovic, *Electrostatic and Stereoelectronic Effects in Carbohydrate Chemistry*,
DOI 10.1007/978-1-4614-8268-0_7,

Fig. 7.1 Hex-5-enyl radical cyclization

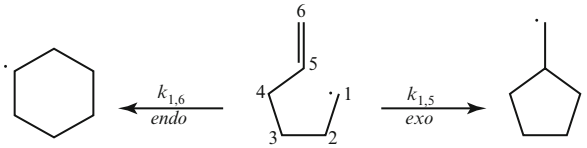

3 *1* *2*

At 60° C, $k_{1,5}$ is approximately 10^5-10^6 sec^{-1}; $k_{1,5}/k_{1,6} = 50$

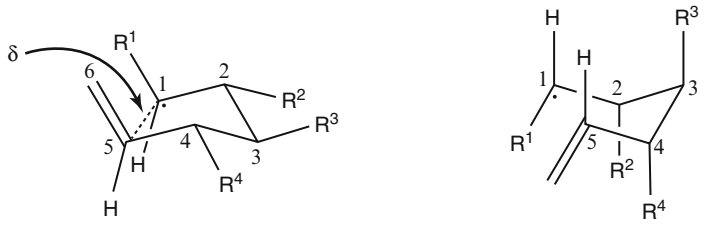

4 *5*

For the transition state, δ = 2.3 A. For cyclohexane C_1-C_5, δ = 2.5 A

Fig. 7.2 Beckwith's transition state model

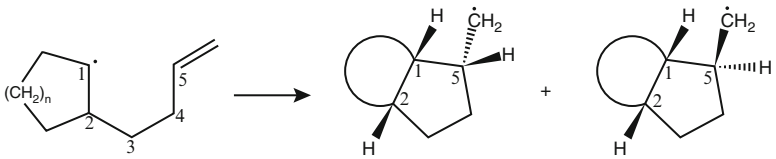

5 *6* *7*

n = 1 cyclopentyl
n = 2 cyclohexyl

1, 2 *cis*; 1, 5 = *cis*

1, 2 *cis*; 1, 5 = *trans*

Fig. 7.3

For example, in the case of a 2-substituted radical (unless otherwise indicated, radical numbering is followed in the text starting with the radical center as 1), structure *4* will be the preferred transition state, leading to 2,5-*trans*-disubstituted cyclopentane.

The ring closure of cyclic 2-but-3-enylcycloalkyl radicals (Fig. 7.3) is similar to that of the open-chain system, except that the constraints of the ring impose an almost exclusive 1,2-*cis* stereochemistry [3, 4]. The critical 1,5-selectivity is still largely *cis*, and it is this selectivity that has found the most use in the synthesis of polycyclic natural products [5, 6]. In the context of the 2-but-3-enylcyclopentyl radical cyclization, it was argued [7] that the 1,5-*cis* stereochemistry is favored because the "chair-like" transition structure *8*a (Fig. 7.4) can achieve effective overlap between the SOMO and the radical center and the olefin π orbitals, with less strain than the other possible chair *8*b.

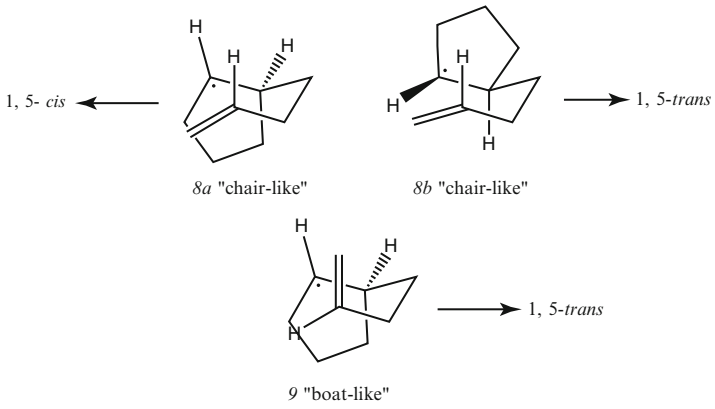

Fig. 7.4

While this is an adequate rationalization, there is yet another plausible explanation for the origin of the minor product: in order to keep the conformation of the cycloalkyl moiety the same, the "chair-like" *8*a or "boat-like" *9* conformation for the cyclization transition state is proposed. The former will lead to a 1,5-*cis* product while the latter will give a 1,5-*trans* product. It is interesting that theoretical calculations of conformations of the hex-5-enyl radical transition states showed that the difference between "chair-like" and "boat-like" transition states is less than 1 kcal/mol. To obtain an answer as to what are the structural features that favor one or the other transition state, highly substituted radicals from carbohydrates were prepared, since the aldopyranose sugars readily undergo a Wittig reaction to give hex-5-en-1-ols [8], which can be converted to highly functionalized hex-5-enyl radicals by any of the variations of the Barton deoxygenation reaction [9] as shown in Fig. 7.5. Due to the availability of pyranose sugars of various configurations, such a protocol is also uniquely suited to study the effect of 1-, 2-, 3-, and 4-substituents on the stereochemistry of the cyclization reaction. Furthermore, the well-established protecting-group strategies in carbohydrate chemistry permit the study of open-chain radicals, as well as cyclic radicals with known absolute and relative stereochemistry.

An example of this is illustrated in Fig. 7.6. Radical *12* (Fig. 7.5) cyclizes to give products *18*, *19*, and *20* in a ratio of 74:14:12 in 61 % overall yield from *11* (Y = H). (The ratios of products are normalized with respect to the cyclopentane isomers.) Likewise, the radical generated from the enol ether *11* (Y = OMe) undergoes facile cyclization to the corresponding products in similar ratios.

In the cyclization of the acyclic radical *17*a (or *17*b) (a: Y = H; b: Y = OMe), the formation of the 1,5-*cis* product *18* can be accounted for by transition state *21*. Note that in this transition state, the (phenylmethoxy)methyl substituent at the C1 position and the C2, C3, and C4 phenylmethoxy groups are all in a quasi-equatorial orientation as suggested by the Beckwith model. The fact that the

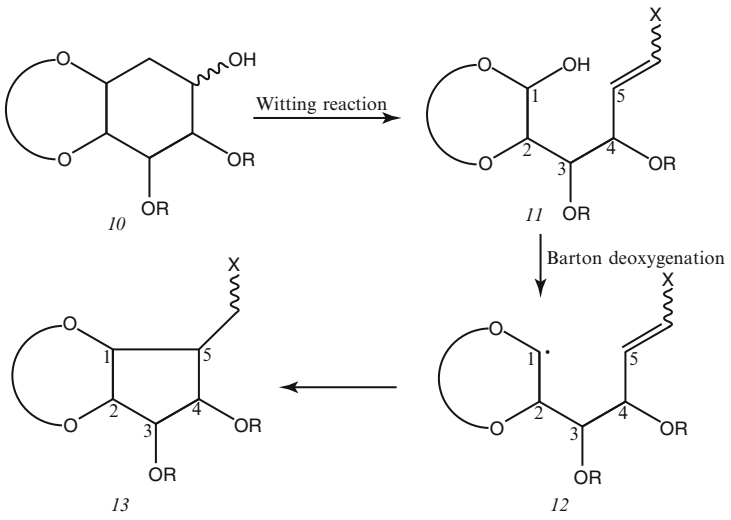

Fig. 7.5

4,5-stereochemistry is overwhelmingly *trans* (combined *18* and *19*: 88 %) can be accounted for by considering the local allylic conformation (C3–C6). As pointed out by other workers [10] in the context of both intra- and intermolecular additions, the conformation with the least allylic strain, in this case *22*, is favored, and this leads to the 4,5-*trans* products.

In sharp contrast to the acyclic radicals, cyclic radicals exhibited much better stereoselectivities. Cyclization of radical *24*a *or24b prepared* from 4,6-*O*-benzylidene-2,3-di-*O*-benzyl-D-glucopyranose *23* gave a single *trans* product (*25*a or *25*b) in each case (Fig. 7.7) [11]. Likewise, a radical with the 3-benzyloxy substituent removed (*26*) also cyclizes to give almost exclusively the 1,5-*trans* product *27*.

Whether or not allylic strain at the olefinic center of hex-5-enyl radical plays a role in formation of *25* and *27* can be probed by studying the cyclization of the radicals *28*a and *28*b, which lack these allylic substituents. These cyclic 4-deoxy radicals (radical numbering is followed in the text, starting with the radical carbon as 1), generated by routes similar to the ones described above, cyclize with predominantly 1,5-*cis* (i.e., *endo*-Me) stereochemistry (Fig. 7.8). The 3-substituent appears to have very little effect on the course of the reaction.

The preponderant formation of the 1,5-*trans* products *25* and *27* is totally unexpected, especially since other structurally related radicals (e.g., *28*a and *28*b) and their carbocyclic analogs give a mixture with mostly 1,5-*cis* products [3, 5, 12–15]. If one assumes that the dioxane ring maintains the chair conformation and that the bulky phenyl and butenyl groups occupy equatorial orientations, then the 1,5-*trans* product can only be rationalized by a boat-like cyclization transition state depicted by structure *34* in Fig. 7.9, in which the pseudoaxial radical attacks the C═C bond in the pseudoequatorial butenyl side chain. The original preference

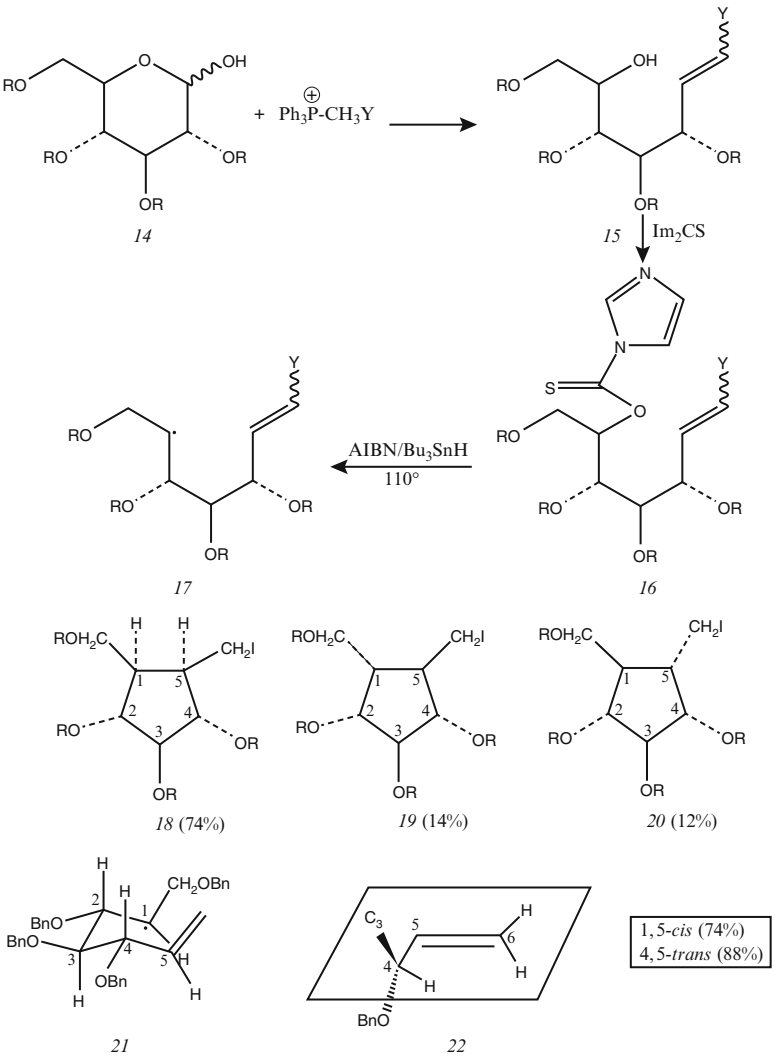

Fig. 7.6 Latent C_5-hydroxy as a radical precursor in pyranosides

for a boat-like transition state in radical *34* was unknown. Some relief of steric compression between the C2 oxygen, i.e., dioxane O, and the C4 benzyl group is expected, as the *cis* decalin-like chair-chair conformation undergoes a change to the chair-boat conformation *34*. However, the conformational studies [16] of various sugar derivatives suggest that this alone would not be sufficient to produce such a dramatic effect. RajanBabu proposed that the local conformation of the allyl ether portion of the molecule (viz., C3–C6) was an important factor in controlling this stereochemistry [17]. The boat-like transition state contains the most favorable allylic conformation [18, 19] for the C3–C6 portion (*33*) of the molecule, whereas

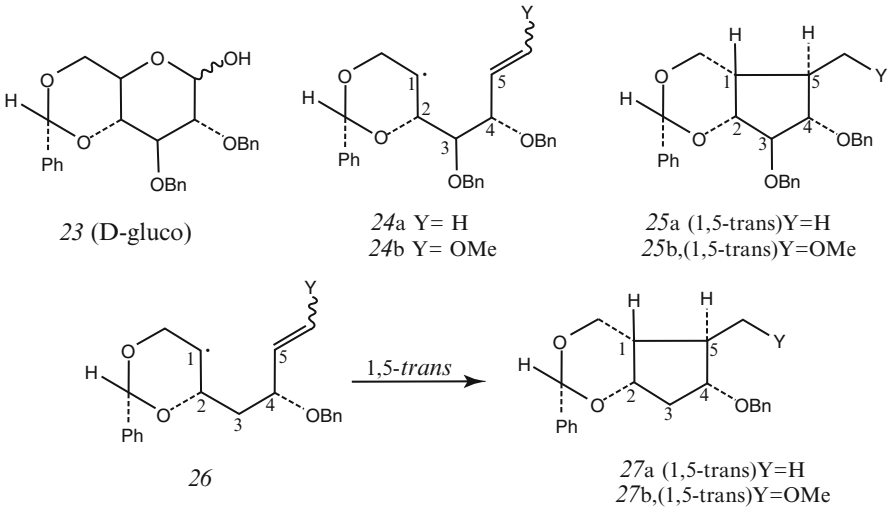

23 (D-gluco)

*24*a Y= H
*24*b Y= OMe

*25*a (1,5-trans)Y=H
*25*b,(1,5-trans)Y=OMe

26

*27*a (1,5-trans)Y=H
*27*b,(1,5-trans)Y=OMe

Fig. 7.7

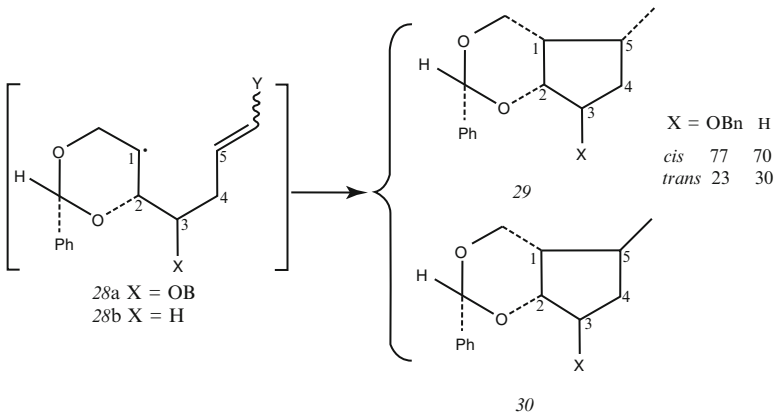

*28*a X = OB
*28*b X = H

29

30

Fig. 7.8 Cyclization of 2-deoxyglucose-derived radicals

the allylic segment *31* in the chair-like transition state *32* has more strain because a bulky group (X = OBn) eclipses one of the vinylic hydrogen atoms. The relief of the allylic strain more than compensates for the formation of the normally unfavorable boat-like transition state. Another hitherto unrecognized stereoelectronic component may be influencing the course of this unusual stereochemical outcome. Additions of alkyl radicals to olefins appear to be nucleophilic in nature [20]; and if so, an activation of olefin π* orbital by the allylic β-CO-σ* may play an important role in acceleration of the reaction rates. In some conformations, e.g., the "boat-like" *34*, the alignment of the β-CO-σ* with respect to the π system is more favorable than in others, and reactions proceeding through these transition states

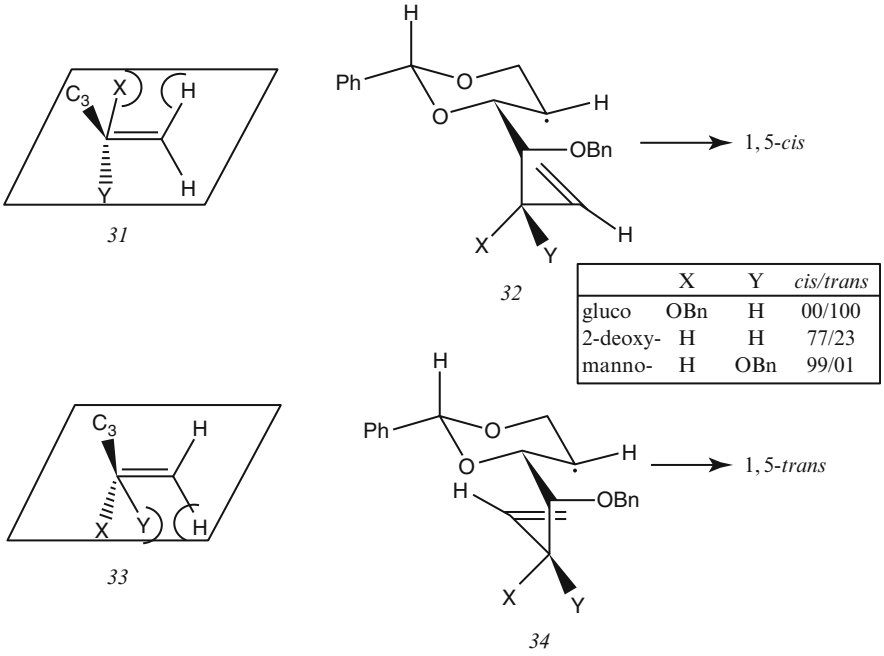

	X	Y	*cis/trans*
gluco	OBn	H	00/100
2-deoxy-	H	H	77/23
manno-	H	OBn	99/01

Fig. 7.9 Transition states for the cyclization of glucose- and mannose-derived radicals

would be expected to be faster. Since the various conformations of the starting material are in rapid equilibrium, these reactions are probably under the Curtin-Hammett regime and these kinetic effects might play an important role in deciding the course of the reaction. Studies on substrates with differing allylic β-CX-σ* bond energies might shed some light on this aspect of reaction. Notably, a slightly lower selectivity is observed in a system that has an allylic CC bond in an analogous steric situation [21]. Presumably a σ*-CC is much higher in energy than a σ*-CO and cannot interact with the π system as favorably as the latter.

In the absence of an allylic alkoxy group, the allylic strain (and the possible stereoelectronic effect) is not present, and the reaction proceeds through low-energy "chair-like" transition state such as *32* to give predominantly the 1,5-*cis* products. This is the case with the 4-deoxy radicals *28*a and *28*b giving *cis*/*trans* ratios of 77:23 and 70:30 (Fig. 7.8). The minor 1,5-*trans* products in these systems could arise via a "boat-like" transition state *34* (X = Y = H). The same rationale applies to the stereochemistry of cyclization of the radical *35* (Fig. 7.10), which is generated by treating the starting epoxide with Cp_2TiCl [11, 22].

Further confirmation that the C4 oxygen is the control element comes from the cyclization of the mannose *38*-derived radical *32* (X = H; Y = OBn). In this case the configuration of the key C4 center is inverted as compared to that of the glucose-derived radical; in accord with the prediction, predominant formation of the 1,5-*cis* product (*cis*/*trans*, 99:1) is observed. As shown in Fig. 7.11, the "chair-like"

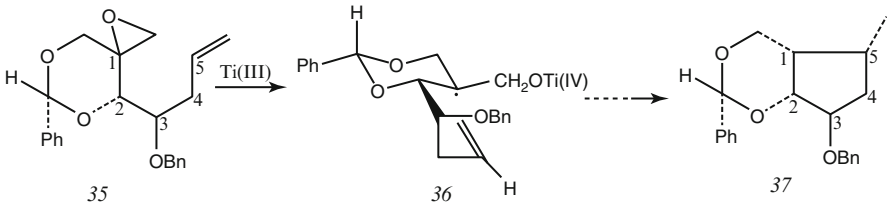

Fig. 7.10 Cyclization of a Ti(III)/epoxy-derived radical

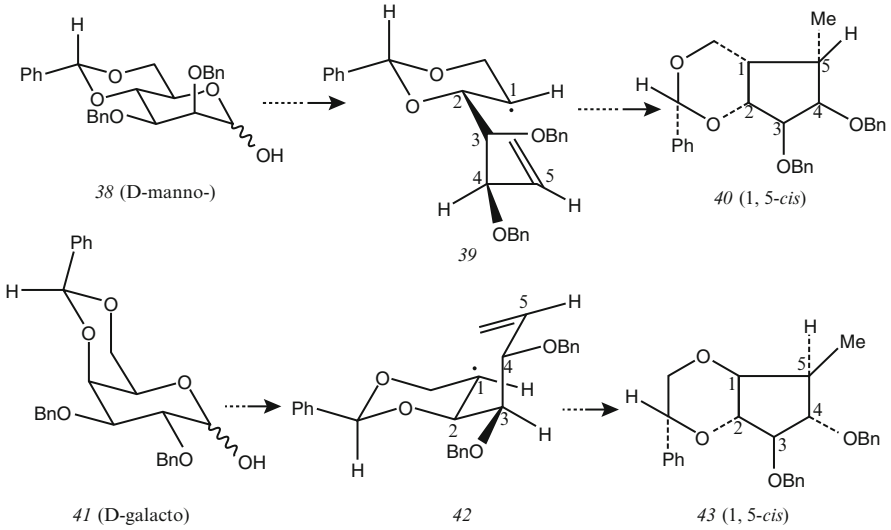

Fig. 7.11

conformation of the transition state 39 incorporates the low-energy conformation of the allylic (C3–C6) segment (i.e., *31*, X = H; Y = OBn). The advantages of using readily available sugars as precursors for substituted radicals are further highlighted by the ease with which one can generate a radical with a totally different structure to test the predictive power of these models. Thus, the radical *42* (Fig. 7.11) which was readily prepared from galactose cyclizes via the chair-chair transition state to give only the 1,5-*cis* product *43*. It is interesting to note that the galactose-derived radical *42* has an enantiomeric relationship with the mannose-derived radical *32*, except for the C3 configuration. Both of these radicals produce almost exclusively the 1,5-*cis* products, again confirming the relative lack of influence of the C3 oxygen substituent on the stereochemistry when a C4 substituent is also present.

The radical cyclization products derived from sugars are useful for the synthesis of cyclopentanoid natural products. For example, the unprecedented 1,5-*trans* stereochemistry seen in the case of 4,6-O-benzylidene-glucose-derived radicals can be used to prepare optically active prostaglandin intermediates such as Corey lactone *44* (Fig. 7.12) [23].

Fig. 7.12

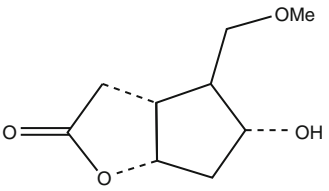

44

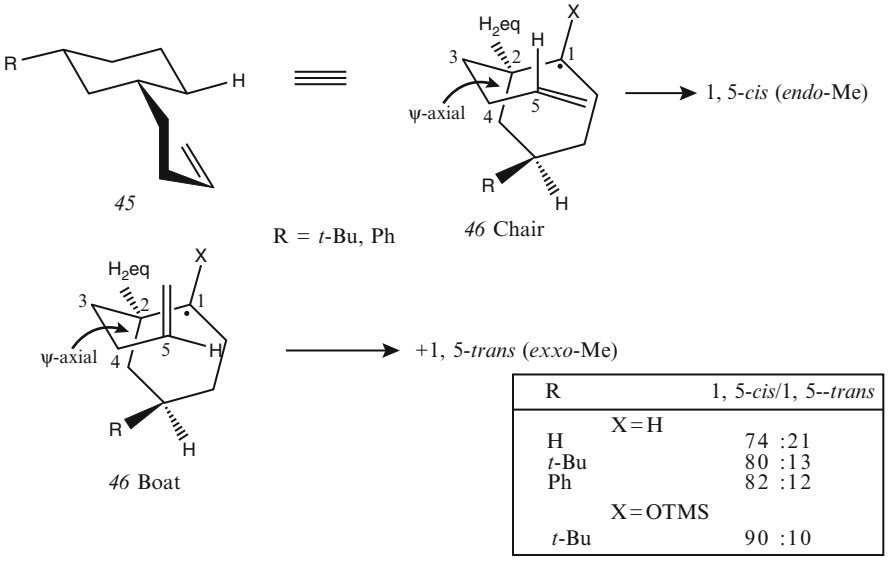

45

R = *t*-Bu, Ph

46 Chair

46 Boat

R	1, 5-*cis*/1, 5--*trans*
X = H	
H	74 :21
t-Bu	80 :13
Ph	82 :12
X = OTMS	
t-Bu	90 :10

Fig. 7.13 Cyclization of equatorial 2-but-3-enylcyclohexyl radicals

In every case of conformationally locked systems reported in the literature [12, 13] and in the ones so far discussed (*34*, *36*, *42*), the but-3-enyl groups are in an equatorial orientation. In the absence of any special effects, such as the allylic strain, all these systems yield 1,5-*cis* selectivity. These results cast some doubt on the original contention [3] that efficient ring closure can occur only through an effective overlap of SOMO of the radical with the p-orbitals of an axially oriented but-3-enyl group. On the contrary, a careful examination of the *cis* decalin-like transition state reveals that if the but-3-enyl group were in an axial orientation, a "chair-like" transition state should yield predominantly 1,5-*trans* product (vide infra, Fig. 7.13).

In an effort to delineate these effects, the ratio of 1,5-*cis* to 1,5-*trans* products in fused bicyclo[4.3.0]nonanes prepared by the radical cyclization of axially and equatorially oriented 2-but-3-enylcyclohexyl radicals, which are conformationally locked, was studied [14]. These results are shown in Figs. 7.13 and 7.14.

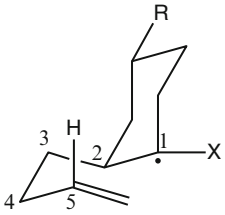

47, Chair
*47*a, X = H
*47*b, X = OTMS

→ 1, 5-*trans* (*exo*-Me)

R	1, 5-*cis*/1, 5-*trans*
X = H	
t-Bu	22:62
Ph	31:61
X = OTMS	
*t*Bu	25:75

Fig. 7.14 Cyclization of axial 2-but-3-enylcyclohexyl radical

As expected, radicals with an equatorial butenyl group (Fig. 7.13) give mostly 1,5-*cis* products, the selectivity being highest in the conformationally rigid systems (4-Ph and 4-*t*-Bu). For the unsubstituted parent system [3], this ratio is 74:21, and for the corresponding 4-phenyl dioxa system (Fig. 7.8), it is 70:30. This is consistent with the fact that the 1,5-*cis* products arise from "chair-like" transition states, depicted by *46*-chair, in which the substituents are all in the most favorable equatorial positions of the cyclohexane ring. The minor ring-closure products may result from "boat-like" transition states (e.g., *46*-boat). As suggested earlier, the energy difference between the chair-like and boat-like transition states could be small relative to the energy of activation for cyclization [24].

In contrast, radicals with axially oriented 2-but-3-enyl group give a higher proportion of the 1,5-*trans* product. This 1,5-*trans* preference in the cyclization of radicals with an axial but-3-enyl group may be most reasonably rationalized by the "chair-like" transition state depicted by structure *47*-chair, which retains the butenyl group in the axial position. However, since the conformational equilibrium may not be so one-sided, as in the case of diequatorial intermediates such as *46*-chair even when an anchoring group is present, 1,5-*trans* selectivity is lower than the *cis* selectivity as observed in the case of equatorially disposed butenyl compounds. This is further reflected in the decrease of the *cis*/*trans* ratio from 1:2 to 1:3 when going from phenyl (A-value, conformational free-energy difference: 3.1 kcal/mol) to *t*-Bu (A-value 5 kcal/mol).

Cyclization of 2-but-3-enylcyclohexanes mediated by zinc in the presence of trimethylsilyl chloride may also be influenced by the same controlling factors. Corey reported [12] that *cis*-2-but-3-enyl-4-*t*-butylcyclohexane gave mostly an *endo*-methyl-*cis*-hydrindanol. The 1,5-*cis*/*trans* ratio was reported to be 66:7.

An unexpectedly high proportion of 1,5-*trans* products was obtained in the cyclization of the α-allyl (axial) glycoside radicals *47a* and *47b* [25]. As the previously discussed model would have predicted, a significant portion of the reaction must proceed through the chair-chair conformation leading to this product. Since the triacetoxy sugar is conformationally flexible (hydroxy and acetoxy groups are small,

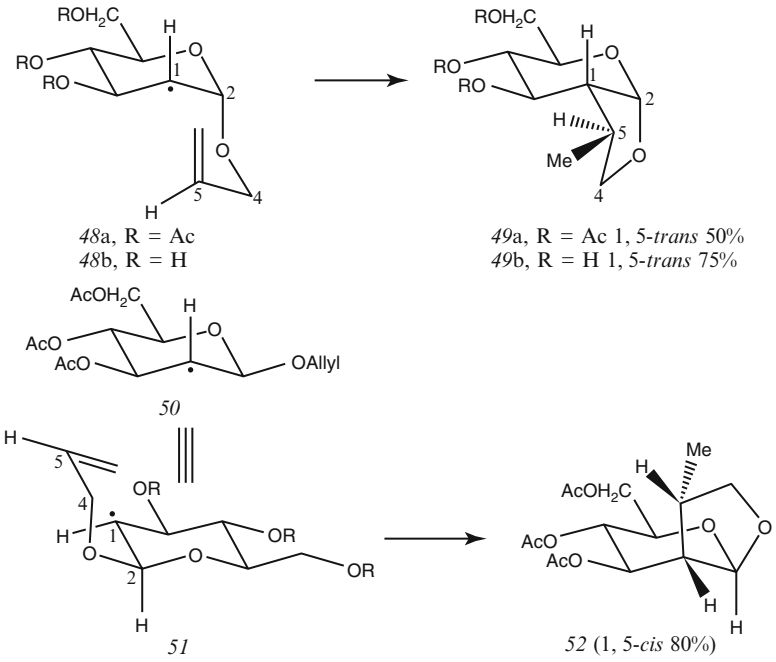

Fig. 7.15 Stereochemistry of intramolecular radical C-glycosidation

(A-value 0.7 kcal/mol)), and it is likely that nonchair conformations are populated at temperatures at which the radicals are generated (see references [16, 27]), especially at the temperatures at which the cyclization is carried out, it is not surprising that the 1,5-*cis* product is also observed, albeit in low yield. The proportion of the 1,5-*trans* product is even greater in the case of the unprotected (R═H) sugar derivative. The stereochemistry of the products from the corresponding equatorial β-allyloxy derivative has not been determined [25]. It can be predicted that the major (75 %) product would be the *endo* isomer *52a* arising through a chair-chair transition state *51*. The special stabilization via β-CO-σ* interaction (see below) is not applicable in this case, since radicals without an α-oxy substituent do not interact with neighboring CO bonds.

In addition to the axial versus equatorial orientation of the but-3-enyl group, special stabilization of an intermediate radical can also play an important role in the stereochemical outcome of hex-5-enyl radical cyclizations. The surprising results of De Mesmaeker [28] on the stereochemistry of intramolecular C-glycosidation reactions (Fig. 7.16) can be satisfactorily explained if one also takes into account this important stabilization effect in considering the described models. For example, the anomeric radical from *53a* would be expected to cyclize via chair-like transition state *55* leading to *56* as the major product, but up to 53 % of the *exo*-isomer *58* is also formed in the reaction.

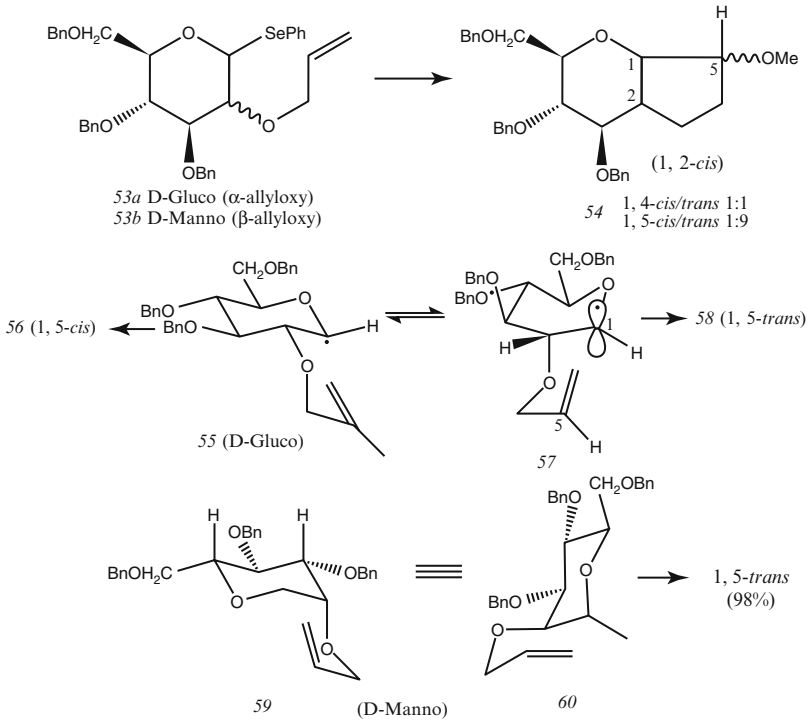

Fig. 7.16

Based on EPR studies carried out on related systems by Giese et al. [29], it can be assumed that an α-oxy radical (glycosyl radical) such as *55* undergoes a conformational change into the boat form *57*. In this form, the electronic stabilization from the β-CO-σ*-SOMO interaction can more than compensate for the apparent strain involved in the high-energy conformation. A chair transition state for the cyclization now leads to the 1,5-*trans* product. A more compelling case for this scenario is provided by the cyclization of the mannose (from *53b*)-derived radical *59*, where this conformational change of the sugar is not needed for the radical stabilization. The stable chair conformation of the sugar radical is helped by the axial nature of the β–CO bond. As expected, very high selectivity (9:1 = *exo*/*endo*) for the 1,5-*trans* product is observed. Such an unusual anomeric radical stabilization is also involved in the formation of *63* (Fig. 7.17) as the major product via the transition state *61* [30]. It should be added that this stabilization does not exist in the case of radicals that lack an electron-withdrawing group (e.g., *305* or *307* [27]).

There are a number of other instances [31–33] where the heuristic models presented above can be used to rationalize unusual stereochemical outcomes in hexenyl radical cyclizations including an interesting case of a tandem cyclization (Fig. 7.18) [34].

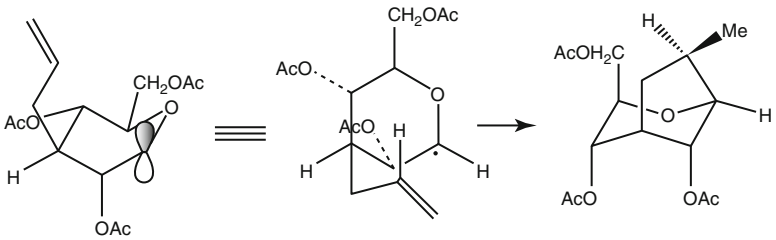

61 *62* *63*, 90%; *exo*-Me

Fig. 7.17

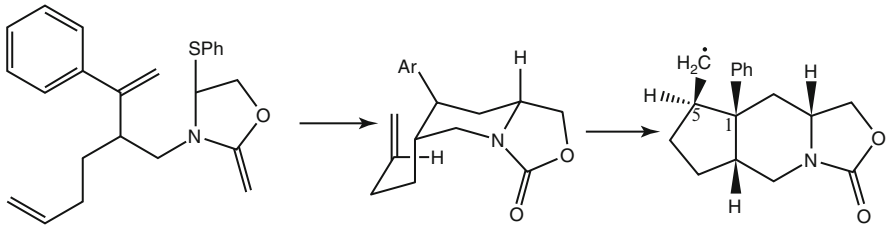

64 *65* *66*

Fig. 7.18

Thus far it has been conclusively shown that the stereochemical outcome of the cyclizations of conformationally rigid 2-but-3-enylcyclohexyl radicals is critically influenced by the orientation of the butenyl side chain; an equatorial butenyl group leads predominantly to 1,5-*cis* cyclization products, whereas an axial butenyl group preferentially gives rise to 1,5-*trans* products. [Since alkylation of cyclohexanones can be carried out to produce axial (kinetic) or equatorial (thermodynamic) 2-but-3-enyl ketones, this control element can be parlayed into annulation stereochemistry by the appropriate choice of radical cyclization methodology.] These stereochemical consequences can be satisfactorily accounted for by the cyclohexane "chair-like" transition states originally proposed by Beckwith et al. for acyclic hex-5-enyl radical cyclization. In related but conformationally less rigid systems, the transition states having an equatorial and an axial butenyl side chain may compete. Minor ring-closure products also may arise from less favorable "boat-like" transition states. As shown in several of the sugar-derived radicals, the formation of these "boat-like" transition states may sometimes be helped by the configuration at the C4 carbon. In the presence of a C4 substituent, the local acyclic conformation dictates the choice between the "chair-like" and "boat-like" transition states, and the one with the lowest 1,3-strain controls the course of the reaction. This results in an unprecedented control of the 1,5-stereoselectivity of the hex-5-enyl radical cyclization. In systems with C3 and C4 substituents, the C4 substituent is the control element and the C3 substituent exerts only a marginal influence on the

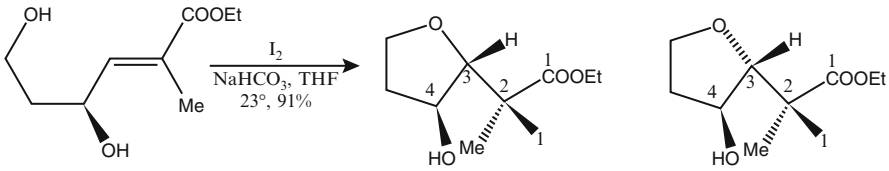

67 *68a* *69b*

Fig. 7.19

1,5-stereoselection. Special effects, such as the stabilization a β-CO-σ* provides for an α-oxy radical, should be taken into account before considering these models.

An iodoetherification reaction (selected examples of an iodoetherification reaction [35–41] of a terminally disubstituted olefin bearing a hydroxyl group at the allylic position) is shown in Fig. 7.19. As illustrated in Fig. 7.19, the reaction of substrate *67* with iodine in the presence of $NaHCO_3$ in THF gives compound *68a* in 91 % yield [42]. The presence of a hydroxyl group induces allylic 1,3-strain to favor a *trans* relative stereochemistry between C3–O and C4–O bonds of the cyclization product (compound *68a*). Furthermore, the antiperiplanar addition of the oxygen to the double bond activated by the iodine (I_2) results in a product with a residual C1 bond *anti* to the newly formed C–O bond as in *68*, *69* (Fig. 7.19).

Transition states **A** and **B** could be used to rationalize *trans* product 68, 69, **A** being favored for steric reasons (Fig. 7.20) [43]. However, considering that the substituent at the allylic position (OH) is an electron-withdrawing group, stereoelectronic arguments could be raised in favor of transition state **B**. It has been shown that the allylic hydroxyl group can have a significant stereodirecting effect on electrophilic additions to double bonds [44–48].

A study has been conducted on whether the hydroxyl group has any stereoelectronic effects [49] that can control diastereoselectivity, an aspect of cyclofunctionalization.

To this end, Guindon et al. [43] have performed cyclofunctionalization reactions using secondary alcohols *72* and *75* (Fig. 7.21). The transition states (cf. transition states **E** (*73*), **F** (*76*), **G** (*78*), and **H** (*79*), Fig. 7.21) involved in these reactions were compared in terms of steric or steric/stereoelectronic effects to determine the relative reaction rates. The reasoning behind this strategy was that the *anti* diol *72* would cyclize faster than the *syn* diol *75* if steric effects were the only controlling factor in the reaction. If both allylic 1,3-strain and stereoelectronic effects were involved, *75* would react more rapidly than *72*. A complementary experiment featuring a bidirectional approach using *80* (Fig. 7.22) was also proposed to ensure that both the *syn* and the *anti* would have the same chemical environment and to further support the findings from the competition reactions of *72* and *75*.

By shedding light on the critical role of stereoelectronic effects involved in the intramolecular addition of a nucleophile to an activated α, β-unsaturated ester, these studies may have contributed to a refinement of the transition state model normally used to rationalize such reactions. Furthermore, these studies may provide an

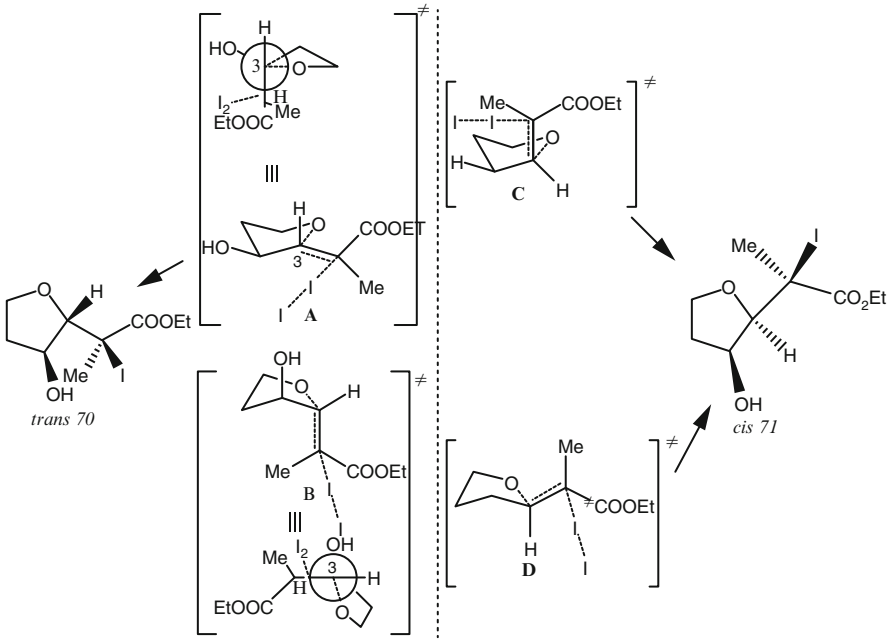

Fig. 7.20

alternative application for bidirectional synthesis in the elucidation of reaction pathways.

The iodoetherification reactions described above normally proceed under kinetic control [50–53], hence the importance of the transition state energy. Complete reversibility of the electrophilic addition to the olefin is implied [54]. In the case of halogen additions, onium intermediates are generally freely reversible, see [55–59], allowing for selectivity during the cyclization step. The allylic hydroxyl group involved in the iodocyclization reaction does not hydrogen bond to the nucleophilic oxygen (H-bond acceptor). (In the cyclofunctionalization reaction of an α,-β-unsaturated ester, similar results were obtained for the free allylic alcohol, the OMe counterpart, and the allylic fluorine. See Ref. [50].) Although the exact nature of the intermediates is not yet known, it has been suggested that the intermolecular haloetherification reaction involves a fully developed halonium ion and that the cyclofunctionalization reaction proceeds through a π-complex before undergoing charge separation (Fig. 7.20) [60]. (It should also be noted that the presence of terminally disubstituted double bond forces the minimization of allylic 1,3-strain, an important steric constraint in the transition states proposed.)

An analysis of these transition states, based on the minimization of the different torsional strains, would suggest that *trans*-predictive transition state **A** (Fig. 7.20) is the lowest in energy while *trans*-predictive transition state **B** suffers from the presence of an axial hydroxyl group and a gauche staggering within the ring.

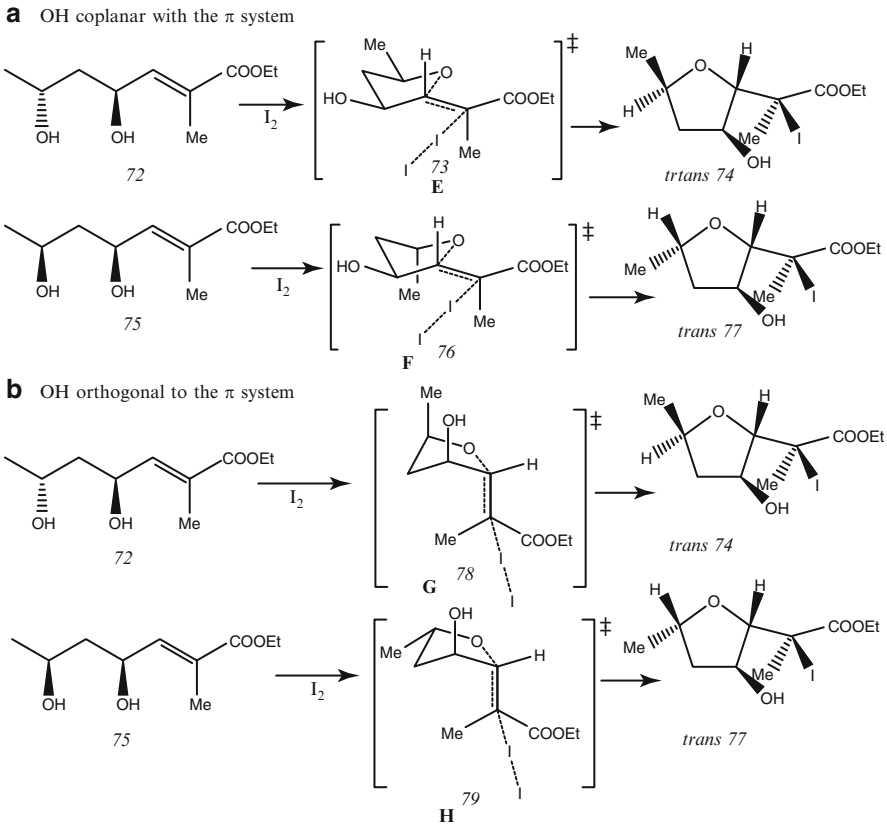

Fig. 7.21 Proposed transition states for the iodoetherification of diols *72* and *75*

Nevertheless, these two transition states are preferred over *cis*-predictive transition states **C** and **D**, which are destabilized by two gauche effects and by allylic 1,3-strain, respectively.

Several additional points should be made about the electronic effects of both the ester (end substituent of the olefin) and the allylic hydroxyl group. First, the presence of the ester renders the olefin less reactive toward the electrophile [51]. Second, most of the positive charge (in the onium or in the π-complex) is found on the β-carbon of olefin. Given this, as well as stereoelectronic reasons, an electron-withdrawing allylic hydroxyl group at the equatorial position (transition state **A**, Fig. 7.20) should be better aligned for maximizing conjugation of the $\sigma^*_{C\text{-}O}$ orbital with either the π-system [61] or the carbonium ion, which results in a decrease in the rate of cyclization or an increase in the energy of the carbonium ion, respectively. Having the electron-withdrawing allylic group in an orthogonal position (i.e., axial as in **B**) with respect to the π-system might avoid the rate-retarding effect (Endo alkoxy effect) [62], which would make transition state **B** the lowest in energy [50]. In support of these orthogonal arguments, see [63]. Since both **A** and **B** lead to the same

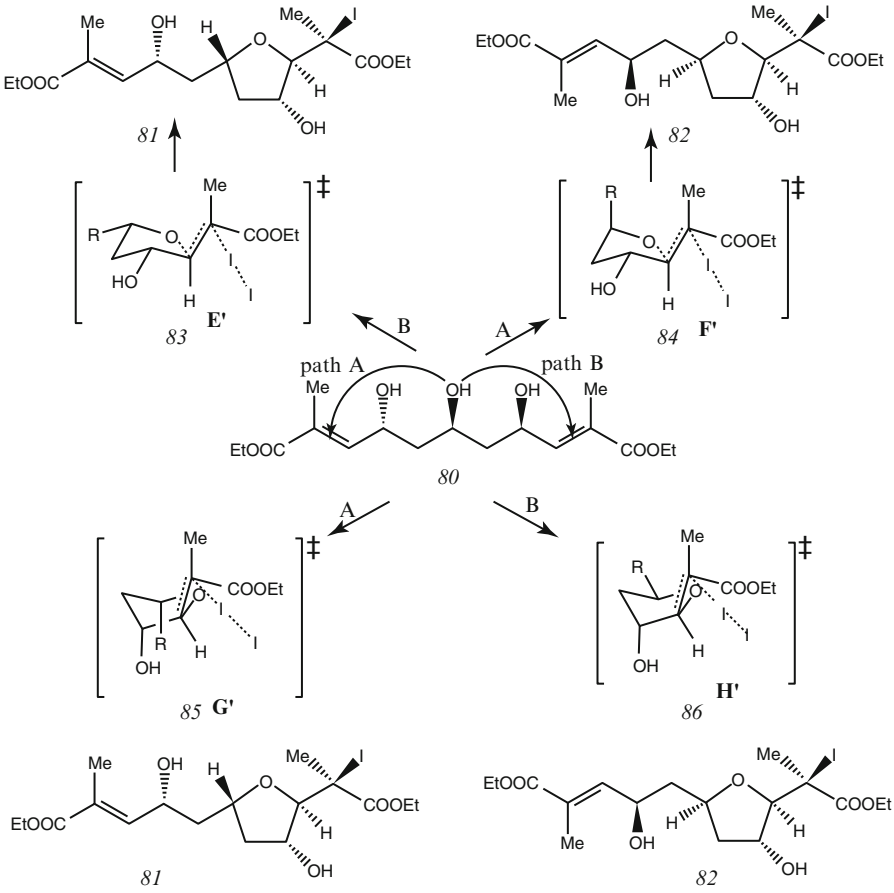

Fig. 7.22 Two-directional synthesis

product, additional stereochemical information must be encoded into the substrates in order to differentiate between the two *trans*-predictive transition states.

The search for the operative *trans*-predictive iodoetherification transition state begins with the following competition experiments involving *anti* diol *72* and *syn* diol *75* (Fig. 7.21). In such competitions, the difference in reactivity of these diols is a reflection of the difference in energy of the respective transition states, which can in turn indicate whether the allylic hydroxyl substituents involved are axial or equatorial. The four possible transition states leading to the cyclized products *74* and *77* from the respective diols *72* and *75* are illustrated in Fig. 7.21.

When minimization of torsional strain is the controlling factor in the iodoetherification reaction, the transition state possessing the equatorial hydroxyl group at the allylic carbon should be preferred (as in **A**, Fig. 7.20). Given the steric interaction in **F** resulting from the presence of an axial methyl group, this transition state should be higher in energy than **E**, where all of the substituents are equatorial.

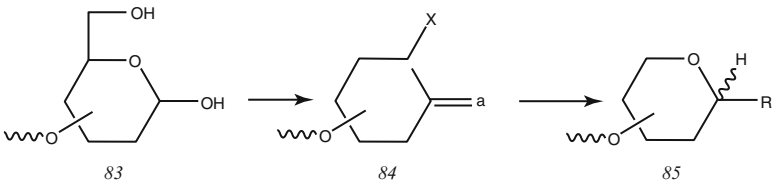

Fig. 7.23

In this case, the *anti* diol *72* will have cyclized faster than the *syn* diol. If both torsional strain minimization and stereoelectronic arguments are involved, then the preferred transition states will be those in which the hydroxyl group is orthogonal (as in **B**, Fig. 7.20) to the π-system of the double bond (**G** and **H**, Fig. 7.21). In this scenario, transition state **G** should be higher in energy than **H** due to development of transannular diaxial interaction, and the *syn* diol will have reacted faster than the *anti* diol *72*.

In summary, the *anti* diol should cyclize faster than the *syn* when steric effects are the only controlling factor in the reaction. If both allylic 1,3-strain and stereoelectronic effects are involved, then the *syn* diol should react more rapidly.

In the 1990s, reports had been published on free radical approach for the synthesis of enantiomeric pure polyhydroxylated cyclohexane rings [64–67]. These authors have shown for the first time the 6-*exo*-trig [5, 20] cyclization of acyclic sugar derivatives *84*. For leading references, see [14, 17, 23, 68–75]. In Fig. 7.23: X = leaving group, a = radical acceptor. This is a reliable and efficient method for the preparation of aminocyclitols [76–86], pseudo-sugars [85–93], and branched-chain cyclitols [94]. The success of this method is governed by the correct choice of radical acceptor. As expected, conformationally restricted precursor with α, β-unsaturated esters [95] as terminal acceptors has provided the best results. In earlier works, the cyclization of fully oxygenated (C2–C5) 6-deoxy-6-halo sugar precursors with gluco-, manno-, or gulo-absolute configurations [64, 66, 67, 96] were analyzed.

In order to evaluate, expand, and exploit the synthetic usefulness of this methodology, a large number of differently substituted and functionalized substrates were needed. In addition, due to scarce examples of synthetically useful 6-exo free radical cyclizations [97], the stereochemical outcome and stereoelectronic effects concerned with this process remain almost unknown, in contrast with the rich literature about the 5-exo ring closure [98]. With these ideas in mind, Marco-Contelles and Sánchez have synthesized and cyclized compounds *86–97* (Fig. 7.24). The authors have found that the absolute configuration at the new stereocenter formed during the carbocyclization of acyclic 6-pentenyl radicals depended upon the stereoelectronic effects of the vicinal substituent at the carbon where the radical is being generated. This is a novel and interesting result in the field of radical chemistry (for an independent and simultaneous approach to this subject, see [99]).

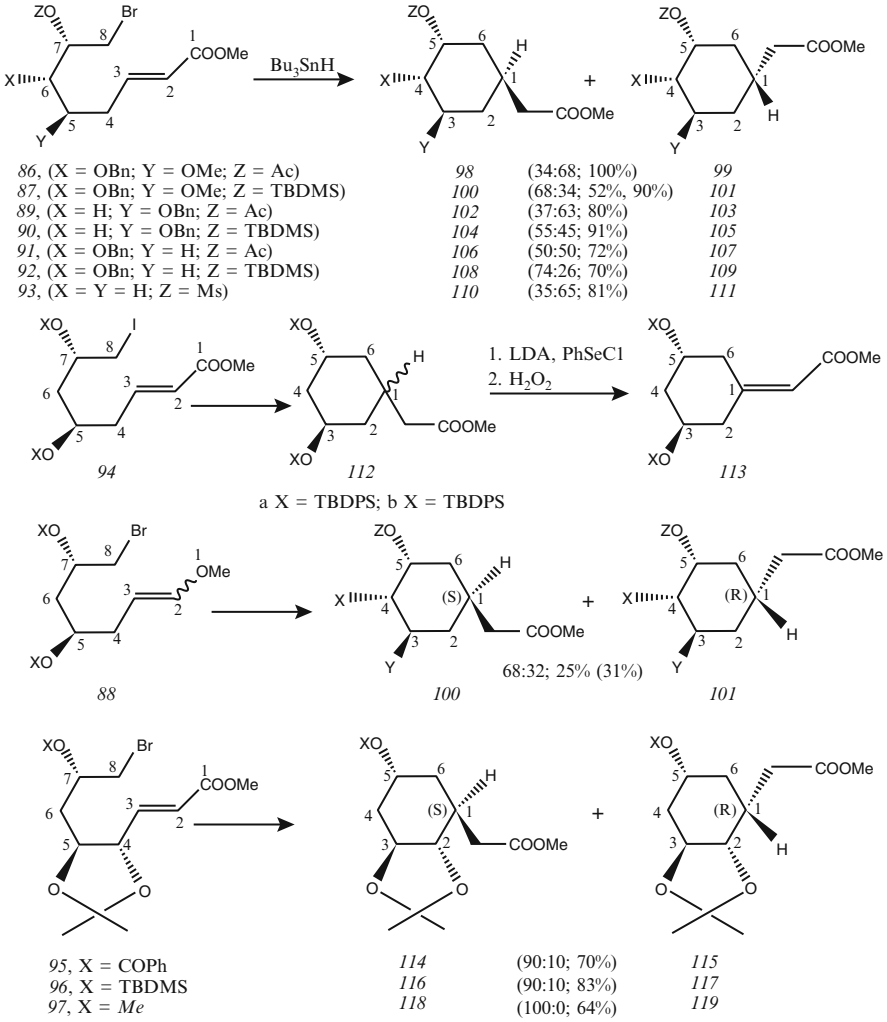

86, (X = OBn; Y = OMe; Z = Ac) *98* (34:68; 100%) *99*
87, (X = OBn; Y = OMe; Z = TBDMS) *100* (68:34; 52%, 90%) *101*
89, (X = H; Y = OBn; Z = Ac) *102* (37:63; 80%) *103*
90, (X = H; Y = OBn; Z = TBDMS) *104* (55:45; 91%) *105*
91, (X = OBn; Y = H; Z = Ac) *106* (50:50; 72%) *107*
92, (X = OBn; Y = H; Z = TBDMS) *108* (74:26; 70%) *109*
93, (X = Y = H; Z = Ms) *110* (35:65; 81%) *111*

94 *112* *113*

88 *100* *101*

95, X = COPh *114* (90:10; 70%) *115*
96, X = TBDMS *116* (90:10; 83%) *117*
97, X = *Me* *118* (100:0; 64%) *119*

Fig. 7.24

The free radical cyclizations were carried out by treatment of the precursors with tributyltin hydride and a catalytic amount of AIBN in refluxing toluene. The resulting carbocycles were obtained as mixtures of isomers (Fig. 7.24). The S/R ratios have been determined in the crude reaction mixtures by ^{1}H NMR analysis. Particularly, the assignment of absolute configuration at the new stereocenter C1 was possible by a detailed analysis of the ^{1}H NMR spectra.

The data reported in Fig. 7.24 deserve some comments: (1) in the 6-*exo* free radical cyclization of precursors *86–97*, acetyl migration was not observed [95] nor 1,5-hydrogen shifts [95]. (2) As expected, the cyclization of the enol ether *88* gave

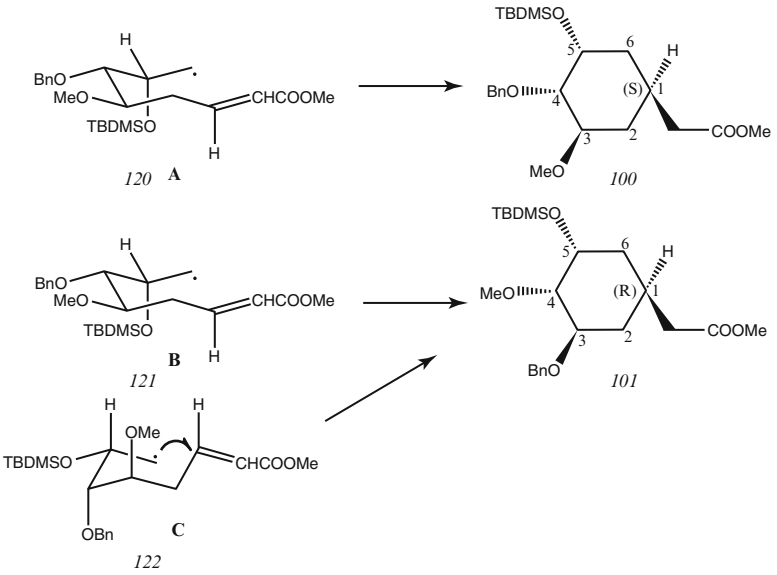

Fig. 7.25

poor yield in comparison with the analogous precursor *87* with an α, β-unsaturated ester as radical acceptor. (3) The *S*/*R* ratios are dependent upon the type of substituents in the acyclic precursor. The highest values have been observed for the conformationally restricted compounds *95–97* having an isopropylidenedioxy group at C4–C5. (4) In the cyclization of sugars *86–94*, the absolute configuration at the new stereo center (C1) depended on the nature of the substituents at C7: a *tert*-butyldimethylsilyl group (*87*, *90*, *92*, *94*) gives major C1 (S) branched-chain cyclitol, while for an acetate or mesylated (*86*, *89, 92*, *93*), a clear inversion of the stereogenic trend is observed and major C1(*R*) isomers result. (5) Cyclization of precursor *94* gave only one isomer (*112a*), a carbocycle with a C2 symmetry axis. This compound was transformed into cyclohexane *113a* by standard α-selenation and elimination [100]. Compound *113a* is related to *113b*, a product that has been used in the preparation of cyclohexane ring analogs of 1α, 25-dihydroxyvitamin D_3 [101].

The different stereogenic results obtained in the cyclization of *86* (*89, 91, 93*) or *87* (*88, 90, 92*) which differ only by the nature of the substituent at C7 were totally unexpected, and no similar stereodirecting properties have been reported in the literature.

Figures 7.25 and 7.26 are proposed as possible explanation of these facts. As reported [102], for these kinetically controlled processes, in the reactant-like transition state, the radical adopts a chair-like conformation with substituents in preferred pseudoequatorial positions. This suggests that, for instance, in precursor *87*, the conformers **B** and **C** are clearly disfavored, as the 1,3-diaxial interactions

Fig. 7.26

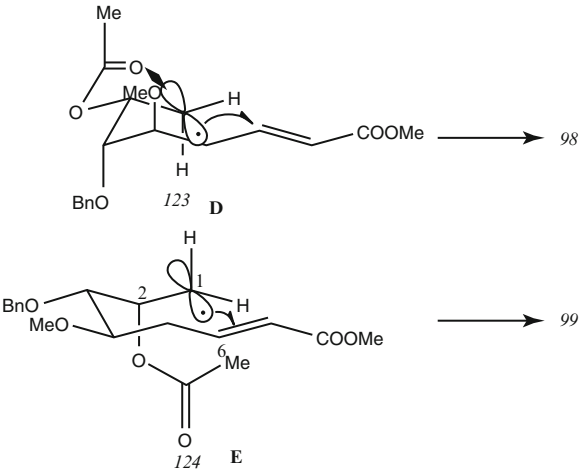

develop in the transition state; in fact, low-energy conformer **A** gives *100* as the major product (Fig. 7.25).

Precursor *86*, with the less sterically hindered acetate group at C2 (hept-6-enyl radical numbering), should also follow the same trend, but in practice the opposite isomer *98* is obtained. To explain this it was proposed that of the two transition states **D** and **E** (Fig. 7.26), **D** is of lower energy than the relatively less stable conformer **E**. This is probably due to the superior stabilizing effect that the electron-attracting acetoxy group gives to the vicinal carbon-centered radical. These effects can be interpreted in terms of stabilizing interaction between the single occupied p-orbital (SOMO) of the radical and the σ* LUMO of the vicinal bonded C–OR bond [103]. This powerful stereoelectronic effect overrides the steric repulsion due to the presence of substituents in the pseudoaxial orientation. In accordance with this, it is known that the stereoelectronic effects of the vicinal acetoxy groups in pyranoid cyclic radicals dramatically change the conformation of these species [104].

It can be concluded that the electronic nature of the substituent vicinal to the radical center has an important qualitative and quantitative effect in the formation of the new stereocenter in the 6-*exo* free radical cyclizations. The magnitude of this effect is related to the structure of the substrate.

Finally, the results presented above in the free radical cyclization of precursors *95–97* can also be rationalized in similar terms (Fig. 7.26). Major isomers have been obtained in the ring closure of carbon-centered radicals in chair-like conformations with the acceptors in preferred pseudoequatorial orientations (conformer **F**, Fig. 7.27). The 4,5-isopropylidenedioxy group restricts here the conformational mobility, and the substituent X at C2 (hept-6-enyl radical numbering), in a pseudoaxial orientation, induces 1,3-steric repulsion with the acceptor at C6 (conformer **G**, Fig. 7.27).

Fig. 7.27

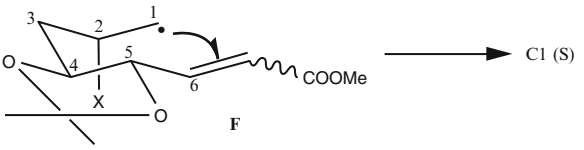

125 X =OTBDMS, OCOPH, OMe

F

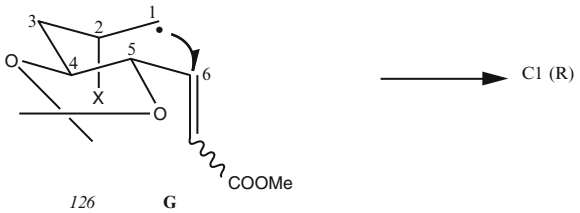

126 **G**

The good yields obtained in the cyclization of appropriate radical precursors show that this is a convenient method for the synthesis of branched-chain cyclitols from carbohydrates. In addition, an interesting stereoelectronic effect in the cyclization of these acyclic sugar derivatives is demonstrated: the stabilizing effect of electron-attracting groups vicinal to carbon-centered radicals determines the preferred conformation in the transition state and the stereochemical outcome of the reaction.

References

1. Beckwith ALJ (1981) Regioselectivity and stereoselectivity in radical reactions. Tetrahedron 37:3073–3100
2. Beckwith ALJ, Easton JC, Lawrence T, Serelis AK (1983) Reactions of methyl-substituted 5-hexenyl and 4-pentenyl radicals. Aust J Chem 36:545–556
3. Beckwith ALJ, Philipou G, Serelis AK (1981) Formation of some bicyclic systems by radical ring-closure. Tetrahedron Lett 22:2811–2814
4. Wolf S, Agosta WC (1981) Stereoselectivity in the cyclization of 2-(bet3-enyl) cyclopentyl radical. J Chem Res Synop 78–79
5. Curran DP (1988) The design and application of free radical chain reactions in organic synthesis, Parts 1 and 2. Synthesis 417–439:489–513
6. Hart DJ, Tsai Y-M (1984) α-Acylamino radical cyclizations: synthesis of isoretronecanol. J Am Chem Soc 106:8209–8217
7. Curran DP, Rakiewicz DM (1985) In: Giese B (ed) Selectivity and synthetic applications of free radical reactions. Tetrahedron Symposia-in-Print, p 3923
8. Wilcox CS, Tomasco LM (1985) New syntheses of carbocycles from carbohydrates. Cyclization of radicals derived from unsaturated halo sugars. J Org Chem 50:546–547
9. Barton DHR, McCombie SW (1975) New method for the deoxygenation of secondary alcohols. J Chem Soc Perkin Trans 1:1574–1585
10. Hoffmann RW (1989) Allylic 1, 3-strain as controlling factor in stereoselective transformations. Chem Rev 89:1841–1860

11. RajanBabu TV, Fukunaga T, Reddy GS (1989) Stereochemical control in hex-5-anyl radical cyclization: from carbohydrates to carbocycles. 3. J Am Chem Soc 111:1759–1769
12. Corey EJ, Pyne SG (1983) Conversion of ketones having δ, ε-π-functions to cyclopentanols by zinc-trimethylchlorosilane. Tetrahedron Lett 24:2821–2824
13. Pradham SK, Kolhe JN, Mistry JS (1982) Trapping of radical intermediate in reaction of sulfonates with sodium iodide/zinc/DME. Total frontier orbital control of stereoselectivity in ring closure. Tetrahedron Lett 23:4481–4484
14. RajanBabu TV, Fukunaga T (1989) Stereochemical control in hex-5-enyl radical cyclizations: axial vs equatorial 2-(1-but-3-anyl)cyclohexyl radicals. J Am Chem Soc 111:296–300
15. Clive DLJ, Beaulieu PL (1983) Formation of carbon-carbon bonds by ring closure of β-phenylselenocrotonates. J Chem Soc Chem Commun 307–309
16. Auge J, David S (1984) Hexopyranose sugars conformation revised. Tetrahedron 40:2101–2106
17. RajanBabu TV (1987) From carbohydrates to optically active carbocycles I: stereochemical control in sugar hex-5-enyl radical cyclization. J Am Chem Soc 109:609–611
18. Karabatsos GJ, Fenglio DJ (1970) Top Stereochem 5:167
19. Cha JK, Christ WJ, Kishi Y (1984) Tetrahedron 40:2247
20. Giese B (1986) Radicals in organic synthesis: formation of carbon-carbon bonds. Pergamon Press, New York
21. Choi J, Ha D, Hart DJ, Lee C, Ramesh S, Wu S (1989) α-acylamino radical cyclizations: application to the synthesis of a tetracyclic substructure of gelsemine. J Org Chem 54:279–290
22. Nugent WA, RajanBabu TV (1988) Transition-metal centered radicals in organic synthesis. Titanium (III)-induced cyclization of epoxy olefins. J Am Chem Soc 110:8561–8562
23. RajanBabu TV (1988) From carbohydrates to carbocycles. 2. A free radical route to Corey lactone and other prostanoid intermediates. J Org Chem 53:4522
24. Spellmeyer DC, Houk KN (1987) A force-field model for intramolecular radical additions. J Org Chem 52:959–974
25. Audin C, Lancelin J, Beau J (1988) Radical cyclization on carbohydrate pyranosides: a controlled formation of functionalized ring-fused bicyclic acetals. Tetrahedron Lett 29:3691–3694
26. De Mesmaeker A, Hoffmann P, Ernst B (1989) Tetrahedron Lett 30:57
27. Korth H, Sustmann R, Groninger KS, Witzel T, Giese B (1986) Electron spin resonance spectroscopic investigation of carbohydrate radicals. Part 3. Conformation in deoxypyranosan-2-, 3-, and 4-yl radicals. J Chem Soc Perkin Trans 2:1461–1464
28. De Mesmaeker A, Hoffmann P, Ernst B, Hug P, Winkler T (1989) Stereoselective carbon-carbon bond formation in carbohydrates by radical cyclization reactions. III. Strategy for the preparation of C(1)-glycosides. Tetrahedron Lett 30:6307
29. Korth H, Sustmann R, Dupuis J, Giese B (1986) Electron spin resonance spectroscopic investigation of carbohydrate radicals. Part 2. Conformation and configuration in pyranos-1-yl radicals. J Chem Soc Perkin Trans 2:1453–1459
30. Groninger KS, Jager KF, Giese B (1987) Cyclization reactions with allyl-substituted glucose derivatives. Liebigs Ann Chem 731–732
31. Hashimoto H, Furuichi K, Miwa T (1987) Cyclopentane-annelated pyranosides. A new approach to chiral iridoid synthesis. J Chem Soc Chem Commun 1002–1003
32. De Mesmaker A, Hoffmann P, Winkler T, Waldner A (1990) Stereoselective carbon-carbon bond formation in carbohydrates by radical cyclization reactions. V. Application for the synthesis of α-C(2)-branched sugars. Synlett 201–204
33. Nouguier R, Lesueur C, Riggi ED, Bertrand MP (1990) Stereoselective free-radical cyclization on sugar template: the sulfonyl radical as a synthetic tool for functionalized glycosides. Tetrahedron Lett 31:3541–3544

34. Kano S, Yuasa Y, Yokamatsu T, Asami K, Shiroshi S (1986) Effect of A-strain on synthesis of cis-fused 4a-aryloctahydro—1H-cyclopenta[c]pyridine derivatives through tandem radical cyclization of an α-acylamino-polyene system. J Chem Soc Chem Commun 1717–1718
35. Tamaru Y, Harayama H, Bando T, Nagaoka H, Yoshida Z (1996) Pronounced electronic effect of allylic amino group on the n-facial stereoselectivity and reactivity of the iodoetherification of N-substituted 3-amino-4-penten-1-ols. Liebigs Ann 223–234
36. Fujioka H, Kitagawa H, Nagatomi Y, Kita Y (1996) Asymmetric induction via an intramolecular haloetherification reaction of chiral ene acetals: a novel approach to optically active 1, 4- 1, 5-diols. J Org Chem 61:7309–7315
37. Seeperausd M, Blumenstein M, Mootoo DR (1997) Tetrahedron 16:5711
38. Marshall JA, Yanik MM (1999) Synthesis of nonracemic β-hydroxy ketones and carbonate derivatives from homopropargylic alcohols through iodolactonization. J Org Chem 64:3798–3799
39. Jordá-Gregori JM, González-Rosende ME, Sepúlveda-Arques J, Galeazzi R, Orena M (1999) Highly regio- and stereoselective iodocyclization of chiral 3-alkoxycarbonyl-4-propenyl-2, 2-dimethyl-1, 3-oxazolidines: a computational investigation. Tetrahedron Asymmetry 10:1135–1143
40. Bew SP, Barks JM, Knight DW, Middleton RJ (2000) Stereochemical features of iodocyclizations of 3-alkene-1, 2-diols to β-hydroxytetrahydrofurans. Tetrahedron Lett 41:4447–4451
41. Bravo F, Castillón S (2001) Synthesis of substituted tetrahydrofuran by electrophile-induced cyclization of 4-pentene-1, 2,3-triols- and example of 5-exo versus 5-endo cyclization governed by the electrophile. Eur J Org Chem 507–516
42. Guindon Y, Lavallée J-F, Llinas-Brunet M, Horner G, Rancourt J (1991) Stereoselective chelation-controlled reduction of α-iodo-β-alkoxy esters under radical conditions. J Am Chem Soc 113:9701–9702
43. Guindon Y, Soucy F, Yoakim C, Oglivie WW, Plamondon L (2001) Diastereoselective synthesis of 2,3,5-trisubstituted tetrahydrofurans via cyclofunctionalization reactions. Evidence of stereoelectronic effects. J Org Chem 66:8992–8996
44. Rollinson SW, Amos RA, Katzellenenbogen JA (1981) Total synthesis of lauraceae lactones: obtusilactones, litsenolides, and mahubanolides. J Am Chem Soc 103:4114–4125
45. Chamberlin AR, Dezube M, Dussault P, McMills MC (1983) Iodocyclization of allylic alcohol derivatives containing internal nucleophiles. Control of stereoselectivity by substituents in the acyclic precursors. J Am Chem Soc 105:5819–5825
46. Tamaru Y, Mizutani M, Furukawa Y, Kawamura S, Yoshida Z, Yanagi K, Minobe M (1984) 1, 3-asymmetric induction: highly stereoselective synthesis of 2,4-trans-disubstituted γ-butyrolactones and γ-butyrothiolactones. J Am Chem Soc 106:1079–1085
47. Tamaru Y, Higashimura H, Naka K, Hojo M, Yoshida Z (1985) Palladium(II)-catalyzed stereoselective dilactonization. Angew Chem 97:1070–1071
48. Ohfune Y, Kurokawa N (1985) Efficient synthesis of naturally occurring 3,4-dihydroxyprolines: electrophile-mediated lactonization of 2-amino-3-hydroxy-4-pentenoic acid derivatives. Tetrahedron Lett 26:5307–5308
49. Deslongchamps P (1983) Stereoelectronic effects in organic chemistry. Pergamon Press, Canada
50. Labelle M, Guindon Y (1989) Diastereoselective synthesis of 2, 3-disubstituted tetrahydrofuran synthons via the iodoetherification reaction. A transition state model based rationalization of the allylic asymmetric induction. J Am Chem Soc 111:2204–2210
51. Guindon Y, Slassi A, Ghiro E, Bantle G, Jung G (1992) Stereoselective silver triflate-mediated iodocyclization of carbamates. Tetrahedron Lett 33:4257–4260
52. Guindon Y, Yoakim C, Gorys V, Oglivie WW, Delorme D, Renaud J, Robinson G, Lavallée J-F, Slassi A, Jung G, Rancourt J, Durkin K, Liotta D (1994) Stereoselective hydrogen transfer reactions involving acyclic radicals. Tandem substituted tetrahydrofuran formation

and stereoselective reduction: synthesis of the C17-C22 subunit of ionomycin. J Org Chem 59:1166–1178
53. Guindon Y, Murtagh L, Caron V, Landry SR, Jung G, Bencheqroun M, Faucher A-M, Guérin B (2001) Cyclofunctionalization and free-radical-based hydrogen-transfer reaction sequence applied to the synthesis of the C7-C-16 subunit of zincophorin. J Org Chem 66:5427–5437
54. Guindon Y, Slassi A, Ghiro E, Bantle G, Jung G (1992) Tetrahedron Lett 33:4257–4260
55. Brown RS, Gedye R, Slebocka-Tilk H, Buschek JM, Kopecky KR (1984) J Am Chem Soc 106:4515
56. Slebocka-Tilk H, Ball RG, Brown RS (1985) The question of reversible formation of bromonium ions during the course of electrophilic bromination of olefins. 2. The crystal and molecular structure of the bromonium ion adamantylideneadamantane. J Am Chem Soc 107:4504–4508
57. Bellucci G, Bianchini R, Ambrosetti R (1985) Direct evidence for bromine-olefin charge transfer complexes as essential intermediates of the fast ionic addition of bromine to cyclohexene. J Am Chem Soc 107:2464–2471
58. Bellucci G, Chiappe C, Marioni F (1987) Evidence for a reversible electrophilic step in olefin bromination. The case of stilbene. J Am Chem Soc 109:515–522
59. Reitz AB, Nortey SO, Maryanoff BE, Liotta D, Monahan R III (1987) Stereoselectivity of electrophile-promoted cyclizations of γ-hydroxyalkenes. An investigation of carbohydrate-derived and model substrates. J Org Chem 52:4191–4202
60. Chamberlin AR, Mullholland RL, Kahn SD, Hehre WJ (1987) Modeling chemical reactivity. 7. The effect of a change in rate-limiting step on the stereoselectivity of electrophilic addition to allylic alcohols and related chiral alkenes. J Am Chem Soc 109:672
61. Danishefasky SJ, Larson E, Springer JP (1985) A totally synthetic route to lincosamine: some observations on the diastereofacial selectivity of electrophilic reactions on the double bonds of various 5-(1-alkenyl)arabinopyranosides. J Am Chem Soc 107:1274–1280
62. Houk KN, Moses SR, Wu Y-D, Rondan NG, Jager V, Schohe R, Fronczek FR (1984) Stereoselective nitrile oxide cycloadditions to chiral allyl ethers and alcohols. The inside alkoxy effect. J Am Chem Soc 106:3880–3882
63. Kahn SD, Pau CF, Chamberlin AR, Hehre WJ (1987) Modeling chemical reactivity. 4. Regiochemistry and stereochemistry of electrophilic additions to allylic double bonds. J Am Chem Soc 109:650–663
64. Marco-Contelles J, Martínez L, Martínez-Grau A, Jimeno ML (1991) Carbocycles from carbohydrates: a free-radical route to aminocyclitols derivatives. Tetrahedron Lett 32:6437–6440
65. Marco-Contelles J, Pozuelo C, Jimeno ML, Martínez L, Martínez-Grau A (1992) 6-Exo free radical cyclization of acyclic carbohydrate intermediates: a new synthetic route to enantiomerically pure polyhydroxylated cyclohexane derivatives. J Org Chem 57:2625–2631
66. Marco-Contelles J, Sánchez B, Pozuelo C (1992) Synthesis of branched chain cyclitols: preparation of some useful chiral building blocks. Tetrahedron Asymmetry 3:689–692
67. Marco-Contelles J, Sánchez B, Ruiz P (1992) Branched chain cyclitols: asymmetric synthesis of a 1α, 25-dihydroxy-19-norvitamin D3 A-ring synthon. Nat Prod Lett 1:167
68. Wilcox CS, Gaudino JJ (1986) New approaches to enzyme regulators. Synthesis and enzymological activity of carbocyclic analogs of D-fructofuranose and D-fructofuranose-6-phosphate. J Am Chem Soc 108:3102
69. Wilcox CS, Gaudino JJ (1990) A concise approach to enantiomerically pure carbocyclic ribose analogs. Synthesis of (4S, 5R, 6R, 7R)-7-(hydroxymethyl) spiro[2,4]heptane-4, 5, 6-triol 7-*O*-(dihydrogen phosphate). J Am Chem Soc 112:4374–4380
70. Othman AA, Al-Masudi NA, Timari US (1978) A new route to the synthesis of cyclitol derivatives. J Antibiot 31:1007–1012
71. Tsang R, Fraser-Reid B (1986) Serial radical cyclization via a vinyl group immobilized by a pyranoside. A route to bis-annulated pyranosides. J Am Chem Soc 108:2116–2117

72. Dickson JK, Tsang R, Llera JM, Fraser-Reid B (1989) Serial radical cyclization of branched carbohydrates. Part 1. Simple pyranoside diquinanes. J Org Chem 54:5350–5356
73. Yeung BWA, Contelles JLM, Fraser-Reid B (1989) A radical cyclization route to Collum's key intermediate for (+)-phyllanthocin: annulated furanoses via radical cyclizations. J Chem Soc Chem Commun 1160–1162
74. Enholm EJ, Trivellas A (1989) Samarium(II) iodide mediated transformation of carbohydrates to carbocycles. J Am Chem Soc 111:6463–6465
75. Alonso RA, Vite GD, McDevitt RE, Fraser-Reid B (1992) Radical cyclization routes to bridged pyranosides as precursors of densely functionalized cycloalkanes. J Org Chem 57:573
76. Suami T, Ogawa N, Saguro M, Rinehart KL (1976) J Am Chem Soc 98:7110
77. Semeira D, Phillippe M, Delaumeny JM, Sepulchre AM, Gero SD (1983) A general synthesis of cyclitols and aminocyclitols from carbohydrates. Synthesis 710–713
78. Knapp S, Sebastian MJ, Ramanathan K (1983) Total synthesis of (±)-deoxyfortamine. J Org Chem 48:4786–4788
79. Kuo CH, Wendler NL (1985) Total synthesis of fortamine, the aglycon of the major aminocyclitols antibiotics fortimicin A and B. Tetrahedron Lett 25:2291
80. Beier B, Schürrle K, Werbintzky O, Piepersberg W (1990) Stereoselective synthesis of (±)-cis-inos-1,3-diamines. J Chem Soc Perkin Trans 1:2255–2262
81. Paulsen H, Röben W, Heiker FR (1981) Cyclitol reactions. VI. Synthesis of enantiomerically pure conduritols and aminoconduritols. Chem Ber 114:3242–3252
82. Schubert J, Schwesinger K, Knothe L, Prinzbach H (1987) Liebigs Ann Chem 65:1443
83. Ferrier R, Stütz AE (1990) Functionalized carbocycles from carbohydrates. 11. Two routes to enantiomerically pure 3-aminoinososе derivatives. Carbohydr Res 200:237–245
84. Shing TKM, Elsley DA, Gilahouley JG (1989) A rapid entry to carbocycles from carbohydrates via intramolecular nitrone cycloaddition. J Chem Soc Chem Commun 1280–1282
85. Tatsuta K, Niwata Y, Umezawa K, Toshima K, Nakata M (1990) Enantiospecific total synthesis of a β-glucosidase inhibitor, cyclophellitol. Tetrahedron Lett 31:1171–1172
86. McIntosh MC, Weinreib SM (1991) A strategy for synthesis of conduritols and related cyclitols via stereodivergent vinylsilane-aldehyde cyclization. J Org Chem 56:5010–5012
87. Barton DHR, Gero SD, Cleophax J, Machado DS, Quiclet-Sire B (1988) Synthesis methods for the preparation of D- and L-pseudo-sugars from D-glucose. J Chem Soc Chem Commun 1184–1186
88. Blattner R, Ferrier RJ (1987) Crystalline pseudo-α-D-glucopyranose. J Chem Soc Chem Commun 1008–1009
89. Köhn W, Schmidt RR (1987) α-Glucosidase inhibitors. 5. Investigations towards a synthesis of C1-branched cyclitols from D-glucose. Liebigs Ann Chem 1045–1054
90. Ogawa S, Orihara M (1988) Pseudosugars. Part XXI. Synthesis of seven penta-*N*, *O*-acetyl-pseudo-2-amino-2-deoxy-DL-hexopyranoses. Carbohydr Res 177:199–212
91. Paulsen H, Deyn W (1987) Cyclitol reactions. XIII. Synthesis of pseudosugars from D-glucose by intramolecular Horner-Emmons olefination. Liebigs Ann Chem 125–131
92. Tadano K, Maeda H, Hoshino M, Yimura Y, Suami T (1987) A novel transformation of four aldoses to some optically pure pseudohexopyranoses and pseudopentofuranose carbocyclic analogs of hexopyranoses and pentofuranose. Synthesis of derivatives of (1S, 2S, 3R, 4S, 5S)-, (1S, 2S, 3R, 4R, 5S)-, (1R, 2R, 3R, 4R, 5S)-, (1S, 2S, 3R, 4S, 5R)-2, 3, 4, 5-tetrahydroxy-1-(hydroxymethyl)cyclohexanes and (1S, 2S, 3S,4S)-2, 3, 4-trhydroxy-1-(hydroxymethyl) cyclopentane. J Org Chem 52:1946–1956
93. Shing TKM, Tang Y (1990) A new approach to pseudo-sugars from (−)-quinic acid: facile synthesis of pseudo-β new approach to pseudo-sugars from (−)-quinic. J Chem Soc Chem Commun 748–749
94. Barton DHR, Dalko P, Gero DS (1991) Synthesis of branched-chain cyclitols using a palladium(0)-catalyzed allylic coupling reaction. Tetrahedron Lett 32:2471–2474

95. Motherwell WB, Crich D (1992) Free radical chain reactions in organic synthesis. Academic, London
96. Marco-Contelles J, Pozuelo C, Jimeno ML, Martinez-Grau A (1992) J Org Chem 57:2615
97. Batty D, Crich D, Fortt SM (1989) Synthesis of 1α, 25-dihydrovitamin D3 ring model by an acyl radical cyclization. J Chem Soc Chem Commun 1366–1368
98. RajanBabu TV (1991) Stereochemistry of intramolecular free-radical cyclization reactions. Acc Chem Res 24:139–145
99. Redlich H, Sudau W, Szardenings AK, Vollerthum R (1992) 5-Carbon analogs of sugars. I. Radical cyclization of hept-1-enitol. Carbohydr Res 226:57–78
100. Svirdov AF, Ermolenko MS, Yashunski FDV, Kochetkov NK (1983) Selenoesters in organic synthesis. 2. Synthesis of α, β-unsaturated ketones. Tetrahedron 24:4359–4362
101. Perlman KL, Swenson RE, Paaren HE, Deluca HF (1990) Novel synthesis of 19-nor vitamin D compounds. Tetrahedron Lett 32:7663–7666
102. Hanessian S, Dhanoa DS, Beaulieu PL (1987) Synthesis of carbocycles from ω-substituted α,β-unsaturated esters via radical-induced cyclizations. Can J Chem 65:1859–1866
103. Giese B (1989) Angew Chem Int Ed Engl 28:989
104. Dupuis B, Giese B, Hartung J, Leising M, Korth HG, Sustmann R (1989) J Am Chem Soc 28:989

.

Chapter 8
Carbohydrate Sulfones

8.1 Michael Additions to Vinyl Sulfones

In the course of total synthesis of maytansine *1* (Fig. 8.1), an ansa-macrocyclic lactam from *Maytenus serrata*, *M. buchananii*, etc., the heteroconjugate addition [1–3] of methyllithium to the pyranosyl heteroolefin such as *2* (Fig. 8.2) proceeded with the complete acyclic stereoselection [1]. The authors explained the high diastereoselective C–C bond formation by efficient conformational and chelational control.

Das and Pathak [4] were interested in the synthesis of amino sugars by diastereoselective addition of amines to sugar vinyl sulfones, extending thus the Michael addition of carbon nucleophiles to nitrogen nucleophiles. They studied first the addition of various primary and secondary amines to α-vinyl sulfone-modified hex-2-enopyranosides *4α* (Fig. 8.3) and found that the primary amines, such as isobutylamine and cyclohexylamine, add in a diastereoselective fashion, producing exclusively C2 equatorial (D-gluco) products (*5*) (Fig. 8.3). The secondary amines- pyrrolidine, piperidine, and morpholine- on the other hand gave a mixture of C2 isomers in which the D-gluco isomers still predominated [5]. The anomeric β-vinyl derivatives (4β) with both primary and secondary amines, such as isobutylamine-, pyrrolidine-, and morpholine – gave only D-gluco derivatives *7* [5].

On the other hand, sterically bulky *tert*-butylamine only reacted with *4β* (and not *4α*) at elevated temperature to give D-gluco derivative *7* in high yield [6]. From these reactions, the authors concluded that the directive effect of the anomeric configuration was determining to a great extent the stereochemical outcome of the reactions, but the nature of nucleophiles, e.g., sterically bulky, also played an important role.

During the synthesis of vinyl sulfone-modified hex-5-enofuranosides, Das and Pathak [4] observed that the variation of the substituent at the C3 carbon of furanoside to some extent affected the E/Z ratios of olefins. Thus, by changing

M. Miljkovic, *Electrostatic and Stereoelectronic Effects in Carbohydrate Chemistry*,
DOI 10.1007/978-1-4614-8268-0_8, © Springer Science+Business Media New York 2014

Fig. 8.1

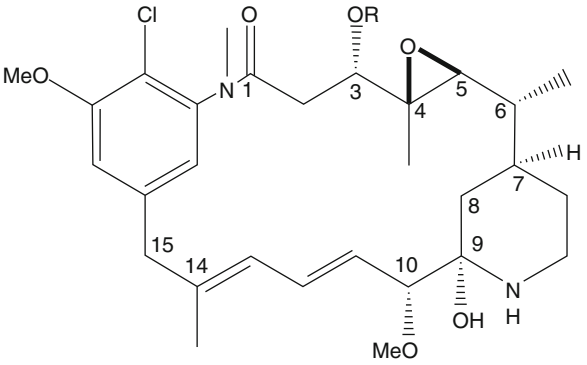

1

Fig. 8.2

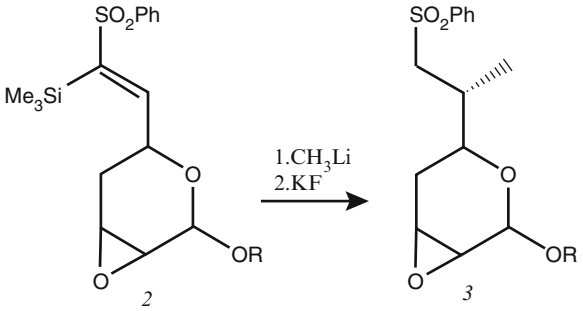

2 *3*

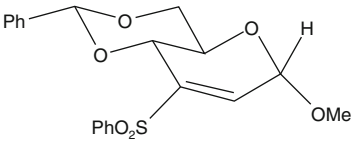

4α

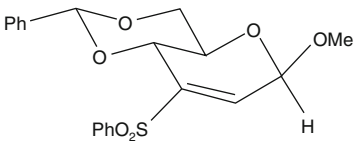

4β

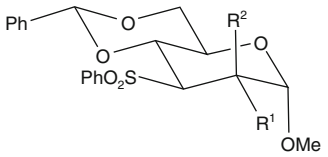

5, R^1= amine; R^2= H
6, R^1= H; R^2= amine

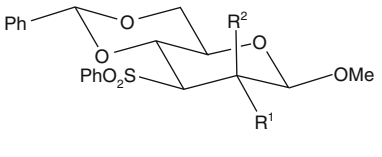

7, R^1= amine; R^2= H
8, R^1= H; R^2= amine

Fig. 8.3

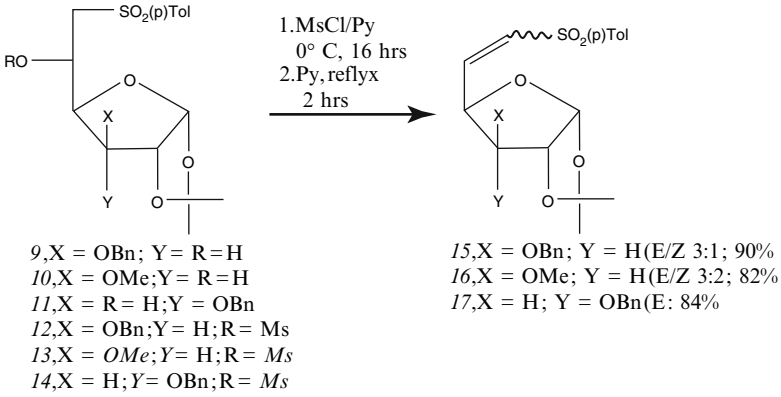

Fig. 8.4

from OBn in *12* to OMe in *13*, the E/Z ratio of olefin changed from 3:1 to 3:2; in the case of *14*, however, only the E isomer could be detected (Fig. 8.4). Since the presence of β-OBn (*12*) or β-OMe (*13*) at the C3 carbon caused the formation of the Z isomer (alongside the E isomer), as opposed to the exclusive formation of the E isomer in the case of *13*, the authors argued that the stereoselectivity of abstraction of protons from the C6 carbon during the elimination reactions of mesylated products of *12–14* (Fig. 8.4) was dictated by stereoelectronic properties of the group present at the C3 carbon on the β-face of furanosides. However, the exact cause for the loss of selectivity of abstraction of protons in the formation of *15* and *16* was not established. The observation related to the influence of C3 substituent on the E/Z ratios for *12–14* led the authors to envisage that the same structural features could also affect the diastereoselectivity of the addition of amines to the C5 of *15–17*. Thus, the 3-*O*-benzylated D-gluco derivative *15* on reaction with the neat benzyl and isopropylamines gave *18* and *19* in 1:9 ratio (yield 83 %). In both cases, the L-ido derivatives *19* were the major products. The 3-*O*-methylated D-gluco derivative *16* gave with benzyl and isopropylamine in 9:1 ratio *21* and *20* (82 % yield). Again, in both cases the L-ido derivatives *21* were the major products (Fig. 8.5).

The authors speculated that the stereoelectronic effect of OMe at C3 (compound *16*) is sufficient to impose diastereoselectivity in favor of the L-ido derivative. However, the allo derivative *17*, where the steric bulk at C3 was significantly reduced because of the presence of a hydrogen atom instead of β-OBn/OMe at the C3 carbon, showed a complete lack of the diastereoselectivity of addition when reacted with benzyl and isopropylamines. In these cases, *22* and *23* were formed in 1:1 and 3:2 ratios, respectively.

To explain the diastereoselectivity of addition of amines to *15–17*, the authors postulated the formation of an H-bonded precursor that has the geometry of a six-membered ring *24* (Fig. 8.6). This system fixes the transition state in the L-ido

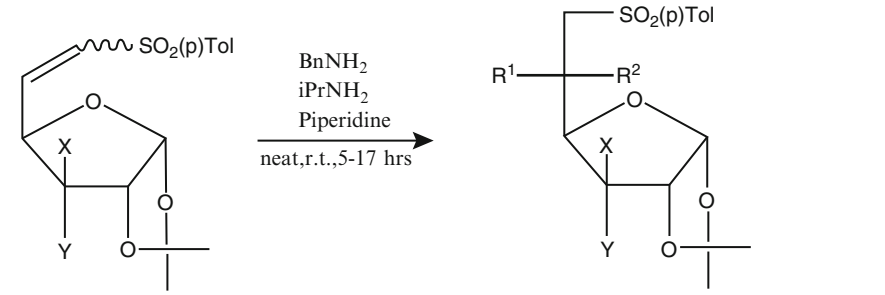

15, X = OBn; Y = H
16, X = OMe; Y = H
17, X = H; Y = OBn

18, X = OBn; R^1 = Y = H; R^2 = BnNH, iPrNH
19, X = OBn; R^1 = BnNH, iPrNH; R^2 = Y = H
20, X = OMe; R^1 = Y = H; R^2 = BnNH, iPrNH
21, X = OMe; R^1 = BnNH, iPrNH; R^2 = Y = H
22, X = R^1 = H; Y = OBn; R^2 = BnNH, iPrNH
23, X = R^2 = H; Y = OBn; R^1 = BnNH, iPrNH

Fig. 8.5

Fig. 8.6

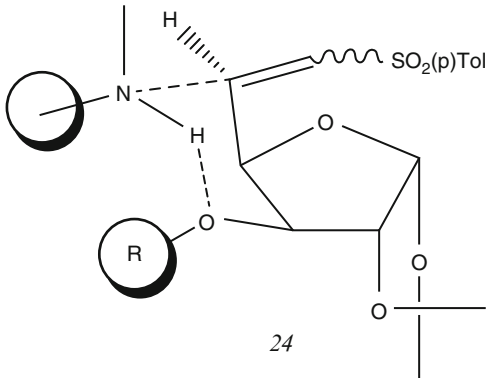

24

configuration. They argued that the stereoelectronic interactions between the R group (OBn/OMe/H) would allow the amine nucleophile to take up the position as shown in Fig. 8.6. Minimum interactions of primary amines with OBn (compound *15*) allow the amines to attack the C5 carbon in diastereoselective fashion via the H-bonded intermediate. A more severe interaction of OBn (compound *15*) with the bulky secondary amine piperidine does not allow the formation of the hydrogen-bonded intermediate, but the highly reactive piperidine reacts with *15* anyway without any selectivity.

The one stereoelectronic or perhaps electrostatic interaction that probably plays a pivotal role in the diastereoselectivity of the addition of amines to sugar vinyl sulfones is the interaction between the sulfonyl group and the ring oxygen of the furanose that fixes the conformation of the vinyl sulfone as shown in Fig. 8.7.

Fig. 8.7

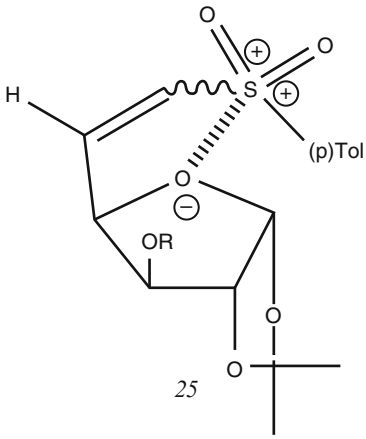

25

If so, then only the Z isomer of vinyl sulfone should react in this way since it is the only one of possible vinyl isomers that can form the above intermediate. However, this seems not to be true. If there exists a stereoelectronic interaction between the C3 and the ring oxygen nonbonding electron orbitals with the olefinic π bond that fixes the conformation of the molecule to conformers *26a* and *27a*, then hydrogen bonding between the C3 oxygen and the incoming amine will position the nitrogen, as the authors suggest, and the diastereoselectivity will be 100 %. The obtained D-gluco/L-ido ratio must then reflect the ratio of E and Z isomers in the starting reaction mixture.

The most common approaches for the synthesis of C5 branched-chain sugars are via the direct attack of carbon nucleophiles at the C5 carbon of a C5 ulose derivative such as *28* (Fig. 8.9). If the attacking carbon nucleophiles are alkyl Grignard reagents, the obtained branched-chain sugar is tertiary carbinol. However, if the attacking carbon nucleophile is alkylidene phosphorane, then the hydrogenation of the obtained olefin will give the 5-deoxy branched-chain sugar (epimeric mixture), as shown in Figs. 8.8 and 8.9.

Michael-type addition of carbon nucleophiles to electron-deficient hex-5-enofuranosyl carbohydrates *31–34* (Fig. 8.10) has been used to a limited extent for the functionalization of the C5 carbon of carbohydrates, with the compound *31* being more widely used as Michael acceptor [7].

The functionalization of an exocyclic carbon atom of the pyranose or furanose ring using vinyl sulfone-modified carbohydrate has not been explored in spite of the efficient use of vinyl sulfone-modified pyranose derivative as a Michael acceptor for the synthesis of maytansinol [1].

After an observation that carbon nucleophiles add to vinyl sulfone-modified hex-2-enopyranosides *35* and pent-2-enofuranosides *36* (Fig. 8.11) in a diastereoselective fashion to the C2 carbon of the olefinic system from a direction opposite to that of the disposition of the anomeric methoxy group [8], Das et al. [9] undertook a study of the addition of carbon nucleophiles to vinyl sulfone-modified

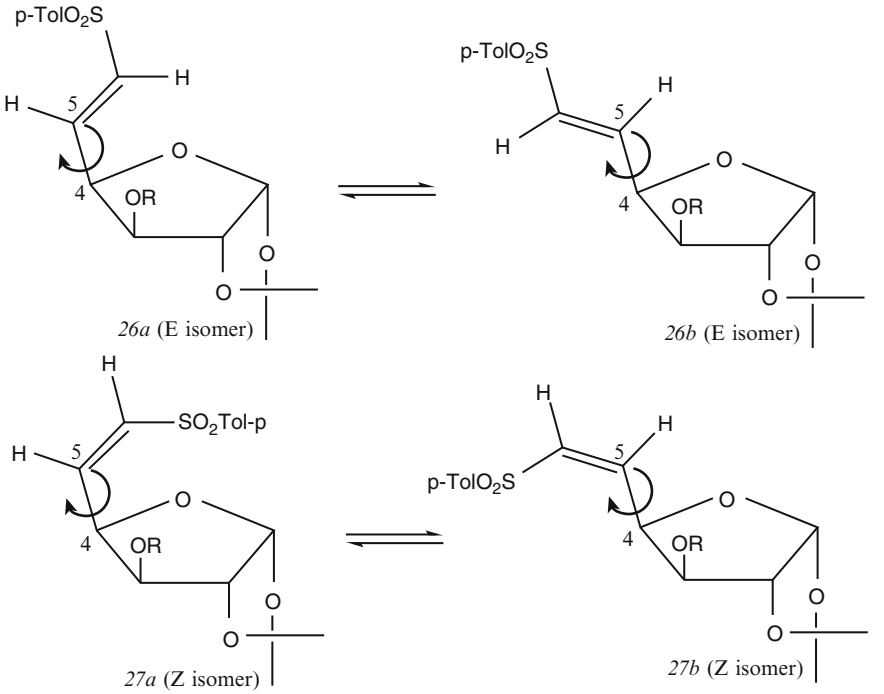

Fig. 8.8

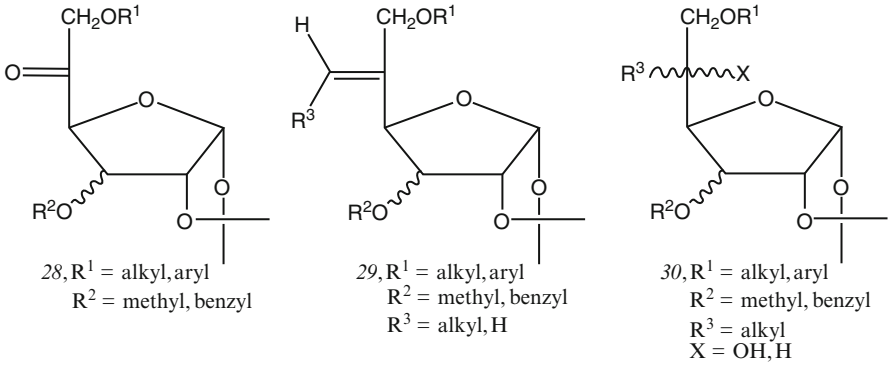

Fig. 8.9

hex-5-enofuranosides *37–39* and *40* (Fig. 8.12) as an extension of their earlier study of the addition of amines to vinyl sulfone-modified hex-5-enofuranosides which proceeded with a high stereoselectivity. Hence, they initiated a study with the carbon nucleophiles generated from nitromethane and dimethyl malonate.

Fig. 8.10

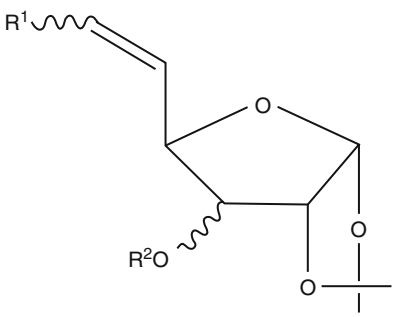

31, R^1 = CHO; R^2 = alkyl

32, R^1 = $COOR^3$, R^2 = alkyl

33, R^1 = CN; R^2 = alkyl

34, NO_2; R^2 = alkyl

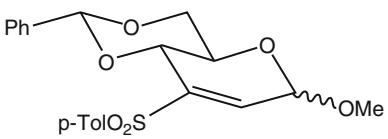

35

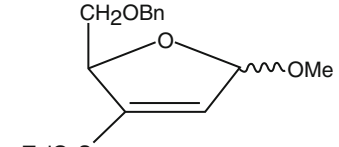

36

Fig. 8.11

Fig. 8.12

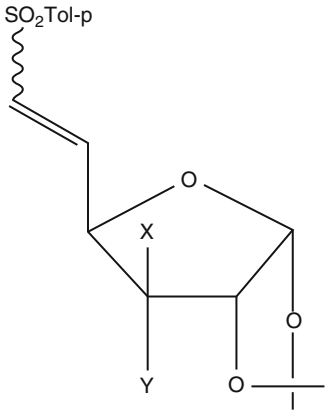

37, X = OBn; Y = H
38, X = OMe; Y = H
39, X = H; Y = OBn
40, X = OAc; Y = H

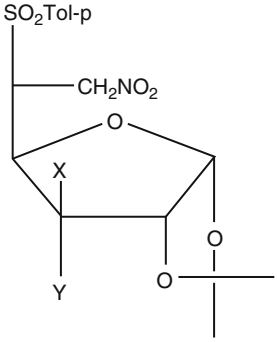

41, X = OBn; Y = H
43, X = OMe; Y = H
45, X = H; Y = OBn
47, X = OAC; Y = H

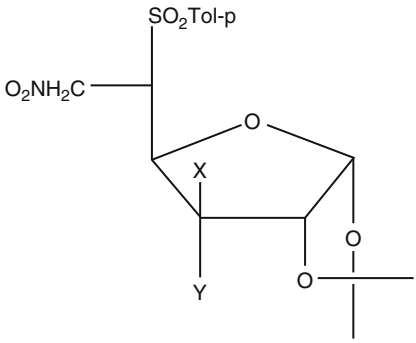

42, X = OBn; Y = H
44, X = OMe; Y = H
46, X = H; Y = OBn
48, X = OAC; Y = H

Fig. 8.13

The vinyl sulfones *37–39* and *40* were reacted with a sodium salt generated from nitromethane in 1,4-dioxane whereby mixtures of addition products were obtained, i.e., *41* and *42* (in 5.5:1 ratio; 86 % yield), *43* and *44* (in <9:<1 ratio; 89 % yield), *45* and *46* (in 1.5:1 ratio; 83 % tiled), and *47* and *48* (in 4.5:1 ratio; 79 % yield).

The authors suggested the following explanation for the observed diastereoselectivity of the Michael addition. A carbon nucleophile would be repelled by OMe group of *43* and would be forced to attack the double bond from the other side, resulting in the formation of the L-ido product preferentially (Fig. 8.13). In the case of *45*, however, the carbon nucleophile would be repelled by the ring oxygen and would attack the double bond from both sides, resulting in a loss of diastereoselectivity of addition. According to authors' opinion, the explanation for the observed loss of diastereoselectivity in the case of *45* does not seem plausible.

The same diastereoselective product formation could be expected from Michael addition to compound *40*, as was the case for *43*. However, the authors presumed that an additional factor such as the equilibrium between rotamers *50a* and *50b* would block both sides of C5, resulting in lower diastereoselectivity but still favoring the formation of L-ido isomer (Fig. 8.14). The acetyl protected *47* behaved more like *41* (Fig. 8.13) and produced mixtures of products with poorer diastereoselectivity. It should be noted that in the above discussion, the authors excluded the contribution of ring conformations to the diastereoselectivity of additions of nucleophiles to vinyl sulfones *41–45* because they presumed that the isopropylidene group would impose partial rigidity to furanose ring. Branched-chain sugars, having carbon substituents at the nonterminal carbon atoms of the carbohydrate chains, are components of many natural products, especially antibiotics [7, 10].

The most common methods for the synthesis of branched-chain sugars involve the reduction of alkylidene glycosides, opening of the sugar oxiranes by carbon nucleophiles, and the addition of organometallic reagents to glycopyranosiduloses [11].

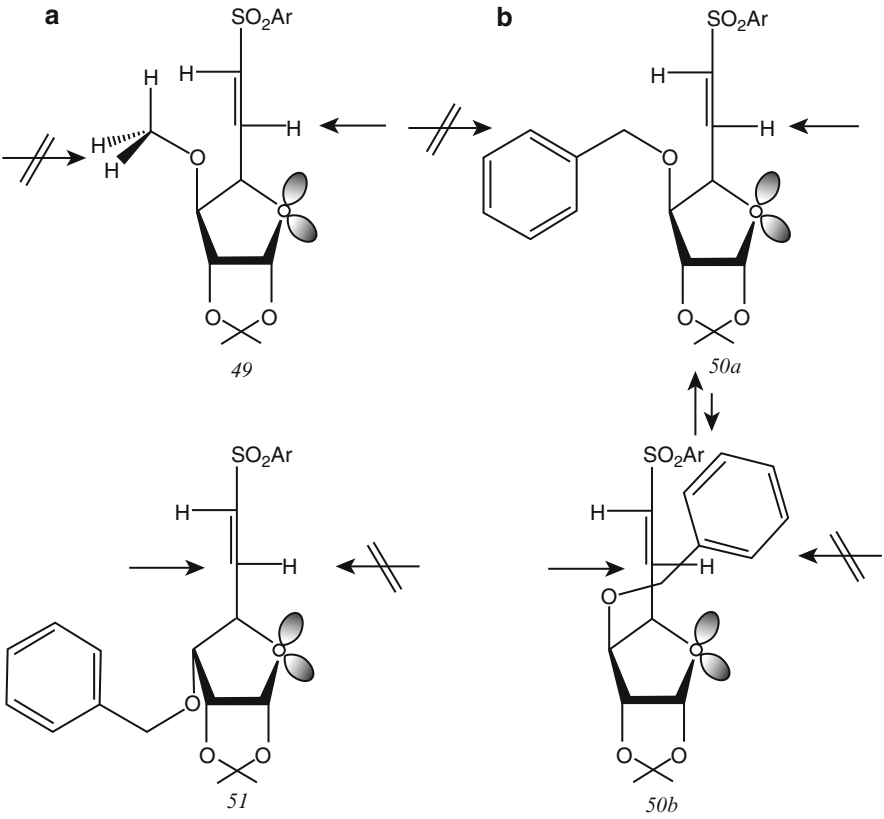

Fig. 8.14

The Michael-type addition reaction of carbon nucleophiles to vinyl sulfone-modified carbohydrates should be considered as an efficient route for the synthesis of branched-chain sugars because almost all carbohydrates in pyranose and furanose form could be converted to their vinyl sulfone derivatives very easily [5, 12–14]. Moreover, the product of the reaction carrying sulfone functionality has the potential to undergo a wide variety of transformations [15]. For a review on desulfonylation reaction, see Ref. [16].

It was reported that a nucleophile attacked the C2′ position of the 2′-enesulfone nucleoside exclusively from the α-face of the pent-2′-enofuranosyl moiety of a β-nucleoside [17, 18]. This observation led to a study of the effect of the anomeric configuration on the stereochemical outcome of the addition of nucleophiles to vinyl sulfone-modified carbohydrates (Fig. 8.15).

Thus, Sanki et al. [19] reported that 1α- and 1β-anomers of a carbohydrate reacted with carbon nucleophiles highly stereoselectively, demonstrating the

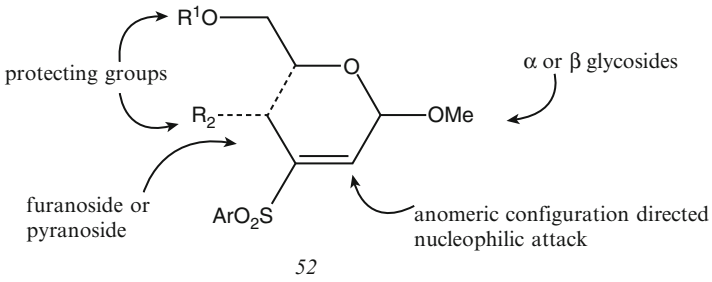

52

Fig. 8.15

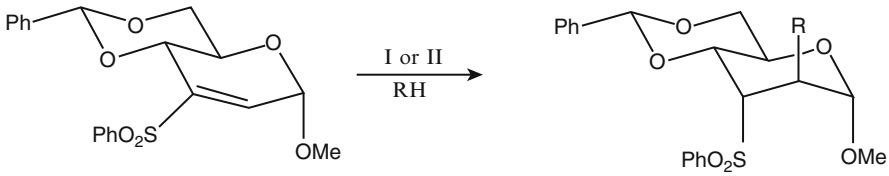

53

54, R = Ch_2NO_2
55, R = $CH(COOCH_3)_2$

I = CH_3NO_2, NaOMe, MeOH, rt., 36 hrs, 60
II = $CH_2(COOCH_3)_2$, NaH, THF, rt., 1.5 hr., 82%

Fig. 8.16

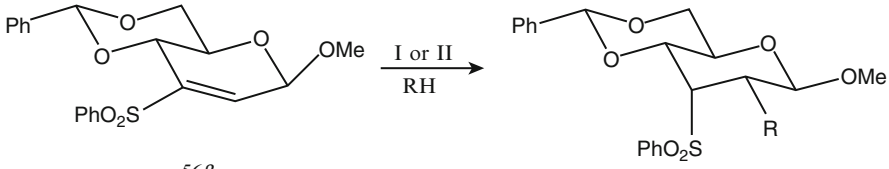

56β

57, R = Ch_2NO_2 *58*, R = $CH(COOCH_3)_2$

I = CH_3NO_2, NaOMe, MeOH, rt., 2 hrs., 56%
II = $CH_2(COOCH_3)_2$, NaH, THF, rt., 2 hrs, 98%

Fig. 8.17

directing effect of the anomeric configuration. In both cases, the carbanion added to the planar olefinic bond to 1α and 1β from a direction opposite of that of the disposition of the anomeric methoxy group (Fig. 8.15).

Thus, the nucleophile generated from CH_3NO_2 and NaOMe reacted with *53α* to produce a single isomer *54* in 60 % yield (Fig. 8.16). The nucleophile generated-from dimethyl malonate and sodium hydride produced exclusively *55* in 82 % yield.

The nucleophile generated from CH_3NO_2 and NaOMe reacted with *56β* to produce single isomer *57* in 56 % yield. The nucleophile generated from dimethyl malonate and sodium hydride produced *58* in 98 % yield. The configuration of the products was established by X-ray crystallography (Figs. 8.17 and 8.18).

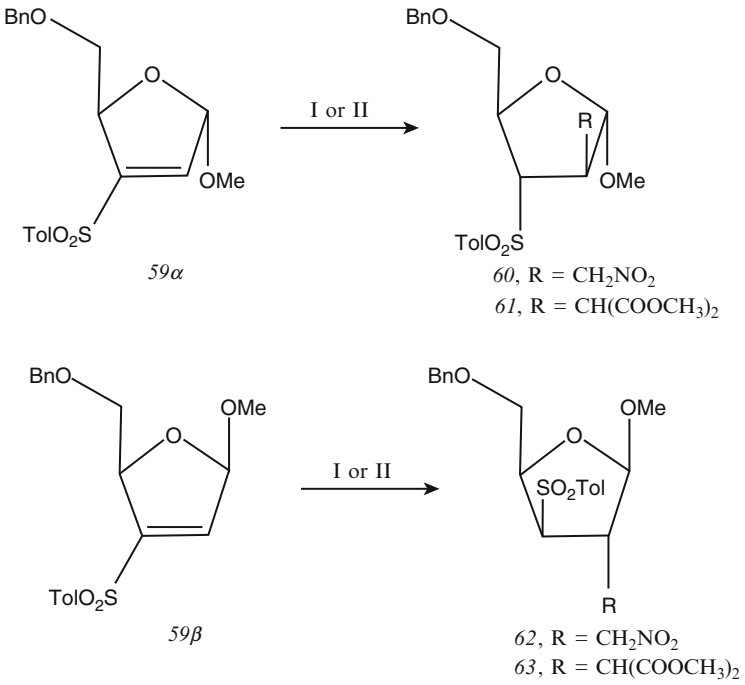

Fig. 8.18

In order to establish the general pattern directing effect of the anomeric configurations, anomeric pure pentofuranoses *59α* and *59β* were synthesized and subjected to reaction with carbanions generated from CH_3NO_2/NaOMe or CH_3NO_2/*t*-BuO^-K^+, and $CH_2(COOCH_3)_2$/NaH [20]. The 2-enesulfonyl furanoside *59α* gave branched-chain sugars *60* and *61* in 73 % and 55 % yield, respectively, whereas the 2-enesulfonyl furanoside *59β* gave adducts *62* and *63* in 74 % and 87 % yield, respectively.

8.2 Glycosyl Sulfones

Chen et al. [21] have studied the Bamberg-Bäcklund reaction on carbohydrate anomeric sulfones and observed that the α-β ratio of unreacted sulfones *64α* and *64β* recovered from the basic reaction mixture was not the same as the starting ratio with the amount of α-anomer enhanced (Fig. 8.19).

This observation could be explained in two ways: (1) the β-isomer was reactive, whereas the α-isomer was not, and (2) the β-isomer was isomerizing to the α-isomer.

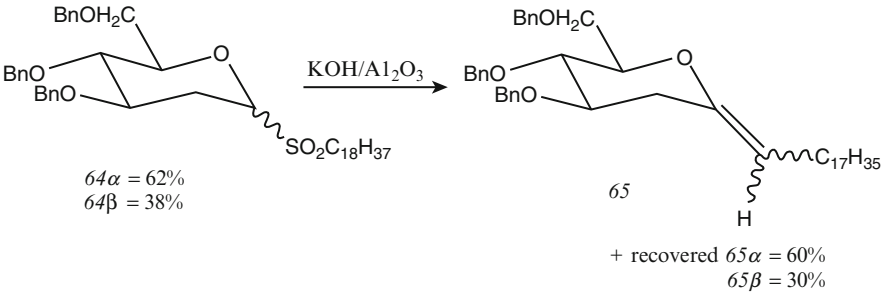

Fig. 8.19

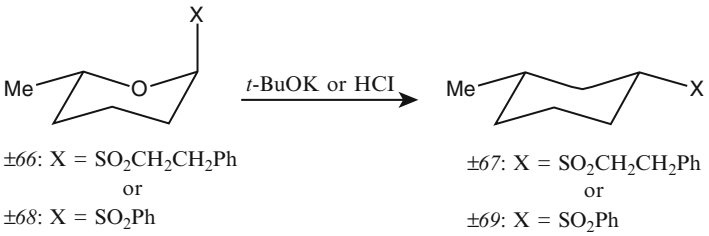

Fig. 8.20

Table 8.1 Base-catalyzed isomerization of sulfones

Starting material	T (°C)	Time	Ratio (*trans*/*cis*)	ΔG° kcal/mol
(±) *64*	85	20 h	1:2.52	−0.658
		5 d	1:2.34	−0.605
(±) *69*	85	20 h	1:5.65[a]	–
		5 d	1:2.52	−0.658
(±) *67*	75	5 d	Only *cis*-isomer[b]	–
(±)*66*/(±)*67* (1:1.32)	75	5 d	1:1.28[b]	–

[a]No equilibrium obtained
[b]No obvious isomerization detected

These two explanations were easily verified. When pure α-isomer *64α* was subjected to the Bamberg-Bäcklund conditions, no reaction was observed, consistent with the first explanation; however, when pure β-isomer *64β* was subjected to the same conditions, the α-isomer was recovered together with Bamberg-Bäcklund product *65*. These reaction conditions were not in equilibrium. The sulfones were, therefore, equilibrated with *t*-BuOK-benzene with no brominating agent present. The equilibrium ratio of β-α in both directions was 57:43. This corresponds to an apparent A-value of 0.167 kcal/mol for dodecyl sulfone group. Simpler tetrahydropyranyl phenyl sulfones *66–69* (Fig. 8.20) gave similar results (Table 8.1), although a different *A*-value was recorded, presumably due to the absence

Table 8.2 Acid-catalyzed sulfone isomerizations

Starting material	T (°C)	Time	Ratio (trans/cis)	ΔG° kcal/mol
(±) *66*	4[a]	7 w	1:3.84	0.741
(±) *66*/(±) *67* (1:1.32)	rt[b]	2 w	1:3.62	0.762
(±) *68*	4[c]	3 w	1:1.27[d]	–
(±) *68*	rt[e]	2 w	1:3.18	0.685
(±) *68*/(±) *69* (1:2.52)	rt[f]	2 d	1:3.15	0.679

[a]$CDCl_3$ (0.5 mL)
[b]$CDCl_3$ (1 mL), TMSCl (1.5 μL), *t*-BuOH (2 μL)
[c]$CDCl_3$ (0.5 mL)
[d]No equilibrium obtained
[e]$CDCl_3$ (1 mL), TMDCl (1.5 μL), *t*-BuOH (2 μL)
[f]$CDCl_3$ (1 mL), TMDCl (12.5 μL), *t*-BuOH (10 μL)

of electronegative substituents found in *64α* and *64β*. Tetrahydropyranyl phenethyl sulfones *66* and *67* failed to equilibrate under basic conditions. It was assumed that proton exchange was not occurring at the anomeric carbon but at the α′-carbon of the phenethyl group. The acid-catalyzed equilibration (Table 8.2) of phenethyl and phenyl sulfones however gave similar *A*-values, and in the former case, the acid- and base-catalyzed isomer ratios were in good agreement.

The evaluation of an anomeric effect for a substituent group requires a comparison of the apparent size of the group in an axial position in cyclohexane (where there can be no effect) to its apparent size in tetrahydropyran where an effect may exist. The *A*-value for CH_3 group in cyclohexane is 1.8 kcal/mol, while that for SO_2CH_3 is 2.5 kcal/mol [22]. Thus, in cyclohexane, sulfone is larger than methyl by 0.7 kcal/mol. From the equilibration and conformational data of the simple methyl tetrahydropyranyl sulfones, it appears that the sulfone is smaller than the methyl group. It was estimated [22] that the apparent A-value for the sulfonyl group is 0.7 kcal/mol. Assuming that the sulfone *A*-value in tetrahydropyran, in the absence of the anomeric effect, should be equal to 2.5 kcal/mol (the same as cyclohexane value), then the anomeric effect for the sulfone is $2.5_{\text{predicted}} - 0.7_{\text{observed}} = 1.8$ kcal/mol. It is known, however, that the apparent size of axial groups in tetrahydropyran is larger than in cyclohexanes. A correction of 1.5 was proposed for converting a cyclohexane value to that of tetrahydropyran. This factor has been derived by comparison of the *A*-value of CH_3 (1.8) in cyclohexane to that of 2.7 at C2 in tetrahydropyran [23, 24]. Hence, the sulfone *A*-value could be as high as $2.5 \times 1.5 = 3.75$ kcal/mol, which leads to an anomeric effect of $3.75_{\text{predicted}} - 0.7_{\text{observed}} = 3.05$ kcal/mol. In either case, the anomeric effect in favor of an axial sulfone is approximately 70 % of the steric effect, favoring the equatorial conformer. Hence, in the parent phenylsulfonyl tetrahydropyran itself, the group will appear to be equatorial. This is a different situation from that of the oxygen anomeric effect, which, although a smaller force, overrides an equivalent or somewhat smaller steric effect. It is therefore possible to detect significant amounts of axial anomeric oxygen species in the parent tetrahydropyran under equilibrium conditions.

Fig. 8.21

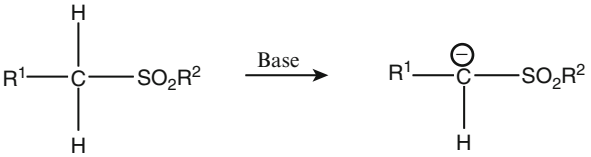

70 *71*

Fig. 8.22

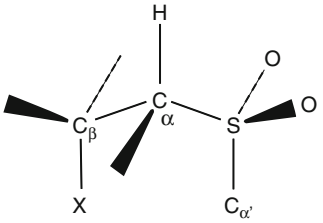

72

It is well known that the ease of formation of an α-sulfonyl carbanion (*71* in Fig. 8.21) depends upon the orientation of the bond being cleaved to yield carbanion [25], with the readiest deprotonations being observed when the C–H bond is as shown in *72* (Fig. 8.22), i.e. aligned with the internal bisector of the O-S-O angle, or equivalently, antiperiplanar to the S–$C_{\alpha'}$ bond. The stereoelectronic control exerted by the sulfonyl group enabled King et al. [26] to find out if any related geometry-dependent factors operate at adjacent carbon centers. The authors have looked at the effect of the geometry of an alkoxy group β to the sulfonyl function as in *72* (Fig. 8.22) (X = OR) and found that the orientation of the alkoxy group with respect to the C-H bond significantly affects the ease of α-sulfonyl carbanion formation, and have suggested that this observation may provide insight into the nature of the polar effect (see Table 8.3).

In NaOD in D_2O at 20 °C, the equatorial hydrogen on C3 of *74* exchanges readily, with first-order dependence on [OH^-]. From the similarly determined rate constants for the exchange of the α-hydrogen in a series of six-membered cyclic sulfones as shown in Table 8.3, it is evident that the α-equatorial hydrogen exchanges faster than the axial, the rate difference in *74*, *76*, *78*, and *79* being, respectively, 200, >25, 90, and ≥80. This result, although surprising in the light of an earlier report [27] that indicated only a small preference for equatorial exchange, is, in fact, precisely what is expected on the basis of (a) the antiperiplanar orientation of the α-equatorial hydrogens with respect to S–$C_{\alpha'}$ bond and (b) the comparative difficulty for the (normally) α-axial hydrogens to achieve this arrangement, e.g., via the twist-boat form. The authors have concluded that in exchange reactions for the other sulfones (*75*, *77*, and *80*), which have two identical chair forms, the rate constants reflect the ease of exchange of α-equatorial hydrogens in the different structures.

Table 8.3 Rate constants for H–D exchange of α-hydrogens in six-membered cyclic sulfones[a]

Compound	Reaction	k_{exch} ($M^{-1}s^{-1}$)
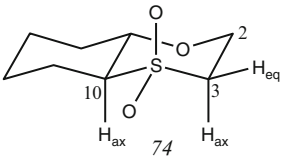 *74*	$C_3\text{-}H_{eq} \rightarrow C_3\text{-}D_{eq}$ $C_3H_{ax} \rightarrow C_3\text{-}D_{ax}$ $C_{10}\text{-}H_{ax} \rightarrow C_{10}\text{-}D_{ax}$	3.2×10^{-2} 1.6×10^{-4} $< 3 \times 10^{-8}$
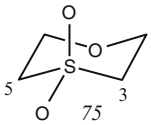 *75*	$(C_3\text{-}H_2 + C_5\text{-}H_2) \rightarrow (C_3D_2 + C_5\text{-}D_2)$	2.15×10^{-2}
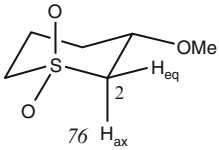 *76*	$C_2\text{-}H_{eq}) \rightarrow C_2D_2$	4.5×10^{-4}
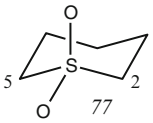 *77*	$(C_2H_2 + C_6\text{-}H_2) \rightarrow (C_2D_2, C_6\text{-}D_2)$	ca. 10^{-6} (ca. 2×10^{-6})
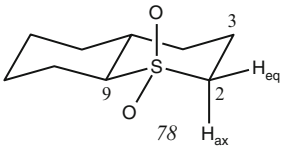 *78*	$C_2\text{-}H_{eq} \rightarrow C_2\text{-}D_{eq}$ $C_2\text{-}H_{ax} \rightarrow C_2\text{-}D_{ax}$	1.2×10^{-6} est. ca. 10^{-8}
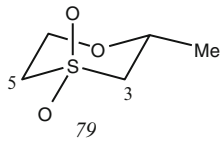 *79*	$C_3\text{-}H_{eq} \rightarrow C_3D_{eq}$ $C_5\text{-}H_{eq} \rightarrow C_5\text{-}D_{eq}$ $(C_3\text{-}H_{ax} + C_5\text{-}H_{ax}) \rightarrow (C_3\text{-}D_{ax} + C_5\text{-}D_{ax})$	1.6×10^{-2} 2.3×10^{-2} ca. 2×10^{-4}
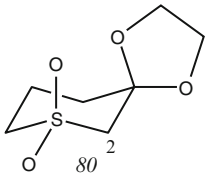 *80*	$C_2H_2 \rightarrow C_2\text{-}D_2$	4.8×10^{-3} (9.6×10^{-3})

[a]From Ref. [26]

Comparison of these rates in *76*, *77*, and *78* shows that the presence of a β-synclinal oxygen atom accelerates the reaction by a factor of >200; another synclinal oxygen on the same carbon, as in *80*, leads to a further 20-fold rate increase. An antiperiplanar oxygen, however, as in *74* and *75* increases the rate more than 10^4 times relative to *77* and *78*. Alternatively, if *74* and *75* are compared with *76*, changing of the oxygen atom from the synclinal to the antiperiplanar orientation increases the rate by 71- and 95-fold. That this

Fig. 8.23

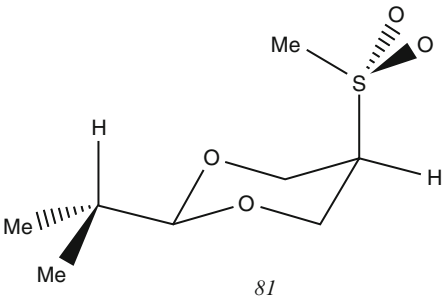

81

substantial rate difference is not primarily due to a simple steric effects or the presence of an extra β-carbon is shown by examining the rates of exchange in *79*; the rate of exchange at the C3 carbon and that at either the C5 or those of the corresponding reactions in *74* and *75* differ by less than a factor of three, showing that neither steric nor electronic effect of the methyl group is of significance in this case. From this, it can be concluded that the important factor in the rapid exchange of the α-equatorial hydrogens in *74* and *75* relative to *76* (and *80*) is the orientation of the hydrogen with respect to the oxygen – specifically, the antiperiplanar geometry in *74* and *75*.

This conclusion suggested that the sulfone *81* (Fig. 8.23) (which has been shown [28] to have the conformation as drawn) would be expected to be well-arranged for the exchange of the α-sulfonyl methine hydrogen; it was found that the exchange in *81* occurs almost 200 times faster than that in *75* (on a per hydrogen basis) [28].

To explain these results, the authors suggest that the incipient carbanion in the transition state is stabilized by donation of its electrons into the carbon-oxygen σ* orbital, i.e., that it is a "kinetic anomeric effect" [29]. A related anomeric stabilization of a sulfonyl carbanion was proposed by Padwa and Wanamaker [30] to explain a strong preference for a syn-periplanar arrangement in methoxy-substituted cyclopropyl carbanion.

The observations reported show the existence of a geometry-dependent substituent effect that an electron pair (incipient or fully formed) is stabilized by antiperiplanar oxygen much more than by clinal oxygen. These observations are not satisfactorily accounted for by the conventional components of the polar effect, i.e., the inductive and field effects [31], and it was concluded that the polar effect of the oxygen atom in these reactions has a stereoelectronic component as well.

8.3 Strecker Reaction

Strecker synthesis [32] is the preparation of α-amino nitriles in one step by treatment of aldehydes or ketones with NaCN and NH_4Cl. It is a special case of the Mannich reaction. Since the CN is easily hydrolyzed to the acid, this is a convenient method for the preparation of α-amino acids. There are two possible

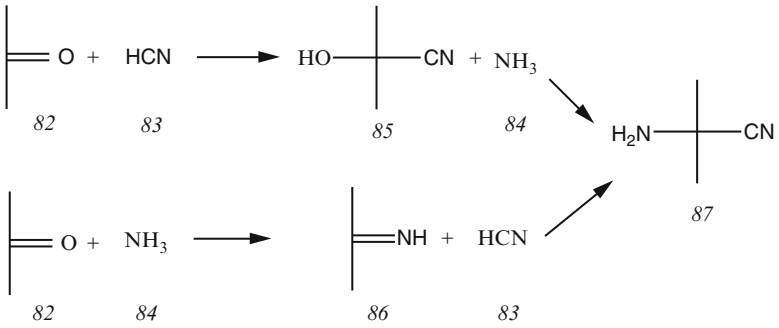

Fig. 8.24

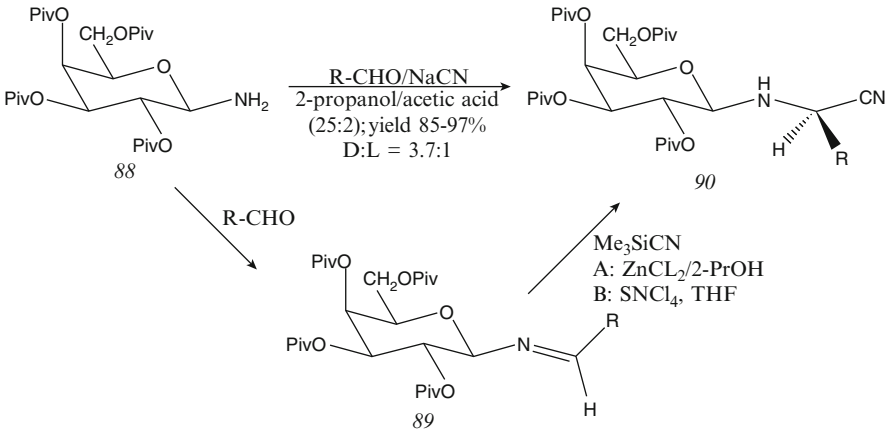

Fig. 8.25

pathways for this reaction. The cyanohydrin may be produced first, and a nucleophilic substitution of an unusually labile hydroxyl group in the α-position to nitrile can be easily effected with ammonia (ammonium chloride), resulting in α-amino nitrile, or ammonia (or the amine) may be added first to the carbonyl group to give an imine to which NaCN is added (Fig. 8.24). Hydrolysis of the nitrile group with a mineral acid to the carboxylic group will finally give the D,L-α-amino acid.

In 1991, Kunz et al. [33] used the 2,3,4,6-tetra-*O*-pivaloyl-β-D-galactopyranosylamine *87* (Fig. 8.25) as the stereodifferentiating template in the asymmetric synthesis of *N*-galactosyl D-α-amino nitriles via the Strecker reaction.

For the synthesis of the 2,3,4,6-tetra-*O*-pivaloyl-β-D-galactopyranosylamine *88* as the chiral template in the asymmetric Strecker synthesis [34], pivaloylated galactopyranosyl fluoride *92* [35] was activated with BF_3-etherate and then reacted with trimethylsilyl azide [36] to give D-galactopyranosyl azide *93* (Fig. 8.26) with a surprising preponderance of the α-anomer. If the reaction was carried out with $SnCl_4$

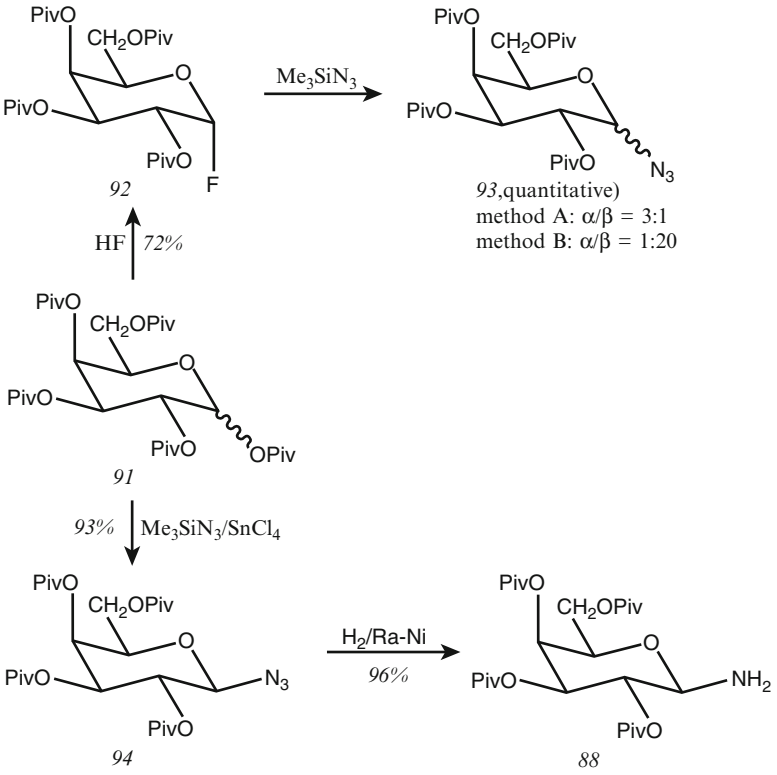

Fig. 8.26

in tetrahydrofuran, the desired β-galactopyranosyl azide *94* was preferably formed, whereby the ratio of the anomers β/α was found to be 20:1. The anomers were separated chromatographically. A selective synthesis of *88* was accomplished by reaction of the penta-*O*-pivaloyl-D-galactopyranose *91* with $SNCl_4$/trimethylsilyl azide according to a procedure described for the synthesis of peracetylated monosaccharides [37].

The pure β-anomeric galactopyranosyl azide *94* was hydrogenated using Raney nickel as the catalyst to give *O*-pivaloylated D-galactopyranosylamine *88* in almost quantitative yield (Fig. 8.26). The obtained β-D-galactopyranosylamine *88* was allowed to react with aldehydes and NaCN in 2-propanol/acetic acid (25:2) (Fig. 5.25). The *N*-galactopyranosyl α-amino nitriles *90* were obtained in almost quantitative yield. However, the completion of the reaction required 2–4 weeks. The diastereoselectivity in these Strecker syntheses ranged from 3:1 to 7:1 in favor of the D-amino nitrile derivative (Fig. 8.25).

The reaction of the β-D-*N*-galactopyranosylamine *88* with trimethylsilyl cyanide (Fig. 8.25) required activation by Lewis acids [38]. The best results were obtained if zinc chloride in 2-propanol at 0 °C (method A) or tin tetrachloride ($SNCl_4$) in

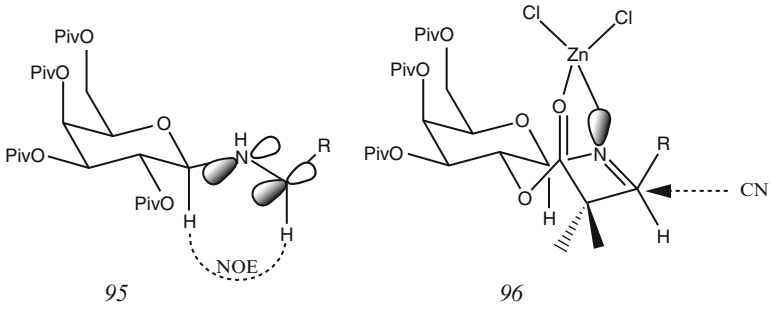

Fig. 8.27

tetrahydrofuran at −30 °C (method B) were used. With 2 mol-% of the Lewis acid, the conversions were complete after 8–12 h. If equimolar or slightly higher amounts of the Lewis acid were added at room temperature, the reactions were completed within a few minutes. The ratios of stereoisomers ranged between 6 and 13:1 with preponderance of the D-nitrile derivatives.

As a rule, the reaction at lower temperature catalyzed by $SnCl_4$ (method B) showed the higher stereoselectivity. Besides small amounts of the starting imine *89*, the crude products *90* only contained a few percent of the corresponding α-anomeric amino nitriles presumably produced by a Lewis acid-catalyzed anomerization of the β-anomeric amino nitriles *90*.

The rationalization of the observed stereoselection during the Strecker reaction (Fig. 8.27) was based upon the NMR experiments on aldimine of galactosamine *95*. A strong NOE between the aldimine and the anomeric proton showed that the Schiff bases *89* prefer a conformation illustrated in formula *95* (Fig. 8.27). Conformation *95* is obviously stabilized by a $\pi \rightarrow \sigma^*$ delocalization of the π electrons of the C═N bond into the σ* orbital of the ring C–O bond. The resulting partial double bond character of the C–N bond at the anomeric center and the population of the σ* orbital of the ring C–O bond account for the increased tendency of the Schiff bases *94* to undergo anomerization.

Due to the arrangement of the polar functions at the carbohydrate framework, the activating catalyst $ZnCl_2$ is obviously fixed to the front side (*95* in Fig. 8.27) coordinating the imine nitrogen and the carbonyl oxygen of the 2-pivaloyl group. Therefore, the ^{1}H-NMR spectrum of the complex *96* in [D_8] tetrahydrofuran is nearly unchanged in comparison to that of the corresponding Schiff base *95*. This complex *96* is preferably attacked by the free cyanide, liberated in the polar medium from its silyl derivative, at the sterically less hindered back side (*96* in Fig. 8.27), i.e., the *Si* side of the imine [39]. $SnCl_4$ presumably forms octahedral complexes, which exhibits analogous asymmetric shielding of the diastereotopic faces of the imines. In tetrahydrofuran solution, the diastereodifferentiating effect of this Lewis acid may be similar to the one observed in the formation of homoallylamines from aldimines [40].

8.4 Mercuration of Carbohydrate Olefins

A convenient procedure for converting carbohydrate derivatives into cyclohexanone analogs (as illustrated in Fig. 8.28) was first observed when the unsaturated sugar *97* was treated in refluxing aqueous acetone with a molar equivalent of mercury (II) chloride [41].

This procedure introduced by Ferrier, involving the mercury salt-mediated ring transformation of 6-deoxyhex-5-enopyranosides into deoxyinososes, has provided a route of wide practical utilization in the field of aminocyclitols [42–46] and pseudo-sugar chemistry [47, 48]. This procedure has led to the preparation [49] of the B-A ring system of the antibiotic b-rhodomycin and has extended [50] to thioglycoside analogs of hex-5-enopyranosides (Fig. 8.29).

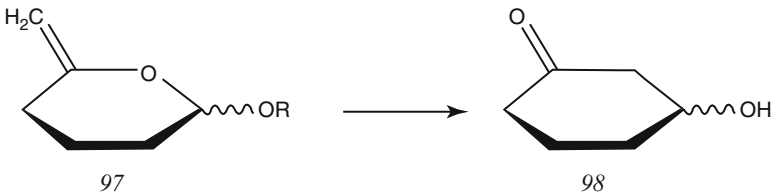

97 *98*

Fig. 8.28

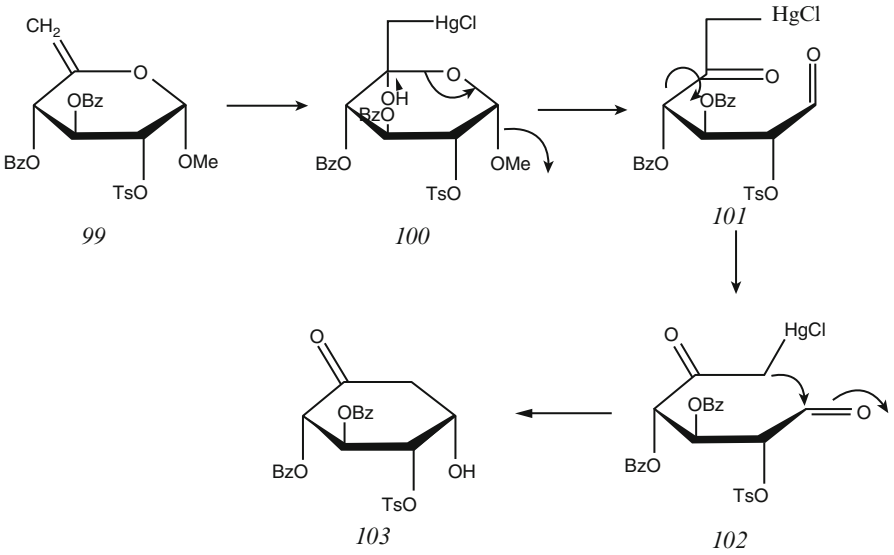

99 *100* *101* *102* *103*

Fig. 8.29

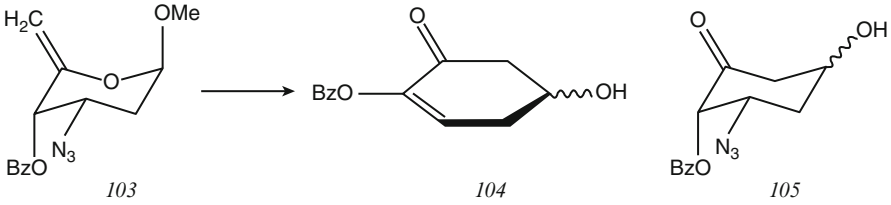

Fig. 8.30

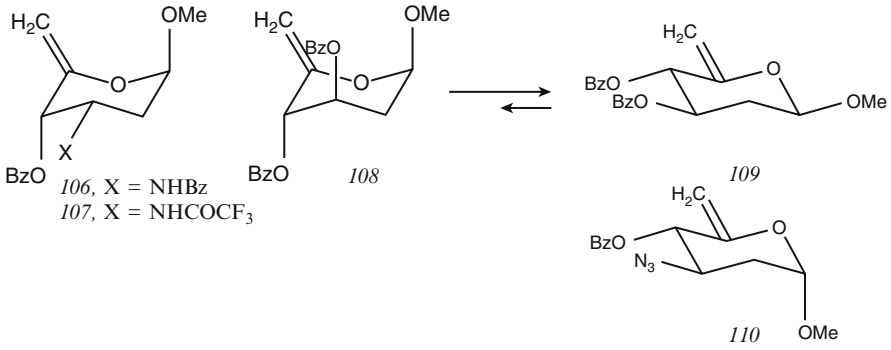

Fig. 8.31

László et al. [51] have treated methyl 3-azido-4-*O*-benzoyl-2,3,6-trideoxy-β-D-*erythro*-hex-5-enopyranoside *103* with an equimolar amount of mercuric chloride in refluxing aqueous acetone [41] and obtained in 78 % yield the crystalline 2-benzoyloxy-5-hydroxycyclohex-2-enone *104* instead of the expected 3-azidocyclohexanone *105* (Fig. 8.30).

The cyclohex-2-enone derivative *104* is a product of the β-elimination process accompanying the ring-closure reaction [45, 52–54], and apparently being favored by the *trans*-relationship of N_3(3) and H(2) in *103*. A similar elimination involving the loss of BzO(3) of methyl 2,3,4-tri-*O*-benzoyl-6-deoxy-α-D-ribo-hex-5-enopyranoside has been reported [55]. Neither the 3-acylamino-β-D-*erythro*-hex-5-enopyranosides *106* and *107* nor the 3,4-di-*O*-benzoyl-β- (*108*) and 3-azido-α-D-threo (*109*) derivatives gave elimination products (Fig. 8.31). Thus, the Ferrier reaction of these compounds gave high yields of (2S, 3S, 5S)-3-benzamido-2-benzoyloxy-5-hydroxycyclohexanone (*111*), (2S, 3S, 5S)-2-benzoyloxy-5-hydroxy-3-trifluoroacetamidocyclohexanone (*112*), (2S, 3R, 5R)-di-2, 3-dibenzoyloxy-5-hydroxycyclohexanone (*113*), and (2S, 3R, 5R)-3-azido-2-benzoyloxy-5-hydroxycyclohexanone (*114*), respectively (Fig. 8.32).

This and previous results are in accord with the finding of Lukacs et al. [55, 56] that an apparent relationship between the stereochemistry at the C5 carbon of the cyclohexanone derivatives produced in the Ferrier reaction and the conformation of

Fig. 8.32

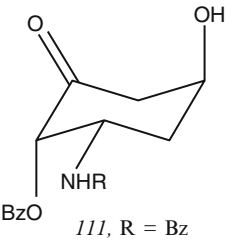

111, R = Bz
112, R = $COCF_3$

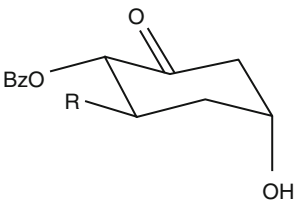

113, R = OBz
114, R = N_3

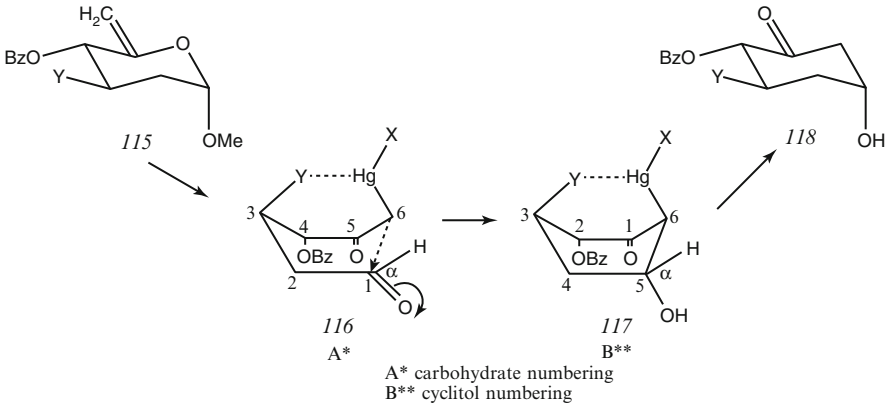

Fig. 8.33

the starting hex-5-enopyranosides. Thus, the exo-methylene sugars in the $^1C_4$ (D) conformation provide cyclohexanones with the HO-5 directed upward, whereas those with the $^4C_1$ (D) conformation gave ketones with the HO-5 directed downward. With a single exception [44], the "Ferrier ketones" so far prepared have the three-substituent *trans* to HO-5. This high stereoselectivity of the ring closure can be explained as follows.

The mercury atom, as a transition element attached to C6 [42, 52], may develop coordination with the lone pair-bearing substituent Y (Y = N or O) at the C3 carbon with the formation of an intermediary six-membered ring (a) (Fig. 8.33) and thus direct the approach of the C6 nucleophile toward the C1 carbon from the same side as the three-substituent is located. The subtended angle (a) between the direction of the approach of the nucleophile and the C1═O bond is maintained during the reaction ("Baldwin's" 6-exo-trig mode of ring closure [57]) and thus represents the angle across C6–C5–O5 in the product. Due to the lesser steric crowding on the opposite side of the ring, HO5 (to be generated via protonation) will be trans to the three-substituent. This mechanism involves an optimal steric arrangement in the transition state, represented by a double-boat conformational system (b in Fig. 8.33).

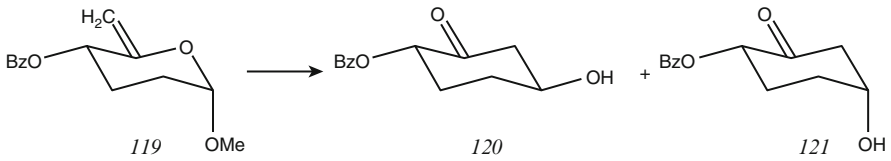

Fig. 8.34

Proof for the stereocontrol exerted by the mercury atom has been obtained from the carbocyclization of methyl 4-*O*-benzoyl-2,3,6-trideoxy-α-D-*glycero*-hex-5-enopyranoside *119* (Fig. 8.34).

Since there is no three-substituent, coordination with the mercury atom cannot occur, so that the nucleophilic attack of C6 on C1 of the ring-opened sugar occurs from both directions and gives 4:3 mixture of (2S, 5S)- (*120*) and (2S, 5R)-2-benzoyloxy-5-hydroxycyclohexanone *120*. Although this mixture of diastereoisomers could not be fractionated by chromatography, the signal of H5 of the newly generated chiral center of both *120* and *121* could be distinguished readily by ^{1}H-NMR (4.02 and 4.55 ppm, respectively). It was also determined by the ^{1}H-NMR that *120* and *121* exist in $^{2}C_5$ conformers.

8.5 1,3-Dipolar Cycloaddition of Chiral N-(Alkoxyalkyl) Nitrones

Vasella [58] has shown that the hydroxy-oxime *122* (2,3-*O*-isopropylidene-5-*O*-trityl-D-ribose oxime) can be, via its tautomeric form α-alkoxy-hydroxylamine *123*, converted by reaction with carbonyl compounds (formaldehyde, acetaldehyde, etc.) to N-(alkoxyalkyl) nitrones *124* which then reacts via 1,3-dipolar cycloaddition with methyl methacrylate to give the protected isoxazolidine ribosides *125*, *126* epimeric at C5. This reaction proceeds in high yield (97 %) and with high stereoselectivity (84:16) (Fig. 8.35).

The high stereoselectivity of cycloaddition of N-(alkoxyalkyl) nitrones obtained by the use of formaldehyde and acetone prompted Vasella to identify the factors that were responsible for this high stereoselectivity.

The hydrolysis of isoxazolidine riboside *127* ($R_1 = H$; $R_2 = CH_3$) obtained by the hydrolysis of the C5′ trityl group from *125*, as well as of *128*, obtained from detritylation of *126*, both isoxazolidines *129* and *130* were obtained (Fig. 8.36).

The only difference between the isoxazolidines *127* and *128* was the configuration at the C5 carbon.

The stereoselectivity of the cycloaddition reaction most likely depends upon the ring oxygen of the five-membered ring furanose. As a matter of fact, in the transition state of cycloaddition, the stereoelectronic effect could be expected to become operational which will, similarly to the anomeric effect, be based upon

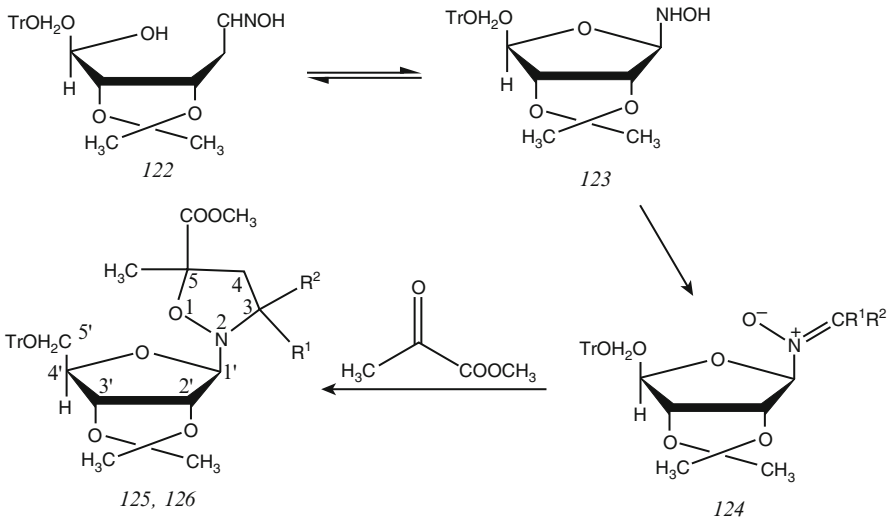

Fig. 8.35

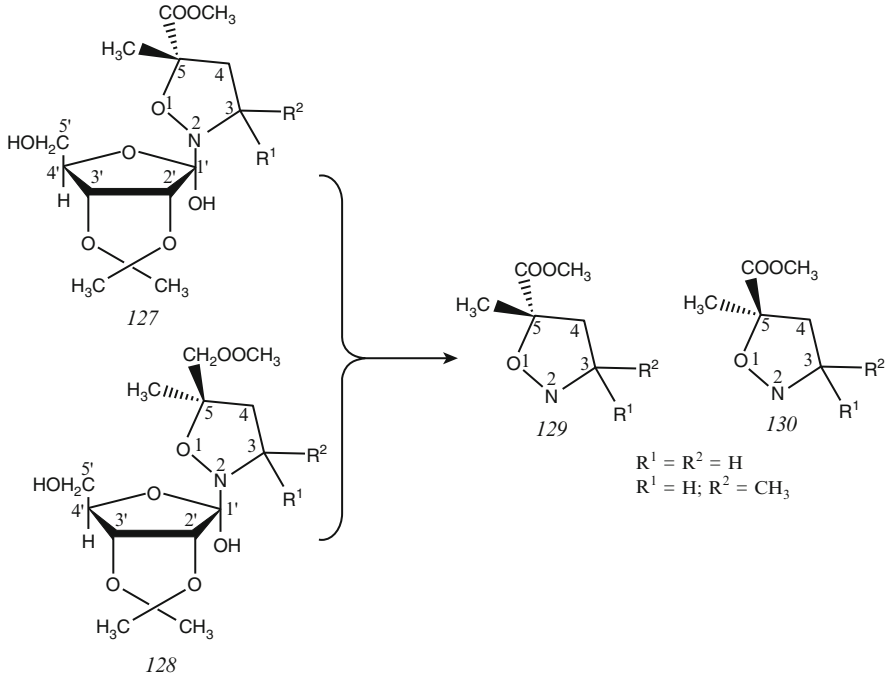

Fig. 8.36

Fig. 8.37

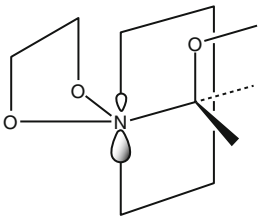

131

Fig. 8.38

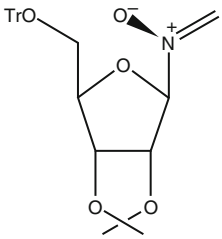

132

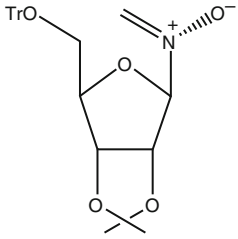

133

conjugative interaction that arises in the course of the reaction between the doubly occupied sp^3 orbital on nitrogen and the σ* orbital of C1–O bond of the sugar residue [59]. In the appropriate geometry of the transition state, namely, at the coplanar (antiperiplanar) position of the mentioned orbitals, the decrease of activation energy should be effected through this conjugative stabilization and should lead to an increase of the electrophilic character of nitrone.

According to a qualitative orbital consideration, the ψ_1 orbital of the π-system of nitrone can interact with the formal nitrogen nonbonding electron pair of cyclo adducts. The anomeric effect (classic and kinetic) that can become operational in the transition state of cycloaddition can stabilize the transition state. On the other side, the unoccupied ψ_3 orbital of the π-system of nitrone through its interaction with the unoccupied σ* orbital of C1–O bond can decrease the activation energy, and with that increase the electrophilic character of nitrone (Fig. 8.37).

The main reason for the stereoselectivity of cycloaddition of nitrone of type 3 is not due to destabilization of alternative transition states due to steric interactions but due to the selective stabilization of one transition state due to the favorable stereoelectronic interactions. Hence, the conformations of N-(alkoxyalkyl) nitrone will be limited to transition states *132* and *133* (Fig. 8.38), which can be named "O-*endo*" (*132*) and "O-*exo*" (*133*), whereby the stereoselectivity of cycloaddition increases with the increase of the number of substituents on the nitrone, indicating also that the reaction proceeds preferably via "O-endo" conformation (*132*).

Vasella has suggested that the observed stereoselectivity is due to a stereoelectronic effect which strongly influences the stereochemistry of the transition state of the cycloaddition reaction. This stereoelectronic effect is caused by the nitrogen electron pair which is oriented antiperiplanar to the C–O bond of the

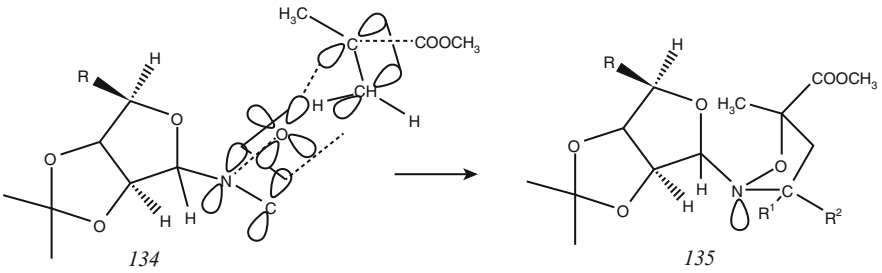

Fig. 8.39

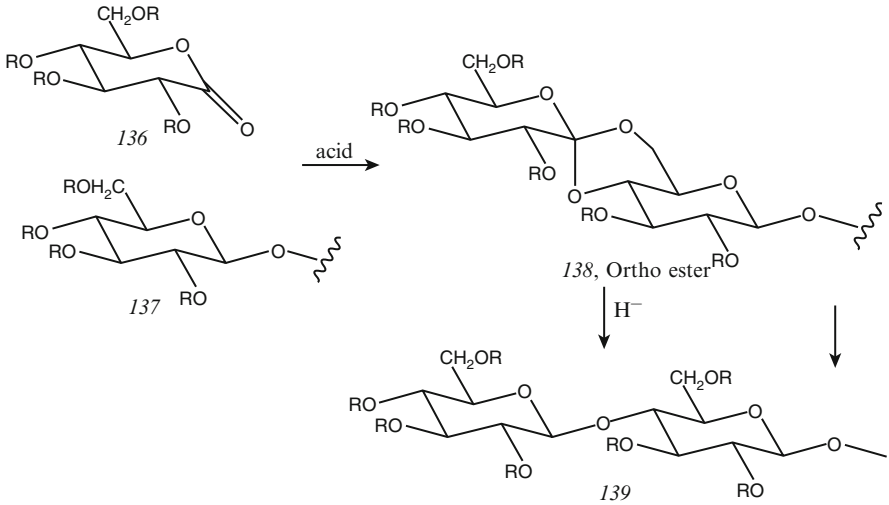

Fig. 8.40

furanose ring during the cycloaddition reaction (*134* → *135*) (Fig. 8.39). When this additional electronic delocalization is operative, the energy of the transition state is lowered accordingly.

8.5.1 Synthesis of Glycosides by Reduction of Sugar Orthoesters

Ohtake et al. [60–63] reported a novel two-step glycosylation procedure as shown in Fig. 8.40.

In the reduction of these sugar orthoesters, there are four possible glycoside products for each orthoester (Fig. 8.41). For example, the possible products of the glycosylidene-glucoside *140* are glucosyl-α- and β-(1 → 4)-glucoside (*141* and *142*) and glycosyl-α- and β-(1 → 6)-glucoside (*143* and *144*) (Fig. 8.40).

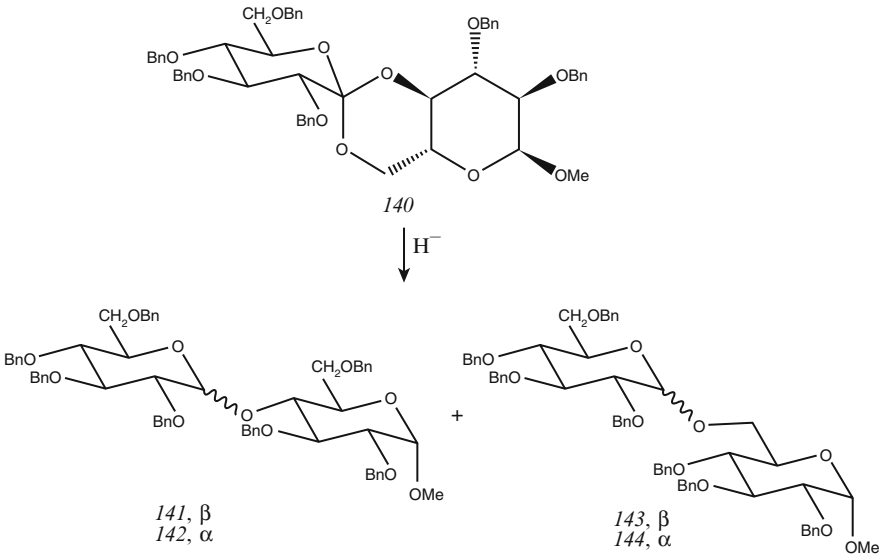

Fig. 8.41

As reported earlier [61], the combination of $LiAlH_4$ and $AlCl_3$ [64, 65] was an effective reagent for selective cleavage of the spiro sugar orthoesters. In Table 8.4 the reduced sugar orthoesters and the obtained products are given.

Table 8.4 summarizes the results of the reduction of the six sugar orthoesters *145–148* and *149*, *150* with $LiAlH_4/AlCl_3$, which were prepared from the corresponding sugar lactones. As can be seen from Table 8.4, the reduction of *145* proceeded smoothly with two equiv. of reagents in 2 h at room temperature to afford glucosyl-β-(1 → 4)-glucoside *151* in 92 % yield, whereas the other possible isomers *143*, *144*, and *145* were not detected. Also in the cases with orthoesters *147*, *148*, and *149*, glycosyl-β-(1 → 4)-glucosides *153*, *154*, and *155* were obtained again in excellent yields (92–98 %) with complete regio- and stereoselectivity. The reduction of the two orthoesters *149* and *150* containing L-sugar moieties proceeded efficiently under the same reaction condition, and glycosyl-β-(1 → 4)-galactosides *155* and *156* were produced selectively again in excellent yields (96–99 %).

The results in Table 8.4 are noteworthy first from the point that the sterically congested 4-O-positions of sugar compounds were efficiently glycosylated by this method. More noticeable was that the resulting disaccharides were obtained with complete β-selectivity even in the cases with mannosyl and rhamnosyl donors.

The reduction of six sugar orthoesters *157*, *158*, *159*, *160*, *161*, and *162* (Table 8.5) with $NaBH_3CN$ proceeded smoothly in the presence of $AlCl_3$. The results are summarized in Table 8.5.

The above results showed that the prepared 12 sugar orthoesters were separated into two groups from the point of reactivity of the reductants and of the

Table 8.4 Reduction of sugar ortho esters with $LiAlH_4/AlCl_3$

Sugar orthoester	Disaccharide obtained	Yield %
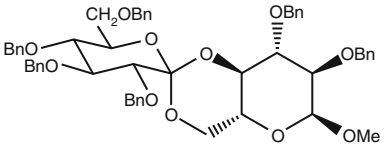 *145*	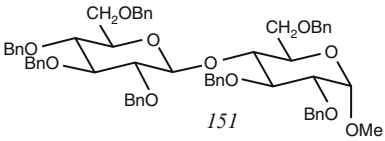 *151*	92
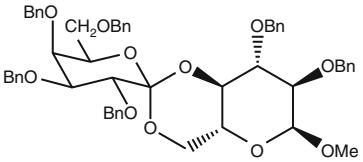 *146*	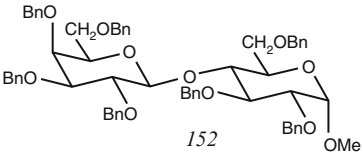 *152*	98
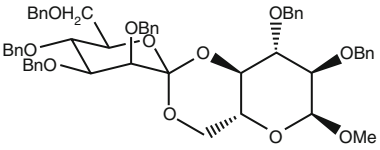 *147*	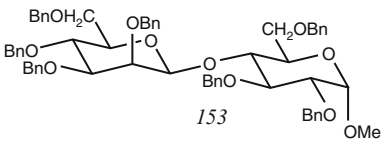 *153*	98
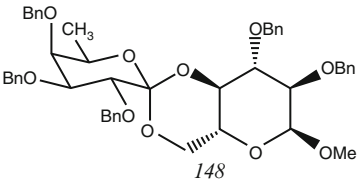 *148*	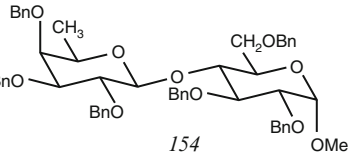 *154*	92
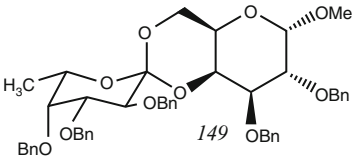 *149*	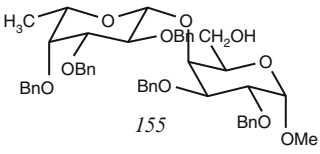 *155*	96
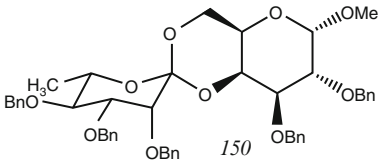 *150*	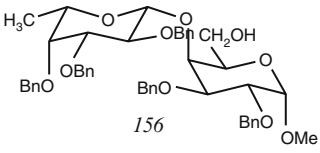 *156*	99

These reactions were carried out for 1 h and rt under Ar in Et_2O/CH_2CI_2 (ortho ester = 50 mM, 2 equiv $LiAlH_4$, 2 equiv $AlCl_3$). Yields are isolated yields

regioselectivity in their reductions. According to the X-ray crystallographic analysis and the molecular modeling studies [66–68], these orthoesters were classified into four groups from the point of the structures of their ring systems. It was shown that these two classifications were closely related and that the difference or similarity among the reactivity of orthoesters was well explained by considering the conformations of the ring systems in these molecules.

Table 8.5 Reduction of sugar ortho esters with $NaBH_3CN/AICI_3$

Sugar ortho ester	Disaccharide obtained	Time h	Yield %
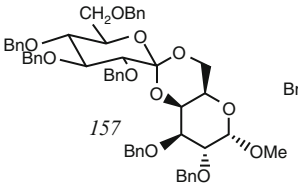	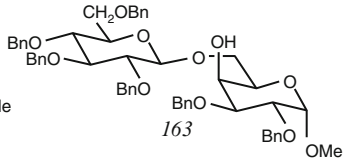	2	93
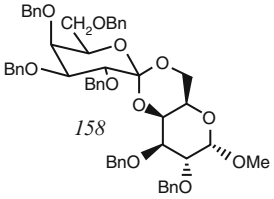	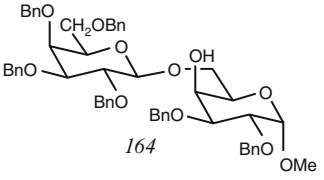	2	97
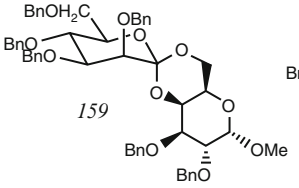	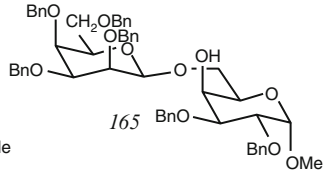	48	42
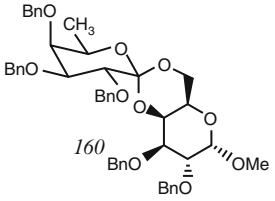	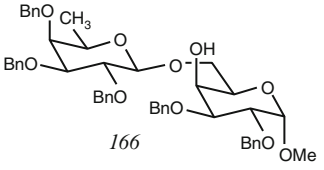	2	88
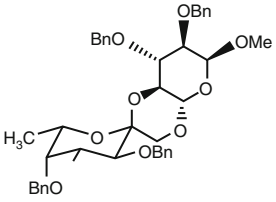	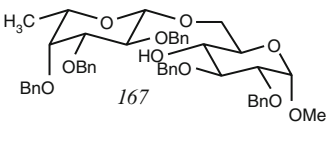	1	88
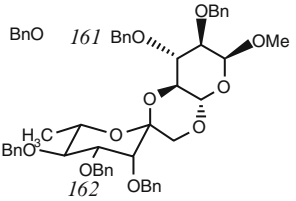	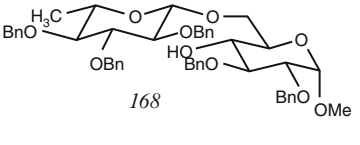	12	88

These reaction were carried out at rt under Ar in toluene/CH_3CN (ortho ester = 50 mM, 7 equiv $NaBH_3CN$, 5 equiv $AICI_3$, 100 mg MS 3A/2 mL solvent). Yields are isolated yields

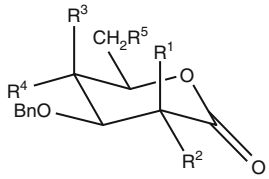

169, $R^1 = R^3 = H$; $R^2 = R^4 = R^5 = OBn$ (Glc)
170, $R^1 = R^4 = H$; $R^2 = R^3 = R^5 = OBn$ (Gal)
171, $R^1 = R^4 = R^5 = OBn$; $R^2 = R^3 = H$ (Man)
172, $R^1 = R^4 = R^5 = H$; $R^2 = R^3 = OBn$ (D-Fuc)

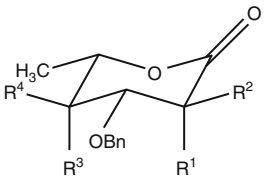

173, $R^1 = R^4 = H$; $R^2 = R^3 = OBn$ (L-Fuc)
174, $R^1 = R^4 = OBn$; $R^2 = R^3 = H$ (Rha)

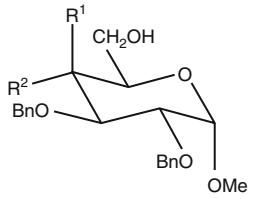

175, $R^1 = H$; $R^2 = OH$ (Glc)
176, $R^1 = OH$; $R^2 = H$ (Gal)

Fig. 8.42

As already reported [68], the structures and conformations of the spiro ring system of the formed orthoesters depended upon whether D- or L-sugar lactones were used as glucosylidene parts and whether glucose or galactose was used as the diol part.

In Fig. 8.42 the structures of both sugar lactones and sugar diols used for the synthesis of sugar orthoesters are given.

For example, the ring systems of the sugar orthoesters *145–148* (Table 8.4) prepared from the sugar lactones *169–172* and *175* (Fig. 8.42) had the same structure.

Reduction results indicated that the orthoesters *145–148* or *149*, *150* were reduced by $LiAlH_4/AlCl_3$ to afford the corresponding glycosyl-β-(1 → 4)-glycosides in excellent yields but that the reduction with these reagents did not proceed efficiently in the case of orthoesters *161*, *162*, or *157–160* with the B- or C-type ring system (Fig. 8.43). Further, it was revealed that the orthoesters with the B- or C-type ring system were efficiently converted into glycosyl-β-(1 → 6)-glycosides by reduction with $NaBH_3CN/AlCl_3$ but that this combination of the reagents was not effective for the efficient and selective reduction of the other two types (A or D) of orthoesters.

All of the products in Tables 8.4 and 8.5 resulted from the selective ring opening at the bonds between the anomeric carbons and the axial oxygen atoms. In the cases of the present reductions, it was appropriate to think that the initial step was the elimination of one of the oxygen atoms in the dioxane ring of each sugar orthoester

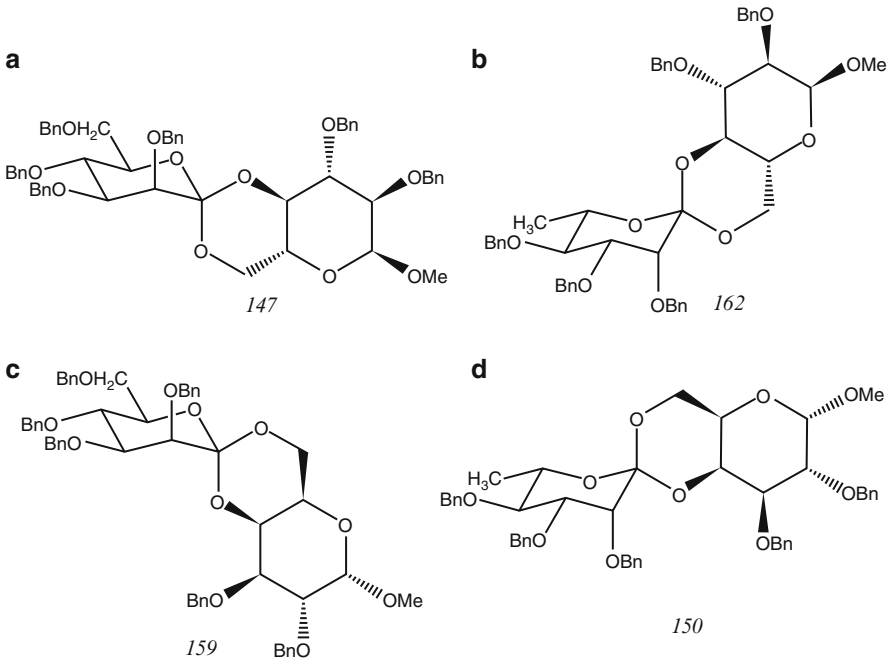

Fig. 8.43

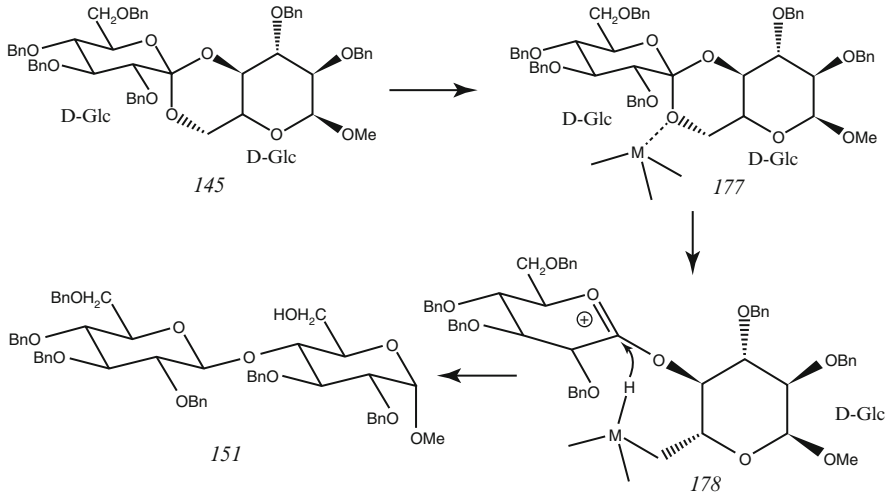

Fig. 8.44

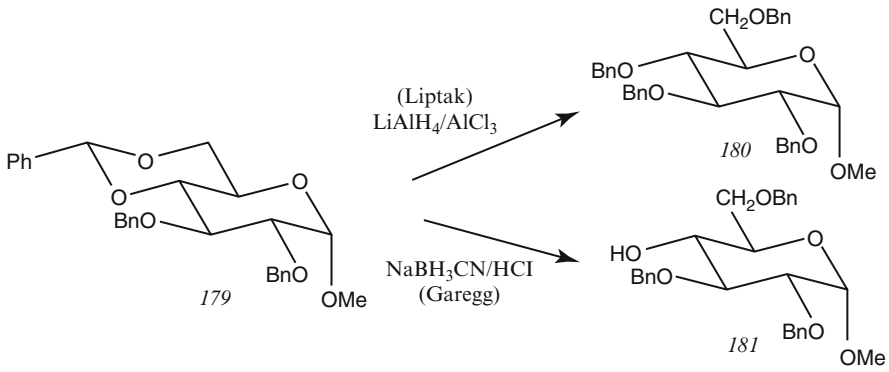

Fig. 8.45

and that the second step was the attack of the hydride anion to a resulting oxocarbenium ion (Fig. 8.44). The higher reactivity of axial substituents of the pyran rings in elimination reactions compared to those at the equatorial positions can be rationally explained by the stereoelectronic effects [69].

The matching or mismatching between the reductants and the substrates in the present reductions was compatible to the well-known selectivity in the reduction of 4,6-*O*-benzylidene glycosides shown in Fig. 8.45 [65, 70].

Although the reasons for the high regioselectivity in the reduction with these reagents have not been clarified even with simple substrates such as *179*, 4- and 6-*O*-benzyl glycosides *180* and *181* were afforded selectively from *179* with $LiAlH_4/AlCl_3$ and $NaBH_3CN/HCl$, respectively.

Finally, the mechanism that accounts for the extremely high β-selectivity should be mentioned. This stereoselectivity could be explained by considering the electronic advantage of the axial anion attack [71]. Moreover, it seemed reasonable to think that a hydride anion on the reducing reagents attacked the intermediates immediately after the dioxane ring opening or that the reactions shown in Fig. 8.46 proceeded concertedly. Thus, the attack from an axial direction from which the eliminated oxygen atoms had been bound would be advantageous. As proton atoms attached to the anomeric carbons from the axial direction, β-glycosides were afforded as the resulting products. The high β-selectivity might be the most interesting and important feature of this reductive glycosylation procedure. This superior selectivity was realized by developing a glycosylation method based on the completely different concept.

Li et al. [72] (Fig. 8.46 and Table 8.6) have studied the relative rate of hydrolysis of the four bicyclic orthoesters *188*, *189*, *190*, and *191* having a six- or a seven-membered orthoester ring (Table 8.6).

The hydrolysis experiments were performed in deuterated acetonitrile/D_2O mixtures (4:1) using HCl as catalyst.

The study of the rate of hydrolysis of *189–191* showed that the orthoacetate *189* was hydrolyzed 40 times faster than the orthobenzoate *200*, whereas the hydrolysis

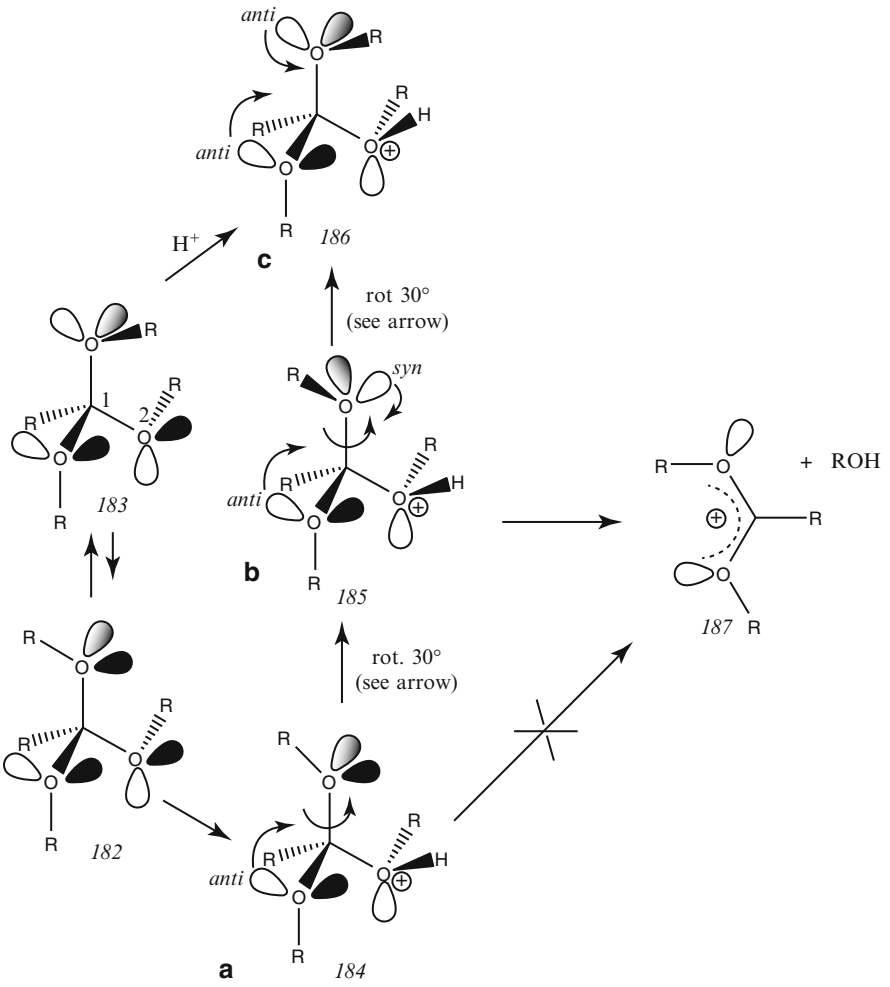

Fig. 8.46

of orthoacetate *191* was 1680 times faster than that of *190*. With regards to the product distribution, the orthoformate *188* gave a mixture (2:1) of the formate *192* and the diol *193*. The orthoacetate *189* gave a mixture (2:1) of acetate *194* and the same diol *193*. These two cases are assumed to be identical, and in the following discussion, the hydrolysis of the orthoformate *188* will be omitted. The acid-catalyzed hydrolysis of orthobenzoate *190* yields benzoate *195* as the only product with no trace of the diol *193*. Finally, the hydrolysis of the orthoacetate *191* affords only the mixture (1:1) of two possible acetates *196* and *197*, with no diol being formed.

In order to understand the mechanism of hydrolysis with the formation of the various products, and since several competing routes may be involved (Fig. 8.47),

Table 8.6 Relative rates of hydrolysis and product distribution in the compounds 188–191

Starting material	Rel rates	Products	
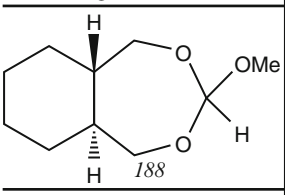 *188*	–	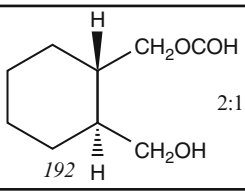 *192* 2:1	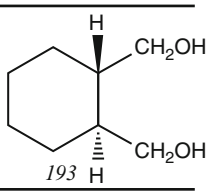 *193*
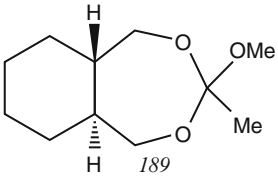 *189*	40	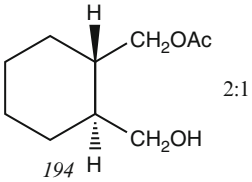 *194* 2:1	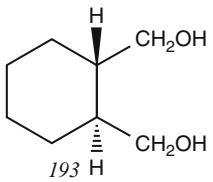 *193*
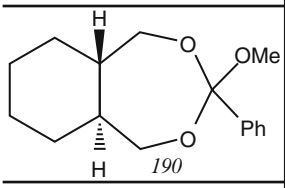 *190*	1	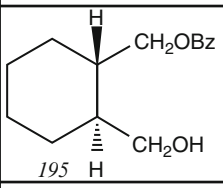 *195*	
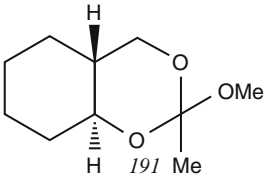 *191* Me	1680	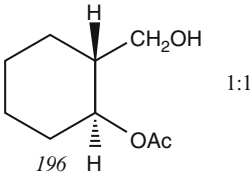 *196* 1:1	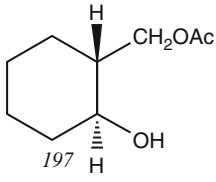 *197*

the hydrolysis of orthoesters *198*(*189*) and *199*(*190*) has been carried out with labeled water (H_2O^{18}).

The orthoesters *198* and *199* can be in principle protonated at either the exocyclic O2 oxygen atom or the endocyclic O3 (or O4) oxygen atoms. Protonation of O2 oxygen yields methanol and the cyclic oxocarbenium cation *201* (R = Me or Ph) which when subsequently attacked by labeled water gives *203* (R = Me or Ph) and then the labeled ester *206**. The protonation of one of the two endocyclic oxygens induces ring opening to afford the acyclic oxocarbenium cation *200* (R = Me or Ph). Labeled water may now attack this cation in two ways: either in an S_N2 fashion on the methoxy carbon (H_3C-O2) leading to the ester *204* (or *206*) or directly at the central carbon atom position C1. In the latter case, the intermediate *202* (R = Me or Ph) can be protonated at the oxygen atom O4 to form diol *205*; protonation can also take place at position O2, yielding the previously described ester *204** or *206**.

The experimental work shows that the orthoester (R = Me) was indeed producing all three products *205*, *204*, and *206** when hydrolyzed in the presence of H_2O^{18}. Therefore, in this case, both cations *200* and *201* contribute to the product distribution. Moreover, the cation *200* (R = Me) must be formed predominantly over the cyclic cation *201* (R = Me) because the labeled ester alcohol *210**,

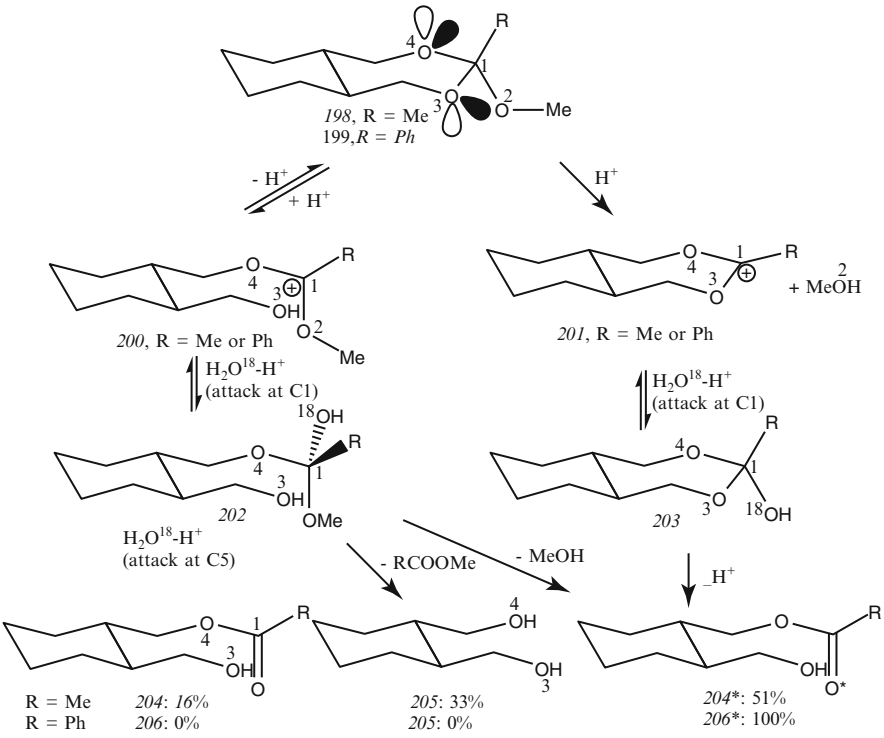

Fig. 8.47 Hydrolysis pathways for the orthoesters *198* and *199*

accounting for 51 % of the mixture, is formed via both cations *200* and *201*. This assumption is very reasonable since the hydrolysis products *206* and *205* (49 % of the mixture) can only arise from the cation *200* too.

Regarding the orthobenzoate *199* hydrolysis, the cation *200* (R = Ph) makes no contribution to the final product distribution, the benzoate alcohol *206** (*195*) being formed via the cyclic cation *201* (R = Ph). This assumption again is very reasonable since neither *205* nor *206** issued from *200* (R = Ph) is present.

In the case of the six-membered ring orthoester *207* (Fig. 8.48), the ester alcohols *213* and *214* are obtained in 1:1 ratio. Since the diol *212* is not present in the hydrolysate, it is reasonable to conclude that cations *208* and *209* do not contribute to the hydrolysis route and that the products *213* and *214* come only from the cyclic cation *210*. In summary, all hydrolysis processes involve the cyclic cations *201* (R = Me or Ph) and *210*, whereas the cation *200* issued from seven-membered ring opening is only observed when R is methyl substituent. These results are now rationalized in the light of stereoelectronic effects and with the help of theoretical calculations.

An AM1 study of the protonated species corresponding to the neutral conformers of *198*, *199*, and *207* that differ in the position of exocyclic substituents was carried out. It was found that all three orthoesters once protonated undergo

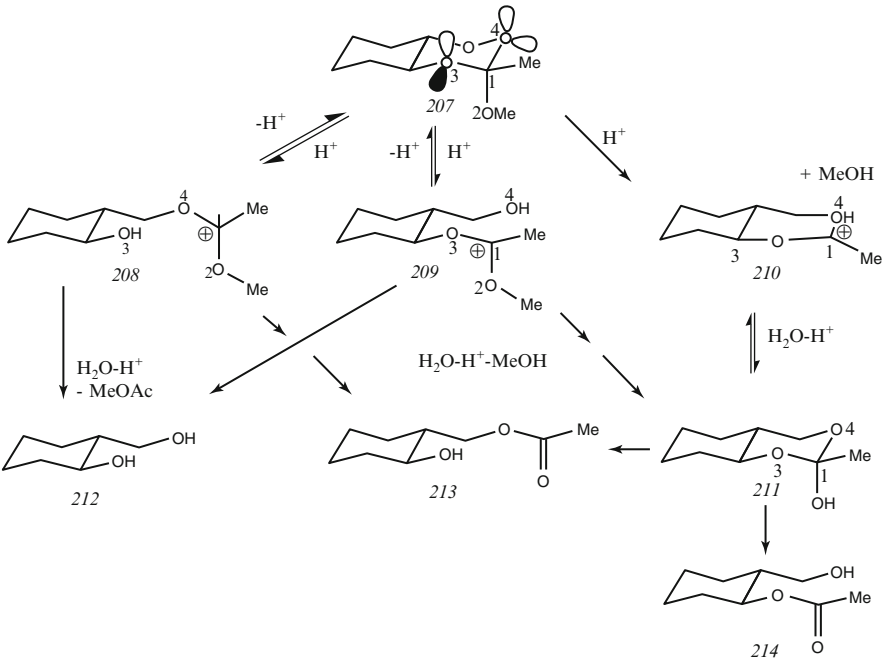

Fig. 8.48

fragmentation without an additional energy barrier along the reaction coordinates to produce cations *200*, *201*, *208*, *209*, and *210*. These results suggest that bond cleavage is not the rate-determining step but rather protonation. This is in agreement with the fact that protonation is known to be playing a key role in the rate-determining step in orthoester hydrolysis [73, 74].

In the case of the seven-membered ring orthoacetates, the two structures *217* and *218* (Fig. 8.49) were found, the latter being favored by AM1 and 3-21G by 1.41 and 1.84 kcal/mol, respectively. The seven-membered ring orthobenzoate can exist as either *218* conformer (preferred 3-21G structure) or conformer *219* (preferred AM1 structure). Both optimization methods are in fair geometrical agreement with the X-ray data.

Each orthoester having three oxygen atoms has six sites (labeled **a** – **f**) that are available for protonation by H_3O^+, yielding in principle six transition structures per orthoester. Study of all these possible sites of protonation by AM1 semiempirical Hamiltonian revealed that some oxygen lone pairs could not be attacked by H_3O^+ for steric reasons. However, rotation of the methoxy group about the C1–O1 bond could relieve these unfavorable interactions and thus make these hindered sites available for protonation. Thus, protonation of orthoester *215* at the endo site **c** was equivalent to protonation at site **e** (the other equivalent positions are indicated in Fig. 8.48). In the case of six-membered orthoester *215* where all bonds are staggered, use of antiperiplanar lone pair hypothesis allows straightforward identification of the most

	ΔHf (kcal/mol)	Calcd. ratio		Exptl. ratio
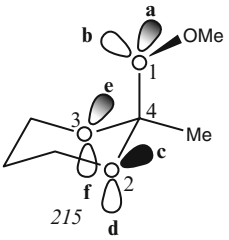 *215*	a - 40.01 b (-40.31) c **215e** d -37.76 e - 34.02 f **215d**	98% - - 2% 0% -	*exo:* *98%* *endo* *2%*	100% 0%
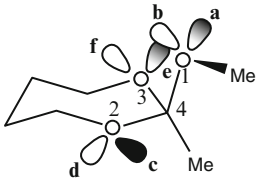 *216*	a - 47.81 b - 48.27 c **217c** d **217c** e - 44.52 f - 49.66	3% 7% - - 0% 76%	*exo:* *12%*	< 51%
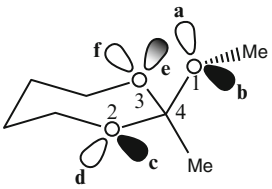 *217*	a - 47.55 b - 45.68 c - 48.55 **218c** **218e** **218f**	2% 0% 12% - - -	*endo:* 88%	> 49%
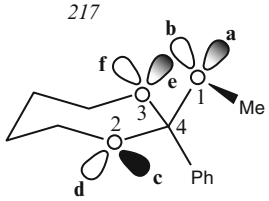 *218*	a - 12.22 b - 12.02 **219d** d - 3.09 e - 9.44 f -13.09	10% 7% - 0% 0% 42%	*exo:* *27%*	100%
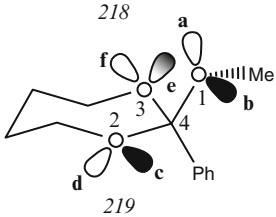 *219*	a - 12.15 b - 10.69 c - 12.98 d - 3.12 **219e** **219f**	9% 1% 31% 0% - -	*endo:* 73%	0%

Fig. 8.49 AM1 Protonation structures characteristics and corresponding heats of formation (ΔHf). Relative energies of the neutral species are indicated on the *left* (kcal/mol; *underline*: AM1, *italics*: 3-21G optimized including ZPE). This structure has a boat conformation and may be disfavored in a bicyclic system (From Li et al. [72])

basic oxygen atoms [75]. The oxygen atom O1 receives two contributions from the lone pairs **d** and **f**, whereas only its lone pair **a** is able to donate electrons. It is therefore O1, which should be the most protonable oxygen atom of the orthoester *215*. Oxygen O2 receives two contributions as well from **a** and **e**, but it also donates

electrons from both lone pairs **c** and **d**. With regards to O3, this atom receives only from **c,** whereas its two lone pairs **e** and **f** can donate electrons; as such, it must be the least basic oxygen atom. These conclusions are confirmed by calculations which show that protonation at position O1 is indeed the most favored process; protonation at positions O2 and O3 is disfavored by 2.56 and 6.30 kcal/mol, respectively.

These stereoelectronic considerations and calculations are in full agreement with the experimental results, because only the C4-O1 bond cleavage is observed and it is a fast process. This latter observation can also be rationalized in terms of stereoelectronic effects, because once protonated at position O1, both lone pairs **f** and **d** (which are already partially responsible for the large basicity of the O1 oxygen) immediately provoke C4–O1 bond breaking without further backbone motion.

All the transition structures (apart from *215b*) calculated indicate that the geometry of the orthoester *215* is not too much altered at the transition state. This observation suggests that protonation, the rate-limiting step, and bond cleavage are distinct, despite the fact that the second step is not accompanied by a barrier on the potential energy surface, as checked by IRC [76] (intrinsic reaction coordinate) studies starting from the transition structures (no intermediates or weak ones were located between the transition structures and the products). All the orthoesters have C4–O bond lengths in the 1.40–1.42 Å bracket. At the transition state, the C4–O bond lengths can be classified into three families: the C4–O bond whose oxygen atom gets protonated has lengthened (1.44–1.48 Å), one of the remaining C4–O bond has shrunk (1.37–1.39 Å), whereas the other one does not change (1.40–1.42 Å).

These figures clearly demonstrate that the bond cleavage is far from being complete at the protonation transition state. It is also worth noting that the distance between water oxygen and the H^+ is 0.202 Å shorter than the distance between the orthoester *215* oxygen O1 and H^+ in *215a*, the most favored transition structure. This proves that the proton affinity of this orthoester is greater than that of water, because it can attract H^+ with equal strength at a longer distance at the transition state level. The same trend is also observed in the case of the seven-membered ring orthoesters *216–219*, although to a lesser extent (0.127, 0.127, 0.160, and 0.143 Å) for *216*f, *217*c, *218f*, and *219*c which are the favored protonation transition structures, likely due to a diminished proton affinity of these orthoesters compared with *215*, as experimentally confirmed by the relative rates of hydrolysis of the orthoesters *198–199* (Table 8.6).

All the observation made in the case of *215* can be applied in the case of the seven-membered ring orthoesters *216–219*. However, due to the much floppier structures of these compounds and also to the fact that *syn*-periplanar lone pairs must also be at work, application of stereoelectronic principles becomes an awkward task.

The calculations show that the seven-membered ring orthoacetate gets mainly protonated in an *endo*-fashion (inside the ring, *216*f and *217*c) rather than at the *exo*-position (*216*b). In this case again, the calculations are in good agreement with the experiments since a Boltzmann distribution of the transition states at 25 °C predicts that 88 % of the protonation should take place at the endocyclic oxygen positions; it is experimentally difficult to estimate accurately the amount of endocyclic protonation versus exocyclic protonation, but at least 49 % of the protonation should be endocyclic, according to the final product distribution.

Fig. 8.50

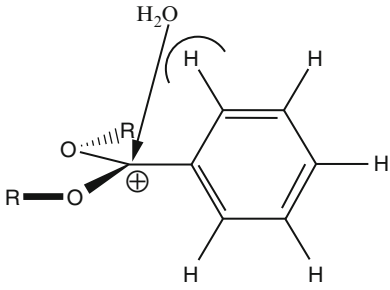

220

In the case of the seven-membered ring orthobenzoate, the exocyclic protonation is predicted to be more favored (27 %) than for orthoacetate. Despite the large apparent difference between the experiment and the calculations, the trend (more *exo*-protonation) is correctly foreseen. There also exists a major difference between orthoacetates and orthobenzoates in that the cations formed after endocyclic protonation and ring cleavage in the case of the orthobenzoate lead to structures extremely unfavorable to water at the central carbon position.

For obvious steric reasons, the plane of the phenyl is nearly perpendicular (49° and 65° in the cases of the cations issued from *218*f and *219*c, respectively) to the plane defined by the two oxygens and their intercalated carbon. This carbon is the preferred site of attack by nucleophiles, for which the best incoming trajectory is also perpendicular to the O-C-O plane.

Clearly, the preferential phenyl orientation is incompatible with nucleophilic attack by water (Fig. 8.50), and ring closure, an intramolecular process, is much preferred, leading back to the original orthobenzoate compound.

Obviously, this steric hindrance to water attack on the cation is not encountered after exocyclic protonation and cleavage of the orthobenzoate since the phenyl ring becomes nearly coplanar with the O-C-O plane (0° in the case of the cation issued from *218*a) leaving both sides of the O-C-O plane completely free to nucleophilic attack. All these considerations dealing with the orientation of the phenyl ring become irrelevant when the phenyl substituent is replaced by methyl group, and in the case of the orthoacetate, protonation is the only factor influencing the product distribution. In that case, the protonation transition state calculations fit perfectly with the experiment.

8.6 Reductive Cleavage of Glycosidic Bond

The reductive cleavage method is one of the important tools for determining the structure of polysaccharides [77]. Various aspects of the method have been studied extensively [78–88]. So far, the investigation has concentrated mostly on the variation of polysaccharides and catalysts, while triethylsilane and dichloromethane are employed as the reducing agent and solvent, respectively.

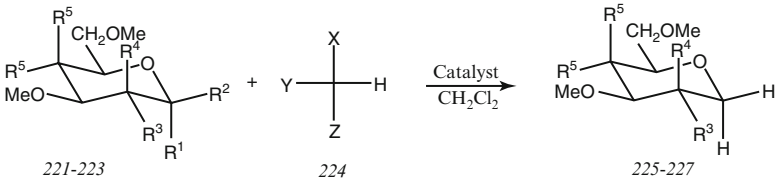

221-223 *224* *225-227*

	R^1	R^2	R^3	R^4	R^5	R^6
*221*α(α-D-Glc)	OMe	H	OMe	H	OMe	H
*222*β(β-D-Glc)	H	OMe	OMe	H	OMe	H
*223*α(α-D-Glc)	OMe	H	H	OMe	OMe	H
*223*α(α–D-Glc)	OMe	H	OMe	H	H	OMe
225(anhydro-D-Glc)	H	H	OMe	H	OMe	H
225(anhydro-D-Man)	H	H	H	OMe	OMe	H
227(anhydro-D-Gal)	H	H	OMe	H	H	OMe

	X	Y	Z
*224*a	C_2H_5	C_2H_5	C_2H_5
*224*b	C_2H_5O	C_2H_5O	C_2H_5O
*224*c	*i*-C_3H_7	*i*-C_3H_7	*i*-C_3H_7
*224*d	C_6H_5	C_6H_5	C_6H_5
*224*e	*t*-C_4H_9	CH_3	CH_3

Fig. 8.51

The method consists of exhaustive methylation of the free OH groups in a polysaccharide, reductively cleaving all glycosidic linkages with Et_3SiH in the presence of Lewis acid catalyst, acylating the free OH groups generated by cleavage, and identifying the partially methylated and acylated 1,5- or 1,4-anhydroalditol products present in the final reaction mixture.

Although a mechanistic aspect of the reaction was not investigated in depth, a cyclic oxocarbenium ion was suggested to be formed during the course of the reaction, based on the stereochemistry of the 1-monodeuterio-1,5-anhydroglucitol produced upon reduction with Et_3SiD [78]. The stereochemistry of the deuterio-1,5-anhydroalditol products seems to support this rationale, because the predominant (>90 %) axial configuration of the deuterium atom in the products could arise from the cyclic oxocarbenium intermediate. As we already know, a cyclic oxocarbenium ion has also been proposed as an intermediate for the anomerization of permethylated methyl D-glucosides, along with an acyclic oxocarbenium ion (Fig. 8.51) [89, 90].

It has also been suggested that a similar cyclic oxocarbenium ion is involved in the process of transglycosylation and acetolysis [91].

The reductive cleavage of methyl glycosides has some analogy with the hydrolysis of acetals and ketals [92]. Since glycosides are acetals, then formation of an oxocarbenium ion in the course of both reactions may imply mechanistic similarities. An A-2 mechanism has been suggested for hydrolysis of methyl (or phenyl) D-glycopyranosides [93]. According to this mechanism for the hydrolysis of

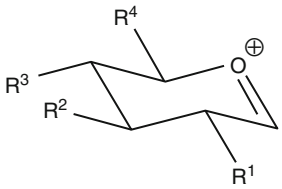

220

cyclic oxocarbenium ion

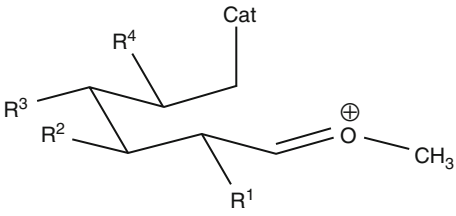

221

acyclic oxocarbenium ion

Fig. 8.52

Fig. 8.53

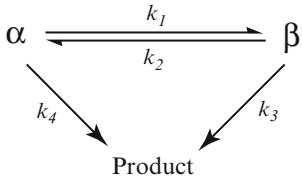

D-glucopyranosides, it is apparent that the pyranoside ring does not open during the course of reaction. It is also important to point out that the attack by a water molecule on the oxocarbenium ion takes place in the rate-determining step. However, this step is a fast one in the hydrolysis of other acetals in general (Fig. 8.52).

It is reasonable to assume that an oxocarbenium ion, either cyclic or acyclic, may be involved in the course of reductive cleavage because the reducing agent itself is anionic by nature. However, the most critical problem to be solved is whether the rate-determining step is the formation of an oxocarbenium ion from the substrate or the reduction of the ion by a silane. This means that the factors which may influence the observed rates should be (1) the structural characteristics of the substrates, especially the configuration of the anomeric carbons; (2) the nature of the reducing agents; and (3) the nature of the catalysts.

The investigation of the rate of anomerization of permethylated methyl glycosides indicates that the rate of anomerization of β to α is about four times faster than α to β for methyl D-glucopyranosides [89]. Furthermore, the former process seems to take place via an acyclic oxocarbenium ion, whereas the latter favors a cyclic oxocarbenium ion [90]. In the presence of a reducing agent, both ions may compete with reduction and anomerization. The cyclic oxocarbenium ion, if formed, should compete with methoxytrimethylsilane and the reducing agent. Since the reducing agent is used at a five or ten times molar excess, it is probable that the rate of reduction is much higher than that of anomerization. The complexity of the kinetics of this reaction is shown in Fig. 8.53.

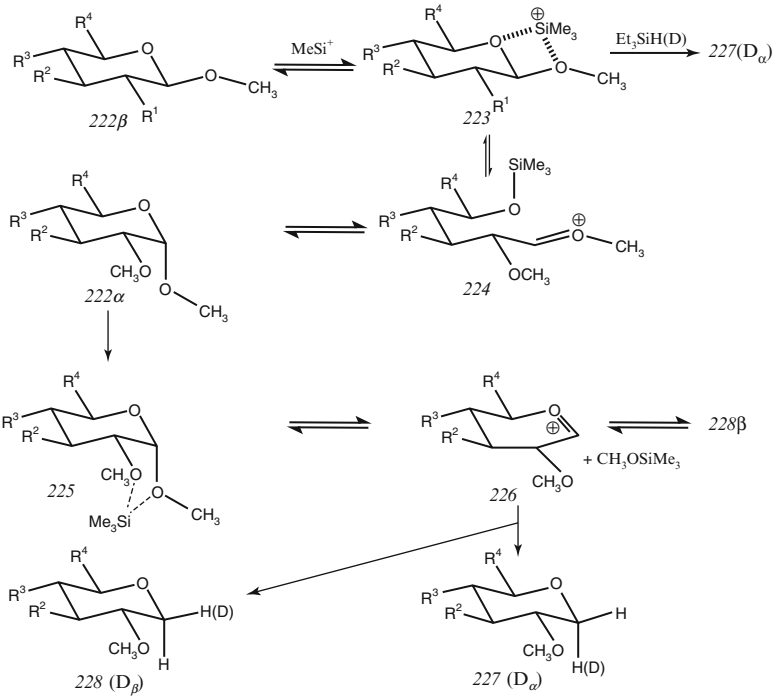

Fig. 8.54

Kinetic measurements have shown that both anomerization and reduction are much slower for the α-anomer than those for the β-anomer. Furthermore, the reduction takes place at far greater rate than the anomerization, regardless of the reducing agent. These results are consistent with the process proceeding via a cyclic oxocarbenium ion. The silane, which is present in fivefold excess, should be a better nucleophile than methoxytrimethylsilane. Consequently, the rate of formation of the product is much greater than that of anomerization.

On the other hand, the β-substrate forms a substantial amount of α-anomer, in addition to *227*, in 1 h. It seems to favor the acyclic oxocarbenium pathway because the intermediate can readily recyclize intramolecularly to the α-anomer. Then the question remains as to whether the cyclic oxocarbenium ion is the sole intermediate for reduction of both α- and β-anomers. This may be true if a weak reducing agent, such triethoxysilane is employed, which gives only 2.6 % and 5.3 % of *227* in 0.5 and 1.0 h, respectively. However, it should be pointed out that the rate of formation from the β-anomer is about twice as high as that from the α-anomer. If the cyclic oxocarbenium ion is the sole intermediate, the rates should be very similar for both the α- and β-anomers.

This observation can be explained by suggesting two reaction pathways, as shown in Fig. 8.54. In the case of the β-anomer, the reduction may take place

Fig. 8.55

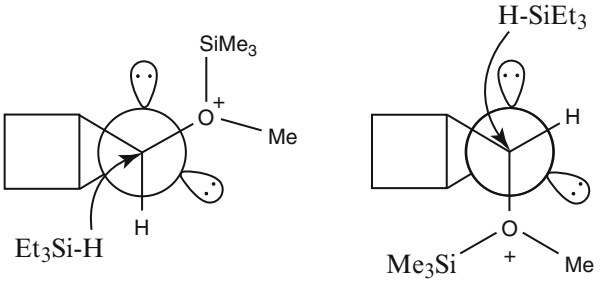

229 *230*

without the formation of the cyclic oxocarbenium ion. The trimethylsilyl cation derived from $Me_3SiOSO_2CF_3$ may coordinate to both O5 and O1 atoms of the β-anomer to form a complex such as *223*. This kind of coordination is plausible if one looks at the spatial arrangement of the lone pair orbitals in the two oxygen atoms. Then the complex *223* may be directly attacked by a silane to form an anhydroalditol product *227* and methoxytrimethylsilane, or the ring may open to form an acyclic oxocarbenium ion *224*.

The direct attack may be considered as an S_N2 process, which can be illustrated as shown in Fig. 8.54. This may be the reason that the 1-deuterio-1,5-anhydroglucitol *227* D_α formed almost exclusively when Et_3SiD was used for the reductive cleavage of *222*β [78]. Also, this is why the reduction takes place much faster than the anomerization. The acyclic oxocarbenium ion *224* may undergo mostly intramolecular recyclization to form the α-anomer.

On the other hand, in the case of the α-anomer, the complexation to O1 and O2 is plausible (such as *225*; Fig. 8.54), and the resulting *anti*-arrangement of the lone pair orbital in the O5 and C1–O bond may readily lead to formation of cyclic oxocarbenium ion *226* (Fig. 8.54). Once it is formed, a silane can readily attack from the axial direction to produce the alditol *227* (and *227*D_α when Et_3SiD is used). An S_N2 type of reaction of *225* with Et_3SiD should give *228*D_β as the major product, and this was not observed. For such a displacement to occur, a silane has to approach from the direction parallel to the one of the lone pair orbitals of the ring oxygen atom, as shown in Fig. 8.55 (*230*). This seems unfavorable because of the repulsive nature of the interaction between the lone pair electrons and the partially negatively charged hydrogen of the reducing agent.

When the substrate was mixed with $Me_3SiOSO_2CF_3$ in the absence of the reducing agent, rapid equilibrium was reached within 1 h [90]. The α/β ratio was approximately 4 for permethylated methyl D-glucopyranoside and 5 for the galactopyranoside, regardless of the anomeric configuration of the starting material. The presence of the silane significantly decreases the rate of anomerization of *222*α to *223*β. This is not surprising because the cyclic oxocarbenium ion intermediate *226* should react with the silane (which should be present in at least fivefold excess) at a higher rate than recombination with methoxytrimethylsilane to form *222*β. The anomerization of *222*β to *222*α is also retarded by the presence of silane, the ratio of

Table 8.7 Rates of formation of 1,5-anhydroalditol by reductive cleavage of permethylated methyl D-glycopyranosides with triethylsilane and $Me_3SiOSO_2CF_3$ (1:5:5 by molar equiv.) at 25 °C

Glycoside	k(min^{-1})
*222*α (α-D-Glc)	9.6 (±0.5) × 10^{-3}
*222*β(β-D-Glc)	3.7 (±0.5) × 10^{-2}
*225*α(α-D-Glc)	2.2 (±0.5) × 10^{-2}
*225*β(β-D-Glc)	1.2 (±0.5) × 10^{-1}

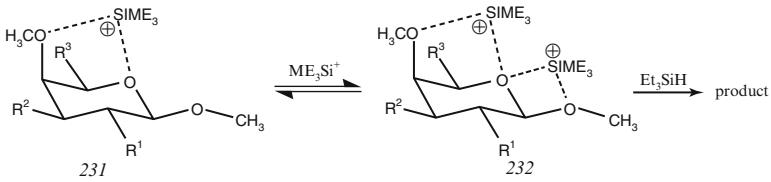

Fig. 8.56

α/β ranging from 0.09 to 1.32. However, the retardation is much less significant than with the case of *222*α to *222*β.

tert-Butyldimethylsilane seems to be the most effective among the reducing agents employed in this investigation. This may be an indication that the silane itself, not the free hydride ion, approaches the anomeric carbon in the rate-determining step. The stereoelectronic factor seems to play an important role. Triethoxysilane, triphenylsilane, and dimethylphenylsilane are less effective than trialkylsilanes. Diphenylsilane seems to be as effective as trimethylsilane in spite of the presence of two phenyl groups. The presence of two hydrogen atoms may increase the reducing power of diphenylsilane.

The rates of the formation of the 1,5-anhydroalditols (*222–225*) are listed in Table 8.7. The highest rate is observed with the β-galactoside, and the α-mannoside shows the lowest rate among the five glycosides examined. The rate enhancement in β-galactoside may be due to the complexation of Me_3Si^+ with the oxygen atom at C4 and the ring oxygen atom, as shown in Fig. 8.56. Such complexation may increase the partial charge at C1, which should be more susceptible to the attack by a silane.

A similar kind of complex formation is also possible with the α-mannoside. Once the complex is formed, the lone pair orbital of the ring oxygen atom, which should be used for complexation with Me_3Si^+ and the oxygen atom of C2–OCH_3, is no longer available to push out the α-methoxy group at C1 to form a cyclic oxocarbenium ion (Fig. 8.57). This may be the reason for the lowest rate of the reductive cleavage of α-D-mannosides.

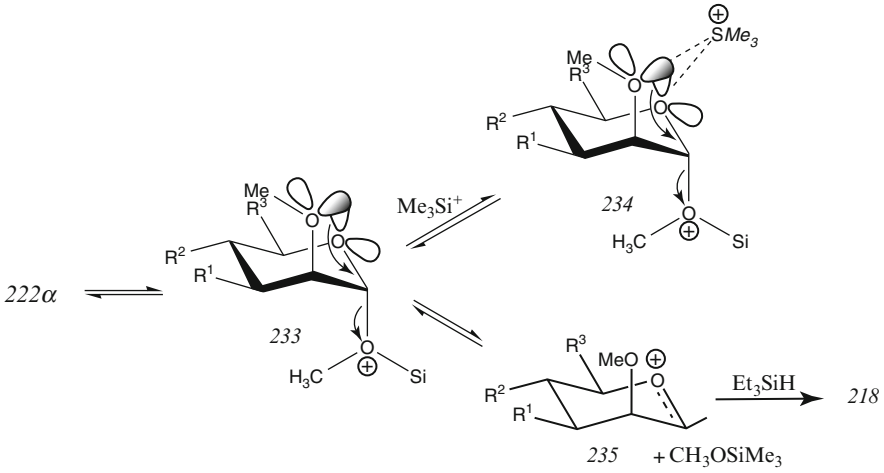

Fig. 8.57

8.7 Carbohydrate Degradation by Oxygen

The severe carbohydrate damage that accompanies oxygen delignification is a serious issue. Carbohydrate degradation is not caused by direct attack of molecular oxygen, but by active oxygen species (AOS) which are mainly generated from reactions between the phenolic molecules in lignin and molecular oxygen [91–93]. Among AOS, the hydroxyl radical ($HO^{\cdot}$) is believed to be the most effective for the degradation of carbohydrates.

It is generally accepted that $HO^{\cdot}$ abstracts a hydrogen on C2 or C3 in carbohydrates, resulting in the introduction of a carbonyl group and consecutive depolymerization via the β-elimination mechanism [94]. In contrast, Guay et al. [95] proposed that hydroxyl radical mainly attacks the anomeric position of methyl β-D-glucopyranoside. Konishi et al. [96] have investigated the abstraction of anomeric hydrogen of methyl α- and β-D-glucopyranosides (*236* and *237*) and methyl α-D-(1-^{2}H) glucopyranoside (*239*) and methyl β-D-(1-^{2}H) glucopyranoside (*238*) with AOS under the simulated industrial oxygen delignification conditions (2,4,6-trimethylphenol *240* and molecular oxygen) (Fig. 8.58).

To examine the stability of the carbohydrate model compounds, MPGα and MPGβ were jointly subjected to oxygen-alkali treatment in the absence of trimethylphenol. The recovery of both compounds was almost 100 %. Therefore, MPGα and MPGβ are not directly attacked by molecular oxygen and do not undergo alkaline-induced reactions. Consequently, the degradations described below are caused exclusively by AOS.

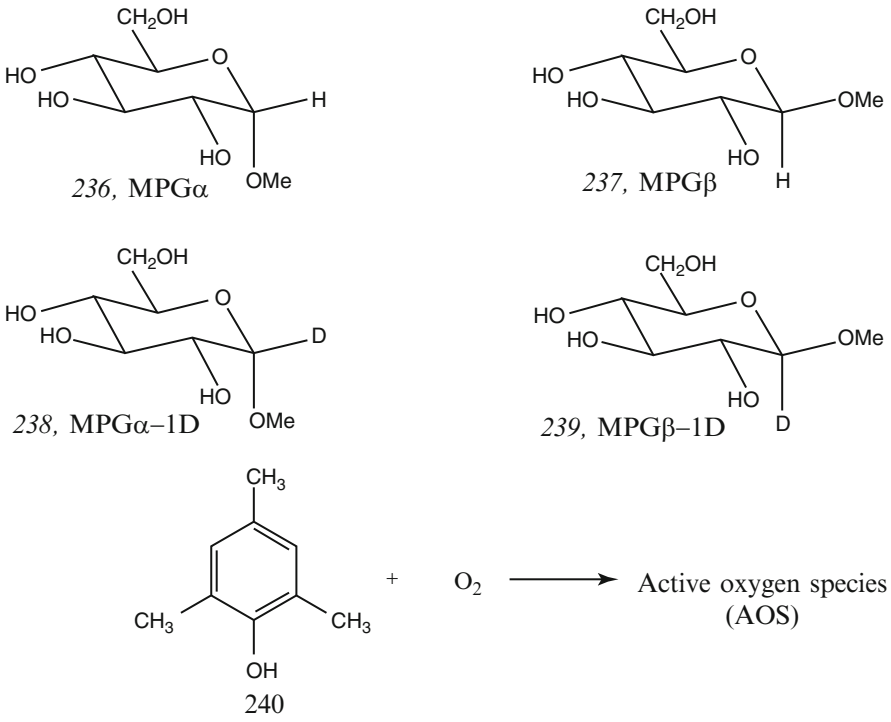

Fig. 8.58

When MPGα and MPGβ were jointly subjected to oxygen-alkali treatment in the presence of trimethylphenol, it was found that the degradation of both compounds was similar, but MPGβ was degraded more than MPGα, suggesting that the configurational difference at the anomeric position has a certain effect on the reaction with AOS. To exclude that the difference in rate of degradation of MPGα and MPGβ is not caused by difference in degradation at other carbon atoms in pyranoside ring, the Konishi et al. [96] have compared the rates of degradation of MPGβ and the deuterated form, MPG-β-1D, by AOS. Thus, when these two compounds were jointly subjected to oxygen-alkali treatment in the presence of trimethylphenol, it was found that the degradation of both compounds was similar, but MPGβ was degraded faster than MPGβ-1D due to the kinetic isotope effect.

The authors explained this observation by postulating that the kinetic isotope effect observed originates from anomeric hydrogen abstraction. No kinetic anomeric effect was observed for degradation of MPGα and MPG-α-1D, which indicates that anomeric hydrogen abstraction from MPG-α by AOS is not more than a very minor reaction. From this, it may be concluded that the anomeric carbon-hydrogen bond of MPG-β must be activated toward AOS attack by the anomeric effect.

8.8 Norrish-Yang Photocyclization

Norrish-Yang photocyclization has been widely used to generate regio- and stereocontrolled C–C bonds under mild conditions, especially when constructing quaternary stereocenters.

Herrera et al. [97, 98] have reported the usage of Norrish-Yang photocyclization for the synthesis of new spirocyclic monosaccharide derivatives of types *243* and *244* via a hydrogen atom transfer (HAT) reaction promoted by a 1,2-diketone *241*, in its excited state, followed by C–C tetrasubstituted bond formation in a diastereoselective manner (Fig. 8.59). Of special interest is the study of the tendency to inversion at C5 (for examples of epimerization of anomeric and pseudoanomeric radicals, see [99, 100]), probably triggered by conformational changes that the 1,4-diradical intermediate *242* undergoes in its triplet state, within its lifetime (for discussions of the lifetime of diradicals in solution, see [101, 102]) before the intersystem crossing (ISC) occurs.

In this regard, the authors probed different substituents and stereochemistries, mainly in position 5, 6, and 9 of the pyranose core of *242*-(Z), to explore the role of the stereoelectronic interactions [102–105], conformational restrictions [106–108], and formation of intramolecular hydrogen bonds in the stereocontrol of this reaction. For the anomeric effect, see [109]. For the anomeric effect of protons, see [110], and for the formation of intramolecular hydrogen bonds [111] in the stereocontrol of this reaction.

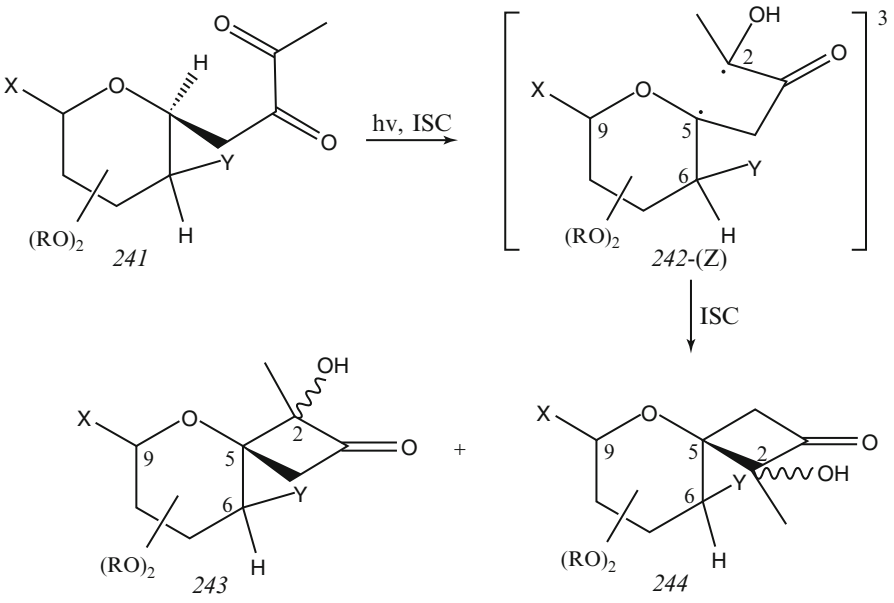

Fig. 8.59

It has been reported that 1,2-diketones mainly abstract hydrogen atoms from their triplet state and with a very small rate constant related to alkyl and aryl ketones [112]. However, in studied cases, the reactions were completed within relatively short times. A new factor has been introduced in these models. The presence of the geminal endocyclic oxygen may specially activate the hydrogen atom transfer. Furthermore, the 1,4-diradical intermediate *242* may be stabilized by a possible conjugative interaction of the SOMO-C5 radical with the lone pair at the ring oxygen and the σ*-LUMO of the C6–O bond (if Y = OR) [103–105], affecting probably the rate of the HAT step and the lifetime of intermediate *242*. Such studies have not been carried out before, although this C5-centered radical resembles the in-depth studied anomeric radical (for recent reviews, see [113, 114]) where the C5–H bond has been replaced a C5-alkyl; thus, it will be termed a pseudoanomeric radical. The photochemical generation of pseudoanomeric radical at C5 of the ribose moiety of a nucleotide, mimicking the 4′-RNA and 4′-DNA radicals, has previously been achieved via Norrish type I cleavage to study the DNA and RNA damage [115].

The compound *245* was selected for photocyclization due to its conformationally restricted $^4C_1$ pyranose ring. The 1,2-diketone *245* was irradiated with outdoor sunlight in its crystalline form for 20 h until the yellow color faded, affording a mixture of compounds from which the main product *247-(2R)* was isolated in moderate yield (42 %) as a sole stereoisomer (Table 8.8, entry 1). A single product *247-(2R)* was obtained in quantitative yield upon irradiation with sunlight in solution with $CHCl_3$ or benzene as solvents (Table 8.8, entry 2). Slightly shorter time was required upon irradiation with the UV lamp (Table 8.8, entry 3). The reaction proceeded with total retention of configuration at C5.

For this model, a C5 radical with very slow isomeric interconversion is formed at the 1,4-diradical intermediate *246* stage (Fig. 8.60). This isomerization is controlled by conformational changes at the ring moiety influenced by its substituents and stereoelectronic effects within the lifetime of this intermediate before the ISC occurs. In this case, four main favorable factors can play a major role leading to the product with retention at C5: stabilizing interaction of the SOMO-C5 radical with the lone pair at the ring oxygen (pseudoanomeric effect) and the σ*-LUMO of the C6-oxygen bond (β-oxygen effect) leading both to an axial C2–C5 bond formation via an early transition state [116, 117], the classic anomeric effect restricting the relative conformation between endocyclic oxygen and the C9 and the possible existence of an intramolecular hydrogen bond C2–OH. . .O(Bn) . . .C6, favoring their *syn* approximation. Moreover, steric hindrance and/or the possible hydrogen bond C2–OH. . .O(Bn)–C6 formation probably enhanced the high stereocontrol at C2 of the product, because the introduction of the protic solvent led to a mixture of diastereoisomers [118] (Table 8.8, entry 4).

The hydroxyl radical is one of the most reactive species known. Many of its reactions, including examples of hydrogen atom abstraction, have rate constants approaching the diffusion-control limit (ca. 10^{10} dm^3 mol^{-1} sec^{-1}). It is believed that the rate of hydrogen abstraction in molecules depends on the polar effects and the electrophilic character of the hydroxyl radical [119]. Steric effects are not

Table 8.8 Photocyclization of 1,2-diketones derived from O-glycosides

Reteention (A/B) Inversion (C/D)

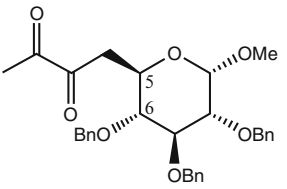

248 (=245)

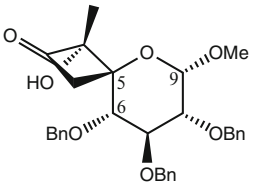

249-(2R)/*250* (2S)

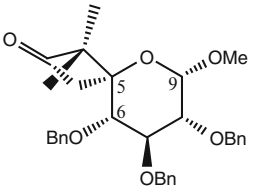

250-(2R)/*250*-(2S)

Entry	Light source	Solvent	Time h	Ratio (A:B:C:D)	Yield %	Retention %
1	sl (sunlight)	neat	21	(1:0:0:0)	42	100
2	sl	$CHCl_3$	2	(1:0:0:0)	100	100
3	UV	$CHCl_3$	1.5	(1:0:0:0)	100	100
4	UV	*t*-BuOH	1.8	(6:1:1:0)	92	87

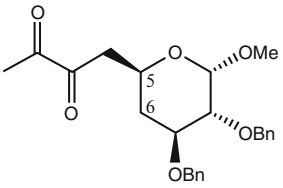

251

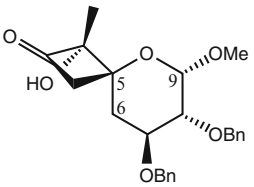

252-(2R)/*252*-(2S)

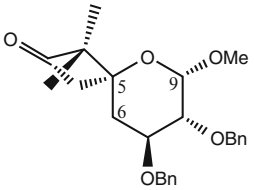

253-(2R)/*253*-(2S)

Entry	Light source	Solvent	Time h	Ratio (A:B:C:D)	Yield %	Retention %
5	sl (sun light)	$CHCl_3$	1.1	(0:2.3:1:0)	61	70
6	UV	$CHCl_3$	0.55	(0:2.3:1:0)	65	70
7	dl(day light)	$CHCl_3$	0.55	(0:2.3:1:0)	55	75
8	dl	$CHCl_3$	4	(0:3:1:0)	55	75

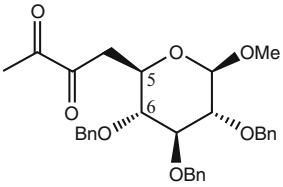

254

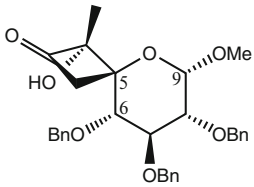

255-(2R)/*255*-(2S)

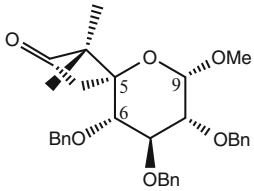

256-(2R)/*256*-(2S)

Entry	Light source	Solvent	Time h	Ratio (A:B:C:D)	Yield %	Retention %
9	UV	$CHCl_3$	0.6	(15:6:1:0)	95	95
10	UV	$CHCl_3$	0.3	(11:3:1:0)	88	93
11	UV	$CHCl_3$	2.0	(1:0:0:0)	80	100

(continued)

Table 8.8 (continued)

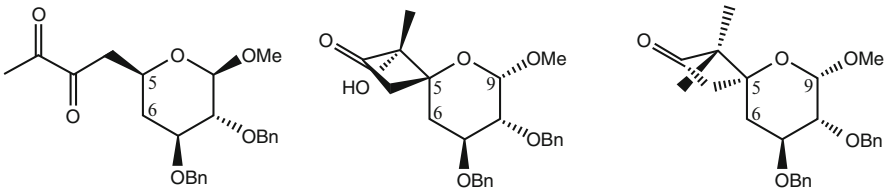

Entry	Light source	Solvent	Time h	Ratio (A:B:C:D)	Yiled %	Retention %
11	UV	$CHCl_3$	1.1	(0:1:1.2:0)	56	45

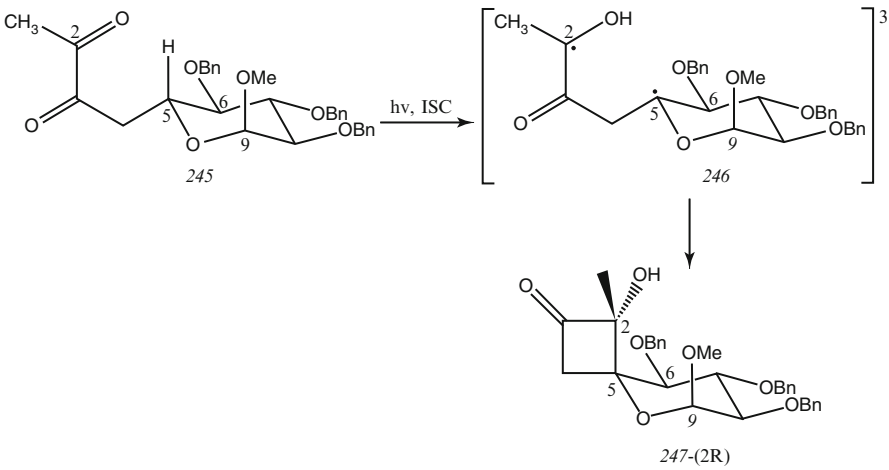

Fig. 8.60

generally thought to be important, but there are reported examples of the influence of stereoelectronic effects including the apparent preference of the attack at the C–H bond adjacent to the ring oxygen in the reaction of furanose sugars (for instance, to give *260* preferentially from β-D-fructofuranose) [120], in contrast to the behavior with pyranose sugars, for which reaction with the C–H bonds appears to be unselective [121] (Fig. 8.61). This selectivity evidently involves optimum overlap between the developing radical center and the lone pair of electrons on the adjacent ring oxygen, because it is also observed in the reactions of *tert*-BuO radical with ethers [122]; the relatively high selectivity for the C–H bond adjacent to oxygen in tetrahydrofuran compared with several other cyclic or acyclic examples

Fig. 8.61

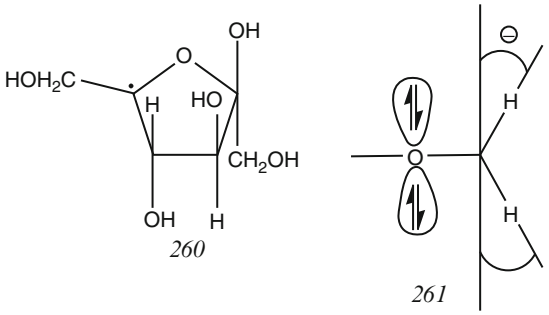

is attributed to the relatively small dihedral angle (θ) between the C–H bond and the p-type orbital on oxygen (*261*) [123].

The radical anion SO_4^- can be generated by photolysis [124] or thermolysis [125, 126] of the peroxydisulfate dianion as well as by the one-electron reduction of peroxydisulfate [127] by low-valent transition metal ions. The use of (catalytic) copper (II) and peroxydisulfate as an oxidant evidently involves similar reactions [128].

In contrast with its reaction with HO· (from which radicals formed by C–H abstraction are observed in relatively unselective fashion) [129], α-D-glucose reacts with SO_4^- to give a spectrum dominated by signals due to the C^1, C^2, C^5, and C^6 radicals (*264, 265*, *266*, and *267*; Table 8.9), the major signals being from the C^2 (*265*) and C^6 radicals (*267*) and the carbonyl conjugated species *268* formed via the rapid acid-catalyzed rearrangement of the C^2 species (see Table 8.9): there was little or no evidence for the C^3- or C^4-derived species. It is not surprising that reaction at C^6 occurs readily (it is sterically and statistically favored) [129]. The dominance of *265* perhaps reflects the stabilizing interaction (SOMO-σ*) between the unpaired electron at C^2 and the (eclipsing) β-OH bond (see *262* in Fig. 138) which makes a contribution to the stabilization of the transition state; similar interaction probably exists between the β-C–O bond in the C^6-derived radical *505* and similarly for the C^5-derived radical *266*. The C^1 radical benefits from conjugation to two α-oxygen atoms.

By comparison, the spectrum from β-D-glucose provides evidence for much greater extent of attack at C^1, to give *264*, and less at C^2, to give *27*. For *264*, susceptibility of the axial C–H bond toward the H abstraction accelerated by development of the overlap with the lone pair of electrons in a p-orbital on the ring oxygen (cf. *263*: see also [130]; with *263* (Table 8.9)) the equatorial β-OH group cannot provide such assistance (Fig. 8.62).

Weaker signals in the spectrum obtained for β-D-glucose were also observed from radicals obtained by abstraction of C^3–H (*270*) as well as C^5–H (*266*) and C^6–H (*267*) (see Table 8.9); signals were also observed for *273*, which is formed by elimination of water from *264*. It is interesting to note the relatively low signal intensity from the C^5-derived species in the spectra from α- and β-D-glucose: this is to some extent unexpected given the potentially stabilizing (and hence activating)

Table 8.9 Structures of radicals observed from the reaction of SO_4^{-} with some simple carbohydrates

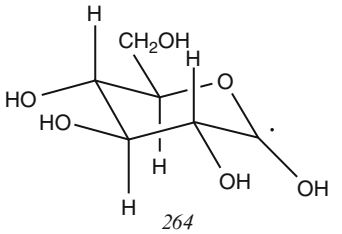

264

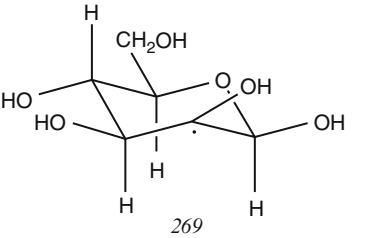

269

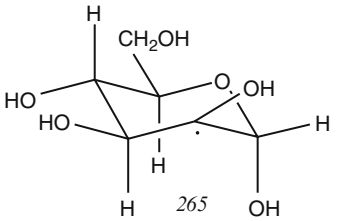

265

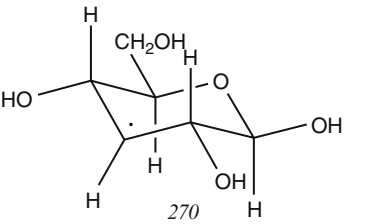

270

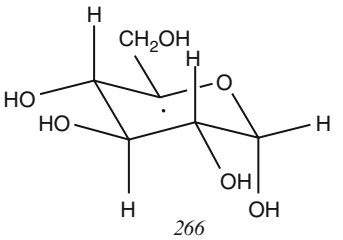

266

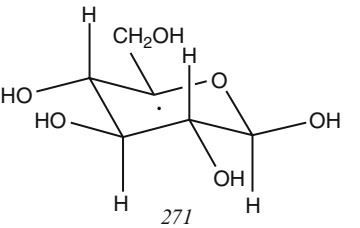

271

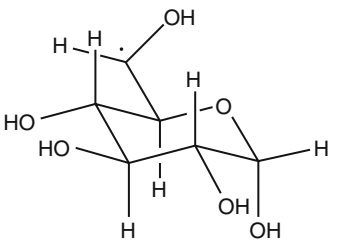

267

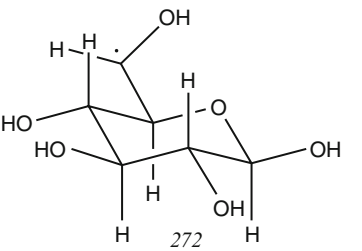

272

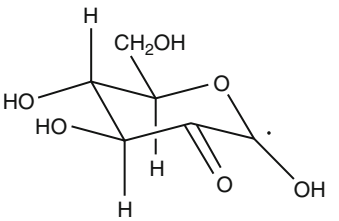

268

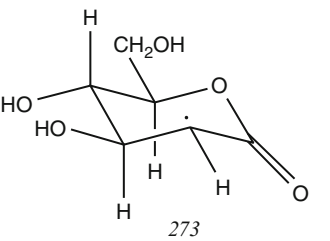

273

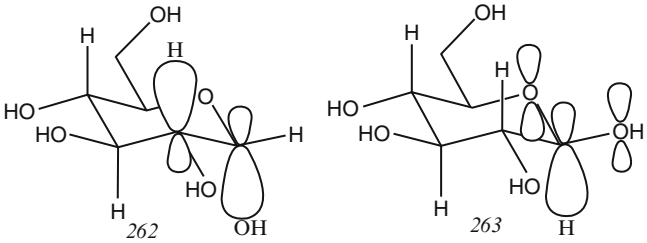

Fig. 8.62

effect of the α-oxygen in the ring and the eclipsing β-OH group at C^6. It is presumed that the β-C^6–OH group does not fully exert its effect in the transition state (unlike C^1–O in the α-glycosyl radical shown in *262* and the two α-oxygens in *263*) because the appropriate conformation is not adopted until the radical is fully formed. This is also true for the C^6 radicals formed from α- and β-D-glucose.

References

1. Isobe M, Kitamura M, Goto T, Goto T (1982) Stereocontrolled total synthesis of (±)-maytansinol. J Am Chem Soc 104:4997–4999
2. Isobe M, Kitamura M, Goto T (1979) Complete asymmetric induction in heteroconjugate addition on an acyclic system. A new synthetic approach directed toward ansamacrolide maytansine. Tetrahedron Lett 36:3465–3468
3. Isobe M, Kitamura M, Goto T (1980) Heteroconjugate addition of lithium alkyls to substituted hetero-olefins conjugated with sulfur and silicon atoms. Chem Lett 331–334
4. Das I, Pathak T (2005) A diastereoselective and general route to 5-amino-5- deoxysugars: influence of C-3 substitution on the addition of amines to C-5 of vinyl sulfone-modified hex-5-enofuranosyl carbohydrates. J Org Chem 70:8047–8054
5. Ravindran B, Sakthivel K, Suresh CG, Pathak T (2000) Diastereoselective addition of amines to vinyl sulfone modified carbohydrates: a highly flexible methodology for the synthesis of new classes of deoxyamino sugars. J Org Chem 65:2637–2641
6. Suresh CG, Ravindran B, Pathak T, Narasimha RK, Sasidhar JS, Lokanath NK (2000) Structural studies on C-2 substitution in a new set of synthetic aminodeoxy sugars: the steric bulk at C-2 influences the puckering of the pyranose ring. Carbohydr Res 337:1507–1512
7. Ferrier RJ (1968–2001) Carbohydrate chemistry: monosaccharides, disaccharides, and specific oligosaccharides, vol 1–32. The Royal Society of Chemistry, Cambridge
8. Sanki AK, Suresh CG, Falgune UD, Pathak T (2003) Org Lett 5:1285
9. Das I, Pal TK, Suresh CG, Pathak T (2007) Diastereoselective C–C bond formation at C-5 of vinyl sulfone-modified hex-5-enofuranosyl carbohydrates: diversity-oriented synthesis of branched-chain sugars and beyond. J Org Chem 72:5523–5533
10. Yoshimura J (1984) Synthesis of branched-chain sugars. Adv Carbohydr Chem Biochem 42:69–134
11. Miljkovic M (2009) Carbohydrates, synthesis, mechanisms, and stereoelectronic effects. Springer, New York
12. Collins PM, Ferrier RJ (1996) Monosaccharides: their chemistry and their role in natural products. Wiley, Chichester

13. Simpkins NS (1993) Sulphones in organic synthesis. Pergamon Press, Oxford
14. Takai I, Yamamoto A, Ishido Y, Sakakibara T, Yagi E (1991) Carbohydr Res 220:195–207
15. Ravindran B, Deshpande SG, Pathak T (2001) Vinylsulfone-modified carbohydrates: first general route to D-lividosamine (2-amino-2, 3-dideoxy-D-glucose) and its new analogs. Tetrahedron 57:1093–1098
16. Najera C, Yus M (1999) Desulfonylation reaction: recent developments. Tetrahedron 55:10547–10658
17. Wu J, Pathak T, Tong W, Vial JM, Remaud G, Chattopadhyaya J (1988) New synthesis of 2′, 3′-dideoxy-2′,3′-disubstituted and -2′-monosubstituted uridines and adenosines by Michael addition reactions. Tetrahedron 44:6705–6722
18. Bera S, Langley GJ, Pathak T (1998) Sugar-modified uridine bisvinyl sulfone: synthesis of a bifunctionalized nucleoside Michael acceptor and its use in stereoselective tandem cyclization. J Org Chem 63:1754–1760
19. Sanki AK, Suresh CG, Falgune UD, Pathak T (2003) Anomeric configuration-directed diastereoselective C–C bond formation in vinyl sulfone-modified carbohydrates: a general route to branched chain-sugars. Org Lett 5:1285–1288
20. Sanki AK, Pathak T (2002) A glycosylation driven strategy for the synthesis of anomerically pure vinyl sulfone-modified pent-2-enofuranoses and hex-2-enopyranoses. Synlett 1241–1244
21. Chen G, Franck RW, Yang G, Blumenstein M (2002) Anomeric effects of sulfone. Can J Chem 80:894–899
22. Bushweller CH (1995) In: Juaristi E (ed) Chapter 5: Conformational analysis and stereochemistry of six-membered rings. Verlag Chemie, New York, p 25
23. Eliel EL, Hargrave KD, Pietrusiewicz KM, Manoharan M (1982) J Am Chem Soc 104:3635
24. Bushweller CH (1995) In: Juaristi E (ed) Chapter 5: Conformational analysis and stereochemistry of six-membered rings. Verlag Chemie, New York, p 157
25. Boche G (1999) Angew Chem Int Ed Engl 28:277–297
26. King JF, Rathore R (1990) Geometry dependence of the effect of a β-substituent on the rate of hydrogen-deuterium exchange: evidence for a stereoelectronic component of the polar effect. J Am Chem Soc 112:2001–2002
27. Brown MD, Cook MJ, Hutchinson BJ, Katritsky AJ (1971) Conformational analysis of saturated heterocycles. XL. Stereochemistry of base-catalyzed hydrogen-deuterium exchange of methylene protons alpha to a sulfonyl group. Tetrahedron 27:593–600
28. Kaloustian MK, Dennis N, Mager S, Evans SA, Alcudia F, Eliel EL (1976) Conformational analysis. XXX. Conformational equilibria of 1,3-dioxanes with polar substituents at C-5. J Am Chem Soc 98:956–965
29. Kirby A (1983) The anomeric effect and related stereoelectronic effects at oxygen. Springer, Berlin, pp 78ff
30. Padwa A, Wanamaker MW (1986) Significance of the anomeric effect on the configurational stability of cyclopropyl carbanions. Tetrahedron Lett 27:2555–2558
31. Stock LM (1972) Origin of the inductive effect. J Chem Educ 49:400–404
32. Strecker A (1850) Ann Chem Pharm 75:27
33. Kunz H, Sager W, Schanzenbach D, Decker M (1991) Carbohydrates as chiral templates: stereoselective Strecker synthesis of D-⟨-amino nitriles and acids using *O*-pivaloylated D-galactopyranosylamine as the auxiliary. Liebigs Ann Chem 649–654
34. Kunz H, Sager W (1987) Diastereoselective Strecker synthesis of α-amino nitriles in carbohydrate matrixes. Angew Chem 99:595–597, Angew Chem Int Ed Engl 26:557
35. Kunz H, Sager W (1985) Stereoselective glycosylation of alcohols and silyl ethers using glycosyl fluorides and boron trifluoride etherate. Helv Chim Acta 68:283–287
36. Birkhofer L, Ritter A (1965) Silylation as an auxiliary method of organic chemistry. Angew Chem 77:414–426, Angew Chem Int Ed Engl 4:417
37. Paulsen H, Györgydeak M, Friedmann M (1974) Conformational analysis. V. Influence of the anomeric and reverse anomeric effect on conformational equilibria on N-substituted N-pentopyranosides. Chem Ber 107:1590

38. Ojima I, Inaba S (1975) Asymmetric synthesis of α-aminonitriles via cyanosilylation of Schiff bases. Chem Lett 737
39. Kunz H, Pfrengle W (1988) Carbohydrates as chiral templates: asymmetric Ugi-synthesis of α-amino acids using galactosylamines as the chiral matrices. Tetrahedron 44:5487–5494
40. Laschat S, Kunz H (1990) Carbohydrates as chiral templates: stereoselective synthesis of chiral homoallyl amines and β-amino acids. Synlett 51–52
41. Ferrier RJ (1979) Unsaturated carbohydrates. Part 21. A carbocyclic ring closure of a hex-5-enopyranoside derivative. J Chem Soc Perkin Trans 1:1455–1458
42. Blattner R, Ferrier RJ, Prasit P (1980) New approach to aminoglycoside antibiotics. J Chem Soc Chem Commun 944–945
43. Sugawara F, Kuzuhara H (1981) Synthesis of potential antimicrobial agents from maltose. Part II. Partial conversion of maltose into cyclohexane derivatives. Agric Biol Chem 45:301–304
44. Semeria D, Phillipe M, Delaumney JM, Spulchre AM, Gero SD (1983) A general synthesis of cyclitols and aminocyclitols from carbohydrates. Synthesis 710–713
45. Mádi-Puskás M, Pelyvás I, Bognár R (1985) Carbocyclic ring closure of an aminodeoxy hex-5-enopyranoside. J Carbohydr Chem 4:323–331
46. Vass G, Krausz P, Quiclet-Sire B, Delaumney JM, Cleophax J, Gero SD (1985) A new approach to the synthesis of cyclitols and aminocyclitols from D-glucose and D-glucosamine. C R Acad Sci Ser II:1345–1346
47. Machado AS, Olesker A, Castillon S, Lukacs G (1985) Hydroxy group directed hydrogenation with rhodium and iridium catalysts. Synthesis of protected chiral carbocyclic analog of daunosamine. J Chem Soc Chem Commun 530–532
48. Barton DHR, Gero SD, Augy S, Quiclet-Sire B (1986) Synthesis of carbocyclic analogs of D-glucosamine and L-idosamine from D-glucosamine. J Chem Soc Chem Commun 1399–1401
49. Dyong I, Hagedorn HW, Thiem J (1986) Antibiotics models. 7. Diastereoselective synthesis of a rhodomycinone model from D-glucose. Liebigs Ann Chem 551–563
50. Sakairi N, Hayashida M, Kuzuhara H (1987) Synthesis of a new antimicrobial aminoglycoside employing maltose as a key starting material. Tetrahedron Lett 28:2871–2874
51. László P, Pelyvás IF, Sztaricskai F, Szilágyi L, Somogyi Á (1988) Novel aspects of the Ferrier carbocyclic ring-transformation reaction. Carbohydr Res 175:227–239
52. Blattner R, Ferrier RJ, Haines SR (1985) Unsaturated carbohydrates. Part. 28. Observations on the conversion of 6-deoxyhex-5-enopyranosyl compounds into 2-deoxyinosose derivatives. J Chem Soc Perkin Trans 1:2413–2416
53. Blattner R, Ferrier RJ (1986) Functionalized carbocycles from carbohydrates. Part 9. Direct synthesis of 6-oxabicyclo[3.2.1]octane derivatives from deoxyinoses. Carbohydr Res 150:151–162
54. Ferrier RJ, Haines SR (1984) Functionalized carbocycles from carbohydrates, part 6. A route to functionalized cyclopentanes from 6-deoxyhex-5-enopyranoside derivatives. Carbohydr Res 130:135–146
55. Machado AS, Olesker A, Lukacs G (1985) Synthesis of two enantiomeric tetrasubstituted cyclohexanones from 6-deoxyhex-5-enopyranoside derivatives. Carbohydr Res 235:231–239
56. Machado AS, Olesker A, Castillon S, Lukacs G (1985) Hydroxy group directed hydrogenation with rhodium and iridium catalysts. Synthesis of protected chiral carbocyclic analog of daunosamine. J Chem Soc Chem Commun 330–332
57. Baldwin JE (1976) Rules for ring closure. J Chem Soc Chem Commun 734–736
58. Vasella A (1977) Stereoselektivität und Reaktivität bei der 1, 3-dipolaren Cycloaddition chiraler N-(Alkoxyalkyl)nitrone. Helv Chim Acta 60:1273–1295
59. David S, Eisenstein WJ, Hehre WJ, Salem L, Hoffmann R (1973) Superjacent orbital control. Interpretation of the anomeric effect. J Am Chem Soc 95:3806–3907
60. Ohtake H, Iimori T, Ikegami S (1997) A highly stereoselective β-(1 → 4)-glycosidic bond formation by reductive cleavage of cyclic orthoesters. Tetrahedron Lett 38:3413–3414

61. Iimori T, Ohtake H, Ikegami S (1997) A highly stereoselective β-(1 → 4)-glycosidic bond formation by reductive cleavage of cyclic orthoesters. Tetrahedron Lett 38:3415–3418
62. Ohtake H, Iimori T, Shiro M, Ikegami S (1998) Synthesis and structure of glycosylidene acetals of galactoside. Heterocycles 47:685–688
63. Ohtake H, Iimori T, Ikegami S (1998) A highly stereoselective construction of glycosyl-β-(1 → 4)-galactoside linkages by reductive cleavage of cyclic orthoesters. Synlett 1420–1422
64. Bhattacharjee SS, Gorin PAJ (1969) Hydrogenolysis of carbohydrate acetals, ketals, and cyclic orthoesters with lithium aluminum hydride – aluminum trichloride. Can J Chem 47:1195–1206
65. Lipták A, Jodál I, Nánási P (1975) Stereoselective ring cleavage of 3-*O*-benzyl- and 2,3-di-*O*-benzyl-4, 6-*O*-benzylidenehexopyranoside derivatives with lithium aluminum hydride – aluminum chloride reagent. Carbohydr Res 44:1–11
66. Kolossváry I, Guida WC (1996) A low mode search. An efficient, automated computational method for conformational analysis: application to cyclic and acyclic alkanes and cyclic peptides. J Am Chem Soc 118:5011–5019
67. Cheng G, Guida WC, Still WC (1989) An internal-coordinate Monte Carlo method for searching conformational space. J Am Chem Soc 111:4379
68. Ohtake H, Ichiba N, Shiro M, Ikegami S (2000) Synthesis and structure of 6-*O*-, 6-*O*-glycosylidene glycosides. J Org Chem 65:8164–8170
69. Deslongchamps P, Chénevert R, Taillefer RJ, Moreau C, Saunders JK (1975) Hydrolysis of cyclic orthoesters. Stereoelectronic control in the cleavage of hemiorthoester tetrahedral intermediates. Can J Chem 53:1601–1615
70. Garegg PJ, Hultberg H, Wallin S (1982) A novel, reductive ring-opening of carbohydrate benzylidene acetals. II. Carbohydr Res 108:97–101
71. Eliel EL, Nader FW (1970) Conformational analysis. XX. Stereochemistry of reaction of Grignard reagent with ortho esters. Synthesis of 1, 3-dioxanes with axial substituents at C-2. J Am Chem Soc 92:584–590
72. Li S, Dory Y, Deslongchamps P (1996) Hydrolysis of cyclic orthoesters: experimental observations and theoretical rationalization. Tetrahedron 47:14841–14854
73. Bunton CA, De Wolfe RH (1965) The hydrolysis of carboxylic ortho esters. J Org Chem 30:1371–1375
74. Eliason R, Kreevoy MM (1978) Kinetic hydrogen isotope effects in the concerted mechanism for the hydrolysis of acetals, ketals, and ortho esters. J Am Chem Soc 100:7037–7041
75. Deslongchamps P (1983) In: Baldwin JE (ed) Stereoelectronic effects in organic chemistry, vol 1, Organic chemistry series. Pergamon Press, Oxford, p 31
76. Schmidt MW, Baldridge KK, Boatz JA, Elbert ST, Gordon MS, Jensen JH, Koseki S, Matsunga N, Nguyen KA, Su SJ, Windus TL, Dupuis M, Montgomery JA (1993) General atomic and molecular electronic structure system. J Comput Chem 14:1347–1363
77. Rolf D, Gray GR (1982) Reductive cleavage of glycosides. J Am Chem Soc 104:3539–3541
78. Rolf D, Benneck JA, Gray GR (1983) Reductive cleavage of glycosides. Stereochemistry of trapping of cyclic oxonium ions. J Carbohydr Chem 2:373–383
79. Bowie JU, Gray GR (1984) Synthesis and mass spectra of partially methylated and partially ethylated anhydro-D-mannitol acetates derived by reductive cleavage of permethylated and perethylated saccharomyces cerevisiae D-mannans. Carbohydr Res 129:87–97
80. Bowie JU, Trescony PV, Gray GR (1984) Analysis of linkage position in *Saccharomyces cerevisiae* D-mannans by reductive-cleavage method. Carbohydr Res 125:301–307
81. Jun J-G, Gray GR (1987) A new catalyst for reductive cleavage of methylated glycans. Carbohydr Res 163:247–261
82. Lee CK, Gray GR (1988) A general strategy for the chemical sequencing of polysaccharides. J Am Chem Soc 110:1292–1293
83. Lee CK, Gray GR (1995) Carbohydr Res 269:163–179

84. Benneck JA, Rice MJ, Gray GR (1986) Analysis of linkage positions in 2-acetamino-2-deoxy-D-glucopyranosyl residues by the reductive-cleavage method. Carbohydr Res 157:125–137
85. Rolf D, Benneck JA, Gray GR (1985) Analysis of linkage positions in D-glucopyranosyl residues by reductive-cleavage method. Carbohydr Res 137:183–196
86. Rolf D, Gray GR (1984) Analysis of linkage positions in D-glucopyranosyl residues by the reductive-cleavage method. Carbohydr Res 131:17–28
87. Rolf D, Gray GR (1986) Carbohydr Res 152:343–349
88. Vodonik SA, Gray GR (1989) Analysis of the linkage positions in D-fructofuranosyl residues by the reductive-cleavage method. Carbohydr Res 172:255–266
89. Lee CK, Kim EJ, Lee I-SH (1993) Anomerization and transglycosylation reactions of permethylated methyl D-glycopyranosides. Carbohydr Res 240:197–206
90. Lee CK, Kim EJ, Lee I-SH (1998) Mechanism of anomerization of permethylated methyl D-glycopyranosides by trimethylsilyl trifluoromethanesulfonate. Carbohydr Res 309:243–250
91. Ericssson B, Lingren BO, Theander O (1971) Factors influencing the carbohydrate degradation under oxygen-alkali bleaching. Svensk Papperstidn 74:757–765
92. Yokoyama T, Matsumoto Y, Yasumoto M, Meshitsuka G (1996) The role of peroxide species in the carbohydrate degradation during oxygen bleaching. Part 2: Effect of oxygen pressure on the degradation of lignin and carbohydrate model compounds and on the reaction selectivity. J Pulp Pap Sci 22:J151–J154
93. Gierer J, Imsgard F (1977) The reaction of lignins with oxygen and hydrogen peroxide in alkaline media. Svensk Papperstidn 80:510–518
94. Gierer J (1997) Formation and involvement of superoxide (O_2./H_2O.) and hydroxyl (HO.) radicals in TCF bleaching processes. Holzforschung 51:34–46
95. Guay DF, Cole BJW, Fort RC Jr, Genco JM, Hausman MC (2000) Mechanism of oxidative degradation of carbohydrates during oxygen delignification. I. Reaction of photochemically generated hydroxyl radical with methyl β-D-glucoside. J Wood Chem Technol 20:375–394
96. Konishi F, Yokoyama T, Matsumoto Y (2009) Investigation of hydrogen abstraction from methyl glycoside by active oxygen species under oxygen delignification conditions. Part 1. Study of the anomeric position. Holzforschung 63:52–60
97. Herrera AJ, Rondón M, Suárez E (2007) Stereocontrolled photocyclization of 1,2-diketones applied to carbohydrate models: a new entry to C-ketosides. Synlett 1851–1856
98. Herrera AJ, Rondón M, Suárez EJ (2008) Stereocontrolled photocyclization of 1,2-diketones: applications of a 1,3-acetyl group transfer methodology to carbohydrates. J Org Chem 73:3384–3391
99. Brunckova J, Crich D, Yao Q (1994) Intramolecular hydrogen atom abstraction in carbohydrates and nucleosides: inversion of and α- to β-mannopyranoside and generation of thymidine C-4′ radicals. Tetrahedron Lett 35:6619–6622
100. Yamazaki N, Eichenberger E, Curran DP (1994) Synthesis of β-mannopyranoside from α-epimers by radical inversion. 1,6-hydrogen transfer reactions of 2-*O*-(2-bromoaryl) dimethylsilyl-α-methyl-D-mannopyranosides. Tetrahedron Lett 35:6623–6626
101. Johnston LJ, Caiano JC (1989) Time-resolved studies of biradical reactions in solution. Chem Rev 89:521, and references cited therein
102. Cai X, Cygon P, Goldfuss B, Griesbeck AG, Heckroth H, Fujitsuka M, Majima T (2006) α-Carbonyl substituent effect on the lifetimes of triplet 1,4-biradicals from Norrish-type-II reactions. Chem Eur J 12:4662–4667
103. Dupuis J, Giese B, Rüegge D, Fischer H, Korth H-G, Sustman R (1984) Conformation of glycosyl radicals: radical stabilization by β-CO bonding. Angew Chem 96:887–888
104. Giese B (1989) Stereoselectivity of intermolecular reactions. Angew Chem 28:993–1004
105. Brunckova J, Crich D (1995) Intramolecular hydrogen atom abstraction: the β-oxygen effect in the Norrish type II photo-reaction. Tetrahedron 51:11945–11952, and references cited therein

106. Griesbeck AG, Mauder H, Stadtmüller S (1994) Intersystem crossing in triplet 1,4-biradicals: conformational memory effects on the stereoselectivity of photocycloaddition reactions. Acc Chem Res 27:70–75
107. Ihmels H, Scheffer J (1999) The Norrish type II reaction in the crystalline state: toward a better understanding of the geometric requirements for γ-hydrogen atom abstraction. Tetrahedron 55:885–907
108. Giese B, Wettstein P, Stähelin C, Barbosa F, Neuburger M, Zehnder M, Wessig P (1999) Memory of chirality in photochemistry. Angew Chem Int Ed Engl 38:2586, and references cited therein
109. Juaristi E, Cuevas G (1992) Recent studies on the anomeric effect. Tetrahedron 48:5019–5087, and references cited therein
110. David S (2005) The evidence for an anomeric effect of the proton. Carbohydr Res 340:2569–2572
111. Walther K, Kranz U, Henning H-G (1987) Photochemistry of amino ketones. X. Preparation and diastereoselective photocyclization of N-(β-benzoylethyl)-N-tosylglycinamides. J Prakt Chem 329:859
112. Turro NJ, Lee T-J (1969) Molecular photochemistry. XX. Intramolecular photoreduction of alkyl α-diketone. J Am Chem Soc 91:5651–5652
113. Giese B, Zeitz H-G (1997) C-Glycosyl compounds from free radical reactions. In: Hanessian S (ed) Preparative carbohydrate chemistry. Marcel Dekker, New York, p 507
114. Pearce AJ, Mallet J-M, Sinaÿ P (2001) In: Renaud P, Sibi MP (eds) Radicals in organic synthesis, vol 2. Wiley-VCH, Weinheim, p 523
115. Strittmatter H, Dussy A, Schwitter U, Giese B (1999) Angew Chem Int Ed Engl 38:135
116. Beckwith ALJ, Duggan PJ (1998) The quasi-homo-anomeric interaction in substituted tetrahydropyranyl radicals: structure and kinetics of formation. Tetrahedron 54:4623–4632
117. Beckwith ALJ, Duggan PJ (1998) The quasi-homo-anomeric interaction in substituted tetrahydropyranyl radicals: diastereoselectivity. Tetrahedron 54:6919–6928
118. Kaanumalle LS, Natarajan A, Ramamurthy V (2005) In: Griesbeck AG, Mattay J (eds) Synthetic organic photochemistry, vol 12, Molecular and supramolecular photochemistry. Macel Dekker, New York, p. 553
119. Norman ROC, Gilbert BC (1967) Electron spin resonance studies of short-lived organic radicals. Adv Phys Org Chem 5:53–119
120. Fitchett M, Gilbert BC, Wilson RL (1988) Fragmentation reactions of radicals formed from sugar phosphates and the hydroxyl radical: an investigation by electron spin resonance spectroscopy and pulse radiolysis. J Chem Soc Perkin Trans 2:673–689
121. Gilbert BC, King DM, Thomas CB (1981) Radical reactions of carbohydrates. Part 2. An electron spin resonance study of the oxidation of D-glucose and related compounds with the hydroxyl radical. J Chem Soc Perkin Trans 2:1186–1199
122. Malatesta V, Ingold KU (1981) Kinetic application of electron paramagnetic resonance spectroscopy. 36. Stereoelectronic effects in hydrogen atom abstraction from ethers. J Am Chem Soc 103:609–614
123. Deslongchamps P (1975) Stereoelectronic control in the cleavage of tetrahedral intermediates in the hydrolysis of esters and amides. Tetrahedron 31:2463–2490
124. Clifton CL, Huie RE (1989) Rate constants for hydrogen abstraction reactions of the sulfate radical, SO_4^-. Alcohols. Int J Chem Kinet 21:677–687
125. Fenton HJH (1894) Oxidation of tartaric acid in presence of iron. J Chem Soc 899–910
126. Fenton HJH, Jackson HJ (1899) The oxidation of polyhydric alcohols in presence of iron. J Chem Soc 1
127. Gilbert BC, Stell JK (1990) Mechanism of peroxide decomposition. An ESR study of the reactions of the peroxomonosulfate anion ($HOOSO_3^-$) with titanium (III), iron (II), and α-oxygen substituted radicals. J Chem Soc Perkin Trans 2:1281–1288
128. Gilbert BC, Stell JK, Jeff M (1988) Electron spin resonance studies of the effect of copper (II) and copper (I) on the generation and reactions of organic radicals formed from the Fenton

reaction and the titanium (III)-hydrogen peroxide and Ti(III)-peroxydisulfate redox couples. J Chem Soc Perkin Trans 2:1867–1873
129. Gilbert BC, Smith JRL, Taylor P, Ward S, Whitwood AC (1999) The interplay of electronic, steric, and stereoelectronic effects in hydrogen-atom abstraction reactions of SO_4^{-}, revealed by EPR spectroscopy. J Chem Soc Perkin Trans 2:1631–1637
130. Hayday K, McKelvey RD (1976) An anomeric effect in photochemical hydrogen abstraction reactions of tetrahydropyranyl ethers. J Org Chem 41:2222–2223

Author Index

M. Miljkovic, *Electrostatic and Stereoelectronic Effects in Carbohydrate Chemistry*,
DOI 10.1007/978-1-4614-8268-0, © Springer Science+Business Media New York 2014

I

L

M

Subject Index

M. Miljkovic, *Electrostatic and Stereoelectronic Effects in Carbohydrate Chemistry*,
DOI 10.1007/978-1-4614-8268-0,